INTERNATIONAL COURT OF JUSTICE

DISPUTE OVER THE STATUS AND USE OF THE WATERS OF THE SILALA

(CHILE v. BOLIVIA)

REJOINDER OF THE PLURINATIONAL STATE OF BOLIVIA

ANNEXES 23.3 TO 23.5

VOLUME 3 OF 6

15 MAY 2019

LIST OF ANNEXES TO THE REJOINDER OF THE PLURINATIONAL STATE OF BOLIVIA

VOLUME 3 OF 6

ANNEX N°	TITLE	PAGE N°
TECHNICAL DOCUMENTS (ANNEXES 23.3 – 23.5)		
Annex 23.3	FUNDECO, "Study of Evaluation of Environmental Impacts in the Silala", May 2018 (English Translation)	5
Annex 23.4	FUNDECO, "Study of Evaluation of Environmental Impacts in the Silala, Palynology", 2018 (English Translation)	131
Annex 23.5	F. Urquidi, "Technical analysis of geological, hydrological, hydrogeological and hydrochemical surveys completed for the Silala water system", June 2018 (English Translation)	233
Annex 23.5 Appendix a	SERGEOMIN (National Service of Geology and Mining), Study of the Geology, Hydrology, Hydrogeology and Environment of the Area of the Silala Springs, June 2000-2001, Final Edition 2003 (English Translation)	333

Annex 23.3

FUNDECO, "Study of Evaluation of Environmental Impacts in the Silala", May 2018

(English Translation)

DIREMAR

ENVIRONMENTAL IMPACT ASSESSMENT STUDY IN SILALA

La Paz - Bolivia

May 2018

Luis Pacheco D.Cs.

Coordinator

Authors:

Luis F. Pacheco, D.Cs. Coordinator. Director of the Institute of Ecology of the Higher University of San Andres (UMSA).
Lic. Rosa Isela Meneses Specialist in high Andean ecosystems and wetlands. Head of the botany unit of the National Museum of Natural History and Researcher of the National Herbarium of Bolivia.
Eng. Lic. Gabriel Zeballos Specialist in Geographic Information Systems. Department of Geography, Ohio State University.
M. Carolina Garcia Lino, PhD. Ecologist of plants of alpine environments. Researcher associated with the National Herbarium of Bolivia.
Susi Loza Herrera, MSc. Biologist – ecologist. Researcher associated with the National Herbarium of Bolivia.
Lic. Loly Vargas C. Socio-environmental biologist
Arely N. Palabral A., MSc. Botanical biologist. Researcher associated with the National Herbarium of Bolivia.
Eng. Ariel Lliully A. Botanical specialist in grasses and graminoids. Re earcher associated to the National Herbarium of Bolivia.
Lic. Jorge Molina Biologist of aquatic ecosystems. Researcher associated with the Limnology Unit (IE-UMSA).
Biol. Jaime Sarmiento Ichthyologist. National Museum of Natural History.
Biol. Alberto Mariscal Ichthyologist.
Lic. James K. Aparicio E. Herpetologist. Head of the Zoology Unit of the National Museum of Natural History. Head and Curator of the Reptile and Amphibian Area of the Bolivian Wildlife Collection.
Lic. Leslie Zegada H. Herpetologist
Lic. M. Isabel Gomez U. Ornithologist. National Museum of Natural History.
Lic. Paola Velásquez Noriega Ornithologist.
Adriana Rico, PhD. Mammal Zoologist. Bolivian Wildlife Collection (IE-UMSA).
Biologist Virginia Sanchez Mammal Zoologist.

Glossary

Bofedal: Type of plant formation dependent on the constant contribution of water and characterized by a high concentration of organic matter.
Ecological quality: The general expression of the structure and function of an ecosystem.

Community: Set of animal populations, plants and/or living beings that share a geographical area in a given time. When living in a territory, the populations share space and other resources and establish different types of relationships. The stability of a biological community is determined by the variety and quantity of populations that form it.

Ecosystem: It is integrated by the community in interrelation with the area or territory occupied by it. Then, in the ecosystem live components are distinguished, which form the community and the lifeless components (abiotic elements).

Macro-invertebrates: They are aquatic invertebrates, larvae, nymphs, naiads or adults that live in the substrate, the column or the surface of bodies of water, which can be seen with the naked eye or through simple magnifying glasses. When they are in the water they can give information about
the health of the ecosystems and the ecological quality of the water, in its physical-chemical and morph-structural components.

Fluvial Habitat Index (FHI): Index designed to assess habitat quality based on seven parameters including: the inclusion of rapids, frequency of rapids, composition of the substrate, velocity/depth regime, percentage of shade in the channel, elements of heterogeneity and coverage of aquatic vegetation.
Population: Set of individuals of the same species that share a geographical space in a given time. A species is a set of beings with similar biological characteristics, which can cross originating fertile offspring. Example: all the lapachos of a certain area form a population. Example: all mice in a certain area.

Physiological unit: Community of plants similar in appearance. For example, because of its growth pattern.

Authors
Glossary
Executive Summary

1. BACKGROUND
2. THEORETICAL FRAMEWORK
3. GENERAL OBJECTIVE
4. STUDY AREA
5. METHODOLOGY
5.1 Diagnosis of abiotic and biotic factors in the Silala area
5.2 Determination of the actual area of the bofedales
5.3 Vegetation map of the area and calculation of the bofedales area in the past
5.4 Current conditions of the bofedales: first line of analysis
Vegetation
Ichthyofauna
Herpetofauna
Avifauna
Mastofauna
DATA ANALYSIS
5.5 Environmental impacts to the bofedal caused by the artificial canal system
Vegetation
Aquatic macro-invertebrates
5.6 Fishes
6. RESULTS
6.1 Historical occupation in the territory of Silala (social area)
6.2 Diagnosis of biotic and abiotic factors
Climatic conditions
Physical-chemical parameters
Canals
Soil
Flora
Fauna
Macro-invertebrates

Ichthyofauna
Herpetofauna
Avifauna
Mastofauna
6.3 Determination of the actual area of the bofedales
6.4 Calculation of the bofedal area in the present and recent past
6.5 Current conditions of the Silala bofedales
Botanical description of the Silala bofedales
Fragments of the South Bofedal
North Bofedal (N)
Confluence between the South and North Bofedales (CONF)
Current status of the bofedales
6.6 Environmental impacts to the bofedal caused by the presence of artificial canals
6.6.1 Ecological quality of the bofedales
6.6.1 Macro-invertebrates
Birds
Mammals
6.7 Planning of the restoration measures that must be carried out to guarantee the conservation
of the ecosystem of bofedales
6.8 Development of an environmental monitoring program for Silala
6.9 Mitigation and control of impacts on the Silala bofedales
7. CONCLUSIONS
8. BIBLIOGRAPHIC REFERENCES
ANNEXES
1. Historical and social aspects
2. Codes and meanings of fragments and abbreviated species
3. Forward selection of PCA analysis with environmental variables that significantly affect plant communities.
4. Photographic guide of the taxa found in the Silala wetlands
5. Physical-chemical parameters of the sampling stations in the Silala wetlands
6. Habitat and morphological-structural parameters of the Silala wetlands

Executive Summary

The results of the report of the consultancy "Environmental Impact Assessment Study in Silala" are presented. This report includes the assessment of the status of bofedales (biotic and abiotic factors), the impacts caused by human activities (mainly the canalization), an assessment of the diversity associated with bofedales, restoring, mitigation and monitoring guidelines and, in addition some historical and social aspects related to the area. The assessment was carried out through field visits between March and April 2018 and analysis of satellite images.

Three zones were differentiated in the Silala bofedales: the South Bofedal, North Bofedal and the Confluence Area. At a landscape level and based on the composition and abundance of species, the three bofedales are described. The South Bofedal is the most degraded and fragmented. In this area six fragments with different plant communities are recognized, which correspond to meadows and grass with different proportions of bare soil and saline outcrops (fragments A, B and C).

Species were found that are not typical of bofedales (such as Deyeuxia curvula), some that are indicative of high soil moisture (such as Xenophyllum incisum), which are usually found at the margins of bodies of water and bofedal margins. Desert and saline areas were found that, due to the presence of the aforementioned species, would have been a bofedal in the recent past (decades). Within the South Bofedal, the D and E fragments represent the areas that still maintain a properly bofedal structure, with a state of conservation from regular to degraded, with the E fragment having the highest ecological quality in the Silala. The D and E fragments of the South Bofedal have a total area of 4,822 m2.

In the North Bofedal, three units were identified: 1) areas with dominance of Oxychloe andina (typical species of bofedales), 2) areas with a high density of open canals with dominance of Deyeuxia eminens var. eminens and 3) semi-dry sectors of margins of bofedales, with Festuca potosiana dominance. The North Bofedal has an area of 2,540 m2. This bofedal is degraded.

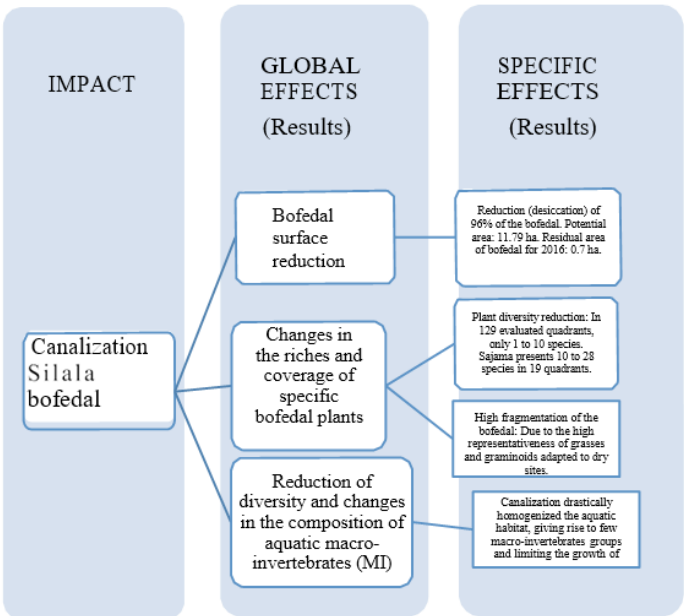
In the bofedal of the Confluence Area there is a higher frequency of Deyeuxia eminens var. eminens (species associated with running waters) and to a lesser extent a mixture of Festuca rigescens and Oychloe andina. This sector is much degraded and poorly preserved.

The assessment at the level of quadrants (129 of 1 m2), shows a high heterogeneity of the vegetation in the bofedales; mainly the North Bofedal, which has a wide range of grasses such as Festuca potosiana. Since it is a species of the margins of bofedales, the presence of Festuca potosiana suggests that the water availability of bofedales has been reduced, compared to a typical bofedal.

The floristic composition indicates a high degree of compaction (which reduces the porosity of the soil), by the dominance of gramineae and graminoid species, such as Carex cf. maritima and frigid Puccinellia; species that form plaques, such as Plantago tubulosa and herbaceous as Gentiana gayi. The North Bofedal and the fragment D of the South Bofedal are the least compacted, although the presence of gramineae typical of dry environments is common, even in the core part of the bofedal.

At the abiotic level, we observe that the physical and chemical characteristics of the water, the relief characteristics (slope of <1 to 7%) and low density of camelid cattle (inferred by the low presence of feces), the bofedales should be in very good conservation conditions and

with very good ecological quality. However, the current status of the Silala bofedales reflects a high degree of fragmentation and desiccation. Below, there is a diagram that summarizes the main environmental impacts found in the components evaluated in the Silala bofedales:



Scheme 1: Own elaboration.

At the socio-cultural level, the Silala bofedales and its surroundings present historical- archaeological and cultural value, given the evidence of human settlements and seasonal occupation; possibly for grazing and/or hunting activities, since Inca times. The geographical position of Silala, in the middle of a desert area, makes its springs a place of great ecological relevance and temporary refuge for several species of fauna; particularly migratory birds.

The Silala bofedales had several human interventions over time, such as: i) the extraction of yareta (Azorella compacta), whose populations seem to have been decimated several decades ago to supply vegetable fuel for human activities; and ii) human settlements, temporary shelters of people and grazing sites, especially by Quetena Chico community members. However, the canalization of the waters at the beginning of the 20th century to supply the railway of the Chilean Company "The Antofagasta and Bolivian Railway Company Limited", who carried out the canalization, is undoubtedly the activity with the greatest impact on the Silala bofedales. These impacts continued with the maintenance of canals throughout almost the last century.

The surface that has 100% clear evidence of having been a bofedal totals 117,934 m2 (11.79 hectares). For 2016 the bofedal covered an area of 7,679 m2 (0.76 hectares). This reinforces the evidence that the canalization was an important factor of degradation of bofedales. The reduction of the bofedal area as a consequence of the infrastructure was of approximately 94%.

In conclusion, there are three areas of bofedal with different degrees of fragmentation and drainage. The abundance of some surrounding plant species suggests a change in the composition of the bofedal. The area has a wealth of 167 species, 86 of flora and 81 of fauna (including macro- invertebrates). The biodiversity of the Silala suggests that this site is a regional oasis, due to the diversity it contains. However, the presence of human activity from the settlements and in particular the canalization modified the area and the typical composition of the bofedal, causing a strong fragmentation. Restoration, mitigation and monitoring measures are suggested according to the assessment carried out.

ENVIRONMENTAL IMPACT ASSESSMENT STUDY IN SILALA

1. BACKGROUND

The canals were built to make the water flow more efficient that, due to the geo-morphological characteristics, has a slope towards Chile. The Bolivian State carried out several studies on hydrological level, soils, temporal analysis of bofedales via images (Normalized Difference Vegetation Index – NDVI), among others (see Table 1).

Table 1. Studies carried out in the Silala area requested by the Strategic Office for the Maritime Claim, Silala and International Water Resources (DIREMAR).

Main Subject	Commentaries	Source
Hydrogeology	It suggests that the groundwater in the Silala area was recharged mainly by glacial melting thousands of years ago. The Silala geomorphology consists of ravines formed by fault action, giving rise to a zone of weakness and erosive action combined fluvioglacial water and mechanical weathering. The fluvioglacial flow derives from the melting that occurred more than 10,000 years BP. Currently no natural fluvial activity is manifested.	SERGEOTECMIN, 2004
Geology	They present a detailed geological map for the Silala bofedales, where the volcanic events and the alluvial and colluvial contributions of the glacial events stand out as a basis for the formation of the ecosystems in the area. The rocks that stand out from the area are of the ignimbrite type Silala 1, 2 and 3, which is the place where the springs are formed.	SERGEOMIN, 2017
Soil	The soils in the Silala area have a typical granulometry of fluvioglacial soils with clasts and angular grains. They were able to organize themselves in the natural bed of a river along hollows.	SERGEOMIN 2017
Soil	The results confirm the drainage of the North and South Bofedales, due to the differences in depth and the water table mainly, where the South Bofedal is shallower and has a deeper water table.	DIREMAR 2017
Multi-temporal landscape analysis	It contains the analysis of high and medium resolution satellite images. Through unsupervised classification and application of the Normalized Vegetation Difference Index (NDVI), the area of the bofedal was estimated at different times and years. A map of susceptibility and vulnerability of bofedales was generated, indicating that the most vulnerable sites are at the margins of the bofedal.	DIREMAR, 2017

Biological aspects of the Silala region are described in this report, which are of great importance to assess the impact of the constructions on the bofedales. For this, a description of the current vegetation and fauna is used, framed in a multi-temporal analysis of the landscape and the most obvious changes, under the current knowledge of the biota associated with bofedales.

2. THEORETICAL FRAMEWORK

The bofedales are a type of plant formation dependent on the constant contribution of water and characterized by a high concentration of organic matter (Squeo 2006, Ruthsatz 2012). The bofedales differ from other plant formations, such as meadows, because they are at higher elevations throughout the Andes (Ruthsatz 2012). They are distributed along the Andean Mountain Range, from Peru and Bolivia to northern Argentina and Chile. In Bolivia, they are found along the Altiplano, between 3,800 and 5,000 meters above sea level. The Puno bofedales are distributed between 3,650 and 4,100 meters and the bofedales from the Andean highlands between 4,100 and 5,200 meters (Garcia & Beck 2006, Meneses 2012); generally covering small areas scattered on slopes and plains permanently saturated with water.

The landscape of the bofedales is characterized by a mosaic of puffed and plaque-shaped cushions, interspersed with water springs and a network of streams or permanent courses of surface water. These ecosystems receive rainwater, water contribution from nearby bodies of water (for example, lagoons and rivers), groundwater and the melting of glaciers (Ostria 1987, Contreras 2007, Zavala & Cepeda 2006).

Specifically, in the High Andean bofedales the dominant and structuring species are of the Juncaceae family: Distichia muscoides, D. filamentosa, Oxychloe andina and Patosia clandestina, which can reach coverage of up to 90 to 95%, depending on the state of conservation of the bofedal and its location (Figure 1). Because of their type of growth and the environmental conditions in which they are found, these species have a high capacity to form peat; in fact, the roots of these species can be alive up to more than 40 cm deep (Figure 2).
Figure 1. Bofedales well preserved. Right. Bofedal of Oxychloe andina in



Aychuta, Sajama, we can see the minimum coverage of low-bearing gramineae and the dominance of cushions (November 2014, photo Oscar Plata). Left. Bofedal dominated by Distichia muscoides, in Tuni Condoriri, Real Mountain Range. The almost null presence of gramineae and the high coverage of water and cushions is seen (March 2013, BIOTHAW project photo).

At the ecosystem level, bofedales are key habitats for the conservation of bio-



Figure 2. Three characteristic species of the Bolivian bofedales. Note the length of the live roots.

diversity in the puna and the high Andean zone. They are water reservoirs and a source of food for many species, especially during the dry season (Squeo et al., 2006). Due to the high content of nutrients in their leaves (e.g. Distichia muscoides and D. filamentosa; Loza-Herrera et al., 2015), plants of the bofedales offer fodder very much desired by domestic camels (llamas, alpacas) and wild camels (vicuñas); as well as for sheep, cattle and horses. In addition, the flora of the bofedales contrasts with other formations of the puna because it has a greater diversity of species typical of these habitats, both at the level of specific wealth and plant endemism (Meneses 2012, Anthelme et al., 2014). In general, wetlands of small extension, such as bofedales, are of great ecological value (Biggs et al., 2017) and the Silala is particularly important, as it is located in a semi-desert region.

3. GENERAL OBJECTIVE

To carry out the Environmental Impact Assessment study, in order to determine the relationship between the artificial canalization of upwelling waters in the Bolivian springs and their effect on the ecosystem of Silala and evaluate if these impacts have put at risk the survival of the bofedales and their interrelation with the species.

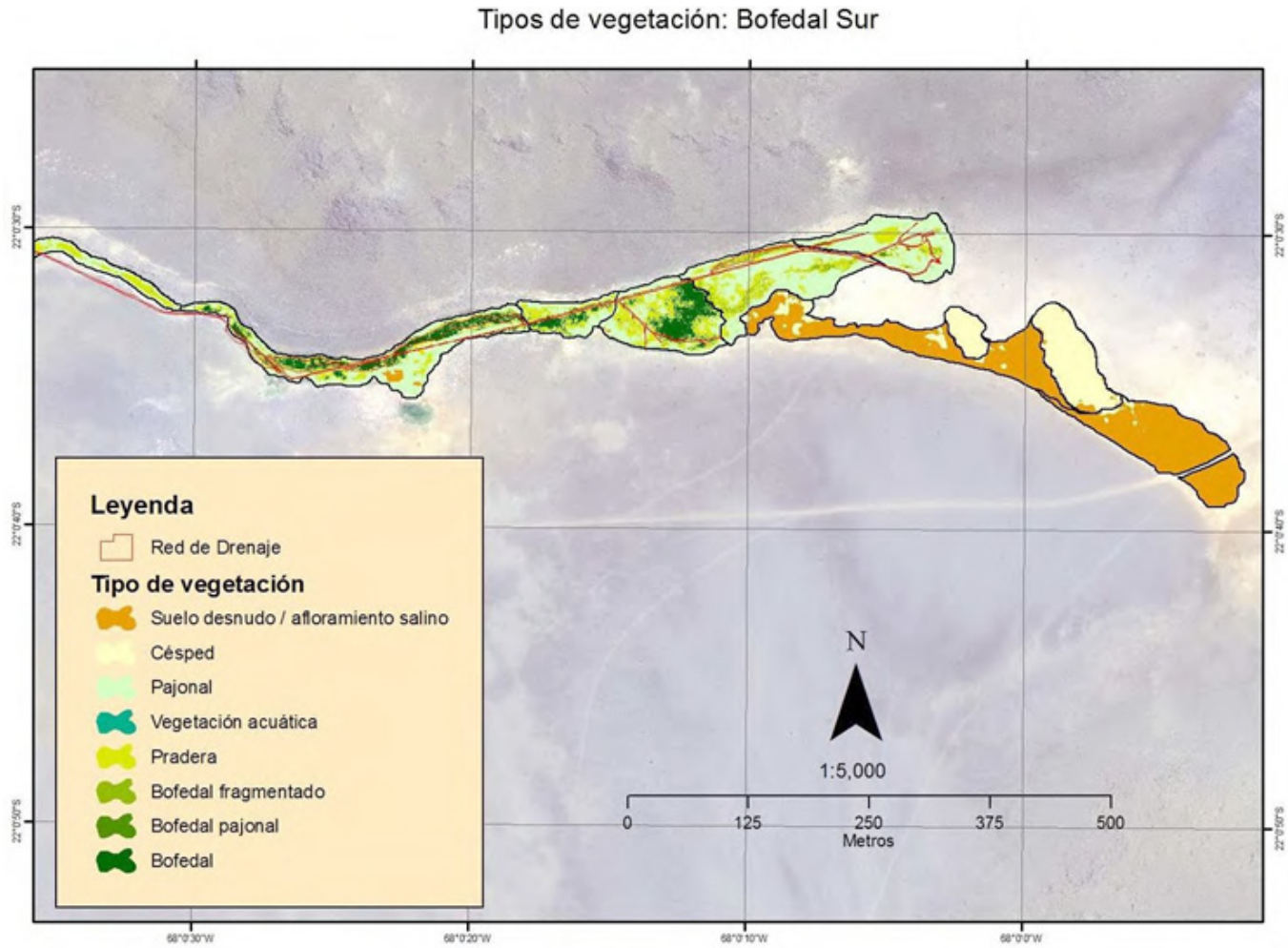
4. STUDY AREA

The Silala area is between 4,200–5,400 meters above sea level, in the canton of Quetena, Municipality of South Lipez of Potosi. The area is located at 26 km from Colorada Lagoon (Laguna Colorada), via secondary dirt roads. The

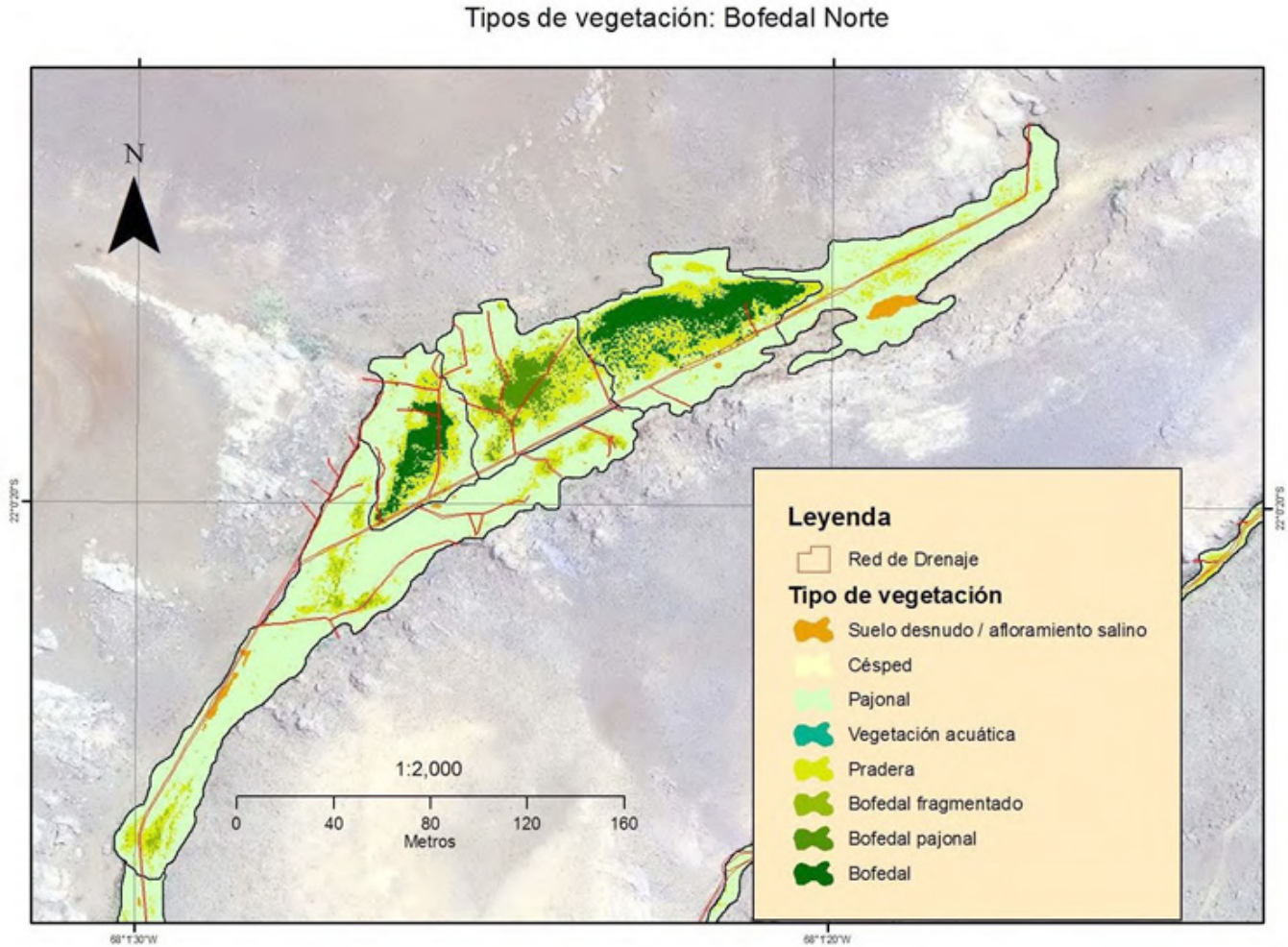
area constitutes a RAMSAR site and is part of the “Eduardo Abaroa Andean Fauna National Reserve.”

5. METHODOLOGY

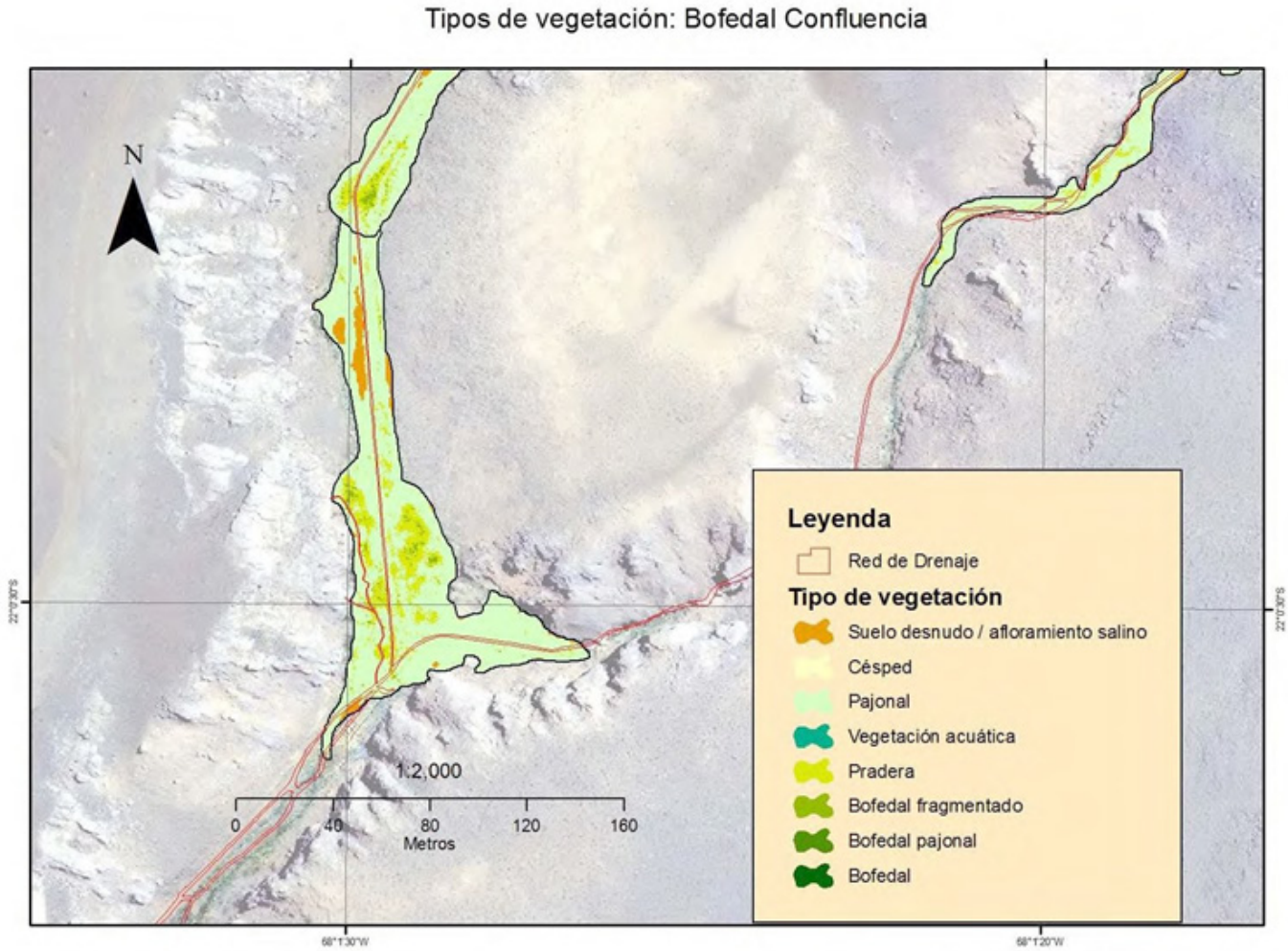
The field work was carried out between March and April 2018. For a better understanding and description of the bofedales fed by the Silala waters, the zone was divided into three areas. The South Bofedal (S) that corresponds to the most fragmented site, the North Bofedal (N) and the Confluence Area (CONF), where the waters coming from the South and North Bofedales converge. The study area covers an area of approximately 120,671 m2, 20,373 m2 in the north, 90,503 m2 in the south and 9,795 m2 in the Confluence Area.



Vegetation type: South bofedal



Vegetation types: North bofedal



Vegetation types: Confluence bofedal

5.1 Diagnosis of abiotic and biotic factors in the Silala area

For the diagnosis of abiotic factors, a compilation of bibliographic information was carried out. The biotic data consider bibliographic review, field data on flora and vegetation. For fauna, information on vertebrates and macro-invertebrates is included.

5.2 Determination of the actual area of the bofedales

The bofedales area was determined from the classification results of the high resolution satellite images (DIREMAR 2016), and with botanical information (indicated in this document), using geo-referenced coverage of springs belonging to DIREMAR. Initially the bofedal identification criteria were defined and later these characteristic elements were identified and geo-referenced during field trips, to then supplement said information with the Normalized Difference Vegetation Index (NDVI) values from satellite images of March 2016 (DIREMAR 2017) (Figure 4).

For the correct delimitation of bofedales, the presence of Oxychloe andina was used as the most important bofedal indicator species in this region (Squeo et al., 2006, Beck 2010, Meneses et al., 2015). Other indicator species of permanent bofedal, and bofedal margins were also identified. The permanent bofedal is one that is always green all year round and besides Oxychloe andina presents species associated with this, such as Phylloscirpus deserticola or Zameioscirpus atacamensis. In the bofedal margins there are other species that resist aridity better, and they are only green seasonally. The most representative grassland indicator species and other margin formations are Carex cf. maritime and Deyeuxia spicigera. These characteristics were used to delimit the area of the bofedal with satellite images and the NDVI that allows recognizing the vegetation with high photosynthetic activity from other types of dry vegetation or bare soil (Jensen 2016). The NDVI is calculated with a mathematical formula that helps to discriminate objects in the landscape according to their spectral reflectance characteristics. The index varies from -1 to +1, values close to +1 indicate that the vegetation is vigorous and with high photosynthetic activity, and values close to 0 indicate presence of dry, degraded vegetation or bare soil or, bodies of clear water or any other body with high absorbance of the infrared band of the electromagnetic spectrum (Jensen 2016). In this study, Pleiades multi-spectral satellite images were used in March 2016, provided by DIREMAR 2017 (Figure 4). This image corresponds to the end of the wet season, and is the most recent, which is why it is completely comparable with the field data of this study (end of the wet season of 2018). The thresholds were calculated at 0.6 for the bofedal, and 0.3, 0.4 and 0.5 for other formations of drier vegetation such as scrublands, grass or meadows. Because in some cases the reflectance between different species may be similar, the classification of thresholds of vegetation types was carried out separately, sector by sector, distinguishing the vegetation types according to their presence in the terrain.

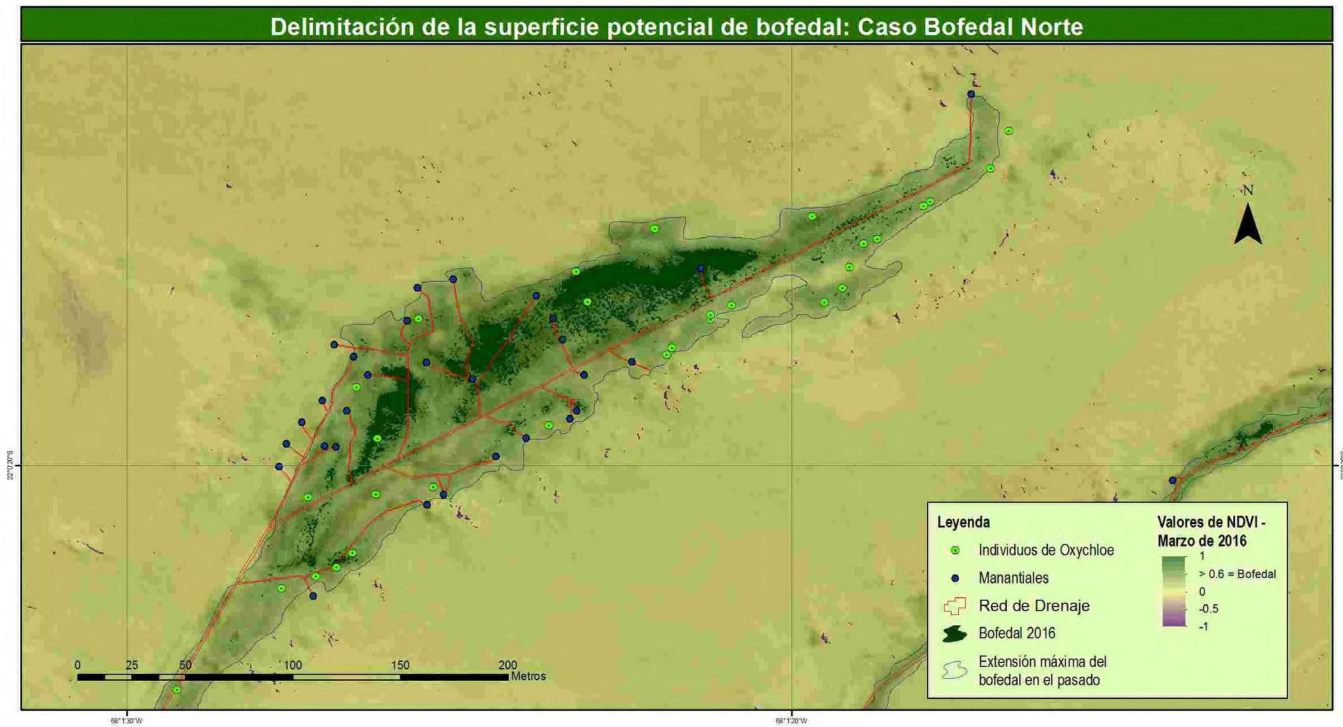


Figure 4. Process of delimitation of the current bofedal. The yellow area corresponds to the classification made by DIREMAR (2017). This coverage was then corroborated, corrected and complemented with data on the location of the springs and the presence of the indicator species, such as *O. andina*. The result of the delimitation is shown in green.

5.3 Vegetation map of the area and calculation of the bofedales area in the past

In order to systematize the analysis process, a reclassification of the values of the Normalized Difference Vegetation Index (NDVI) was carried out. The NDVI is a mathematical formula that is applied to discriminate objects in the landscape according to their spectral reflectance characteristics. The index that varies from -1 to +1, it indicates vigorous vegetation with high photosynthetic activity when the values are close to +1, and dry, diseased vegetation or bare soil in the values close to 0 (Jensen 2016).

5.4 Current conditions of the bofedales: first line of analysis

This process consisted of two parts. Initially, different vegetation types were identified in the field (March 2018) and thereafter, during the office work stage, the coverage area was interpolated with the help of satellite images of 2016 and 2004, through a Geographic Information System (GIS).

The 2004 image was chosen because it is the oldest of the high resolution images available. Using these two years it was possible to carry out a comparative analysis with the images obtained in 2014. The values used to make the comparison were those of the Normalized Difference Vegetation Index obtained by DIREMAR (2017). Below are two scenes of images of the South Bofedal, in 2004 and in 2014 (Figure 5). At first glance it can be observed that notorious changes occurred in the vegetation cover in said period.

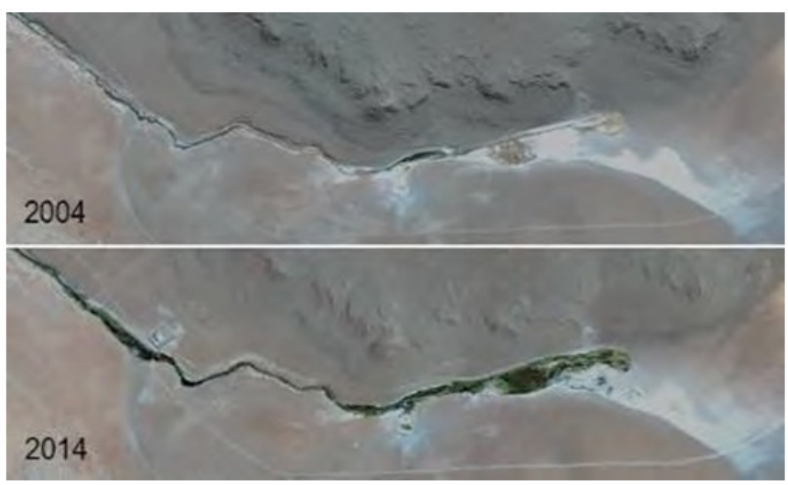


Figure 5. Vegetation coverage of the soil in the South Bofedal. Above: before the presence of the Bolivian State in the area (dry season, 16 June 2004). Below: after 8 years without maintenance of the artificial canals (wet season, 14 March 2014, image corrected for changes in humidity). The images are of high resolution (Quick Bird II) and are in true color. The intense green color shows the vegetation in the bofedal areas and in white the areas of dry or degraded bofedal. Source: DIREMAR (2017).

The identification of the vegetation types was carried out through the survey in the field of indicator species. In addition, panoramic photographs of the study site were taken, and these species were geo- referenced through a Garmin S60 GPS navigator. The position values were programmed to be captured using the datum and ellipsoid WGS84 (World Geodetic System 1984) and the UTM19s projection system (Universal Transverse Mercator Projection, South Zone 19).

The global position files were generated in GPX format as waypoints and tracks. The waypoints were marked throughout the perimeter area in each location where individual Oxychloe andina –a bofedal indicator species– were found. In addition, according to the geo-morphological and physiognomic characteristics, the tracks were marked on foot in order to delimit the sectors in which the study area was subdivided.

Additionally, and only as a form of non-technical exploration, interviews were carried out with local inhabitants, with whom the entire area, which, according to them, covered the bofedal in 1970, was demarcated (with GPS); before the availability of satellite images. The description of this tour is detailed in historical and social aspects (Annex 1).

Through desk work, the spatial analysis was carried out in order to determine the bofedal area. The information used consisted of spatial files in vector format, satellite images, and raster images of the Normalized Difference Vegetation Index (NDVI). The files obtained with the GPS navigator were converted to SHP format, using the DNRGarmin software. Additionally, there was spatial information in vector format with the location of springs and canals (IGM 2016), and in raster format (image) of high resolution satellite images and NDVI (DIREMAR 2017). The Auto-Sync tool of the ERDAS IMAGINE 2014 software was used for a geometrical correction of spatial co-registration of the NDVI images. All images were co-registered using one of them (March 2016) as the referential image (Table 2). The Arc-Map 10.3 program was used for spatial analysis. This analysis consisted of: 1) reclassification of the NDVI image[s], 2) identification of the threshold that best fits the presence of bofedal and other types of vegetation, and 3) selection and measurement of the area corresponding to each type of vegetation.

In order to be consistent with the time of year in which the field trip was made, the March 2016 image was used and the threshold of the Normalized Difference Vegetation Index (NDVI) corresponding to bofedal type vegetation was determined. Panoramic photographs were used to corroborate the result obtained in Arc-Map. Based on this coverage, and assuming that the spatial displacement of the bofedales is limited, the NDVI threshold of bofedales was determined for a dry season, using the June 2004 image. This analysis allowed us to identify that the threshold corresponding to the regions in which there is important Oxychloe coverage is 0.3.

Table 2. Characteristics of the satellite images used for the analysis of the Normalized Difference Vegetation Index (NDVI).

Date	Type	Spatial Resolution (m)	NDVI threshold for bofedales
16/06/2004	QB02	0,5	> 0,3
02/03/2016	GE01	0,5	> 0,6

Source: Own elaboration based on field control and satellite images of DIREMAR (2017)

Vegetation

An initial tour was carried out in order to verify the sites with canalization, the size of the bofedales area and based on observations the design was adjusted in the field. For each sector a physiognomic delimitation was carried out, in each delimited sector two methods were used: transects and quadrants.

Transects: Transverse lines (not permanent) were installed along the bofedales, according to the size of each sector (Figure 6). The longest lines reached 50 meters long in some sectors. In each transect, an attempt was made to accumulate 100 records (approximately one record every 50 cm), which includes both species and other abiotic components (bare soil, organic matter, feces of herbivores), and all types of anthropic interventions in the bofedal: type of canals with and without stone bedding and its dry, drying or active state. This method allows visualizing the change between the margin and the center of the bofedal.

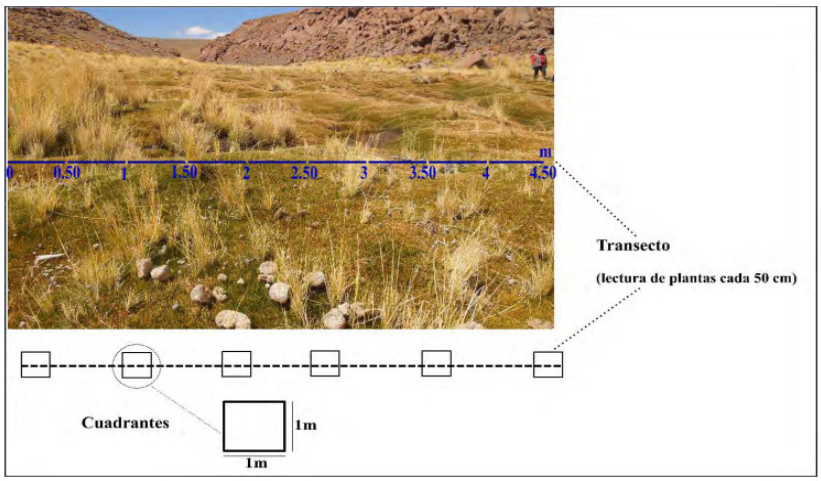


Figure 6. Transects along with the layout of quadrants evaluated in the North Bofedal of Silala. Every 50 cm the dominant physiognomic unit was recorded (unit of relatively homogeneous vegetation). A detailed description was made in quadrants of 1 m2, separated on average between 6-8 meters apart.

Quadrants of 1x1 meters were placed on each transect. The quadrants were arranged as shown in Figure 6.

Physical measures of the bofedales: Compaction (kpA) was measured in the quadrants with vegetation representative of bofedal, with a compactometer (Agratronix, Streetsboro Model OH 44241, USA). Between 2 to 5 measurements were performed, distributed uniformly in each quadrant (Meneses et al., 2014). The depth of the organic sediment was measured with a steel penetration rod at different points located on the transects.

With the same quadrant data, a map of the status of the bofedal was prepared, according to the categorizations of the plants registered in Silala. The categorization was based on the natural history of the plants, differentiating particularly if these were typical of bofedal or of dry sites. Subsequently, "weighted weights" were assigned to each species in each quadrant evaluated, multiplying the value assigned by the relative area that each species covered in the quadrant, in order to evaluate the conditions of the bofedales spatially. Values close to 1 indicate good status and values close to 4 indicate degraded bofedales. In order to reflect this information better, different colors were assigned. The "degraded" sites were colored in red, the "dried" ones in orange, the "regular" ones in yellow, the "good" ones in light green and the "very good" ones in dark green.

Ichthyofauna

In order to determine the presence of fish, surveys were conducted with hand nets in different habitats and micro-habitats in the area. So as to determine the populations of trout (Oncorhynchus mykiss), visual censuses were carried out in different reaches of canals, including natural canals and zones of canalized areas. Additionally, measurements were made of the main physical-chemical parameters: pH, conductivity, dissolved solids and temperature. The measurements were made at noon in different micro-habitats.

Herpetofauna

The collection was made with the free capture method, which consists of an intensive search in habitats and micro-habitats with high probability of presence of individuals (Heyer et al., 1994), through day and night walks to different areas of the bofedales and the surrounding slopes. The margins and potholes around the bofedales were surveyed. For the data collection, different techniques were used, ranging from the use of sieves to capture amphibians within the bodies of water, to the manual trapping of lizards and amphibians (Scrocchi & Kretzshmatr, 1996).

The relative abundance of the species was estimated according to the following criteria:

- Common (c), > 2 individuals registered every day.
- Frequent (F), registered at least twice a day.
- Rare (R), no more than 3 individuals throughout the study period.
- Exceptional (E), registered only once during the survey.

Photographic records were also taken and in all cases the greatest possible biological and ecological information of the specimen collected or observed was recorded.

The collected specimens were prepared and transported using standardized techniques (Pisani & Villa 1974, Gaviño et al., 1979). The identification was made using taxonomic keys, bibliographic descriptions and comparisons with specimens deposited in the previously determined Bolivian Collection of Fauna.

Avifauna

For the assessment of birds, the transect count method was used. A single transect was established that traversed the different habitats of each of the Bofedales (South and North) and the area where the waters converge (Confluence Area). The transect was traveled once a day, adding three repetitions. All birds detected were recorded while walking at a constant speed (approximately 1 km/hour). For each observation, time, species, number of individuals and type of habitat were recorded. Identification at the species level was made by direct observation using 10 x 35 binoculars and field guides (Fjeldså & Krabbe 1990, Herzog et al., 2017). The assessments were mainly conducted between 8:00 and 17:00, except for one hour at noon. The nomenclature of the South American Classification Committee was used (Remsen et al., 2018).

Mastofauna

First, a tour of the entire work area was carried out in order to establish the sampling sites for micro- mammals, in relation to the canalization sites and the bofedales area. In this

way, we worked in the South Bofedal, the Central Canal (CC) and the North Bofedal. The presence of medium to large mammals was established through signals (feces, tracks and dens), during the entire stay in the field, after the setting of traps for micro-mammals. The sampling of micro-mammals was carried out with 100 snap traps (museum special and Victor), in each of the sectors.

In the South Bofedal, the traps were placed in four lines that ran along the canals, separated by about 10 meters, from the water springs (nascent) in a northwest direction. In each line, 25 traps were placed, separated from each other by about 10 meters, making a total of 100 traps, covering an approximate area of 1.4 hectares.

In the Central Canal, 52 traps were placed, separated approximately 10 meters from each other, along 600 meters; in two parallel lines on each side of the course of this canal, covering an approximate area of 1.6 hectares.

Sampling in the North Bofedal was done in a single line, which ran from the center of the bofedal towards the canal near the border with Chile; in a length of approximately 1 km. 109 traps were placed, separated from each other by about 10 meters, covering an area of approximately 1.5 hectares.

All traps used as bait a mixture of oatmeal with tuna and drops of vanilla essence. The traps were activated around 5 pm and checked and deactivated early the next morning. The traps of the South and North Bofedales were activated for two nights; while the Central Canal traps, for three nights. In total a catch effort of 681 traps per night was completed.

All the specimens that fell into the traps were collected and taken to the camp for further analysis and preparation. The standard measurements were taken: length of the body, length of the tail, length of the hind leg and the ear, in addition to the weight. Sex and reproductive status were also determined.

DATA ANALYSIS

Vegetation

The field work and the vegetation analyzes took into account only vascular plants. This level of life organization is one of the most complexes to analyze and its importance lies in the fact that it allows us to infer the natural and human-induced impacts, because we know the type of ecosystem that different species usually inhabit with preference.

For the case of the Silala wetlands, abundance range curves or Whittaker curves were developed (Feinsinger 2004), that give us a visual idea of the composition, richness and equitability of elements in a given area. In our case we graphed the composition and abundance of both species (in black in all the figures), as abiotic components (bare ground, stone, canals, etc. all in red in the figures). The water is highlighted in light blue and the dead species, burned or organic matter in yellowish green.

If the slope of the graph is pronounced it indicates low equitability, with some species very abundant and other species that are not abundant or rare (Feinsinger 2004). If, on the contrary, the slope is almost zero, a high level of equitability is inferred, since all species register similar abundances. In that sense, equitability is the degree to which the abundance of different species differs (Feinsinger 2004). Additionally, the length of the curve will give us an idea of the richness of the elements that make it up; the longer a curve, the greater

the number of elements that make up the community. Finally, the order in which the components appear shows us that the species located in the upper part are the most abundant and the species of the tail or lower part are those of lower abundance. An additional advantage of abundance range curves is that they clearly show the identity of the species, which helps distinguishing the relative abundance of typical bofedal species, from others whose presence indicates that the wetland would be drying up.

In order to explore the existence of general patterns in the composition of plants in the South and North and the Confluence Area, a Principal Component Analysis (PCA) was applied. This analysis gives us a global panorama of the vegetation and helps to visualize patterns of organization of the species. It uses calculations on the differentiation of sites based on an index (in this case the Euclidean distance). In order to correct for the presence of double zeros between pairs of sites, the data matrix with the species and their coverage were transformed with the Hellinger formula (Legendre & De Caceres 2013).

Subsequently, in order to understand which environmental variables measured in the field explain the patterns of plant communities, a Coronary Canonical Analysis (CCA) was used, which performs calculations using both groups of data and determines which environmental variables significantly affect plant communities. Two CCA analyzes were run separately: the first with the average and the standard deviation of the compaction and the second with variables associated with the type of substrate (Annex 2), as independent variables. The second CCA was run with the option "Forward selection", with $\alpha = 0.05$, to see the types of substrate that contributed to better explain the composition and abundance of plant communities (Leps & Smilauer 2003).

5.5 Environmental impacts to the bofedal caused by the artificial canal system

Vegetation

In order to assess the impacts, quadrant data were used and multivariate analyzes were applied. While with the data of transects, the different physiognomic vegetation units were coded first. These units are composed of one, two or even five species or abiotic elements, among of which are bare soil, sandy soil and organic matter. For example, the unit composed of Oxychloe andina and Festuca rigescens was coded as: oand_frig. In this way, the frequency of units was quantified. Subsequently, the frequency of these units was calculated and an Analysis of Correspondence with data on the composition and abundance of the most frequent units was applied, thus avoiding methodological errors in the analysis. These analyzes were carried out separately for the South and North Bofedal. In the South Bofedal, only the first 15 units were considered more frequently and in the North Bofedal only the first 12 units were considered.

Subsequently, with the help of the values proposed by Meneses et al. (2015), the ecological quality of the different areas of the Silala bofedal was evaluated qualitatively. This analysis was supported by revisions of the collections of the National Herbarium of Bolivia.

Aquatic macro-invertebrates

The aquatic macro-invertebrates (Annex 5) are invertebrates, larvae, nymphs, naiads or adults that live in the substrate, the column or the surface of bodies of water, and that can be seen with the naked eye or with simple magnifying glasses (Figure 7). Since they are in the water they can provide information about the health of the ecosystems and the ecological quality of the water, in its physical-chemical and morphological-structural components.



Figure 7. Aquatic macro-invertebrates of Silala. Photograph taken with 6X stereo-microscope.

In order to evaluate the effect of the canalization on aquatic communities of macro-invertebrates, the bodies of water of the North and South Bofedales and the canal were categorized into three types of canals: canalized with stone (CP), canalized without stone (SP) and natural or naturalized sections (N) (Figure 8). The latter corresponds to sections of canals that are more similar to the natural environments of a bofedal not intervened, which we assume are like this for the time elapsed without canal maintenance.



Figure 8. Categorization of the types of canals in the Silala bofedal.



Figure 9: Sampling design in the sections of the modified canals from left to right: canals with stones, canals without stones and naturalized canals.

Collection and metrics of macro-invertebrates

The fauna of macro-invertebrates was collected with a Surber net (15 x 15 cm, 0.02 cm2, with mesh size 250 µm). In each of the 20 sampling stations, three subsamples were taken distributed in the different micro-habitats of the section of the canals and ravines (Figure 9). The samples were fixed with 4% formaldehyde and transported to the Limnology Unit of the Institute of Ecology of the Higher University of San Andres, where they were evaluated. The samples were separated and identified at the highest possible taxonomic resolution, with the help of specialized bibliography (Dominguez et al., 2006, Dominguez & Fernandez 2009, Stark et al., 2009 and Prat et al., 2011). The taxonomic richness, Shannon-Weiner diversity index, was calculated. In order to see the difference between the three categories (canalized with stone (CP), canalized without stone (SP) and naturalized sections (N)) the Kruskal-Wallis statistic was used.

Physical-chemical and morphological-structural parameters

The physical-chemical parameters considered for this study were: pH, Electrical Conductivity (EC), Total Dissolved Solids (TDS), Salinity (PSU), Oxide Potential Reduction (OPR), Dissolved Oxygen (DO) Dissolved Oxygen Percentage (DO%) and temperature (Multi 3630 IDS SET G, Germany). Among the morphological-structural parameters were measured: the width of the river (measuring tape, m), depth (graduated rod, m), velocity (Global Water FP111, m/s). The type of substrate was evaluated in three transects of 10 meters with granulometer: Block (B), Large Stone (LS), Fine Stone (FS), Coarse Debris (CD), Fine Debris (FD), Coarse Gravel (CG), Fine Gravel (FG), Coarse Sand (CS), Fine Sand (FS), Silt (S), Clay (C). A Substrate Diversity Index (SUDI, using Simpson's inverse index) was also calculated.

5.6 Fishes

The only exotic species detected in the Silala area is rainbow trout. In that sense, this section refers to this species only. Rainbow trout (Oncorhynchus mykiss) is an exotic species, which was widely introduced into aquatic systems of the Bolivian Altiplano since the 1940s (Loubens 1989). Currently there is a small "wild" population in canals and aquatic systems.

According to the results of the counts made during the fieldwork, the current density of "wild" trout is very low, varying between 20 and 54 trout per kilometer. The observed sizes vary between 9 and 25 cm in standard length, approximately.

The same species of trout was introduced into aquatic systems of the Chilean Altiplano (Vila et al., 2007). The trout found in rivers feed mainly on aquatic insects and, probably, when they exist, on small native fish.

Trout is usually found in cold water river systems (streams, large and small rivers) and also in lakes. The preferred temperature of this species varies between 13 – 18 ºC (Garside & Tait 1958, Loubens 1991). Reproduction can occur at temperatures below 13 ºC, up to 5 ºC (Luna & Valdestamon 2018). Consequently, the physical conditions of the biotope in Silala are favorable for the development of the species. On the other hand, considering the current density of trout, there are still abundant populations of some invertebrates (such as amphipods) and, probably, some vertebrates such as amphibian larvae, which can be used as a food source (Lippolt et al., 2011, Buria et al., 2009). On the other hand, the species usually reproduces in sandy bottom fluvial systems (Luna & Valdestamon 2018); consequently,

it can also be considered that there are areas that could be used for reproduction. In addition, there are some areas, for example near the military post, where there are some lateral water overflows that the fingerlings can use in order to protect themselves from predation by adults and also use as a growing area. In other places, such as the Pampalarama Lagoon in the La Paz Valley, trout fingerlings were observed in this type of habitats, where they remain protected from adults. Although during this campaign –as mentioned in the report– it was not possible to verify the presence of trout fingerlings in Silala.

Life cycle of rainbow trout

Males reach sexual maturity at 2 years and females at 3 years. The maximum age recorded is 11 years in anadromous individuals and six years in non-anadromous individuals (Luna & Valdestamon 2018, Lippolt et al., 2011). In Andean systems, a period of reproduction is reported between April and July until September, with a period of migration, from the lake to the rivers where they breed, between November and March (Liberoff et al., 2014, Riva-Rossi et al. 2003, Loubens 1992). There are other references of reproduction at the end of the dry season, between August and November, in the southern hemisphere (Luna & Valdestamon 2018).

The trout reproduction occurs in sandy bottom fluvial systems (Riva-Rossi et al., 2003). When they reach sexual maturity, the adults migrate to the rivers; the female digs a nest where she deposits the eggs that are fertilized by the male. Subsequently, the eggs are covered again. When the hatching occurs, the fingerlings migrate downstream (Luna & Valdestamon 2018). In the region of Pampalarama in the La Paz Valley, it was observed that the fingerlings penetrate, at least temporarily, in bofedales and flood areas bordering rivers, probably as protection from predation by adults.

Cultivation and maintenance of "wild" trout populations in Silala

Fish populations and fishing in mountainous systems (rivers, lakes and reservoirs), depend on uncontaminated water; expedited migratory routes and sustainable fishing pressure (Vila 2007). The development of extensive fish farming depends on an abundant and healthy stock, of physical factors such as temperature (between 13 and 18 ºC to cultivate trout), adequate availability of food and conditions for natural reproduction. It is necessary to have a stock of reproducers for the production of fingerlings or the periodic breeding of juveniles, for a process of growth in ponds.

The trout in the Silala area comes from a fish farming program that was launched in 2013 (ERBOL 2016), with the inauguration of a pond system for trout farming. Currently, the presence of trout in the area is limited to a small wild population in the canals of anthropic origin built in the area of bofedales and a very small population (< 50 individuals) that is maintained in an artisanal pond. Although the physical conditions (temperature of 17 ºC at noon) are within the appropriate range for extensive or intensive trout farming, the observed specimens do not exceed 25 cm in standard length; although different size classes are found.

Unfortunately, an official report on the number of trout introduced in the area could not be found. According to press reports, in March 2013, 50 individuals were introduced, without

specific origin (La Razon newspaper 2013). The same reference mentions the transfer of another 60 specimens from Lake Toro in Potosi, although there are no references on the concretion of this fact. Although it was not possible to confirm the presence of fingerlings, which could indicate the occurrence of reproduction processes in the area, the current density of 20 to 54 trout per linear kilometer and approximately 50 trout in ponds, could represent that the trout was successfully established in the area and that there is reproduction, which would have allowed the population to grow. This aspect seems to be confirmed by the presence of individuals of different size classes, both in ponds and in the canals of the area.

The impact of trout on the environment and aquatic biota

The activity of trout on canal margins could accelerate the erosion processes and, consequently, the runoff of water from the canals. Taking into account the refuge behavior of trout in cavities and their digging capacity (for example, for the construction of nests for spawning), the physical influence of the species on the canal infrastructure is likely. However, the current density of the population does not seem significant for the production of a physical impact on the canals. Consequently, it can be considered that the current erosion processes are mainly due to a process of water erosion.

On the other hand, the likely impact of trout on other elements of the aquatic biota should be considered. Numerous works in different regions where Oncorhynchus mykiss and other trout species demonstrated the impact on amphibian populations, due to four main factors: 1) direct depredation of eggs and larvae, 2) alteration of reproductive behavior, 3) the effect on the morphology of the larvae and 4) introduction of pathogenic organisms, such as Saprolegnia diclina, which can produce a high mortality in eggs (Martin-Torrijos et al., 2016, Bosch et al., 2006). Consequently, the likely impact of introducing trout on amphibian populations in the area should be assessed in greater detail.

Additionally, considering the evolution of the aquatic systems in the area, in the absence of trout predators, the possible impact on some invertebrate species should be considered, mainly a species of Trichoptera (Neotrichia sp.), naturally rare in Silala.

On the other hand, taking into account the characteristics of the marsh systems in the Southern Altiplano of Bolivia, the past presence of populations of Orestias sp. (gr. agassii) in the Silala is likely. The study of ancient environmental DNA is an alternative for the study of past biota. Ancient environmental DNA can be found in sedimentary environments and its analysis can potentially reveal the presence of fractions of biological communities (Haile et al., 2009, Willerslev et al., 2014, Zobel et al., 2018). Consequently, the application of these methodologies could represent an opportunity to confirm the past presence of fish, particularly Orestias, as well as other species of fauna such as aquatic snails.

6. RESULTS

6.1 Historical occupation in the territory of Silala

The Silala bofedales and its surroundings present evidences of human settlements and seasonal occupation, possibly for grazing and/or hunting activities. This background gives the region a high historical-archaeological and cultural value. The Silala bofedales suffered several human interventions over time, among which we can mention:

The canalization of the Silala waters, which undoubtedly had the greatest impact on the Silala bofedales. This canalization was authorized by Bolivia in 1908, with the sole objective that the Chilean Company "The Antofagasta and Bolivia Railway Company Limited" to use the Silala waters for the filling of steam locomotive cauldrons (Orellana et al., 2013). The artificial canalization of water sources covers almost the entire surface of the Silala bofedal (Figure 10).

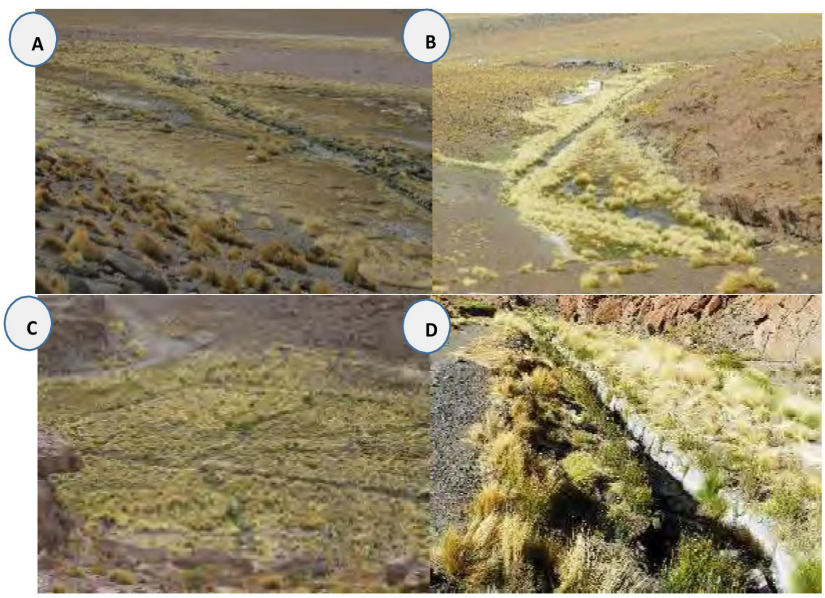


Figure 10 Canalization of Silala bofedales. A) South Bofedal, B) Canals near the Silala Military Outpost, C) North Bofedal and D) Canal in the Cajon Ravine. (Photo: A. C. Simon Pfanzelt and B. D. Loly Vargas Callisaya).

According to the perception of the local people interviewed (Joaquin Estelo and Primo Berna, community members of Quetena Chico), the size of the bofedal diminished from 1970 to 1978, and the typical vegetation of these bofedales was in the process of drying out.



Figure 11. Water springs abstracted and canalized towards a main canal (Photo: Loly Vargas Callisaya).

During the fieldwork and thanks to the community members, it was possible to highlight and geo- reference the remains of six landmarks (cement structures 1.5 meters high), which according to the testimonies of the community members were 15 landmarks that surrounded the South Bofedal and were built by the Chileans.

Another relevant historical antecedent that occurred in Silala was the extraction of yareta, in the years before 1945. The interviewees indicated that the extractions were made by people from Chile and, as evidence, they pointed out the roads that lead to Chile, from the Silala hill.

It was also possible to identify settlements and temporary shelters in Silala of people who made trips and tours as part of their livestock activities. The transfer of livestock allowed them access to agricultural resources produced in other eco-zones. The traditional destinations of the Quetena llama breeders were: Toconao, San Pedro de Atacama and populations of the Loa River in the west (today Chile), and Pirquitas, Rinconada and San Antonio de Los Cobres (Argentina) to the south. More rarely, they also traveled to the valleys of the eastern Andean slope, such as Tupiza or Tarija (Nielsen et al., 1981).

According to the interviewees, the people of Quetena Chico also used the Silala bofedales as a stay and grazing site for their cattle. In the field we managed to find traces of the small shelters (five caves or houses); which are no longer used by the community members. Between the people of Quetena who lived or traveled in different periods of time by the Silala bofedales, the following were mentioned: Felix Berna, Hilarion Bern, Ladislao Bern Alvares, Remigio Bern Ezquibel and Primo Bern. The latter inhabits his stay in Silala, between April and September.

6.2 Diagnosis of biotic and abiotic factors

6.2.1 Abiotic factors

Climatic Conditions

According to data from the Laguna Colorada station (Urquidi 2004), the average annual temperature ranges between -15 °C and 14 °C, the average annual rainfall is 59.1 mm and the average annual evaporation is 914 mm. Based on climatic data, the size of the drainage basin and the expected infiltration, Urquidi (2004) estimated that a drainage area of at least 4.7 times the current size of the drainage area would be needed to maintain the flow of water measured in the region (164 l/s). This means that the existence of the bofedal in the Silala is due to the existence of a fossil aquifer and that the contribution of the current rainfall is minimal.

Physical-chemical parameters

Below are the average physical-chemical parameters, taken from the work of Urquidi (2004) and the work carried out in the field; the data correspond to three stations in the North Bofedal (N), eight in the South Bofedal (S) and three below the confluence. Additionally, the same parameters were taken at the fishing sites in potholes (aquatic habitats with low velocity), rapids (deep aquatic habitat and with greater velocity) and bofedales.

Table 3. Physical-chemical parameters of the Silala bofedales. Data for 2004 (Urquidi 2004) and 2018 are shown.

Parameters	Urquidi (2004)	N Bofedal (2018)	S Bofedal (2018)	Confluence (2018)	Pothole (2018)	Rapid (2018)	Bofedal (2018)
Average pH	7,7	7,6 ± 1	8,47 ± 0,4	8,7 ± 0,1	8,3	8,3	8,4
Average temperature (ºC)	16	13,5 ± 4,4	15,3 ± 0,9	14,5 ± 3,4	16	16	17
Conductivity (µS/cm)	Between 80 and 350	187 ± 30	301 ± 28	262 ± 44	257	260	255
Total Dissolved Solids (TDS, mg/l)	37 and 150	122 ± 18	122 ± 18	127 ± 11	139	129	128

Canals

The Silala hydraulic system on the Bolivian side consists of three open canals covered with ignimbrite stones: Main Canal, North Canal and South Canal.

The Main Canal is built along the main ravine from the confluence of the North and South Canals to the borderline between Bolivia and Chile. It has a length of 690 meters, an average width of 0.80 meters and an average depth of 0.50 meters. The side walls and the floor of the canal are made of ignimbrite stone of different sizes that, in some places, are joined with mortar.

On the Main Canal, 31 meters from the confluence of the North and South Channels, there is a disused desiltation chamber. The desiltation chamber is made of stone covered with cement, with four cells. The internal walls of the desiltation chamber are stained with copper sulphate, which was used as flocculator and disinfectant of the desiltation chamber. Overlying the stone canal, two iron pipes of 8 and 10 inches in diameter emerge, that are cut and partially buried in many stretches of the ravine (Urquidi 2004).

Currently the Main Canal has a great deterioration and growth of grasses on its margins, but the stone soles are in good condition. The interior of the canal has aquatic plants that reduce the flow of water (Urquidi 2004). Parallel to the Main Canal there is a dirt road that continues to be passable and continues to the Inacaliri Post, in Chilean territory.

The North Canal is built of ignimbrite stone (walls and sole) and has an average width of 0.57 meters, with an average depth of 0.36 meters. It has a length of 650 meters and collects water with water conveyance canals from 25 springs that emerge in the North Bofedal. In this bofedal there are 4 piezometric wells 10 meters deep, with 2.5-inch iron pipe. The measurements in these wells indicate piezometric levels between 0.40 and 0.67 meters above the surface. These wells were installed by the Antofagasta-Bolivia Railway Company (FCAB) (Urquidi 2004). The North Canal is in the same conditions as the Main Canal.

Already 14 years ago, Urquidi (2004) reports that the South Canal was completely deteriorated and its soles had almost completely disappeared. In this section of the ravine, of the walls or cliffs of ignimbrites, there were 18 springs or water springs, all with water conveyance canals or stone collectors connected to the conveyor canal. The density of springs in this section was extremely high, having been inventoried up to 3 springs per linear meter (Urquidi 2004).

Soil

The following table summarizes the main characteristics of the Silala soils, both of the North Bofedal and the South Bofedal, according to the report by DIREMAR (2017), from whose report we summarize the following, which we consider pertinent to our own work.

Table 4. Main soil characteristics in the North and South Bofedales of Silala. LCA: Environmental Quality Laboratory of the Institute of Ecology of the Higher University of San Andres (UMSA), CIAT: Center for Tropical Agricultural Research of the Autonomous Government of Santa Cruz.

Characteristics	**Silala North Bofedal**	**Silala South Bofedal**
Depth (m)	Ave. =0,88 n=15 Values of 0,55 to 1,4 m	Ave.=0,64 n=15 Values of 0,2 to 1,2 m
Water table (m)	Ave.=0,29 n=15 Values of 0,1 to 0,4 m	Ave.=4,14 n=15 Values of 0,15 to 50 m
Organic matter (%)	Ave.=11,23 n=12 Values of 0,17 to 71	Ave.=1,78 n=12 Values of 0,1 to 11
pH (LCA)	From 5,6 to 8,9	From 6,2 to 8,4
pH (CIAT)	From 5,2 to 8,5	From 7,4 to 7,6
Electric conductivity (µS/cm)	Ave.=266,25 n=12 Values of 26 to 785	Ave.=129,67 n=15 Values of 61 to 290
Permeability (cm/s)	Average = 2,656E-07	Average = 1,146E-07
Hydraulic conductivity (cm/s)	Average = 4,99E-05 n=3	Average = 2,24E-04 n=3
Apparent density (gr/cm^3)	Ave.=1,28 n=7 Values of 0,87 to 1,5	Ave.=1,47 n=11 Values of 1,09 to 1,8
Porosity (%)	Ave.=51,85 n=7 Values of 43,27 to 67,28	Ave.=44,6 n=11 Values of 32,07 to 58,82
Capillarity (per velocity cm/min)	Ave.=0,625 n=2 Values of 0,42 to 0,83	Ave.=0,26 n=4 Values of 0,04 to 0,5

Source: Data from the DIREMAR Report, 2017.

The texture is predominantly sandy, with values between 70%, and 95%, and a layer of organic matter that reaches 100% for several areas sampled in the North Bofedal and one point in the South Bofedal (DIREMAR, 2017).

The pH and electrical conductivity vary directly in relation to the depth of the soil. The pH is more acidic in deeper horizons. The neutral and acid values have been measured in the sand layer, inferring that these are influenced by the washing of the bases, due to the movement of sub-surface waters (DIREMAR, 2017).

The hydraulic properties are typical of sandy soils, with infiltration velocities above 30 mm/h, due to the type of soil that predominates in the bofedales. The Field Capacity (FC) and Permanent Wilting Point (PWP) were also determined, in order to determine the water available for plants in the bofedales.
The greater impact to the soil is translated in the removal or de-structuring of the surface layer of the soil, which becomes more vulnerable to the erosion by the strong winds, and a simultaneous phenomenon of compaction of the deepest layers of the soil. Likewise, the deterioration of bofedales due to wrong practices causes the salinization of bofedales by accumulation of sodium and potassium salts, as well as other minerals.

Finally, due to extreme climatic conditions and poorly structured soils, there are no agricultural practices in the area (SERNAP 2006). And soil formation is characterized by intense abiotic weathering, but with very slow biotic processes (humification).

6.2.2 Biotic factors

Flora

Until 2016, only a preliminary survey of the flora and fauna present in the Silala in a report presented to the Foreign Ministry (Palabral-Aguilera et al., 2016) would have been carried out. These authors registered a total of 36 plant species (Palabral-Aguilera et al., 2016), which included species specific to the bofedal (where the greatest sampling effort was made) and some species from surrounding areas. With this work that figure increases to a total of 86 species of plants (vascular and non-vascular), reported for the Silala area (Table 5). The increase is explained by a greater sampling effort. It is important to note that many of the reported species have some degree of threat (Table 5).

In the Silala, 86 species have been registered, in 65 genera of 35 families (Figure 12). The most diverse family is Poaceae, with 23 species; followed by Asteraceae with 15 species, and then Cyperaceae (with 6 species) (Table 5). At the level of genera, the most diverse is Deyeuxia, with 11 species, followed by Festuca and Senecio with 4 species each, and Werneria, Pycnophyllum and Parastrephia with two species each, the rest of genera have only one representative (Table 5).

Table 5. Species of plants registered in Silala until May 2018. The categorization of species corresponds to: 1 = typical of bofedal; 2 = transition zone between the bofedal and the dry zone; 3 = dry zone; 4 = salinized areas; and 5 = only in water courses and springs. The column "Code" indicates the abbreviation used in the abundance range graphs and the column "Threat category" indicates whether the species has any degree of threat, according to the red book of plants of Bolivia (Ministry of Environment and Water, 2012).

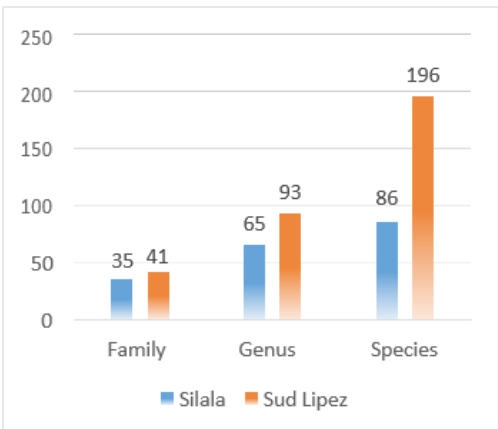
Family	**Species**	**Code**	**Categorization**	**Threatened Species**
Apiaceae	*Azorella compacta*	Acom	3	ENDANGERED
	Lilaeopsis macloviana	Lmac	1	
	Mulinum ulicinum	Muli	3	
Araceae	*Lemna minuta*	Lmin	5	
Asteraceae	*Baccharis tola var. viscosissima*	Btol	3	
	Comp.			
	Leucheria daucifolia	Ldau	3	
	Oriastrum revolutum	Orev	3	
	Parastrephia lucida	Pluc	3	
	Parastrephia quadrangularis	Pqua	3	VULNERABLE
	Perezia purpurata	Ppur	3	
	Senecio		3	
	Senecio adenophyllus	Sade	3	
	Senecio chrysolepis	Schr	3	
	Senecio puchii	Spuc	3	
	Werneria apiculata	Wapi	1, 2 and 3	
	Werneria glaberrima	Wgla	3	
	Werneria pygmaea	Wpyg	1 and 2	
	Xenophyllum incisum var. incisum	Xinc	2	
Brassicaceae	*Descurainia myriophylla*	Dmyr	3	
	Menonvillea virens	Mvir	3	
	Mostacillastrum dianthoides	Mdia	3	
	Petroravenia friesii	Pfri	1 and 2	
Bryaceae	*Bryum*		1	
Cactaceae	*Cumulopuntia boliviana*	Cbol	3	
Calyceraceae	*Calycera pulvinata*	Cpul	3	
Campanulaceae	*Lobelia oligophylla*	Loli	1	
Caryophyllaceae	*Arenaria digyna*	Adig	1 and 2	
	Colobanthus quitensis	Cqui	1 and 2	
	Pycnophyllum bryoides	Pbry	3	
	Pycnophyllum macropetalum	Pmac	3	
Cyperaceae	*Carex cf. maritima*	Cmar	1 and 2	
	Eleocharis atacamensis	Eata	1	
	Phylloscirpus deserticola	Pdes	1	ENDANGERED
	Schoenoplectus californicus	Scal	5	
	Zameioscirpus atacamensis	Zata	1	ENDANGERED
	Zameioscirpus muticus	Zmut	1	

Family	Species	Code	Categorization	Threatened Species
Ephedraceae	*Ephedra breana*	Ebre	3	
Fabaceae	*Adesmia spinosissima*	Aspi	3	
Gentianaceae	*Gentiana gayi*	Ggay	1 and 2	
Haloragaceae	*Myriophyllum quitense*	Mqui	3	
Hydrophyllaceae	*Phacelia nana*	Pnan	3	
Indet.	*Indet.*			
Juncaceae	*Juncus stipulatus*	Jsti	1	
	Luzula vulcanica	Lvul	1 and 2	
	Oxychloe andina	Oand	1	ENDANGERED
Loasaceae	*Caiophora coronata*	Ccor	3	
Malvaceae	*Nototriche auricoma*	Naur	3	VULNERABLE
Montiaceae	*Calandrinia acaulis*	Caca	3	
Nostocaceae	*Nostoc*		5	
Onagraceae	*Epilobium denticulatum*	Eden	3	
Orobanchaceae	*Castilleja pumila*	Cpum	1 and 2	
Oxalidaceae	*Oxalis pycnophylla*	Opyc	3	IN DANGER
Phrymaceae	*Mimulus glabratus*	Mgla	3	
Plantaginaceae	*Plantago tubulosa*	Ptub	1 and 2	
Poaceae	*Aciachne pulvinata*	Apul	3	
	Anatherostipa bomanii	Abom	3	
	Deyeuxia			
	Deyeuxia breviaristata	Dbre	3	
	Deyeuxia chrysantha	Dchr	1	
	Deyeuxia chrysophylla	Dchr	3	
	Deyeuxia crispa	Dcri	3	
	Deyeuxia curvula	Dcur	3	
	Deyeuxia eminens	Demi	5	
	Deyeuxia eminens var. eminens	Demi	5	
	Deyeuxia filifolia var. festucoides	Dfil	3	
	Deyeuxia nitidula	Dnit	3	
	Deyeuxia spicigera var. cephalotes	Dspi	1 y 2	
	Dielsiochloa floribunda	Dflo	3	
	Festuca chrysophylla	Fchr	3	
	Festuca orthophylla	Fort	3	
	Festuca potosiana	Fpot	3	VULNERABLE
	Festuca rigescens	Frig	1	
	Gram.			
	Nassella aff. rupestris		3	
	Pappostipa frigida	Pfri	1 and 2	
	Poa lepidula	Plep	3	
	Puccinellia frigida	Pfri	4	

Family	Species	Code	Categorization	Threatened Species
Potamogetonaceae	*Stuckenia pectinata*	Spec	5	
Pteridaceae	*Argyrochosma nivea*	Aniv	1 and 2	
Ranunculaceae	*Ranunculus uniflorus*	Runi	5	
Rosaceae	*Polylepis tarapacana*	Ptar	2	VULNERABLE
Salviniaceae	*Azolla filiculoides*	Afil	5	
Solanaceae	*Jaborosa squarrosa*	Jsqu	3	
Valerianaceae	*Valeriana petersenii*	Vpet	3	
Verbenaceae	*Junellia pappigera*	Jpap	3	

Source: Own elaboration based on field data and the records of Palabral *et al.,* (2016).

Regarding the diversity of plants for the South Lipez Province, based on a bibliographic review and the database of the National Herbarium of Bolivia, a total of 41 families, 93 genera and 196 species have been registered (Figure 12). In this context, the flora of Silala comprises 85% of the families, 70% of the genera and 44% of the species of the entire South Lipez region.



Of the total species registered in Silala, and after comparing the species with the data from the catalog of vascular plants of Bolivia (Jørgensen et al., 2014), 17 species are new records for the Department of Potosi (Table 6) and two of these are new records for Bolivia (Menonvillea virens and Mostacillastrum dianthoides), both of the Brassicaceae family. These species were confirmed by the Brassicaceae family specialist, Diego Salariato.

Table 6. New species records for the Department of Potosi. The species that are also new record for Bolivia are highlighted with an asterisk.



Petroravenia friesii



Arenaria digyna



Deyeuxia filifoia var. *festucoides*

Familia	Especie
Brassicaceae	*Menonvillea virens* *
	Mostacillastrum dianthoides *
	Petroravenia friesii
Campanulaceae	*Lobelia oligophylla*
Caryophyllaceae	*Arenaria digyna*
Cyperaceae	*Phylloscirpus deserticola*
Gentianaceae	*Gentiana gayi*
Juncaceae	*Juncus stipulatus*
	Luzula vulcanica
Plantaginaceae	*Plantago tubulosa*
Poaceae	*Deyeuxia filifolia* var. *festucoides*
	Deyeuxia nitidula
	Deyeuxia spicigera var. *cephalotes*
Potamogetonaceae	*Stuckenia pectinata*
Ranunculaceae	*Ranunculus uniflorus*
Salviniaceae	*Azolla filiculoides*
Solanaceae	*Jaborosa squarrosa*



Lobelia olygophylla



Luzula vulcanica



Deyeuxia nitidula

By categorizing the species registered in the bofedales, according to the place where they can generally develop, we find that there are more species typical of dry places (18), than typical species of bofedal (13). Eight generalist species were recorded, which can be found in bofedales as well as in transition zones, which have lower humidity and could become dominant species in meadows. Seven other species are only found in water courses and springs, a species found only in transitional zones and a species that develops only in saline areas (Table 5).

Eight species present in the Silala region are in some category of danger: four in the category IN DANGER and four as VULNERABLE (Figure 13). In relation to South Lipez there are eleven species IN DANGER and seven in VULNERABLE.

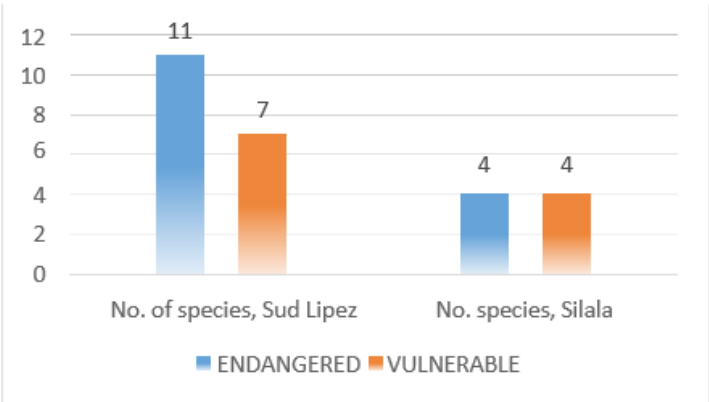


Figure 13. Number of threatened species in South Lipez and Silala.

Fauna

Macro-invertebrates

A total of 13,765 individuals were collected and 26 taxa could be identified. 60% correspond to the Insect Class, of which five taxa correspond to Ephemeroptera, Plecoptera and Trichoptera (EPT). The remaining 40% corresponds to other invertebrates: Amphipoda, Oligochaeta, Hirudinea, Nematoda and Trematoda (Table 7). All the taxa mentioned in the table are new records for the area.

Table 7. Taxonomic list of macro-invertebrates in the Silala bofedales.

Order/Group	Family	Sub-family	Genre
Plecoptera	Gripopterygidae		*Claudioperla*
Ephemeroptera	Baetidae		*Andesiops*
Trichoptera	Hydroptilidae		*Metrichia*
			Neotrichia
	Hydrobiosidae		*Cailloma*
Hemiptera	Corixidae		*Ectemnostega*
Coleoptera	Elmidae		*Austrelmis*
Diptera	Chironomidae	Diamesinae	*Paraheptagyia*
		Tanypodinae	
		Orthocladiinae	*Corynoneura*
			Orthocladiinae
		Chironominae	*Tanytarsus*
	Simuliidae		*Simulium*
	Limoniidae		*Hexatoma*
	Dolichopodidae		
	Tabanidae		
	Empididae		
	Ephydridae		
Amphipoda	Hyallelidae		*Hyallela*
Oligochaeta	Naididae		*Dero*
	Naididae		*Homochaeta*
	Enchytraeidae		
Hirudiea	Glossiphonidae		

Nematoda	Dorylaimidae		*Dorylaimus*
Trematoda	Dugesiidae		*Dugesia*
Hydracarina			

Ichthyofauna

The aquatic systems of Silala are characterized by a basic pH, which varies between 8.31 and 8.41; relatively low temperatures (16 to 17 ºC measured at noon); low conductivity (255 - 267 µS) and presence of dissolved solids (128 - 139 ppm) (see Table 3).

Only one species of fish was recorded in the area, the trout (Oncorhynchus mykiss), a species widely used in fish farming activities in the high Andean area of Bolivia.

Although in systems of the southern Altiplano in Bolivia and in the north of Chile, records of Orestias and Trichomycterus species, native to the Andean region, are known. During the current campaign, no native species were recorded in Silala. We do not have an explanation for the absence of native fish in Silala, since these have been recorded in several sites not far from the Silala bofedal (Figures 21 and 22). The nearest towns in which populations of Orestias are found are between 65 km (Ascotan salt flat, in Chile) and the towns of Alota and Quetena in South Lipez (approximately 71 km). In closer systems such as Pastos Grandes or Laguna Colorada, there are no records of fish.

Considering the characteristics of the aquatic systems of the Silala area (mainly the presence of highly degraded bofedales) and the water quality, it is presumed that there were favorable conditions for the presence of Orestias species in that area. Currently, however, most systems have been modified by the presence of canals. The velocity of water in this type of systems, despite the presence of vegetation, is a strongly limiting factor for the current presence of Orestias species, which are mainly associated with lentic systems (bofedales). When this native species is found in running water systems, it is associated with areas of stagnated water (pothole), with presence of vegetation and low current speed. One of the important problems to evaluate is the introduction of species (such as trout), usually associated with the introduction of parasites such as the white spot disease or Ich (Ichthyophthirius multifiliis) or the saprophyte Saprolegnia difilis, which can have effects on populations of native species of fish and amphibians (Wurtsbaugh & Alfaro 1988).

Populations of Trichomycterus species were recorded in aquatic systems of the southern Altiplano of Bolivia and northern Chile and Argentina (Figure 14). The closest towns to the Silala in which populations of Trichomycterus were registered are approximately 71 km away, in the area of Alota and Quetena in southern Bolivia. Considering the current characteristics of the Silala's aquatic systems (mainly the presence of canal systems with running water) and the water quality, currently there are favorable conditions for the presence of species of the Trichomycterus genre in the area. In general, species of this genre are considered indicators of running water systems (rivers and streams). The absence of Trichomycterus species allows us to speculate that the zone included mainly lotic systems (bofedales), in which the presence of said genre is less likely.

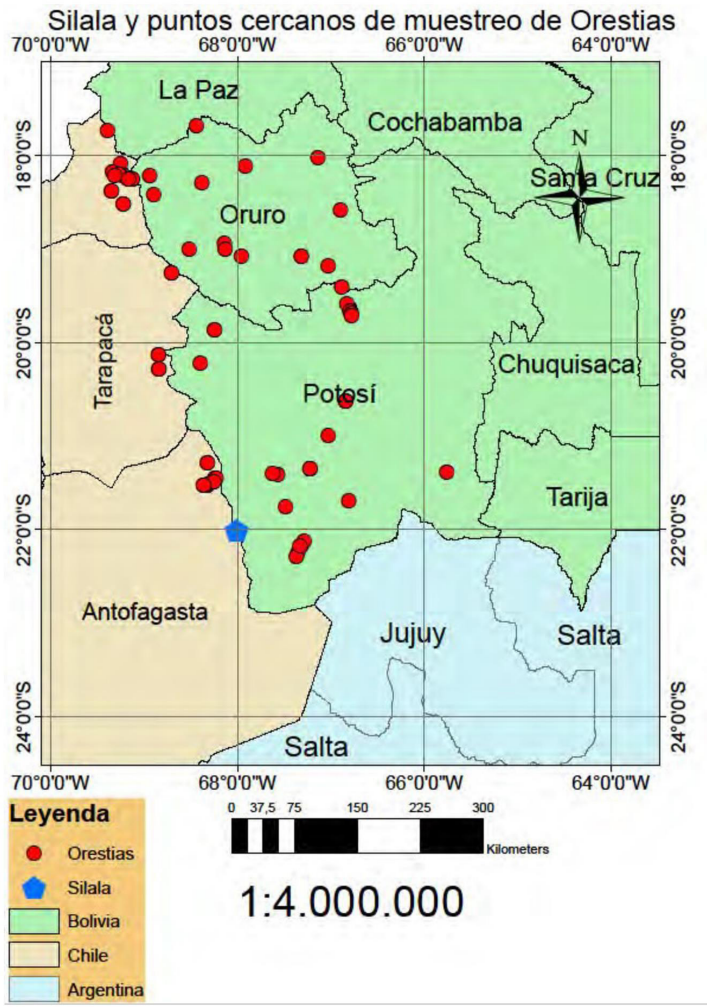


Figure 14. Distribution map of *Orestias* species in the southern Altiplano of Bolivia and northern Chile. Map prepared by A. Mariscal with data from the collections of the National Museum of Natural History.

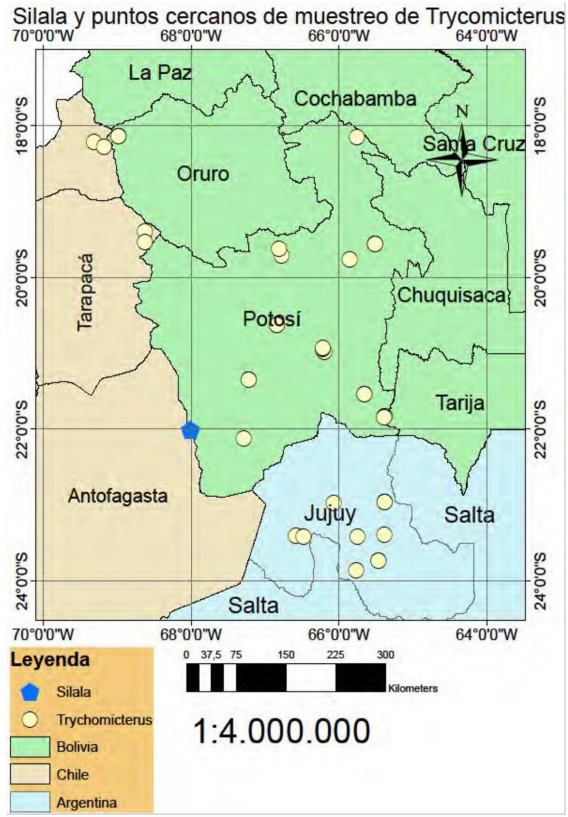


Figure 15. Distribution map of *Trichomycterus* species in the southern Altiplano of Bolivia and northern Chile. Map prepared by A. Mariscal with data from the collections of the National Museum of Natural History.

Herpetofauna

In the four days of sampling, it was possible to register only one species of amphibian (Rhinellaspinulosa), which was observed frequently along the bofedales (n = 33 observations, Fig. 42), and two species of reptiles: Liolaemus puna, distributed mainly in the areas of rocky slopes of the northeast slope (n = 9), and Liolaemus schmidti (n = 1) that was observed in an area of scrublands (Fig.42). None of the registered species is found in the Red Book of Vertebrates of Bolivia, nor is it an endemic species, but all three are listed in the category "Deficient Data (LC)" of the IUCN (Table 8).

In the last decades, the local disappearance of the Rhinella spinulosa toad in other areas of the Bolivian Altiplano has been seen with concern. Reason why we consider very important for its conservation the registration of a population of this species in the Silala area and it would be important to generate actions in order to guarantee its conservation in this area.

a) b)



Figure 16. The *Rhinella spinulosa* toad, with an abundant population in the area. a) Female, b) Male (Photos L. Zegada).

Table 8. List of amphibian and reptile species captured in the Silala locality.

ORDER/FAMILY	GÉNRE	SPECIES	HÁBITAT	RELATIVE ABUNDANCE	UICN CATEGORY
ANURA					
Bufonidae	*Rhinella*	*Rhinella spinulosa*	Bofedal	F	LC
SAURIA					
Liolaemidae	*Liolaemus*	*Liolaemus puna*	Roquedal	F	LC
		Liolaemus schmidti	Scrubland	C	LC

Relative abundance: Common (C); Frequent (F); Rare (R); Exceptional (E). Deficient Data (LC)

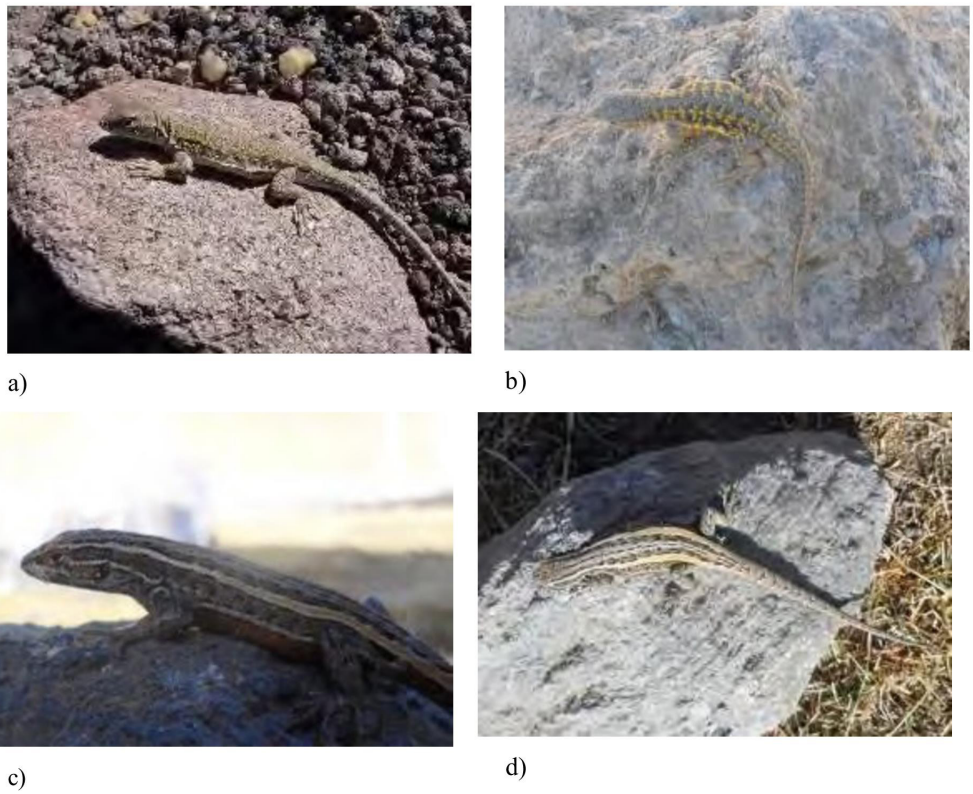


Figure 17. a) *Liolaemus schmidti* (Photo Ariel Liully); b) *L. schmidti*, which is abundant in the scrublands of the area (Photo L. Zegada); c) *Liolaemus puna found on rocky hillsides (Photo L. Zegada)*; d) *Liolaemus pachecoi* present in in the rocky areas, which are used as refuge (Photo: Tamara Perez).

Through a review of the published and relevant information, it has further been possible to observe the presence of the Liolaemus pachecoi in rocky hillsides (Palabral-Aguilera et al. 2016) of the Silala area. Similarly, considering the possible distribution according to the environmental conditions and the types of habitats present in the area, the species that are likely to be found in this area, with additional work efforts, are: Telmatobius huayra, an amphibian endemic to Bolivia and found in the Vulnerable category in the Red Book of Vertebrates of Bolivia; the Tachymenis peruviana snake of wide distribution and presence in these regions of the Altiplano, and the Liolaemus hajeki lizard, registered on the other side of the border, in the Silala basin itself. Likewise, the presence of some other species of the Liolaemus genre cannot be ruled out, which is the most representative within the herpetofauna of the region.

Avifauna

According to the rarefaction curve and the Chao index (30.5 ± 3.5), in the 2018 sampling > 70% of the avifauna in the Silala area was recorded. During this study 389 individuals were observed, of 26

bird species. The greatest abundance of birds was observed in the bofedales, with 180 individuals (101 records), followed by the rocky places with 122 individuals (74 records) and pastures with 79 individuals (41 records) (Table 9). Nine of the 26 species were recorded only in one type of habitat, with two or more records and could be considered as habitat specialists. Six of these nine species were observed

only in bofedales: including two species of ducks (Anas flavirostris, Lophonetta specularioides) (Figure 17A), species that depend on bodies of water, such as the White Wing Remolinera (Cinclodes atacamensis), species that use cushions and other vegetation in the bofedales, such as the Ochre-Naped Ground Tyrant (Muscisaxicola flavinucha), the Andean Negrito (Lessonia oreas), and the Rufous- bellied seedsnipe (Attagis gayi) (Figure 17). Three other species were observed only in rocky outcrops: two species of raptors (Falco femoralis, Geranoaetus polyosoma) and the Gray-faced Goldfinch (Sicalis uropygialis). Five species were recorded in three habitats and can be considered as habitat generalists: cordilleran canastero (Asthenes modesta) (Figure 17 E), and Finches (Phrygilus atriceps, Phrygilus dorsalis, Phrygilus plebejus and Phrygilus unicolor) (Figure 17 F-H), which were observed in large numbers feeding on seeds in different habitats.

More than 80% of the individuals observed in the Cream-winged Cinclodes (Cinclodes albiventris) (Figure 18) and the Grey-breasted Seedsnipe (Thinocorus orbignyianus) (Figure 17 B) were recorded only in the bofedales, while the Rufous-naped Ground Tyrant (Muscisaxicola rufivertex) was only observed in the rocks, capturing insects; thus, these three species could be considered as almost habitat specialists (Table 9). It is highlighted the abundance of the different species of Finches (Phrygilus atriceps, Phrygilus dorsalis, Phrygilus plebejus and Phrygilus unicolor), that were observed feeding on the seeds of grasses in the bofedal. The presence of these grasses between the cushions of the bofedal indicates some degradation of the habitat. Both Phrygilus atriceps and Phrygilus dorsalis are found in different habitats, including pastures and bofedales; on the other hand, Phrygilus plebejus and Phrygilus unicolor are not typical species of bofedales and are observed in pastures and bushes (Herzog et al., 2017).

Together with the observations made during 2016 (Palabral-Aguilera et al.), a total of 35 species of birds have been recorded in Silala. Four families are the dominant ones (with the largest number of species): Thraupidae (5 species), Furnariidae (5 species), Tyrannidae (5 species) and Anatidae (4 species) (Table 9). Two species registered in the Silala are under threat categories, the Darwin's rhea (Rhea pennata) (considered In Danger in the Red Book of Vertebrates of Bolivia) and the Diademed Plover (Phegornis mitchellii) (considered Near Threatened in both the Red Book of Vertebrates of Bolivia, and the Red List of IUCN) (Figure 17 C). Six species are considered endemic to the Central Andes zoogeographic region (CAN). Seven species have migratory movements, the Baird's sandpiper (Calidris bairdii) (Figure 17 D) and the Solitary Sandpiper (Tringa solitaria) are boreal migrants, the Rufous-naped Ground Tyrants (Muscisaxicola flavinucha, Muscisaxicola cinereus and Muscisaxicola rufivertex) are southern migrants and the Andean Negrito (Lessonia oreas) has altitudinal movements (Table 9).

Table 9. List of birds registered in the Silala.

FAMILY	SPECIES	HABITAT			CONSERVATION CONDITION			MIGRATORY	SOURCE
		BOFEDAL	PASTURE	ROCKY OUTCROPS	UICN (2018)	Red Book of Bolivia (2009)	Endemic CAN		
Rheidae	*Rhea pennata*					EN	x		2
Tinamidae	*Tinamotis pentlandii*		x				x		1
Anatidae	*Oressochen melanopterus*	x							1, 2
	*Lophonetta specularioides**	x							1, 2
	*Anas flavirostris**	x							1, 2
	Anas georgica								2
Columbidae	*Metriopelia aymara*			x					1
Trochilidae	*Oreotrochilus estella*	x							1
Charadriidae	*Phegornis mitchellii*				NT	NT			2
Scolopacidae	*Calidris bairdii*							Boreal Migration	2
	Tringa solitaria							Boreal Migration	2
Thinocoridae	*Attagis gayi**	x							1, 2
	Thinocorus orbignyianus	x	x						1, 2
Laridae	*Chroicocephalus serranus*								1, 2
Ardeidae	*Egretta thula*								2
Accipitridae	*Geranoaetus polyosoma**			x					1, 2
Falconidae	*Phalcoboenus megalopterus*		x						1, 2
	*Falco femoralis**			x					1
Psittacidae	*Psilopsiagon aurifrons*								1
Furnariidae	*Geositta punensis*		x				x		1

FAMILY	SPECIES	HABITAT			CONSERVATION CONDITION			MIGRATORY	SOURCE
		BOFEDAL	PASTURE	ROCKY OUTCROPS	UICN (2018)	Red Book of Bolivia (2009)	Endemic CAN		
	Ochetorhynchus ruficaudus		x						1
	Cinclodes albiventris	x		x					1, 2
	*Cinclodes atacamensis**	x							1, 2
	Asthenes modesta	x	x	x					1, 2
Tyrannidae	*Lessonia oreas**	x					X	Altitudinal migration	1, 2
	Muscisaxicola cinereus							Partial austral Migration	2
	*Muscisaxicola flavinucha**	x						Austral Migration	1, 2
	Muscisaxicola rufivertex	x		x				Partial austral Migration	1
	Agriornis montanus			x				Altitudinal migration	1
Thraupidae	*Sicalis uropygialis**			x			x		1
	Phrygilus atriceps	x	x	x					1, 2
	Phrygilus dorsalis	x	x	x			x		1, 2
	Phrygilus unicolor	x	x	x					1, 2
	Phrygilus plebejus	x	x	x					1
Fringillidae	*Spinus atratus*		x	x					1, 2

Legend:
* Habitat specialists (species registered only in one type of habitat with two or more records).
Threat Category: EN (Endangered), NT (Near Threatened)
Endemic CAN: Endemic of Central Andes zoogeographic region (CAN) (Stotz *et al.*, 1996)
Source of Information: 1. Registration during 2018 assessment; 2. Report (Palabral-Aguilera *et al.*, 2016)



Figure 17. Birds observed in the Silala bofedales. A) *Lophonetta specularioides* B) *Thinocorus orbignyianus*; C) *Phegornis mitchellii*; D) *Calidris bairdii*; E) *Asthenes modesta*; F) *Phrygilus unicolor*; G) *Phrygilus atriceps*; H) *Phrygilus dorsalis* (Photos: Omar Rocha).

A)  B) 

Figure 18. Birds observed in the Silala bofedales. A) *Cinclodes albiventris*; B) *Oressochen melanopterus* (Photos: M. Isabel Gomez).

Mastofauna

In relation to medium and large mammals, the presence of southern viscacha (Lagidium viscacia) was visually evident in the area, mainly in the cliff of the North Bofedal and vicuñas (Vicugna vicugna) in the South Bofedal. In addition, viscacha feces were found in the Central Canal and in the South Bofedal, near the rocky outcrops. In the Central Canal, bone remains of tuco-tuco (Ctenomys sp.) were found, but the species cannot be identified. In this canal there were a large number of dens, possibly associated with these rodents. We also found feces and bone remains of Andean fox (Lycalopex culpaeus) in the North Bofedal and Central Canal, as well as bone remains of vicuñas, which could indicate the presence of pumas in the area.

Until this study, there was no report of the micro-mammal species for the area. With a total effort of 681 traps per night, 94 individuals were captured, giving a capture success of almost 14%; which is quite high, considering that the average capture success is 10%. (http://www.openepi.com/v37/SampleSize/SSPropor.htm). However, most of the individuals collected correspond to two species.

The North Bofedal is the site with the largest number of individuals captured (67 individuals and a capture success > 30%), belonging to four genera (Phyllotis, Tapecomys, Calomys, Abrothrix, all Cricetidae). In the Central Canal, 23 individuals were captured (capture success > 9%), belonging to the same four genera of the North Bofedal. The South Bofedal was the site with the least capture success (2%), with only four individuals captured belonging to two genera (Calomys, Abrothrix). The genus with the highest number of captures was Phyllotis and Calomys had the least number of individuals captured (Figure 19).

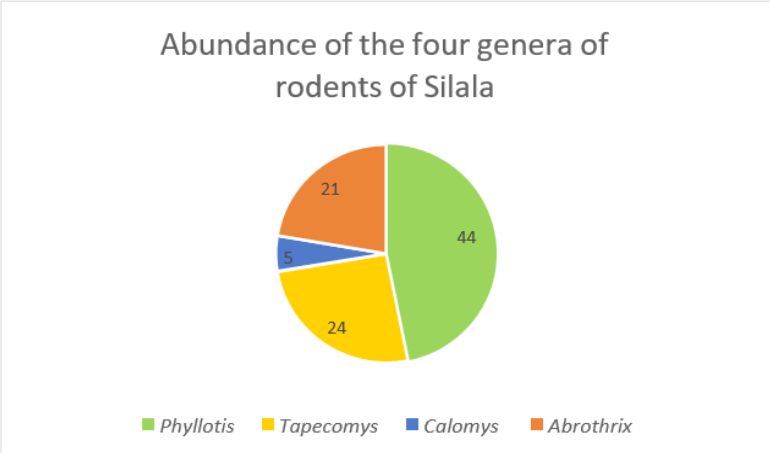


Figure 19. Pie chart showing the abundance of the four genera found in Silala.

Within the Phyllotis genre two species were identified (P. xanthophygus -> 85% of the captured individuals and P. cf. xanthophygus), which are typically high Andean, common near sites with rocky outcrops (Anderson, 1997) (Figure 20). The species P. xanthophygus (Figure 21a) is generally associated with scrublands and tola formations, in addition to stony areas, which could explain its great relative abundance in the North Bofedal.

The presence of Abrothrix andinus is registered for the area of Los Lipez (Anderson, 1997), for which we suppose that the two specimens collected in the North Bofedal belong to said species (Figure 21b). In addition to this species, 19 individuals of the Abrothrix genre were captured, but their taxonomy is not clear, although it is clear that they do not correspond to Abrothrix jelskii, a species that would be expected to be found in the area (Figure 20; D'Elia et al., 2015). For Bolivia, only these two species of Abrothrix are registered (Anderson, 1997), so it would be very important to fully determine the identity of the other 16 specimens, which morphologically seem to represent four species (Figure 21c, d, e, f).

The presence of Tapecomys wolffsohni (Figure 21g) extends its range of distribution (described for this species by Anderson, 1997), since their previous records reached only 2,800 meters above sea level. Despite being the second most abundant species in the area (Figure 20), very little is known about its biology and ecological aspects.

Regarding individuals of the Calomys genre, five individuals were identified as Calomys musculinus (Figure 21h), whose presence had already been registered southeast of the Department of Potosi; even at more than 4,000 meters above sea level (Anderson, 1997). It is possible that Calomys Lepidus is also found in the area, since this is a species that can be found at more than 4,000 meters above sea level (Anderson, 1997).

Andean mouse (Andinomys edax) is a monotypic species that could be found in Silala, since it inhabits mountainous areas of Potosi and Chuquisaca, at more than 3,700 meters above sea level; although there are no records in the drier part of Potosi (Anderson, 1997). Another species that could be found in the Silala area is the Andean big-eared mouse (Auliscomys sublimis),

which is common over 3,800 meters above sea level. It lives near bofedales, associated with rocks and vegetation of low bearing and scrublands; and can get to use the tuco-tuco (Ctenomys) tunnels.

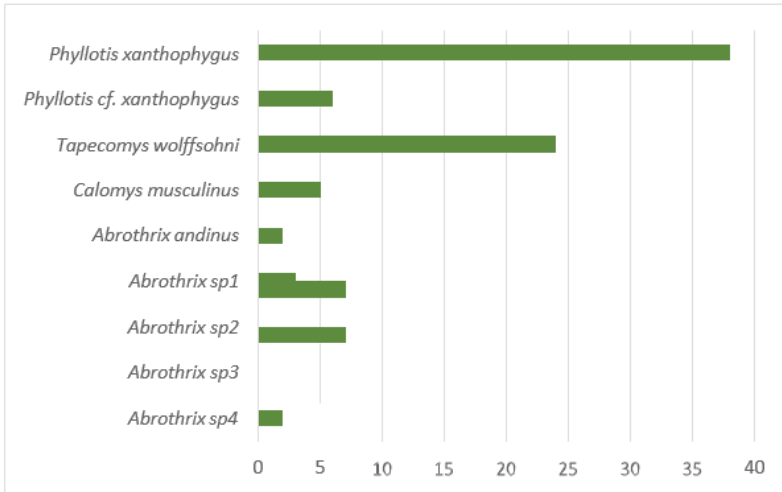


Figure 20. Species of micro-mammals found in Silala. The bars represent the relative abundance (captures) of each of the species.

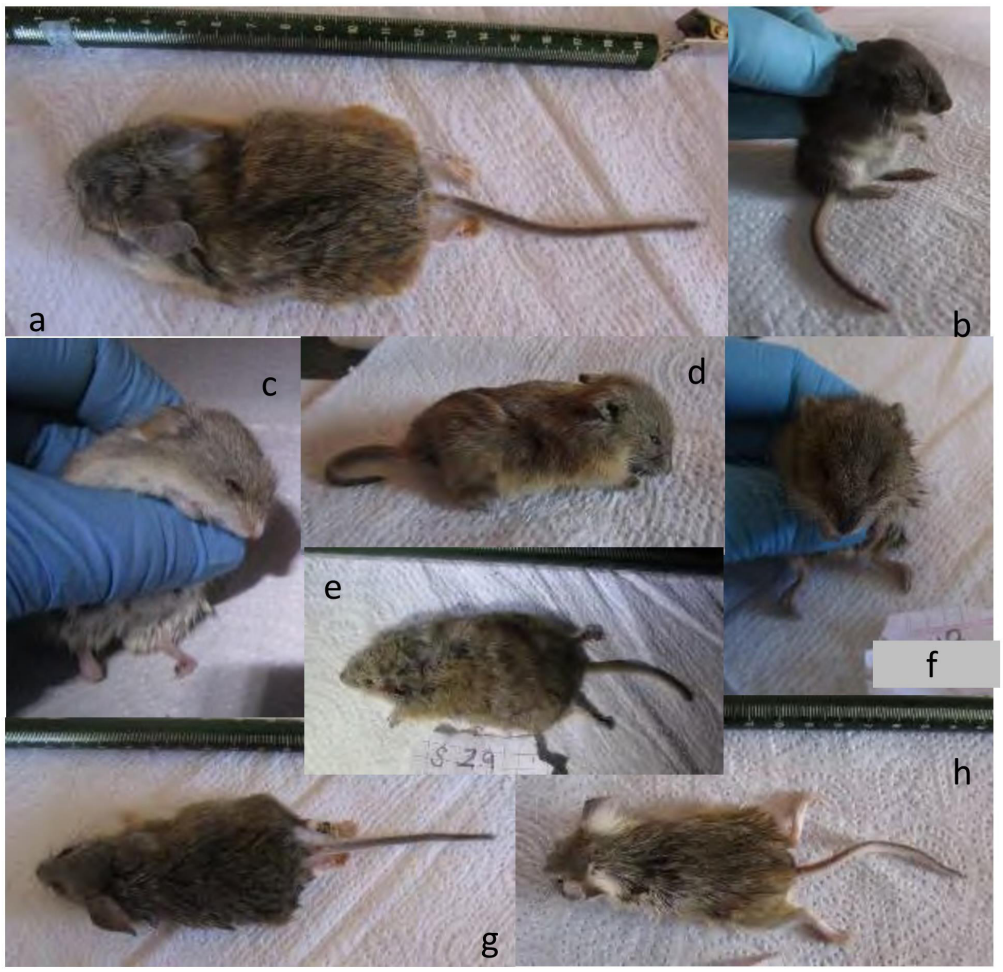


Figure 21. Species of micro-mammals found in Silala. a) *Phyllotis xanthophygus*, b) *Abrothrix andinus*, c) *Abrothrix sp1*, d) *Abrothrix sp2*, e) *Abrothrix sp3*, f) *Abrothrix sp4*, g) *Tapecomys wolffsohni*, h) *Calomys musculinus*.

In summary, the wealth of species (flora and fauna) currently present in the Silala area is as follows:

Table 10. Summary of the biodiversity recorded in Silala.

Taxonomic Group	N° of total species	N° of endemic species for Bolivia	N° of endangered species	New records for Potosi	New records for Bolivia	N° of typical bofedal species
Flora	86	1	9	17	2	13
Macro-invertebrates[¥]	26	0	1	15	1	6
Fish	1	-	-	-	-	-
Amphibians	2	1	1	-	-	-
Reptiles	4	-	2	-	-	-
Birds	35	-	2	-	-	19
Mammals	13*	1	1	#	#	0

[¥] In the case of macro-invertebrates, the determination is at the level of genera or families, due to the the difficulty of obtaining codes for Bolivia.

* Considering the four morph-types of Abrothrix as distinct species.

6.3 Determination of the actual area of the bofedales

In the study area, individuals of Oxychloe andina were found, which is a kind of bofedal plant sensu strict (i.e., plants strongly adapted to water saturation, which form peat-like soils, and which are rich in organic matter); and also species of margin plants, referred to a more general type of wetland, that includes vegetation from less organic soils and that does not form peat. In this sense, the current total area of the bofedal is very limited and its spatial distribution is highly fragmented in several sectors. The rest of the surface is covered by the other generalist species, which indicates that the bofedal has undergone a process of drainage and regression. In sum, the following types of vegetation were found: bofedal, mixed bofedal, scrubland bofedal, wet scrubland, dry scrubland, meadow, grass, areas with saline outcrops. In addition, portions without vegetal cover were found, with sandy soils of volcanic origin, bare rock and organic matter without vegetation (Table 11).

Adding all types of soil cover, the total area of study in Silala covers 114,817 m2 (11.48 hectares) (Table 11). Most of the wetland corresponds to the South Bofedal (87,892 m2), while the North Bofedales and Confluence Area are smaller (20,290 m2 and 6,635 m2, respectively). Of this total, only 7,680 m2 (0.76 hectares) correspond to actual bofedal at present. In conclusion, it can be affirmed that 107,137 m2 (10.7 hectares) of bofedal have been lost due to canalization.

Table 11. Surface area (m^2) of the different Silala bofedal fragments.

Type of vegetation	South A	South B	South C	South D	South E	South F	North	Confluence	Total
Bofedal	-	-	-	2.512	2.310	-	1.779	-	6.601
Scrubland Bofedal	-	151	-	-	-	-	584	-	735
Fragmented Bofedal	-	-	-	-	-	68	177	99	344
Scrubland	53	-	6.149	3.864	5.134	14.750	13.522	6.214	49.686
Meadow	-	-	-	-	2.447	12.802	3.820	-	19.069
Mixed Meadow	-	6.073	781	3.957	-	-	-	-	10.811
Grass	7.811	-	2.222	-	-	-	-	-	10.033
Saltpeter bed	2.878	-	-	-	-	-	-	-	2.878
Bare soil	12.463	22	1	65	239	558	408	322	14.078
Aquatic Vegetation	-	-	-	-	-	582	-	-	582
Sector Total	23.205	6.246	9.153	10.398	10.130	28.760	20.290	6.635	**114.817**

Source: Own elaboration based on field data and satellite images.

Although the largest bofedal is the South Bofedal, it is the one that is most affected, followed by the Confluence Area. Both bofedales have a dominant presence of generalist species, which form scrublands or meadows.

In conclusion, taking into account that: 1) a bofedal has peat-like soils, which have plant material that is not completely decomposed, and 2) only certain plant species, such as Oxychloe andina and, to a lesser extent, Zameioscirpus atacamensis, form this type of soils. It can be concluded that the bofedal area identified in the study area is highly degraded and fragmented because it is surrounded by scrublands and other types of vegetation, which indicate draining processes.

6.4 Calculation of the bofedal area in the present and recent past

Throughout the study area there are artificial canals built during the last century. These canals continuously diverted the water that naturally irrigated from the bofedal, modifying the natural hydrological conditions of the region, causing the drainage of the soils and changes in the vegetation. The process of invasion of scrubland and meadow species is a result of this draining process.

According to the floristic and spatial analyzes of the study area, the three areas of the Silala were at one time large and continuous peatlands that covered practically the entire area of the three plains analyzed (North, South and Confluence). This is supported by the fact that, in all the margin of the study area, there are isolated individuals of bofedal plants (Oxychloe andina) (Figure 23). These individuals grow by rhizomes, that is to say that they reproduce mainly in a vegetative way through the prolongation of subterranean stems. For this reason, it can be affirmed that these isolated groups could not appear individually, but they had to have conformed at some time in the past a continuous structure or much less fragmented than what is observed in the present. For this reason, it can be affirmed that the true bofedal area was much wider in the past. The

satellite images analyzed by DIREMAR indicate that this sector is dry at least since 1975 (the year in which the Landsat satellite began capturing images of the Earth) (DIREMAR 2017).

The absence of images or photographs makes it impossible to know the exact date when was the last time the dead plants in this sector were wet and vigorous. However, a comparison of aerial-photogrammetric flight images of 1967 and 2001 suggest that the bofedal was dry since 1970 (Figure 22). This shows that the bofedal was almost completely dry since the 60s. It can be seen in the same figure that the canals were clearly defined, and they were the cause for the degradation of the bofedal.

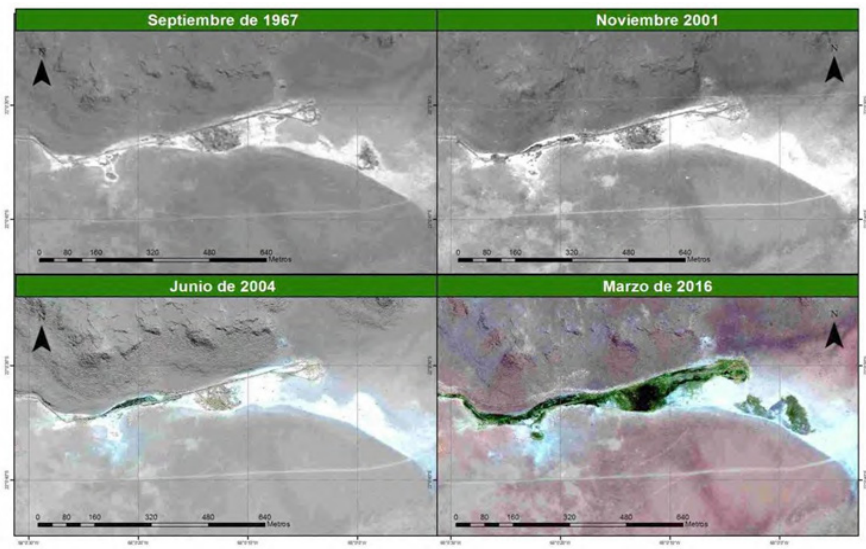


Figure 22. Detail of images of the South Bofedal during 1967, 2001, 2004 and 2016. Note that the images correspond to different seasons of the year (1967, 2001, 2016 wet season) and 2004 (dry season). The images of 1967 and 2001 correspond to aero-photogrammetric flights and have a spatial resolution of 1 meter. The images of 2004 and 2016 correspond to Quick Bird II satellite images of 0.5 meters of spatial resolution and true color combination. The recovery of vegetation in 2016 is evident, though minimal. Source: Satellite Images: DIREMAR 2017. Aerial photographs: Photographic Archive of the Military Geographical Institute (MGI) – Bolivia.

Table 12. Values of the potential areas of the bofedal (m^2) in 2004, in 2016, and the maximum extension that could have been reached before 1975.

Bofedal	South A	South B	South C	South D	South E	South F	North	Confluence	Total
Maximum possible extension*	23.205	6.246	9.153	10.398	10.130	28.759	20.291	9.752	**117.934**
2004**	0	63	0	1.247	1174	0	2.012	107	**4.603**
2016***	0	151	0	2.512	2.310	68	2.540	99	**7.679**

* According to flora and landscape indicators, it is estimated that the area of the bofedal covered this area.
** Year with the oldest high resolution image.
*** Year with the high resolution image in the most recent wet season.
Source: Own elaboration based on high resolution images (DIREMAR 2017), and field data collection.

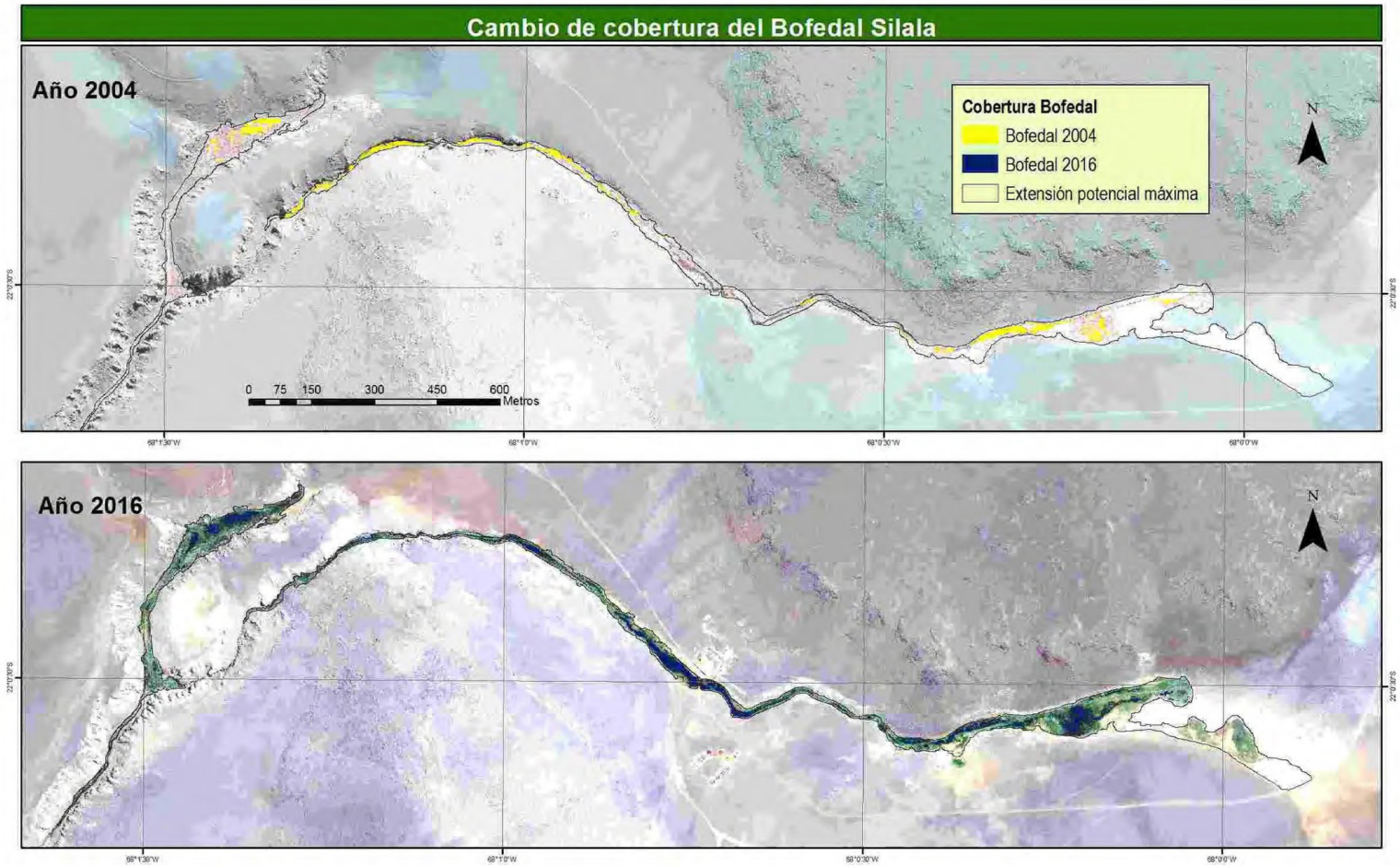


Figure 23. Potential area of the bofedal in the past (black contour). In 2004 (yellow fill) and in 2016 (blue fill). Source: Own elaboration based on high resolution images (DIREMAR 2017).

In conclusion, the presence of isolated individuals of Oxychloe throughout the entire margin of the study area is a landscape indicator that the bofedal could occupy the entire surface that today occupies the scrublands, meadows and grasses. If we consider that Oxychloe only grows in conditions of permanent or semi-permanent water saturation, it can be affirmed that, the bofedal regression process allowed the invasion of other species, which survive better in drier conditions, due to a significant decrease in water supply. This decrease is clearly related to the construction of the canals, because elements that altered the natural drainage of the bofedal can be recognized. The result was a degraded area, with artificial drainage in the form of a fishbone.

6.5 Current conditions of the Silala bofedales.

For its altitudinal range (between 4100-4300 meters) and for the species present, the Silala bofedales are considered high Andean.

Botanical description of the Silala bofedales

In Silala, fragments were delimited according to the physiognomy and the dominant plants (see methodology). The following describes the flora of each fragment of the South Bofedal, North Bofedal and Confluence Area, which are related to the vegetation map (Figure 24).

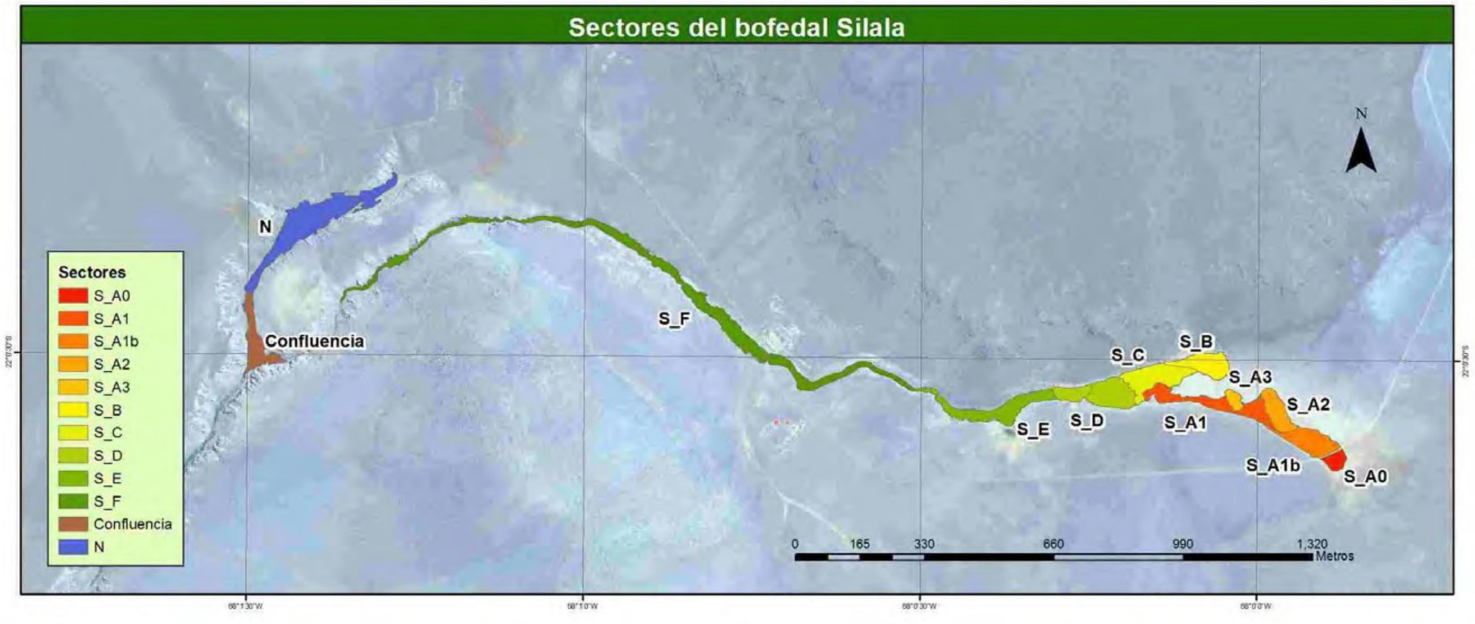


Figure 24. Differentiation of the fragments in the North Bofedal, South Bofedal and Confluence Area. The characteristics of the fragments are detailed in table

Table 13. Coverage of species and abiotic elements found in the different fragments of the Silala bofedal. These fragments were differentiated at the landscape level on basis of their physiognomy.

Fragment	Species	Surface Area m^2	Altitude m	Gradient %	Organic matter cm	Percentage of coverage of common to bofedals	Percentage of coverage of other species, as an degradation	Percentage abiotic elements
Deserted areas (before the road) (S_A0)	*Xenophyllum incissum var. incissum Deyeuxia curvula Junellia pappigera Nototriche auricoma Nasella aff. rupestris* Bare soil	1444	4410	<1%	Unavailable		3 2 1 >1 >1	95
Open meadow in which the *Deyeuxia curvula* species predominates (following the road) (S_A1)	Sandy soil Saline outcrop Stone Camelid feces *Deyeuxia curvula* *Xenophyllum incissum* var. *incissum* *Eleocharis atacamensis* *Festuca potosiana*	6208	4409	<1%	Unavailable		45 2 3 >1	45.5 3 1 0.5
Salinized grass in which the *Carex* species and isolated *Oxychloe* cushions predominate S_A2	Bare soil Stone *Carex* cf. *maritima* *Oxychloe andina* *Deyeuxia curvula* *Festuca potosiana*	5438	4409	<1%	Unavailable	50 5	2 1	42 >1
Salinized grass in which the *Carex* species predominates S_A3	Bare soil *Carex* cf. *maritima* *Deyeuxia curvula*	3761	4409	<1%	Unavailable	89	2 2 >1	7

Meadow with isolated cushions of *Oxychloe* S_B (below the fenced water spring)	Artificial canals	6268	4407	<1%					10
	Oxychloe andina				Average: 49.1	1			
	Festuca				maximum: 74		>1		
	potosiana Carex				minimum: 19	89			
	cf maritima						>1		
	Xenophyllum incissum var. *incissum*								
Low salinized grass dominated by *Carex* cf. *maritima* S_C species (following SENAMHI's gauging site)	Bare soil	9170	4405	<1%				25	
	Carex cf.					67			
	maritima					>1			
	Deyeuxia				Average: 61.6	5			
	chrysantha				maximum: 86		1		
	Plantago tubulosa				minimum: 30	>1			
	Puccinellia frigida						>1		
	Stuckenia pectinata					>1			
	Xenophyllum incissum var. incissum						2		
	Zameioscirpus muticus					>1			
Bofedal S_D	Dry canals								2
	Active canals								4
	Bare soil								10
	Organic matter, dead *Oxychloe* cushions								2
	Carex cf. *maritima*						5		
	Deyeuxia chrysantha						1		
	Festuca potosiana				Average: 44.5	30			
	Festuca rigescens				maximum: 64		1		
	Oxychloe andina	10421	4403	<1%	minimum: 25	40			
	Plantago tubulosa						>1		
	Puccinellia frigida						>1		
	Ranunculus						>1		
	Xenophyllum incissum var. incissum						>1		
	Zameioscirpus muticus						>1		
Bofedal S_E	Active canals								8
	Festuca rigescens					55			
	Oxychloe andina					20			

	Lemna minuta					5		
	Stuckenia	10236	4394	2%	Unavailable			
	Lobelia oligophylla					1		
	Plantago tubulosa					1		
	Phylloscirpus deserticola					1		
	Xenophyllum incissum var. incissum						2	
Degraded bofedals – watercourse margins S_F	Active Canals							49
	Organic matter							7
	Stone				Unavailable			5
	Submerged algae	28890	4382	1%				15
	Ranunculus uniflorus					20		
	Deyeuxia chrysantha					4		
	Oxychloe andina					>1		
North Bofedal (N)	Active canals							2
	Water springs							2.5
	Peat							0.5
	Festuca potosiana						20	
	Deyeuxia eminens					10		
	Festuca chrysophylla				Average: 111.1		20	
	Festuca ortophylla				maximum: 268		20	
	Carex cf maritima	20373	4355	5%	minimum: 20		>1	
	Festuca rigescens					5		
	Lobelia oligophylla					>1		
	Aciachne						>1	
	Oxychloe andina					15		
	Phylloscirpus deserticola					3		
	Zameioscirpus atacamensis					2		
Confluence between the South and North Bofedal (CONF)	Canals					5		
	Organic matter					1		
	Sandy soil					0.5		
	Deyeuxia eminens					70		
	Deyeuxia spicigera	6678	4320	7%	Unavailable	3		
	Festuca potosiana					10		

	Gramineas quemadas	5
	Lobelia oligophylla	3
	Phylloscirpus deserticola	3

South Bofedal fragments

Six fragments distinguishable at the landscape level have been delimited in this area on basis of the physiognomic units of the vegetation (Table 13). The first four fragments can be recognized in Figure 25.



Figure 25. Panoramic view of the first four fragments that can be distinguished at the landscape level in the South Bofedal. The different color contours mark the different fragments. Red—Prairie with isolated cushion plants of Oxychloe; blue—salinized Carex grass with isolated cushion plants of Oxychloe; brown—salinized low grass of Carex cf. maritima; green—bare soil/saline outcropping]

Deserted area S_A0



Figure 26. Fragment of the deserted bofedal, before the road.

This sector is physiognomically characterized by open areas, with 95 % of bare and sandy soils 5% of vegetation cover, 3% of the Xenophyllum incissum var. incissum—a species characteristic of lagoon margins and bofedals of the southern region of Bolivia—and 2% of Deyeuxia curvula— species commonly dominant at bofedal margins under drying out processes of the Xerophytic puna. This sector also comprises species with a vegetation cover smaller than the 1 %, such as Junellia pappigera, Nototriche auricoma, Nasella aff. rupestris. These species are commonly found in dry and sandy plains and hillsides of Sur Lipez.

Deserted areas (following the road)

Three different physiognomic units have been differentiated. These reflect a visual gradient of desiccation, that range from very dry (S_A1), in the central part, with fragmented cushions of the O. andina (S_A2) species surrounded by species of Carex cf. maritima (S_A3). Each of these units is described below:

Open meadow with a predominance of the Deyeuxia curvula S_A1 species



Figure 27. Deserted bofedals (following the road).

This fragment is physiognomically characterized by presenting 45,5% of Sandy and bare soil, 3% of saline outcrops, 1% of stones, 0,5% camelid feces, a n d 50% of vegetation cover. The predominant species is the Deyeuxia curvula (porke), covering 45 % of the area, followed by the Xenophyllum incissum var. Incissum with 2%, Eleocharis atacamensis 3%, and the Festuca potosiana, with a cover of less than 1%.

Salinized grass, where the Carex species and isolated Oxychloe cushions (S_A2) predominates



Figure 28. View of the S_A2 fragment.

This fragment is physiognomically characterized by 58 % of total vegetation cover, 42% of bare soil, and 0.1% of stone. The predominant species is the C. cf. maritima, covering 50% of the area. This species can generally be found in high Andean bofedals, covering less than 1% of the area. This sector also comprises fragmented cushions of the O. andina species, reaching as much as 5% of the total vegetal cover, Gramineae, such as the D. curvula, with a coverage ratio of 2%, and F. potosiana,1%.



Figure 29. View of the S_A3 fragment.

This sector comprises dry Stone Canals. It is physiognomically characterized by presenting 7% of bare soil and 93% of vegetation cover. The predominant species is the Carex cf. marítima with a coverage ratio of 90%, followed by the Deyeuxia curvula, 2%, the Xenophyllum incissum var. Incissum, 1%, and the Puccinellia frigida less than 1% of coverage ratio.

Following a detailed examination of these species' composition , the rank-abundance curves for the South Bofedal fragments (S) A1, A2 and A3 show a similar species composition and abiotic elements (Figure 30). All of these species have few elements and a high ratio of sandy soils (sare) and saline outcrops (asal). The predominant species of sites S_A2 and S_A3 is the Carex cf. marítima, though it takes a secondary predominance at the A1 transect, following the Deyeuxia curvula. The three transects comprise Xenophyllum incissum var. incissum (Xinc) species and Werneria pygmaea (Wpyg), to a lesser extent. The presence of Oxychloe andina is an indication of the presence of a bofedal and is found in the A2 fragment, with a low abundance ratio.

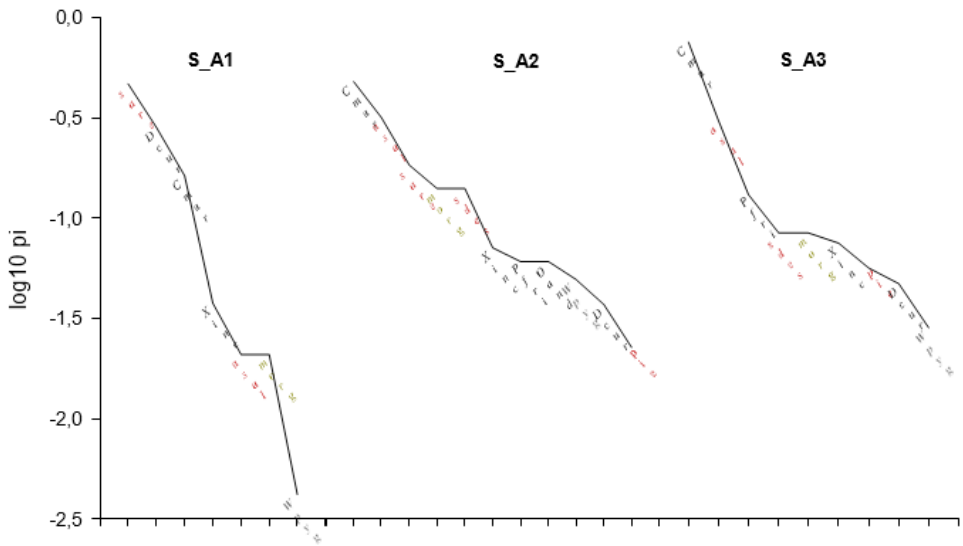


Figure 30- Rank-abundance curves for the flora found in the transects of fragments A1, A2 and A3, within the South Silala Bofedal.

Figure 31 shows the different components, such as, soils, plants, and saline outcrops present in a longitudinal profile that extends from A0 t o A3, which depicts a desiccation gradient that ranges from very high to intermediate dryness.



Figure 31. Longitudinal profile of the A sector. Schematics of the main vegetation components and abiotic elements.

Meadow comprising isolated cushions of the Oxychloe - S_B species (below the fenced water spring)

This bofedal is surrounded by Festuca potosiana and Deyeuxia curvula, and comprises canalized springs and dispersed cushions of Oxychloe andina, of a diameter of 1 x 1 m and 0,5 x 0,5 m. This fragment comprises 10% of manmade canals and 90% of vegetation, where the Carex cf. maritima predominates with 89 % of coverage ratio, followed by the Oxychloe andina (1%) and the Festuca potosiana and Xenophyllum incissum var. incissum (less than 1%). Note that water springs are absent in this sector.



Figure 32. View of the meadow that comprises isolated cushions of *Oxychloe*.



Figure 33. Cross profile of the B fragment (meadow with isolated cushions). Note the presence of different semi-naturalized canals that penetrate the bofedals, some of which are dry while some that present varying amounts of water.

Low salinized grasses dominated by the Carex cf. maritima species

Physiognomically, this fragment comprises 25% of open, salinized soils and 75% of total vegetation cover. The predominant species is the Carex cf. maritima (67%), Deyeuxia curvula (5%), Xenophyllum incissum var. incissum (2%), Festuca potosiana (1%), and Plantago tubulosa, Puccinellia frigida, Stuckenia pectinata, Zameioscirpus muticus, Deyeuxia chrysantha (less than 1%). The area also comprises camelid feces (less than 1%).



Figure 34. View of the S_C fragment.



Figure 35. Cross profile of the C fragment (saline grasses, with a predominance of the *Carex* cf. *maritima* species). Note the open areas, Canals, and saline outcrops.

Bofedal (S_D)



Figure 36. View of the S_D fragment.

This bofedal comprises 2 % of dry canals and 4 % of active canals, open areas with 10% of bare soil, 2 % of organic matter, 5% of dead Oxychloe andina cushions, and 77% of total vegetation cover. The predominant species are O. andina (40%) and Festuca potosiana (30%), followed by Carex cf. maritima (5%), Deyeuxia chrysantha (1%), Festuca rigescens (1%), and Ranunculus, Xenophyllum incissum var. incissum, Puccinella frigida, Plantago tubulosa and Zameioscirpus muticus (less than 1%).

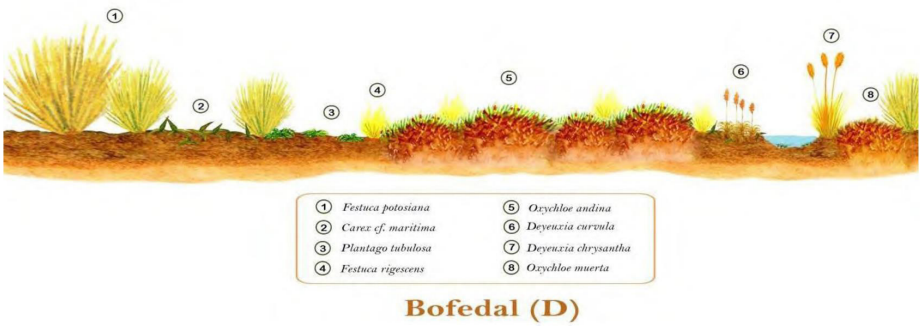


Figure 37. Cross profile of the D fragment. Note the presence of *Oxychloe andina* cushions and peat (dead *Oxychloe*), canals and the predominance of Gramineae in the bofedal margins and Gramineae common of bofedals in-between the cushions.

Scrubland Bofedal S_E



Figure 38. View of the S_E fragment.

This bofedal comprises 8 % of active canals and 92 % of total vegetation cover. The predominant species are Festuca rigescens (55 %) and fragmented O. andina cushions (20 %). The water in the active canals is covered by Lemna minuta (5 %) and Stuckenia pectinata (7%)—a submerged species. The area also comprises species as the Lobelia oligophylla, Plantago tubulosa, Phylloscirpus deserticola (1% of coverage ration each), and Xenophyllum incissum var. incissum.

Degraded bofedals – watercourse margins S_F



Figure 39. View of the S_F fragment.

This watercourse comprises 25 % of open canals, 7% of organic matter, 5 % of rocks, 15% of submerged algae, 20 % of Ranunculus uniflorus—floating at the canal margins—and 4% of Deyeuxia chrysantha, at the watercourse margins, with small cushions of O. andina (less than 1%).

The rank-abundance curves show that the B to F fragments of the SE bofedal comprise 12 and 24 species, respectively. Abundant Carex cf. maritima species are present in all fragments, followed by Gramineae as Deyeuxia curvula (B), Festuca potosiana (D and F), F. rigescens (E) or Pucinellia frigida (C). These Gramineae generally grow in meadows and their presence is an indication that the bofedal is under a desiccation process.

In the D and E fragments, the O. andina is the most abundant species, while it only takes the fifth place among other dominant species in the B fragment, is almost absent in fragment C and is completely inexistent in the F fragment (Figure 40).

The C fragment (S_C) comprises 12 species, five of which are reduced in proportions (Arenaria spp., Ranunculus uniflorus, Calandrinia acaulis, Lilaeopsis macloviana and Oxychloe andina). This fragment also comprises a great extent of bare soil, organic matter, saline outcrops and stones. The presence of Oxychloe andina is significantly reduced and presents indications of having endured recent burning by burnt Gramineae (qgram).

The S_B fragment presents a heterogeneity of species, which are, in some cases, associated to the water springs and saline outcrops, in other. In the S_B and S_C, the Lilaeopsis macloviana and Ranunculus uniflorus species—which develop in water springs or courses—are the least abundant ones (Figure 40).

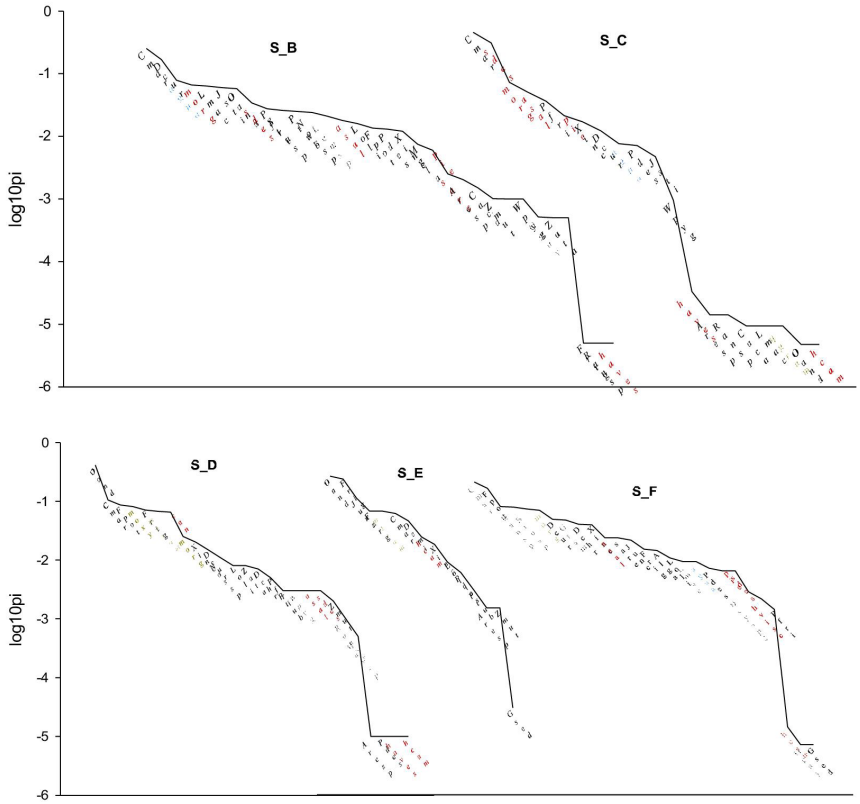


Figure 40. Rank-abundance curves for the South Bofedal fragments: S_B, S_C, S_D, S_E and S_F.

General remarks on the South Bofedals

Most of the Canals constructed in the South Bofedal do not comprise ignimbrite structures, as opposed to the North Bofedal. Several areas with saline outcrops can be found in the lower area of the south bofedal.



Figure 41. Details of the two sectors found in the South bofedal: a) Area comprising cushion fragments of *Oxychloe andina* and b) fragmented cushions developed in a canalized patch of the South Bofedal.

The decision was made to denominate the S_B fragment as a meadow, owing to its reduced coverage ratio of cushions and the predominance of Gramineae. Salt outcrops can also be found in-between the bofedal fragments and the surrounding area.

The S_D fragment is the only one that can be denominated as a bofedal. This fragment is not, however, in good conditions, due to the presence of Gramineae in its crest.

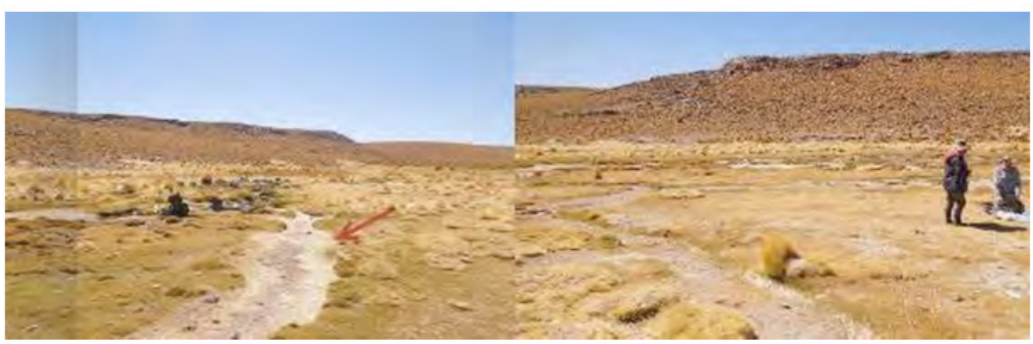


Figure 42. Desiccated section of the S_C fragment. The desiccation was provoked by a diversion made to measure the flowrate of the area.

North Bofedal (N)



Figure 43. View of the North fragment.

This bofedal comprises 75% of Gramineae, 20% of cushions (O. andina, P. desertícola y Z. atacamensis), 2% of canals, 2.5% of water springs, and 1% of peat. The cushions are found in the south central portion and are surrounded by Festuca potosiana in areas of mild humidity. A canal is found on the margins of these cushions. Close to the Canals, the dominant species is the Deyeuxia eminens. Tussoks of Festuca chrysophylla and F. orthophylla can be found throughout bofedal margins. Carex cf. maritima, Festuca rigescens, D. eminens, and Lobellia oligophylla can be found in flooded areas, and Aciachne (though in a reduced amount) in areas that are enduring a desiccation process.

This is currently the largest fragment of the Silala bofedals. Thirty-four elements have been observed in this area, including abiotic species and characteristics. A high density of springs (up to three per lineal meter according to Urquidi 2004) has also been recorded

This fragment presents the greatest amount of species typical of bofedals, such as: Oxychloe andina, Zameioscirpus muticus, Eleocharis atacamensis, and Phylloscirpus desertícola, although the predominant species is the Gramineae Festuca potosiana, followed by the Oxychloe, and the Deyeuxia eminens var. Eminens Gramineae, both common of bofedals. Despite this predominance mentioned, equitability is high in this fragment. The presence of organic matter, bare soils, stones, canals, and sandy soils is noted (Figure 44).

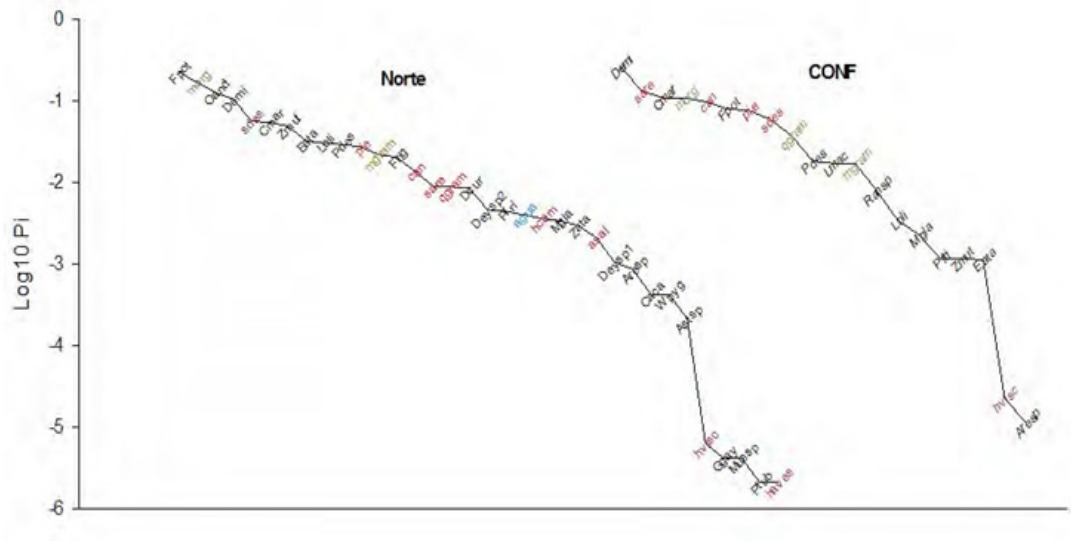
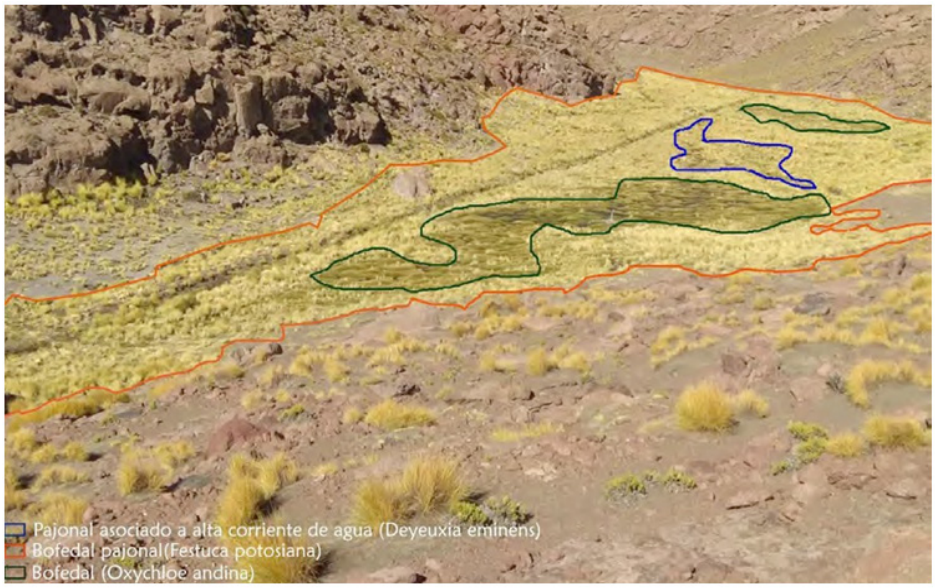


Figure 44. Rank-abundance curve for the North bofedal (N) and the confluence of both canals (CONF).

Physiognomically, three vegetation units are distinguished (Figure 60): a) two bofedal patches in good conditions and dominated by O. andina cushions; b) a unit comprising the greatest amount of canals, where Gramineae associated with flowing water bodies (D. eminens) can be found; and c) a unit of dry-portion Gramineae (F. potosiana).



[Map legend, from top to bottom: Blue—Scrubland associated with a high water current (Deyeuxia eminens); red—scrubland, bofedal (Festuca potosiana); green—Bofedal (Oxychloe andina)]

Figure 45. North Bofedal, Silala. The contours in different colors represent the patches that can be distinguished at the landscape level.

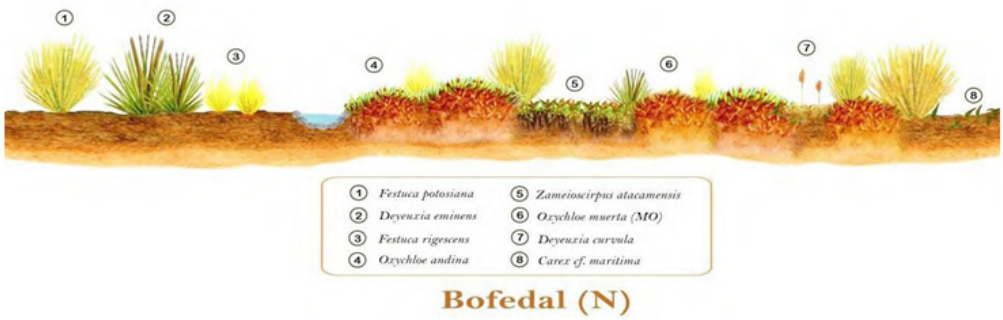


Figure 46. Cross profile of the North bofedal. Schematics of the main vegetation and abiotic element components. Note the presence of *Oxychloe andina* and *Zameioscirpus* spp. cushions, dry areas and canals lined with stones.

South and North Bofedal Confluence (CONF)

This fragment is found in the area in which the waters of the South Bofedal enter a naturally- formed ravine and merge with the North canal, converging to flow in direction to Chilean territory. Although smaller fragments of 2 m2, approximately, can be observed, the partial absence of O. andina is notiecable in this area. The most abundant species is the D. eminens, followed by the Carex cf. maritima and F. potosiana.



Figure 47. View of the confluence area.

Current state of the bofedals

The composition of species in the Silala varies in each bofedal. Many smaller proportion species can be found throughout the North, South and Confluence quadrants. Nevertheless, 41% of C. cf. maritima, particularly, and O. andina and F. potosiana, to a lesser degree, determine the bofedals composition (Figure 48).

The multivariate Principal Component Analysis provides general insights on the composition and abundance of plants in the Silala. Four major groups of plant communities can be distinguished. The First Axis (24% of the total variance) is dominated by the Carex cf. maritima, Festuca potosiana, and—to a lesser degree—by Oxychloe andina. On the right side of this axis, the main set of areas affected the most by the different canalization works stands out with a quadrant dominion of C. cf. maritima (8). These areas are scattered throughout different sectors of the South Bofedal. This species is associated with more open areas, namely, with exposed organic matter and saline outcrops. The second set, with a high abundance of Puccinellia frigida, is found close to this C. cf. maritima dominated quadrant.

The third group is characterized by a predominance of D. eminens, the most abundant in northern quadrants, close to the stone-lined Canals, which are in turn characterized by a greater water flow (see results with macroinvertebrates).

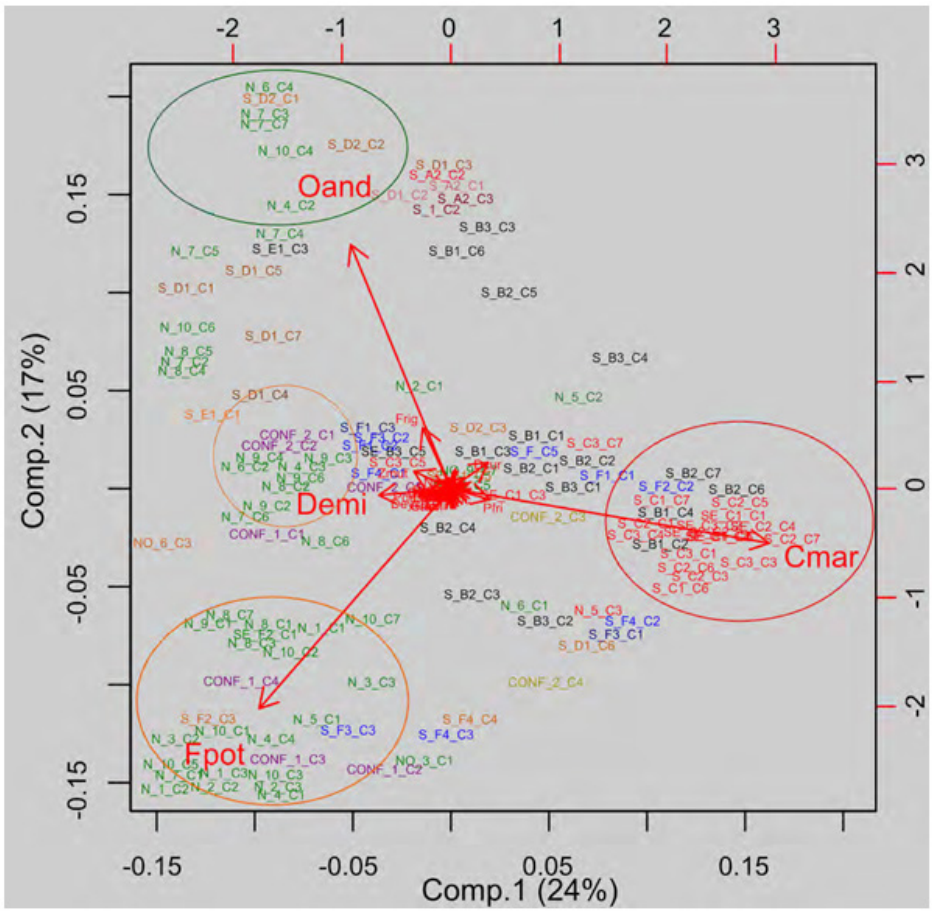


Figure 48. Articulation of the plant species examined as a function of the dominant species of the North (N) and South (S) bofedals and the Silala Confluence (Biplot). To carry out the analysis, 126 quadrants were employed. The circles depict the different plant groups. This analysis allows depicting the differential impacts of the canalization works on the plant species of the South and North bofedals. The direction and length of the arrows show the correlation between the variables and the principal components. The codes are presented in Annex 2. Color Green depicts the quadrants of the North (N) fragment; Pink represents the S_A quadrants; Black the S_B quadrants; Red the S_C quadrants; Brown the S_D quadrants; cherry the S_E quadrants; Blue the S_F quadrants; and purple the confluence sites (CONF).

The 2nd component of the analysis of principal components (17% of the total variance) is dominated by O. andina and F. potosiana. The North (N) bofedal quadrants are mainly found in the lower left side of the biplot, which corresponds to areas with a reduced presence of C. cf. maritima and/or areas where F. potosiana predominates. These areas are enduring a desiccation process and are generally to be found in bofedal margins. Their presence is also of importance in the confluence. The last group comprises a predominance of O. andina, which is mainly found in the

North and S. D. fragments. The spatial distribution of bofedal species is not uniform throughout its areas.

The analysis demonstrates that the composition of species in the North and South Bofedals and Confluence areas is mainly determined by C. cf. maritima, and O. andina and F. potosiana to a lesser degree, as clearly evidenced by their proportion of data variation (41%). Nevertheless, there are many smaller proportion species scattered throughout the North and South bofedals, and the Confluence area. The spatial distribution of bofedal species is not uniform throughout its areas, There are areas where species are mixed and others where some of the species highlighted in the biplot arrows predominate (C. cf. maritima, F. potosiana and, to a lesser degree, O. andina).Thus, the multivariate Principal Component Analysis evidences the high degree of fragmentation of the Silala bofedals and allows visualizing the differential effects of the canalization works between the South and North bofedals, demonstrating that the South bofedal is the one that has been affected the most, owing to the abundance of C. cf. maritima, which is also reported as a species typical of dryer areas that only have semi-permanent humidity.

The above explains the compaction into different fragments determined at the global level (49). The North and S_D bofedals present the least compaction (233,1 ± 273,3; 104,4 ± 179,7) kPa, respectively. While the most compacted fragments are the S_F (216,1±191,3), S_C (915,6±374,9), S_A and S_B (625±107; 561,3±455) kPa, respectively.

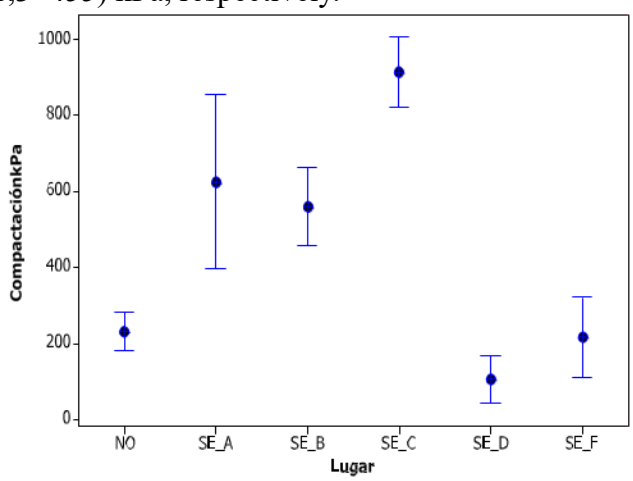


Figure 49. Compaction in vegetation quadrants measured in different fragments of the North (N) and South (S) bofedals of Silala. Only the areas where it was possible to use a compaction meter are included. The codes are presented in Annex 4.

Consistently with our results, Coronel (2010) reports that the C. cf. maritima species is one of the most abundant ones in driest areas as evidence of the effects of the Mauri river diversion. Likewise, Buttolph (1998) found in Cosapa (Potosi) that the C. cf. maritima and D. curvula species are abundant in the driest areas. In the case of the Silala, the surveys were completed long after the canalization works were installed, which is why it is likely that species as the W. pygmaea and P. tubulosa (which

recorded a low abundance rates in our examinations) were more abundant, inasmuch as they are indicative of reductions in the water table. Our examinations in the Silala bofedals have resulted in concerns regarding the total absence of Distichia muscoides, a cushion plant that is more susceptible to reductions in water availability and climate change (Loza Herrera et al. 2015) and is displaced first after water availability is reduced.

The canonical correspondence analysis (CCA), which accounts for the variations in abundance and species compositions as a function of environmental variables measured, demonstrates that the species are organized on basis of a compaction gradient. The presence of Carex cf. maritima, Puccinellia frigida, Plantago tubulosa and Gentiana gayi species is to be noted in the most compacted areas, while that of the O. andina, muticus, E. atacamensis and W. pygmaea species is most manifest in the least compacted one (Figure 50).

These results are evidence of the effects that the canalization works have had on the vegetation, inasmuch as there is a positive feedback between reduced water supply and changes in the vegetation. The greater degree of compaction entails an additional problem, as it reduces the soil porosity necessary for the free circulation of water and air, and restricts the growth of plant roots in compacted surfaces. Thus, in areas where the amount of water has depleted, plants that require less water develop in the Silala (Carex cf. maritima, Puccinellia frigida, Plantago tubulosa). The least compacted areas, on the contrary, are dominated by species that require higher amounts of water that are common of bofedals—the O. andina, Z. muticus, and E. atacamensis species in the case of Silala. These are found precisely where the presence of stone-lined canals is reduced (central part of the North bofedal), and in some areas of the S-D wetland. However, although these areas were the least compacted one in the Silala bofedals, the compaction degree is high compared to referential areas of the Cordillera Real, where compaction in Oxychloe andina cushions is 117.5 ± 122.4 kPa. In addition, loose cushions of this species, which are common in the Cordillera Real due to their high water content (Loza Herrera et al., 2015), have been found in the Silala.

Supporting these results, a second canonical correspondence analysis generated with all the abiotic variables related to the substrate has led to the observation that the species characteristic of more compacted areas, such as. P. frigida, C. maritima, W. pygmaea, and X. incisum, are also the species associated with saline outcrops. Organic matter is mainly associated with Deyeuxia sp. 1 and 2, P. deserticola, Z. atacamensis (Figure 51) where the degree of compaction is inferior.

It should further be noted that, out of the purely aquatic plant species, S. pectinata, Myriophyllum sp. L. minuta, Ranunculus and M. glabratus were observed in the area; mosses species were nevertheless absent in our evaluations, though they are usually present in bofedal watercourses (Gonzales 2014) and are very common in pooling waters (Loza Herrera 2012). From the literature read, according to Rambaud et. al. (2009), this group of organisms is among those that are affected the most by canalization works in wetlands, constituting another piece of evidence of the negative effect of canalization works.

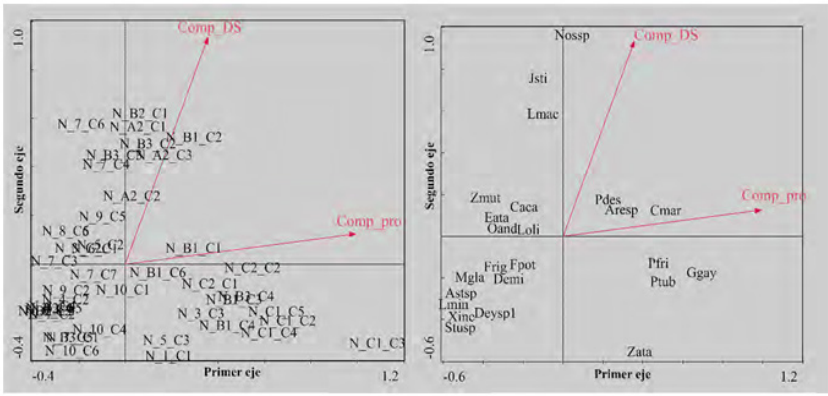


Figure 50. Analysis performed to explain the abundance and composition variations on basis of the main substrate types found in the Silala bofedals. Biplot of the canonical correspondence analysis, presenting the environmental variables ([based on the Spanish acronyms] morg: organic matter; hcam: camelid feces; asal: saline outcrops). To the left, species and environmental variables biplot (morg and hcam). To the right, quadrants present in the bofedals and environmental variables. By applying the "forward selection" option, it was found that only the saline outcrop and the organic matter are significantly associated with the vegetation cover, Annex 3 (Trace=0.43, F=2.09, P<0.05). The environmental variables are indicated with arrows (hcam y morg). The abbreviated name of each of the species is detailed in Annex 2.

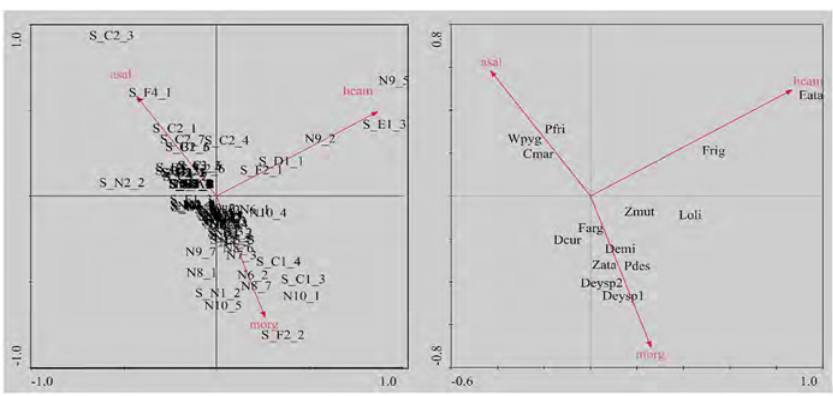


Figure 51 . Analysis performed to explain the abundance and composition variations on basis of the main substrate types found in the Silala bofedals. Biplot of the canonical correspondence analysis, presenting the environmental variables ([based on the Spanish acronyms] morg: organic matter; hcam: camelid feces; asal: saline outcrops). To the left, species and environmental variables biplot (morg and hcam). To the right, quadrants present in the bofedals and environmental variables. By applying the "forward selection" option, it was found that only the saline outcrop and the organic matter are significantly associated with the vegetation cover, Annex 3 (Trace=0.43, F=2.09, P<0.05). The environmental variables are indicated with arrows (hcam y morg). The abbreviated name of each of the species is detailed in Annex 2.

Map of the bofedal state

The map generated on basis of the vegetation cover and the categorization performed completely supports the findings of the multi-variate analysis and compaction data. The areas that have been degraded the most are found in the A fragment of the South Bofedal. Evidence of this assertion is the presence of small O. andina cushions (< 1 m2) and the traces of canals that stretched from this fragment to the South Bofedal. It has been observed that the latter was almost dry (orange squares) and that O. Andina cushions, in a regular state, were completely absent (yellow squares, Figure 52). Site C presented a degraded to dry state with a complete absence of plant cushions. Site D, the one with the best state of preservation within the South bofedal, owing to a greater coverage ratio of O. Andina cushions, but with a high risk of fragmentation due to the fact that degraded bofedal patches were found in the adjacent quadrants, presented a dry to regular state. Site F, close to the military post, presented a dry to regular state. Due to its reduced width, it is likely that this area might suffer more negative effects at the margins, as O. andina cushions were not found at its core, only some P. deserticola and Z. atacamensis, which do not compose a high amount of organic matter, as the Juncaceae (see section 6.2.2).



Figure 52. State of the Bofedal: Quadrant-based analysis of the vegetation cover. The category values are low if the bofedal is dry, or degraded, and high if the bofedal is in a good state (Degraded = 0 - 100, Dry = 101-200, Regular = 201 - 300, Good = 301-400, Very good = 401-500). The values of 0 to 500 are the result of the sum of the vegetal species product in percentages multiplied by assigned weights (the weights are: 0=bare soil; 1=dry vegetation; 2=margin vegetation; 3= bofedal vegetation; 5= *O. andina*) en each quadrant

6.6 Environmental impacts on the bofedals derived from the presence of artificial canals

6.6.1 Ecological quality of the bofedals

The current state of the Silala bofedals presents a high degree of fragmentation and desiccation. Of the 10 fragments examined, five are highly degraded; one is in a degraded state; three are in a regular state, and only one fragment is in good conditions (Figure 53)—though its quality is too low in comparison to the Sajama bofedals (see Meneses et al. 2014), which is the most comparable area where systematic appraisals have been completed.

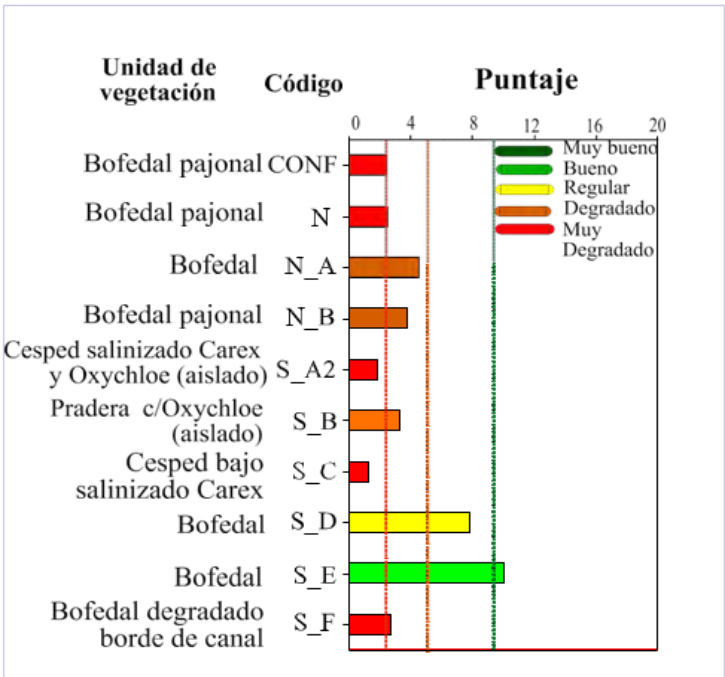


Figure 53. Mean ecological quality of the three different fragments of the Silala on basis of the transects examined. The scores were averaged to obtain a single value for each fragment. CONF: confluence, N: north, S: south. The fragments were coded in alphabetical order according to their order of appearance from the starting point to the endpoint of each bofedal.

Supporting these data, we found that in the South bofedal, the most frequent units are the Carex.cf maritima (6.5%) and Deyeuxia curvula (5%) species. However, in this bofedal, the cushions have less than 2% of frequency ratio (Figure 54). The disruption only allowed the Carex cf. maritima and D. curvula to persist in the area, despite the high number of dry canal systems and saline outcrops.

In the North Bofedal, the trend is similar, and the coverage ratio of the Carex. cf maritima species— in the system of dry canals—is very high (15%), just like the Deyeuxia curvula—sandy soil— (10%) and Festuca potosiana (8%). All of these are not typically found in preserved bofedales. In addition, the cushions frequency is so low that it is not among the first 20 units of higher

frequency, which is why it is not seen in Figure 54. The less degraded areas are found in the central part of the bofedal. The high frequency of Carex cf. maritima (cmar) is an indication of the high frequency of dry and salinized areas (Coronel 2010, Buttolph 1998, Meneses et al., 2014).

From the appraisal made in the Silala bofedals, the total absence of Distichia muscoides, a cushion plant that is more susceptible to water depletion, climate change (Loza Herrera et al., 2015) and salinization (Ruthsatz 2012) and that is the first to be displaced following a depletion of water availability, has arisen concern. Although low in abundance, DIREMAR (2017), Lliully (2018) and Ortuño T. (2018) back up the presence of this cushion in the Villamar (Silala region), Canchilla, Villamar (Laguna Colorada influence area) and Quetena Grande bofedals, respectively.

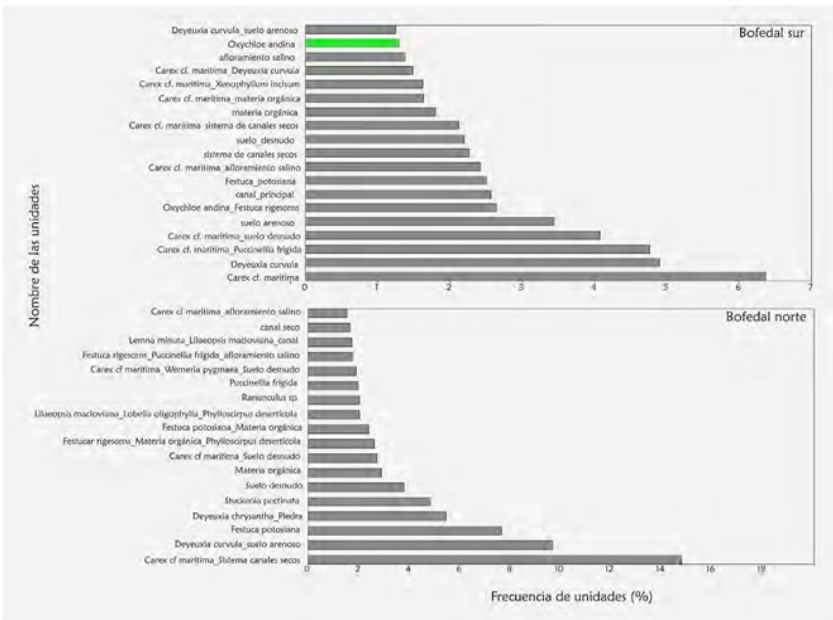


Figure 54. Global frequency of the units found in the South and North Silala bofedals. This graph presents only the 20 first most frequent units for each bofedal. The units typical of preserved bofedals are presented in green.

The desiccation effects that take place in the Silala bofedals have also affected their forage quality, which was considered of a very high quality (Alzerreca et al 2001, Meneses et al 2012, Beck et al 2010, Villarroel 1997, Mamani s/a). Fragmentation and desiccation of the bofedals reduce the ecosystem's capacity to retain water (Squeo et al., 2006, Meneses et al., 2014), which constitutes one of the most severe impacts on ecosystems such as bofedales, with highly significant effects for human beings and activities, particularly in arid regions.

6.6.1 Macroinvertebrates

The taxonomic richness (H = 12.8, p <0.05) and diversity (H = 13.8, p <0.05) both differ among the three canal types. It is clear that these two indicators of biodiversity present higher ratios "naturalized" canals, which are more similar to a natural bofedal (Fig. 67). This is not the case for the abundance of individuals, which does not differ between the three types of canal (H = 3.1, p = 0.2; Figure 55). This final finding suggests that stone-lined canal (CP) environments are not so heterogeneous, but have a similar productivity.

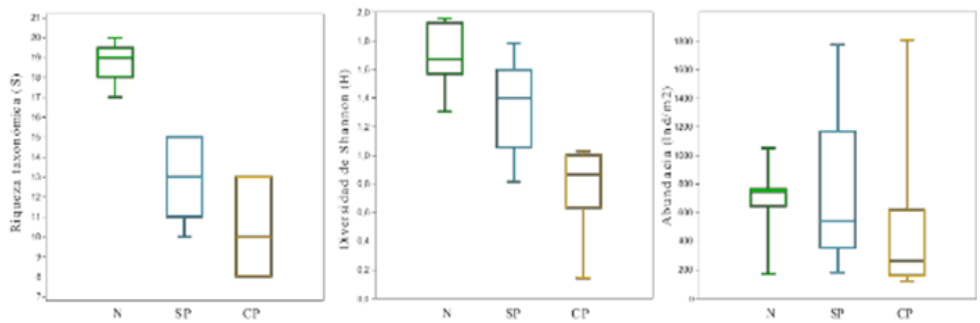


Figure 55. Graphs that present the richness, diversity, and abundance (mean and ranges), compared among the sites: naturalized canals (N), canalization without stone-lining (SP) stone-lined canalization (CP)

Using an NMDS, with the Bray-curtis linkage, it was possible to demonstrate that the composition and relative abundances of taxa assemble similar sets of species among the samples taken from stone- lined canalization (CP), canalization without stone-lining (SP), and naturalized sections (N). This assembling was corroborated with an ANOVA of similarity (ANOSIM-Bray-Curtis, 999 permutations) (Table 14). The macroinvertebrate group that characterizes the naturalized canalization
(N) section is composed of: Austrelmis, Hyallela and Simulium. It is very similar to the community of macroinvertebrates of the bofedal pools (EBNL), which are characterized by: Hyallela, Dero and Glossiphonidae. The canals without stone-lining (SP) are characterized by: Hyallela, Austrelmis and Metrichia species. The stone-lined canals (CP) are characterized by: Hyallela, Andesiops and Austrelmis species; however, the canalized section further south are characterized by: Paraheptagyia, Claudioperla and Hydrobiosidae

Table 14. Significance of the ANOSIM among proposed groups.

ANOSIM R2 = 0,5	SP	CP
N	0,033	0,0033
SP		0,0011

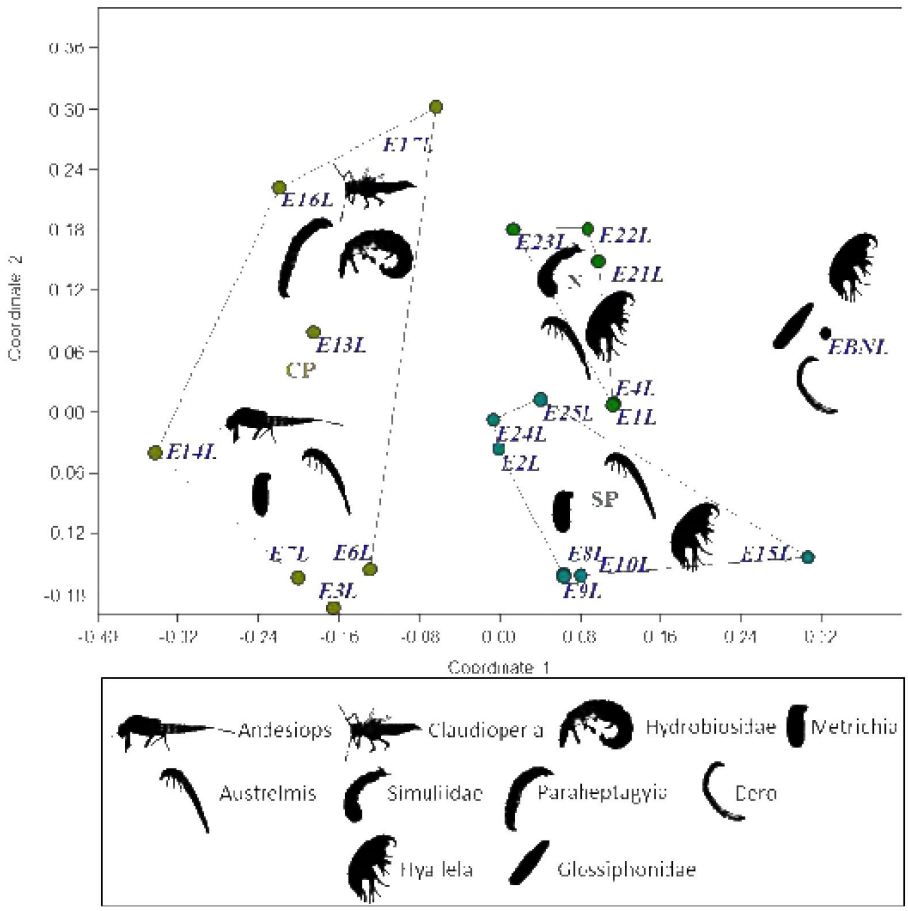


Figure 56. NMDS completed using the Bray-Curtis linkage; sections with stone-lined Canals (CP), sections where stone-lining is absent (SP) and naturalized sections (N).

Environmental parameters

Within the environmental parameters, the physical-chemical parameters (Annex 2) and the morpho-structural parameters (Annex 3) were both separated, followed by a Principal Component Analysis (PCA) with seven environmental parameters and 20 sampling stations. During the analysis, it was observed that the electrical conductivity (EC) is closely related to the altitude; i.e. the areas with low altitudes present the lowest EC values. This may be due to the fact that the EC is related to the presence of ions (sulphate and nitrates, for example) in water. The vegetation absorbs these nutrients from groundwater sources, which decreases at the lowest points. The low values of Fluvial Habitat Index are due to the medium's homogenization with the percentage of blocks and stones. Finally, as expected, the highest flow is found in the lowest sections.

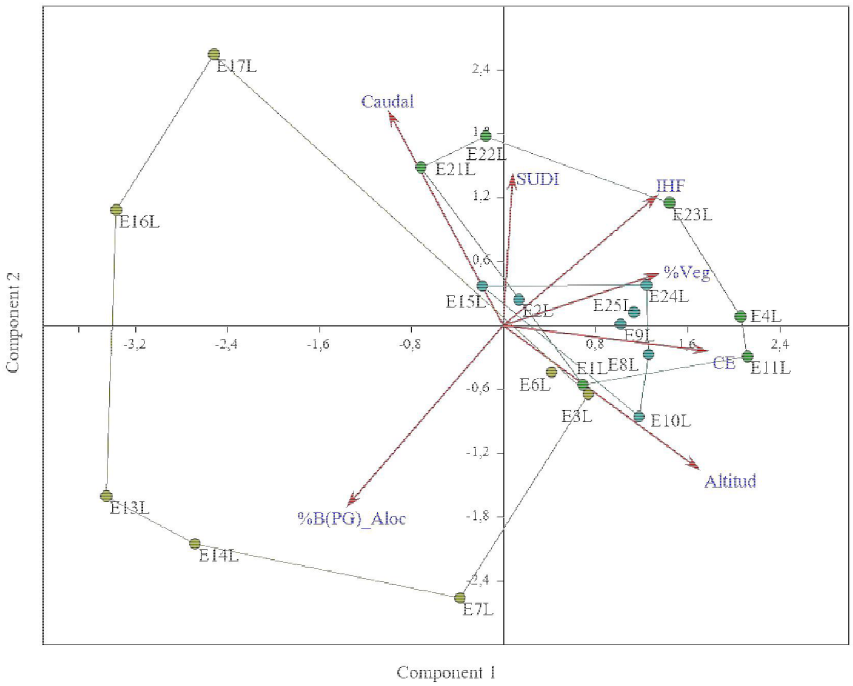


Figure 57. Analysis of the principal components for the environmental parameters of the Silala bofedals. Note that the naturalized and stoned-lined canalization sites (in green) present the highest fluvial habitat values, percentage of vegetation (Veg. %), and electrical conductivity (EC), and a reduced percentage of large stone blocks. The stoned-lined canalized sites, on the other hand, are characterized for presenting a high percentage of blocks and large stones and low values of habitat stability (FHI) [sic, there seems to be a contradiction].

Relation of macroinvertebrates with environmental parameters

In order to examine the relation that macroinvertebrates have with environmental parameters, an analysis of canonic correspondence (CCA) was completed between the most representative PCA variables and the macroinvertebrate fauna. The Cailloma, Claudioperla, and Paraheptagyia genuses present a positive relation with the flowrate (Flow (Velocity)) and a negative relation with the altitude and electrical conductivity. The Ectemnostega, Empididae, Hydracarina and Neotrichia taxa present a positive relation with the fluvial habitat stability (FHI) and a negative relation with the amount of blocks and large stones. These taxa are found in naturalized sites. (Figure 58).

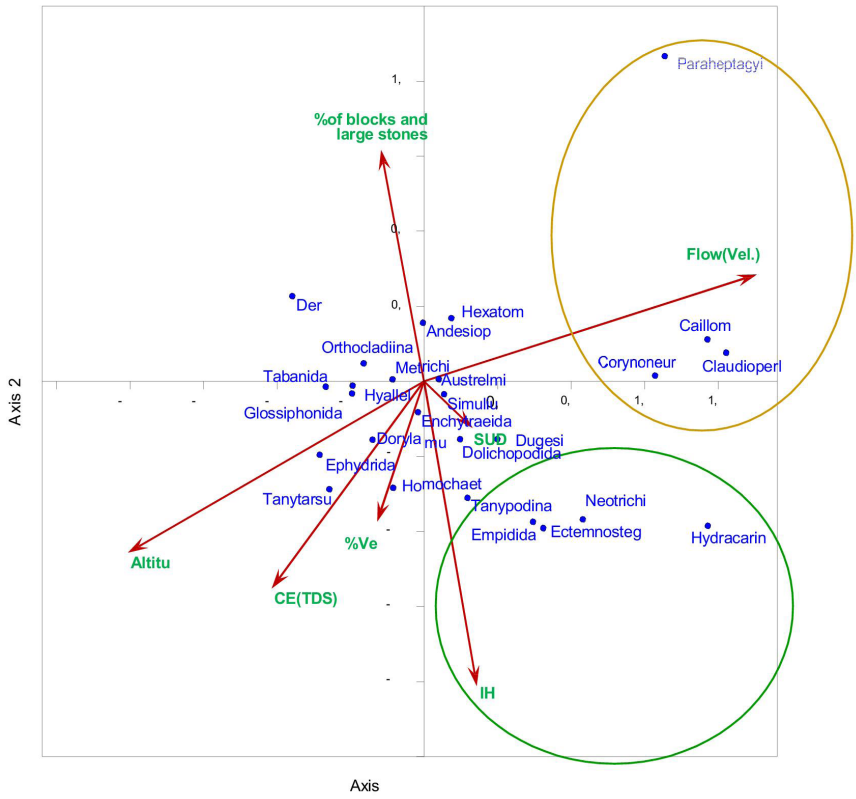


Figure 58. Principal Component Analysis completed to relate the taxa with the environmental variables of the Silala bofedals. Note the positive relation of Cailloma, Claudioperla and Paraheptagyia with the flow and velocity (beige color circle) and a negative relation with altitude. The Ectemnnostegam Neotrichia, Hydracarina and Empididae have a positive relation with the high fluvial habitat values (FHI) and a negative one with the percentage of blocks and stones.

Birds

A comparison between the bird species found in three bofedals comparable to the Silala (Silala, Eduardo Avaroa Natural Andean Fauna Reserve (Hennessey et al 2003) and the northern region of Chile (Innova Chile, 2010), it has been found that 19 bird species inhabit the Silala, 29 the Eduardo Avaroa reserve and 18 the northern region of Chile (Table 15). Fifteen common species were found in the three bofedals surveyed.

Ten of the bird species recorded in the Eduardo Avaroa Reserve were not found in the Silala bofedals (Table 15). It should be noted that the Muscisaxicola juninensis and Gallinago andina species, which are all characteristic of bofedals, are completely absent in the Silala bofedals. This could be to the degraded state and/or reduced extent of the bofedals. The other four species that were not observed in the Silala are migratory birds, so they might arrive to the site in a different season (the Vanellus resplendens and Pygochelidon cyanoleuca cyanoleuca (altitudinal migratory birds), Muscisaxicola frontalis (austral migratory species that might be observed in the site between June and September), and Hirundo rustica (boreal migratory species, rare to abundant from September to March (Herzog et al. 2017)). It should be noted that the difference between bird species groups could be due to different variables, such as: (1) disturbance or degradation state of the habitat, which could affect the vegetation and resource availability for the birds, (2) differences in sampling efforts (the Eduardo Avaroa Reserve bofedals have been visited for many years, during different times of the year and by different researchers), (3) the surface area of the bofedals and species- area relation suggest that larger bofedal areas, as those of the Eduardo Avaroa Reserve, have a greater diversity of bird species, and (4) the closeness among bofedal areas (the closest they are, the easier the movement and arrival of bird species).

Table 15. Bird species that use bofedals as habitats (A10), according to Stotz et al. (1996), in the Silala; the table includes the birds of the Eduardo Avaroa Reserve and Northern region of Chile only by way of comparison.

Family	Scientific name	Silala	EA Reserve	North of Chile	Migratory birds
Anatidae	*Oressochen melanopterus*	x	x	x	
	Anas flavirostris	x	x	x	
Columbidae	*Metriopelia aymara*	x	x		
Charadriidae	*Vanellus resplendens*		x		M. altitudinal
	Phegornis mitchellii	x	x	x	
Scolopacidae	*Gallinago jamesoni*		x		
	Gallinago andina		x		M. altitudinal
Thinocoridae	*Attagis gayi*	x	x	x	
	Thinocorus orbignyianus	x	x	x	
	Thinocorus rumicivorus		x		
Accipitridae	*Geranoaetus polyosoma*	x	x		
Strigidae	*Athene cunicularia*		x		
Picidae	*Colaptes rupicola*		x		
Falconidae	*Phalcoboenus megalopterus*	x	x		
Furnariidae	*Geositta punensis*	x	x	x	
	Cinclodes albiventris	x	x	x	
	Cinclodes atacamensis	x	x	x	
	Asthenes modesta	x	x	x	
Tyrannidae	*Lessonia oreas*	x	x	x	M. austral
	Muscisaxicola juninensis		x		
	Muscisaxicola cinereus	x	x		M. austral
	Muscisaxicola flavinucha	x	x	x	M. austral
	Muscisaxicola rufivertex	x	x	x	M. austral
	Muscisaxicola frontalis		x	x	M. austral
	Agriornis montanus	x	x	x	
Hirundinidae	*Pygochelidon cyanoleuca*		x	x	M. austral
	Hirundo rustica		x	x	M. boreal
Thraupidae	*Phrygilus atriceps*	x	x	x	
	Phrygilus unicolor	x	x	x	
	Nº of species	**19**	**29**	**18**	

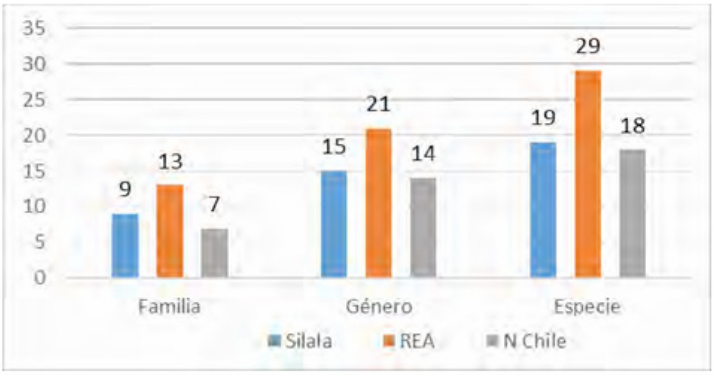


Figure 59. Number of families, genuses, and species observed in the Silala bofedals, the EA Reserve, and the Northern region of Chile. Source: Prepared by the authors.

Mammals

The Silala region is remarkable for its abundance and diversity of rodents (Table 16), though the North and South bofedal mammal species need to be contrasted and compared. The differences between both these bofedals allows suggesting that the South Bofedal (where only two genuses and a maximum of four species can be observed) could be a reflection of what might happen to the rodent diversity of the area if the North Bofedal dried out. It should be recalled that the North Bofedal comprises the greatest vegetation diversity, which is reflected in a more significant productivity, and rodent abundance and diversity.

Table 16. Mammals of the Silala bofedals.

Order/Family	Genus	Species	Log type	Location		
Carnivorous				BN	CC	BS
Canidae Family	*Pseudalopex*	*Pseudalopex culpaeus*	Feces, bone remains	X	X	
Artiodactyla						
Camelidae	*Vicugna*	*Vicugna vicugna*	Direct observation, bone remains		X	X
Rodentia						
Chinchillidae	*Lagidium*	*Lagidium viscacia*	Direct observation, feces	X		
Cricetidae	*Phyllotis*	*Phyllotis xanthophygus*	Capture	29	9	
		Phyllotis cf. *xanthophygus*	Capture	6		
Cricetidae	*Tapecomys*	*Tapecomys wolffsohni*	Capture	16	8	
Cricetidae	*Calomys*	*Calomys musculinus*	Capture	3	1	1
Cricetidae	*Abrothrix*	*Abrothrix andinus*	Capture	2		
		sp 1	Capture	2		1
		sp 2	Capture	5	1	1
		sp 3	Capture	2	4	1
		sp 4	Capture	2		

It is likely that the Silala bofedal rodents migrated progressively from Chile, long before the Chilean bofedals dried out, or that the mammal diversity of the Silala constitutes a lateral relict from the retrogression of the Ballivian lake. These hypotheses could be determined through DNA samples, in order to find evidence of either bottlenecks (first hypothesis), or genetic erosion (second hypothesis). Regardless of the actual cause, the Silala bofedals constitute a type of productive desert oases, that are home to and sustain a great amount of life forms, some of which have been found to be new to the diversity of the State and must thus be preserved and protected.

6.7 Preparation of restoration measures that should be implemented to ensure the survival of the bofedal ecosystems

In order to address the preparation of restoration measures, a definition of preparation and restoration is first herewith presented. Below, following said definition, a series of actions are proposed on basis of the problems observed in the Silala area (Table 17) and some necessary considerations to implement a restoration plan successfully are suggested.

Preparation: Determination of objectives, and what should be done, how and when to do it, and following which order (Bernal, 2012).

Restoration: Process to contribute to the restoration of a certain degraded, harmed or destroyed area, ecosystem, or landscape for the purpose of helping the system retake its ecological

pathway, maintain its resilience, preserve the biological diversity, and reestablish their functionality (SEMARNAT, 2013).

Bearing the above definitions in mind, and based on our field observations, the authors hereby propose the following two restoration components: A) abiotic restoration of the area and b) biotic restoration (Table 17).

Table 17. Preparation of restoration measures based on the problems observed in the Silala and including recommendable terms for their implementation.

Objectives	Problem	Specific objectives	Actions	Term
To implement actions that promote the abiotic restoration of the bofedals	The presence of water abstraction canals. The North Bofedal comprises 25 canalized springs. The South Bofedal comprises 18 canalized springs.	To eliminate and/or reduce the presence of artificial canals and reestablish the natural water flows.	To properly remove the current ignimbrite lining of the canals and fill them with organic matter to allow water to naturally irrigate the area.	Short-term
	Alteration of the hydric regime of the springs	To return the springs' natural flow to its natural conditions	To extend the current irrigation area of the canals, allowing the springs to naturally irrigate the bofedals.	Mid-term

	The high evaporation rate and desertification processes that will only intensify the deterioration of the bofedals.	To protect the bofedal eroded areas	Protecting coconut or jute sheets can be used on bare surfaces to control water losses to evaporation (Aguirre et al. 2018). The North bofedal comprises areas with a high amount of organic matter and remains of bofedal vegetation which could be selected to cover them with jute sheets (Figure 60).	Mid-term
		To excavate infiltration ditches	The water can be conveyed to cover the entire potential surface area of the bofedal.	Mid-term
		To slow down the water flow	Permeable embankments (made of stone or wood with small holes) could be installed to collect sediments, regenerate the soil at the canal base, and allow the latter to be re-colonized by vegetation (Figure 61). It is, however, recommended to perform pilot tests, inasmuch as excess use of this embankments could destroy these habitats.	Mid-term
	Bofedal compaction as a result of stamping	Delimitation of pathways to prevent dispersed transit.	To create a signaled path for human transit, preventing the bofedals and their surroundings from being disturbed	Short-term
To implement biotic restoration actions and improve the vegetation quality of the bofedals	The presence of species characteristic of bofedal margins at the heart of the bofedals (the North Bofedal, particularly, has been invaded by Gramineae characteristic of bofedal margins, e.g. *F. potosiana*, which compete for water and resources against species characteristic of the bofedal nuclei.	To reduce the interference of species uncommon to bofedals.	To eliminate species that compete with the plants typical of bofedals by, for instance, cutting the invasive grasses. This action must be implemented with the supervision of an expert in Gramineae and vegetation uncommon to bofedals.	Mid-term
	Bofedal fragmentation.	To promote the reproduction of dominant species of the bofedals and bush species of the margins (seed planting *in situ*). The presence of seeds in the soil favors natural regeneration	Seeds of species typical (*Oxychloe andina*, *Zameioscirpus* spp. *Phylloscirpus deserticola*) of bofedals should planted in areas where organic matter is present Plant nurseries of typical bush species should formed on the margins (*Parastrephia lucida*, *P. quadrangularis*, *Junellia*	Mid-long term

			species succession.	
	Bofedal fragmentation.	To promote vegetation reproduction. An increase vegetation cover prevents water losses and soil erosion, and promotes water retention.	To increase the density of typical vegetation species (Oxychloe andina, Zameioscirpus muticos, Z. atacamensis, Phylloscirpus deserticola). Patches of cushion plants could be removed from altered areas (presenting evidence of desiccation and destruction by stomping) of the Silala bofedal and relocated in areas where they are more likely to survive.	Mid-lo term
		Proper criteria must be applied to select species to be used for restoration	To compete surveys on the vegetal reproduction of the species that predominate the bofedals, in plant nurseries and in situ.	Mid-long term
		To study the viability of seeds typical of margins and bofedals.	To conduct germination viability and seed production rate tests, in parcels, *in situ*, and in laboratories to make the work and experiments effective.	Long-t
		Proper criteria must be applied to select species to be used for restoration	To define criteria for the selection of species, which should have the following characteristics: high survival ration, extended root systems, fast biomasses production, and a high flower and fruit generation rates at early ages. To avoid using invasive species (*Trifolium, Phalaris*, etc.).	Mid-te
	The presence of trout (*Oncorhynchus* sp), an exotic species that might alter the native aquatic fauna of the area.	To gradually reduce this fish species from the natural flows and pools of the Silala bofedal.	Intensive fishing of sub-adults and alevins with sieves.	Short-t

Some remarks:

The restoration process described herewith encompasses several disciplines, as a result the preparation and implementation of the Project must be carried out with the help of a multidisciplinary team (Montes et al. 2007). More specific remarks are detailed below:

- The restoration costs (budget) necessary for the short, mid and long-term implementation and monitoring must be duly considered, looking forward to reaching the goals set.
- The feasibility of reaching each of the objectives and goals set for the Project must also be borne in mind.
- It is necessary to count on the views of all those who are directly concerned (local communities, the regional and national government).
- The expectations and willingness of those concerned to monitor and reach the goals set must be duly considered.



Figure 60. Protection of eroded areas with coconut fiber sheets (Photograph: Aguirre et al. 2018).



Figure 61. Permeable embankments used to slow down flowing water (Photograph: Aguirre et al. 2018)

6.8 Preparation of an environmental monitoring programme for the Silala

Monitoring is essential to assess the efficacy and efficiency of restoration efforts, as well as to systematically follow through the state of the bofedals, the region's biodiversity response to climate change (bearing in mind that this is one of the regions that presents the most water deficit in Bolivia), and future surveys that might help find ways to mitigate the harm and help the environment adapt to the restoration efforts. It must, nevertheless, be noted that, in order to have a proper monitoring plan, it is necessary

to know the budget, time and work force available. The authors hereby proposed, based on their research, some potential variables for a monitoring programme.

-Monitoring the phreatic level related with the bofedal productivity: The phreatic level is an indicator of the availability of water for vegetation throughout the year. This indicator can help attain knowledge on: the amount of water available yearly for certain predominant and/or key bofedal species and the vegetation's response to these changes (in terms of biomass and reproduction).

The authors propose that thirty 1-m2 quadrants were Oxychloe andina is present be selected. These quadrants should be located randomly in the North and South bofedals. Each of the quadrants must be related to a piezometer to measure to phreatic level. The response variables shall encompass biomass, reproduction and phenology. This will help assess what the minimal water conditions for a certain species to develop and reproduce.

-Desertification advance monitoring. 25 x 25 m parcels must be established, in four different environment types: hillsides, bofedals, plains, saline areas, each with their respective replicas (at least three for each environment type). These parcels must be used to assess the vegetation cover (its richness and abundance) and the humidity and temperature variables at different soil depths. The measurements must be performed at least twice a year (during wet and dry seasons). This monitoring programme will allow appraising the variations of desertification in different micro-habitats of the Silala. It will further help attain knowledge of the most vulnerable areas and serve as a monitoring point to follow through the restoration measures proposed.

Simultaneously with the parcel-based measurements, it is necessary to set up a weather station in the region in order to count on systematic measurements of the environmental variables throughout the year (temperature, wind, precipitation). These variables are of importance to analyze their influence in the region's vegetation and fauna.

-Quantification of degraded peat: Bofedals that accumulate peat present a low organic matter decomposition rate. The degree of disturbance can be quantified by calculating the percentage of exposed peat (see results, below), which is actually completely degraded (soft substrate, lacking a particular structure; this peat transudes when squeezed). Throughout the Silala region, there is a significant cover of dry organic matter, which is more susceptible to eolian erosion. Some of these sites where peat is present (areas where there once were bofedals, and that now comprise either no bofedal at all or degraded bofedals) could be selected to carry out this quantification, by measuring the bofedals actual extent and delimitating it. Yearly measurements must be completed to verify if changes have occurred in their extent.

- Key bird species monitoring in the Silala bofedals. The abundance of bird species should be estimated employing the transect method in three areas of the Silala and quantifying the number of individuals for the following species: Oressochen melanopterus, Cinclodes albiventris, Lessonia oreas, (Muscisaxicola flavinucha), (Muscisaxicola juninensis), Phrygilus atriceps, Phrygilus plebejus, and Phrygilus unicolor. This estimation should be performed every two years during the

same months and applying the same sampling efforts.

The sampling route should cover the ravine, starting at the South bofedal, in direction to the area where the waters merge (confluence area) and ending in the North bofedal (Figure 62); the quantification should be repeated for three consecutive days. This route should cover 3,7 km and must be completed at a constant pace (1 km per hour, approximately) between 8:00 and 12:00, keeping a record of each observed bird as follows: time, species amount of individuals and habitat. The objective of monitoring these key species is to count on an additional measure of the state of the bofedals. If the amount of birds characteristic of bofedals (Oressochen melanopterus, Cinclodes albiventris, Lessonia oreas, Muscisaxicola flavinucha and Muscisaxicola juninensis) increases, it could be inferred that the bofedals are improving. If the amount of granivorous species increases (Phrygilus atriceps, Phrygilus plebejus and Phrygilus unicolor) within the bofedals, it would mean that the Gramineae species have also increased and that the bofedals continue degrading. The data contained in this report could serve as a baseline.



Figure 62. Monitoring route to quantify the bird species of the Silala bofedals

Monitoring of the bofedal extent (in situ) and contrasting the data obtained with satellite images, particularly during dry and humid seasons
In case restoration measurements are implemented, the following are hereby proposed:

-The development of seedlings (initial number, mortality, etc.) should be monitored in the hillsides and the reproduction of vegetation (clods) in the bofedals should also be supervised.

-Intensive trout farming requires a monitoring programme and properly prepared management plans should the idea to implement it stand.

6.9 Mitigation and control of the impacts on the Silala bofedals

The following environmental problems have been identified in the area, and some actions and plans are proposed to address them:

Problem	Plan	Action
Bofedal areas (particularly the South bofedal) where solid waste is accumulated	Waste management	Creation of reuse, management and recycling deposits. The bofedals must be cleaned and the inorganic waste should be collected.
The natural aquatic vegetation cover has been eliminated. The current cleansing of aquatic plants within the canals destroys the habitats necessary for the aquatic fauna and prevents them from retaining sediments.	Cleansing of aquatic plants that grow in the canals must be stopped.	Actions in the bofedals must be implemented so as to avoid eliminating the plants from the canals. Implementation of signaling that explains what should be done and not in each area.
The main water source of the South Bofedal has been restricted throughout its perimeter to ensure water availability [for the canals]. Such action is not advisable to preserve the water quality in its source, inasmuch as this artificial restriction [made of concrete] could alter the physical-chemical characteristics of the water and contaminate it.	The water quality must be evaluated	The works must be implemented after the water source is abstracted and the impact these works have on the water quality must be evaluated.
The enhancement of the flowrate disturbs amphibian species reproduction (*Rhinella spinulosa*).	The natural flows must be restored to reduce the flowrate pace.	The materials and stone lining must be removed from the water courses in order to restore them to their natural state and allow the growth of aquatic plants.

7. CONCLUSIONS

■ The Silala bofedals have been fragmented and degraded, and are highly vulnerable; actions are required to restore them, their biodiversity, their general physiognomic appearance, and the functions of their ecosystems.

■ The evidence suggests that the bofedals once covered a larger extent before the canalization works were introduced. It is estimated that the bofedals once covered a potential Surface area of 11,48 hectares and that only 0,76 hectares of bofedal extent remains at present, which, nevertheless, is not in proper preservation conditions. It can thus be claimed that more than 10 hectares of bofedals have been lost due to the canaliza-

tion works.

■ The apparent, though minimal, regeneration of the bofedal[s] in the past 15 years reinforces the recommendation that restoration measures be implemented to ensure the bofedals' preservation.

■ The Silala bofedals constitute a desert-area productive "oasis" species, are home to and ensure the sustainability of a significant amount of life forms—some of which have been proved to be new to the State's diversity records. If canalization continues, the bofedal vegetation and fauna will remain threatened.

Biotic and abiotic factors

■ The species found to inhabit the Silala include 86 flora species and 81 fauna species, making a total of 167.
■ Thirteen species of plants common of bofedals and 18 bofedal margin species have been registered. Four of these are categorized as Threatened species, i.e. Azorella compacta, P. deserticola, Z. atacamensis and O. andina), while other four are categorized as Vulnerable (P. quadrangularis, N. auricoma, F. potosiana and P. tarapacana).
■ Seventeen plant species have been recorded for the first time within the Potosi department (Table 7); two of these constitute new recorded species for the Bolivian State (Menonvillea virens and Mostacillastrum dianthoides).
■ An abundant population of the Rhinella spinulosa amphibian has been registered reproducing in the Silala water bodies.
■ Three lizard species of the Liolaemus genus have been found, together with a fourth species (Liolaemus hajeki), making the Silala one of the areas of greater diversity of species of this genus in the south Altiplano region of Bolivia.
■ The Silala bofedals, and their vicinities, provide resources for 35 bird species. Two of these are categorized a s Threatened species, i.e. Rhea pennata (Threatened) and (Phegornis mitchellii) (Near-threatened). Six are considered endemic species of the Central Andes zoogeographic region. Seven of these are boreal, austral and altitudinal migratory species. The presence of Oressochen melanopterus, Cinclodes albiventris, Lessonia oreas and Muscisaxicola flavinucha and the absence of Muscisaxicola juninensis and Gallinago andina both call for attention, as they would be an indication of the degraded state and/or reduced extent of the Silala bofedals.
■ The rodent species found in the Silala are those characteristic of the Andean region (Potosi and Oruro, under similar conditions); however, unidentified species of the Abrothrix genus might constitute new observed species for the area, or State.
■ Species of Heleobia (Caenosgastropoda; Cochliopidae) and mollusks commonly linked with bofedals have not been observed.
■ The waters of the Silala bofedals are of a basic type; with a pH between 8 to 9 in the South bofedal and between 7 to 8 in the North bofedal. The alkalinity ratio is high, making the bofedal ecosystem susceptible to saline outcrops.
■ The general conductivity is low, i.e. 160-300 µs/cm; these waters have a reduced content of nutrients, which tend to diminish downstream of the canal.

Current state

■ Three different bofedal areas have been distinguished, the North, South and Confluence areas.
The vegetation of these bofedals is generally fragmented.

Environmental harm derived from the effect of the hydraulic infrastructure

■ The scientific evidence demonstrates that the bofedals have fragmented as a result of the hydraulic infrastructure. This can be further ascertained based on the following evidence: 1) the absence of species characteristic of these environments, e.g. Distichia muscoides (Juncaceae), Werneria spathulata, Cuatrecasasiella argentina (Asteraceae); the large presence of Carex cf. maritima and gramineae as Festuca potosiana (an endemic specie, though common of bofedal margins), which are not characteristic of bofedal environments and are indications of the degradation of the Silala derived from the hydraulic infrastructure. This in turn caused a reduction of the potential extent for species common of bofedals and an increased soil compaction, reducing its water retention capacity.
■ The hydraulic infrastructure drastically homogenized the aquatic environment, giving place to fewer macroinvertebrate groups characteristic of bofedals. Of the groups associated with bofedal waterbodies, it was possible to find only: Austrelmis, Hyallela and Simulium. In the stone canals, on the other hand, the following species were mainly found: Paraheptagyia, Claudioperla and Hydrobiosidae, which are groups associated with the enhanced water flow provoked by the hydraulic infrastructure.
■ The canalization works introduced in the upwelling waters increased the flowrate downstream, affecting the availability of water for the cushions of plants common of bofedals
(e.g. at the South _ C fragment), reducing aquatic diversity (E11L), and potentially disturbing the reproduction and larval development (metamorphosis) of the Rhinella spinulosa amphibian—threatening its survival at the C fragment.
■ The only ictic species found in the area is the Oncorhynchus mykiss trout, which originates from an intensive and extensive trout farming programme promoted by the Potosi Departmental Government. Wild trout populations can currently be found in the artificial canals of the area.
■ The introduction of this trout farm seems to have had an impact on the Silala ecosystem, which is hard to measure in concrete terms due to the absence of past data on aquatic biodiversity (invertebrates, and the possible presence of Orestias in the area) preceding the instalment of the trout farm. It is highly recommendable that the trout population and invertebrate communities be monitored in order to obtain more evidence on the possible impacts.

8. BIBLIOGRAPHIC REFERENCES

Aguirre M. Benito I. & Galera A. Tour of the Zalama peatland (Bizkaia) in the last thirty years. 2018. In: Chico, Guaduneth & Clutterbuck, Ben & Midgley, Nicholas & Labadz, Jillian. Identification, assessment and restoration of peatlands: recent contributions, pp. 23-34.

Albarracín-Jordan J & Capriles J. 2011. The Paleo-American occupation of Cueva Bautista: Late- Pleistocene Human evidence from the Bolivian Highlands. Current Research in the Pleistocene 28: 95-98.

Alzerreca, H. and Luna, D. 2001. Cattleman's Manual for the Management of Bofedales. La Paz, Bolivia, p.40.

Alzerreca H., G Prieto, J. Laura, D. Luna & S. Laguna. 2001. Characteristics and distribution of bofedales in the Bolivian area. Final Report. Integral Association of Cattlemen of the High Andes (AIGACAA), p. 176.

Arratia G. 1982. Fish of the Chilean Altiplano. pp. 93-133 in: Veloso A & Bustos E (editions) Vegetation and ectothermic vertebrates of the Arica–Chungara Lake transect. Synthesis Volume MAB Project 6 UNEP – UNESCO.

Arratia G. 1983. Trichomycterus chungarensis n.sp. and Trichomycterus laucaensis n.sp. (Pisces:Siluriformes: Trichomycteridae) from the High Andes range. Studies on Neotropical Fauna and Environment 18: 65-87.

Arratia G. 1990. The South American Trichomycteridae (Teleostei: Siluriformes) a problematic group. Pp. 395-493 en: Peters G & Hutterer (eds.) Vertebrates in the tropics. Museum Alexander Koening. Bonn.

Argollo J. et al., 1987, Plioquaternary Geology of Bolivia. Unpublished.

Argollo J. and Iriondo G., 1987, Plioquaternary Geology of Bolivia. Unpublished. Bazoberry, Q. A. 2003, The myth of Silala. Plural Editorial. La Paz, Bolivia.

Beck, S., A. Domic, C. Garcia, R. I. Meneses, K. Yager & S. Halloy. 2010. The Sajama National Park and its plants. National Herbarium of Bolivia, La Paz, p. 250

Bernal M. 2012. Planning: basic concepts, principles, components, characteristics and development of the process. Santa Maria University.

Biggs, J., S. von Fumetti y M. Kelly-Quinn. 2017. The importance of small water bodies for biodiversity and ecosystem services: implications for policy makers. Hydrobiology 793:3–39.

Bosch J, Rincon PA, Boyero L, and Martínez-Solano I. 2006. Effects of Introduced Salmonids on a Mountain Population of Iberian Frogs. Conservation Biology 20(1): 180–189.

Buria LM, Albariño RJ, Modenutti BE & Balseiro EG. 2009. Temporal variations in the diet of the exotic rainbow trout (Oncorhynchus mykiss) in an Andean-Patagonian canopied stream. Chilean Magazine of Natural History 82: 3-15.

Bustamante E & Treviño H. 1980. Description of the fisheries in Lake Titicaca 1975-79. Institute of the Sea of Peru - Puno.

Buttolph, L. 1998. Rangland Dynamics and Pastoral Development in the High Andes: The Camelids Herders of Cosapa, Bolivia. Thesis for Doctorate in Philosophy, Utah State University. Logan, Utah, p. 286.

Campos H, Dazarola G, Dyer B, Fuentes L, Gavilan J, Hauquin L, Martinez G, Melendez R, Pequeño G, Ponce F, Ruiz W, Sielfeld W, Soto D, Vega R & Vila I (1998). Conservation categories of native fish of inland waters of Chile and Bolivia. National Museum of Natural History of Chile 47: 101- 122.

Coronel J. 2010. Bofedales of the Mauri River basin: Vegetation and physical-chemical characteristics. Sustainable water. Cochabamba, Bolivia, p. 32

Costa WJM. 2003. Family Cyrpinodontidae (Pupfishes). Pp. 549-554 in: Reis RE, Kullander SO & Ferraris CJ (eds.). Check List of the freshwater fishes of Central and South America. Porto Alegre – Brazil, EEDIPUCRS.

Dangles, O., Rabatel, A., Kraemer, M., Zeballos, G., Soruco, A., Jacobsen, D., & Anthelme, F. (2017). Ecosystem sentinels for climate change? Evidence of wetland cover changes over the last 30 years in the tropical Andes. PloS one, 12(5), e0175814.

DIREMAR, 2017. Multi-temporal analysis by means of satellite images of the bofedales of the Silala springs, Potosi - Bolivia. Technical Report.

DIREMAR, 2017. Final Report: Characterization of the soils of the Silala bofedales and surrounding areas. Strategic Office for the Maritime Claim, Silala and International Water Resources, p. 121.

Dorador C, Pardo R & Vila I (2003). Temporal variations of physical, chemical and biological parameters of a lake of height: the case of Chungara Lake. Chilean Journal of Natural History 76: 15-22.

ERBOL 2016. Potosi will redirect the trout farming project. ERBOL, 6 April 2016.

Eigenmann CH. 1918. The Pygidiidae, a family of South American catfishes. Mem. Carnegie Museum /: 259-398.

Eguino, Z. F. 1964. Synopsis of the History of Bolivia, 2nd Edition, La Paz - Bolivia.

Feinsinger, P. 2004. The design of field studies for the conservation of biodiversity. FAN. Santa Cruz – Bolivia.

Fjeldså, J. & N. Krabbe. 1990. Birds of the high Andes. Apollo Books, Svendborg, Denmark. p. 876.

Flores E. (1986) Bolivia, pp. 43-62 in: Scott D. A. & Carbonell M. (Compilers). Inventory of wetlands of the neo-tropical region. IWRB Slimbridge and IUCN, Cambridge.

Haile J, Froese DJ, MMacPhee RDE et al. (2009) Ancient DNA reveals late survival of mammoth and horse in interior Alaska. Proc. Natl. Acad. Sci. USA 106: 22352–22357.

Hennessey, B., S. K. Herzog & F. Sagot. 2003 Annotated list of birds of Bolivia. Harmony Association, Santa Cruz de la Sierra, p. 238.

Herzog, S. K.; R. S. Terril; A. E. Jahn; J. V. Remsen Jr.; O. Maillard; V. H. Garcia Soliz; R. Macleod; A. Maccormick & J. Q. Vidoz, 2017. Birds of Bolivia: Field Guide. Civil Action Harmony, Santa Cruz.
Garside ET & Tait JS. 1958. Preferred temperature of rainbow trout (Salmo gairdneri Richardson) and its unusual relationship to acclimation temperature. Can. J. Zool. 36: 563-567.
Gonzales, R. K. 2013. Temporal and spatial variability of the macrophyte and macro-invertebrate communities of water courses of the Quetena Bofedal - Barrancas Sector (South Lipez – Potosi). Master's thesis in Ecology and Conservation. CPEC-UMSA.
Gutierrez-Viñuales A. 2008. Chuquicamata: industrial heritage of copper mining in Chile. In: APUNTES (NOTES) Vol. 21, N° 1 (2008): 74-91.
http://www.chululo.cl/pages/recortes2.php?id=28102015_021810
Innova Chile 2010. Base characterization of high Andean meadows and bofedales for a sustainable management of water resources. First Part: Antofagasta Region. Final Report, p. 112.
Jørgensen, P. M., M. H. Neey S. G. Beck (Editions) 2014. Catalog of vascular plants of Bolivia, Monographs in Systematic Botany. Missouri Botanical Garden, 127(1–2): I–VIII, 1–1744. Missouri Botanical Garden Press, St. Louis.
Lauzanne L. (1982). Orestias (Pisces, Cyprinodontidae) of Little Lake Titicaca. Tropical Hydro-biological Magazine, 15: 39-70.
Lauzanne L. (1991). Native species: Orestias, pp. 409-421 in Dejoux C. and Iltis A. (Editions). Lake Titicaca, Summary of the current limnological knowledge. ORSTOM – Hisbol. La Paz, Bolivia.
Legendre, P., & De Caceres, M. 2013. Beta diversity as the variance of community data: Dissimilarity coefficients and partitioning. Ecology Letters, 16, 951–963. https://doi.org/10.1111/ele.12141
Leps J. & Smilaeur P. (Editions), 2003. Multivariate analysis of ecological data using CANOCO. Cambridge University Press, United Kingdom. 267p.
Liberoff A. L., Miller J. A., Riva-Rossi C. M., Hidalgo F. J., Fogel M. L. and Pascual M. A., 2014.
Transgenerational effects of anadromy on juvenile growth traits in an introduced population of rainbow trout (Oncorhynchus mykiss). Can. J. Fish. Aquat. Sci. 71: 398–407. dx.doi.org/10.1139/cjfas-2013-0466.
Lippolt G. E., Vigliano P. H., Alonso M. F., Macchi P. J., Milano D., Denegri M. A. a n d Garcia Asorey M., 2011. Comparative analysis between gill netting and sport fisher catches in a small patagonic Andean lake: its implications for resource evaluation and management. Southern Ecology 21:71- 85.
Lliully A. 2018. Environmental and social impact assessment of the Laguna Colorada transmission line and other socio-environmental documents. Activity Report. La Paz.
Loubens G. (1989). Observations on fish from the Bolivian part of Lake Titicaca. IV. Orestias spp, Salmo gairdneri and management problems. Tropical Hydro-biological Magazine 22: 157-177.
Loubens, G. & Sarmiento J., 1985. Observations on fish from the Bolivian part of Lake Titicaca. II. Orestias agassii Valenciennes 1846 (Pisces: Cyprinodontidae). Tropical Hydro-biological Magazine 18: 159-171.
Loubens G. 1991. Introduced species. 1. Salmo gairdneri (rainbow trout), pp. 425-430 in Dejoux C. & Iltis A. (Editions) Lake Titicaca. Summary of current knowledge. ORSTOM – HISBOL, La Paz – Bolivia.
Loza Herrera, S., R. I. Meneses & F. Anthelme, 2015. Plant communities of the bofedales of the Real Mountain Range (Bolivia) under global warming. Ecology in Bolivia, 50 (1): 39-56.
Loza Herrera, S. 2012. Diversity, composition and abundance of macrophytes and filamentous macro-algae in the bofedales of two micro-basins in Tuni-Condoriri and their relationship with the environmental variables in the dry, transitional and humid periods, Department of La Paz. Bachelor thesis, Higher University of San Andres, La Paz, p. 64.
Luna SM & Valdestamon RR. 2018. Oncorhynchus mykiss (Walbaum, 1792). Rainbow trout. In: Froese, R. and D. Pauly. Editors. 2018. FishBase. World Wide Web electronic publication (02/2018). (Available in: www.fishbase.org) [Consulted on: 23-May-2018).
Mamani P. 2016. Evaluation of native forage resources with satellite images in the Alto Peñas community of the Batallas Municipality, Los Andes Province. Bachelor thesis, Higher University of San Andres, La Paz, p. 141.
Martin-Torrijos L., Sandoval-Sierra J. V., Muñoz J., Dieguez-Uribeondo J., Bosch J. and Guayasamin J. M., 2016. Rainbow trout (Oncorhynchus mykiss) threaten Andean amphibians. Neotropical Biodiversity, 2(1): 26–36.
Mealla L. 2013. Since 2015, it is planned to "cut" 100% of the Silala water. La Razon newspaper, 17 March 2013.
Meneses, R. I. 2012. State of art of the bofedales in the Real Mountain Range in the area that covers the Khara Khota basin up to the Choqueyapu basin. Unpublished technical document. Inter-American Development Bank (IDB), La Paz, p. 74.
Meneses, R., Loza Herrera, S., Lliully A., Palabral A. & Anthelme F., 2014. Methods to quantify the plant diversity and productivity of bofedales in the face of climate change. Ecology in Bolivia, 49 (3), 42-55.
Meneses R. I., A. Palabral, A. Lliully, J. Molina, J. Acho, O. Plata, S. Loza & V. Urrelo, 2014. Floristic and limnological characterization of bofedales in the Municipalities of Turco, Pelechuco, Curva, Charazani and Curahuara de Carangas for the second phase of the National Bioculture Program (PNB). Unpublished technical document. Sustainable Water. La Paz, p. 167.
Ministry of Environment and Water, 2009. Red book of the vertebrate wildlife of Bolivia. La Paz, Bolivia.

Ministry of Environment and Water (MMAyA), 2012. RED BOOK of the threatened Flora of Bolivia. Vol. I. Andean Zone. La Paz, p. 600.
Montaje, J. 1977. Outline of the Chilean Prehistory in "PUMAPUNKU Magazine", Official Magazine of the Aimara Culture Institute, La Paz – Bolivia, pp. 69-84.
Montes C., Rendon-Martos M., Varela L. and Cappa M. J., 2007. Manual of Mediterranean wetland restoration. Ministry of Environment, Seville.
Muñoz J., 2000. General Geomorphology. Ed. Synthesis S. A. Madrid.
Nelson J. S. 2006. Fishes of the World (Fourth Edition). New Jersey. John Wiley and Sons.
Nielsen A. & E. Berberian, 1995. The Mallku Manor Revisited, Contributions to the knowledge of the late pre-Hispanic history of Lipez, in "Archeology Magazine of the Highlands, Inter-Andean Valleys and Lowlands of Bolivia", Memoirs of the congress of archeology of Bolivia, La Paz – Bolivia, pp. 145-166.
Nielsen, A. E., Vazquez M. M., Avalas J. C. and Angiorama C. I., 1999. Archaeological Surveys in the "Eduardo Abaroa" Reserve (South Lipez, Department of Potosi, Bolivia). In: Relations of the Argentine Society of Anthropology XXIV, Buenos Aires.
Nielsen, A. 2009. Training occupations in the Altiplano of Lipez-Potosi, Bolivia. In Journal of Anthropological Texts Vol. 13, N° 1-2, La Paz – Bolivia, pp. 265-285.
Orellana, R. Yañez N., Montero Y., Weisner R., Hantke M., Del Castillo L., Rovere & M., 2013. Conflicts and Agreements on Transboundary Waters. Regulatory Frameworks and International Regulatory Practices. Cordillera University – Sustainable Water, La Paz, Bolivia.
Parenti L. R., 1984. A taxonomic revision of the Andean killifish genus Orestias (Cyprinodontiformes: Cyprinodontidae) Bull. Amer. Mus. Nat. Hist. 178: 107-2014.
De Pinna MCC & Wosiacki W. 2003. Family Trichomycteridae (Pencil or parasitic catfishes), p p. 270-290. In: Reis RE, Kullnader (SO) & de Ferraris CJ (Editions) Check List of the Freshwater Fishes of South and Central America. Porto Alegre. PUCRS.
Palabral-Aguilera A., O. Rocha, F. Guerra, G. Siebel, K. Gonzales, A. Lliully, L. Moya a n d F. Varela, Noviembre 2016. Preliminary Report: Evaluation of the biodiversity of the Silala springs, southwest of Potosi – Bolivia, p. 41.
RAMSAR, C. 2005. Ninth meeting of the conference of the Contracting Parties to the Convention on Wetlands.
Rambaud, M., S. Pavoine, N. Machon, J. Moret & I. Combroux, 2009. Does canalization alter spatial and temporal dynamics of macrophyte communities and their physical habitat? Fundamental and Applied Limnology/Archiv für Hydrobiologie, 174(2), 159-172.
Remsen, J. V., Jr., C. D. Cadena, A. Jaramillo, M. Nores, J. F. Pacheco, M. B. Robbins, T. S. Schulenberg, F. G. Stiles, D. F. Stotz, & K. J. Zimmer. 2018. A classification of the bird species of South America. American Ornithologists' Union.
Riva-Rossi C, Arguinbau M & Pascual M. 2003. The spawning migration of anadromous rainbow trout in the Santa Cruz River, Patagonia (Argentina) through radio-tracking. Southern Ecology 13:151- 159.
Robbins S.P. & Coulter M., 2005. Administration. 8th Edition. Mexico: Pearson Education.
Ruthsatz B. 2012. Vegetation and ecology of the high Andean bofedales of Bolivia. Phytoecology 42: 133- 179.
Santoro, M & A. Romero, 2009. Social interaction in the Late and Late Intermediate Periods, Lluta Valley, Northern Chile, in "Archeology and Ethnohistory an Andean encounter", Institute of Peruvian Studies, Lima – Peru, pp. 81-141.
Sarmiento J. 1991. Fish, pp. 469-481 in: Baudoin M. & Forno E. (Editions) Natural History of a Valley in the Andes: La Paz. La Paz, Bolivia. Quipus Graphics Services.
Sarmiento J. 1992. Aquatic ecosystems and hydro-biological resources, pp. 293-320 in: Marconi M. (Edition). Conservation of Biological Biodiversity in Bolivia. CDC-Bolivia/USAID-Bolivia. La Paz, Bolivia.
Sarmiento J. 2006. Fish, pp. 162-166 in: Olivera M., Ergueta P. & M. Vilca Sanjines (Editions). Conservation and sustainable development in the southwest of Potosi, Bolivia. Prefecture of the Department of Potosi/ TROPIC. La Paz, Bolivia.
Sarmiento J. & Barrera S., 1996. Fish, pp. 33-65 in: Erqueta P. & Morales C. (Editions). Red Book of Vertebrates of Bolivia.
Sarmiento et al., 1999. Plan of Action for the Endangered Species of Bolivia.
Secretary of Environment and Natural Resources (SEMARNAP), 2013. Guidelines for a restoration strategy in protected natural areas. National Commission of Natural Protected Areas Secretariat of the Environment and Natural Resources. Camino al Ajusco N° 200 Jardines en la Montaña CP 14210 Tlalpan, Mexico D.F. http://www.conanp.gob.mx.
SENAMHI, 2017. Continuous monitoring of levels, flows and provision of meteorological information in the area of the Silala springs, Potosi, p. 55.
SERGEOMIN, 2017. Geological structural mapping of the area surrounding the Silala springs, p. 90.
SERGEOTECMIN, 2004. Preliminary report on the hydrological and hydro-chemical investigations carried out in the field of Silala, pp. 193-207.
SERNAP, 2006. Updated Management Plan for the Eduardo Abaroa National Andean Fauna Reserve. Bolivia

National Service of Geology and Mining, 1996. Geological Letter of Bolivia. Sheet 5927–6027 Inca Hill – Khara Lagoon, Scale 1: 100 000.
National Service of Geology and Mining, 2003. Geological Letter of Bolivia. Sheet 5928–6028 Silala – Sanabria, Scale 1: 100 000.
National Service of Geology and Mining, 2003. Study of Geology, Hydrogeology and Environment of the Area of the Silala Springs (Regional Integration Project) Study of Hydrographic Basins - Basin of the Silala Springs, Basin 20. June 2000–2001.
Squeo F., E. Ibacache, B. Warner, D. Espinoza, R. Aravena & J. Gutierrez, 2006. Productivity and floristic diversity of the Tambo meadow. Geo-ecology of the Andean deserts. The High Mountain of Elqui Valley. CEPEDA P., J. (Edition). Editions of the University of La Serena. La Serena, Chile, pp. 325-351.
Stotz, D. F., Fitzpatrick, J. W., Parker III, T. A., & Moskovits, D. K. 1996. Neo-tropical birds: Ecology and conservation. University of Chicago Press.
Tchernavin VV (1944b). A revision of the Trichomycterinae based on material preserved in the British Museum (Natural History). Proc. Zool. Soc. London 114: 234-275.
Thornbury W., 1960. Principles of Geomorphology. Kapelusz S.A Edition. Buenos Aires.
UICN, 2017. The IUCN Red List of Threatened Species. Available in http://www.iucnredlist.org, 2017-3 Version. Downloaded: 27 May 2018.
UNEP. 2007. Hydropolitical Vulnerability and Resilience along International Waters (Nairobi: UNEP Publications).

Urquidi F. 2004. Report of the trip to Silala. Additional field work, pp. 170-192.
Valladares, M., Cruz-Jofre F., Barrera S. & Sarmiento J., 2017. Phylogenetic relationships and historical biogeography of the genres Heleobia Stimpson, 1865 (Caenosgastropoda, Cochliopidae) and Orestias Valenciennes, 1839 (Cyprinodontiformes: Cyprinodontidae) of the Andean Altiplano. (Project in execution)
Vila I., Pardo R. & Scott S., 2007. Freshwater fishes of the Altiplano. Aquatic Ecosystems Health & Management 10(2): 201-211.
Villarroel J. 1997. Fodder and nutritional balance in production areas of Ulla Ulla alpacas. Bachelor thesis, Higher University of San Simon, Cochabamba, p. 111.
Willerslev E., Davidson J., Moora et al., 2014. Fifty thousand years of Arctic vegetation and mega-faunal diet. Nature 506: 47-51.

Wurtsbaugh W. A. & Alfaro T. R., 1988. Mass mortality of fishes in Lake Titicaca (Peru–Bolivia) associated with the protozoan parasite Ichthyophthirius multifiliis. Transactions of the American Fisheries Society 117: 213-217.
Zobel M., Davidson J., Edwards M. E. et al., 2018. Ancient environmental DNA reveals shifts in dominant mutualisms during the Late Quaternary. Nature Communications |DOI: 10.1038/s41467-017- 02421-3

ANNEXES
Annex 1

1. Historical and social considerations

In order to obtain information on the historical aspects and possible past impacts on the Silala, primary and secondary information was collected. The formed was obtained from interviews to the people of the area during two field visits, 25 March–4 April and 19–23 April 2018, and the latter included data on the socioeconomic activities of either the existing communities, or those that interfered the area surveyed. Data on the possible threats and impacts derived from the different socioeconomic activities and historical information was also collected.

The field works comprised different stages: the first consisted performing interviews and polls at the military post, Laguna Colorada and Quetena Chico community. The second consisted in the coordination and actual field trip to the Silala bofedals, accompanied by inhabitants of the Quetena Chico community to get information on the historical aspects and preservation state of the bofedals.

Contacts with people from Laguna Colorada were also made to complete interviews to Mr. Jacobo Berna (51 years old) and his family, who provided the authors with historical information of the Silala based on their wide knowledge of the area. From 1 to 4 April, semi-structured interviews were completed with the people of the Quetena Chico community. Telephone contact was first made with Mr. Aurelio Berna to inform him of the projected interviews, particularly concerning a Quetena individual that visits the Silala bofedals more frequently. During the authors'' stay at the community, the latter's authorities were first contacted, and the objective of the work to be completed was communicated and socialized with the people.

The people of the community were then interviewed and a meeting was scheduled with Mr. Primo Berna (63) and his family to complete the semi-structured interview referred to above at his home in Quetena Chico (Figure 1). Several people of the Quetena community were interviewed, separating them into: 1) people who did not know the Silala bofedals; 2) people who had been to the Silala bofedals in one opportunity; and 3) people who had been to the bofedals on different opportunities.



Figure 1. Interview to Primo Berna and his wife in Quetena Chico (Photograph: Loly Vargas Callisaya).



Figure 2. Field visit to the Silala bofedals with Primo Berna, inhabitant of Quetena Chico (Photograph: Loly Vargas Callisaya).

Perception of the community people on the Silala Bofedals: In order to obtain this information, semi-structured interviews were completed with people who had been to the Silala bofedals on several opportunities. These interviews were made to obtain information on the activities performed in the Silala bofedals area, the local historical aspects of the area surveyed, the people's perception on the state of preservation of the region, and the changes perceived throughout the years.

It was also possible to contact another people group that had been to the bofedals since 1948, and whose family had temporally lived in the Silala area since 1970. A field visit to the Silala bofedals was then scheduled with these community people (Figure 2). The observations made during the different field visits to the bofedals and their vicinities, accompanied by Joaquin Estelo (83) and Primo Berna (63) are detailed below:

- The characteristics of the bofedals since 1948.
- The surface area covered by the bofedals in 1970-1978.
- The historical and sociocultural aspects of the Silala.
- The historical aspects and specifics of the canalization works and the exploitation of the waters of Silala by Chile.
- The traditional management and preservation of the bofedals.

Clearly, this information is not technical in nature, but it might be useful to correlate the findings of this report with the events recalled by the people of the area.

2. RESULTS

2.1. Historical settlements in the Silala region (social field)

The Silala bofedals and their vicinities have a historical-archeological value inasmuch as evidence of human settlements and seasonal habitation has been found, likely connected with cattle raising and/or hunting near the water course and bofedal areas. These findings bear a relation with the following periods: the late formative, the late regional development and the Inca periods (SERNAP, 2006).

The Silala bofedals area has received different human interventions throughout the time, among which the following can be mentioned: a) Chile's introduction of canalization works in 1908 (Orellana et al. 2013), b) "yareta" (Azorella compacta) exploitation before 1945 by the Chuquicamata mining company (Gutierrez-Viñuales 2008), and c) sporadic human settlement by llama cattle raisers (Nielsen et al. 1981).

2.2. Canalization of the Silala waters

The introduction of canalization works in the bofedal area that was authorized in 1908 by Bolivia was intended to allow The Antofagasta and Bolivia Railway Company Limited to build canals to exploit the waters for their steam engines (Orellana et al 2013).

According to Messrs. Joaquin Estelo and Primo Berna, the canals built by Chile in the Silala bofedals cover almost the entirety of their Surface area. During the field work completed for this study, it was possible to corroborate the existence of artificial canals in the South and North bofedals, in the vicinities of the military post and Silala waterfall, and throughout the Cajon ravine (Figure 3). The spring waters were abstracted from their main upwelling pools at the South bofedal as far as the border between Bolivia and Chile.

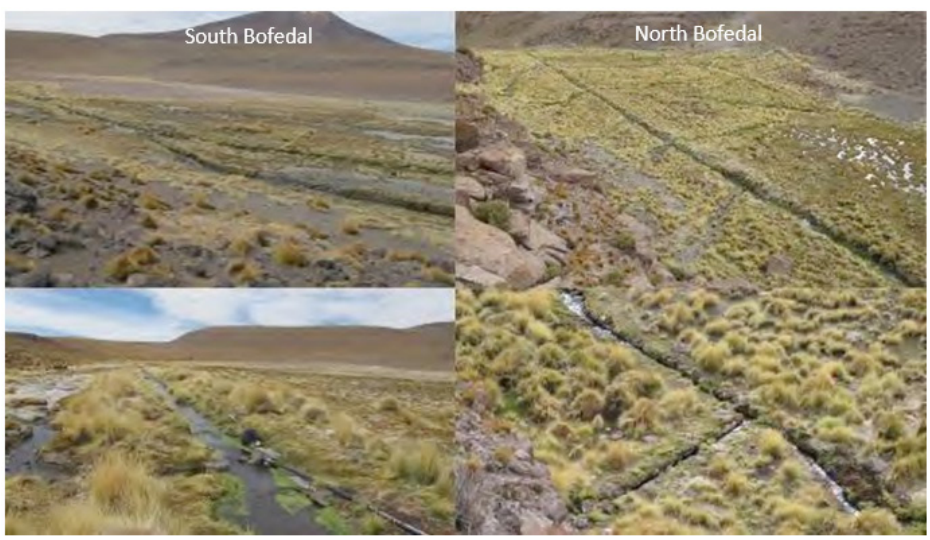


Figure 3. Artificial canals built in the South and North bofedals. Note that the canals of the North bofedal form a clear fishbone shape to abstract all the water course and take the water to the main canal. (Photograph: Simon Pfanzelt).

During the interviews, settler Joaquin Estelo (83) said that he had been to the Silala springs in 1945, when the bofedals were still guarded by the Chilean police forces and maintenance works for the artificial canals were still performed by Chilean people.

The canalization of these water sources was made with stones. Most of the pooling waters were canalized and driven top the main canal (Figure 4). The cleaning and maintenance of the canals was made with a brush, and the Chilean stuff also extracted the aquatic vegetation and everything that could obstruct the flow of water in the canals (fact noted by Joaquin Estelo).



Figure 4. Abstracted and canalized pooling waters driven to the main canal. A). South bofedal; B). North bofedal (Photograph: Loly Vargas Callisaya).

The people interview noted that the canals were intended to abstract as much water as possible and drive it to a main canal. They also said that, in some areas of the bofedals, the water was also collected by means of pipes that were buried underground. During the field visit completed, it was possible to observe remains of pipes in the North bofedal, in Cajon ravine (Figure 5), which, together with artificial canals conveyed the water to a desilting chamber.

According to Bazoberry (2003), once in Chilean territory, the water was collected in a storage reservoir and distributed by means of pipelines to the Chuquicamata mining fields, by a drinking water aqueduct to Antofagasta; and to Inacaliri dam.



Figure 5. Artificial canals installed to abstract the water. A) water abstraction pipeline. B) "desilting chamber" built in the Cajon ravine (Photograph: Loly Vargas Callisaya).

2.3. Surface area of the bofedals between 1970-1978

In order to obtain information of the state of the bofedals during the 1970-1978 period, interviews and site visits were completed with Primo Berna, employing a GPS system and marking the [original] bofedal limits based on his perception and memory. The results have been mapped on Figure 8. According to the mapping completed, back in 1970, the bofedals were more reduced in extent in comparison to what was observed in the field—an interesting account that could be contrasted with technical data. The community inhabitants stated that the bofedal vegetation was enduring a desiccation process and said that dry peat could be observed in the bofedals. They further stated that the vegetation was already reduced in extent at one meter of distance from the main canals.

2.4. Traditional management and preservation of the bofedals.

The people interviewed stated that they perform a traditional management of the bofedals to preserve them; these activities include: opening irrigation channels, irrigating the bofedals and planting seeds in them. Each of the families makes use of a specific bofedal section to graze their cattle and are in charge of that particular section.

Since 1997, following the denouncement put forward by the national press regarding the use of the Silala waters by Chile, the Quetena Chico community had Primo Berna stay in the Silala region to exert sovereignty.

2.5. Boundary stones set up by Chile

The people interviewed mentioned the presence of boundary stones surrounding the South bofedal. These boundary milestones (15, approximately) were 1.5 m-high concrete structures built by the Chileans to guard the bofedals.

They further noted that the Chilean policemen once patrolled the vicinities of the bofedals. During the field visit, and with the help of the people from community, it was possible to corroborate and obtain geographical references (Table 1) of the remains of six of these stone structures (Figure 9) in the South bofedal.

Table 1. Geographical coordinates of the remains of boundary stones found in the south bofedal.

Boundary stone	**Area**	**Coordinate X**	**Coordinate Y**	**Altitude MASL**
1	19 K	0603358	7566074	4415
2	19 K	0603357	7566067	4414
3	19 K	0603345	7566053	4414
4	19 K	0603320	7566023	4425
Silala Hill	19 K	0602817	7665963	4444
Vicinities of the road	19 K	0602837	7565689	4421



Figure 6. Evident remains of boundary stones of the South Bofedal. A) stone marker in the hill found close to the South bofedal. B) stone marker close to the road to the military post (photograph: Loly Vargas Callisaya).

2.6. Yareta extraction

Another relevant historical antecedent that occurred in the Silala was the extraction of yareta, in the years before 1945. The interviewees indicated that the extraction of yareta (Azorella compacta) was done using carts and as evidence, there are currently cart roads called the "yaretales", located on the Silala hill (Figure 10). These cart roads are the silent witnesses of the intensive extraction of Azorella compacta and, according to Jacobo Berna, Joaquin Estelo and Primo Berna these plants were used by the Chuquicamata copper mining company.



Figure 7. Silala hill; note the roads to transport yareta in carts (Photograph: Loly Vargas Callisaya).

2.7. Temporal settlements and shelters in the Silala

The community of Quetena Chico made long trips to Chile, transporting their animals, charque [dry meat] and saltpeter to trade them for Chilean products: apples, pears, wheat, corn. These last two were milled in Chile to make flour and gather bread for their communities. These trips made by the people of Quetena Chico

in the past, were based on livestock activity and were traditionally complemented by seasonal caravans, which allowed access to agricultural resources produced in other eco-zones.

According to Joaquin Estelo, he would travel to Chile to buy basic foods, which took him four days from Quetena Chico to Silala (Figure 26); during these trips made with the animals, would he always head to the Silala waters in order for the animals and people to be able to drink water. After reaching the Silala, they would more to the Chilean towns of Toconao and Caspana.

According to Nielsen et al. 1981, the traditional destinations of the Quetena llama cattle raisers were: Toconao, San Pedro de Atacama, communities of Rio Loa, in the west (currently Chile), and Pirquitas, Rinconada and San Antonio de Los Cobres (Argentina) to the south. They also made less frequent trips to the valleys of the eastern Andean slope, such as Tupiza or Tarija. This information is consistent with the testimonies of the people interviewed.

Ribera & Liberman 2006, highlight that this activity had a high cultural heritage value that was lost and that was part of the survival strategies of highland and dry valleys carried out through exchange routes.



Figure 8. On the right side, Joaquin Estelo, inhabitant of Quetena Chico, who told the authors about the trips he would make to Chile when transportation was yet not available in the area (Photograph: Loly Vargas Callisaya).

Among the testimonies and stories told by the interviewees, the Quetena Chico community people indicate that, before 1940, their grandparents already made trips to the Silala, because that area was an important shelter due to its water resources. This is consistent with the ruins or shelters (caves) found near the Silala Bofedals (Figure 12). These "caves" comprised a dormitory (a cave) of 3 x 3 meters, approximately, and a kitchen where people prepared foods (according to Primo Berna). Five shelters were registered and georeferenced around the Silala; these are no longer used by the community members. According to interviewees Primo Berna, Joaquin Estelo and archaeologist Angela Lanza, these visits to the Silala had different reasons:

- Some people used “caves” as a temporary shelters, when they brought their products to trade them for basic foods in Chile (Joaquín Estelo).
- Some community members of Quetena Chico used the bofedales of Silala, as a temporal shelter and grazing site for their livestock.



Figure 9. Temporal shelters used by the people of the Quetena Chico community in the Silala (Photograph: Loly Vargas Callisaya).

Among the people of Quetena who lived or traveled in different periods of time by the bofedals of Silala since 1940, mention can be made to: Felix Berna, Hilarion Berna, Ladislao Berna Alvares, Remigio Berna Ezquibel and Primo Berna. The latter currently lives in the Silala from April to September, since 1997.

Another trace of human settlements found in Quebrada Cajon, about 200 meters from the border between Bolivia and Chile, corresponds to household ruins (Figure 13). This ruin is found in Bolivian territory and the testimonies indicate that a Chilean person inhabited it (Jacobo Berna, Joaquin Estelo, Primo Berna and second lieutenant Victor Astete).



Figure 10. Traces of human settlement in Cajon Ravine (ancient house that was once inhabited by a Chilean national) (Photograph: Loly Vargas Callisaya).

3. References

Bazoberry, Q. A. 2003, The myth of Silala. Plural Editorial. La Paz, Bolivia.

Nielsen, A. E., Vazquez M. M., Avalas J. C. and Angiorama C. I., 1999. Archaeological Surveys in the "Eduardo Abaroa" Reserve (South Lipez, Department of Potosi, Bolivia). In: Relations of the Argentine Society of Anthropology XXIV, Buenos Aires.

Orellana, R. Yañez N., Montero Y., Weisner R., Hantke M., Del Castillo L., Rovere & M., 2013. Conflicts and Agreements on Transboundary Waters. Regulatory Frameworks and International Regulatory Practices. Cordillera University – Sustainable Water, La Paz, Bolivia.

Ribera M. O. and Liberman M., 2006. The use of land and biodiversity resources in the protected areas of Bolivia. A critical analysis with proposals for its conservation and sustainable management. SERNAP-GEF II. La Paz, Bolivia.

SERNAP, 2006. Updated Management Plan for the Eduardo Abaroa National Andean Fauna Reserve. Bolivia Gutierrez-Viñuales A. 2008. Chuquicamata: industrial heritage of copper mining in Chile. In: APUNTES
(NOTES) Vol. 21, N° 1 (2008): 74-91.

Annex2:Codes and meaning sof fragment sand abbreviated species

Species	Acronym	abiotic	Acronym	Site	Acronym
Algae	Alga	Saline outcrop	asal	South_A	S_A
Arenaria sp.	*Aresp*	Water	agua	South_B	S_B
Astragalus sp.	Astsp	Canal	can	South_C	S_C
Calandrinia acaulis	*Caca*	Bird feces	haves	South_D	S_D
Carex cf. *maritima*	*Cmar*	Camelid feces	hcam	South_E	S_E
Deyeuxia chrysantha	*Dchr*	Viscacha feces	hvisc	South_F	S_F
Deyeuxia curvula	Dcur	Organic matter	morg	North	N
Deyeuxia 1 sp.	*Deysp1*	Dead gramineae	mgram	Confluence	CONF
Deyeuxia 2 sp.	*Deysp2*	Dead *Oxychloe*	moxy		
Eleocharis atacamensis	*Eata*	Stone	pie		
Festuca potosiana	*Fpot*	Burned gramineae	qgram		
Festuca rigescens	*Frig*	Sandy soil	sare		
Gentiana gayi	*Ggay*	Baresoil	sdes		
Gentiana sedifolia	*Gsed*				
Juncus stipulatus	*Jsti*				
Lemna sp.	*Lemsp*				
Lilaeopsis macloviana	*Lmac*				
Lobelia oligophylla	*Loli*				
Mimulus cf. glabratus	*Mgla*				
Moss	*Mussp*				
Nostoc	*Nossp*				
Oxychloe andina	*Oand*				
Gramineae sp.	*Gram*				
Phylloscirpus deserticola	*Pdes*				
Plantago tubulosa	*Ptub*				
Pucinellia frigida	*Pfri*				
Deyeuxia eminens var. eminens	*Demi*				
Ranunculus sp.	*Ransp*				
Stukenia sp.	*Stusp*				
Werneria pygmaea	*Wpyg*				
Xenophyllum incissum var. incissum	*Xinc*				
Zameioscirpus atacamensis	*Zata*				
Zameioscirpus muticus	*Zmut*				

Annex 3: Forward selection of PCA analysis with environmental variables that significantly affect plant communities.

Variable	Var. N	Lambda A	P	F
Camelid feces (hcam)	5	0.19	0.071	2.78
Saline outcrop (asal)	1	0.13	0.091	1.78
Organic matter (morg)	7	0.11	0.050	1.67
Dead gramineae (mgram)	8	0.09	0.159	1.34
Dead *Oxychloe* (moxy)	9	0.09	0.222	1.27
Stone (pie)	10	0.07	0.322	1.05
Viscacha feces (hvisc)	6	0.07	0.228	0.99
Water	2	0.06	0.449	0.84
Burned gramineae (qgram)	11	0.04	0.446	0.67
Canal (can)	3	0.04	0.677	0.53
Sandy soil (sare)	12	0.03	0.771	0.39

Annex 4: Photographic guide of the taxa found in the Silala wetlands.



Claudioperla (Gripopterygidae-Plecoptera)



Andesiops (Baetidae-Ephemeroptera)



Metrichia (Hydroptilidae-Trichoptera)



Neotrichia (Hydroptilidae-Trichoptera)



Cailloma (Hydrobiosidae-Trichoptera)



Ectemnostega (Corixidae-Hemiptera)



Austrelmis (Elmidae- Coleoptera)



Paraheptagyia (Diamesinae, Chironomidae- Diptera)





Tanypodinae (Chironomidae- Diptera)



Tanytarsus Chironominae, Chironomidae- Diptera)



Hexatoma (Limoniidae-Diptera)



Tabanidae (Diptera)



Ephydridae (Diptera)

Orthocladiinae (Chironomidae- Diptera)



Simulium (Simuliidae- Diptera)



Dolichopodidae (Diptera)



Empididae (Diptera)



Hyallela (Hyallelidae-Amphipoda)



Dero (Naididae-Oligochaeta)



Homochaeta (Naididae-Oligochaeta)



Enchytraeidae (Oligochaeta)



Glossiphonidae (Hirudinea)



Dorylaimus (Nematoda-Dorylaimidae)



Dugesia (Dugesiidae-Trematoda)



Hydracarina (Acari)

Annex 5: Physical-chemical parameters of the sampling stations in the Silala wetlands.

Parameter	CANAL	NORTH BOFEDAL	SOUTH BOFEDAL
pH	9	8	9
OD	7	6	7
CE	264	188	293
TDS	174	123	188

Annex 6: Habitat and morphological-structural parameters of the Silala wetlands.

Parameter	CANAL	NORTH BOFEDAL	SOUTH BOFEDAL
Average vel.	0	0	0
Flow	0	0	0
%B Aloc	5	33	11
%PG Aloc	9	33	14
P%F Aloc	6	0	1
%CG	8	0	4
%CF	14	0	3
%GG	10	0	12
%GF	8	7	16
%A	0	13	6
%Silt	0	7	0
%Veg	27	7	32
IHF	51	39	45

Annex 23.4

FUNDECO, "Study of Evaluation of Environmental Impacts in the Silala, Palynology", 2018

(English Translation)

DIREMAR

SURVEY OF ENVIRONMENTAL IMPACT ASSESSMENT IN THE SILALA

Palynology

Luis Pacheco D.Cs.
Coordinator

Authors:

Luis F. Pacheco, D.Cs.
Coordinator

MSc. Teresa Ortuño *Specialist in high Andean ecosystems and wetlands and in Palynology*

Lic. Mariela Escobar Torrez
Botanist - Specialist in Palynology

Lic. Katerine Escobar Torrez
Ecologist - Specialist in Palynology

Univ. Diego Martinez
Geologist Specialist

Univ. Jeanette Pacajes
Biologist - Palinologist

Authors:

Luis F. Pacheco, D.Cs.	**Coordinator**. *Director of the Institute of Ecology of the Higher University of San Andres (UMSA).*
Teresa Ortuño, MSc.	**Botanical biologist specialized in Palynology (current and past) and Systematics of vascular plants (*Gomphrena*, *Amaranthaceae*),**
Lic. Katerine Escobar Torrez	**Biologist specializing in Palynology (current and past) in High Andean eco-regions, Puna (bofedals) and the Amazon**. *Researcher associated with the National Herbarium of Bolivia.*
Lic. Mariela Escobar Torrez	**Ecologist biologist specializing in animal-plant relationship (pollination) and palynological (current pollen) studies.** *Researcher associated with the National Herbarium of Bolivia.*
Univ. Diego Martinez	**Geologist - graduated formation directed to studies of paleontology and geology of the Quaternary.** Investigations and independent consultancies.
Univ. Jeanette Pacajes	**Biologist - graduated. Training aimed at palynology and dendrochronology. Laboratory assistant.** *Thesis student at the Palynology Unit of the National Herbarium of Bolivia.*
External Collaborators	
Marie-Pierre Ledru, PhD.	**Paleontologist specializing in studies of ecosystem dynamics and global changes.** *Director of Investigation in the Institute of Research for Development (IRD). Researcher at the Institute of Evolutionary Sciences of Montpellier (ISE-M)*
Stéphane Guédron, PhD.	**Geochemist specialized in metals and metalloids in the current environment and past eras.** *Investigator at the University of Grenoble Alps and Research Institute for Development (IRD)*

FINAL REPORT
SURVEY OF ENVIRONMENTAL IMPACT ASSESSMENT IN THE SILALA INDEX

EXECUTIVE SUMMARY

Palynology

1. Background
2. Theoretical framework
3. General objective
4. Area surveyed
4.1. Description of the area surveyed
5. Methods
6. Sampling Points
7. Results and interpretation
7.1. Interpretation/stratigraphic description of the soil in the South bofedal (profiles BSP2 and BSP14) 7.2. Interpretation of the relationship of the stratigraphic profiles – extent of the South Bofedal
7.3. Paleoecological interpretations and age-depth models for the South Bofedal (profiles BSP2 and BSP14)
7.3.a. Age-depth model based on 14C dating in the South Bofedal
7.3.b. Geochemical analysis (XRD) for the South bofedal (profiles BSP2 and BSP14)
7.3.b.1 Geochemical analysis in soil profile BSP2
7.3.b.2 Geochemical analysis in soil profile BSP14
7.3.c. Zoning of palynological samples from the South Bofedal (profiles BSP2 and BSP14)
7.3. c.1. Zoning of soil profile BSP2
7.3. c.2. Zoning of soil profile BSP14
7.3.d. Changes observed in the vegetation of the South Bofedal (profiles BSP2 and BSP14)
7.3. d.1. Vegetation changes observed in soil profile BSP2
7.3. d.2. Vegetation changes observed in soil profile BSP14
7.4 Effects of canalization on the South Bofedal
7.4.a. Effects of canalization on soil profile BSP2
7.4.b. Effects of the canalization on soil profile BSP14
7.5. General conclusions on the changes recorded in the South Bofedal
7.6. Stratigraphic interpretation of the soil in the North Bofedal (BNP7)
7.7 Interpretation of stratigraphic profile relationship – extent of the North Bofedal
7.8 Paleoecological interpretations and age-depth model for the North Bofedal

7.8.a. Age-depth model based on 14C dating in the North Bofedal (profile BNP7)
7.8.b. Geochemical analysis of the North bofedal (profile BNP7)
7.8.c. Zoning of palynological samples from the North Bofedal (profile BNP7)
7.8.d. Vegetation changes observed in the North Bofedal (profile BNP7)
7.9 Effects of the canalization on the North Bofedal (profile BNP7)
7.10. General conclusions on the changes occurred in the North Bofedal
8. Determination of the historical environmental impacts caused by the presence of the artificial canals system
8.1. Environmental impacts recorded in the South Bofedal 8.1.1. Impacts detected in BSP2 profile
8.1.2. Impacts detected in BSP14 profile
8.2. Environmental impacts recorded in the North bofedal 8.2.1. Impacts detected in BNP7 profile
9. General conclusions of the survey
10. Technical summary: Result Interpretation 11. Bibliography
Annex 1
Annex 2
Annex 3
Annex 4

TABLE AND FIGURE CONTENTS

Table 1. Profiles and trial pits selected for the South Bofedal

Table 2. Comparative summary of the composition and abundance of palynomorph pollen taxa found in each profile studied in the different periods of time

Table 3. Summary of interpretations and reconstruction of past vegetation through pollen analysis. Vegetation profile BSP2

Table 4. Summary of interpretations and reconstruction of past vegetation through pollen analysis. Vegetation profile BSP14

Table 5. Summary of interpretations and reconstruction of past vegetation through pollen analysis. Vegetation profile BNP7

Table 6. Summary of interpretations and reconstruction of XRD geochemical analysis

Figure 1. Schematic summary of the methodological protocol used in the stratigraphic geochemistry palynological section

Figure 2. Area surveyed with the sampling points in the South Silala Bofedal. Longitudinal transect sampling for the South Bofedal. B) Transverse and longitudinal transect of samples for the North Bofedal. The points correspond to the sampling of stratigraphic profiles (Table 1)

Figure 3. Graphical representation of the stratigraphic description of BSP2 profile in relation to the profile depth (cm) A. Lithological relationship of the profile with the age model from 1880; B. equivalent to the last 17 cm of the stratigraphic profile

Figure 4. Graphical representation of the stratigraphic description of BSP14 profile in relation to the profile depth (cm), where the 14C dating points are punctually highlighted

Figure 5. Image taken from the IEIA Silala 2 report, from figure 24, showing the differentiation of the fragments in the North, South and confluence Bofedals

Figure 6. Stratigraphy of profiles of the South Bofedal and their location in the areas defined in the vegetation survey from the Silala environmental impact report, where A) shows the profile BSP8, B) profile BSP6, C) profile BSP2, meticulously studied, and D) BSP4 profile

Figure 7. Age-Depth model of the sediment profile of the South Bofedal BSP2

Figure 8. Trace elements found in the geochemical analysis of BSP2 profile, in concentration per second (cps)

Figure 9. Mn/Fe ratio in a soil profile from the South Bofedal (BSP2) of the Silala region – Bolivia. In the x-axis, the age scale is observed in years AD and in the y-axis and the values of the Mn/Fe ratios

Figure 10. Concentration in cps of trace elements found in the geochemical analysis of BSP14 profile

Figure 11. Percentage of representative pollen taxa found in sediment profile BSP2. On the left, it is possible to observe the AD time scale accompanied by the lithology of the profile studied, and to the right the zonation that defines the changes in vegetation, extended in the diagram with red lines

Figure 12. Pollen diagram of the concentrations of pollen, spore, algae and ameba taxa (palynomorphs) counted in the profile and related to Lycopodium spore counting to calculate the amount of palynomorphs that exist in a cm3 of sediments treated in the BSP2 laboratory. To the left, the time scale in AD years, and to the right, the zoning that defines the vegetation changes extended in the diagram with red lines

Figure 13. Percentage of representative pollen taxa found in sediment profile BSP14. To the left, the depth in cm accompanied by the lithology of the profile studied and the points at which dating was completed

Figure 14. Stratigraphy of profiles of the North Bofedal and their location in the areas defined in the vegetation study of the Silala environmental impact report, where A) shows BNP1 profile, B) BNP3 profile, C) BNP4 profile and D) BNP7

Figure 15. Age-Depth model of the sediment profile of North Bofedal BNP7

Figure 16. Trace elements found in the geochemical analysis of BNP7 profile, in concentrations per second (cps)

Figure 17. Percentage of representative pollen taxa found in sediment profile BNP7. To the left, the time scale in AD accompanied by the lithology of the profile studied and, transversally, the zonation that defines the changes in the vegetation, extended in the diagram with red lines

Figure 18. Wealth analysis based on the Chao index in the three profiles evaluated by means of palynological analysis

EXECUTIVE SUMMARY

We present the final results, corresponding to the third report of consultancy entitled "Survey of Environmental Impact Assessment in the Silala." This report focuses on the analysis of the historical changes recorded in the bofedal[s] during the last 100 years and is based on a palynological analysis of sediment profiles sampled in the South and North Bofedals, complemented with stratigraphic and geochemical analyzes focused mainly on soil profiles: in the South Bofedal, profile 2 (BSP2), South Bofedal, profile 14 (BSP14) and, in the North Bofedal, profile 7 (BNP7).

The collection of soil profile samples and the soil stratigraphic description was performed in March 2018, after which the chosen profiles were selected and divided in two equal parts. One sample was sent to the EDYTEM laboratory in Savoie (France) for its geochemical analysis, and another was left in Bolivia as a "witness" for the palynological survey and to refer the samples for their 14C dating. With these analyzes, it has been possible to infer the changes that took place in past vegetation and the effects caused by the canalization on the South and North bofedals.

Seven profiles were sampled in the South Bofedal and four in the North Bofedal, using a "RUSSIAN perforator"; plus, two additional profiles from trial pits in the South Bofedal. The sampling strategy included following a longitudinal transect with a desiccation gradient through the South and North Bofedals. From all the samples, four profiles were selected for the South Bofedal (BSP8, BSP6, BSP2 and BSP14) and four additional ones for the North Bofedal (BNP3, BNP4 and BNP7 [sic]), on basis of the organic matter proportions of the soil profiles' superficial layers.

In the South Bofedal profiles, carried out in places where the degree of desiccation was very high, it was possible to observe an unexpected presence of organic matter. In these sites, it has not been possible to find bofedal-characteristic vegetation, which is an indication that the bofedal might have been larger before canalization. The presence of organic matter in these profiles is clear evidence that the area of the bofedal was wider and that it probably decreased as a consequence of canalization; thus, the presence of organic matter served to support the calculation of the estimated area that the South Bofedal covered originally, which was carried out as part of this survey's vegetation study.

Four profiles were sampled in the North bofedal, showing stratification processes with variations in organic matter thickness; this can be attributed to changes in water availability in earlier times. The upper stratum of the four profiles presents a high proportion of organic matter, which is an indication of the fact that the desiccation process had a smaller impact on the North Bofedal—as opposed to the South Bofedal. This can be attributed to factors such as the gradient and the geomorphology (a more closed valley), where most of the canalized water sources converged in a main canal that passed through the North Bofedal. These factors must have influenced water availability positively, for the preservation of the North bofedal in certain areas near the main canal.

The samples for the 14C analysis were sent to the Beta Analityc Laboratory, in Florida (United States). The profiles selected for dating were profiles BSP2 and BSP14, for the South Bofedal, and BNP7, for the North bofedal; 2 samples were taken from each profile to complete the dating and calibration (see Table 1 in Annex 3). The results of the calibration of 14C dating were analyzed with the Clam program (Blaauw, 2010) and age-depth models were developed for soil profiles BSP2 and BPN7. The age model for BSP2 soil profile, based on 14C dating, was compared with the variation of atmospheric lead (Pb) concentrations found in the geochemical analysis in this same profile. Atmospheric Pb was deposited between 1930 and 1980, due to its presence in the atmosphere derived from Pb use as an enhancer in gasoline during those years. Subsequently, the use of Pb in gasoline was banned in many countries, due to its negative effects on the environment and the proliferation of disease—fact that resulted in a gradual decrease in Pb deposition.

The age model for the BNP7 profile was collated by means of a geochemical analysis, where an increase in the Iron/Titanium (Fe/Ti) ratio was detected. This finding is explained by the occurrence of greater aerobic oxidation in the medium, which is an indication of water scarcity. This interpretation is supported by a comparison with other works carried out in high mountain bofedals of Peru and Argentina, as well as on the experience of the experts who contributed to this work. This indication of water reduction concurs in time with the event known as the Little Ice Age (LIA), which had a dry phase from 1750 to 1850. This event occurred regionally and has also been detected by other authors who have completed works on Andean bofedals.

The collection of samples for the geochemical analysis (XRD) was performed every 0.5 cm, from the surface to the deepest profile base, providing high resolution to our interpretations.

Through this analysis, changes in the environment can be detected by the concentration of the different elements (metals) in the soil profiles, which are in turn related with [radiocarbon] dating. This allows inferring what happened in the environment in the past, with a main focus on the last 100 years.

The geochemical survey results show a clear process of gradual desiccation, which is more evident in the South Bofedal. This period of desiccation began around 1908, which is a clear sign of the effects that canalization had on the Silala springs. The concentrations of terrigenous metals indicate that desiccation was more severe during the 50s and 60s and that it continued until the 1990s, which can clearly be observed in iron fluctuations (Fe). This period is considered as the critical stage of the impacts of canalization. The bofedal desiccation process is also reflected in the increase in bromine and nickel concentrations, which respond to an accelerated process of humification, caused by dryness in the environment. Similarly, the Fe/Ti ratio shows high values, due to the oxidation caused by the reduction of water levels; and, conversely, a reduction in the ratio of Mn/Ti and Mn/Fe, which is an indication of a decrease in water inflows to the bofedal.

In order to compare vegetation composition before and after the canalization works were installed, a palynological analysis was carried out, with pollen readings every 0.5 cm, for the first 17 cm of the BSP2 profile, the first 20 cm for the BSP14 profile and the first 16 cm for the BNP7 profile; this was done for the purpose of studying, in greater detail, the history of the South and North bofedals in the last 100 years. Overall, the results of the three profiles provide evidence of a period with higher regional humidity before canalization was introduced in 1908. This interpretation is based on the presence of thola plants in greater quantity, verified by pollen from plants of the Asteraceae families (Parastrephia) and Solanaceae (Fabiana dense), and a reduction of species of the Poaceae and Cyperaceae families, which are known as plants that colonize fragmented bofedals. This also concurs with an increase in the presence of algae, which develop in humid environments, which correspond to the bofedals before 1908. From 1908 onwards, a gradual desiccation process took place and is evidenced by the change in palynomorph composition, reflected in the increase of Palaeoarcella sp, which is a protozoan indicator of water stagnation. This desiccation process reached its climax around 1950, when the eutrophication processes of these stagnant waters, together with desiccation, allowed the colonization and predominance of plants of the Cyperaceae family in both the South and North bofedals. The Cyperaceae species are

opportunistic plants that thrive in humid soils, but with lower water levels than those existing in the bofedals.

In conclusion, the results of the stratigraphic, metal and palynological analyzes indicate that, compared to previous periods of natural dryness—as the Little Ice Age dry phase—the effects of canalization had a greater impact on the availability of water and the state of preservation of the Silala bofedals. In turn, this decrease in water availability is likely to have affected the microclimate and vegetation within the bofedal and in the surrounding areas.

Our results clearly show that the canalization process had a greater impact on the South Bofedal, which cannot be attributed to climatic, or any other, changes.

Finally, Figure a) summarizes the results of this study, which are shown separately for each of the three profiles studied in detail (BSP2, BSP14 and BNP7), to show the coincidences. The red color indicates drier stages and the dark blue color indicates periods with higher humidity. The critical desiccation period is clearly distinguished in the three profiles. Said period occurred between 1950 and 1990 and can clearly be attributed to the canalization of the Silala Befalls water springs and not to climatic effects.

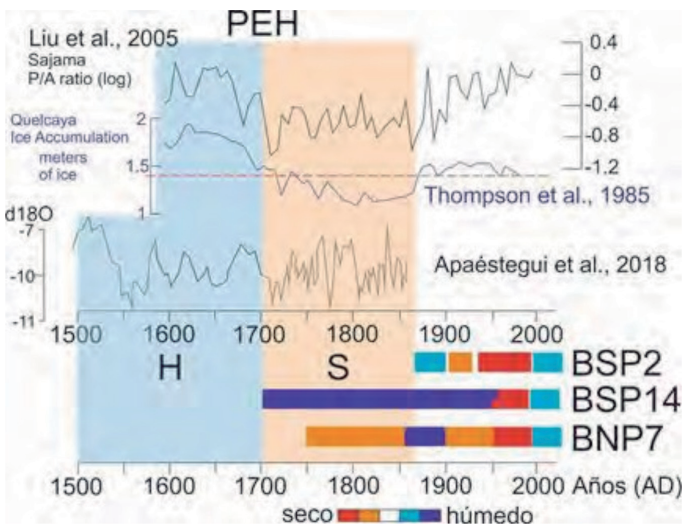


Figure a. Summary in time scale in years AD of the historical reconstruction of profiles BSP2 and BSP14 of the south bofedal and profile BNP7 of the north bofedal compared with regional climatic events detected in the last 500 years. LIA [PEH] = Little Ice Age; S = dry; H = humid.

1. Background.

The present document constitutes the final report and corresponds to the third product of the environmental impact study carried out in the Silala, which is focused on the palynological study of the South and North Bofedals. This work was completed in coordination with the vegetation team. It describes the results of the stratification, palynology and geochemistry studies (X-ray diffraction), which were applied to detect the effects that the canalization introduced in the Silala area had since 1908.

In the present report, the results are arranged following a rationale that is consistent with the methodological scheme and are divided into two parts i) the South Bofedal and ii) the North Bofedal, which respond to the terms of reference (hereinafter, TOR) listed below (1 to 5). In order to facilitate following up their respective responses, the subtitles that cover each of the TOR are presented below:

1. Estimation of plant diversity in the region in the last 100 years, comparing the surface areas of the current bofedals, scrublands and degraded bofedals of the Silala, through a pollen and fossil spores (palynology) survey. This survey is compared with results from other bofedals in the area: 7.3.c and 7.8.c (see index).

2. Paleoecological interpretations of the bofedal and Age/Depth model corresponding to the bofedal: 7.3, 7.8.

3. Reconstruction of past vegetation and interpretation of possible anthropic or climatic changes: 7.3.d and 7.8.d.

4. Analysis of the metal composition by X-ray diffraction (XRD); supplementary analysis for the pollen analysis, which will allow to better understand the changes in the vegetation, determining if they are due to natural or anthropic causes: 7.3.b, 7.4, 7.8.b., 7.9.

5. Determination of the historical environmental impacts caused by the presence of the system of artificial canals on the vegetation: 8.1 and 8.2.

Additionally, subtitle 10 includes a summary of the results, following the order presented in the TOR.

2. Theoretical framework

According to DIREMAR (2017), currently, the predominant species found in the South and North bofedals are Distichia muscoides, Oxyclhoeandina and/or Plantago tubulosa in bofedal areas in

associations such as a) Distichia muscoides – Oxychloe andina, in saturated hydromorphic soils and phreatic levels with surface runoff; b) Plantago tubulosa – Gentiana sp, on hydrothermal soils that do not present submergence and superficial phreatic level.

The studies completed by Diremar (2017) provide information on the soils' characteristics and their depth. These data were used as baseline information to locate the drilling tests of the soil profiles for the palynological study. According to this study, the North Bofedal presents a greater soil depth, where most of the sampled points were deeper than 0.80 m, reaching the deepest place at 1.40 m, while the South Bofedal presented lower soil depth—the shallowest depth was of 0.40 m and the greatest depth surpassed the 1.20 meters. The sediment profiles present coincidences; a depth of 1.50 m was obtained in the North Bofedal, while, in the South Bofedal, it was possible to obtain profile drillings no deeper than 0.50 m due to the soil compositions, with the highest percentage of sand and stones, confirming the previous study on the depth in the North and South Silala bofedals. On the other hand, the organic matter (OM) vs. depth values show that the soil in the North Bofedal is more homogeneous, with soils with higher OM, near the 0.70 cm, while the South Bofedal presents greater sand with depth and a presence of Maximum OM at 0.24 cm. Sediment deposition varies a lot from bofedal to bofedal and it is therefore important to perform tests to obtain a good soil profile to be studied and complete dating surveys for each profile studied, given the heterogeneity in the sediment deposition found in Andean bofedals, including the Silala.

At this point, it should be noted that geochemical studies the variations of the elements are quite subtle to detect concentration changes in detail [sic], allowing to perform a more detailed reconstruction. On the other hand, it can be observed that the water table levels in the Silala bofedals are more heterogeneous than those of other bofedals with different characteristics, as the Villamar bofedal for instance, which displays more homogeneous levels. Thus, the Silala bofedals have been reported as bofedals that are undergoing a degradation process as a result of the canalization works, which have caused a reduction in the groundwater levels and, particularly, a reduction in the characteristic vegetation layer. Despite this, these bofedals currently have sufficient water storage capacity.

The study of the "Environmental Impact Assessment in the Silala" (Silala EEIA 2) shows more specific vegetation data with the detailed identification of species that can be

considered as indicators of degradation in the bofedals, e.g. species that colonize the bofedal when a drying process is recorded, i.e. Cyperaceas (Carex cf. maritima), Poaceae, as the Deyeuxia curvula, Deyeuxia eminens var. eminens, Festuca potosiana, as well as those which, on the contrary, are considered typical and bofedal-forming, where the Juncaceae and Xenophyllum incisum are found, which are a humidity indicator.

Palynology is a discipline that studies pollen from a Paleoecological point of view, and can be used in studies of paleoclimate and past vegetation reconstructions, due to the close relationship between the flora and the processes of the terrestrial system, and mainly because the structure of pollen and spores allows them to be preserved and fossilized. This fact allows, through pollen analysis, inferring the vegetation composition in a system under study over time (Seppa, 2007, Brewer et al., 2007, Twidle, 2012). The investigations carried out in the reconstruction of past environments are carried out in places where a stratification of soil can be distinguished, allowing to obtain sediment profiles with a continuous, stable and low oxidation sedimentation process (less oxygen and greater preservation), as is the case of the vegetation of high Andean bofedals. Given the importance of data on the type of sedimentation that took place, it is advisable to make precise stratigraphic descriptions in the areas studied, which can give indications of the mechanisms that gave rise to sedimentation on basis of a textural analysis of the clastic components (composition of the rocks found in the sedimentation of the superficial layers represented in soil profiles). Soil profiles have different shapes (rounded, angled, etc.), and they also vary in the percentage distribution of their components and color.

Sediment profiles are dated through different methods, the best known being Radiocarbon dating (14C), which is an isotope present in sediment samples that contain organic matter. This method was used to date samples with a maximum of 40,000 years of age (Cook & van der Plitch, 2007, Hattle & Jull, 2007), but currently 14C dating can be used for more recent times with low error margins, facilitating the reconstruction of more modern vegetation. To this end, calibration programs are used, where the age-depth model results are obtained by precise statistical means (https://www.radiocarbon.com). These models give an age equivalence for the different depths of soil profiles as a function of the sediment deposition time. However, to have more certainty on the sample ages, it is desirable to complete the dating with other dating methods, such as the 210Pb (Espi 1997).

Modern palynological studies also use other complementary methods to give greater precision to the interpretations of environment reconstruction, one of which is the analysis of the composition of metals by X-ray diffraction (XRD). This analysis can detect the concentrations of metals in sediments, to allow the possibility of determining whether their presence is due, for example, to plant bioaccumulation, metal accumulation from the atmosphere, or whether the accumulation derives from other anthropogenic disturbances (mining, industrial waste, among others).

Complementary studies, of pollen with metal analysis, conducted in the bofedals of the Peruvian, Chilean and Argentine Andes (Schittek et al., 2015, Schittek et al., 2016) demonstrate the effectiveness of the combination of these methods to infer climate changes or the effects recorded in vegetation due to changes in hydrological regimes, especially in a type of azonal vegetation, such as bofedals. However, few of these surveys comprise recent reconstructions in time—as is done in the present survey.

This study has been designed to study the soil profiles of the Silala region bofedals in order to assess whether the canalization works, introduced in the area surveyed at the outset of the twentieth century, had the impacts that can be detected in the changes recorded in the pollen deposited in the vegetation and the accumulation of metals in the soil.

3. General objective

The objective of the present work was to carry out a palynological and geochemical study (XRD) in the Silala bofedals in order to reconstruct the history of the vegetation and see if it is possible to detect some of the effects caused by the canalization of the springs—which has been in place in the area surveyed since 1908.

In order to achieve said objective, and with the help of earlier geographical information system surveys and the characterization of the current vegetation of the area, the questions that are sought to be answered are:

Does the stratigraphic description of soil profiles in a longitudinal transect in the South and North bofedals support the presence of wetlands (bofedals) in the area studied?

Does the interpretation of the geochemical analysis of metals give any indications of anthropic disturbance focused on the fluctuation in the wetlands' water levels?

Do the changes in the composition of palynomorphs in the sediment profiles, of the South and North bofedals, provide any signs of anthropic disturbance derived from the canalization of water sources during the last 100 years?

4. Area surveyed

4.1. Description of the area surveyed

The area surveyed is part of the southern block of the Western Maintain Range, and corresponds to a Volcanic Zone of the Central part of the Andes, with exposed rocks (ignimbrite, andesite and dacite) that belong to the Miocene (23 to 5 ma) (Baker Y Francis 1978). The geomorphology of the region is the result of different—particularly volcanic—processes (predominance of volcanic craters, lava flows and pyroclastic deposits). Other important processes are the successive glaciations that took place between the Pliocene and Holocene that defined the wide and U-shaped valleys, as well as the formation of deposits of lateral moraines and the superposition of fluvioglacial, alluvial, colluvial and eolian materials. The deposits in the bofedales are constituted by sand, silt and clay (D., Martinez Obs. Pers.).

The few palynological studies in the area allow recognizing different Holocene periods (the last 10,000 years before the present) in the highland region. Lake Titicaca is a reference of these regional changes that are also reflected in the south of Bolivia and north of Chile. The progressive increase of aridity in the environment, from the beginning of the early Holocene, continued during the period of extreme aridity in the Middle Holocene (8000 to 3500 years BP) [sic, the sentence is incomplete] (Mouguiart et al., 1997; 1998; Abbot et al., 2000; 2003 Saez et al., 2007; Moreno et al., 2007; Pueyo et al., 2011).

During the mid and early Holocene, an increase in the activity of the Parinacota volcano was detected (Moreno et al., 2007). Subsequently, during the late Holocene, an increase in rainfall was recorded, coinciding with the settlement of human populations in Chile's northern region, and the occurrence of brief arid intervals (Messerli et al., 1993). However, the data obtained from the late Holocene has very low resolution and the increase in the settlement of human population is not quite clear, particularly for the last 300 years.

5. Methods

The methodological sequence is presented in Figure 1. Annex 2 presents the methodology employed in extenso.

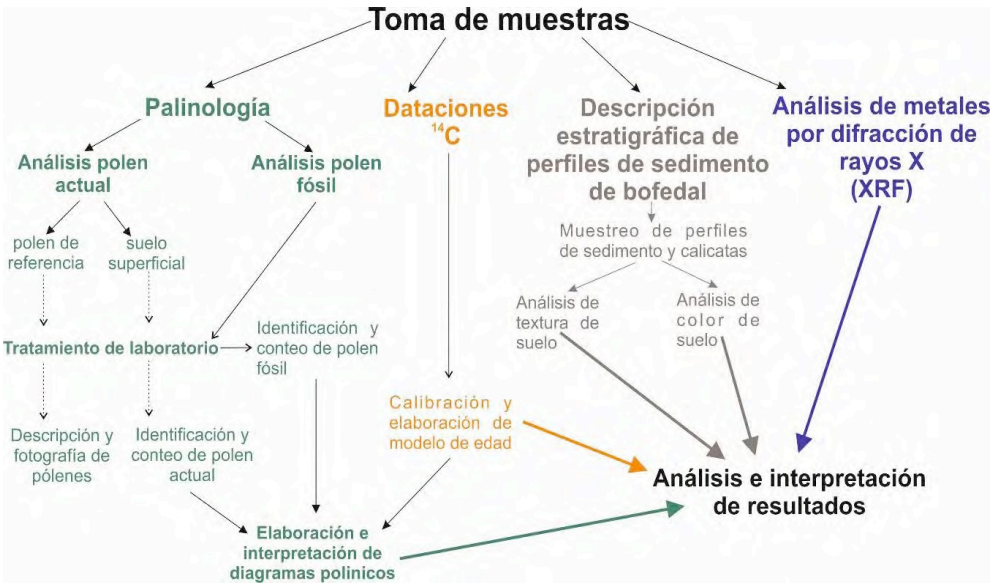


Figure 1: Schematic summary of the methodological protocol used in the palynological study, including the stratigraphic and geochemical sections.

1. Stratigraphic analysis: Although stratigraphic analyzes are not contemplated in the terms of reference, it is essential to have this information, as it is necessary to describe the characteristics of the soil more accurately and perform an effective interpretation of the historical reconstruction of palynology and geochemistry.

Several soil profiles were made, as indicated in section 6 (surveyed area, Figure 2). Each of the soil profiles was described on basis of the soil characteristics and stratigraphy. The information was used as a basis to select the most consistent soil profiles in order to perform a paleo-ecological reconstruction. In some occasions, the soil profiles used in pollen studies can come from areas where the soil may have been affected by landslides or other forms of soil removal, either by natural or anthropic events. These events generate “hiatus” within the profile and can result in inconsistencies in the age-depth models. Therefore, in order to reduce

the possibility of making this mistake, it is necessary to consider the completion of a stratigraphic study that allows having greater certainty of using the appropriate profiles. It is also important to verify the presence of organic matter, which is necessary to carry out 14C dating. Organic matter can ensure efficient preservation of fossil palynomorphs, which improves the accuracy of studies. In the case of this project, the identification of the strata with greater presence of organic matter was especially useful for the vegetation team to perform an approximate calculation of the area that the bofedal might have had before the canalization works were introduced in the Silala area (see subtitle 7.2 of this report).

2. 14C dating: With the data from the dating completed (Annex 4) and the stratigraphy, the age- depth model was constructed by means of the Clam program (Blaauw, 2010), for the South bofedal BSP2 profile and the North bofedal BNP7 profile. The BSP14 profile does not have an age model, due to a slow sedimentation process (see section 7.3.a). The calculations of age models were completed on basis of the dating available per profile, before making the pollen diagrams. Therefore, the age model is first performed in order to be able to relate [it] to the profile depth. Finally, this relationship is used to interpret and compare the palynological and geochemical data (XRD).

3. Geochemical analysis: The profiles selected for the geochemical analysis are: BSP14, located in the South bofedal area, with current vegetation in good condition; the BSP2 profile, located in a degraded area of the South Bofedal, with saline outcrops; and the BNP7 profile, located in a currently stable vegetation area, in the North bofedal.

The XRD geochemical analysis is a method that measures the concentration of chemical elements and their changes over time. The presence of the different elements constitutes indicators of impacts or effects that occurred in the environment. To visualize the information, the data are presented in a chemical element diagram that allows relating the concentrations with the age models (see figures 7, 12). In the case of the Silala, the results of the records obtained for the period following 1900 are the ones used to interpret the effects of canalization (BSP2, BSP14 and BNP7). Additionally, the BNP7 profile recorded a climatic event related to the dry phase of the Little Ice Age.

4. Palynological analysis: The percentages of relative abundance of the palynomorphs found during pollen counts are plotted in the polynomial diagrams. These values represent the relative abundance of the different taxa represented by pollen, spores, algae and amoebas generally denominated palynomorphs. In the case of algae and amoebas, these are not pollen elements, but rather palynomorphs that are useful for interpretations, since they are indicators of the environmental conditions of interest, such as water availability and others. The pollen count was performed with a high resolution level, determining approximately 300 grains of pollen every 0.5 centimeters; in addition, markers of Lycopodium spores, added to the samples, were also counted during the chemical treatment of the sediment in the laboratory; this marker is counted within the samples to obtain pollen concentration (see Annex 2). To carry out a proper vegetation reconstruction, the age calibration model and the soil stratification profile are added to the right side of the pollen diagram.

Additionally, a figure of the pollen count diagram was added as a function of the total pollen concentration for each taxon for the BSP2 profile. In this case, the relationship between the pollen count values and the Lycopodium count values is used; the value provides the amount of pollen that is found in 1 cm-3 of the sample.

In the pollen diagram, a zoning was carried out, which defined several “zones”, which were used as a basis to describe the results and reconstruct the vegetation. These zones were defined as a function of the changes recorded in the composition of taxa identified in the pollen count and their relation in a determined period of time. Four pollen zones were identified in the BSP2 and BNP7 profiles, and three in the BSP14 profile, which correspond to periods of time with evident changes in the composition of pollen taxa. Annex 3 presents some of the pollens determined in the study, as well as some photos of the pollen obtained from reference plates of plants collected in the Silala, during the field work.

6. Sampling points

For the sampling of the profiles in the South Bofedal, an approximately longitudinal transect was followed from the first water springs to the border, along which seven profiles were obtained and two trial pits were dug and sampled. The criterion used to carry out the transect was based on the assumption that the southeastern part of the Silala suffered a strong drying effect, which is currently observed in the vegetation map and corresponds to the bare soil area (see Figure 2).

The South bofedal presents an irregular and reduced depth, reaching a maximum of 1m in the deepest parts (DIREMAR 2017). The depth of the soil profiles that were drilled reached 60 cm. On the other hand, the physiognomy of the vegetation shows a visible degree of impairment, due to the severe desiccation of the bofedal, as a result of the water canalization and diversion. Of the seven profiles made in the South Bofedal, four were identified and were thoroughly studied from the stratigraphic point of view of the soil (BSP2, BSP6, BSP8, BSP10, BSP14) (Figure 2A), in addition to the trial test pits BSP7, BSP9 (see Table 1 and Fig.2). Profiles BSP2 and BSP14 were studied with palynological methods, dating and heavy metal studies.

Table 1: Profiles and trial pits selected for the South Bofedal (analyzed in depth for this report). The dated profile (analyzed in depth for the present report) is shown in italics and the trial pits are presented in bold letters.

Code	**Geographical reference (UTM) 19K**		**Altitude (m)**	**Depth (cm)**
	E	**N**		
BSP2	602984	7565848	4412	42, 0
BSP6	603110	7565799	4416	58, 0
BSP8	603331	7565708	4413	24, 0
BSP10	602901	7565841	4415	41,6
BSP14	602846	7565820	4412	43,5
BSP7	603331	7565713	4413	63, 0
BSP9	603382	7565700	4416	44, 0
BNP7	600842	7566289	4364	73,5
BNP1	600931	7566328	4367	48, 0
BNP3	600758	7566262	4352	22,2
BNP4	600846	7566295	4354	150,9



Figure 2. Area surveyed with the sampling points in the South Silala Bofedal. A) Longitudinal transect sampling for the South Bofedal. B) Transverse and longitudinal transect of samples for the North Bofedal. The points correspond to the sampling of stratigraphic profiles (Table 1). The orange line indicates the transect direction.

Four profiles were carried out in the North Bofedal, bearing the codes BNP1, BNP3, BNP4, BNP7 (Table 1, Fig. 2B); the sampling was carried out in such a way that the profiles are located longitudinally in the bofedal, except for the BNP6 profile made close to the edge (Figure 2B). Of these profiles, BNP7 was dated and studied with palynological methods and with a heavy metal survey. The physiognomy of the vegetation shows a greater drying effect on the far ends of the North bofedal main canal, while the cushions bordering the main artificial canal remain in good condition (Figure 2B).

The depth of the soil in the North Bofedal is irregular, like the South bofedal; however, the profiles reached greater depth, reaching 151 cm in the BNP4 profile. According to the vegetation and soil report records (DIREMAR 2017), the average depth in the North Bofedal is 111 cm.

7. Results and interpretations

7.1. Interpretation/stratigraphic description of the soils in the South Bofedal (profile BSP2 and BSP14)

The BSP2 profile has a depth of approximately 40 cm, dominated mainly by fine sand, from the profile base to a depth of 8 cm, when the substrate is dominated by organic matter towards the profile surface (Figure 3A) (Annex 1). This variation in the deposition of sedimentary material shows a change in the water flows, which reduced with the settlement of organic matter. In addition, with the help of the age model, it is possible to demonstrate that the last 20 cm of the profile represent the last 120 years of the bofedal (Figure 3B).

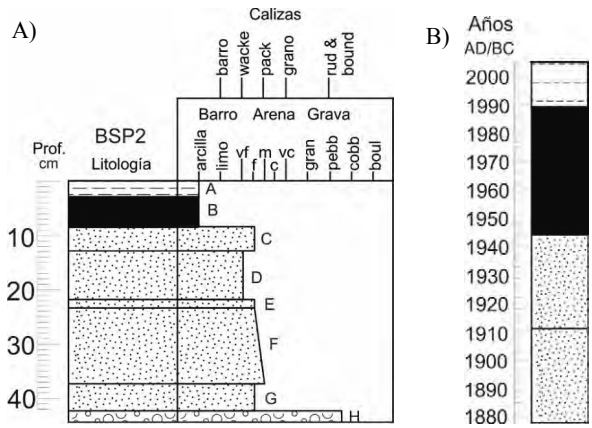


Figure 3. Graphical representation of the stratigraphic description of BSP2 profile in relation to the profile depth (cm) A). Lithological relationship of the profile with the age model from 1880. B) The same as A, but for the last 17 cm of the stratigraphic profile.

On the other hand, the BSP14 profile shows two layers of organic matter, one between 1-10 cm of depth and another between 16-22 cm (see Figure 4) (Annex 1). These layers indicate the development of a bofedal in these areas, which might have been interrupted during some periods of time.

The first change of soil stratum happened near the point with dating that corresponds to an age of 680 – 862 years ago, and therefore in a period prior to the canalization process; the first change of stratum in the soil can be evidenced. The change that occurred was from a high percentage of organic matter to a soil with a higher percentage of fine sand particles, in a clay-silty matrix. The beginning of this process indicates that the bofedal-characteristic vegetation is likely to have stopped developing, due to the presence of more water, derived from the reactivation of water flows at this point. This type of stratum continued until the next change, which occurred between 1960 – 1980 years (Figure 6). This period corresponds to the critical period, due to a lack of water, that occurred approximately 50 years after the canalization works were installed—which remain in operation until the present time.

The increase in organic matter at this stage suggests a new reduction in water availability, which caused a desiccation at the site and led to the re-establishment and/or re-colonization of typical bofedal species. This process was accompanied by a change in the soil structure, with an increase in organic matter. In this period, a process of eutrophication seems to have occurred, which occurs when a waterbody dries up and puddles of stagnant water are produced.

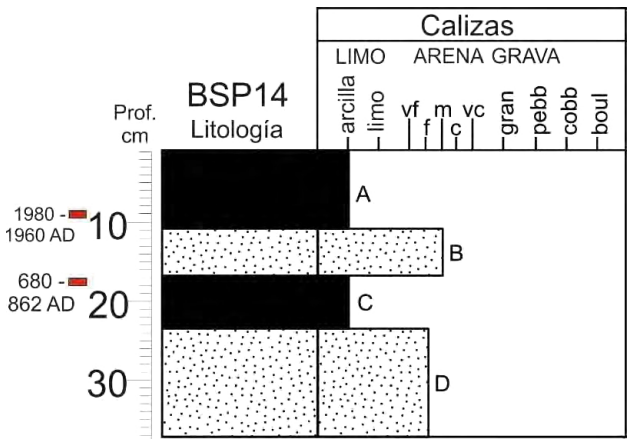


Figure 4. Graphical representation of the stratigraphic description of BSP14 profile in relation to the profile depth (cm), where the ^{14}C dating points are punctually highlighted

7.2. *Interpretation of the stratigraphic profile relation – extent of the South Bofedal*

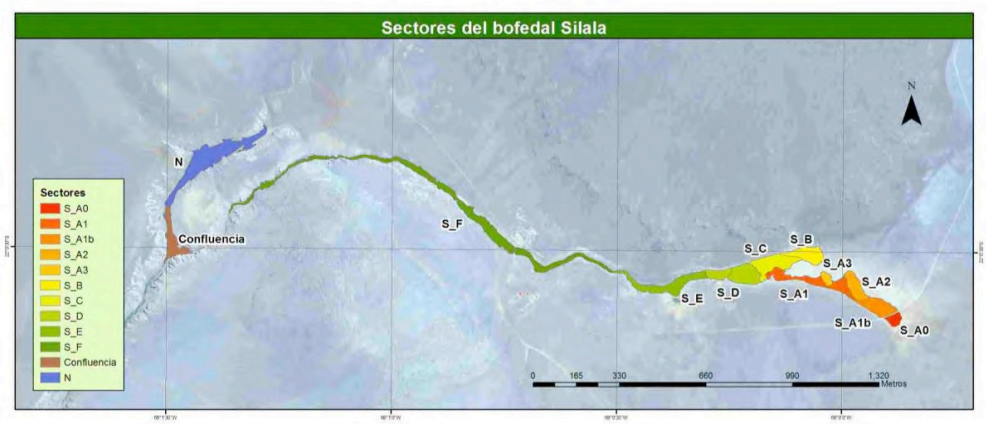


Figure 5. Image taken from the IEIA Silala 2 report (figure 24), showing the differentiation of the fragments in the North, South and confluence Bofedals. The characteristics of the fragments are detailed in table 13 of the final report: "Survey of Environmental Assessment in the Silala" (IEIA Silala).

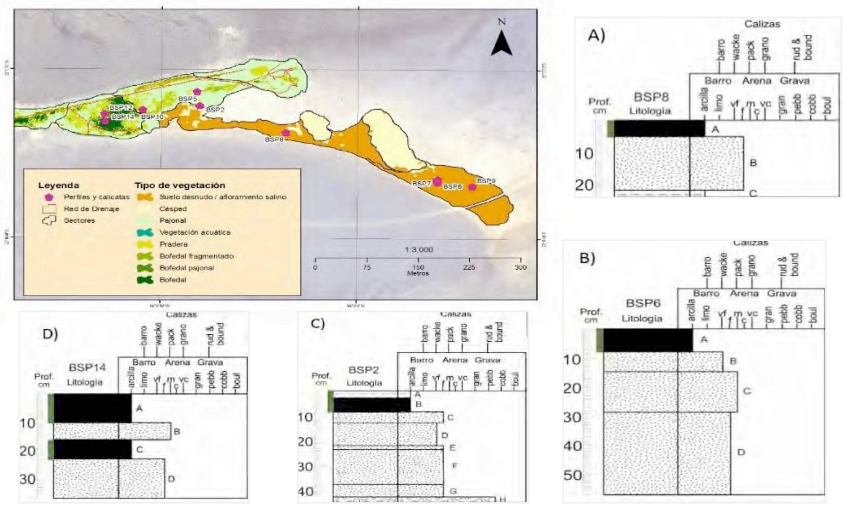


Figure 6. Stratigraphy of profiles of the South Bofedal and their location in the areas defined in the vegetation survey from the Silala environmental impact report, where profiles BSP8 (A), BSP6 (B), BSP2 (C) and D) BSP4 (D) are shown.

In the second environmental impact report of the Silala study (IEIA Silala 2, section 6.5), different patches of plant communities were differentiated in the South Bofedal (Figure 5). The longitudinal transect of the collection of profile samples for the present study follows a gradient of reduction of humid conditions, which are reflected in the physiognomy of the vegetation towards the southeast of the area surveyed.

In the last point, area S_A0 (Figure 5), it was difficult to obtain a compact soil profile, because the substrate of that site had a high percentage of sand, supported by a silty matrix; thus, a trial pit had to be made at that point (profile BSC9). This type of soil is usually found in sites with water accumulation. On the surface of the S_A0 area (Figure 5) substrates of reduced vegetation were found in areas of bare soil, represented mainly by Deyeuxia curvula. The tillers of this species are shown inclined towards the direction of the wind, because they are exposed to wind currents. Wind erosion is a very strong environmental pressure in the study area; it promotes a slow formation of soils, which occurs almost only in sites with vegetation.

Soil profile BSP8 (Figure 6A) is found in vegetation type S_A1b (Figure 5), which has a predominance of Deyeuxia curvula and the presence of Xenophyllum incisum var. incissum, which is

a species that is an indicator of high humidity in the soil inasmuch as it grows on edges of waterbodies and/or bofedals (IEIA Silala 2).

Coincidentally, the first 5 cm of the BSP8 profile presented organic matter, which was not found in the BSC9 profile. This suggests that the establishment of bofedal species occurred in the S_A1b patch, capable of contributing to the formation of soil rich in organic matter. This hypothesis is based on the fact that the study area is in an arid environment, where there is strong soil erosion and slow humification processes, which reduce the likelihood of soil formation with a high amount of organic matter. Therefore, in the absence of bofedal vegetation, which contributes to the formation of organic matter, the soil would present a high percentage of sand, as observed during field work on the slopes (rocky and scrub) that surround the bofedals. These interpretations indicate that vegetation patch S_A1b was part of the extent of the south bofedal, as indicated in the vegetation report (IEIA Silala 2).

Unlike profiles BSC9 and BSP8, profiles BSP2 (Figures 6C) and BSP6 (Figure 6B) are found in areas with remnants of cushions of Oxychloe andina (a species characteristic of bofedals). At present, these areas are found in bare soils with saline outcrops (see Figure 5 and 6) and were classified as open pastures of sectors enduring a desiccation process (IEIA Silala 2). However, the thickness of the layers of superficial organic matter found in these profiles (8 and 7 cm, respectively) indicate that these areas comprised bofedals in the past.

7.3.Paleoecological interpretations and age-depth model for the South Bofedal (profiles BSP2 and BSP14)

With the information of the dating and stratigraphy, the age-depth model was built for the BSP2 profiles of the South Bofedal. The BSP14 profile does not have an age model, due to a slow sedimentation process (see section 7.1). The calculations of the age models were based on the dating available per profile before making the pollen diagrams. Therefore, the age model was first performed in order to relate it to the profile depth. Finally, this relationship is used to confirm with the palynological and geochemical data (XRD).

7.3.a. Age depth model based on 14C dating in the South Bofedal

The BSP2 and BSP14 soil profiles were dated in the South bofedal. The results of the calibration of 14C dating were analyzed in the Clam program (Blaauw, 2010), on basis of two dating surveys

completed at different depths for each profile. For the BSP2 profile, the first dating was performed at 7 cm depth and corresponds to the year 1958 AD. The second dating was 38 cm deep and corresponds to 1711 AD. The age-depth model shows a linear relationship with constant sedimentation, where it can be inferred that every 5 mm of depth in the profile there is sediment accumulation that corresponds to a period of 8 years (Figure 7).

The model is supported by the concentration of atmospheric lead (Pb) obtained from the geochemical analyzes (Figure 9), which shows a high coincidence with the atmospheric accumulation of Pb, which increased between 1930 and 1970-80, due to the use of Pb to improve gasoline (Espi et al., 1997). This atmospheric accumulation of Pb was reduced from 1980 onwards, when the use of Pb was banned, due to its negative effects on the environment. In profile BSP2, the atmospheric deposition of Pb increases from approximately 1935 to 1980 to then decrease. These results concur with other scientific investigations (Espi et al., 1997), which corroborates the high reliability of the model used in this study.

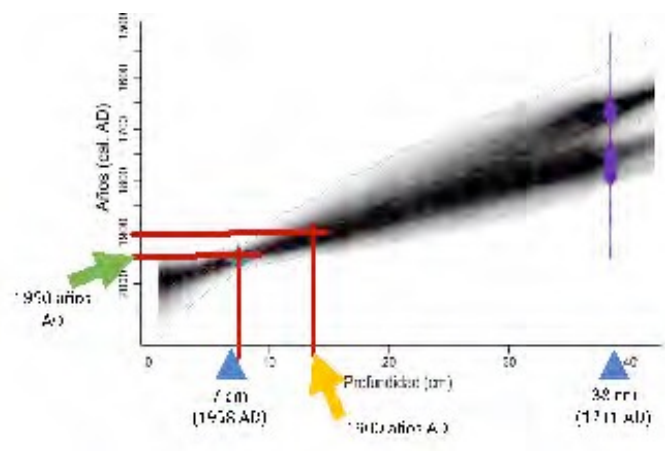


Figure 7. Age-Depth model of the BSP2 sediment profile of the South bofedal.

For the BSP14 profile, the calibration results based on 14C dating show a large difference in ages between the two dating points (> 1000 years between each point, Figure 4). The most superficial dating point (9.5 cm depth) corresponds to the period between 1980-1960, with a reliability of 84.6%. The second dating (at 17.5 cm depth) corresponds to an age between 680-862 years, with a reliability 95.4%.

Due to the short difference in depth between the two points submitted to dating, it is not advisable to develop an age-depth model, as in the case of the BSP2 profile, since in this case it would be necessary

to have a greater number of dating surveys. For this reason, the interpretation of the historical reconstruction in this profile will be carried out on basis of the relation of variations obtained from the other (stratigraphic, geochemical and palynological) analyzes and the intervals that are observed before and after the points where the dating surveys were completed The interpretations are made in a depth scale of centimeters.

7.3.b. Geochemical analysis (XRD) of the South bofedal (profile BSP2 and BSP14)

7.3.b.1. Geochemical analysis in the BSP2 soil profile

The age-depth model indicates that a depth of approximately 17 cm corresponds to 1880 AD (AD = anno dominia = after Christ = current calendar, all ages mentioned below correspond to AD). According to the same model, a depth of 8 cm would correspond to 1950. For the following interpretations, we take these points as a reference (Figure 7).

Figure 8a shows that the concentrations of lead (Pb) present fluctuating values between 1880 and 1975, approximately; with peaks in 1935 and 1953. From 1975 onwards, the values of lead begin to drop, coinciding with a decrease in the use of lead in gasoline globally.

Iron (Fe) values remain high from 1880 to 1906, with a peak towards the end of that period. Subsequently, the concentration of Fe declined steeply until 1925 to then rise again to reach another peak in 1938. This high iron value was remained the same until 1953 and then fell continuously until 1990, when a slight increase can be observed, lasting until the present (Figure 8b).

The concentration of bromine (Br) shows stable values between 1906 and 1948; it then presents slight oscillations in its concentrations until 1940, when it began to increase, reaching a peak in 1958. These values of Br remain high, with slight changes, until 1982, and then drop up to the present time (Figure 8c).

The concentration of nickel (Ni) remained stable from 1878 to 1906. Subsequently, the nickel values dropped markedly until 1925. From that date on, the values began to

increase following the same pattern of bromine, reaching high values from 1968 to 1990, with more marked fluctuations than Br (Figures 8c and d).

The ratio between silicon and titanium (Si/Ti) remains constant from 1880 to 1916. From 1916 onwards, a slight increase began and remained the same until 1950. From 1950 onwards, the Si/Ti ratio increased drastically until 1985. Subsequently, the Si/Ti values decreased until 2004, to slightly increase again, up to the present (Figure 9e).

The ratio between iron and titanium (Fe/Ti) remains constant from 1880 to 1916. As of that date, the Fe/Ti values increase slightly until 1925, with a peak in 1935. A decrease is then observed until 1978, prolonging up to the present (Figure 8f).

The ratio of manganese and titanium (Mn/Ti) remains stable in the same period as Fe/Ti. As of approximately 1916, a slight increase in the Mn/Ti ratio has been recorded, reaching its maximum point in 1980. It subsequently decreased until 2004, when a new increase started and remained up to the present (Figure 8f and g).

The Mn/Fe ratio shows a pattern similar to of the Mn/Ti ratio, but it is not as marked as the former (Figure 9).

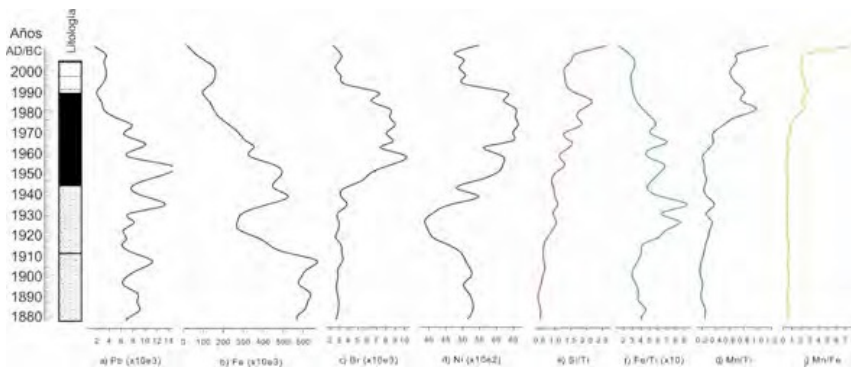


Figure 8. Trace elements found in the geochemical analysis of BSP2 profile, in concentration per second (cps)

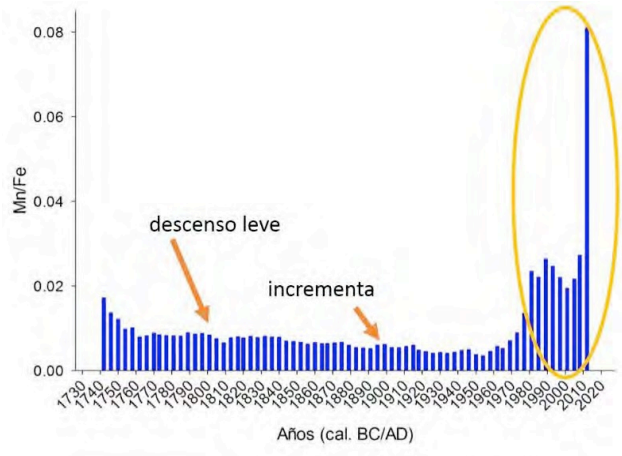


Figure 9. Mn/Fe ratio in a soil profile from the South Bofedal (BSP2) of the Silala region – Bolivia. In the x-axis, the age scale is observed in years AD and in the y-axis and the values of the Mn/Fe ratios

7.3.b.2. Geochemical analysis of soil profile BSP14

The silicon/titanium (Si/Ti) ratio presents a peak prior to the 680 – 862 period. The Si/Ti ratio then presents a reduction and a subsequent stabilization between 1960 and 1980. From this point onwards, the values increase gradually (Figure 10a).

The iron/titanium (Fe/Ti) ratio remains stable until the period between 1960 – 1980, when a gradual increase is observed, reaching a maximum peak at 4 cm depth (after 1960-1980), to then decrease towards the present profile (Figure 10b).

The variations in the manganese/titanium (Mn/Ti) and manganese/iron (Mn/Fe) ratios show similar stable values up to the 1960-1980 calibrated years, with a subsequent increase in both ratios' fluctuations (Figures 10 c and d, respectively).

The lead concentration (Pb) presents fluctuating values from the lowest profile levels, with a high peak in the period of stratification profile change, which took place before the 680 and 862 period. Subsequently, an interval of decrease in the deposition of Pb is registered until the 1960-1980 period, when the Pb concentration increased abruptly, with another peak at 8 cm depth (after 1960-1980), to then decrease and fluctuate towards the present time (Figure 10 e).

The iron (Fe) concentration presents low values in the profile base, increasing abruptly in the 680 and 1980 period, although with strong fluctuations. Subsequently, the concentration of Fe is reduced towards the upper levels of the profile, corresponding to more recent times (Figure 10 f).

The concentration values of Br and Ni follow the same pattern, with fluctuating values until a period before the 680-862 interval. Since then, a reduction in the concentration of Br and Ni is registered, coinciding with the change of soil from organic material to sand and prolonging up to 1960 to 1980. Subsequently, the concentrations of Br and Ni increase and remain stable up to the surface of the profile (Figures 10 g and h respectively).

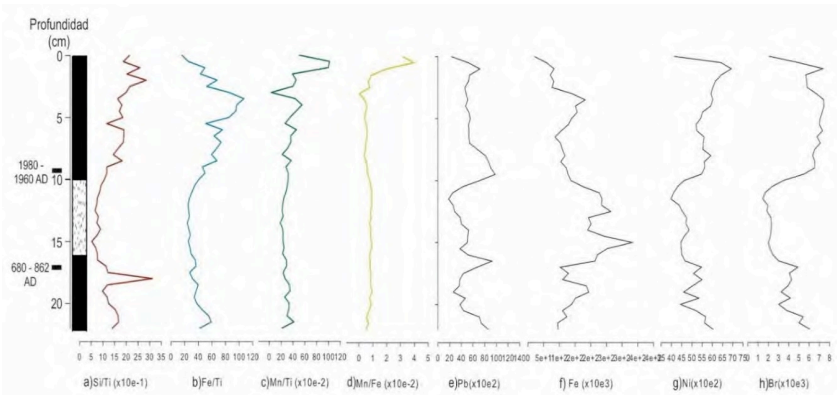


Figure 10. Concentration in cps of trace elements found in the geochemical analysis of BSP14 profile

7.3.c. Zoning of palynological samples from the South Bofedal (profiles BSP2 and BSP14)

7.3.c.1. Zoning of soil profile BSP2

The results of the counting of palynomorphic counts, described according to the zonation (zones) that indicate taxon changes in certain time spaces (Figures 12 and 13) are presented below.

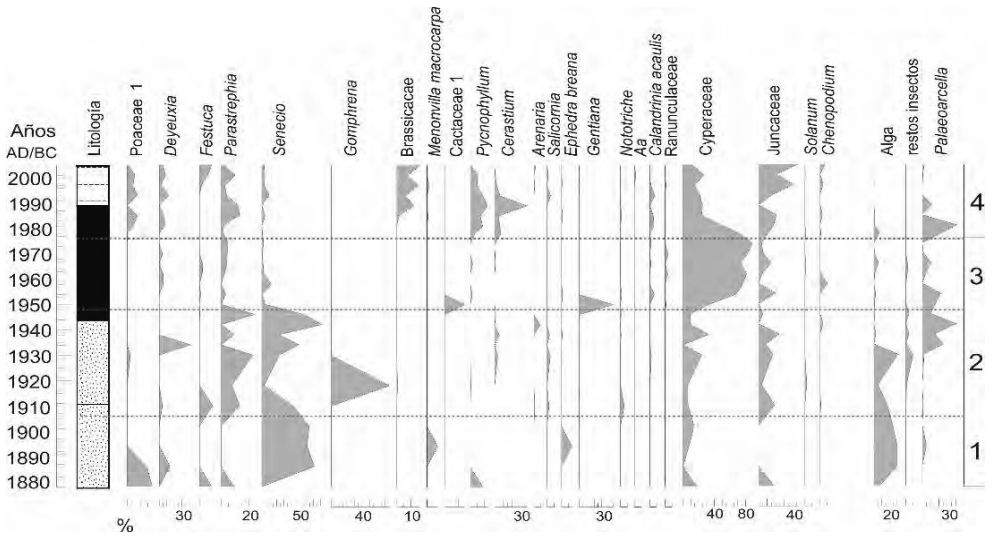


Figure 11. Percentage of representative pollen taxa found in sediment profile BSP2. On the left, it is possible to observe the AD time scale accompanied by the lithology of the profile studied, and to the right the zonation that defines the changes in vegetation, extended in the diagram with red lines.

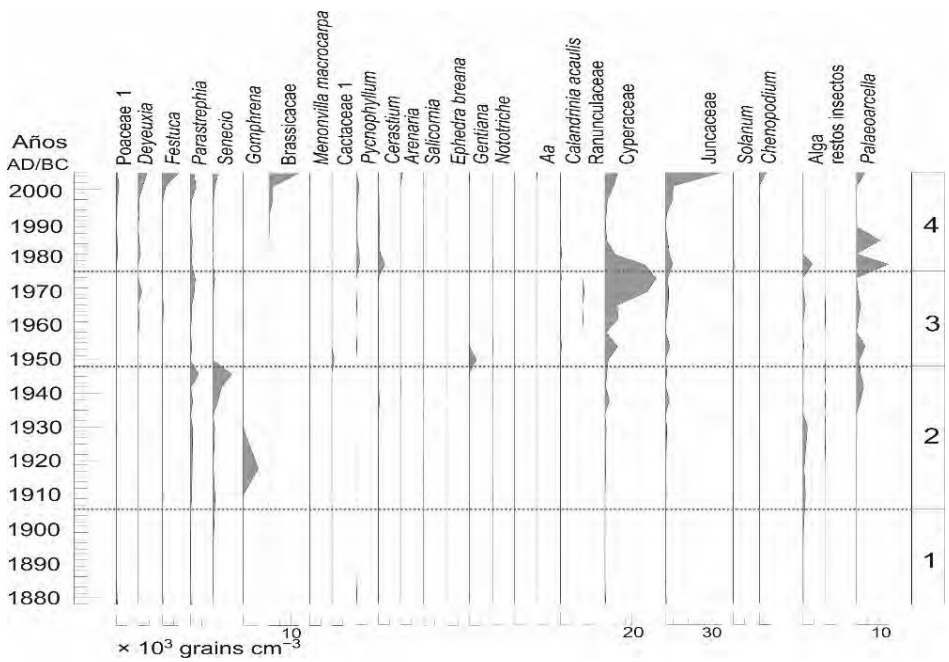


Figure 12. Pollen diagram of the concentrations of pollen, spore, algae and ameba taxa (palynomorphs) counted in the profile and related to Lycopodium spore counting to calculate the amount of palynomorphs that exist in a cm3 of sediments treated in the BSP2 laboratory. To the left, the time scale in AD years, and to the right, the zoning that defines the vegetation changes extended in the diagram with red lines

Zone 1 (1878-1906 AD): predominance of terrestrial species of Asteraceae (Senecio), and also percentages > 20% of algae, but in low concentrations that correspond to less than 1000 grains of palynomorphs per cm3 of soil sample treated in the laboratory.

Zone 2 (1906-1948 AD): the percentages of algae decrease (<10%), fluctuating until almost, from 1935 to approximately 1950 [sic]. While, the values of terrestrial plants increase, Gomphrena (Amaranthaceae), Parastrephia (Asteraceae) and Senecio (Asteraceae) as of 1935, where the pollen concentration of Asteraceae increases, together with Cyperaceae and Palaeoarcella amoeba; it is worth noting that the amoeba is not pollen, but a palynomorph, which in this case constitutes a protozoan that has a carapace or teak, and that is preserved in a similar way as pollen (Silva Do Santos et al., 2011). In this zone, the pollen concentration increases, mainly for terrestrial pollen (> 5000 grains per cm3).

Zone 3 (1948-1976 AD): in this age range, there is a considerable increase in the presence of Cyperaceae (which reaches a percentage greater than 60%). At the same time, it reduces the presence of terrestrial pollen and increases the presence of Palaeoarcella ameba carapaces. Pollen concentrations increase progressively, showing a concentration of > 5000 grains per cm3 of soil to > 25,000 grains per cm3 towards the end of the zone.

Zone 4 (1976 AD - present): an abrupt reduction of Cyperaceae (<20%) and of Palaeoarcella, coinciding with an increase in the presence of terrestrial taxa (Parastrephia, Senecio, Brassicaceae, Pycnophyllum and Cerastium), as well as Poaceae, in addition to an increase of Juncaceae from 1997 to the present; the concentrations drop again until the end of the zone that they increase, mainly due to the presence of Juncaceae, accompanied by Cyperaceae and Brassicaceae (> 30,000 grains per cm3).

7.3.c.2. Zoning of soil profile BSP14

The percentages obtained from the pollen counting are outlined in the pollen diagram as a function of their depth (Fig. 13). To The lithology and dating values obtained in the chosen depths – performed through the 14C method – are presented on the left side of Figure 16.

The zonings were performed as a function of a change in the composition of taxa identified at different depths. The pollen diagram for the South Bofedal (BSP 14) corresponds to a depth of 20 cm, allowing to focus on a period of time of 100 years—although from the dating results,

the profile is older than 1000. Annex 3 presents some palynomorph records found in the countings. The palynological interpretations were performed in the same way as for the XRD analysis, taking into account three phases with evident changes in the pollen taxa composition.

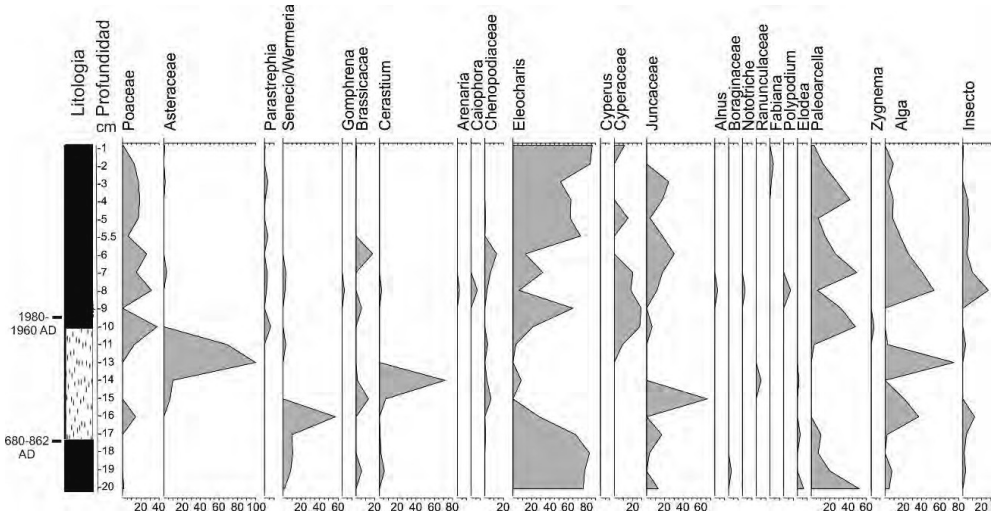


Figure 13. Percentage of representative pollen taxa found in sediment profile BSP14. To the left, the depth (in cm) accompanied by the lithology of the profile studied and the points at which dating was completed

The description of the counting of palynomorph counts, described as a function of the zonings (zones) and indicating taxa changes in determined time spaces, is presented below.

Zone 1 (20 - 18 cm deep, stage prior to the 680 – 862 period): in this temporal zone, the dominant pollen is Eleocharis (Cyperaceae) (~ 80%), accompanied, in smaller proportion, by Paleoarcella (~ 10 – 40%) and Juncaceae (<10%). In addition, the presence of Senecio and Cerastium (<10%) is verified.

Zone 2 (18 – 10 cm deep, between 680-862 to 1980-1960): predominance of taxa of Cerastium (~ 60%), Brassicaceae (20%), Senecio (~ 50%) and other Asteraceae (~ 80%). Eleocharis is very reduced (<5%), along with the Paleoarcella amoeba, which disappears in this period. In contrast, Juncaceae increases with a high peak (~ 60%) and an increase in the presence of algae is observed (~ 40%).

Zone 3 (10 – 0 cm of depth, second period, subsequent to the 1960 – 1980 calibrated years): The decrease or disappearance of taxa of Asteraceae, Gomphrena, Brassicaceae and Cerastium (with values <5%) is verified. On the other hand, there is an increase of Eleocharis (~ 20 – 80%), Juncaceae (~ 20%), Poaceae (> 20%) and Paleoarcella amoeba (~ 20 - 40%). In addition, there is a progressive reduction in the presence of algae (<40%) and aquatic insects (<20%).

7.3.d. Changes observed in the vegetation of the South Bofedal (profiles BSP2 and BSP14)

7.3.d.1. Vegetation changes observed in soil profile BSP2

In general, low concentrations of pollen and palynomorphs were found during the period prior to the canalization (between 1878 and 1906), this is due to the fact that the geochemical analysis indicates a deposition of terrigenous elements, which are small rock and mineral fragments, among others that are dragged from a terrain by erosion and that are constantly deposited in the sediment; this deposition in the stratification is interpreted as the circulation of water with more stable levels in this period.

The results as a whole show that part of the pollen determined belongs to a local vegetation that is currently found in areas near this point of the BSP2 profile and is represented mainly by shrubs of Asteraceae, such as Senecio, Parastrephia lepidophyla and P. quadrandularis, and some Poaceae (Festuca and Deyeuxia)—species that have a high ecological value for presenting adaptations that allow them to develop in arid ecosystems (IEIA silala2); the presence of the pollens of these species indicate that the site surveyed had a larger cover of this type of vegetation and, consequently, higher humidity than that observed in stages subsequent to the canalization, 1906 approximately.

The presence of these thola-forming species before the introduction of canalization works seems to indicate that, at this stage, their development was favored mainly by a scarce anthropic use that intensified thereafter, following the canalization, for its use as firewood, markedly reducing the pollen percentages of these species. Asteraceae pollen has higher percentages between 1880 and 1930, remaining the same until the 1950s, when its abrupt reduction began, which is the most critical stage of the canalization effects.

Between 1910 and 1930, an increase of Gomphrena pollen is observed. Due to the location of these sites, it is likely that this corresponds to the Gomphrena umbellata species, which is an annual species that sprouts in large quantities when there is abundant precipitation. This observation supports the interpretation of the existence of higher humidity conditions in the environment before the 1950s. In addition, in the pollen counts, it is also possible to observe the presence of algae (non-pollinic palynomorphs), between 1880 and 1906, which it reduces from approximately 1908, to then almost disappear towards 1935.

In the palynological survey, it is possible to distinguish four stages of humidity changes in the environment, which have occurred gradually: i) The first one lasted from 1880 to 1930, showing higher levels of water at the site, identified by the high percentages of algae. ii) The second occurred between 1930 to 1950, where a gradual reduction of water flows is detected, producing stagnant waters (puddles), identified by the presence of Palaeoarcella, an amoeba that grows in this type of water [and] is used as an indicator of these aquatic environments (Traverse 2007), in addition to the presence of macroinvertebrate remains, (the dipterous larvae of the Chironomidae family), typical of these environments, all these palonimorphs decrease in percentage from 1950 onwards [sic]. iii) The third stage coincides with a critical dry environment, from 1950 onwards, when a reduction of pollen and palynomorphs, indicating wet environments, is observed. iv) The fourth stage occurred between 1990 to present, approximately, identified by the reduction of Cyperaceae pollen and which is almost replaced Juncaceae since 1997, accompanied by the increase of taxa of terrestrial shrubs (Parastrephia, Senecio, Brassicaceae, Pycnophyllum) and graminoids (Deyeuxia, Festuca), in minor concentration; this stage coincides with the canalization dismantling process in the bofedals.

The third stage, identified in the palynological analysis, coincides with the increase in the concentrations of nickel (Ni), bromine (Br) and manganese (Mn) after 1950, attributed to the accelerated humification. On the other hand, in this stage, it is possible to observe an abrupt increase in the percentages of Cyperaceae in the pollen diagram, a family whose species found in the Silala have been classified as opportunistic since they invade areas rich in organic matter and moisture, easily invading bofedals that are undergoing a fragmentation process. Another indicator of disturbance and fragmentation in the bofedals, after 1950, is the progressive increase of graminoids, which is related to an increase in the values of the Silicon/Titanium (Si/Ti) ratio attributed here as the deposition of phytoliths coming from the graminoids.

With these results we propose a hypothesis, based on the interpretation of the BSP2 profile, which indicates that the area flooded from the beginning of the 20th century to the 50s, which then gradually decreased. After the 50s, a drier environment is observed, favoring the increase of plants of the Cyperaceae family, soil salinization and a greater oxidation in the environment.

7.3.d.2. Vegetation changes observed in the BSP14 soil profile

In the first period (prior to the calibrated age of 680-862), it is possible to observe a predominance of Eleocharis (Cyperaceae), a plant that colonizes disturbed bofedals (IEIA Silala 2). On the other hand, the presence of Paleoarcella is also verified, which is related to stagnant waters and is an indication of a desiccation process in the middle. The intermediate period is related to a wet phase, suggested by the reduction in pollen of bofedal species (Eleocharis and Juncaceae) and the increase in the presence of algae.

The wet phase of this intermediate period (between the calibrated ages of 680-862 to 1962-1980) is supported by an increase in the presence of pollen of Parastrephia, Senecio, other Asteraceae and Cerastium [sic]. These groups decrease in subsequent stages, suggesting that, before canalization, thola shrubs and other composite and herbaceous shrubs were more abundant in the surrounding areas. The reduction of these palynomorphs is more marked after the 1960-1980 period and is attributed to the anthropic use of these resources, which is likely to have caused a reduction in the plant cover of these species.

In the third period (following the calibrated age of 1980-1962), and towards the present, it is possible to observe a gradual process of desiccation in the environment and the surrounding areas, with a reduction of shrub vegetation (thola shrubs). In addition, there is a predominance of Eleocharis and Poaceae, associated to a process of bofedal fragmentation, which was probably exploited by graminoids that colonized those bofedal areas. Another identified palynomorph that reaches high percentages in this period is the Palaeoarcella amoeba, which is also an indication of water stagnation and desiccation at the site.

7.4. Effects of canalization on the South Bofedal

7.4.a. Effects of canalization on soil profile BSP2

The geochemical study of the BSP2 profile evidences the effects of canalization (Figure 9). Changes are observed in the concentrations of terrigenous elements such as iron, bromine and nickel, which are indicators of the processes that occurred due to the canalization of the Silala springs. The mineral elements that were deposited by erosion, such as titanium, aluminum, zirconium and rubidium (not graphed), follow the same pattern as iron concentrations (Figure 10b), found along the entire BSP2 profile. These patterns give evidence of three changes, the first two are abrupt reductions in the deposition of these minerals: i) the first between 1908 to 1925, as a first effect of the canalization process, ii) the second coincides with the photo of the image satellite data taken in 1960, where it can be observed that the South bofedal was very dry (IEIA Silala2) and that the artificial canals were clearly defined. In this context, our results strongly suggest that the construction of canals led to bofedal desiccation and degradation, and influenced the increase in aridity in the surrounding areas. The third change iii) occurs from 1993 onwards, when a slight increase in the concentrations of terrigenous elements is observed, coinciding with the period of bofedal recovery, which occurred after 1995, according to historical data.

In nature, Bromine is found in the form of salts or organic substances. These substances are produced by various organisms. Bromine is mainly found in water soluble salts and is obtained from the oxidation of saline waters; in addition, it has been observed that humification processes promote the formation of bromine, by forming humic acids (Zaccone et al., 2008). The processes of humification occur due to a rapid decomposition of the organic matter for the formation of peat. The increase in bromine (Figure 9c), recorded between 1940 and 1982, must be related to the bofedal desiccation process and, consequently, to the accelerated humification, which occurred as a result of the canalization of the bofedals and/or springs and that promoted – in the area where the profile was made – the deposition of bromine as a result of the process of formation of humic acids and oxidation of salty waters.

Nickel accumulates in the sediments from the high flow of particles highly related to the presence of organic carbon and the chlorophyll fluxes, which occur due to the decomposition of diatoms and/or plants in saline waters: for this reason, nickel is considered a good paleo-indicator of organic carbon production; although due to elements such as Cu and Zn,

it tends to be masked with anthropic uses, creating confusion in the interpretation of the origin of its deposition (Böning, et al., 2015). In the profile studied, the age interval (1940 to 1982), in which an increase in nickel is observed (Figure 9d), coincides with the one that has the highest concentration of bromine, caused by the decomposition of plant matter. The changes in the concentrations of both elements, Br and Ni, indicate that there was a eutrophication process in the wetlands, which perhaps was accelerated by the humification process, increasing the total organic carbon.

Silicon is common in environments of volcanic origin (quartz sandstone), but it can also be of organic origin, as it is an abundant component of graminoid species (in phytoliths, Schittek et al., 2014). In dry environments, as in the Silala, silicon is found in the plants of the graminoid group, which are part of the characteristic vegetation (tillers) that grasslands form on slopes and plains. These graminoids colonize the bofedals that are undergoing a fragmentation process due to lack of water. In this sense, the presence of graminoids within the Juncaceae cushions is considered as an indicator of bofedal degradation as said family predominates in well preserved bofedales (IEIA Silala 2). The increase in the values of the Si/Ti ratio in the profile coincides with periods in which the environment underwent a desiccation process. This fact allows deducing that this increase was associated with the phytolith deposition that occurred gradually since the beginning of the 20th century, but with greater intensity from 1950 to 1985 (Figure 9e), when the effects of canalization were critical. The Si/Ti ratio then decreases towards the present time. This signal given by the Si/Ti relationship fully concurs with the other aspects that are indications of bofedal fragmentation following the introduction of canalization works.

According to Schittek et al. (2015, 2016), well-preserved bofedals generally have stable water levels and anoxic conditions. In these bofedals, the values of the iron and titanium (Fe/Ti) ratio are reduced, unlike the values of manganese/titanium (Mn/Ti) and manganese/iron (Mn/Fe), which are high. Based on the results obtained by Schittek et al. (2015, 2016), it is possible to interpret that the increase in the Fe/Ti ratio (Figure 9f) indicates greater Fe oxidation on the surface derived from water level changes, which are in turn the result of canalization. These alterations in water availability began in stages subsequent to 1925 and lasted until the 1980s, showing some consistency with the values of Mn/Ti and Mn/Fe (Figures 9j and 10), whose values are visibly reduced from 1960 onwards.

7.4.b. Effects of the canalization on soil profile BSP14

The interpretation for this profile was made in three parts, i) the period preceding the canalization, corresponding to 680 – 862; ii) an intermediate period between 680 – 862 and the most recent period of 1960 – 1980, where it was possible to observe, as has already been noted, a change in the stratigraphic composition, with an increase in sand and silt particles; and iii) a third period following 1960 and 1980.

In the first period, the dominance of organic matter is observed. However, the values of the ratio of Fe/Ti, Mn/Ti, and Mn/Fe remain stable, accompanied by the Si/Ti ratio. All these indicators suggest that the bofedal was firmly established at that time; this is confirmed by a reduced input of terrigenous elements at the site: low concentrations of iron and moderate concentrations of nickel and bromine.

The intermediate period shows a change in the sediment deposition, with an increase in the concentrations of the typically terrigenous element, iron and reductions of other elements (Br and Ni) and the ratio of Mn/Ti and Mn/Fe, which are characteristic of the presence of bofedals. Additionally, stability was observed in the Fe/Ti ratio, which, as a whole, strongly suggests a change in sediment deposition and reflects the inflow and stability of the water flow at this site.

The third period, the most recent one, is related to the effects that followed the canalization. To demonstrate these effects, two aspects are initially considered:

1) Our interpretation was made from the most recent dating time, which is found at 9 cm of depth and corresponds to a period calibrated between 1960 and 1980, which is related to the "second desiccation period" caused by the canalization and is observed in the BSP2 profile. This period was interpreted as a stage of bofedal degradation, which is also likely to have caused desiccation in surrounding areas.

2) Profile sampling location. In the case of the BSP2 profile, it was a point found far from the channel, while the BSP14 profile was performed at a site with vegetation in a good state of preservation, in the South bofedal.

Taking these two aspects into account, it can be concluded that most of the values of the geochemical survey support the assumption of a change that took place in the landscape derived from canalization.

On the one hand, an increase in the Si/Ti ratio following the 1960-1980 period, related to the greater deposition of phytoliths by graminoid species, which have become predominant in degraded bofedales. On the other hand, an increase in the concentrations of Br and Ni is also observed, above what was found for the first period. This is clearly related to the formation process of humic acids by the decomposition of vegetal matter, which is an indication of a process of eutrophication in the wetlands. Additionally, the change in water availability, which results in desiccation in areas far from the main canal, is detected by an increase in the Fe/Ti ratio and the fluctuations of the Mn/Ti and Mn/Fe ratio (Schittek et al., 2015; 2016). Finally, the decrease in the deposition of terrigenous elements, such as Fe and other geochemical elements, clearly marks a stage of greater aridity, related to the critical period of dryness already reported in the BSP2 profile.

7.5. General conclusions on the changes recorded in the South Bofedal

The south bofedal shows a clear desiccation process observed in the vegetation changes and in the variation of water levels derived from the effects of the canalization works.

In both profiles (BSP2 and BSP14), a subsequent critical phase is recorded around 1950, which persisted until the 90s, a decade in which interventions to recover the watercourses of the bofedal are took place.

Evidently, in past times, it is also possible to observe variations in the water level (groundwater table), which may be due to other climatic events (profile BSP14); however, our results indicate that the effect of these events did not have a major impact on the vegetation, as a re-establishment of the latter is observed in subsequent stages. And that the critical stage is definitely the one in which the most significant impact for vegetation change at the local level, in and around the South bofedal, is recorded [sic].

7.6. Stratigraphic interpretation of the soil in the North bofedal (BNP7).

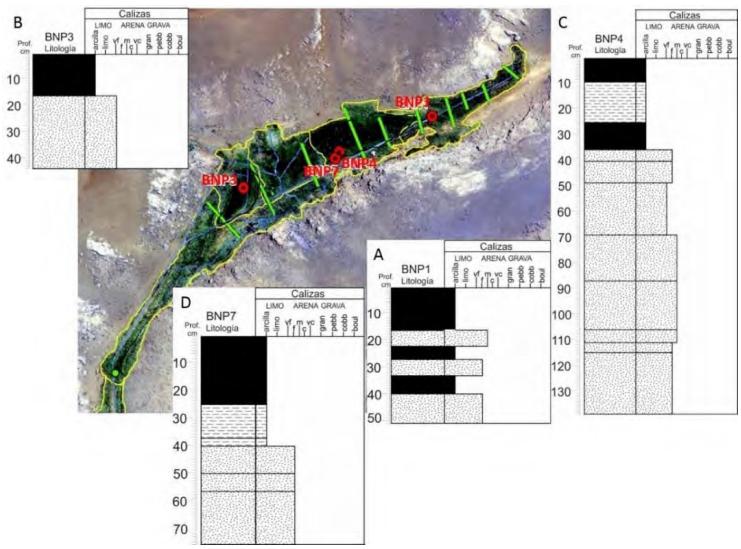


Figure 14. Stratigraphy of the North Bofedal profiles and their location in the areas defined in the vegetation survey of the Silala environmental impact report, where A) shows BNP1 profile, B) BNP3 profile, C) BNP4 profile and D) BNP7, which was carefully studied.

Figure 14 presents a map of the North Bofedal, in which vegetation surveys are identified with green bars and the codes of the profiles are presented in red. The schemes of the profiles performed are also shown, with the different strata found at different depths. A more specific characterization of each of these profiles is found in Annex 1, which presents the descriptions of the textural characteristics for each level or stratum of all the profiles studied. At the end of each description, an interpretation of the sedimentary mechanism that might have allowed its development is included.

The BNP7 soil profile, with a depth of 70 cm, has a greater depth of organic matter near the surface; therefore, it was selected as the most suitable for the study.

In this profile, it is to be expected that the palynomorphs are likely to have remained in good conditions, as there was less oxidation.

Currently, in the area where the BNP7 profile was sampled, the current vegetation shows the development of cushions of Oxychloe andina and Zameoscirpus muticus on the margins—which are both species characteristic of wetlands in good condition. However, it is also possible to observe patches of Poaceae, such as Festuca potosiana, F. rigecens and Cyperaceae, such as Eleocharis, Carex, Phylloscirpus. These species are considered indicators of bofedal degradation.

7.7. Interpretation of stratigraphic profile relations – extent of the North Bofedal

In the North bofedal, four profiles were sampled, showing stratification processes with variations in the thickness of organic matter; this can be attributed to changes in water availability in earlier times. In the upper stratum of the four profiles, it has a high proportion of organic matter, which indicates that the drying process had less impact on the north bofedal, compared to the south bofedal. This can be attributed to factors such as slope and geomorphology (more closed valley), where most canalized water sources converged on a main canal that crossed the north bofedal. These factors must have positively influenced the availability of water, for the maintenance of the North bofedal in certain areas near the main canal. All together we would indicate that the extension of this bofedal was not affected, however some change in the watercourse promoted the strata variability (exchange between sandy material and organic matter) in some areas of the bofedal (BNP1 and BNP4).

7.8. Paleo-ecological interpretations and age-depth model for the North Bofedal

7.8.a. Age-depth model based on 14C dating in the North Bofedal (profile BNP7)

With the dating obtained for the BNP7 soil profile, an age model has been developed, which allows us to reconstruct the changes that have taken place in the environment of the North bofedal for the last 100 years. Two dates were made, the first at 4.5 cm and the second at 44.5 cm in depth, with ages calibrated to 1943 and 1193, respectively (Figure 15). Based on these two dating, the age-depth model was elaborated, which allows us to infer a sedimentation rate of 5 mm every 19 years.

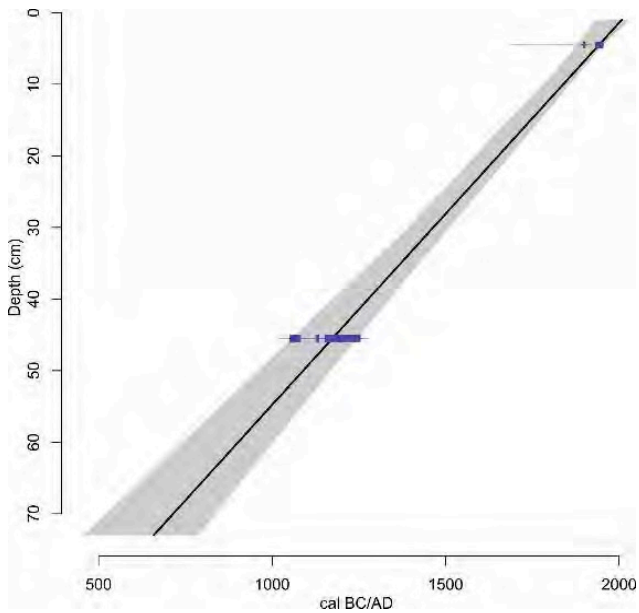


Figure 15. Age-Depth model of the sediment profile of North Bofedal BNP7

In addition, based on our geochemical study, the proposed age model is supported by elevated values of iron concentration (Fe) and the increase in the iron/titanium ratio (Fe/Ti) between the years 1750 to 1850 (Figure 16). This increase in the Fe/Ti ratio indicates a greater oxidation of these elements on the surface and corresponds to a dry phase already known in the Andean region, called the Little Ice Age (LIA; Abbot et al., 1997; Liu et al., 2005).

7.8.b. Geochemical analysis of the North Bofedal (BNP7 Profile)

The results of the geochemical analysis of the BNP7 profile are interpreted from the year 1720 to the present.

The Si/Ti relation presents two intervals of increase and stability (Figure 17a). In 1750 a very low value is recorded which rises and fluctuates until ca. 1847. Subsequently, stable values were observed with slight fluctuations until ca. 1950. In more recent times, the maximum Si/Ti ratio is observed, which is maintained until 1990, then drastically reduced until the present. We have already mentioned that the increases in the Si/Ti relation indicate a greater abundance of gramineous plants, which would have dominated the bofedal, due to their degradation when the water supply and decrease of juncaceous species was reduced.

The Fe/Ti ratio (Figure 17b) shows low and stable values up to ~1775, increasing suddenly thereafter, with a peak in 1847. Subsequently, the Fe/Ti ratio drops towards 1860 and remains stable to the present. Similarly, the Fe concentration values show similar behavior (Figure 17f).

The ratio patterns of Mn/Ti (Figure 17c) and Mn/Fe (Figure 17d) are similar, remaining stable until 1850, then increasing until 1900. Subsequently an abrupt reduction is observed in both relations, which lasts until 1950. These values increase slightly between the 70s and 80s and decrease towards the present.

The Br and Ni deposition patterns show a similar pattern, with little variation in the sample (Figure 17g and h respectively). Finally, Pb (Figure 17e) presents a weak deposition signal compared to the profile of the south bofedal BSP2. Considering that, the origin of Pb deposition is purely atmospheric and the low concentrations of Pb could be explained by the fact that this is an area with dense vegetation cover, which prevents Pb from being deposited directly in the sediment. This would not have happened in the BSP2 profile. This interpretation is supported by the stratigraphic description, which shows that the presence of a good layer of organic matter was permanent during the period studied.

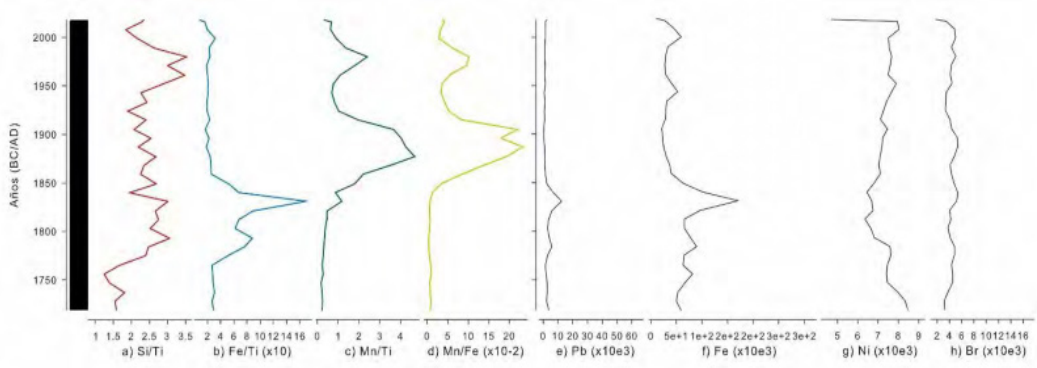


Figure 16. Trace elements found in the geochemical analysis of BNP7 profile, in concentrations per second (cps)

7.8.c. Zoning of palynological samples from the North Bofedal (profile BNP7)

The percentages obtained from the pollen count are plotted in the pollen diagram (Figure 18). Annex 2 shows some records of the palynomorphs found in the counts.

The zoning was done in a similar way as for BSP2, based on a period of time in which we interpreted a change in the composition of identified taxa. The North Bofedal pollen diagram corresponds to a period of 300 years before the present, but we focus mainly on the last 100 years.

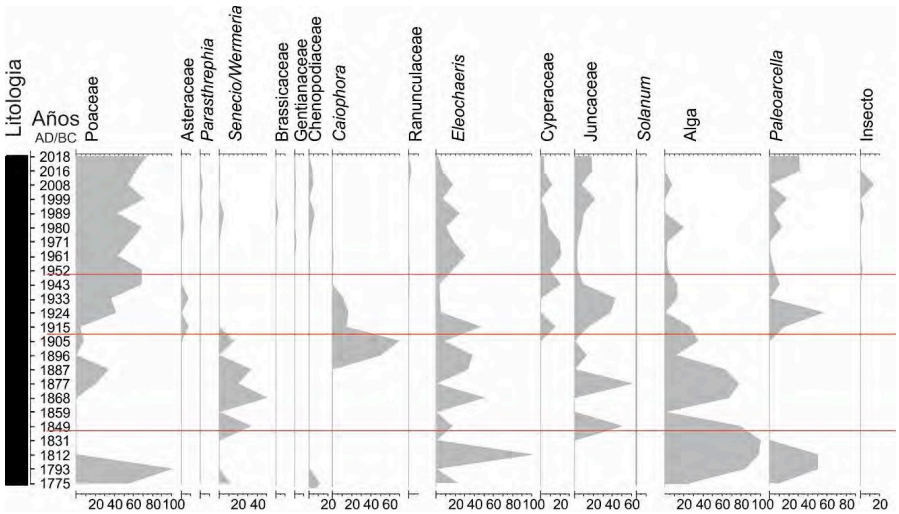


Figure 17: Percentage of representative pollen taxa found in sediment profile BNP7. To the left, the time scale in AD accompanied by the lithology of the profile studied and, transversally, the zonation that defines the changes in the vegetation, extended in the diagram with red lines

Zone 1 (1750-1850 AD) - The pollen with the greatest relative abundance corresponds to Poaceae and Eleocharis (Cyperaceae), both taxa with 80%. The presence of Chenopodiaceae (Amaranthaceous), Senecio (Asteraceae), and algae and Paleoarcella in smaller percentage (10%) is also observed. Algae were abundant near the end of the most recent zoning boundary and contrary to the reduction in the percentage of Paleoarcella.

Zone 2 (1850-1909 AD) - In this period Asteraceae and Juncaceae are observed, both with ca. 40%; and a slight decrease of Eleocharis from 80 to 40%. Towards the upper limit of the temporal zone, from 1875, the presence of Poaceae and Caiophora (Loasaceae) is verified. During this period, the presence of algae decreases gradually, until the end of the upper limit of the zoning.

Zone 3 (1909-1950 AD) - In this period the pollen of Juncaceae dominates (40 %) and the presence of Asteraceae is observed, which shows two small peaks (5%); in addition to the presence of the genus Senecio. In this temporal range, there is a marked reduction in the presence of algae from 25 to 10%, together with a reduction in the presence of Palaeoarcella from 40 to 10%. Additionally, there is a progressive increase of Poaceae from 5 to 70%.

Zone 4 (1950 AD - present) - Dominance of Poaceae (approx. 80%) is verified, which increases gradually until the present. Cyperaceae species present a higher percentage at the beginning of the temporal zone, with 40% and then decreasing towards 1990 by 20%. Simultaneously, the percentage of Juncaceae increases by 20%. The presence of typical hillside elements (external to the bofedal) such as Brassicaceae, Chenopodiaceae, Senecio and Parastrephia is also observed; represented with percentages less than 5%. Additionally, there is a reduction in the presence of algae (< 10%) and a gradual increase in the amoeba Paleoarcella (30%).

7.8.d. Vegetation changes observed in the North Bofedal (BNP7 Profile)

In the period between 1750 and 1850 a dry environment is evident, identified by the values described in the geochemical study (Fe, Fe/Ti, Si/Ti), which coincides with the Little Ice Age (LIA). Pollen indicators of dry climate are observed in the dominance of Eleocharis and Poaceae, species that have been identified as colonizers of degraded bofedales. Also noteworthy is the high percentage of Paleoarcella amebas that show a drying process in a period coinciding with the HSP, between 1783 and 1812. Conversely, around 1830, the percentages of algae increase, indicating a reestablishment of humidity in the medium.

Between 1850 and 1909, wet conditions continued to be restored, favorable for the development of the bofedal, as evidenced by the presence of Juncaceae in a greater percentage than Cyperaceae; in addition, there was an increase in the coverage of shrub vegetation in surrounding areas, represented by the presence of Asteraceae. Additionally, the presence of algae and the disappearance

of the amoeba Paleoarcella coincide with the same pattern of a re-establishment of favorable conditions for the development of the bofedal.

From 1908 (beginning of the canalization) and until 1950, it is observed that the presence of Poaceae pollen, initially reduced, increases gradually, indicating the colonization of grasses in the bofedal. This coincides again with the decrease of algae, and an increase in the presence of amoebas. However, in this stage a transition process of a high percentage of Juncaceae and the simultaneous deposition of Asteraceae pollen from nearby areas is observed. The latter decreased significantly in the next temporal range, between 1950 and the present.

We want to emphasize the reduction of Asteraceae, as it shows us the reduction of shrubs on the slopes. In the last phase, between 1950 and 1990, the most critical effect of the canalization is observed, when the percentage of Juncaceae is considerably reduced and replaced by Cyperaceae, which coincides with an increase in Poaceae, reflecting this drastic change in bofedal vegetation. In addition, the presence of the Paleoarcella amoebas indicates a stagnation of water, probably occurring in areas farther from the main canal, which in this zone had a constant supply of water from the canalized waterways; therefore, it is logical that the bofedal have remained on the banks of this canal. Finally, in the last stage, starting in 1998, the presence of Chenopodiaceae is observed, which tends to grow in places that are more saline or may come from cultivated areas.

7.9 Effects of the canalization on the North Bofedal (BNP7 Profile)

The interpretation of the results of the geochemical analysis of the BNP7 profile is divided into two stages. The first, older, indicates a climatic effect and the second after the canalization that reflects the anthropic effect.

The first stage occurs approximately from 1775 to 1850, coinciding with a change in the regional climate historically known as the Little Ice Age (LIA). This was divided into two phases: a wet phase followed by a dry phase (Abbot et al., 1997; Liu et al., 2005; Apaestegui et al., 2018). During the dry phase a change in iron (Fe) concentrations and the Fe/Ti relation can be seen (Figure 17 b and f), suggesting fluctuations in the surface water level that lasted for approximately 75 years. In addition, an increase in the Si/Ti ratio is also observed during this period (Figure 17a), which indicates greater deposition of graminoids phytoliths (Cyperaceae and Poaceae), which give greater support to the occurrence of a dry stage during this period.

In the post LIA stage, between 1850 and 1900, the Mn/Ti and Mn/Fe ratio indicate that an increase in water levels occurred, which is reflected in a period of bofedal stability (Schittek et al., 2016). From the year ca.1900 a decrease in both relations is observed, which indicates a decrease in the levels of water contribution to the bofedal (Schittek et al., 2016). Towards 1950, it is observed that the values of the ratios Mn/Ti and Mn/Fe increase, which coincides with a period of increase in the exploitation of the bofedales in the Silala, also observed in the south bofedal (BSP2 Profile). During this period, the area's shrub resource was exploited, in addition to maintaining the canals.

The anthropic effect detected by the ratio Si/Ti shows us period was critical of aridity between 1950 and 1990, which can be attributed to the effects of the canalization, detected already in the South Bofedal (BSP2 Profile). Again, this indicates an increase in the number of gramineae that colonized the degraded bofedal.

7.10. General conclusions on the changes occurred in the North Bofedal

The paleo-ecological analysis of the north bofedal records two important historical stages in and around the bofedal. The first related to an event recorded as the Little Ice Age, which between the years 1750 - 1850 is recorded as the dry phase of this event, is reflected in the bofedal with a decrease in the entry of terrestrial elements in response to a decrease in the water table, resulting in a change in the composition of the vegetation of the bofedal and its surroundings, with a decrease in shrubs (thola formations).

The second stage began in the 1950s, and in the South Bofedal is recognized as a critical stage of the canalization effect. It is observed that in the north bofedal this stage also had consequences on the availability of water and the vegetation of the bofedal and surrounding areas, which in comparison with the climatic event (LIA) had a greater impact.

8. Determination of the historical environmental impacts caused by the presence of the artificial canals system

8.1. Environmental impacts recorded in the South Bofedal

8.1.1. Impacts detected in BSP2 Profile

Stratification analyses suggest that the southern bofedal was larger, covering area S_A1b (Figure 3). The results of this report support the estimate of the surface area of the south bofedal before the canalization, which was made in the second report of the project; that is, before the canalization, the south bofedal must have covered about 23,205 m2 (IEIA Silala 2).

XRD analyses indicate that, approximately since 1908 and during the following 20 years, there was a decrease in the deposition of terrestrial elements, such as iron (Fe), titanium (Ti), aluminum (Al), zirconium (Zr) and rubidium (Rb); and that, starting in 1925, a gradual process of soil drying occurred, which became critical around 1950 and remained until about 1997. Since then, there has been a slight increase in water levels that have influenced the deposition of these terrestrial elements.

The values of nickel (Ni), bromine (Br), manganese (Mn) indicate that a humification process occurred from 1945 until the 90s, which coincides with the increase of organic matter in the stratigraphic description of the profile. This process is very possibly the result of the canalization, due to the drying of this zone, which caused the stagnation of waters and the establishment of opportunistic plants.

In summary, large areas of the bofedal were progressively drained since 1908 and had a maximum of draining by 1950. This would have promoted the eutrophication of some springs, through which water probably still flowed from springs, which facilitated the entry of grass (Graminoids) to this site.

Conditions that are slightly more humid have been observed since the 1990s, which coincides with the dismantling of canals, which would have favored the growth of typical bofedal plants, such as Juncaceae, as well as the growth of shrubs in nearby areas.

The changes in vegetation recorded in the palynological analysis suggest, as did the XRD analysis, that there was a drying process due to canalization. Four stages are distinguished: i) the first was a wet stage, between 1880 and 1930, ii) the second occurred between 1930 and 1950, during which there was a gradual reduction in water availability and iii) after 1950, which coincides with the dry stage, with a marked reduction in water availability and finally,

iv) after 1990, when water levels at the site increase, possibly due to the absence of maintenance of the canals.

8.1.2. Impacts detected in BSP14 Profile

Three marked periods are observed that are evidenced in soil, metal and palynological stratigraphy analyses: a period before 680 - 862, an intermediate between 680 - 862 and 1960-1980, and a third from 1960-1980 to the present. These periods are characterized by changes in water availability in the bofedals.

In the first period, it is determined that the bofedal was already established in the area, but suffered a period of drought due to natural climatic events. This is based on the greater presence of phytoliths, evidenced by the increase in the Si/Ti ratio and the higher concentration of Br and Ni, and the decrease in Fe.
Subsequently, in the intermediate period, a re-establishment of wet conditions is observed, verified by the stable values of the Si/Ti, Fe/Ti, Mn/Ti ratio and the decrease of Br and Ni.
In the third period, there is an evident drying process due to the effect of the canalization due to the increase in the Si/Ti ratio, Fe/Ti, and higher concentration of Br and Ni.

Palynological analyses of the BSP14 Profile show that the composition of the bofedal changed in each of the defined periods. The first one was a dry period, followed by a wet period, in the intermediate period related to a higher water intake, which helped the development of typical bofedal plants (Juncaceae).

It is evident that there is a greater effect of the canalization in the third period (1960-1980 to present), observed in the increase of Cyperaceae, Poaceae and the presence of the amoeba Paleoarcella, in addition to the reduction of shrub forms coming from the neighboring vegetation.

8.2. Environmental impacts recorded in the North bofedal

8.2.1. Impacts detected in BNP7 Profile

The analysis of XRD records the effects of HSP between 1775 and 1850, evidenced by changes in the Fe/Ti ratio and the concentration of Fe that suggest changes in water levels caused by the dry phase of LIA, which would imply lower water availability in this period and which coincides with other paleoclimatic surveys in the Andes (Liu et al., 2005). In addition, the interpretation is reaffirmed with the increase in the Si/Ti ratio, associated with the increase in graminoids in the medium, which is an indicator of fragmented and degraded bofedals.

The palynological survey coincides with the geochemical analysis, detecting a dry phase in the period between 1750 and 1850, due to the dominance of Eleocharis and Poaceae, and the presence of the Paleoarcella ameba between 1783 and 1812. Thus, the available information suggests the existence of a drying process in an interval coinciding with the LIA.

The effect of the canalization is reflected in two stages marked by the analysis of XRD and the palynological survey: a transition stage between 1909 and 1950, when the bofedal and surrounding areas show an environment with persistent humidity, evidenced in the ratio of Mn/Ti and Mn/Fe and the increase of Juncaceae and presence of Asteraceae (shrubs); and a second critical stage, from 1950 to 1990, which suggests a reduction in the nearby vegetation cover, and a decrease in Juncaceae, accompanied by the increase of Poaceae and Cyperaceae that colonized the bofedal and Cyperaceae that colonized the bofedal, and the increase of Poaceae and Cyperaceae that colonized the bofedal. This critical period is also observed in the increase in the Si/Ti ratio interpreted as the increase in phytoliths indicating fragmented bofedals.

The geochemical and palynological analyses show a coincidence in the reconstruction interpreted for these periods, clearly evidencing that the effect of the canalization had a greater impact on the wetlands and the surrounding vegetation than the regional climatic changes that occurred during the LIA

9. General conclusions of the survey.

The three profiles analyzed show us a different evolution at the level of deposition of sediments, different ages and geochemical and pollen composition. This was expected, since it is a palynological survey carried out in high altitude bofedals in the Andes, where in each profile there is a different story. Therefore, it is not possible to compare aspects such as the type of sedimentation that directly influences the dating, which is why it was necessary to carry out dating for each profile.

In three soil profiles, it was possible to reconstruct the environment based on pollen indicators of current bofedal species in good condition (current minimum areas), scrublands, thola formations, and degraded bofedals. The reconstruction mainly focused on the last 118 years (from the year 1900). The calculation of the ages was carried out based on 14C dating. With these dating, the age-depth models for the profiles were elaborated. The calibrated ages proposed in the age models were supported by the geochemical results of the concentrations of elements such as lead, iron and the iron/titanium ratio, which are coincidentally related to historical periods registered regionally in other surveys, ensuring high reliability in our data.

The stratification analyzes provide solid evidence that the South Bofedal was more extensive before the canalization, covering the S_A1b area (Figure 3). The results of this report support the estimated calculation of the area of the South Bofedal before the canalization, which was made in the second report of the survey. That is, before the canalization, the South Bofedal must have covered about 23,205 m2 (IEIA Silala 2). This shows a high coincidence between the stratigraphic analyzes carried out on the soil profiles, with the results obtained on the current vegetation.

The three surveyed profiles, despite being located in different areas of the bofedals and showing different stratification, register a high coincidence in the responses to climate changes and the effects caused in the bofedals. This was due to the changes in the water contributions that occurred during the canalization process, which began in 1908.

The results are summarized in two stages from the beginning of the canalization. The first stage, from 1908 to 1950, shows a slow decrease of humidity in the environment in relation to the next stage. Two of the profiles analyzed, BSP2 and BNP7, show this gradual and progressive change of desiccation in relation to the BSP14 profile, this due to the location of the profiles in the bofedal. The BSP14 profile located near the main canal has been able to influence the desiccation process in order to make it slower.

The second stage covers a period from approximately 1950 to the year 1990. The geochemical and palynological analyzes for that period show high coincidence in the three surveyed profiles: a critical period of desiccation in the environment and reduction of water input levels. These changes were more evident in the profiles of the South Bofedal than in the profiles of the North Bofedal. This period is considered critical, because the climatic effects historically registered as the small ice age had

effects and repercussions of smaller scale, in comparison to those registered after the canalization. The canalization modified the landscape on a larger scale and affected plant diversity in the bofedal and surrounding areas.

In the three surveyed profiles, it can be observed that the pollen belonging to vegetation of areas near the bofedals, such as the taxa of the families Asteraceae (Senecio, Parastrephia), Caryophyllaceae (Cerastium, Arenaria), Gomphrena, present in previous periods and in the first stage of the canalization, it is greatly reduced after the critical stage (1950 to 1990). This suggests that, since the beginning of the canalization, the vegetal cover found around the bofedals was affected by the anthropic use.

In the palynological and geochemical survey of the Silala, indicators have been recorded that allow us reaching solid conclusions regarding the effects caused by the canalization of the Silala springs. These indicators are based on the current analogues, based in turn on the current vegetation descriptions (IEIA Silala 2), reference samples obtained in the survey, and references of geochemical surveys in other Andean bofedals. The most important indicators of the geochemical survey recorded in this survey are the concentration values of iron, nickel, bromine, lead and the ratios of iron/titanium, manganese/titanium, manganese/iron and silicon/titanium. From the palynological analysis, it was important to record the percentages of Poaceae and Cyperaceae as indicators of fragmented bofedals, Juncaceae as indicators of bofedals in good condition, Asteraceae and vegetation pollen from areas near the bofedals, which indicate the state of the local terrestrial vegetation, humidity indicator algae, and protozoa such as amoebae (Paleoarcella) and insect remains indicating water stagnation. In general, the results of all these indicators, described in detail in the preceding pages, are congruent and support the general conclusions of this survey and those of the vegetation team.

10. Technical summary: Interpretation of results

1. The estimation of the diversity of plants in the region in the last 100 years, comparing the areas of current bofedals, scrublands and degraded bofedals in Silala, through the survey of pollen and fossil spores (palynology). Survey compared with results from other bofedals in the area.

The profiles of the South and North Bofedals evaluated in the palynological survey show different stages of the composition (Table 2) and wealth (Figure 18) of pollen taxa, and therefore in the diversity of the bofedals. The results vary according to the location of the profiles in the bofedals, as expected. Let us recall that the BNP7 and BSP14 profiles were closer to current water sources and the BSP2 profile was in an area of the bofedal that is currently degraded. However, the three profiles coincide with the change in composition and decrease in wealth, from the beginning of the canalization in 1908, and that the changes have become critical since 1950.

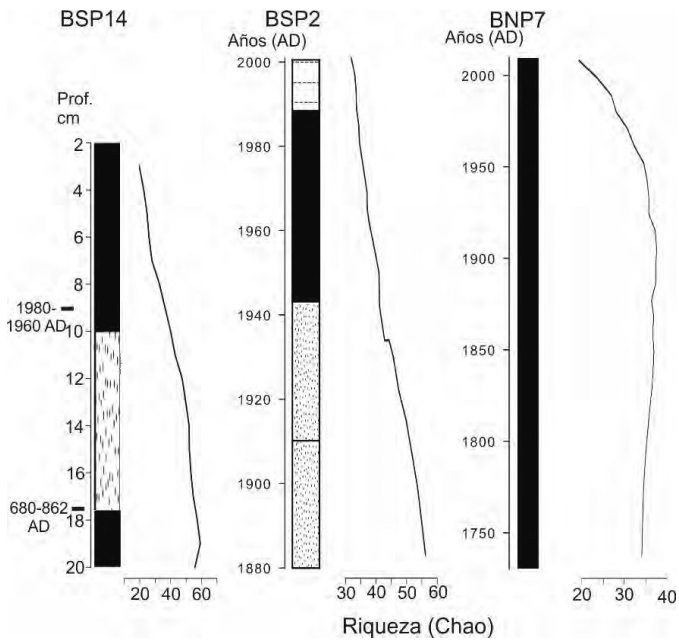


Figure 18: Wealth analysis based on the Chao index in the three profiles evaluated by means of palynological analysis

Table 2: Comparative summary of the composition and abundance of palynomorph pollen taxa found in each surveyed profile in the different periods.

SP2 Profile		**BPS14 Profile**		**BNP7 Profile**	
ime one	**Pollen and palynomorphic diversity**	**Time zone**	**Pollen and palynomorphic diversity**	**Time zone**	**Pollen and payinomorpl diversity**
one 4 976 AD present)	Reduction of *Cyperaceae* (<20%) and *Palaeoarcella* (<20%). Increase in terrestrial taxa (*Parastrephia*, *Senecio*, *Brassicaceae*, *Pycnophyllum* and *Cerastium*) and *Poaceae* (~ 10%), in addition to the increase in *Juncaceae* from 1997 to the present (> 40%).	Zone 3 (10 - 0 cm deep, second period, after 1960 - 1980 calibrated years)	The decrease and disappearance of pollen taxa of Asteraceae, *Gomphrena*, *Brassicaceae* and *Cerastium* (values < 5%), contrary to the increase of *Eleocharis* (~20–80%), *Juncaceae* (~20%), *Poaceae* (> 20%) and the amoeba *Paleoarcella* (~20–40%). In addition, a progressive reduction in the presence of Algae (< 40%) and aquatic insects (< 20%).	*Zone 4 (1950 AD – present)*	*Poaceae* (approx. 80%) dominates, *Cyperaceae* w the highest percentage at t beginning of the zoning (< decreasing in 1990 (20%) *Juncaceae* increases by 2(The presence of *Senecio*, *Parastrephia*, *Brassicace* and *Chenopodiaceae* is observed in percentages l than 5%. Additionally, th reduction of algae (<10%) the gradual increase of *Paleoarcella* (30%) is observed.

Zone 3 (1948 – 1976 AD)	Increase in the presence of *Cyperaceae* (> 60%). Reduction of terrestrial pollen (< 10%) and the presence of *Palaeoarcella* (> 20%) is increased.	Zone 2 (18 - 10 cm deep, intermediate period)	*Cerastium* (~60%), *Brassicaceae* (20%), *Senecio* (~50%) and other *Asteraceae* (~80%) dominate. *Eleocharis* is reduced (< 5%), and conversely *Juncaceae* increases up to ~60%. An increase in the presence of algae is observed (~40%).	*Zone 3 (1909 – 1950 AD)*	The pollen of *Juncaceae* (40%) dominates and the presence of *Asteraceae* with two small peaks (5%). The presence of algae (25-10%) and *Palaeoarcella* (40-10%) is reduced, and there is a progressive increase in *Poaceae* (5-70%).
Zone 2 (1906 – 1948 AD)	Reduction of algae (< 10%), which fluctuates from approximately 1935 to 1950. Terrestrial plants increase, *Gomphrena* (*Amaranthaceous*) (60%), *Parastrephia* (*Asteraceae*) (20%) and *Senecio* (*Asteraceae*) (> 50%), from the year 1935 *Cyperaceae* (> 10%) and the *Palaeoarcella* amoeba (> 20%) increase.	Zone 1 (20 – 18 cm deep, first period, previous to 680 – 862 calibrated years)	*Eleocharis* (*Cyperaceae*) dominates this area (~80%), *Paleoarcella* (~10–40%) in smaller proportion and *Juncaceae* (< 10%). In addition, there is a continuous presence of *Senecio*, *Brassicaceae* and *Cerastium* (< 10%).	Zone 2 (1850 – 1909 AD)	Presence of *Asteraceae* and *Juncaceae* both approximately 40%, and a slight decrease of *Eleocharis* (80–40%). As of the year 1875, *Poaceae* and *Caiophora* (*Loasaceae*) (> 20 and 40%, respectively). The presence of algae decreases gradually (50–10%).
Zone 1 (1878 – 1906 AD)	Dominance of terrestrial taxa, *Asteraceae* (mainly *Senecio*) (> 60%) and algae (> 20%).			Zone 1 (1750 – 1850 AD)	Dominance of *Poaceae* and *Eleocharis* (*Cyperaceae*) (80%). In addition, there is the presence of *Chenopodiaceae* (*Amaranthaceous*), *Senecio* (*Asteraceae*) in lower percentage (10%). The presence of Algae (~80%) and *Paleoarcella* (~40%), the first abundant near the end of the upper limit of zoning contrary to the reduction of the percentage of *Palaeoarcella*.

2. Paleo-ecological interpretations of the bofedal related to the Age/Depth model corresponding to each bofedal, and 3. The reconstruction of past vegetation and interpretation of possible anthropic or climate changes.

Table 3: Summary of interpretations and reconstruction of past vegetation through pollen analysis. Vegetation Profile BSP2.

Age Ranges	SOIL PROFILE – SOUTH BOFEDAL – PROFILE 2 (BSP2)
Time Range 4 (1976 AD – present)	Reduction of pollen of *Cyperaceae* that is almost replaced by *Juncaceae* approximately from 1997, accompanied by the increase of taxa of shrubs: *Parastrephia*, *Senecio*, *Brassicaceae* and *Pycnophyllum*. The *Poaceae* (*Deyeuxia*, *Festuca*) are present in smaller percentage. This stage coincides with the process of dismantling the canals.
Time Range 3 (1948 – 1976 AD)	It presents a critical dry environment due to the canalization effect since 1950. There is a reduction of pollen and palynomorphs, indicators of humid environments. There is a reduction of *Asteraceae*, associated with the presence of tola formations; there is an increase of the *Cyperaceae* species, which are opportunistic plants that colonize bofedals in process of fragmentation and degradation, by reduction of water supplies.
	It is interpreted that there was waterlogging at the beginning of the 20th century, but water supplies were gradually reduced, reaching a critical stage towards the 1950s. The environment was definitely drier after the 1950s, which favored the abrupt increase of *Cyperaceae*.
Time Range 2 (1906 – 1948 AD)	The pollen of Asteraceae presents higher percentages between 1880 and 1930, maintaining until the 1950s. Between the years 1910 and 1930 an increase of pollen of *G. umbellata* is observed, which is an annual species that sprouts in large quantities when there is high rainfall or water contributions. This observation supports the existence of greater humidity in the environment before the 1950s.
	Between the years 1930 and 1950, a gradual reduction of the water contributions and appearance of stagnant waters (puddles) is detected, which is verified by the presence of *Palaeoarcella*, an amoeba that is considered an indicator of this type of environment (Traverse 2007). This observation is supported by the presence of macro-invertebrate remains, (i.e., dipterous larvae of the *Chironomidae* family) typical of stagnant water. All these palynomorphs decrease in percentage from the year 1950.
Time Range 1 (1878 – 1906 AD)	The period between 1880 and 1930 shows higher levels of water, which is verified by the high percentages of algae between 1880 and 1906. Subsequently the presence of algae is reduced, almost disappearing around 1935.
	The presence of pollen of species that form tola formations (mainly *Asteraceae*) presents higher percentages between 1880 and 1930, which is maintained until the 1950s. Subsequently, the pollen of *Asteraceae* is reduced, indicating less humidity and possible anthropic use.

Results 2 and 3 are summarized in Tables 3, 4 and 5, which show high coincidence in the interpretations for the three surveyed profiles. A gradual desiccation throughout the Silala region culminates with a critical stage of desiccation from the 1950s. This stage is coincident in all the indicators (stratigraphy of soils, metals and pollen).

Evidence suggests that the impact was greater in the South Bofedal due to its geo-morphological characteristics. Another recurring result is that, in periods before the canalization, vegetation on the slopes showed higher pollen taxa wealth, as evidenced by the three surveyed profiles. Finally, it is important to record the regional climate event, the Little Ice Age (LIA), in the reconstruction of the BNP7 profile. As pointed out, the LIA did not have such a strong effect on the vegetation, nor the bofedal, as the canalization of the springs carried out at the beginning of the 20th century.

To conclude, it is important to take into account that there is a different sedimentation process in the surveyed soil in the bofedals, in terms of stratification and calibrated ages at depth; therefore, great care must be taken in the comparison between the soil profiles of the same bofedal and, therefore, with other bofedals in the area. However, we can find a coincidence with respect to the indicators (pollen, metals).

Table 4: Summary of interpretations and reconstruction of past vegetation through pollen analysis. Vegetation Profile BSP14

Age Ranges	**SOIL PROFILE – SOUTH BOFEDAL – PROFILE 14 (BSP14)**
Time Range 3 (10 - 0 cm deep, third period, after the interval 1960 - 1980)	A critical drying stage is detected after 1950 to the present. A gradual process of desiccation is observed in the bofedal and in the surrounding areas, with shrub vegetation reduction of the tola formations. The vegetation of the bofedal presents dominance of *Cyperaceae* and *Poaceae*, which indicates a process of fragmentation and degradation of the bofedal.
	Palaeoarcella reaches high percentages in this period. This amoeba is indicative of stagnant water and drying at the site.
Time Range 2 (18 – 10 cm deep, intermediate period after dating, previous to 680 – 862)	This period is related to a wet phase due to the increase in the presence of algae, which indicates an increase in water levels at the site.
	It is a wet stage, which is verified by the increase in the presence of the pollens of *Parastrephia*, *Senecio* (*Asteraceae*) and *Cerastium* (*Caryophyllaceae*). All this period prior to the canalization shows that the tola formations and other compounds and herbaceous shrubs had greater coverage on the slopes of the areas surrounding the bofedal.
Time Range 1 (20 – 18 cm deep, first period, before the interval 680 – 862)	The dominance of *Cyperaceae* is observed, associated with the colonization of fragmented bofedals. There is the presence of *Paleoarcella*, which is related to the stagnation of waters, indicating a drying process.

Table 5: Summary of interpretations and reconstruction of past vegetation through pollen analysis. Vegetation Profile BNP7

Age Ranges	SOIL PROFILE – SOUTH BOFEDAL – PROFILE 7 (BSP7)
Time Range 4 (approx. 1997 – present)	Approximately, as of 1997, the presence of Chenopodiaceae is observed, which grows in places that are more saline or that come from areas of cultivation (quinoa).
Time Range 4 (1950 AD – present)	A reduction of *Juncaceae* is observed, which is replaced by *Cyperaceae*, and there is an increase in pollen of Poaceae, with a drastic decrease in *Asteraceae*, which is vegetation from nearby areas. The presence of *Paleoarcella* indicates stagnant waters and a drying process in the area.
Time Range 3 (1909 – 1950 AD)	It includes the beginning of the canalization in the area. There is a low presence of *Poaceae* pollen at the beginning of the period and a gradual increase after the canalization. At the same time, the algae decrease, indicating a reduction in humidity. On the other hand, the presence of amoeba increases, indicating the presence of stagnant water. In this stage of gradual transition, there is a high percentage of *Juncaceae* and *Asteraceae* from nearby areas.
Time Range 2 (1850 – 1909 AD)	Between 1850 and 1909, the reestablishment of humid conditions is observed, after the dry phase of the Little Ice Age (LIA). There is a higher percentage of *Juncaceae* than of *Cyperaceae* and the presence of *Asteraceae*, related to nearby tola formations.
	In 1830, the percentages of algae increase, and the *Paleoarcella* amoeba disappears, which would indicate a reestablishment of humidity in the environment.
Time Range 1 (1750 – 1850 AD)	High percentages of *Eleocharis* and *Poaceae*, which are indicators of dry climate. High percentage of *Paleoarcella* amoeba between the years 1783 and 1812.
	This period of desiccation coincides with the climatic event of the Little Ice Age.

4. The analysis of the composition of metals by X-ray diffraction (XFR) is a complementary analysis to the analysis of pollen, which will allow better understanding the changes in the vegetation, determining if they are due to natural or anthropic causes.

The results of the XRD analysis in the three profiles (Table 6), give us evidence of drying processes, by changes in the water supply, in the Silala North and South Bofedals. These processes are of different origins. The first drying period corresponds to a process of natural origin, in a previous time (between 1775 and 1850), which is registered in the North Bofedal (BNP7 Profile). This period of desiccation coincides with the already surveyed Little Ice Age, which determined a change in the regional climate recorded in previous surveys in the region (Liu et al., 2005; Apaéstegui et al., 2018). The second period of desiccation is after the canalization that began in 1908. This period is gradual and shows its most critical stage from the year 1950, continuing until the year 1990. This critical period is observed in the three profiles, with change in the concentrations of trace elements.

5. The determination of the historical environmental impacts caused by the presence of the system of artificial canals on the vegetation.

Impacts detected in the South Bofedal

The results indicate that the impacts of the canalization are more evident in the South Bofedal. The BSP2 and BSP14 Profiles indicate that, before the canalization, the species from the surrounding areas deposited a greater quantity of pollen from tola formations or nearby zones, than in periods after the canalization. Likewise, in figure 18 of this technical summary, it is observed that the profiles of the South Bofedal show lower pollen wealth in relation to the profile of the North Bofedal. This decrease can be interpreted as a reduction effect on the vegetation cover of areas around the bofedal.

On the other hand, XRD analyzes show consistently that, since 1908 and for the next 20 years, there was a decrease in the deposition of terrigenous elements such as iron (Fe), titanium (Ti), aluminum (Al), zirconium (Zr) and rubidium (Rb); and that from 1925 a gradual process of soil drying occurred, which increased in 1950 until about 1997. Since then, there has been a slight increase in water levels, which have influenced the deposition of iron, aluminum, zirconium and rubidium.

Table 6: Summary of interpretations and reconstruction of the XRD geochemical analysis

Profile	Geochemical Interpretations (XRD)
BSP2	The terrigenous elements (Ti, Al, Zr, Rb and Fe) follow the same pattern of variation in their concentrations, evidencing three changes: *i)* a reduction between 1908 and 1925, as a first effect of the canalization process, *ii)* an even greater reduction, from 1938 to 1993, where the dryness in the environment increases; these changes show the effect of canalization in the bofedal and the increase in dryness in surrounding areas. The third change *iii)* occurs from 1993, with a slight increase in the concentrations of the terrigenous elements, coinciding with the recovery period of bofedals, which occurred according to historical data after 1995. Accompanying these variations in the concentration of terrigenous elements, elements such as Br and Ni are observed. An increase of these elements translates as acceleration of humification processes and organic matter. In addition, the greatest increase of these elements is observed between the years 1940 and 1983, considered the critical period of desiccation of the bofedal. On the other hand, the increase in Silicon between the years 1950 and 1985, verified in a comparative way in the Si/Ti ratio, indicates a process of colonization of graminoids in areas of the bofedal, which gives clear evidence of degradation of the bofedal. Finally, the Fe/Ti ratio, which indicates fluctuations in water levels, coincides in indicating a drying period from 1925 to 1980. Conversely, the values of the Mn/Ti and Mn/Fe ratios, indicators of bofedals stability, show a marked reduction starting in 1960.
BSP14	The geochemical analysis of this profile shows three periods: *i)* The first period is focused on a period prior to channeling (calibrated years 680 – 862). *ii)* An intermediate period between the calibrated ages of 680 – 862 and 1960 – 1980, where a change in the stratigraphic composition is observed, with the increase in sand and silt particles. *iii)* And a third period after the time of the channeling (1960 – 1980).

	In the first period, the dominance of organic matter supports the stable values of the Fe/Ti, Mn/Ti and Mn/Fe ratios. The slight increase in the Si/Ti ratio, the moderate concentration of Ni and Br and the decrease in the entry of terrigenous elements (Fe), suggests that at this time the bofedal was already established in the area. We consider that the Silala bofedal is more than 1,000 years old. The intermediate period suggests a change in deposition of sediments, with the increase of iron concentrations, a terrigenous element, and in the decrease of other elements characteristic of the presence of bofedals, verified by the Mn/Ti, Mn/Fe ratios and the presence of Br and Ni; in addition to the stability in the Fe/Ti ratio, which reflects the intake and stability of the water supply in this site. In the third period, the increase in the Si/Ti ratio (after the 1960 – 1980 interval) is observed, accompanied by a greater increase in the concentrations of Br and Ni, high values in the Fe/Ti ratio and an increase in the fluctuations of the Mn/Ti and Mn/Fe ratios. These data together indicate a dry stage, coinciding with the critical period of dryness observed in the BSP2 Profile.
BSP7	Two stages are observed, the first –the oldest– that indicates a climatic effect (the Little Ice Age - LIA) and the second, after the canalization, which reflects the anthropic effect. In the first stage (climatic effect), approximately between the years 1775 and 1850, an increase in the concentrations of Fe is verified, and in the Fe/Ti and Si/Ti ratios; that together indicate a stage of desiccation of the bofedal. This stage clearly coincides with a change in the regional climate historically recorded as the Little Ice Age (LIA). In turn, the Little Ice Age was divided into two phases: a wet phase, followed by a dry phase (Abbot *et al.*, 1997, Liu *et al.*, 2005, Apaestegui *et al.*, 2018), the dry phase being the one registered in this survey. Subsequently, the values of the Mn/Ti and Mn/Fe ratios show a period of bofedal stability between 1850 and 1900. As of this year, there is a decrease in these ratios, which reflects a decrease in water levels. From 1950 to 1990 (second stage), the Mn/Ti, Mn/Fe and Si/Ti ratios increase simultaneously; which indicates desiccation and colonization by graminoids species in the bofedal. All this coincides with the critical period detected in the South Bofedal.

The values of nickel (Ni), bromine (Br), manganese (Mn) indicate that there was a process of humification, from 1945 to the 1990s, which coincides with the increase of organic matter in the stratigraphic description of the soil. This process is possibly the result of the canalization, due to the drying up of this area that caused the stagnation of waters and the settlement of opportunistic plants, in addition to soil salinization.

It should be clear that large areas of the Silala bofedal have progressively dried out since 1908 and had a maximum level of drying by 1950. This would have promoted the eutrophication of some spring waters, through which waters of the springs probably still flowed, which facilitated the entry of opportunistic plants to the bofedals (Poaceae) resulting in its fragmentation and degradation.

The changes in vegetation recorded in the palynological analysis suggest –as in the XRD analysis– that there was a drying process due to the canalization. We have managed to distinguish four stages: i) the first stage was humid, between 1880 and 1930; ii) in the second stage, between 1930 and 1950, there was a gradual reduction of water supply; iii) after 1950, which is the driest stage; and iv) approximately from the 1990s, when an increase in water contributions was detected, probably due to the dismantling of the canals.

Impacts detected in the North Bofedal.

The XRD analysis records the effects of the dry phase of the Little Ice Age (LIA) between the years 1775 AND 1850, evidenced by changes in the Fe/Ti ratio and Fe concentration. The palynological survey also gives evidence of this dry stage, with the presence of Eleocharis and species of the Poaceae family, and of the amoeba Paleoarcella. This period coincides with other paleo-climate surveys in the Andes. In addition, the interpretation is reaffirmed with the increase of the Si/Ti ratio, associated with the increase of graminoids in the environment, which is a good indicator of fragmented and degraded bofedals.

The effect of the canalization is reflected in two stages marked by the XRD analysis and the palynological analysis. A transition stage between 1909 and 1950 is distinguished first, when the bofedal and the surrounding areas showed an environment with persistent humidity, evidenced in the Mn/Ti and Mn/Fe ratio and the increase of Juncaceae and presence of Asteraceae (shrubs), but in process of gradual desiccation. In addition, there was a second critical stage –from 1950 to 1990 AD– that suggests a decrease in the nearby vegetation cover and a decrease in Juncaceae, accompanied with the increase of Poaceae and Cyperaceae, which colonized the bofedal. This critical period is also observed in the increase of the Si/Ti ratio, interpreted as the increase of phytoliths, which indicate a state of fragmentation and degradation of bofedals.

11. Bibliography.

Abbott MB, Binford MW, Brenner M, and Kelts KR (1997) A 3500 14C years high-resolution record of lake level changes in Lake Titicaca, Bolivia/Peru. Quaternary Research 47(2): 169–180.

Abbott MB, Wolfe BB, Aravena R, Wolfe AP y Seltzer, G. O. 2000. Holocene hydrological reconstructions from stable isotopes and paleolimnology, Cordillera Real, Bolivia. Quaternary Science Reviews, 19, 1801–1820.

Abbott MB, Wolfe BB, Wolfe AP, Seltzer O, Aravena R, Mark BG, Polissar, P. J., et al. 2003. Holocene paleohydrology and glacial history of the central Andes using multiproxy lake sediment studies. Palaeogeography, Palaeoclimatology, Palaeoecology, 194, 123–138. doi:10.1016/S0031- 0182(03)00274-8

Apaéstegui J, Cruz FW, Vuille M, fohlmeister J, Espinoza JC, Sifeddine A, Strikis N, Guyot JL, Ventura R, Cheng H y Edwards L. 2018. Precipitation changes over the eastern Bolivian Andes inferred from speleothem (δ18O) records for the last 1400 years. Earth and Planetary Science Letters: 404: 124 – 134.

Arche A. (Coord.) 1992. Sedimentology Vol. 1. Higher Council of Scientific Research, Madrid.

Baker, M. C. W.; Francis, P. W. 1978. Upper Cenozoic volcanism in the Central Andes—ages and volumes. Earth and Planetary Science Letters, vol. 41, no 2, p. 175-187.

Blaauw MB (2010) Methods and code for classical age-modelling of radiocarbon sequences.Quaternary Geochronology.5: 512–518.

Böning, P., Shaw, T., Pahnke, K., & Brumsack, H. J. (2015). Nickel as indicator of fresh organic matter in upwelling sediments. Geochimica et Cosmochimica Acta, 162, 99-108.

Brewer, S., J. Guiot, & D. Barboni. 2007. Pollen methods and studies. pp. 2497 – 2508. En: Elias, S.A. (ed.), Encyclopedia of Quaternary Science. vol. 1, Elsevier Science Publishers B.V. (North- Holland), Amsterdam.

Compton R. 1962. Field Geology. Pax Editorial, Carlos Cesarman Bookstore.
Court, P. (1974). Nouvelles techniques de detection des flux et des retombees polliniques: e tude de la se dimentation des pollens et des espores a la suface du sol. Pollen et spores, XVI, 103-141.

Cook, R. D. (2007). Concepts and applications of finite element analysis. John Wiley & Sons.

DIREMAR, 2017. Soil Characterization of the Silala Bofedals and Surrounding Areas. Consultancy Product, Strategic Office for the Maritime Claim, Silala and International Water Resources. Technical report.

Espi E, Boutroun C.F., Hong S., Pourchet M, Ferrart C, Shotyk W y L. Charlet. 1997. Changing contentrations of Cu, Zn, Cd, and Pb in a high altitude peat bog from Bolivia during the past three centuries. Water, Air, and Soil Pollution, 100: 289 – 296.

Faegri K. & J. Iversen (1989). Textbook of pollen analysis. New York, John Wiley and Sons. Hatté, C., and A. J. T. Jull. "Radiocarbon Dating Plant Macrofossils." (2007): 2958-2965.

Heusser, C. 1971. Pollen and Spores of Chile: Moderm Typos of thePterudophyta, Gimnospermae and Angiospermae. The University of Arizona Press. Tucson. p. 167.

Liu K, Reese C and Thompson LG (2005) Ice-core pollen record of climatic changes in the central Andes during the last 400 yr. Quaternary Research, 64(2): 272–278.

Miall, A. 1978. Lithofacies types and vertical profile models in braided rivers: a summary. En A. Miall (editor): "Fluvial Sedimentology", Can. Soc. Of Petrol. Geol, Memoir 5, pp. 597-604.

Miall, A. 1996. The Geology of Fluvial Deposits. Sedimentary Facies, Basin Analysis, and Petroleum Geology. Springer eds. 582 p.

Messerli, B., Grosjean, M., Bonani, G., Bürgi, A., Geyh, M. A., Graf, K., & Vuille, M. (1993). Climate change and natural resource dynamics of the Atacama Altiplano during the last 18,000 years: a preliminary synthesis. Mountain Research and Development, 117-127.

Moreno A, Giralt S, Valero-Garcés B, Sáez A, Bao R, Prego R, Pueyo JJ, Gonzáles-Sampériz P y Taberner C. 2007. A 14 kyr record of the tropical Andes: The Lago Chungará sequence (18°S, northern Chilean Altiplano). Quaternary International, 161:4–21.

Mourguiart P, Argollo J, Gorrege T, Martin L, Montenegro ME, Abdelfettah S y Wirrmann D. 1997. Limnological and climatological changes in the Lake Titicaca basin (Bolivia) during the last 30.

Mourguiart P, Correge T, Wirrmann D, Argollo J, Montenegro ME, Pourchet M y Carbonel P. 1998. Holocene palaeohydrology of Lake Titicaca estimated from an ostracod-based transfer function. Palaeogeography, Palaeoclimatology, Palaeoecology, 143, 51–72.

Munsell Color Co. (1976). Munsell book of color. Macbeth, a Division of Kollmorge. Corp., Baltimore, MD.

Pueyo JJ; Sáez A, Giralt S, Valero-Garcés BL, Moreno A, Bao R, Schwalb A, Herrera C, Klosowska, B. y Taberner C, 2011. Carbonate and organic matter sedimentation and isotopic signatures in Lake Chungará, Chilean Altiplano, during the last 12.3 kyr. Palaeogeography, Palaeoclimatology, Palaeoecology, 307: 339–355.

Reading, H. 1996. Sedimentary Environments: Processes, Facies and Stratigraphy. Blackwell Science eds. 688 p.

Roubik, D. & P. Moreno. 1991. Pollen and Spores of Barro Colorado Island. Monographs in Systematic Botany from the MissouriBotanical Garden. 270p.

Sáez A, Valero-Garcés BL, Bao R, Pueyo JJ, Gonzáles-Sampériz S, Girtalts S, Taberners C, Herrera C y Gibert RO. 2007. Lacustrine sedimentation in active volcanic settings: the Late Quaternary depositional evolution of Lake Chungará (northern Chile). Sedimentology, 54: 1191–1222.

Sandoval, P., L. Marconi & T. Ortuño. 2010. Pollen Flora of bofedals and surrounding areas of the Tuni Condoriri. National Herbarium of Bolivia. Institute of Ecology. Higher University of San Andres and National Museum Natural History. La Paz, Bolivia.

Schittek K,Forbriger M, Mâchtle B, Schâbitz F, Wennrich V, Reindel y B. Eitel. 2014. Holocene environmental changes in the highlands of the southern Peruvian Andes (14° S) and their impact on pre-Columbian cultures. Clim Past Discuss 10:1707–1746.

Schittek, K., et al.2015. “Holocene environmental changes in the highlands of the southern Peruvian Andes (14 S) and their impact on pre-Columbian cultures.” Climate of the Past 11.1: 27-44.

Schittek, Karsten, et al. 2016. A high-altitude peatland record of environmental changes in the NW Argentine Andes (24° S) over the last 2100 years. Climate of the Past, vol. 12, no 5, p. 1165-1180.

Seppa, H. 2007. Pollen analysis, principles. pp. 2486–2497. En: Elias, S.A. (ed.), Encyclopedia of Quaternary Science. vol. 1, Elsevier Science Publishers B.V.

Traverse, A. 2007. What Paleopalynology Is and Is Not. En Paleopalynology. Springer, Dordrecht. p. 1-43.

Twidle, C.L. 2012. Chapter 4, Section 1.4: Pollen Analysis: Not Just a Qualitative Tool. En: Geo- morphological Techniques, Edited by Andrew Goudie, British Society for Geomorphology, ISSN 2047-0371

Urquidi F. 2004. Report on the field visit to the Silala. Additional Field Works. Pp. 170 – 192.

Wentworth Ch. 1922. "A Scale of Grade and Class Terms for Clastic Sediments". The Journal of Geology.

Zaccone, C., Cocozza, C., Shotyk, W., & Miano, T. M. 2008. Humic acids role in Br accumulation along two ombrotrophic peat bog profiles. Geoderma 146.1-2 (2008): 26-31.

Annex 1

Stratigraphic Description of the South Bofedal profiles.

BSC9 Trial pit:

A. Depth: 0 – 12.5 cm; texture: fine sand, grain supported with planar and specific contacts in a silty matrix. The lithic fragments represent around 30%. Isolated clays composed of ignimbrite with diameters ranging between 7 to 12 millimeters, rounded with low sphericity. There is no evidence of organic matter forming soil. It has a strong reaction to acid attack. Grayish-brown color (Hue 7.5 YR 4/2). Deposits formed by material fall in sub-aquatic environment contributed by wind currents with contributions of colluvial material.
B. Depth: 12.5 – 24.5 cm; texture: massive clay, with silty component and isolated grains of different sizes of sand. Presence of isolated roots. Reddish-brown matte color (Hue 2.5 YR 4/3). Sedimentation by decantation of material contributed by wind developed in floodplains.

C. Depth: 24.5 - 44 cm; texture: fine to very fine sand, supported grain, planar and specific contacts in silty matrix. The lithic fragments are present in about 30%. Isolated clasts of up to 4 millimeters in diameter, sub-rounded with high sphericity, composed of ignimbrite. Isolated presence of roots. Dark- reddish color (Hue 2.5 YR 3/2). Deposits formed by the fall of material in the sub-aquatic environment contributed by wind currents.
D. Depth: 44 - 52 cm; texture: level formed by large clasts (ranging in diameter between 13 to 16.5 centimeters) of ignimbrite composition, clasts supported with specific contacts on medium to coarse sand matrix, sub-rounded with low sphericity, the major axis parallel to the horizon. Dark orange color (Hue 5 YR 6/3). Deposits formed by detritus flow in high energy systems. Reduced transport.

BSP7 Trial pit:

A. Depth: 0 - 12 cm; texture: medium sand, supported grain, planar and specific contacts in a silty matrix. Lithic fragments present in around 20%. Clasts of up to 9 millimeters in diameter, very angular with low sphericity and quartz compounds. There is no soil development and there is a moderate presence of roots. There is a reaction to the attack with acid (10% HCl) throughout the level. Grayish- brown color (Hue 5 YR 4/2). Sedimentation by traction and decantation of materials product of turbulent flows. Sub-aerial exhibition without soil development. The presence of carbonates indicates photosynthesis and precipitation of carbonates by evaporation in the aquatic system.
B. Depth: 12 - 31 cm; texture: sand from fine to very fine grains; grain supported with planar and punctual contacts in a sandy silt matrix. Lithic fragments present in around 40%. Clasts of up to 6 millimeters in diameter composed of low sphericity sub-angular ignimbrite. Moderate presence of roots. Brown color (Hue 7.5 YR 3⁄4). Deposits formed by the fall of material in the subaqueous medium contributed by wind currents.
C. Depth: 31 - 45 cm; texture: very fine sand, grain supported with specific and planar contacts in clay loam matrix. Lithic fragments representing about 40%. Isolated roots. Dark brown-black color (Hue 10 YR 3/3). Deposits formed by the fall of material in the subaqueous medium contributed by wind currents. Minimal decrease in the energy of the medium.
D. Depth: 45 - 58 cm; texture: very fine sand, grain supported with specific and planar contacts in silty clay matrix. The lithic components represent around 15%. Isolated clasts up to 7 millimeters in diameter, it is angular with low sphericity and ignimbrite compounds. Isolated roots. Dark brown- black color (Hue 10 YR 3/3). Deposits formed by the fall of material in the sub-aquatic environment contributed by wind currents.
E. Depth: 58 - 63 cm; texture: sediment composed of small ridges (diameter between 7.5 to 12.5 centimeters), clasts supported with specific contacts, without preferential orientation,

on medium to coarse sand matrix, very angular sphericity clasts and ignimbrite compounds. Opaque orange color (Hue 5 YR 6/3). Deposits formed by detritus flow in high energy systems.

BSP8 Profile:

A. Depth: 0 - 5 cm; texture: organic matter, clastic fraction composed of heterogeneous sands ranging from very fine to medium, matrix supported in silty matrix. Lithic fragments with a presence of around 20%. Gray-yellowish brown color (Hue 10 YR 5/2). Development of soil with periods of sedimentation.
B. Depth: 5 - 22 cm; texture: medium to very thick fine sand, matrix supported on sandy silt matrix with specific contacts (isolated character). The lithic fragments represent approximately 30%. Presence of roots. Gray-yellowish brown color (Hue 10 YR 4/2). Material traction deposits of episodic turbulent gravity flows and decantation when the system energy has been reduced.
C. Depth: 22 to 35 cm; texture; clay with isolated grains of coarse sand. Light gray color (Hue 10 YR 7/1). Sedimentation by decantation of material contributed by wind developed in floodplains.

BSP6 Profile:

A. Depth: 0 - 8 cm; texture: organic matter, lithic fraction composed of clay and very fine sand. Lithic fragments up to 3 millimeters in diameter. Opaque yellow-orange color (Hue 10 YR 7/3). Development of soil without total sedimentation interruption.

B. Depth: 8 - 15 cm; texture: very fine to fine sand, supported grain, planar, specific contacts in clay matrix with around 20% lithic components. Isolated clasts of 3 to 5 millimeters in diameter, sub- angular of high sphericity. Moderate presence of organic matter. Reddish-gray color (Hue 2.5 YR 4/1). Decantation of sub-aquatic grains contributed by wind, periods of stability with sub-aerial exposure and soil formation.

C. Depth: 15 - 29 cm; texture: medium coarse sand, clasts supported with planar and specific contacts on very thin silty sand matrix. The lithic components represent around 20%. Isolated clasts of between 5 to 9 millimeters in diameter, very angular to round with low sphericity, composed of ignimbrites and Andesite in a smaller quantity. Presence of roots. Dark reddish-gray color

(Hue 2.5 YR 3/1). Deposit by traction and decantation of materials product of turbulent flows.

D. Depth: 29 - 57.5 cm; texture: fine to medium sand, grain supported with planar and specific contacts on very thin silty sand matrix. It presents about 30% of lithic fragments. Frequent clasts with diameters between 5 to 11 millimeters, angular and sub-angular of high and low sphericity in the clasts composed of ignimbrite and sub-angular high sphericity in clasts composed of quartz. Isolated presence of roots. Dark reddish-gray color (Hue 2.5 YR 3/1). Deposit by traction and decantation of materials product of turbulent flows.

BSP2 Profile:

A. Depth: 0 - 3 cm; texture: organic material with silty clastic-clay material. Brown color (HUE 7.5 YR 4/3). Consolidation of soil development with interruption in the sedimentation rate and sub-aerial exposure

B. Depth: 3 - 8.3 cm; texture: organic matter, clastic material composed of clay. Homogeneous deposit. Reddish-black color (HUE 10R 2/1). Development of soil with sedimentation present but decrease of the sedimentation rate.

C. Depth: 8.3 - 12 cm; texture: fine sand in silty clay matrix, grain supported with high organic content, base of the irregular segment. Very dark black-reddish color (HUE 2.5 YR 2/2). Deposit by traction and decantation of materials product of turbulent flows.

D. Depth: 12.5 - 21.5 cm; texture: very fine sand on silty clay matrix, supported matrix, lithic around 30%. Lithologically homogeneous segment with an irregular base. Presence of roots. Dark reddish- gray color (HUE 7.5 R 4/1). Decantation of sub-aquatic grains contributed by wind, intermittent flows with local reworking and little transport.

E. Depth: 21.5 - 23 cm; texture: fine to medium sand, grain supported with silty matrix, clasts isolated up to 7 mm with high sphericity and sub-rounded, irregular base. Brownish-gray color (HUE 5YR 4/2). Deposit by traction and decantation of materials product of turbulent flows, with erosion of the bed and reworking without considerable transport.

F. Depth: 23 - 37 cm; texture: section of decreasing grain, described in three parts: Base: Medium to fine sand, grain supported with planar contact, silty matrix, with lithic fragments close to 35%. Clasts up to 1 cm in diameter whose presence represent up to 15% of the total, it has an ignimbrite composition. Medium: Fine grain sand, grain supported with silty matrix, lithic fragments

around 30%. Very isolated clasts up to 3 mm in diameter, high sphericity and sub-angled. Top: Fine to very fine sand in silty clay matrix, supported matrix, with lithic fragments around 30%. Presence of isolated roots. Dark gray-reddish color (HUE 7.5 R 3/1). Deposit by traction and decantation of materials product of turbulent long-term flows, with progressive decrease in the energy of the medium giving way to a deposition by decantation.

G. Depth: 37 - 42 cm; texture: fine sand, supported grain, silty matrix, planar and specific contacts, with lithic fragments around 20%. Irregular base. Dark reddish color (HUE 2.5 YR 2/1). Decantation of sub-aquatic grains contributed by wind, reworking of bed material.

H. Depth: 43 cm - profile base; texture: very coarse gravel, clasts up to 4 cm in diameter of ignimbrite composition, low sphericity and angled. Medium to fine sand matrix. Red-grayish color (HUE 2.5 YR 6/2). Detritus flow reservoirs in a medium of high energy and low transport.

BSP10 Profile:

A. Depth: 0 - 4.5 cm; texture: organic matter with little sediment composed of clay. Brown color (Hue 7.5 YR 6/3). Soil development and sub-aerial exposure.
B. Depth: 4.5 - 10.5 cm; texture: organic matter with higher sedimentation of clays. Presence of roots. Dark brown color (Hue 7.5 YR 3/1). Development of soil with occurrence, even sedimentation of very fine material as wind contribution.
C. Depth: 10.5 - 19 cm; texture: fine sand, heterogeneous (grains of very coarse sand), grain supported with planar contacts on a very fine silty sand matrix. The lithic fragments represent up to
20%. Abundant roots. (Hue 7.5 YR 7/5). Sedimentation by traction and decantation of materials product of turbulent flows.
D. Depth: 19 - 23 cm; texture: very fine sand, grain supported in chaotic arrangement with planar contacts, specific and locally without contact. Clay matrix and presence of lithic fragments of around 25%. Moderate presence of roots. Gray-brown color (Hue 7.5 YR 4/2). Deposits formed by falling material in sub-aquatic environment contributed by wind currents.
E. Depth: 23 - 33.5 cm; texture: coarse gravel (clasts from 15 to 32 mm); matrix supported with floating clasts. The matrix is constituted by medium to fine sand (lithic fragments around 30%). The clasts are composed of ignimbrite, very angular and with high sphericity. Abundant presence of roots. Dark brown color (Hue 7.5 YR 3/3). Deposits formed by detritus flow in high energy systems.

F. Depth: 33.5 - 44 cm; texture: fine to very fine sand, grain supported with specific contacts in clay loam matrix, lithic fragments present in around 30%. Floating clasts of 9 to 14 millimeters in diameter, angled with high and low sphericity. Moderate presence of roots. Dark brown color (Hue
7.5 YR 3/3). Deposits formed by material fall in sub-aquatic environment contributed by wind currents with alluvial material contribution.

BSP-14 Profile:

A. Depth: 0 - 10 cm; texture: organic matter with little sediment composed of clay. Dark brown color (Hue 10 YR 2/2). Soil development and sub-aerial exposure.
B. Depth: 10 - 16 cm, texture, medium to fine sand, grain supported on silty clay matrix, specific contacts; the lithic fragments make up about 30%. High organic content. Yellow-grayish brown color (Hue 10 YR 5/3). Sedimentation by traction and decantation of materials product of turbulent flows. Reactivation of a gravity flow system.
C. Depth: 16 - 23 cm; texture: organic matter. Dark brown color (Hue 10 YR 2/2). Soil development and sub-aerial exposure.
D. Depth: 23 - 37 cm, texture, medium to coarse sand, heterogeneous, grain supported with specific planar contacts, on a silty sand matrix. The lithic fragments make up about 25%. Clasts of up to 11 mm composed of Andesite and ignimbrite, very angular with high sphericity. Yellow-grayish brown color (Hue 10 YR 4/2). Sedimentation by traction and decantation of materials product of turbulent flows.

Stratigraphic Description of the North Bofedal profiles.

In the North Bofedal, soil profile samples distributed longitudinally were obtained. The textural characteristics of each level or stratum of each profile surveyed are summarized below.

BNP 1

A. Depth: 0 - 16cm; texture: organic matter with clastic-clayey material. Brownish-black color. Interpretation, soil development with interruption in sedimentation rate and sub-aerial exposure.

B. Depth: 16 - 22 cm, texture, medium to fine sand, in silty matrix, supported grain, planar contacts, with lithic fragments around 40%. Isolated clasts up to 7 mm of ignimbrite, angular and of low sphericity. Brownish-black color. Interpretation, deposition by traction and decantation of materials product of turbulent flows, with erosion of the bed and reworking without considerable transport.

C. Depth: 22 - 27 cm; texture: organic material with clay clastic material. Brownish-black color. Interpretation, soil development with interruption in sedimentation rate and sub-aerial exposure.

D. Depth: 27 - 33 cm; texture: fine sand in silty matrix, grain supported, lithic around 35%. Isolated clasts of up to 10 mm of ignimbrite, very angular and of low sphericity. Black-brownish color. Interpretation, decantation of sub-aquatic grains contributed by wind, intermittent flows with local reworking and little transport.

E. Depth: 33 - 40 cm; texture: organic material with clay clastic material. Black-brownish color. Interpretation, soil development with interruption in the sedimentation rate and sub-aerial exposure.
F. Depth: 40 - 51 cm; texture: fine to very fine sand, grain supported on silty matrix, with lithic fragments present in 30%. Black-brownish color. Interpretation, decantation of sub-aquatic grains contributed by wind, intermittent flows with local reworking and little transport.

BNP 3

A. Depth: 0 - 16 cm; texture: organic material with clay-silty clastic material. Isolated clasts up to 14 mm of ignimbrite, angular and with low sphericity. Reddish-gray color. Interpretation, soil development with interruption in sedimentation rate and sub-aerial exposure.

B. Depth: 16 - 44 cm; texture: very fine sand, grain supported on silty matrix, lithic fragments present in 30%. Dark gray-reddish color. Interpretation, soil development with sedimentation present but decrease in the sedimentation rate.

BNP 4

A. Depth: 0 - 9 cm; texture: organic material with clay clastic material. Brown-reddish color. Interpretation, consolidation of soil development with interruption in the sedimentation rate and sub- aerial exposure.

B. Depth: 9 - 25 cm; texture: organic matter, clastic material composed of clay. Reddish-black color. Interpretation, soil development with sedimentation present but decrease in the sedimentation rate.

C. Depth: 25 - 35.5 cm; texture: organic matter, clastic material composed of clay. Reddish-black color. Interpretation, soil development with sedimentation present but decrease in the sedimentation rate.

D. Depth: 35.5 - 40 cm; texture: fine to medium sand in clay matrix, supported matrix, lithic fragments around 30%. Reddish-black color. Interpretation, material traction deposits of episodic turbulent gravity flows and decantation when the energy of the system has decreased.

E. Depth: 40 - 48.5 cm; texture: fine to very fine sand, grain supported with silty clay matrix, lithic fragments around 10%. Reddish-black color. Interpretation, deposits formed by material fall in sub- aquatic environment contributed by wind currents.

F. Depth: 48.5 - 69 cm; texture: fine to very fine-grained sand, grain supported with clay matrix, lithic fragments around 25%. Dark gray-reddish color. Interpretation, deposit by traction and decantation of materials product of turbulent flows of long duration, with progressive decrease of the energy of the environment giving way to a deposition by decantation.

G. Depth: 69 - 87 cm; texture: medium grain sand, supported grain, silty matrix, planar and specific contacts, lithic fragments around 30%. Reddish-black color. Interpretation, deposition by traction and decantation of materials product of turbulent flows, with erosion of the bed and reworking without considerable transport.

H. Depth: 87 - 106 cm; texture: medium sand, grain supported with silty clay matrix, lithic fragments around 20%. Reddish-black color. Interpretation, detritus flow deposits in an environment of high energy, of low transport.

I. Depth: 106 - 111 cm; texture: fine sand in silty clay matrix, supported grain, lithic fragments around 30%. Dark gray-reddish color. Interpretation, deposits formed by material fall in sub-aquatic environment contributed by wind currents.

J. Depth: 111 - 115 cm; texture: fine to medium grain sand in clay matrix, supported matrix, lithic fragments around 10%. Reddish-black color. Interpretation, material traction deposits of episodic turbulent gravity flows and decantation when the system energy has decreased.

K. Depth: 115 - 139 cm; texture: fine sand, grain supported with clay matrix, lithic fragments around 40%. Reddish-black color. Interpretation, deposits formed by material fall in sub-aquatic environment contributed by wind currents.

BNP 7

A. Depth 0 - 25 cm; texture: organic material with clay-silty clastic material. Dark reddish brown color. Interpretation, soil development with interruption in the sedimentation rate and sub-aerial exposure.

B. Depth: 25 - 37.5 cm; texture, organic material with clay-silty clastic material. Dark reddish brown color. Interpretation, soil development with interruption in the sedimentation rate and sub-aerial exposure.

C. Depth: 37.5 - 40.5 cm, without data. Sample thickness removed.

D. Depth: 40.5 - 50.5cm; texture: fine sand matrix supported on clay-silt matrix. Brownish-gray color. Interpretation, deposits formed by material fall in sub-aquatic environment contributed by wind currents.

E. Depth: 50.5 - 57 cm; texture: fine sand, matrix supported on a clay matrix, specific contacts and no contacts. Dark reddish brown color. Interpretation, deposits formed by material fall in sub-aquatic environment contributed by wind currents.

F. Depth: 57-76.5 cm; texture: fine grain sand, matrix supported with clay matrix, lithic fragments around 10%. Dark reddish gray color. Interpretation, deposits formed by material fall in sub-aquatic environment contributed by wind currents.

ANNEX 2

METHODOLOGY

1. FIELD VISIT

In March of this year, a visit was made to the study area for sampling, as well as identifying and describing the ecological and geological characteristics of the area, which allowed an interpretation of the results more appropriate to the nature of the place.
In this way it was observed that in the study area the main course of the Silala flows for around 50 kilometers where two main bofedals named South Bofedal and North Bofedal have been identified.

1.1 SAMPLING

For the fulfillment of the proposed objectives, the sampling was mainly oriented to the Palynology that includes floral samples for reference pollen, soil samples to obtain surface pollen and sediment samples from bofedals for fossil pollen. And as a complement, the stratigraphic description of sediments was made in the profiles obtained and in two trial pits.

1.1.1 PALINOLOGY

1.1.1.1 REFERENCE POLLEN

Species of greater presence and/or own of the zone were identified, from which floral samples were taken; those mature but not open flowers in such a way that intact stamens are conserved inside (containing the pollen grains). In this way contamination of the samples is also avoided. The flowers were deposited in properly coded paper envelopes. In some cases, a complete fertile plant sample was taken.

1.1.1.2 SURFACE POLLEN

In each bofedal studied different plant communities were identified, according to the predominance of a certain type of vegetation. Within each plant community an approximate area of one hectare was established, where the vegetation is physiognomically homogeneous. Within this area ten samples of surface soil were randomly taken with a small spoon, an approximate quantity of 10 g, introduced in Ziploc bags with their respective sampling codes.

1.1.1.3 FOSSIL POLLEN

For the sediment sampling of the bofedals, two Russian-type drills were used. One of 50 cm and one of 100 cm in length. The dimensions of the profiles are 5 cm in diameter and variable length according to the consistency of the sediment in each bofedal.
In both bofedals, the sampling transect was defined according to the criterion of affectation by drying observed. Thus, in the South Bofedal, the sampled transect is longitudinal, while in the North Bofedal this transect is transversal. A total of 26 profiles of variable length (10- 139 cm) were taken, which were deposited in longitudinal sections of 1.5-inch PVC pipes and covered with plastic film to conserve their moisture and avoid contamination.
This number of samples includes the replicas of several profiles.

1.2 STRATIGRAPHICAL DESCRIPTION

The stratigraphic description of some profiles was carried out in the field with the purpose of defining the viability of success in the subsequent required analyzes.
Additionally, we made the description in two trial pits, both located in the South Bofedal, this due to the marked drying of said bofedal.

Both trial pits with a dimension of 50 x 40 cm, one of 52 cm and another 63 cm deep. For the description of the color of sediment the Munssell Book (1976) was used, for the size of the textural grain Chilingar was used (1956), this allows to locate it in Wentworth's scale (1922). The Compton manual (1962) was used to describe the shape of the particles.

1.3 PHOTOGRAPHS TAKING

Photographs were taken in strategic places in order to obtain representative views of our samplings.
The profiles obtained were also photographed in order to capture the coloration at the time of extraction.

2. LABORATORY WORK

The profiles obtained and transported to the city of La Paz, were conserved in facilities of the Institute of Geological Sciences and the Environment (IGEMA), where we made the selection of those profiles suitable for the realization of the proposed analyzes. In this way, for the detailed stratigraphic description, 5 profiles (BSP2, BSP6, BSP8, BSP10, BSP14) and the two trial pits (BSP7, BSP9) were selected in the South Bofedal, while in the North Bofedal, 4 profiles were selected (BNP1, BNP3, BNP4, BNP7).

The profiles BSP2, BSP14 (South Bofedal) and BNP7 (North Bofedal) in addition to the detailed stratigraphic description were studied with palynological methods, 14C dating and X-ray diffraction analysis of metals (XRD).

These profiles were divided into two equal halves, one half was sent to France for the XRD analysis and the other half was left in Bolivia as a control copy for the palynological study and the sending of samples for 14C dating.

2.1 POLLEN EXTRACTION

In the cases of surface pollen and fossil pollen, Lycopodium tablets (allochthonous pollen) were used in order to facilitate the calculation of the concentrations of the different palynomorphs identified (Court, 1974).

2.1.1 REFERENCE POLLEN

Under a stereomicroscope, the anthers of the flowers that are soaked are separated. The product obtained is introduced into properly coded test tubes where it is crushed with the aid of a glass rod. Finally, we continue with the protocol of Faegri & Iversen.

Laboratory protocol for sediment samples (modified by Erdtman in 1954 and by Faegri & Iversen in 1989)

1. Take a small amount of sediment (1 cm3).
2. Place the sediment in test tubes.
3. Assign correlative codes to each sample.
4. Put the sediments in a 400 cm3 glass. Add 50 cm3 of 10% KOH.
5. Put the glasses in a hot stove for 5 to 10 minutes.
6. Filter with distilled water through a 180 μm metal mesh. Centrifuge the filtered material and repeat as many times as necessary until a clear solution is obtained.
7. Add 10% hydrochloric acid (HCl) to balance the tubes and centrifuge.
8. Add pure HCl and heat in a water bath for 10 minutes. This treatment eliminates carbonates,
but is susceptible to the degradation of exine.
9. Wash with distilled water and centrifuge.
10. Carefully add a 70% HF solution and let it work overnight.
11. Wash twice with distilled water.
12. Acetolysis: First, prepare in a Pyrex glass of 600ml anhydrous acetic acid and then carefully drip H2SO4 concentrate. For this action, glasses and protective gloves should be used (9 ml of acetic acid anhydride and 1 ml of H2SO4 are required for each sample). After mixing with the rest of the sample, heat in a pot for 5 minutes (in this way the organic material is destroyed with the exception of pollen grains). Then it is centrifuged.
13. Add concentrated acetic acid and centrifuge.
14. Wash twice with distilled water.

15. Add pure alcohol and centrifuge (in this way the sample is dried).
16. Put glycerin in the test tubes according to the amount obtained.
17. Assembly: wash the coverslips in 96% alcohol.
18. On the coverslip, place a small tube of glycerin gelatin and a drop of the sample 55 µl.
19. Heat the coverslip in an oven at 80°C.
20. In order to seal the plate melted paraffin, glass glue or fine nail polish can be used, which is
carefully placed on the edge of the coverslip.
21. Leave one hour in a horizontal position, with the coverslip facing up.

2.1.2 SURFACE POLLEN

In test tubes with distilled water 2 grams of soil were introduced together with a Lycopodium tablet (allochthonous pollen), when the tablet is dissolved, proceed with the complete protocol of Faegri & Iversen.

2.1.3 FOSSIL POLLEN

Longitudinally the profiles were divided into portions every 0.5 cm to the depth of 10 cm and towards the base every 1 cm. These portions were stored in Ziploc bags labeled with sample code and depth. 0.5 cm3 was taken from each portion with evident organic content, 1 cm3 was taken from those portions with little organic matter. In both cases, the sample was soaked in distilled water together with a Lycopodium tablet and when this was dissolved, the Faegri & Iversen protocol was followed. In case of enough organic matter, exposure to HF is avoided, proceeding directly to acetolysis.
The protocol of Faegri & Iversen allows obtaining the aforementioned, where the pollen grains without plasmatic content are conserved. This residue was diluted with glycerin and reserved in appropriately coded Eppendorf tubes until the plates were assembled, the identification and counting of the existing palynomorphs.

2.2 STRATIGRAPHICAL DESCRIPTION

The detailed stratigraphic description of the selected profiles was based on the description of the textural characteristics of the levels identified in the sections according to the following parameters:

2.2.1 TEXTURE

2.2.1.1 GRAIN SIZE

The size of the diameter of the grains, clasts or detritus is described.
Initially (determination in the field) the grain size is determined by making a comparative observation with the graph in order to determine the size of sedimentary particles established by Chilingar (1956). Once the particle size is obtained, it is classified including the sample in a category of the Wentworth Grade Scale (1922) (see Figure 1).

Millimeters (mm)		Micrometers (μm)	Phi (ϕ)	Wentworth size class		Rock type
	4096		-12.0	Boulder	Gravel	Conglomerate/ Breccia
	256		-8.0	Cobble		
	64		-6.0	Pebble		
	4		-2.0	Granule		
	2.00		-1.0	Very coarse sand	Sand	Sandstone
	1.00		0.0	Coarse sand		
1/2	0.50	500	1.0	Medium sand		
1/4	0.25	250	2.0	Fine sand		
1/8	0.125	125	3.0	Very fine sand		
1/16	0.0625	63	4.0	Coarse silt	Silt	Siltstone
1/32	0.031	31	5.0	Medium silt		
1/64	0.0156	15.6	6.0	Fine silt		
1/128	0.0078	7.8	7.0	Very fine silt		
1/256	0.0039	3.9	8.0			
	0.00006	0.06	14.0	Clay	Mud	Claystone

Figure 1: Wentworth Grain Scale (1922)

2.2.1.2 SHAPE OF THE COMPONENTS

The shape of the sediment components is described considering the roundness or angularity and the sphericity of the grains, clasts or detritus by direct observation and its comparison with the scheme of Sphericity, Roundness and Degree of Selection instituted by Compton (1962) (see Figure 2).

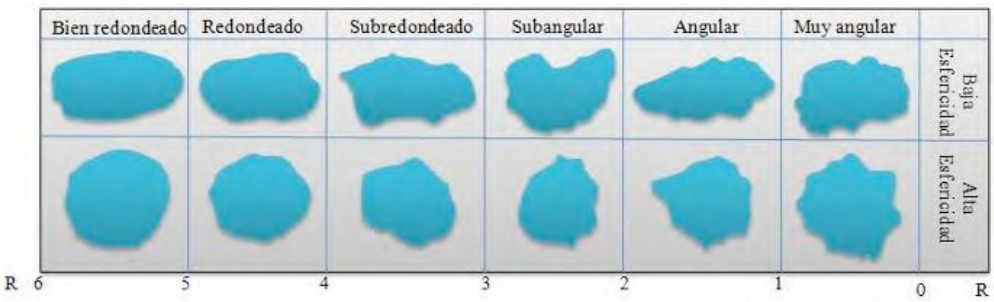


Figure 2: Shape diagram of the clasts.

2.2.1.3 PERCENT RATIO OF COMPONENTS

The sediments surveyed are mainly composed of quartz grains, lithic fragments (resulting from the erosion and weathering of surrounding rocks that are ignimbrites and andesites), silt and clay. The percentage estimate is made by observation and comparison with the Graph for the Estimation of Percentages (see Figure 3).

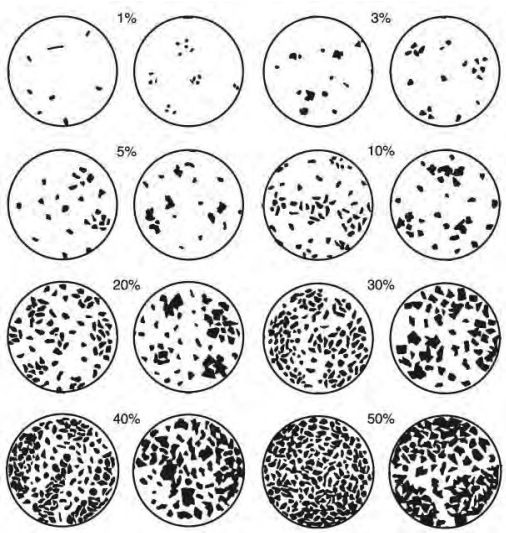


Figure 3

Figure 3: Estimation of components by percentages

2.2.2 ESTIMATION OF SEDIMENT COLOR

The color of the different segments of the obtained profiles was determined by direct visual comparison with the Munsell Color Chart and described with the corresponding code.

2.3 14C DATING

For the 14C dating, 5 grams of sample were taken at the points where a marked change in stratification was observed, and then these were dried in an oven at 25°C and later sent to the Beta Analytic Laboratory, Florida-United States.
In the BSP2 profile, two samples were taken, one at 7 cm and the second at 38 cm in depth. In the BNP7 profile, 2 samples were taken at 4 cm and 45 cm depth and finally in the BSP14 profile, 2 dating were carried out at the depths of 9 and 17.5 cm.

2.4 X-RAY DIFFRACTION ANALYSIS OF METALS (XRD)

A complete longitudinal section of the BSP2, BNP7 and BSP14 profiles were reserved and sent for the XRD analyzes carried out every 0.5 cm in facilities of the EDYTEM Laboratory in Savoie, France.

3. OFFICE WORK

3.1 PALINOLOGY

3.1.1 REFERENCE POLLEN

We proceeded to make the microscopic plates in order to observe the structural characteristics of the pollen of each species sampled. Then we proceeded to the description and obtaining of photographs. These remain as a record of the identification of the diversity of pollens in the surveyed area.

3.1.2 SURFACE AND FOSSIL POLLEN

Microscopic plates were made using 25 μm of pollen extract and under different light microscopy the different palynomorphs were identified. The identification of pollen grains is based on the description of the exine's own characteristics: structure, ornamentation, grain position, openings, shape and size. For identification, photographs of the obtained reference plates and the database of other works carried out in similar environments were used. Identification keys Heusser (1971), MarkGraf (1978), Roubik & Moreno (1981) and pollen catalog Sandoval (2010).
The count of the different identified palynomorphs was done following the line method, trying to count a minimum of 300 pollens per prepared sample (Court, 1974).

Once the palynomorph count is complete, this database is introduced to the Psimpoll program for the calculation and layout of the percentages and the concentration of each palynomorph.
For a better interpretation, the data of the stratigraphic description of each profile and the estimated age according to the obtained age model were added to the diagram.

3.2 STRATIGRAPHICAL DESCRIPTION

The descriptions allowed elaborating graphic schemes of the texture of the ground in relation to the depth. In addition, in the case of BSP2, BSP14 and BNP7 profiles, it can also be related to the age of the profile.

3.3 14C DATING

The results sent by the Beality Analytical Laboratory were calibrated and analyzed in the Clam program (Blaauw, 2011) (Table 1), thus, the age-depth model was obtained, which shows a linear relationship with constant sedimentation, as a consequence of an insufficient number of points analyzed.

Bofedal	Profile	Depth	^{14}C Age	Calibrated Age
South	BSP2	7-7.5	103.29 ± 0.39 pMC	1956-1957 AD
	BSP2	38-38.5	240 ± 30 BP	1726 - 1806 AD
	BSP14	9-9.5	124.50 ± 0.46 pMC	1980-1962 AD
	BSP14	17.5-18	240±30BP	680-862AD
North	BNP7	4 - 4.5	133.28 ± 0.50 pMC	1976 - 1978 AD
	BNP7	45-45.5	860 ± 30 BP	1176-1274 AD

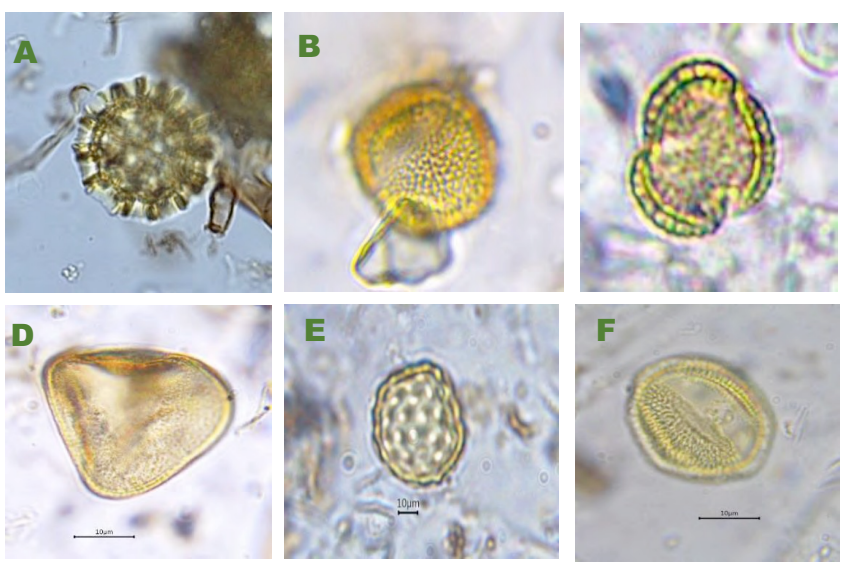
3.4 X-RAY DIFFRACTION ANALYSIS OF METALS

The results sent by the EDYTEM Laboratory allowed elaborating graphs of the behavior of the metals analyzed in relation to the time and to the lithological characteristics of the samples.
Due to the characteristics of the area, important events marked in the global history and recent studies carried out in the continent were identified as relevant metals for our results; Pb, Fe, Br, Ni, Ti, Al, Zr and Rb. Also Si/Ti, Fe/Ti and Mn/Ti ratios.

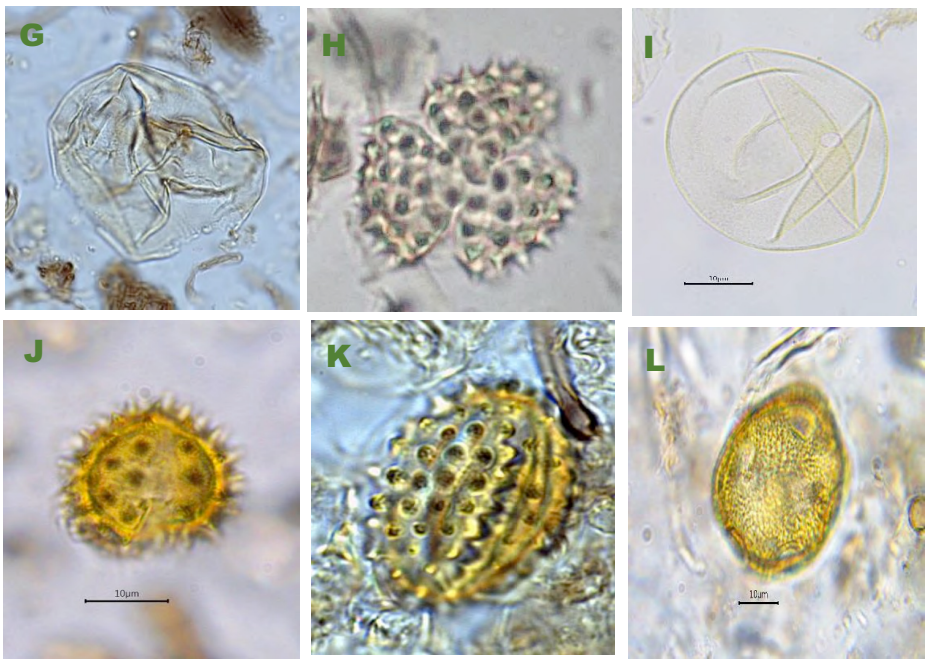
Annex 3

Fossil pollen

Photos registered in this survey



A. Amaranthaceae, Gomphrena. Monad grain, spherical shape with a diameter of 10-13 µm, Spherical-hexagonal field, pantoporated and fenestrated exine.
B. Caryophyllaceae, Pycnophyllum. Monad grain, oblate-spheroidal shape, equatorial length 15um, circular lobed field, tricolpate, prominent colpos, circular pores and reticulated-tilted exine with a thickness of 1.5 µm.
C. Brassicaceae, monad grain, oblate-spheroidal shape, circular lobed area, equatorial length 20 µm, tricolpate, narrow colpos, microreticulated-tilted exine of <2 µm thickness.
D. Cyperaceae, Eleocharis, pseudo-monad grain, unperturbed, triangular field, round edges, convex base, uneven and thin exine (Sandoval et al., 2010, Roubik 1991). Size: 55x40 µm.
E. Chenopodiaceae, spherical monad grain, pantoporated exine, circular pores of 1-2 µm in diameter with thin annulus, a number of approx. 65 pores, exine thickness of 2-2.5 µm.
F. Gentianaceae, monad grain, oblate-spheroidal shape, reticulated exine, sub-circular field, tricolpate, moderately long and broad colpos, circular pores, 2 µm exine thickness (Roubik 1991, Heusser 1981). Size: 33x35 µm.

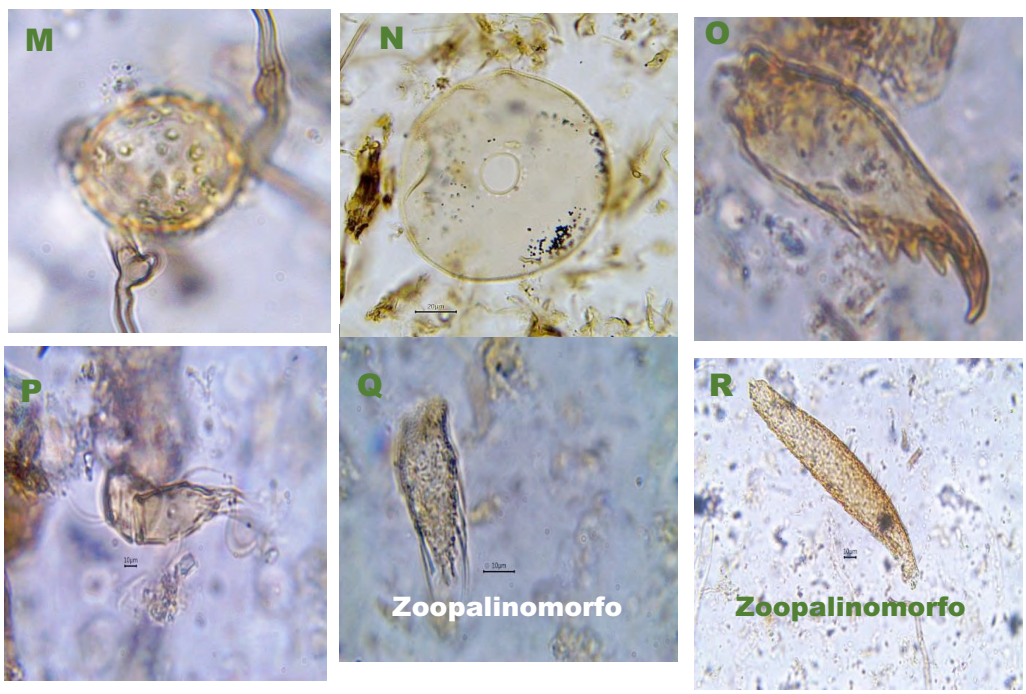


G. Juncaceae, monad grain, aberrant shape, heteropolar, monoporated, non-annular circular pore, psilate exine of <1 µm thickness (Sandoval et al., 2010). Size: 37X35 µm.

H. Asteraceae, Parastrephia quadrangularis, monad grain, sub-prolate to prolate-spheroidal, circular field, tricolpate, pantoporated, equine exine, conical equids of obtuse apex, length of thorns of approximately 3 µm (Collao-Alvarado et al. 2015, Sandoval et al., 2010). Size: 21x38 µm.
I. Poaceae, Festuca, monad grain, prolate-spheroidal shape, psilate exine of <1 µm thickness, circular field, monoporated, circular pore, annulated and operculated (Heusser, 1981).
J. Asteraceae, Werneria, monad, radiosymmetric, spheroid field, tricolporate, easily distinguishable colpos, equine ornamentation with spines of 4 µm and distance of 6 µm between thorns (Collao- Alvarado et al., 2015, Sandoval et al., 2010). Size: 37x38 µm.
K. Asteraceae, Senecio, monad, radiosymmetric, spheroid field, tricolporate, equine ornamentation with thorns of 3 µm and distance of 5 µm between the thorns (Sandoval et al., 2010). Size: 43x42 µm.
L. Montiaceae, Calandrinia, monad, apolar, spheroid field, pantoporated, pores of variable size, granulated surface, micro-equidated tectum exine (Heusser 1981). Size: 66 µm

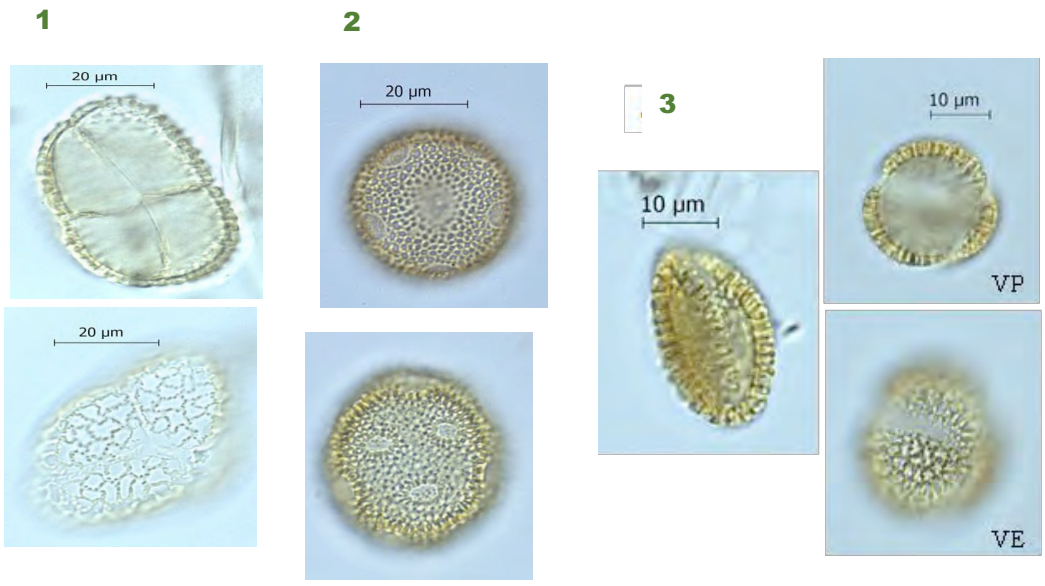
Palynomorphs

Photos registered in this survey

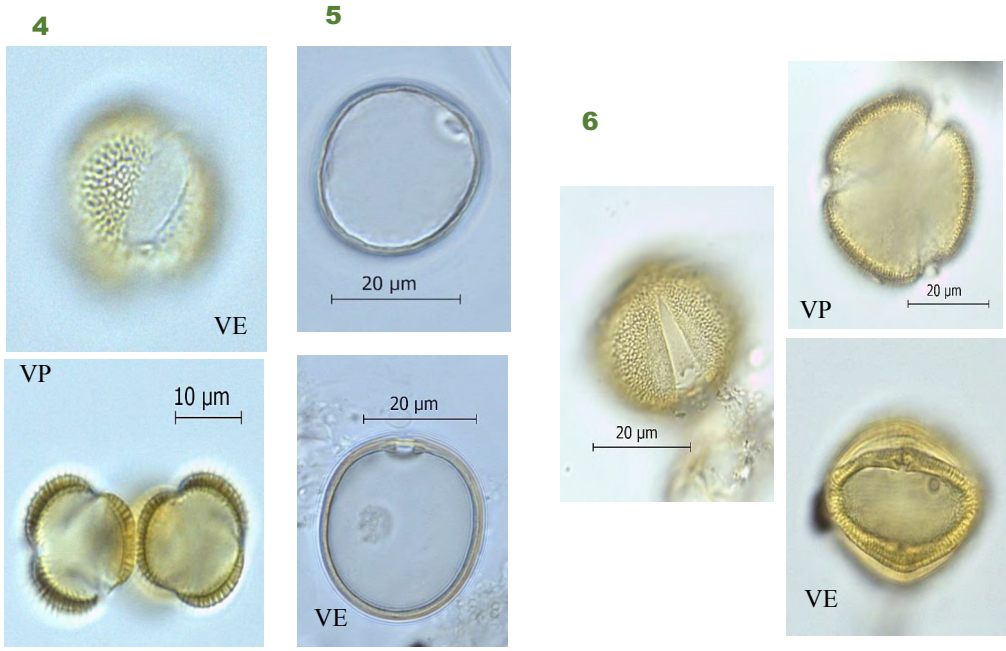


Reference Pollen

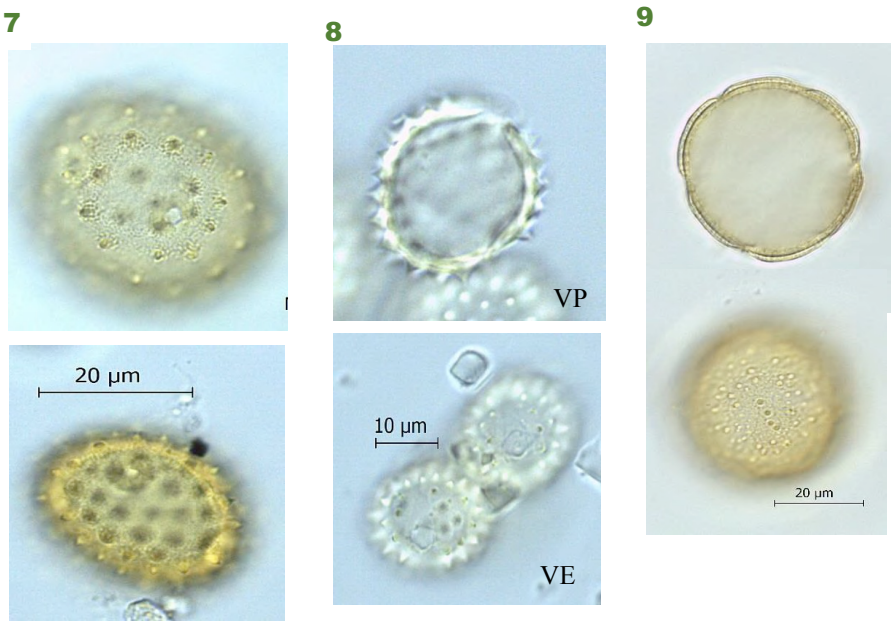
Photos registered in this survey



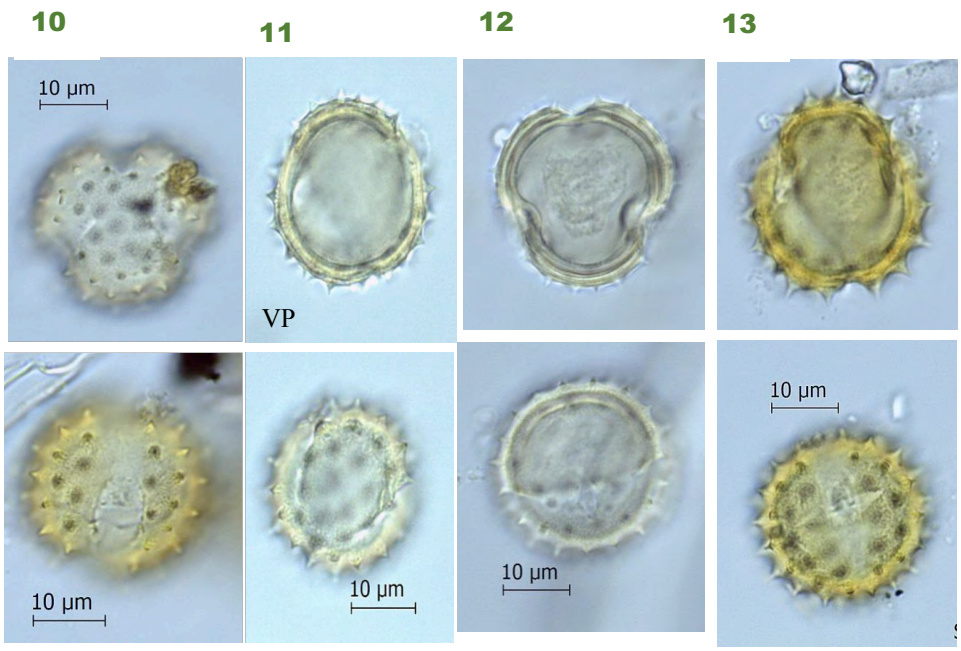
1. Orchidaceae, Myrosmodes paludosa, pollen in tetrads, kidney shape, each unperturbed unit with triangular shape of obtuse angles. Reticulated structure, exine thickness of 2.5 µm. Size 54.26 ± 6 µm.
2. Caryophyllaceae, Cerastium peruvianum, monad pollen, spherical shape, pantoporated, annular circular pores with a diameter of 5 µm. Reticulated homo-broached structure. Exine thickness of 3 µm. Size 33 ± 4 µm.
3. Brassicaceae, Menonvillea macrocarpa, monad pollen, prolate spheroidal shape, circular field, tricolpate, wide colpos of narrow ends. Reticulated and tilted hetero-broached structure, staff length of 1 µm. Exine thickness of <1 µm. Size 22.18 ± 2.33 µm.



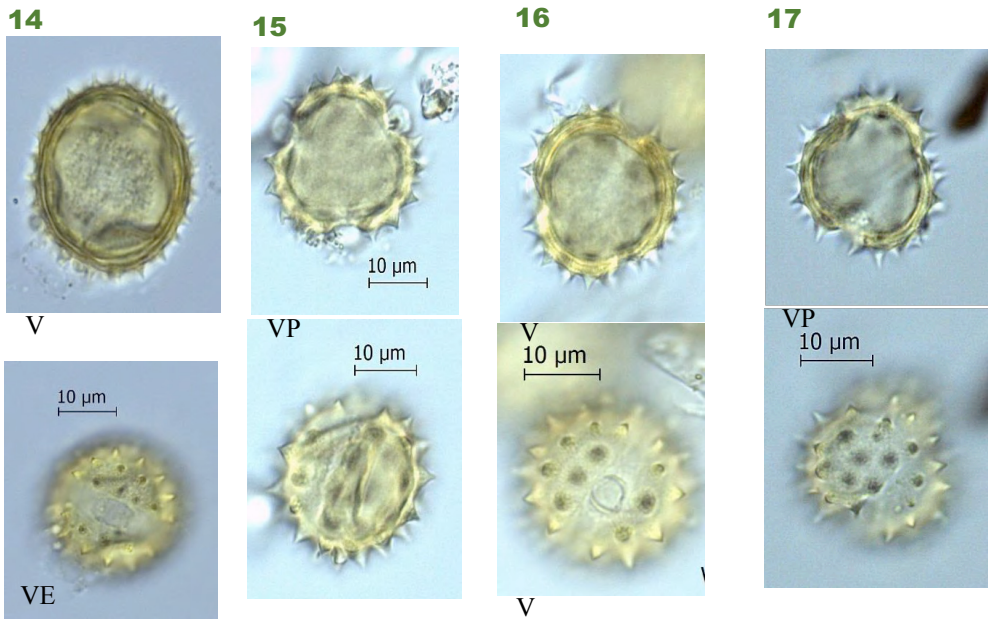
4. Brassicaceae, Mostacillastrum dianthoides, monad grain, oblate-spheroidal shape, circular field, tricolpate, wide colpos of round ends, reticulated and tilted homo-broached exine, staff length of 2 µm. Thickness of the exine of 1.5 µm. Size 14.48 ± 0.23 µm.
5. Poaceae, Festuca potosiana, monad, circular shape, circular area, monoporated, circular pore with prominent annulus, psilate exine. Size 32.36 ± 1.18 µm.
6. Gentianaceae, monad, sub-prolate shape, sub-circular field, tricolporate, long and wide colpos, circular pores of 7 µm in diameter. Micro-reticulated – tilted structure, staffs of 1.5 µm length. Exine thickness of <1 µm. Size 32.2 ± 2.87 µm.



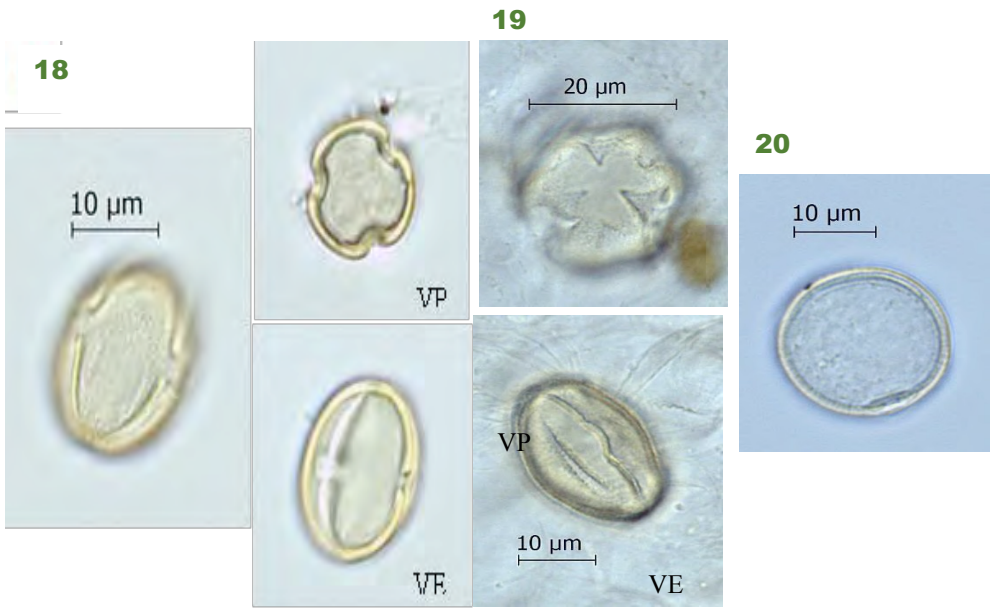
7. Malvaceae, Nototriche auricoma, monad pollen grain, spherical shape, spheroidal field, pantoporated, circular pores 3 µm in diameter, thin annulus. Equine structure, conical equines 2.3 µm long. Exine thickness of <1 µm. Size 35.18 ± 5.47 µm.
8. Asteraceae, Parastrephia lepidophylla, monad grain, spherical oblate shape, circular field, tricolporate, broad colpos as long as the pollen grain, elongated pores, equine exine, spines wider than long. Size 17 ± 1.32 µm.
9. Ranunculaceae, Ranunculus praemotus, monad pollen grain, spherical shape, spheroidal field, zono-colpate, six short colpos. Micro-equine structure, equines of obtuse apex. Exine thickness of 1.5 µm. Size 45.05 ± 3.21 µm.



10. Asteraceae, Senecio candollei, monad pollen grain, oblate spheroidal shape, circular field, tricolporate, elongated pores, long and wide colpos. Equine structure, triangular equines, 2.5 µm wide base, sharp apex, length of 3 µm, separation of 2 µm between equines. Exine thickness of 2 µm. Size 26.16 ± 0.61 µm.
11.Asteraceae, Senecio chrysolepis, monad grain, oblate spheroidal shape, circular field, tricolporate, long and wide colpos, elongated pores. Equine structure, conical equines with acute apex, base 2.5 µm, length 2.5 µm, separation between equines of 1.5 µm. Exine thickness of 1.5 um. Size 23.43 ± 1.6 µm.
12. Asteraceae, Senecio comoris, monad grain, oblate spheroidal shape, circular field, tricolporate, long and relatively narrow colpos, elongated pores. Equine structure, conical equines with acute apex, 2 µm base, length of 2.2 µm, separation between equines of 2.5 µm. Exine thickness of 2 µm. Size 25.6 ± 0.8 µm.
13. Asteraceae, Senecio rufescens, monad grain, oblate spheroidal shape, circular field, tricolporate, long and wide colpos, elongated pores. Equine structure, conical equines, 3.5 µm base, length of 3 µm, separation between equines of 1.5 µm. Exine thickness of 1.5 µm. Size 23.61 ± 1.4 µm.



14. Asteraceae, Perezia ciliosa, monad grain, oblate spheroidal shape, circular field, tricolporate, long and narrow colpos, elongated pores. Micro-reticulated–tilted structure, staffs 1.5 µm long. Exine thickness of 1.5 µm. Size 27.6 ± 4 µm.
15. Asteraceae, Werneria glaberrima, monad grain, oblate spheroidal shape, circular field, tricolporate, large and long colpos, circular pores. Equine structure, conical equines, 3 µm base, length of 4 µm, equine separation of 2 µm. Exine thickness of 2 µm. Size 23.43 ± 1.48 µm.
16. Asteraceae, Werneria pygmaea, monad grain, oblate spheroidal shape, circular field, tricolporate, long and relatively narrow colpos, circular pores with a diameter of 3 µm. Equine structure, conical equines, 2 µm base and length of 2 µm, equine separation of 1.5 µm. Exine thickness of 1.5 µm. Size 21.83 ± 1.45 µm.
17. Asteraceae, Xenophyllum incisum, monad grain, oblate spheroidal shape, circular scope, tricolporate, long and relatively narrow colpos, elongated pores. Equine structure, conical equines, base 3 µm, length 4 µm, equine separation 3 µm. Exine thickness of 2 µm. Size 21.62 ±
1.76 µm.



18. Loasaceae, Caiophora coronata, monad, radiosymmetric sub-prolate shape, circular field, tricolporate, long colpos, pores at the equator of the colpos (Heusser, 1981). Size: 18.89 ± 0.97 μm.
19. Hydrophyllaceae, Phacelia nana, monad pollen grain, prolate shape, circular field, tricolporate, long and narrow colpos. Micro-reticulated structure. Exine thickness of 1.5 μm. Size 23.26 ± 1.84 μm.
20. Poaceae, Puccinellia frigida, monad grain, spherical shape, monopod, circular pore, inconspicuous angle, micro-striated exine. Size 23-24 μm.

ANNEX 4

Results of the 14C Analysis

Beta Analytic Inc
4985 SW 74 Court
Miami, Florida 33155
Tel: 305-667-5167
Fax: 305-663-0964
beta@radiocarbon.com

Mr. Darden Hood
President

Mr. Ronald Hatfield
Mr. Christopher Patrick
Deputy Directors

Beta Analytic
RADIOCARBON DATING

ISO/IEC 2005:17025-Accredited Testing Laboratory

REPORT OF RADIOCARBON DATING ANALYSES

Katerine Escobar Torrez
Herbario Nacional de Bolivia

Report Date: May 16, 2018
Material Received: April 18, 2018

Laboratory Number	Sample Code Number	Conventional Radiocarbon Age (BP) or Percent Modern Carbon (pMC) & Stable Isotopes Calendar Calibrated Results: 95.4 % Probability High Probability Density Range Method (HPD)	
Beta - 492440	**BSP2 7**	**103.29 +/- 0.39 pMC**	IRMS δ13C: -27.5 o/oo

(95.4%) 1956 - 1957 cal AD(-7 - -8 cal BP)

Submitter Material: Organic Sediment/Gyttja
Pretreatment: (organic sediment) acid washes
Analyzed Material: Organic sediment
Analysis Service: AMS-Standard delivery
Conventional Radiocarbon Age: -260 +/- 30 BP
Fraction Modern Carbon: 1.0329 +/- 0.0039
D14C: 32.90 +/- 3.86 o/oo
Δ14C: 24.44 +/- 3.86 o/oo(1950:2,018.00)
Raw pMC: (without d13C correction): 102.76 +/- 0.39 pMC
Calibration: BetaCal3.21: HPD method: SHCAL13 + SHZ1_2

Beta Analytic Inc
4985 SW 74 Court
Miami, Florida 33155
Tel: 305-667-5167
Fax: 305-663-0964
beta@radiocarbon.com

Mr. Darden Hood
President

Mr. Ronald Hatfield
Mr. Christopher Patrick
Deputy Directors

Beta Analytic
RADIOCARBON DATING

ISO/IEC 2005:17025-Accredited Testing Laboratory

REPORT OF RADIOCARBON DATING ANALYSES

Katerine Escobar Torrez
Herbario Nacional de Bolivia

Report Date: May 16, 2018
Material Received: April 18, 2018

Laboratory Number	Sample Code Number	Conventional Radiocarbon Age (BP) or Percent Modern Carbon (pMC) & Stable Isotopes Calendar Calibrated Results: 95.4 % Probability High Probability Density Range Method (HPD)	
Beta - 492442	**BSP2 38**	**240 +/- 30 BP**	IRMS δ13C: -26.1 o/oo

(64.9%) 1726 - 1806 cal AD(224 - 144 cal BP)
(30.5%) 1640 - 1692 cal AD(310 - 258 cal BP)

Submitter Material: Organic Sediment/Gyttja
Pretreatment: (organic sediment) acid washes
Analyzed Material: Organic sediment
Analysis Service: AMS-Standard delivery
Percent Modern Carbon: 97.06 +/- 0.36 pMC
Fraction Modern Carbon: 0.9706 +/- 0.0036
D14C: -29.44 +/- 3.62 o/oo
Δ14C: -37.39 +/- 3.62 o/oo(1950:2,018.00)
Measured Radiocarbon Age: (without d13C correction): 260 +/- 30 BP
Calibration: BetaCal3.21: HPD method: SHCAL13



REPORT OF RADIOCARBON DATING ANALYSES

Katerine Escobar Torrez — Report Date: May 16, 2018

Herbario Nacional de Bolivia — Material Received: April 18, 2018

Laboratory Number	Sample Code Number	Conventional Radiocarbon Age (BP) or Percent Modern Carbon (pMC) & Stable Isotopes Calendar Calibrated Results: 95.4 % Probability High Probability Density Range Method (HPD)	
Beta - 492443	**BNP7 4**	**133.82 +/- 0.50 pMC**	IRMS δ13C: -28.0 o/oo

(89.7%) 1976 - 1978 cal AD(-27 - -29 cal BP)
(5.7%) 1963 cal AD(-14 cal BP)

Submitter Material: Organic Sediment/Gyttja
Pretreatment: (organic sediment) acid washes
Analyzed Material: Organic sediment
Analysis Service: AMS-Standard delivery
Conventional Radiocarbon Age: -2340 +/- 30 BP
Fraction Modern Carbon: 1.3382 +/- 0.0050
D14C: 338.17 +/- 5.00 o/oo
Δ14C: 327.21 +/- 5.00 o/oo(1950:2,018.00)
Raw pMC: (without d13C correction): 133.01 +/- 0.50 pMC
Calibration: BetaCal3.21: HPD method: SHCAL13 + SHZ1_2



REPORT OF RADIOCARBON DATING ANALYSES

Katerine Escobar Torrez — Report Date: May 16, 2018

Herbario Nacional de Bolivia — Material Received: April 18, 2018

Laboratory Number	Sample Code Number	Conventional Radiocarbon Age (BP) or Percent Modern Carbon (pMC) & Stable Isotopes Calendar Calibrated Results: 95.4 % Probability High Probability Density Range Method (HPD)	
Beta - 492444	**BNP7 45**	**860 +/- 30 BP**	IRMS δ13C: -25.9 o/oo

(95.4%) 1176 - 1274 cal AD(774 - 676 cal BP)

Submitter Material: Organic Sediment/Gyttja
Pretreatment: (organic sediment) acid washes
Analyzed Material: Organic sediment
Analysis Service: AMS-Standard delivery
Percent Modern Carbon: 89.85 +/- 0.34 pMC
Fraction Modern Carbon: 0.8985 +/- 0.0034
D14C: -101.53 +/- 3.36 o/oo
Δ14C: -108.89 +/- 3.36 o/oo(1950:2,018.00)
Measured Radiocarbon Age: (without d13C correction): 870 +/- 30 BP
Calibration: BetaCal3.21: HPD method: SHCAL13

Beta Analytic
RADIOCARBON DATING

Beta Analytic Inc
4985 SW 74 Court
Miami, Florida 33155
Tel: 305-667-5167
Fax: 305-663-0964
beta@radiocarbon.com

Mr. Darden Hood
President

Mr. Ronald Hatfield
Mr. Christopher Patrick
Deputy Directors

ISO/IEC 2005:17025-Accredited Testing Laboratory

REPORT OF RADIOCARBON DATING ANALYSES

Katerine Escobar Torrez
Herbario Nacional de Bolivia

Report Date: August 09, 2018
Material Received: July 20, 2018

Laboratory Number	Sample Code Number	Conventional Radiocarbon Age (BP) or Percent Modern Carbon (pMC) & Stable Isotopes Calendar Calibrated Results: 95.4 % Probability High Probability Density Range Method (HPD)	
Beta - 499941	**BNP14 17.5-18**	**124.50 +/- 0.46 pMC**	IRMS δ13C: -27.9 o/oo
(84.6%)	**1981 - 1984 cal AD**	**(-32 - -35 cal BP)**	
(10.8%)	**1962 cal AD**	**(-13 cal BP)**	

Submitter Material: Peat
Pretreatment: (organic sediment) acid washes
Analyzed Material: Organic sediment
Analysis Service: AMS-Standard delivery
Conventional Radiocarbon Age: -1760 +/- 30 BP
Fraction Modern Carbon: 1.2450 +/- 0.0046
D14C: 244.95 +/- 4.65 o/oo
Δ14C: 234.76 +/- 4.65 o/oo(1950:2,018.00)
Raw pMC: (without d13C correction): 123.76 +/- 0.46 pMC
Calibration: BetaCal3.21: HPD method: SHCAL13 + SHZ1_2

Beta Analytic
RADIOCARBON DATING

Beta Analytic Inc
4985 SW 74 Court
Miami, Florida 33155
Tel: 305-667-5167
Fax: 305-663-0964
beta@radiocarbon.com

Mr. Darden Hood
President

Mr. Ronald Hatfield
Mr. Christopher Patrick
Deputy Directors

ISO/IEC 2005:17025-Accredited Testing Laboratory

REPORT OF RADIOCARBON DATING ANALYSES

Katerine Escobar Torrez
Herbario Nacional de Bolivia

Report Date: August 09, 2018
Material Received: July 20, 2018

Laboratory Number	Sample Code Number	Conventional Radiocarbon Age (BP) or Percent Modern Carbon (pMC) & Stable Isotopes Calendar Calibrated Results: 95.4 % Probability High Probability Density Range Method (HPD)	
Beta - 499942	**BSP14 9-9.5**	**1300 +/- 30 BP**	IRMS δ13C: NA
(95.4%)	**680 - 862 cal AD**	**(1270 - 1088 cal BP)**	

Submitter Material: Peat
Pretreatment: (organic sediment) acid washes
Analyzed Material: Organic sediment
Analysis Service: AMS-Micro-sample Analysis; Standard delivery
Percent Modern Carbon: 85.06 +/- 0.32 pMC
Fraction Modern Carbon: 0.8506 +/-
D14C: -149.42 +/- 3.18 o/oo
Δ14C: -156.39 +/- 3.18 o/oo(1950:2,018.00)
Measured Radiocarbon Age: (without d13C correction): NA
Calibration: BetaCal3.21: HPD method: SHCAL13

Results of metal analysis (XRD)

ResultsoftheBSP2Profile

Depth	Years BP	Years AD-BC	Fe	Ni	Br	Pb	Si/Ti	Fe/Ti	Mn/Ti	Mn/Fe
0	-62	2012	15006	5482	2330	1498	2.6482	14.3051	1.1592	0.081
0.5	-58	2008	55734	4756	3159	3430	1.6679	26.2525	0.715	0.0272
1	-55	2005	97063	5032	3119	3208	1.5275	32.4083	0.7002	0.0216
1.5	-51	2001	153692	4893	2579	3414	1.2931	32.1061	0.6236	0.0194
2	-47	1997	158513	5080	3211	3439	1.3021	28.1051	0.6181	0.022
2.5	-43	1993	140579	5043	3662	2720	1.3468	29.3178	0.7218	0.0246
3	-39	1989	95234	6278	7265	1871	1.6318	30.7603	0.8107	0.0264
3.5	-35	1985	124048	6205	6426	2672	2.1689	34.8058	0.7685	0.0221
4	-31	1981	148331	6563	8438	3117	1.8627	41.9844	0.9825	0.0234
4.5	-28	1977	176571	6558	8420	5160	1.7019	51.4484	0.6952	0.0135
5	-24	1973	228167	6638	9027	7865	1.823	56.7862	0.5042	8.88E-03
5.5	-20	1969	276511	6484	8052	6440	1.2735	50.9228	0.3576	7.02E-03
6	-16	1965	314769	6444	8781	9707	1.509	70.1513	0.3633	5.18E-03
6.5	-12	1962	353338	5624	7423	8934	1.4246	54.2013	0.3086	5.69E-03
7	-8	1958	326932	6136	10162	7157	1.1271	46.738	0.2097	4.49E-03
7.5	-4	1954	440230	6196	8773	13922	1.3012	66.21	0.2313	3.49E-03
8	0	1950	493123	6043	6527	13910	1.0339	62.3417	0.2339	3.75E-03
8.5	4	1946	466451	5474	5470	9636	0.887	53.1992	0.2636	4.95E-03
9	8	1942	453969	4816	3500	7692	0.9552	47.546	0.2275	4.78E-03
9.5	12	1938	524233	5471	3234	10514	0.9946	64.331	0.2766	4.30E-03
10	16	1934	415598	4638	3837	13177	1.0804	93.5821	0.3783	4.04E-03
10.5	20	1930	297649	4135	2848	7271	0.927	63.1951	0.2675	4.23E-03
11	24	1926	271253	3878	2957	8168	1.0343	84.6872	0.3437	4.06E-03
11.5	28	1922	274825	3964	2910	6357	0.9172	70.2698	0.3125	4.45E-03
12	32	1918	369414	4106	2617	6919	0.7483	59.6406	0.2879	4.83E-03
12.5	36	1915	421817	4479	3168	6145	0.6511	42.9461	0.2546	5.93E-03
13	40	1911	503855	4916	3273	7931	0.6182	40.2762	0.2301	5.71E-03
13.5	44	1907	663727	5070	3401	11215	0.6313	36.8553	0.1976	5.36E-03
14	48	1903	625039	5212	2910	9130	0.6759	31.4358	0.1722	5.48E-03
14.5	52	1899	590762	5250	2874	6847	0.5932	29.853	0.1841	6.17E-03
15	56	1895	579671	5024	2725	6467	0.5469	34.5948	0.2091	6.04E-03
15.5	60	1891	634268	5167	2787	8755	0.4654	36.9104	0.189	5.12E-03
16	64	1887	621626	5277	2947	8681	0.4684	37.4835	0.2001	5.34E-03
16.5	68	1883	607599	5306	2909	9105	0.5347	45.479	0.2487	5.47E-03
17	72	1879	565430	5196	2728	7185	0.5334	40.5094	0.2427	5.99E-03

ResultsoftheBSP14Profile

Depth	Pb	Fe	Ni	Br	Si/Ti	Fe/Ti	Mn/Fe	Mn/Ti
0	2325	20542	4149	2087	2.1349	16.1114	0.0319	0.5137
0.5	5200	59168	6422	4885	1.876	25.6583	0.0396	1.0169
1	7184	83115	6930	7367	2.58	49.7993	0.02	0.9964
1.5	5390	71533	6436	5680	2.0332	43.2224	9.09E-03	0.3927
2	5241	82370	6157	5754	2.8539	67.6273	6.73E-03	0.4548
2.5	4627	76543	6025	5795	2.1556	52.2478	7.68E-03	0.4014
3	4823	140272	5933	6682	1.9878	85.4796	3.78E-04	0.0323
3.5	5101	182580	6025	7409	1.6305	107.085	4.07E-03	0.4358
4	4726	151227	5909	7443	1.8125	96.4458	5.74E-03	0.5536
4.5	5293	157113	5524	7274	1.7093	95.1623	4.77E-03	0.4543
5	5511	138821	5430	7084	1.8494	85.0098	4.11E-03	0.3497
5.5	5244	128600	5202	7011	1.171	51.0317	5.26E-03	0.2687
6	5294	105808	5243	7303	1.8963	75.6853	6.07E-03	0.4592
6.5	5273	86298	5605	6772	1.8981	63.2683	5.72E-03	0.3622
7	5420	103992	5558	7095	1.8698	73.5966	4.97E-03	0.3659
7.5	6814	109532	5538	6536	1.6571	67.1975	4.56E-03	0.3067
8	8116	117998	5929	6342	1.445	59.5348	3.69E-03	0.2195
8.5	8700	104468	5612	6559	1.8244	67.4422	5.51E-03	0.3719
9	9073	122752	5627	6527	1.1685	46.1821	6.06E-03	0.2799
9.5	9800	127563	5469	5511	1.1674	49.7904	6.41E-03	0.3193
10	7153	136692	4626	3520	1.0617	40.9257	7.81E-03	0.3195
10.5	4234	175358	4301	2373	0.9127	34.8624	8.74E-03	0.3046
11	2510	228106	4105	1684	0.8614	30.9087	9.20E-03	0.2844
11.5	1819	235946	3978	1449	0.7566	27.2361	9.06E-03	0.2468
12	2608	234324	4376	1946	0.7363	25.04	9.15E-03	0.2292
12.5	2856	264240	4532	1862	0.6612	25.8628	8.40E-03	0.2172
13	3827	192459	4741	2254	0.8052	26.9853	8.76E-03	0.2363
13.5	4004	201360	4714	2293	0.7429	23.8578	7.81E-03	0.1864
14	5259	190189	4872	2280	0.8975	26.0497	8.70E-03	0.2267
14.5	5091	242968	4630	2217	0.7515	28.4506	8.25E-03	0.2347
15	5023	333389	4465	2001	0.5228	25.3991	9.16E-03	0.2327
15.5	3773	252454	4481	2156	0.6893	27.9263	8.97E-03	0.2504
16	5175	221122	4507	2445	0.7635	29.4084	7.69E-03	0.2262
16.5	9240	213520	4661	3014	0.7676	35.7775	8.07E-03	0.2887
17	6633	102473	5478	4903	1.1345	36.8475	7.95E-03	0.2931
17.5	4337	129171	5078	4053	1.2139	27.5477	8.58E-03	0.2363
18	3731	110657	5491	4291	3.1235	31.4188	8.43E-03	0.2649
18.5	3633	185907	5038	3934	1.1924	39.8685	8.52E-03	0.3397

18.5	3633	185907	5038	3934	1.1924	39.8685	8.52E-03	0.3397
19	2630	193638	4598	3259	0.9801	36.9891	9.51E-03	0.3519
19.5	4690	151702	5342	4152	1.183	34.0139	7.67E-03	0.261
20	3776	138289	4434	3012	1.2473	37.7942	8.90E-03	0.3364
20.5	4377	110107	5192	3788	1.5289	45.3862	7.24E-03	0.3285
21	7096	124274	5674	5417	1.6507	55.2329	5.41E-03	0.2987
21.5	7421	94532	5625	5004	1.6744	59.0825	7.02E-03	0.415
22	8634	95869	6032	6043	1.3958	42.345	5.10E-03	0.216
22.5	10394	92615	6482	6535	1.3217	40.4786	8.47E-03	0.3427
23	8678	119565	6058	5563	1.0416	31.6477	5.85E-03	0.1853
23.5	4766	138418	5035	3334	0.9841	37.9227	8.34E-03	0.3162
24	2614	109106	3893	2406	1.0784	28.8031	8.60E-03	0.2476
24.5	6356	128599	4665	3460	0.9374	28.3445	8.77E-03	0.2486
24.5	6464	128256	4598	3734	0.941	28.4444	8.37E-03	0.2382
24.5	6416	128096	4616	3721	0.9603	27.9442	7.60E-03	0.2125
24.5	6306	127698	4411	3390	0.9977	29.1615	8.55E-03	0.2494
25	4350	148174	4524	3084	0.9972	27.8575	9.43E-03	0.2626
25.5	5539	174132	4271	2963	1.0331	27.6049	7.99E-03	0.2207
26	13243	152591	4723	3856	1.15	25.8366	8.72E-03	0.2252
26.5	4819	192550	4603	2755	1.5455	28.6447	8.77E-03	0.2513
27	3089	191058	4547	2729	1.1134	24.0173	9.60E-03	0.2307
27.5	2561	221974	4460	2457	1.0069	23.6823	9.67E-03	0.2291
28	2883	228981	4419	1887	0.9748	23.0039	8.57E-03	0.1971
28.5	2193	217467	4469	2298	0.9636	19.8148	8.86E-03	0.1756
29	2729	217337	4444	2439	1.0322	20.9947	9.01E-03	0.1891
29.5	1917	270226	4445	1880	1.063	22.7616	9.45E-03	0.215
30	2010	266750	4399	2024	1.0643	24.0532	9.18E-03	0.2207
30.5	2457	214052	4274	2064	1.1663	26.3028	0.0104	0.2739
31	1996	233933	4415	1846	0.9969	21.9573	9.15E-03	0.201
31.5	2522	210485	4219	2183	0.9771	21.5484	0.0102	0.2208
32	3150	178712	4254	2281	0.7342	21.3006	9.15E-03	0.195
32.5	1789	159398	4229	1759	0.8675	22.9614	9.76E-03	0.224
33	1696	139153	4251	1906	0.9291	18.6582	9.78E-03	0.1825
33.5	2241	185864	4338	2083	0.9986	22.0767	9.80E-03	0.2164
34	2756	182420	4179	2047	1.0873	23.7341	9.37E-03	0.2224
34.5	2869	158386	4274	2086	1.2222	23.9761	0.0101	0.2425
35	2024	172567	4160	1895	1.1694	23.8188	9.82E-03	0.2338
35.5	2588	166584	4404	2415	1.1398	23.5521	0.0105	0.2467
36	3337	179362	4588	2673	0.7593	23.3757	9.32E-03	0.2179
36.5	4355	191905	4689	2660	0.9816	25.2706	9.04E-03	0.2283
37	3435	207693	4489	2244	1.0117	23.9858	9.12E-03	0.2188

19	2630	193638	4598	3259	0.9801	36.9891	9.51E-03	0.3519
19.5	4690	151702	5342	4152	1.183	34.0139	7.67E-03	0.261
20	3776	138289	4434	3012	1.2473	37.7942	8.90E-03	0.3364
20.5	4377	110107	5192	3788	1.5289	45.3862	7.24E-03	0.3285
21	7096	124274	5674	5417	1.6507	55.2329	5.41E-03	0.2987
21.5	7421	94532	5625	5004	1.6744	59.0825	7.02E-03	0.415
22	8634	95869	6032	6043	1.3958	42.345	5.10E-03	0.216
22.5	10394	92615	6482	6535	1.3217	40.4786	8.47E-03	0.3427
23	8678	119565	6058	5563	1.0416	31.6477	5.85E-03	0.1853
23.5	4766	138418	5035	3334	0.9841	37.9227	8.34E-03	0.3162
24	2614	109106	3893	2406	1.0784	28.8031	8.60E-03	0.2476
24.5	6356	128599	4665	3460	0.9374	28.3445	8.77E-03	0.2486
24.5	6464	128256	4598	3734	0.941	28.4444	8.37E-03	0.2382
24.5	6416	128096	4616	3721	0.9603	27.9442	7.60E-03	0.2125
24.5	6306	127698	4411	3390	0.9977	29.1615	8.55E-03	0.2494
25	4350	148174	4524	3084	0.9972	27.8575	9.43E-03	0.2626
25.5	5539	174132	4271	2963	1.0331	27.6049	7.99E-03	0.2207
26	13243	152591	4723	3856	1.15	25.8366	8.72E-03	0.2252
26.5	4819	192550	4603	2755	1.5455	28.6447	8.77E-03	0.2513
27	3089	191058	4547	2729	1.1134	24.0173	9.60E-03	0.2307
27.5	2561	221974	4460	2457	1.0069	23.6823	9.67E-03	0.2291
28	2883	228981	4419	1887	0.9748	23.0039	8.57E-03	0.1971
28.5	2193	217467	4469	2298	0.9636	19.8148	8.86E-03	0.1756
29	2729	217337	4444	2439	1.0322	20.9947	9.01E-03	0.1891
29.5	1917	270226	4445	1880	1.063	22.7616	9.45E-03	0.215
30	2010	266750	4399	2024	1.0643	24.0532	9.18E-03	0.2207
30.5	2457	214052	4274	2064	1.1663	26.3028	0.0104	0.2739
31	1996	233933	4415	1846	0.9969	21.9573	9.15E-03	0.201
31.5	2522	210485	4219	2183	0.9771	21.5484	0.0102	0.2208
32	3150	178712	4254	2281	0.7342	21.3006	9.15E-03	0.195
32.5	1789	159398	4229	1759	0.8675	22.9614	9.76E-03	0.224
33	1696	139153	4251	1906	0.9291	18.6582	9.78E-03	0.1825
33.5	2241	185864	4338	2083	0.9986	22.0767	9.80E-03	0.2164
34	2756	182420	4179	2047	1.0873	23.7341	9.37E-03	0.2224
34.5	2869	158386	4274	2086	1.2222	23.9761	0.0101	0.2425
35	2024	172567	4160	1895	1.1694	23.8188	9.82E-03	0.2338
35.5	2588	166584	4404	2415	1.1398	23.5521	0.0105	0.2467
36	3337	179362	4588	2673	0.7593	23.3757	9.32E-03	0.2179
36.5	4355	191905	4689	2660	0.9816	25.2706	9.04E-03	0.2283
37	3435	207693	4489	2244	1.0117	23.9858	9.12E-03	0.2188
37.5	2094	216141	4156	2088	1.0436	23.9385	9.50E-03	0.2275

38	1813	277605	4380	1804	1.0266	24.8238	9.52E-03	0.2363
38.5	1567	286329	4306	1634	1.0341	23.1583	9.35E-03	0.2165
39	1703	319763	4425	1552	1.2065	24.276	0.0101	0.2457
39.5	1505	321057	4574	1778	1.0283	21.9256	9.70E-03	0.2126
40	1510	304032	4177	1671	1.0971	22.9736	9.95E-03	0.2285
40.5	1443	337886	4323	1832	0.976	21.5365	9.47E-03	0.204
41	1511	328818	4377	1644	0.8929	20.5114	0.0102	0.2095
41.5	1297	356157	4415	1711	0.8148	19.9483	9.76E-03	0.1947
42	1467	349798	4211	1855	0.7947	21.1627	0.01	0.2121
42.5	1397	341594	4299	1302	0.9031	24.1341	0.0109	0.2636
43	1484	317331	4146	1510	0.6592	25.6616	0.0103	0.2631

ResultsoftheBSP7Profile

Depth	Years BP	Years AD-BC	Fe	Ni	Br	Pb	Si/Ti	Fe/Ti	Mn/Ti	Mn/Fe
0	-61	2018	11581	4706	1804	2680	2.3368	8.57216876	0.3235	0.0377
0.5	-60	2016	27259	7950	3483	1483	2.2895	16.0725236	0.6757	0.042
1	-59	2008	45051	8042	4873	1483	1.8425	19.6557592	0.6357	0.0323
1.5	-49	1999	59395	7510	5022	1456	2.1588	31.6435802	0.8998	0.0284
2	-40	1989	33623	7552	4341	1040	2.6322	22.4452603	1.3685	0.061
2.5	-31	1980	29125	7669	5060	1114	3.5256	23.6981286	2.4052	0.1015
3	-21	1971	27465	7609	4314	1367	3.0007	18.6709721	1.7988	0.0963
3.5	-12	1961	28520	7496	4179	1021	3.4725	20.084507	1.093	0.0544
4	-3	1952	40044	7894	4410	1452	2.8696	21.0536278	0.7739	0.0368
4.5	7	1943	52662	7661	3514	822	2.263	20.7657729	0.6995	0.0337
5	16	1933	31039	7412	3448	1130	2.4265	19.4115072	0.8243	0.0425
5.5	25	1924	29690	7268	3378	871	1.9012	19.5586298	1.0303	0.0527
6	35	1915	28658	7117	4086	985	2.4036	23.6062603	1.9465	0.0825
6.5	44	1905	21440	7465	4386	653	2.0729	16.6330489	3.6649	0.2203
7	53	1896	23530	7229	5307	619	2.5416	22.5167464	4.0316	0.179
7.5	63	1887	24872	7195	5377	975	2.1903	18.2747979	4.252	0.2327
8	72	1877	30001	7107	4834	1034	2.6756	24.2726537	4.682	0.1929
8.5	82	1868	36919	7039	4116	1181	2.3462	25.356456	3.4979	0.138
9	91	1859	40234	7116	4329	1560	2.2567	25.6922095	2.2133	0.0861
9.5	100	1849	63206	6793	4783	2405	2.686	52.3661972	1.7829	0.034
10	110	1840	101716	6447	5362	6808	1.9475	67.5853821	0.8645	0.0128
10.5	119	1831	170927	6688	5215	12521	3.005	169.907555	1.175	6.92E-03
11	128	1821	96229	6755	4017	5947	2.6627	88.6903226	0.4691	5.29E-03
11.5	138	1812	65535	6356	4246	3740	2.7467	67.492276	0.4573	6.78E-03
12	147	1803	65779	6638	3776	2986	2.5194	62.1142587	0.3805	6.13E-03

12.5	156	1793	77606	6824	4145	4203	3.0569	88.3895216	0.3417	3.87E-03
13	166	1784	89839	7588	4823	5937	2.4686	76.1347458	0.3119	4.10E-03
13.5	175	1775	65172	7635	4819	2950	2.3944	50.9953052	0.2793	5.48E-03
14	184	1765	63381	7456	4363	1553	1.665	26.8449809	0.2351	8.76E-03
14.5	194	1756	81736	7417	4542	1953	1.2483	27.9534884	0.2869	0.0103
15	203	1747	67144	7456	4552	2747	1.3907	28.7308515	0.1836	6.39E-03
15.5	212	1737	52948	7973	3767	2870	1.8121	30.712297	0.2291	7.46E-03
16	222	1728	50173	8331	3193	2289	1.5502	26.9312936	0.2496	9.27E-03
16.5	231	1719	58917	8468	3205	3804	1.584	29.2102132	0.2291	7.84E-03

Annex 23.5

F. Urquidi, "Technical analysis of geological, hydrological, hydrogeological and hydrochemical surveys completed for the Silala water system", June 2018

(English Translation)

TECHNICAL ANALYSIS OF GEOLOGICAL, HYDROLOGICAL, HYDROGEOLOGICAL AND HYDROCHEMICAL SURVEYS COMPLETED FOR THE SILALA WATER SYSTEM

Eng. FERNANDO URQUIDI BARRAU, Ph.D.

Geologist Consultant – **DIREMAR**

June 2018

GLOSSARY

Aquifer: A permeable area of rock or soil capable of storing, transmitting and supplying ex-ploitable quantities of groundwater through springs or streams.
Shared aquifer: A permeable rock or soil capable of storing, transmitting and supplying ex-ploitable quantities of groundwater distributed or located between cities, localities, re-gions, districts or independent states.
Aquifer in ignimbrite: The rock that stores the aquifer is an ignimbrite with secondary porosity. This must be highly faulted, fractured nd jointed to allow storage, transmission and supply of groundwater.
Perched aquifer: Underground body of water, generally of modest dimensions, supported by a relatively impermeable stratum and located between a deeper groundwater table and the surface of the ground.
Stagnant groundwater: Water present in low permeability rocks where the flow or movement of water is extremely low.
Alkalinity: The name given to the quantitative ability of an aqueous solution to neutralize an acid.
Anion: Ionic species, with a negative net charge.
Bofedal: This term used for high altitude Andean wetlands with vegetation: it is very typical of the Andean Region of Bolivia, Chile and Peru. It is used to identify a certain type of permanently wet (saturated) natural meadow.
Headwater: A tributary stream of a river, near or part of its source.
Carbon 14 - 14C: A radioactive isotope of the chemical element carbon used to determine the ages of non- metallic organic objects, as well as the age of the water.
Isotopic characterization: The identification of the isotopic signature, the distribution of certain stable isotopes and radioactive isotopes within the chemical components.
Cation: An ionic chemical species with a positive charge.
Volcanic ash: Also known as núess ardent (burning clouds) or ash from a volcano.
Ionic Chromatography: A chromatographic process that separates ions and polar molecules based on their affinity with an ionic exchanger.
Discharge: Upwelling groundwater in the terrestrial surface from an aquifer forming springs or streams.
Deuterium: A radioactive isotope of hydrogen.
Plasma emission spectrometry: An analytical technique used for the detection of trace ele-ments. It is a type of emission spectrometry that uses inductively coupled plasma to pro-duce stimulated atoms and ions to emit electromagnetic radiation characteristic wave-lengths of a particular element.
Excess of deuterium: The concept of deuterium excess (d) is defined as $d=\delta 2H-8\delta 18O$. Excess deuterium
can be used to identify regions that are sources of vapor for air masses that produce pre-cipitation and contribute to the recharge of groundwater.
Hydro-chemical: This covers the chemical characteristics of waterbodies.
Ignimbrite: The igneous rock formed on the earth‘s surface by the deposition and consolida-tion of flows
of volcanic ash and burning clouds. It is only partially synonymous with welded tuffs.
Isotope: One or more species of the same chemical element that has the same numbers of protons in the core, but that differ from each other for having different numbers of neutrons. Due to their

differences in masses, the isotopes of an element have slightly different physical properties, which is why they can be separated.
Stable isotope: An isotope that does not transmute into another element with the emission of corpuscular or electromagnetic radiation.
Radioactive isotope: A radioactive form of an element. It consists of atoms with stable cores, which pass through a radioactive descent into stable forms, emitting characteristic alpha, beta, or gamma radiation. These can occur naturally, as in the cases of tritium and radiocarbon, or can be created artificially.
Meteoric water line: A linear equation that defines the average ratio between the hydrogen and oxygen rates in the surface waters of a defined area.
Global Meteoric Line: An equation defined by the geo-chemist Harmon Craig to establish the average ratio between isotope radios of hydrogen and oxygen in natural and surface waters. The equation is expressed as a global average: $\delta 2H = 8\delta 18O + 10‰$.
l/sec.: Liters per second.
Weathering: The natural destructive process by which earth materials exposed to atmospheric agents (water, wind, temperature, etc.) at or near the surface of the earth are changed in composition, color, texture, firmness, or shape, with little or no transportation of loosened or altered material.
Silicate Weathering: The destructive process by which silicates exposed to atmospheric agents (changes in water, wind, temperature, etc.) at or near the earth‘s surface are changed in color, texture, composition, firmness, or shape, with little or no transport of loosened or altered material.
Volumetric method: A quantitative chemical analysis that involves measuring the volume of a solution of known concentration that is used to determine the concentration of the analyte.
Silicate minerals: Silicate minerals are minerals that form rocks, composed of silicate groups. They are the largest and most important type among the minerals that form rocks and make up approximately
90% of the earth‘s crust.
Mineralization: Process by which groundwater, through interaction with minerals in the aquifer, incorporates chemical elements into the water.
Modern carbon percentage: Unit to report carbon dating. The reference is the radiocarbon content of
atmospheric CO2, defined as 100 percent modern carbon before 1950.
Recharge: Groundwater recharge (or deep drainage or deep percolation) is a hydrological process whereby the water that has infiltrated the surface moves down from the non-saturated area to the groundwater. The recharge is the main method by which water enters an aquifer. Its source can be precipitation or surface water.
Salinity: The concentration of dissolved salts in water.
Silicate: A compound whose crystalline structure contains tetrahedral SiO4, either in isolation or joined to more oxygen atoms to form groups, chains, layers, or three-dimensional structures with metallic elements.
Volcanic tuff: Ash emitted by a volcano, deposited and compacted. Sediment composed of crumbly volcanic ash.
Tritium: A radioactive isotope of hydrogen. The tritium core contains one proton and two neutrons.Tritium of natural occurrence is rare on earth, where minimal amounts are formed as a result of the interaction of the atmosphere with cosmic rays.

TABLE OF CONTENTS

GLOSSARY
TABLE OF CONTENTS

1. INTRODUCTION
1.1. LOCATION OF THE SURVEYED AREA
2. GEOLOGY
2.1. IMPORTANCE OF THE SILALA IGNIMBRITE
2.2. GEOLOGY OF THE SILALA NEAR FIELD
2.2.1. IGNEOUS ROCKS
2.2.2. QUATERNARY SEDIMENT DEPOSITS
2.3. FORMATION OF THE SILALA RAVINES
2.4. STRUCTURAL GEOLOGY OF THE AREA OF THE SILALA SPRINGS
2.4.1. FAULTS FOUND IN THE SILALA IGNIMBRITE AREA
2.4.2. SILALA IGNIMBRITE JOINTS
2.5. HYDROGEOLOGICAL UNITS
3. HYDROLOGY
3.1. BASIN
3.2. CLIMATE
3.3. SURFACE WATERS VOLUME
3.4. INVENTORY OF GROUNDWATER SOURCES
3.4.1. SOUTH BOFEDAL – FIRST BOFEDAL
3.4.2. SOUTH CHANNEL – SECOND BOFEDAL
3.4.3. SOUTH CHANNEL – THIRD BOFEDAL
3.4.4. NORTH BOFEDAL
3.4.5. MAIN CHANNEL
4. HYDROGEOLOGY
4.1. HYDROGEOLOGICAL RESEARCHES
4.1.1. PIEZOMETER DRILLING AND DEVELOPMENT
4.1.2. SLUG TESTS
4.1.3. PACKER TESTS
4.1.4. PUMPING TEST IN THE AQUIFER
4.1.5. CONSTANT FLOW TEST
4.2. AQUIFER TEST ANALYSIS METHODS
4.2.1. ANALYSIS AND DATA REPORTS
4.2.2. PUMPING TEST RESULTS
4.2.3. ANALYSIS METHODS FOR THE STEP TEST
4.2.4. ANALYSIS METHODS FOR THE CONSTANT FLOW TEST
4.3. WATER QUALITY SAMPLING
4.4. THE SILALA AQUIFER
4.4.1. AQUIFER STORAGE
4.4.2. HYDROGEOCHEMICAL RESULTS
4.5. NEGRA RAVINE IN THE CHILEAN-SIDE SILALA
5. HYDROCHEMISTRY OF THE SILALA FLOWS
5.1. ANALYSIS OF HYDROCHEMICAL RESULTS
5.1.1. PHYSICAL-CHEMICAL CHARACTERISTICS OF THE SILALA WATERS
5.1.2. WATER TYPE CLASSIFICATION
5.2. DATA AND ANALYSES OF ENVIRONMENTAL ISOTOPES
5.2.1. STABLE ISOTOPES OF OXYGEN AND HYDROGEN

5.2.2. STABLE ISOTOPES OF TRITIUM
5.2.3. RATIO OF THE CARBON-13 AND CARBON-14 ISOTOPES
6. GENERAL CONCLUSIONS
7. BIBLIOGRAPHY

FIGURES

Figure 1: Location of the Silala Springs area.
Figure 2. Location of the springs in the Silala North and South Bofedals. Figure 3. Geological Map of the Silala Study Area, 2003
Figure 4. Generalized stratigraphic column of geology in the Silala, 2003
Figure 5. Generalized stratigraphic column of geology in the Silala, 2017
Figure 6. Geological Map of the Silala Near Field. Figure No. 7. 1st Domain Joints
Figure No. 8. 2nd Domain Joints Figure No. 9. 3rd Domain Joints Figure No. 10. 4th Domain Joints
Figure No. 11. Structural Geology – Stress ellipsoid
Figure No. 12. Structural Geology – Fracture rose diagrams
Figure 13a. Fracture Rose Diagram of the Normal faults of the Silala ignimbrites Figure 13b. Fracture Rose Diagram of the Reverse Faults of the Silala Ignimbrites
Figure 14. Joint Rose Diagram of the area of the Silala ignimbrite
Figure 15a. Delineation of Hydrogeological Units (HGU) in the Silala area, DHI.
Figure 15b. Images of the Silala area superposed by the HGUs, delineated by DHI.
Figure 16. Silala Near Field Topographical basin and Far Field hydrological basin
Figure 17. Hydrological basin (violet), topographical basin of the Silala river provided by Arcadis (blue) and Silala Near Field (yellow)
Figure 18. Location of the springs, bofedals and ravines on both sides of the international border.
Figure 19. General map of the South Bofedal in which the extent, springs, network of channels and the general directions of the flow are presented.
Figure 20. General map of the North Bofedal in which the extent, springs, network of channels and the general flow directions are presented.
Figure 21. Map of the location of the wells with the hydraulic tests carried out. DHI, 2018
Figure 22. Hydrogeological Units: geometric mean for the measured hydraulic conductivity (K) obtained from small-scale hydraulic tests. HGU7 - Fault Zones.
Figure 23: Stiff diagrams for the Springs, Channel and Groundwater of the Silala Near Field. DHI, 2018
Figure 24. Mapping of flows and net tributaries based on simultaneous measurements of the average channel flow (in l/sec.). DHI, 2017.
Figure 25. Map presenting the location of the sampling points for the hydrochemical and isotopic analyzes
Figure 26. Piper Diagram – Campaign 1
Figure 27. Piper Diagram – Campaign 2
Figure 28. Piper Diagram – Campaign 3
Figure 29. Piper Diagram – Campaign 4
Figure 30. Schoeller Diagram – Campaign 1
Figure 31. Schoeller Diagram – Campaign 2
Figure 32. Schoeller Diagram – Campaign 3

Figure 33. Schoeller Diagram – Campaign 4
Figure 34. Wilcox Diagram – Campaign 1
Figure 35. Wilcox Diagram – Campaign 2
Figure 36. Wilcox Diagram – Campaign 3
Figure 37. Wilcox Diagram – Campaign 4
Figure 38. Stiff Diagram of sample Si-2 from the South Bofedal. As a reference sample
Figure 39. Stiff Diagram of sample Si-6 from the North Bofedal. As a refernce sample
Figure 40. Map of the Springs including the Stiff Diagrams for the Samples from the First Field Cam-paign in the Silala Near Field
Figure 41. Map including the Stiff Diagrams for the samples taken in the Second Field Campaign in the
Silala Near Field
Figure 42. Maps including the Stiff Diagrams for the samples taken from the Third Field Campaign in the
Silala Near Field
Figure 43. Maps including the Stiff Diagrams for the Fourth Campaign in the Silala Near Field
Figure 44. Oxigen-18 (δ 18O) ratio versus Deuterium (δ 2H) of the total samples
Figure 45. Ratio of the Oxigen-18 (δ 18O) samples versus Deuterium (δ 2H) taken in 2016. Figure 46. Ratio of the Oxigen-18 (δ 18O) samples versus Deuterium (δ 2H) taken in 2017
Figure 47. Ratio of the Oxigen-18 (δ 18O) samples versus Deuterium (δ 2H) in the samples taken from the
Drilled Wells.
Figure 48. Map with the results of the relation of the frequency of oxygen and hydrogen isotopes –
Campaign 4
Figure 49. Map with the results of the relationship of the frequency of the isotopes of oxygen and hydro-gen from drilled wells (2017).
Figure 50. Ratio of carbon-13 and carbon-14 isotopes in the waters of the North and South Bofedals
Figure 51. Relationship of carbon-13 and carbon-14 isotopes in waters of nine wells drilled in the two
Bofedales North and South

TABLES

Table 1. Hydrogeological units (hgu)
Table 2. Location of the field parameters and hydrochemical data from the third field campaign and negra
ravine samples. (the source is the author‘s)
Table 3. Location of the field parameters and hydrochemical data from the fourth campaign
Table 4. Characteristics of the Silala waters
Table 5. Results from the stable isotopes of the first (c1) and fourth (c4) campaigns
Table 6. Isotopic parameters (δ 18o) and (δ 2h) of the waters of silala
Table 7. Samples taken in 2016
Table 8. Samples taken in 2017
Table 9. Results of the stable isotopes from the drilled wells

PHOTOGRAPHS

Photograph 1: Headwaters of the Main Ravine with the ―U-Shaped‖ valley profile, 2000.
Photograph 2: Sample at the headwaters of the Main Ravine, near the intersection of the North and South
Channels, the typical profile of a U-shaped valley is ob-served, 2000

Photograph 3: Trial Pit excavated in the Main Ravine, a deposition of sedimentary-glacial and fluvial- glacial material is observed in the profile. Depth: 3.30 meters, 2000
Photograph 4: Main Ravine on the Chilean side with the vertical ignimbrite wall (Silala Fault) and springs emerging from it with collecting channels. The iron pipeline, parallel to the Main Channel, conveys the water to Antofagasta for FCAB company. October, 2000
Photograph 5. Spring that emerges in the North Channel (showing the secondary conveyance channel); the ignimbrite mantel can be seen in the back.
Photograph 6. The South Bofedal – First Bofedal
Photograph 7. South Ravine, presenting channeliza-tion. 2000. Photograph 8. Waterfall in the South Ra-vine and Channel. 2000
Photograph 9. Springs in the North Bofedal. With stagnant water, without movement. Photograph 10. Main Silala Channel. Open Channel coated with Ignimbrite rocks. 2017
Photograph 11. Springs in the Main Ravine on the Chilean side emerging in the joints of the Silala ignimbrite with its collecting canals. 2000
Photograph 12. Main Channel on the Chilean side. Springs in the fractured Ig-nimbrite. 2000
Photograph 13. Negra Ravine on the Chilean Side with its unmodified Bofedal, October 2000

ANNEXES

ANNEX 1. SERGEOMIN, ―Survey of Geology, Hydrology, Hydrogeology and Environment of the Silala
Springs Area‖, 2003.
ANNEX 2. SERGEOMIN, ―Structural Geological Mapping of the Area Surrounding the Sila-la Springs‖,
2017. Tomas Frias Autonomous University, ―Hydrogeological Characterization of the Silala
Springs‖, 2017.
ANNEX 3. Tomas Frias Autonomous University, ―Hydrogeological Characterization of the Silala
Springs‖, 2018.
ANNEX 4. Results from the water analyses completed by Hydroisotop Laboratory, 2018.

TECHNICAL ANALYSIS OF GEOLOGICAL, HYDROLOGICAL, HYDROGEOLOGICAL AND HYDROCHEMICAL SURVEYS COMPLETED FOR THE SILALA WATER SYSTEM

1. INTRODUCTION

The Strategic Office for the Maritime Claim, Silala and International Water Resources (DIREMAR) requested Geologist Eng. Fernando Urquidi Barrau (PhD), Member of Number of the National Academy of Sciences of Bolivia, to perform a technical analysis of the geological, hydrological, hydrogeological and hydrochemical surveys completed in the area of the Silala Springs.

This report includes an analysis of geological studies carried out by the National Geology and Mining Service (SERGEOMIN, for its Spanish acronyms) in 2003 and 2017 and by the Tomas Frias Autonomous University of Potosi (UATF, for its Spanish acronyms) in 2018. In addition, this report includes an analysis of the hydrological and hydrogeological surveys carried out by the Danish Hydraulic Institute (DHI)— DIREMAR's main consultant in this regard. Finally, this report also presents an interpretation of the isotopic hydrochemistry of the surface and groundwater of the Silala Springs, which had been analyzed by HIDROSITOP and IBTEN.

It should be emphasized that the current conditions of the quantity of surface water flows were highly modified by the artificial channelization and the drainage network built in the last century by The Antofagasta (Chili) and Bolivian Railway Company Ltd. (FCAB), which have been used and maintained by this company and its successors up to the present.

1.1. LOCATION OF THE SURVEYED AREA

The surveyed area of the Silala Springs is located in Canton Quetena Grande, South Lipez Province, of Potosi Department. It is geographically located in the Western Cordillera of the Andes, at reference coordinates 7566000 North and 602000 East, UTM WGS84 ZONE 19 SUD. The area borders the international border with the Republic of Chile to the west, passing through boundary landmarks LXXIII, LXXIV and LXXV; the North Lipez province to the north; the San Antonio de Lipez and San Antonio de Esmoruco Cantons to the east; and the International border with the Republic of Argentina to the south.[1]

The Silala is a groundwater system, whose waters well up from several and different aquifer levels that are located on the international border between Bolivia and Chile. The Silala Aquifer is a very unique case in the hydrogeology of the two countries' Volcanic Area of the Central Andes , since it is a unique system of potable groundwater located in highly fractured and jointed ignimbrite igneous rocks that date back from the Upper Miocene age.[2]

1 Tomas Frias Autonomous University, ―Hydrogeological Characterization of the Silala Springs‖, 2018. P. 1.

2 Choque, M.N., 1996; Lema, Z., Ramos, C., 1996; Richter, D.H., et at., 1992.

The Silala Springs form bofedals, denominated high-altitude wetlands because they are located at more than 4,000 meters above sea level (m.a.s.l.), on the southwestern end flank of the Western Cordillera of the Central Andes, in the South Lipez Province of the Department of Potosi, Bolivia. This highland region has an arid and desert climate that presents low temperatures and high solar radiation. Currently, the groundwater of the Silala Aquifers emerges on the surface in more than 70 springs, with variable volumes inside Bolivian territory, forming a negligible surface water flow that has been modified by channelization works. In this system, water flows towards the border with Chile by means of a network of stone channels that drain the Silala bofedals and transport water efficiently from the individual springs found in the North Bofedal (also known as Cajones) and the South Bofedal (also known as Oriental), towards a water intake in Chilean territory, located downstream crossing the border. The springs and bofedals are located at an altitude of 4,386 m.a.s.l. and of 4,435 m.a.s.l., respectively (See Figures 1 and 2).

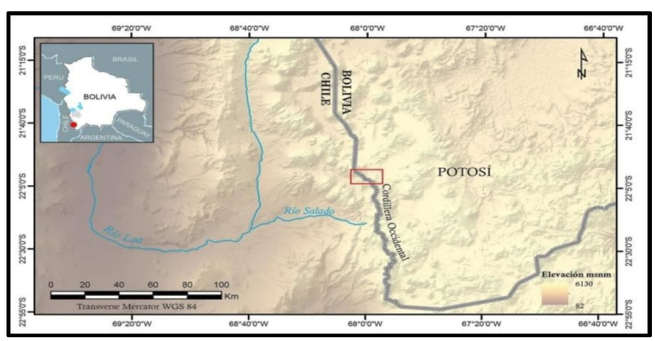


Figure 1: Location of the Silala Springs area

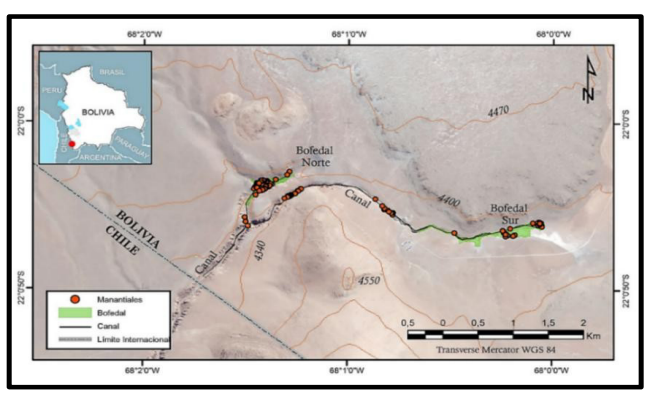


Figure 2. Location of the springs in the Silala North and South Bofedals

2. GEOLOGY

Geological information is fundamental to know the textural characteristics of the volcanic rocks of the area and their influence on the recharge, circulation and discharge of water from the aquifers that make up the upwelling springs or streams in the Silala.

The geological framework of the Silala area in Bolivia is very well detailed and presented in three surveys performed to that end[3] (See Annexes I, II and III of the present report). Both the summary of the mapped and re-interpreted regional geology of previous works, as well as the geomorphology and the detailed regional structural features, indicate that the volcanic events in the Silala area are the primordial activity developed from the Upper Miocene to the Lower Pleistocene. Their igneous volcanic products were emplaced and deposited on a substrate of Paleozoic and Paleogenic rocks that are not exposed in the area, but that can be observed in neighboring areas.

In the Silala region, this important and intense magmatic activity began with an explosive volcanism of the Plinian type, forming large calderas (as exemplified by the calderas of Pastos Grandes, Guacha, Cerro Panizo, Capina and others) and producing the effusion, deposition and consolidation of flows of volcanic ash and burning clouds in extensive ignimbrite plains that correspond to extra caldera facies, which are denominated as Silala Ignimbrite. Regionally, these ignimbrite deposits are monotonous, of dacite composition and calc-alkaline rhyolites rich in sodium and potassium. Their importance is its level of welding and its fracture intensity. (See Figures 3 and 6).

3 See SERGEOMIN, ―Survey of Geology, Hydrology, Hydrogeology and Environment of the Silala Springs Area‖.
2003; SERGEOMIN, ―Structural Geological Mapping of the Area Surrounding the Silala Springs‖, 2017; Tomas
Frias Autonomous University, ―Hydrogeological Characterization of the Silala Springs‖, 2017.

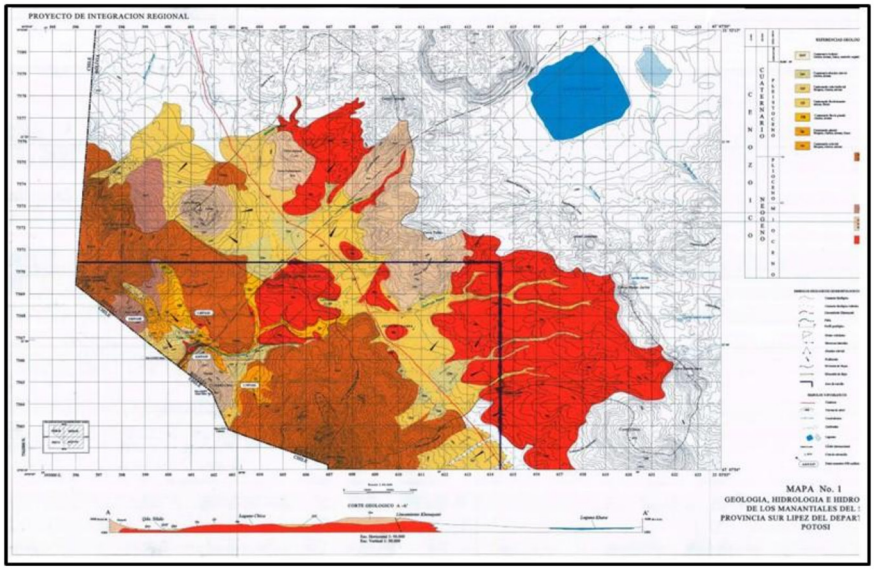


Figure 3. Geological Map of the Silala Study Area, 2003[4]

Subsequently, the gradual reduction in the volatile content of the magma caused volcanism to change to an effusive type. This second volcanic activity emplaced volcanic domes, as the Silala Chico and Torito Hills, and emitted lava flows of andesitic-dacitic composition that formed stratovolcanoes, as the Inacaliri and Silala Grande. This second igneous activity is not so relevant for this report.

In contrast, the tectonic structural features are very important, particularly the lineament pattern of Pastos Grandes–Cojina, to the East, and the Khenayani–Uyuni lineament (fault) to the Southeast, which forms a vertex that has a direction to the Pacific Ocean. The structural or tectonic geology of the region is linked to the subduction of the Nazca Plate, under the South American Plate, and the uplift of the Andes Mountain Range, with the specific development of the Southern Altiplano and the Volcanic Belt during the Andean Cycle II of the Upper Oligocene and the Basal Miocene (23 to 19 Ma BP – millions of years before the present).

In a transgressive tectonic environment, tensional areas are also developed, facilitating the emission or effusion of volcanic products, as the circular collapse structures of the large calderas, which

4 SERGEOMIN. ―Survey of Geology, Hydrology, Hydrogeology and Environment of the Silala Springs Area‖, 2003.

stage of resurgence.[5] Two preferential directions of faulting and fracturing are defined: NW-SE and NE- SW. The first is more evident and, although both control the magmatism of the region, they are combined in a series of dextral course faults.

Figure 4 shows the stratigraphic column of the Silala area of the geological map represented in Figure 3 and prepared by SERGEOMIN in 2003. It describes the geo-morphological processes that occurred in the area, which is why it is presented here.

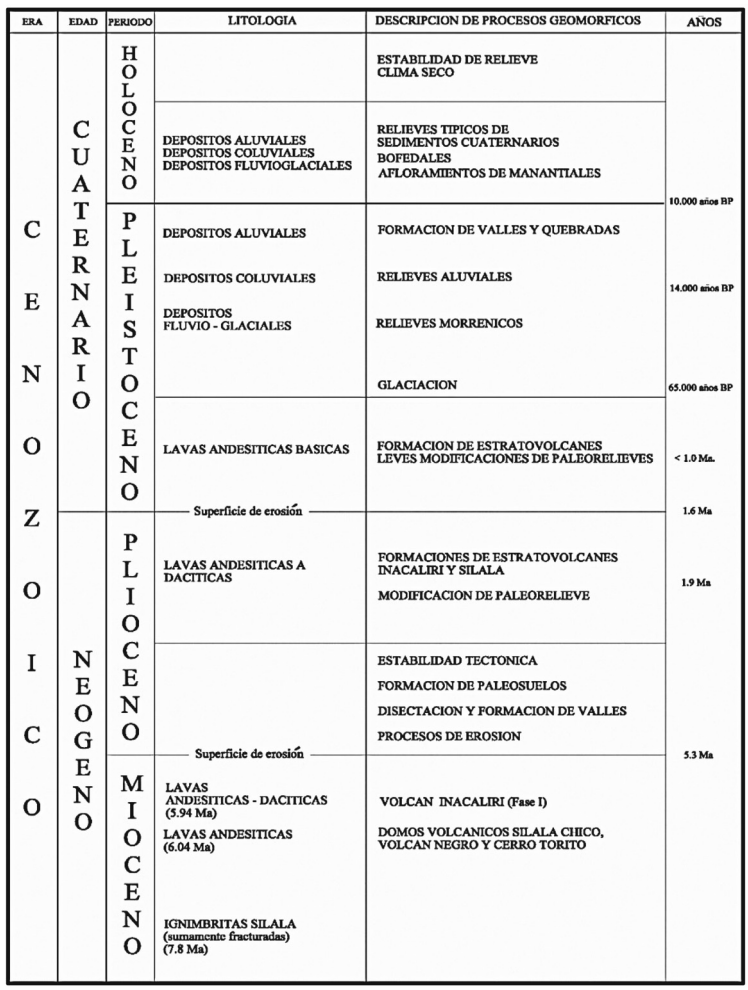


Figure 4. Generalized stratigraphic column of geology in the Silala.[6]

5 Baby et al. 1990. Session Accountability. Series 2, Vol. 311, pp. 341-347.

The following Figures, 5 and 6, show the generalized stratigraphic column of the geology in the Silala and the geological map re-interpreted by SERGEOMIN in 2017.

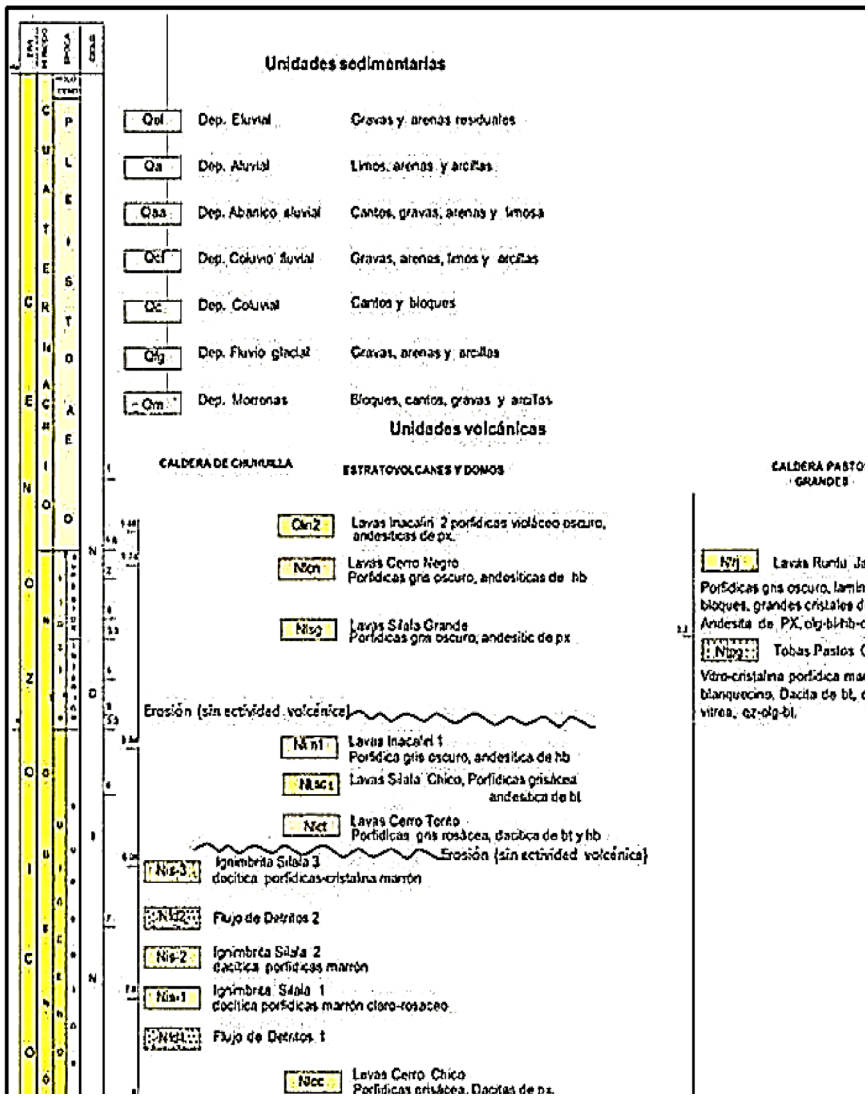


Figure 5. Generalized stratigraphic column of geology in the Silala, 2017.[7]

6 SERGEOMIN, —Survey of Geology, Hydrology, Hydrogeology and Environment of the Silala Springs Areal, 2003. P. 12.
7 SERGEOMIN, —Structural Geological Mapping of the Area Surrounding the Silala Springs. 2017, p. 24

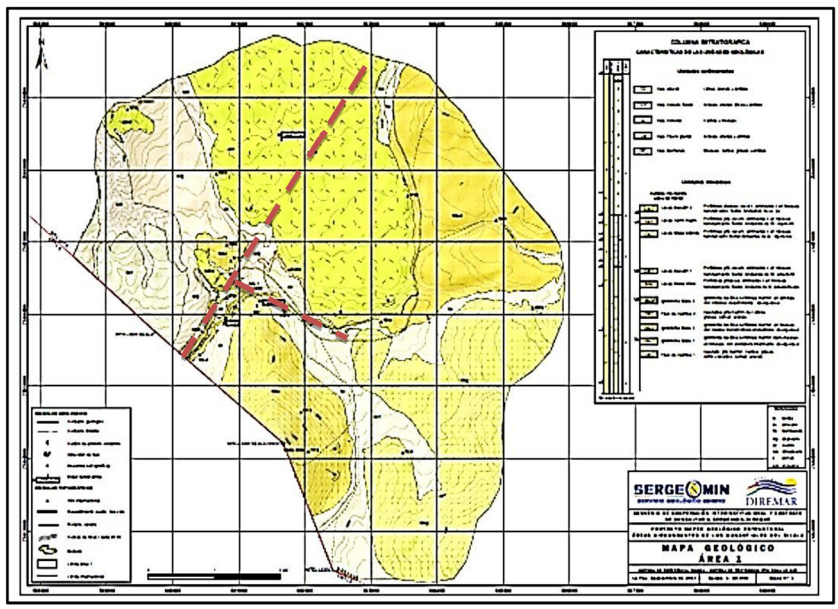


Figure 6. Geological Map of the Silala Near Field[8]

2.1. Importance of Silala Ignimbrites

The geological basement of the Silala area is made up of three layers of semi-welded volcanic ash called Silala Ignimbrite 1, 2 and 3 (Nis1, Nis2 and Nis3). These are dacitic-andesitic in composition and consist mainly of plagioclase, quartz, biotite and hornblende, in a semi-fine matrix of volcanic ash. Previous works have found them to date back to between 7.8 Ma. BP. to 6.6 Ma. BP.[9] Likewise, SERGEOMIN states that, interspersed between the first two mantles of ignimbrites that emerge in the streams, there are two flows of volcanic detritus (Nfd1 and Nfd2), which are welded formations of small fragments of rocks within a volcanic ash. The first volcanic debris flow (Nfd1) is mapped at the base of the Silala Ignimbrite 1 (Nis1) and the second debris flow (Nfd2), 50 to 180 centimeters thick, outcrops on both sides of the Main Ravine on the Silala Ignimbrite 1 and, like windows, surround the lavas of the Inacaliri Volcano, on its southern margin and around the Silala Chico dome. In addition, a thin Silala Crystalline-Vitreous Tuff (Nts) is observed below the second detritus flow(Nfd2).

8 SERGEOMIN, ―Structural Geological Mapping of the Area Surrounding the Silala Springs‖. 2017, Annex A: Map 1.
9 SERGEOMIN, ―Structural Geological Mapping of the Area Surrounding the Silala Springs‖, 2017. p. 25.

During the Holocene, the climate became arid and desert-like—very similar to On the Bolivian side, the Silala Ignimbrite 3 (Nis3) constitutes the largest outcrop of ignimbrite in the Silala area; it is located in the North-East sector, outside the South Channel and Bofedal, and is presented in the form of a fan with the apex in the direction of the Silala South Channel. The base of this unit does not outcrop and its thickness is unknown, but it is assumed that it is concordant with the Silala Ignimbrite 2 (Nis2).[10] The Nis3 ignimbrite unit—constituted by an ignimbrite or a moderately welded tuff flow of reddish to pinkish color and which is whitish pinkish on a fresh surface, is mapped and described in Chilean geological maps as the Cabana Ignimbrite.[11]

Further complicating the geological framework and the hydrogeological environment, it has been determined that the tectonic faults of the Silala area provide a conduit for groundwater flow. In addition, the discharge of the latter, which was recharged regionally in the Silala area, is related to the high fracturing degree of the rocks. The hydraulic properties of rocks in the Silala suggest that faults and related fracture networks (joints), or the so-called high secondary permeability, exert the greatest influence on groundwater flow. Therefore, erosion and extensive fracturing have resulted in a highly eroded ignimbrite area and in superficial fragments of ignimbrite rocks that probably act as a very important equivalent porous medium (EPM).

Conceptually, the welding degree of the ignimbrite is of importance, as it significantly affects the rock‘s hydraulic behavior. The more welded the ignimbrite, the more competent and fragile the rock, which will lend itself to fracturing and, generally, to a greater hydraulic conductivity (Belcher, 2001); this is exemplified in the ignimbrite and the brittle and weathered tuff, which are observed in many of the shallow wells of the Silala Near Field, and which are highly conductive (for example, 2 x 10-2 to 2 m/d).[12] In addition, it is expected that the storage characteristics of the welded ignimbrite versus friable ignimbrite will be quite different with a much lower storage capacity in the welded ignimbrite and a much higher one in the friable and eroded one.

2.2. Geology of the Silala Near Field

2.2.1. Igneous Rocks[13]

A summary description of the local geology surrounding the springs shows that it is similar to the regional geology. Although the base of Ignimbrite 1 (Nis1) does not outcrop in the Silala Ravine, geophysical surveys have found that there is lithological continuation with depth. For conventional purposes, the description of the local geological column will begin with the description of the

10 SERGEOMIN, ―Structural Geological Mapping of the Area Surrounding the Silala Springs‖, 2017. p. 27.
11 CM, Annex II. ARCADIS. Detailed Hydrogeological Study of the Silala River. 2017. Figure 4-2. P. 16.
12 Lewis, 1989.
13 See SERGEOMIN, ―Structural Geological Mapping of the Area Surrounding the Silala Springs‖, 2017. Pp. 23-39.

Debris Flow 1 (Nfd1)

The horizon of Debris Flow 1 (Nfd1) outcrops on both banks of the Silala Main Ravine. It presents a reddish brown color on an altered surface and a reddish salmon color on a fresh surface and is composed of clasts of igneous rocks with sub-angular to sub-rounded morphology, with diameters of a few centimeters to 25 centimeters, dispersed in a terrestrial sandy-clayey matrix with a low degree of compaction. The thickness of this level fluctuates between 60 to 140 centimeters; this variation in thickness is due to the paleo-relief that existed when they were deposited and to the amount of material dragged by the flow.

Silala Ignimbrite 1 (Nis1)

The ignimbrite deposits of the Silala Springs are pyroclastic flows of Neogene age. They appear in the three channels of the Silala (North, South and Main) and were found to date back to 7.8 Ma., within the Upper Miocene. Their base does not outcrop, but in some sectors it is found above the Debris Flow (Nfd1) in discordant contact.

The unit is composed of ignimbrites or moderately welded flow tuffs, of pinkish brown color. It presents a certain banding, the band color of which range between light and brown, with vertical parallel to sub- parallel fractures, and presents a porphyritic texture with feldspar phenocrysts, quartz, biotite and few pyroxenes, in a proportion of 35%, lithic rocks of igneous rocks 2%, scarce pumice 5%, a 58% matrix composed of micro crystals, vitreous fragments and a ferruginous paste.

The exposed (outcropping) thickness varies from 3 to 8 meters and has a sub-horizontal arrangement with a slight inclination towards the center of the ravine. The importance of this unit lies in its lithology since – with a higher fracture index– it becomes the host rock of the Silala Springs. This theory is confirmed by the number of streams mapped along the ravines and in the bofedals found above the Nis1 ignimbrite.

Crystalline-Vitreous Tuff (Ntcv)

This unit overlaps the Silala Ignimbrite 1 in almost all of the Main Ravine. It consists of a fairly thin, compact tuff fall, with an average thickness of 15 centimeters, and intermediate composition, with fine-to- medium phaneritic texture.

This tuff level is very important and constitutes a guiding horizon due to its stratigraphic position, areal extension and sub-horizontal disposition. It allows subdividing the Silala Ignimbrites into two members (Nis1 and Nis2) and is an indicator of possible vertical displacements produced by faulting or landslides of the rock mass.

Silala Ignimbrite 2 (Nis2)

The ignimbrite deposits (Nis2) outcrop along the Silala Main Ravine. They consistently overlap the level of the Crystalline-Vitreous Tuff (Ntcv) at the base and are crowned by the Debris Flow 2 (Nfd2) towards the top.

It is composed of ignimbrites or quite welded tuff flows, of a reddish to pink color and somewhat rusty. They have a massive structure and are banded in some sectors. They have a porphyritic texture with plagioclase phenocrysts, quartz, pyroxenes and amphiboles. They are also lithic, with very variable diameters; they correspond to andesites and pumice stone of up to 10 cm of length. Their degree of welding is shown when they are crushed or deformed. The matrix occupies 65% of the rock and is composed of micro-crystals of plagioclase and volcanic glass.
Its thickness can reach 10 meters. Unlike the overlapping ignimbrites, they present an inverse gradation to their lithic [elements] and a lower degree of fracturing, reason why they are more competent or welded and less permeable.

Debris Flow 2 (Nfd2)

This unit outcrops in both walls of the Main Ravine and, as windows, surrounds the lavas of the Inacaliri on its southern margin. It presents a reddish brown color, on an altered surface, and a grayish brown color, on a fresh surface. It is composed of clasts of igneous rocks, with sub-angular to sub-rounded morphology, and with a chaotic distribution. Their diameters range from a few centimeters to 40 centimeters, and they are dispersed in a sandy-clayey and ferruginous matrix, somewhat earthy with a good degree of compaction. The thickness of Debris Flow 2 (Nfd2) varies between 50 to 180 centimeters.

It should be mentioned that, in the Silala area, this flow has a wider distribution than the Nfd1 flow. In addition, it has a greater thickness and a better welding degree. It also evidences a surface that is more polished by glacial processes since it presents a gloss similar to desert varnish, faceted faces and striations.

Silala Ignimbrite 3 (Nis3)

The rocks of this unit constitute the largest outcrop of ignimbrites in the Silala area, and are located in the north-east sector of the ravines. They have the shape of a fan with the apex in the direction to the South Ravine. Its base practically does not emerge to the surface, but it is assumed that it is concordant with the Nfd2 and Nis2 units. On the other hand, its contact with the upper unit forms an angular misalignment. It is constituted by ignimbrites or moderately welded tuff flows, of reddish to pinkish color, and has a splinted structure that resembles a pseudo-stratification in the sectors in which it becomes massive. Its matrix is abundant and consists mainly of glass, limonite and hematite, with massive structure. Sporadically, it presents spherulites and pieces of pumice stone. They have inclusions of biotite and plagioclase. Finally, its lithic composition corresponds to that of volcanic rocks (andesites and dacite).

In the Nis3 unit no outcrops of groundwater have been found and it has been designated in Chilean geological maps as the Cabana Ignimbrite (Hauser, A. Y. 2004 and SERNAGEOMIN 2017). Geo- chronological analyzes

(age of the rock) should be performed in order to determine its exact stratigraphic position.

Silala Chico Lava (Nlsc)

The Nlsc unit emerges mostly in the southern part of the ravines. In fact, half of the volcanic rock cone is located in Chilean territory (Silala Chico Hill), although there are also some rel-icts in the northern sector. In both cases, in the Silala Main Ravine, they flank the Silala Ig-nimbritas 1 and 2.

Therefore, it is inferred that the Silala Aquifer passes below these lavas, bordering the volcanic cone, into Chilean territory. Crossing the Bolivia-Chile international border, the waters of Silala Aquifer emerge in the springs of the Negra Ravine and in the 37 springs of the Main Ra-vine. Of these, 27 emerge from the joints in the ignimbrite on the walls of the ravine, and 10 emerge as a flow from the ground, on the sides of the ravine, or as fluvial deposits at the base of the ravine.[14]

2.2.2. Quaternary Sediment Deposits

The following description of these deposits cover the regional geology of the Silala area.

Glacial Deposit – Mo-raines (Qg-m)

The glacial activity is represented by erosion and accumulation geo-forms, located in the vicini-ty of the stratovolcanoes and in the Silala Main Ravine. Within the first ones, glacial cirques are observed, developed in the Inacaliri and Silala Grande Stratovolcanoes. Another effect of glacial erosion is the deepening and widening of pre-existing valleys; the typical ―U-shaped‖ profile.

There are three groups of moraines encased in glacial valleys. The outermost or distal one is found at approximately 4,500 m.a.s.l. and corresponds to the ―Last Glacial Maximum‖ which, in the Central Andes, occurred 14,500 years BP and caused strong alterations in the landscape due to the movement of the ice masses and thawing, forming large lakes, lagoons and deep val-leys (Argollo, J., 1991). This age was determined, in other studies, by radio-carbon methods car-ried out mainly in peats and shells, both in the Western Mountain Range and in the Eastern Mountain Range. The second moraine is located at 4,600 m.a.s.l. and the last at 4,800 m.a.s.l.—they correspond to a Late-Glacial.

The thawing activity had a significant influence in the formation of the Silala Ravines. It is a typical example of a ravine carved by ice and melt-water that exploits areas of weakness (faults and fractures). However, the current design of the Main Ravine shows a ―U-shaped‖ cross sec-tion, with almost vertical side walls and a flat floor. It is important to mention that the water produced

14 CM. Annex II. Arcadis. Detailed hydrogeological survey of the Silala River, 2017.

by glacier mass melting was a very important source of the current groundwater stored in the Silala Ignimbrites of the Silala Aquifer.

Fluvial-Glacial Deposit (Qfg)

The fluvial-glacial sediments are present in the accumulation of volcanic and pyroclastic rocks of almost heterogeneous size with respect to their granulometry, which were deposited at the outlet of the glacial valleys that surrounded the stratovolcanoes and the Silala Ravines. These deposits are composed of some silt, sand with clasts, ridges and boulders of volcanic rocks of different diameters. The larger blocks show glacial striations that reflect the movement of ice masses, while the smaller granulometry material shows fluvial-glacial transport and erosion.

Colluvial-Fluvial Deposit (Qcf)

Deposit present in the embankment, with a gentle slope, where the sediment accumulated as a result of the transport of rocky material resulting from gravity and the action of intermittent runoff water. They are the product of melting and snowfall.

Colluvial Deposit (Qc)

The colluvial sediments are located in different parts of the area with gentle and steep slopes. These are colluvial cones, commonly called sallerios (stony grounds), in quite extended areas. These accumulations present incipient sedimentary deposits, which are heterometric and frequently polygenic. They are constituted by blocks, boulders, pebbles and gravels of outcrops of volcanic rock that come from the inactive volcanoes, such as the Silala Chico, Silala Grande, Inacaliri and others.

Alluvial Fan Deposit (Qaa)

The alluvial activity is represented by the runoff of fluvial-glacial waters that gave rise to forms of erosion and accumulation 10,000 years BP. Large alluvial fans can be observed, reflecting somewhat more temperate climatic conditions that produced the melting of ice masses and, therefore, the amount of runoff water, which is totally different from the current one, which in turn formed deposits of various materials of medium to fine granulometry (gravel, sand, silt and clays) that are arranged in a decreasing grain form from top to bottom, with the apex in the highest area.

Alluvial Deposit (Qa)

These deposits are mostly located in the areas that surround the springs that exist in the surveyed area, and can also be observed in upwelling streams, forming the bofedals. In them, it is possible to observe very fine sediments, but mostly organic matter.

2.3. Formation of the Silala Ravines

The survey of the formation of the three Silala Main, North and South Ravines is based on field work carried out between 2000 and 2005 and recent geological-tectonic works provided by SERGEOMIN (2017) and the Tomas Frias Autonomous University (2018).

In the Altiplano of the Central Andes, two extensive humid facies have been related to the records of large lacustrine fluctuations,15 the Minchin Facie (approximately 35,000 to 23,000 years BP) and the Tauca Facie (beginning 15,400 years BP, maximum between 13,000 and 12,000 years BP). These were followed by the Coipasa Event that was less humid, between 11,300 and 10,400 years BP.16

In the area surrounding the Silala Springs, the most outstanding structural and geo-morphological features are influenced by the movements of glaciers and their thawing, which slide through faults (See Photographs 1, 2, 3 and 4). The three Silala Ravines, which are formed on igneous ignimbrite rocks (Nis1 and Nis2), have two very well-known geo-morphological features; the first is that they occurred 15,000 years BP, with the radical change of climate, when a period of warming began and caused the melting of continental glaciers that covered a large part of the planet. The three Silala Ravines were formed at the end of the ice age (Late-Glacial between 12,000 to 8,000 years BP), known as the Tauca Facie. They are a typical example of the action of ice and melt-water that benefit from areas of weakness in the outcropping ignimbrite rock; exemplified by the Silala Fault, with a NNE-SSW course, and the transverse E-W readjustment faults.[17] However, in the current design of the Main Ravine, with a ―U-shaped‖ geo- morphological cut and almost vertical side walls (15 to 100 meters high and a floor of more than 40 meters wide)[18], the flat floor is covered with glacial and fluvial-glacial sediments that show the combination of several other weathering factors and not only glacial action (See Photograph 3).

It is important to emphasize that the abundant water derived from thawing and the copious rain of the Tauca Facie were the biggest charge of the current groundwater stored in the Miocene ignimbrite rocks and led to the formation of the Silala Aquifer, which now outcrops through the Silala Springs on both sides of the border.

Both the description of the geological and geo-morphological features of the Silala Ravines, including the structural geology of the area, the igneous rocks and the mapped Quaternary Glacial sediments, and the description of the other structures identified in the Silala ignimbrites, allow a correct interpretation of the formation of the Silala Ravines.

15 U.S. Geological Survey, Bulletin 1975. 1992, pp. 19 – 23.
16 Servant et al., 1995; Sylvestre et al., 1996, 1999.
17 Ministry of Environment and Water (MMAyA, hereinafter), 2016. Geophysical Prospecting Survey by the Electrical Tomography Method. ―Silala Valley Bofedals and Adjacent Sectors‖. Abel Sangueza Antezana, p. 37.
18 SERGEOMIN, ―Survey of the Geology, Hydrology, Hydrogeology and Environment of the Silala Springs ar ea‖. 2003. P. 16.

The Main and North Ravines, located in the Silala Near Field, were formed by the action of the glacial movement that slid, mainly from the Inacaliri Volcano, before 15,000 years BP. The ice slid through the ravine formed by the Silala Fault. Photographs 1 and 2 show the valley of the Main Ravine with a ―U-shaped‖ profile, typical of ice formation in motion. Photograph 3 shows the trial pit excavated near the border with a typical glacial soil profile.

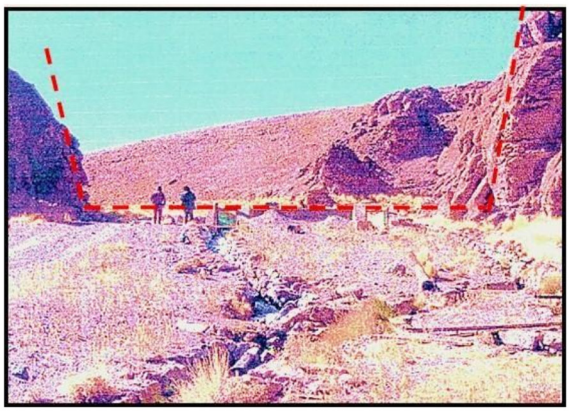
According to surveys of the Pleistocene geology, the valley of the South Ravine was formed by a collapse fault that was later extended by the movement of the glacier and by the large amount of melt-water—as also happened in the Minchin and Tauca lake formations in the Central and SW regions of the Bolivian Altiplano. In that period, the melting and torrential rains produced huge volumes of water, leaving traces of alluvial-fluvial erosion in the vertical north wall of the valley (near the waterfall also formed by a small normal fault across the channel). In addition, due to the volume and velocity of the descending water, no alluvial sediments were deposited in its narrow valley. These glacial and fluvial features ended in the same way they started 8,400 years ago.

Surveys completed on the Chilean side indicate that there is geological and geo-morphological evidence of an active fluvial system in the Silala Main Ravine and show even four surfaces of fluvial terraces cut by water or four Pleistocene sedimentary sequences.[19] However, on the Bolivian side these terraces have not been found on the walls of the ignimbrites. Photograph 4 shows the upwelling groundwater from the aquifer, which is not observed in the Main Ravine, on the Bolivian side.



Photograph 1. Headwaters of the Main Ravine with the “U-Shaped” valley profile, 2000.[20]

19 CM, paras. 2.11-2.12.
20 The source is the author‘s.



Fotografía 2. Muestra en la cabecera Quebrada Principal, cerca de la intersección del Canal Norte y Sur, se observa el perfil típico de un valle en "U", año 2000[21]



Fotografía 3. Calicata excavada en la Quebrada Principal, se observa en el perfil una deposición de material sedimentario glaciar y fluvio-glaciar. Profundidad: 3.30 metros, año 2000.[22]

[20] The source is the author's.
[21] The source is the author's.



Photograph 4. Main Ravine on the Chilean side with the vertical ignimbrite wall (Silala Fault) and springs emerging from it with collecting channels. The iron pipeline, parallel to the Main Channel, conveys the water to Antofagasta for FCAB company. October, 2000[23]

2.4. Structural Geology of the Area of the Silala Springs

The Rose Fracture Diagram was prepared by SERGEOMIN (2017) and the Tomas Frias Autonomous University (UATF, for its Spanish acronyms), and its interpretation concurs in the Map of Lineaments and Faults of the Silala Springs area. It shows a general fracture system that presents four structural trends:

- The first and main system has a general NE-SW (40 ° -70 °) trend; it presents discontinuous and shorter features and is represented in the South and North sector of the area, including the Uyuni- Khenayani system fault.

- The second system has a longitudinal NW-SE (100 ° -140 °) direction and includes the main volcanic centers of the area; it is more frequent and continuous in the Northwest and Northeast sectors of the area.

- The third system has a general N-S (340 ° - 360 °) trend; it is chiefly present to the south of the area;
some volcanic cones are aligned in this direction.

- The fourth system – which is not predominant and presents an E-W to E-NE direction – is infrequent and transverse to the previous ones. It is present in the central part of the area and cuts off some longitudinal N-S trend lines.

The survey completed by the Tomas Frias Autonomous University (2018) describes the local geological structure as follows: 1,500 fractures were mapped throughout the study area. Following their interpretation, it was concluded that the maximum stress axis has a preferred E-W direction,

23 The source is the author‘s.

which gave rise to four structural domains, each with particular characteristics. For example, fault mirrors were mapped in the 4th domain. These determined the current position of the structural canyon, as well as the secondary porosity of the whole ignimbrite complex that allows the springs to well up.

The position of the fault mirrors (striae) shows that the fractures of the 4th domain were activated by the action of shear stresses, which formed the current geomorphology of the canyon (tectonic pit/structural gully). The fault mirrors mapped have an average dipping direction of 140/48° (azimuth of the dipping direction), a trend with an azimuth of 225, and a plunge (subsidence) of 110; with a raque of 110 SW, conditioning a structural control for the upwelling of the springs of the NWW sector.

The Tomas Frias Autonomous University Survey described the following domains of the fracturing system.

a) 1st Domain[24]
Fractures ―b‖ and ―c‖ respond to shear fractures with respect to the main stress axis of a NE trend of 81°;
fractures ―a‖ and ―d‖ respond to shears of a second order in relation to the shear stresses (see Figure No. 8.
1st Domain Joints).

From an interpretation of the direction frequency Rose, it can be perceived that the ruling fracture direction is 80° N – 85° W. The latter is the reason why the flow of the SEE sector springs (South Springs) has a higher rate, inasmuch as water always flows to areas where there is less resistance. These extension fractures are open fractures that enable the upwelling of the springs because of their high secondary permeability rate (See Figures No. 9, 12, 13, Structural Geology).

b) 2nd Domain[25]
The 2nd domain is characterized for having a 1st δ (maximum effort axis) of an 85° NE direction and a Plunge of 12° NE, a 2nd δ of an 85° NE direction and a Plunge of 78° SW, and a 3rd δ of an 5° NW direction and a Horizontal Plunge. These caused fractures ―b‖ and ―e‖ to be shear fractures, fractures ―a‖ to be compression fractures, and ―e‖ to be second order shear fractures.

From an interpretation of the Rose diagram (see Rose Diagram, Annex A. 1., p. 29), it is possible to perceive a predominant Rb [Direction] in a range of 0° N – 10° W, which matches the compression fractures, and a fracture frequency in a range of 60° N – 68 ° W—matching the shear fractures.

The above provides an explanation as to why the 2nd domain (Figure No. 8) section does not comprise any springs, i.e. this domain presents closed fractures, unlike the 1st Domain. (see Figures Nos. 11 and 12, Structural Geology).

24 Tomas Frias Autonomous University, ―Hydrogeological Characterization of the Silala Springs‖, 2018. p. 7.

25 Tomas Frias Autonomous University, ―Hydrogeological Characterization of the Silala Springs‖, 2018. p. 7.

c) 3rd Domain[26]

The 3rd domain (see Figure No. 9) is characterized for presenting a maximum stress axis (δ1) with a NE 75° direction and a Plunge of 10° SW, a 2nd δ of a 75° NE direction and a Plunge of 80° NE, and a 3rd δ of a 15° NW direction and a Horizontal Plunge. These caused fractures —a‖ and —d‖ to be first order shear fractures, fractures —b‖ and —c‖ to be second order shear fractures, and fracture —e‖ to be compression fractures.

From an interpretation of the Fracturing Frequency Rose, it can be perceived that there is a predominant NS fracture Rb [direction], which corresponds to compression fractures, and NW fractures that correspond to shear fractures, to a lesser degree. This is why springs do not well up in this domain (see Figures Nos. 11 and 12, Structural Geology).

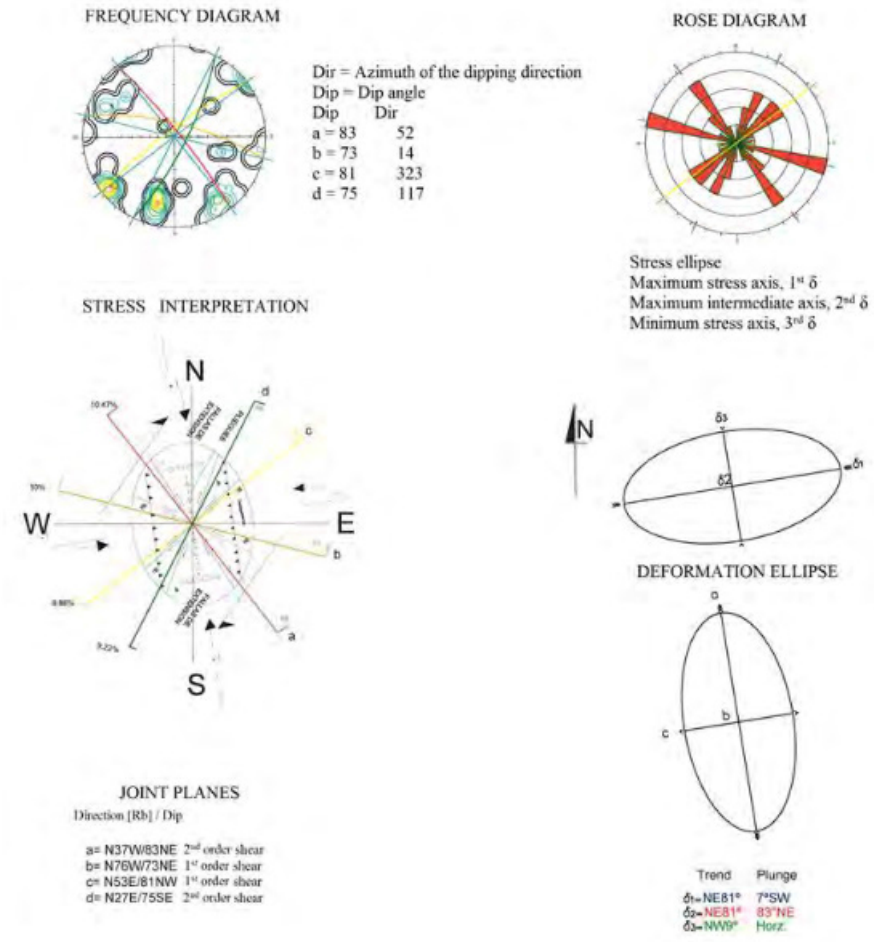
d) 4th Domain[27]

Fractures —a‖, —b‖ and —c‖ are first order shear fractures, with respect to the 1st δ. Fractures —e‖ and —d‖ are
second order shear fractures activated by shear stresses. These have activated the predominant faults in the

4th Domain (see Figure No. 10), as a result of the action of shear stresses, where a fault mirror was mapped with a dipping direction of 140°/148°, a 225° trend, a 11° plunge, and a SW 11° raque. This structural control predetermines the emergence of the NWW sector springs (see Figures Nos. 11 and 12. Structural Geology).

26 Tomas Frias Autonomous University, ―Hydrogeological Characterization of the Silala Springs‖, 2018. p. 8.
27 Tomas Frias Autonomous University, ―Hydrogeological Characterization of the Silala Springs‖, 2018. p. 8

1ST DOMAIN JOINTS
SILALA PROJECT



Interpretation

Based on the structural interpretation, it can be perceived that fractures ~~–b~~" and ~~–c~~" respond to shear fractures in relation to the main axis of a NE 81° trend; fractures ~~–a~~" and ~~–b~~" respond to second order sheers in relation to shear stress.

There are fractures of angle strike extension, which fluctuate from 81° N – 85° E and concur with the direction of the topographic depression of the area in which the springs flow, with a preferential Rb [direction] of N 81° E.

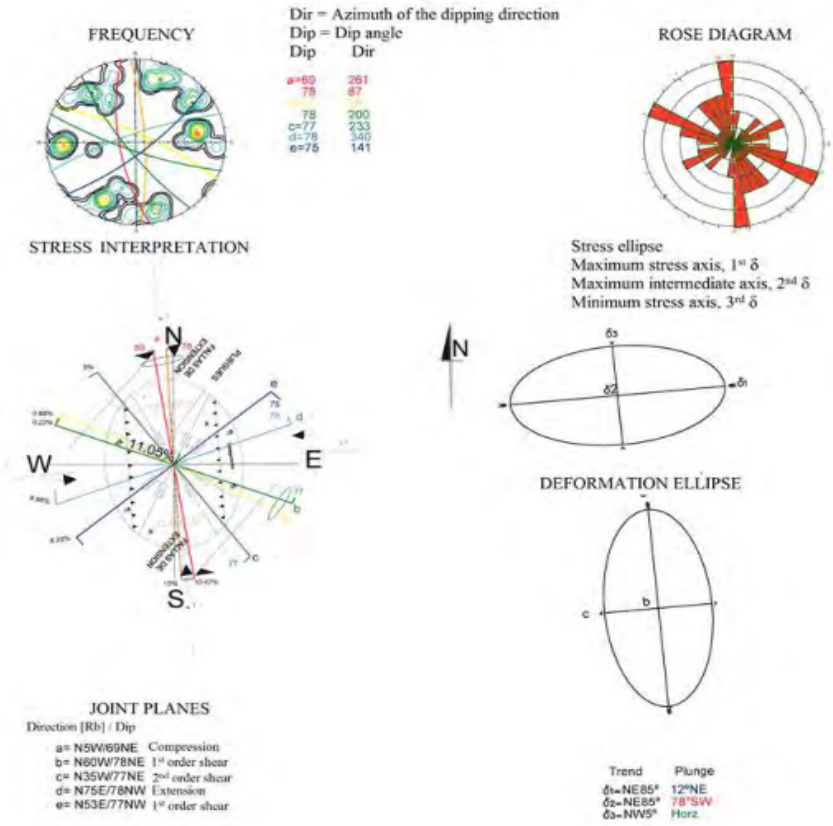
From an interpretation of the Rose diagram, it can be perceived that the ruling fracture direction is 80° N – 85° W. The latter is the reason why the flow of the SEE sector springs has a higher rate, inasmuch as water always flows to areas where there is less resistance. These extension fractures are open fractures that enable the upwelling of the springs because of their high secondary permeability rate.

Figure No. 7. 1st Domain Joints[28]

[28] Tomas Frias Autonomous University, ~~–H~~ydrogeological Characterization of the Silala Springs", 2018. Annex A. 1.

2ND DOMAIN JOINTS

SILALA PROJECT



INTERPRETATION

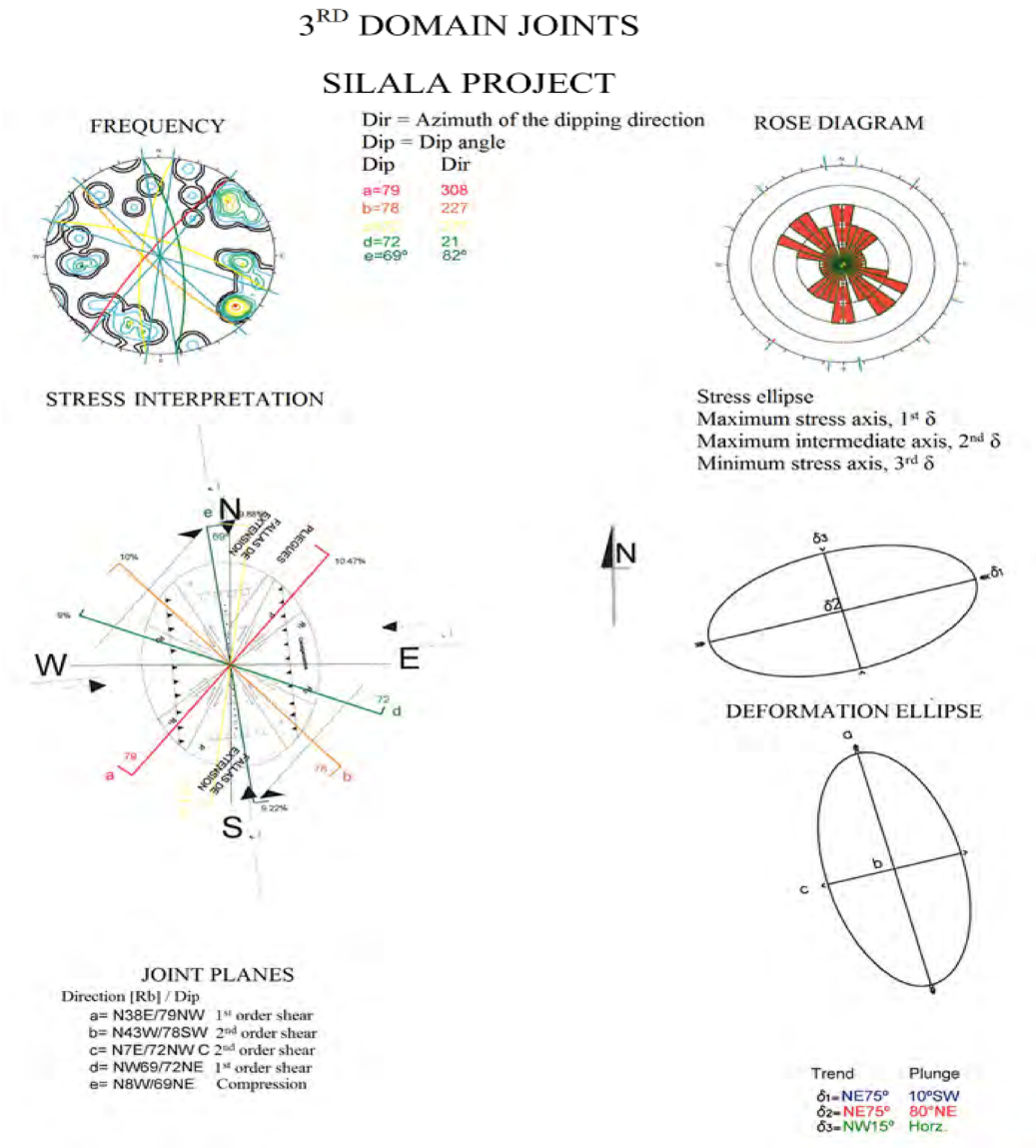
2nd Domain: it is characterized for having a 1st δ (maximum effort axis) of an 85° NE direction and a Plunge of 12° NE, a 2nd δ of an 85° NE direction and a Plunge of 78° SW, and a 3rd δ of an 5° NW direction and a Horizontal Plunge. These caused fractures ~~"b"~~ and ~~"e"~~ to be shear fractures, fractures ~~"a"~~ to be compression (closed) fractures, and ~~"c"~~ to be second order shear fractures.

From an interpretation of the Rose diagram (see, Annex A. 1., p. 29), it is possible to perceive a predominant Rb [Direction] in a range of 0° N – 10° W, which matches the compression fractures, and a fracture frequency in a range of 60° N – 68 ° W—matching the shear fractures.

The above provides an explanation as to why the 2nd domain section does not comprise any springs, i.e. this domain presents closed fractures, unlike the 1st Domain.

Figure No. 8. 2nd Domain Joints[29]

[29] Tomas Frias Autonomous University, ~~"H~~ydrogeological Characterization of the Silala Springs", 2018. Annex A. 1.



INTERPRETATION

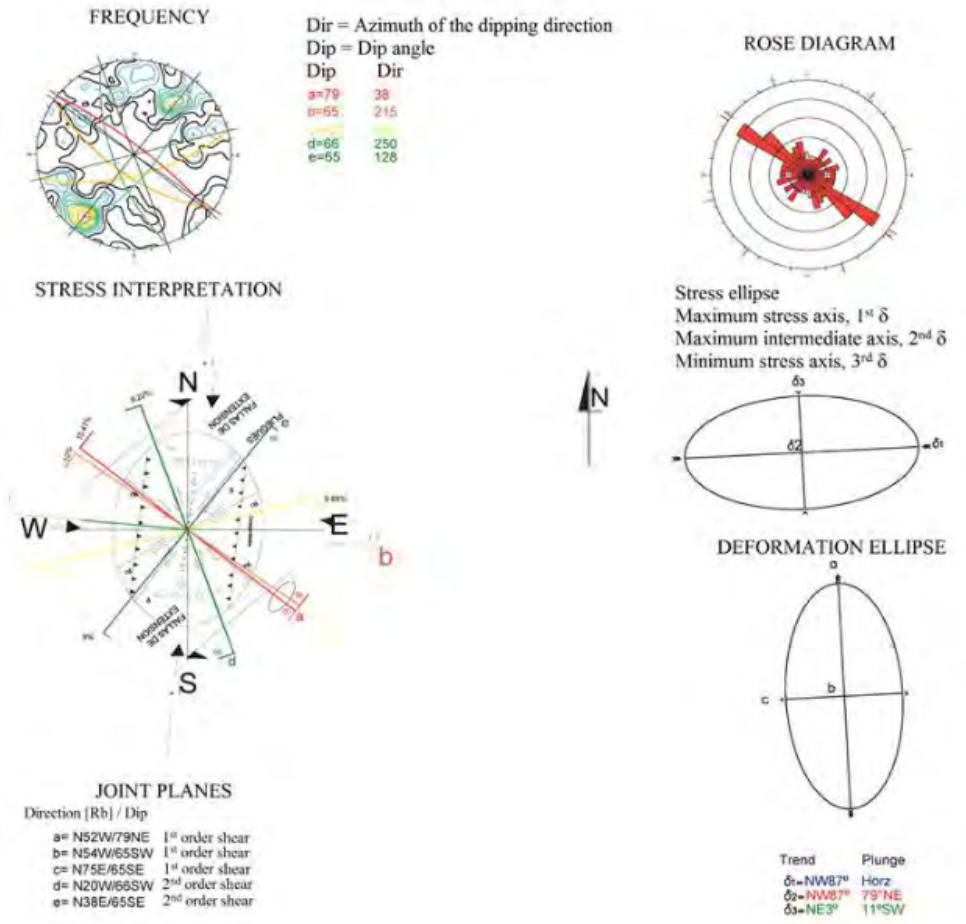
3rd domain: it is characterized for presenting a 1st δ of a 75° NE direction and a Plunge of 10° SW, a 2nd δ of a 75° NE direction and a Plunge of 80° NE, and a 3rd δ of a 15° NW direction and a Horizontal Plunge. These caused fractures ~~–a~~" and ~~–d~~" to be first order shear fractures, fractures ~~–b~~" and ~~–c~~" to be second order shear fractures, and fracture ~~–e~~" to be compression fractures.

From an interpretation of the Rose diagram, it can be perceived that there is a predominant NS fracture Rb [direction], which corresponds to compression fractures, and NW fractures that correspond to shear fractures, to a lesser degree. This is why springs do not well up in this domain.

Figure No. 9. 3rd Domain Joints[30]

[30] Tomas Frias Autonomous University, ~~–H~~ydrogeological Characterization of the Silala Springs", 2018. Annex A. 1.

4TH DOMAIN JOINTS
SILALA PROJECT



INTERPRETATION

Fractures –a", –b" and –c" are first order shear fractures, with respect to the 1st δ.

Fractures –e" and –d" are second order shear fractures activated by shear stresses.

These have activated the predominant faults in the 4th Domain, as a result of the action of shear stresses, where a fault mirror was mapped with a dipping direction of 140°/148°, a 225° trend, a 11° plunge, and a SW 11° raque. This structural control predetermines the emergence of the NWW sector springs.

Figure No. 10. 4th Domain Joints[31]

[31] Tomas Frias Autonomous University, –Hydrogeological Characterization of the Silala Springs", 2018. Annex A. 1.

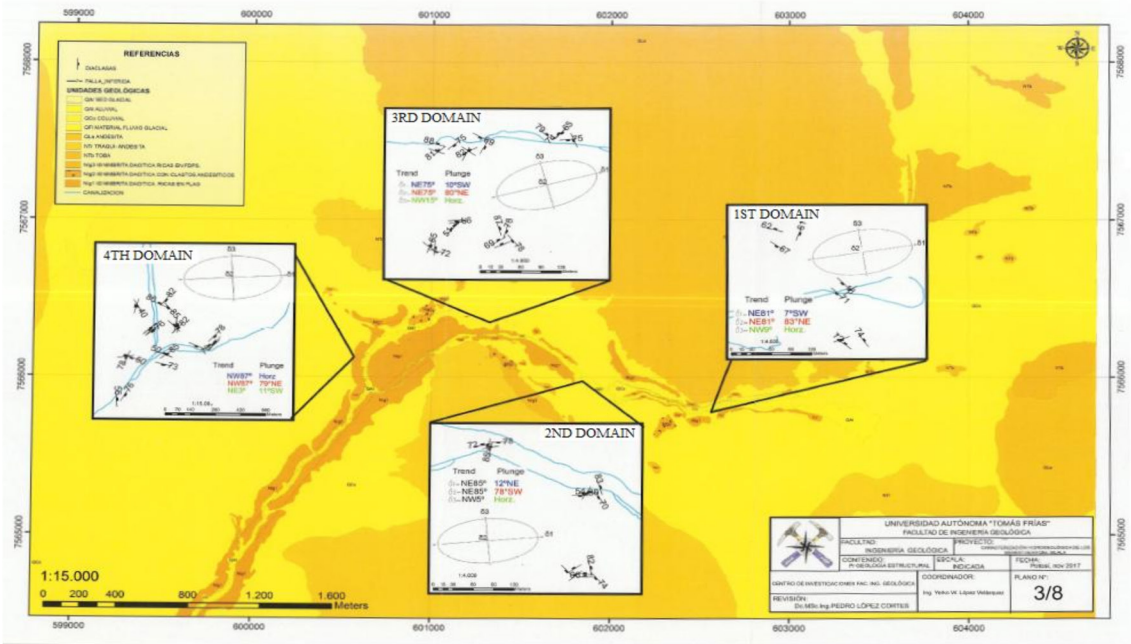


Figure No. 11. Structural Geology – Stress ellipsoid[32]

[32] Tomas Frias Autonomous University, "Hydrogeological Characterization of the Silala Springs", 2018. Annex A. 2.

English translation prepared by DIREMAR. The original-language text remains the authoritative one.

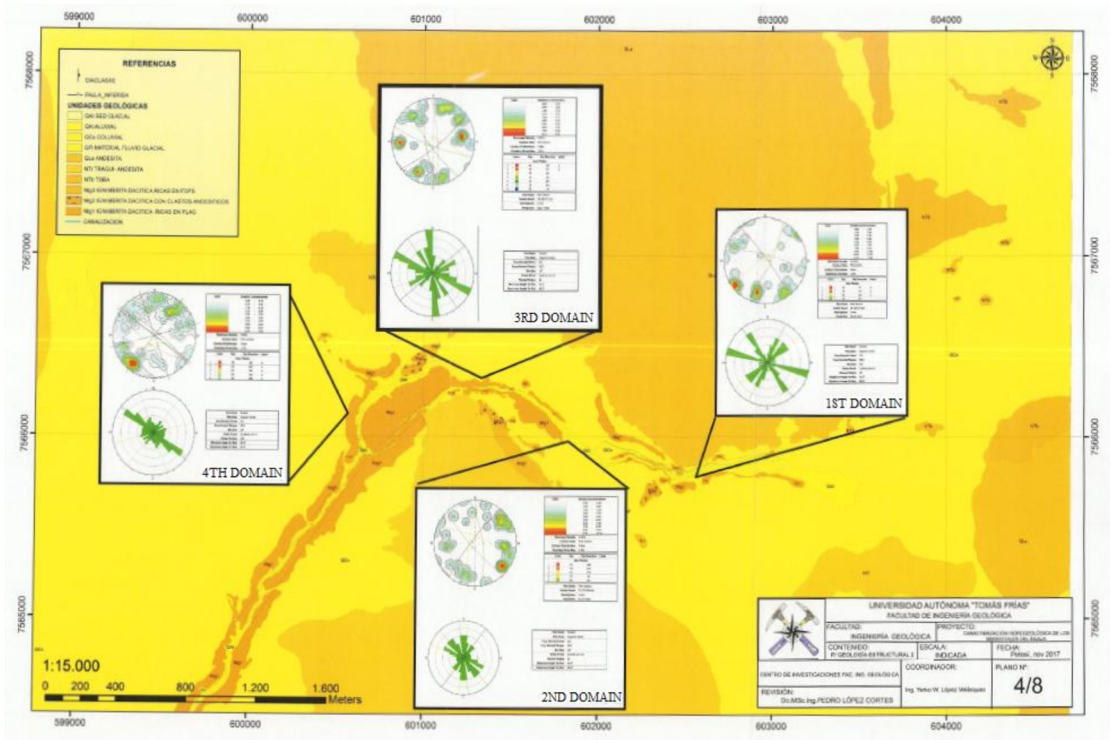


Figure No. 12. Structural Geology – Fracture rose diagrams[33]

[33] Tomas Frias Autonomous University, "Hydrogeological Characterization of the Silala Springs", 2018. Annex A. 2.

The sector studied is located at the base of the Inacaliri and Silala Chico hills. It is elon-gated and narrow and extends to the NE through the ravine upstream as far as the bofedales. From the bofedales, it expands and forms a regular surface with a positive slope towards the East. The rocky outcrops that are present in this sector are the pyroclastic deposits arranged sub-horizontally. In these outcrops, there are fractures that have a sub-vertical position, shaping column-like forms of heights that surpass the 5 m and that are fused in sets of mi-nor fractures – discontinuously and with greater inclinations.[34]

To the east of this sector, the outcrops are quite weathered and appear as a foliation in the shape of very fractured tables. At the northern limit of the area, it was possible to record da-ta on the outcrops that are mainly dispersed. The ignimbrites have a massive structure and moderate hardness; they have a moderate fracturing degree; however, it is possible to ob-serve joints and faults in varied directions throughout their thickness.[35]

The fracture density is determined by the number of cooling joints, the rearrangement frac-tures and the reduced minor faults that are continuous and interconnected. In general, the fractures are closed and occasionally unfilled; They are not very rough, with variable conti-nuity and their frequency of fracturing fluctuates from 2 to 4 per 10 m, on the side of the station cell. Consequently, the rocky massif is characterized as a moderately frac-tured one.[36]

2.4.1. Faults found in the Silala Ignimbrite area

According to the SERGEOMIN (2017) report, 185 faults were identified in the Silala Ignim-brite area: 85 normal faults, 26 inverse faults, 11 lateral faults and 63 faults that do not pre-sent displacement kinematics. These faults present relative movements or displacements of few inches caused mainly by displacements derived from gravity. In addition, it has not been possible to identify the direction of the striations in the fault planes, because the events that occurred in this sector are not differentiated.

A structural analysis was carried out in the areas with the most data available to process and create the fracture rose diagram. Consideration was given to the data that represents the pre-dominant structures of the unit to relate them to faults and lines at the macrostructural lev-el, defined on basis of an analysis of satellite images.

The fracture rose diagram presented in Figure 13 a shows normal faults (n = 85) that make up the first subgroup of fractures measured in the Silala Ignimbrite sector. These preliminary show the following trend directions: NW-SE (125 ° -305 °); N-S (175 ° -355 °); NE-SW (35 ° -215 °). Figure 13b shows the stereographic projection of inverse faults (n = 26) that form the second subgroup of fractures measured in the Silala ignimbrite, and presents the following trends: NE-SW (55 ° 235); NW-SE (325 ° -145 °). The number of inverse faults recorded in this sector is small, com-pared to the normal faults,

34 SERGEOMIN, ―Structural Geological Mapping of the Area Surrounding the Silala Springs‖. 2017. P. 58.
35 SERGEOMIN, ―Structural Geological Mapping of the Area Surrounding the Silala Springs‖. 2017. P. 58.
36 SERGEOMIN, ―Structural Geological Mapping of the Area Surrounding the Silala Springs‖. 2017. P. 58.

which allows us todeduce that the stress regime in the area is distensive in kind.37

The frequency in the normal faults of the first NW-SE trend (125 ° -305 °) shows the immediate directional relationship with the traces of the Inacaliri graben of a NW-SE direction (300 °), which is located to the north of the area. Another N-S trend, represented in the normal fault rose diagram, even with a lower frequency, shows the relationship with the N-S lineaments parallel to the Linzor stratovolcanoes and others of shorter length, to the South and Center of the area.38

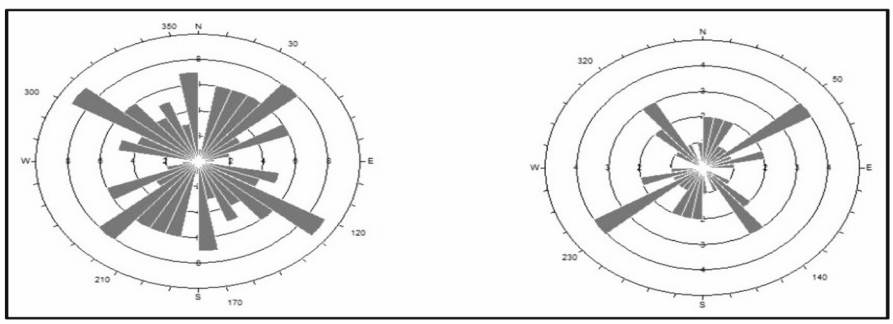


Figure 13a. Fracture Rose Diagram of the Normal faults of the Silala ignimbrites
Figure 13b. Fracture Rose Diagram of the Reverse Faults of the Silala Ignimbrites

Due to its tectonic and volcanic activity, the fracturing degree in the Silala Ignimbrites is potentially suitable for the transport and circulation of water fluids. This relationship leads us to postulate that the Silala-Llancor lineament – with an ENE-WSW (70°) direction – is likely to behave like a left lateral fault. The fault crosses the central sector of the area; it coincides pro-parte with the channel of the Silala Spring; passing through the middle of the Silala Ignimbrites and the lavas of Silala Grande Hill[39].

2.4.2. Silala Ignimbrite Joints

The joints have the characteristics of planar forms; they are continuous and bigger than 5 m; they have frequencies of 10 to 15 joints in every 10 m and persist in the whole ravine; the openings that they present are minimal, ranging from millimeters to 20 cm, occasionally.

The vast majority of these joints do not show any type of infilling; the percentage of those that present clays infilling millimeter separations is reduced. The roughness of the walls is of two types: those formed by cooling are smooth, and those formed by stress have moderate roughness. The presence

37 SERGEOMIN, ―Structural Geological Mapping of the Area Surrounding the Silala Springs‖. 2017. P. 59.
38 SERGEOMIN, ―Structural Geological Mapping of the Area Surrounding the Silala Springs‖. 2017. P. 61.
39 SERGEOMIN, ―Structural Geological Mapping of the Area Surrounding the Silala Springs‖. 2017. P. 31.

of water and humidity only occurs in the northern sector of the ravine - from the bifurcation of the ravine onwards.[40]

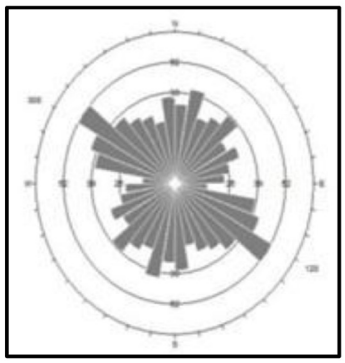


Figure 14. Joint Rose Diagram of the area of the Silala ignimbrite[41]

In Figure 14, the joint rose diagram of the Silala Ignimbrite sector was established on basis of 637 measured planes, at stationary points. It also contains the joints formed by cooling and weathering events; which makes their frequency chaotic with respect to their directions.

According to what is observed in the joint rose diagram, formed mainly by cooling joints, a predominant direction similar to that of the normal NW-SE faults (305°) is shown, which has been directly related to the Inacaliri Graben structure and the regional lineaments – which have the same direction (Tibaldi et. al 2008).[42]

2.5. Hydrogeological Units

To complement the geological framework, and due to the importance of the hydrology of the Silala Near Field, it is necessary to classify the geological sequence into hydrogeological units. The definition of hydrogeological units for the study area is based on the characteristics of the rocks, the tectonic history of the area, and the capacity to store and transmit water – that is, the capacity of rocks and unconsolidated deposits to store and transport groundwater. Based on the hydrogeological characteristics measured and, in other cases, interpreted from the geological units, the Danish Hydraulic Institute (DHI) [sic] has grouped the geological units into eight (8) Hydrogeological Units (HGU). In this report, seven (7) Hydrogeological Units (HGU) have been modified (Figure 15 A), because only these units were used as parameters in the development of the hydrogeological framework model and in the DHI groundwater flow modeling[43]. In Figure 15 B, where the Silala area is superimposed by the seven hydrogeological units delineated by DHI, the ignimbrite deposits are shown with a high degree of welding (upper or lower) and approximate thickness. It is known that the hydrogeological properties of ignimbrites and tuffs are heterogeneous in nature, and that the hydraulic conductivity can vary by more than 14 orders of magnitude.

40 SERGEOMIN, ―Structural Geological Mapping of the Area Surrounding the Silala Springs‖. 2017. P. 61.
41 SERGEOMIN, ―Structural Geological Mapping of the Area Surrounding the Silala Springs‖. 2017. P. 61.
42 SERGEOMIN, ―Structural Geological Mapping of the Area Surrounding the Silala Springs‖. 2017. P. 61.

43 DHI, 2018. Product No. 2. Final Report, p. 35.

The complete and detailed descriptions of the seven Hydrogeological Units (HGU) are provided in Product No. 1 on ―Groundwater Flows‖ prepared by DHI, 2018. The table below presents the Hydrogeological Units and maps with their delineation in the Silala area.

TABLE 1. HYDROGEOLOGICAL UNITS (HGU)

TABLE 1. HYDROGEOLOGICAL UNITS (HGU)

Hydrogeological units	Basic Lithology	Approximate thickness (m)
HGU1	Colluvial and alluvial deposits	1 to 10 m
HGU2	Glacial deposits, sandy loams	1 to 10 m
HGU3	Weathered lava flows	1 to 30 m
HGU4	Felsic volcanic sequences	Up to 600 m
Higher HGU6	Ignimbrite deposits with a high degree of welding	Up to 150 m
HGU5	Ignimbrite deposits with a low degree of welding	10 to 120 m
Lower HGU6	Ignimbrite deposits with a high degree of welding	Up to 300 m.
HGU7	Fault zones regarded of importance for the groundwater flow	50 to 100 m of width, depth to the ignimbrite base (assumed)

Figure 15-A shows the delineation of the Hydrogeological Units (HGU) established by DHI. It can be observed that HGU 7 (red color) is the most important because it is the one that allows the aquifer's groundwater springs to outcrop. HGU 2 (green color) shows the glacial deposits in the base of the ravines. HGU 3 (pink color) and HGU 5 (purple color) show the surface area of the potential Silala Aquifer.

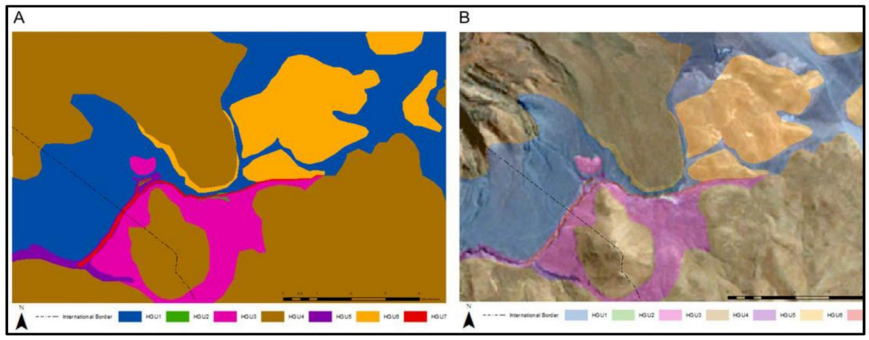


Figure 15. A) Delineation of Hydrogeological Units (HGU) in the Silala area, DHI.
B) Images of the Silala area superposed by the HGUs, delineated by DHI.

3. HYDROLOGY

The Silala springs are fed by groundwater in which the contributions from surface runoff are minimal compared to the contribution of groundwater flow.[44] The Silala has a desert climate with low precipitation, low temperatures and a high evaporation potential.[45]

The so-called Laguna Blanca and Laguna Chica are not waterbodies, but rather topographical depressions that do not bear any surface water. The surface of the Laguna Blanca is covered with clasts of 2 to 20 cm of chert or amorphous quartz that produce the whitish color that can be seen in satellite images and aerial photographs.[46]

3.1. Basin

The Chilean Memorial[47] presents a strictly topographic basin delineated for the Silala Springs, upstream of the Inacaliri police station, with an area of 95.5 km2. From this basin, Chile has calculated that 59 km2 found on the Bolivian side are contributing to the discharge at the international border. The recharge of rain on this topographic basin (59 km2) cannot, in itself, explain the observed transboundary flows and, therefore, the flows of the groundwater basin discharging to the Silala Springs must be, or are, much bigger, upstream.[48]

The Danish Hydraulic Institute (DHI) has adopted the definition of a ‗Near Field' and ‗Far Field' area for its survey of the Silala Springs. The DHI studies have digitally delineated a possible hydrological basin of 234 km2 (Silala Far Field) that is likely to allow the flow of groundwater from aquifers to the Silala Springs through faults and joints. This hydrological basin has been used for the recharge assessment and water balance of these waters. It is estimated that recharge to the aquifers in this basin is able to sustain a discharge of the same order of the magnitude as the transboundary surface waters (see Figures 16 and 17).

44 DHI, 2018. Final Report, p. 10.
45 DHI, 2018. Final Report, p. 10.
46 SERGEOMIN, ―Survey of Geology, Hydrology, Hydrogeology and Environment of the Silala Springs Area‖, 2003.
P. 25.
47 Peach, Denis & Wheater, Howard. 2017. The Evolution of the Silala River, Basin and Ravine. Expert Report 2. P. S/No.
Chile's Memorial (CM).
48 49 DHI, Final Report, p. 10.

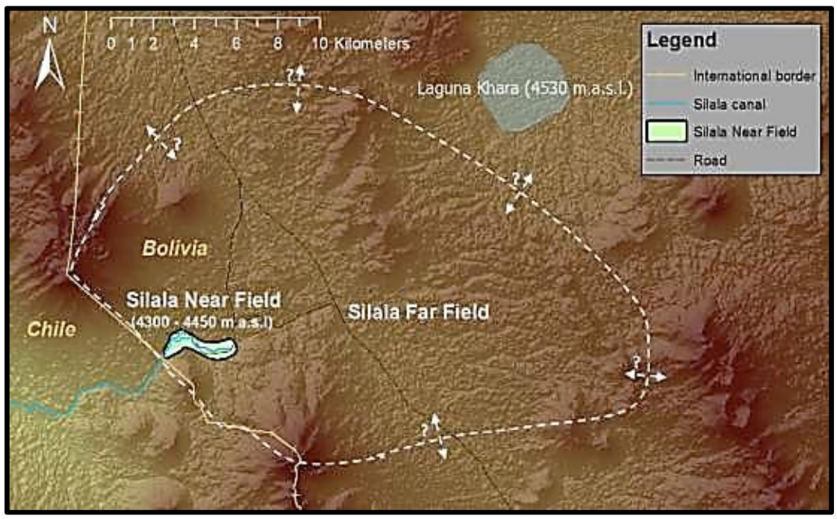


Figure 16. Silala Near Field Topographical basin and Far Field hydrological basin[49]

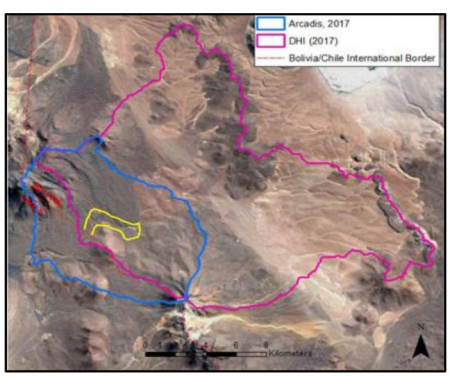


Figure 17. Hydrological basin (violet), topographical basin of the Silala river provided by Arcadis (blue) and Silala Near Field (yellow)[50]

49 DHI, Final Report, p. 7.
50 DHI, 2017, Provisional Report 4, p. 14.

3.2. Climate

The DHI has estimated an average precipitation derived from the basin of 125 mm/year for the period from 1969 to 2017; the inter-annual variation of precipitation is very high, ranging from precipitations close to 0 mm/year in 2009-2010 and higher than 300 mm/year in 1997 and 1999.51 Likewise, DHI has also esti-mated the records of average annual temperature of 2.2 ° C for 1969-2010, with maximum and minimum temperatures between +19.6 ° C and -19.6 ° C.52 The potential evapotranspiration rate (Et0) is 1472 mm/ year which varies from 2-2.5 mm/day in the austral winter months to 5-5.5 mm / day in the summer.[53]

3.3. Surface Waters Volume

In 2017, technical reports on water sampling conducted by the Vice Ministry of Water Resources and Ir-rigation identified 23 streams in the North Bofedal and 21 in the South Bofedal. In each stream, a collector channel of about 0.30 m wide, with variable depths, has been installed. This channel then joins another primary collector channel and forms a secondary channel, or directly joins with the main channel that collects all possible water from the springs. The main channel has a width of 0.80 to 1.00 m. All the channels were covered with ignimbrite stone, reducing the percentage of water infiltration and evapo-ra-tion.[54]

The main channel of the South Bofedal has a length of approximately 2,876 meters, sup-plemented by 265.55 meters of secondary channels that form the entire network of secondary collector channels. The main channel of the North Bofedal is 703 meters long and has a network of sec-ondary channels (See Photograph 5) that add up to a total of 423.10 meters. The two channels join and form the 706-meter long Main Silala Channel which reaches the border with the Re-public of Chile.[55]

According to DHI[56], continuous flow measurements for the Main Channel are available at two permanent measurement stations located near the international border between Bolivia and Chile, respectively. Despite the independent continuous and simultaneous flow measurements carried out on the Bolivian side of the border, the actual channelized flow on the border re-mains uncertain; measures of 160 to 210 l/sec have been calculated.

Dense artificial drainage networks are functioning in the South and North Bofedals. The drain-age channels have been dug as second and third order branches to collect the water directly from the individual springs draining them efficiently towards the South and North Channels, which in turn transport water to the border through the Main Channel.

51 DHI. Final Report. Product 2. 2018. p. 13.
52 DHI. Final Report. Product 2. 2018. p. 14.
53 DHI. Final Report. Product 2. 2018. p. 14.
54 Vice Ministry of Water Resources and Irrigation, ―Technical Report. Second Campaign of Water Sampling for the Hydrochemical and Isotopic Analysis and Diagnosis of the Channels in the Silala Springs‖, 2017, p. 9.
55 Vice Ministry of Water Resources and Irrigation, ―Technical Report. Second Campaign of Water Sampling for the Hydrochemical and Isotopic Analysis and Diagnosis of the Channels in the Silala Springs‖, 2017, p. 9.
56 DHI. Final Report. Product 2. 2018. p. 18.

The current surface flow that flows in the Silala of Bolivia does it through the Main, North and South Channels that were built along the streams of the same name (see Figure 18.). The Main Ravine and Canal of Silala have a longitudinal extension of 3.15 km from the upper limit of the South Bofedal to the border with Chile. The Main Channel has a 0.85 km long tributary that descends from the North Bofedal through the North Ravine to its confluence with the South Channel of the South ravine. The South Channel drains the flow produced by the South Bofedal springs as well as by other springs located downstream of the Military Post in the same channel; these latter waters have been called ―diffuse waters‖ in the DHI reports.

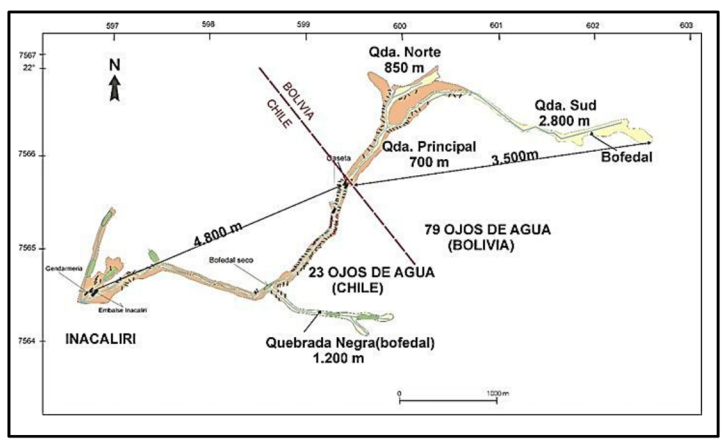
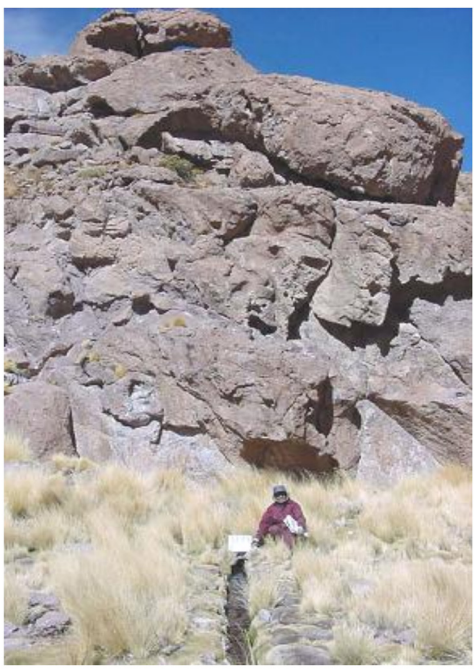


Figure 18. Location of the springs, bofedals and ravines on both sides of the international border.[57]

57 The source is the author‘s.

3.4. Inventory of groundwater sources

To assess the quantity and quality of the groundwater sources, a detailed inventory of the number of springs has been prepared. In 2001, the location of the springs that outcrop in the bofedals and streams of the study area was carried out by Mining Technical Service technicians (SETMIN, for its Spanish acronyms) through a detailed topographic survey with a first order precision GPS system.



Photograph 5. Spring that emerges in the North Channel (showing the secondary conveyance channel) the ignimbrite mantel can be seen in the back.[58]

To measure the physical-chemical parameters of the water, a BWS Multiparameter equipment was used in the field, measuring the temperature, pH, dissolved oxygen, salinity, TDS and electrical conductivity. In addition, gauging was completed with small propellers in almost all springs or inventoried springs. Their number, location, origin and all the physical characteristics

58 SERGEOMIN, ―Study of the Geology, Hydrology, Hydrogeology and Environment of the Silala Springs area‖, 2003. P. 36.

were established and hydrochemical properties of the waters of the springs or groundwater streams that emerge in the Silala area were analyzed.[59]

Based on deductions and observations, it is estimated that the bofedals located in the Silala are hydrogeologically interconnected to adjacent masses of groundwater, although it is be-lieved that this degree of interaction varies from one bofedal to another. In other words, both Bofedals (North and South) depend on the water transfer mechanism and the type of groundwa-ter emergence under any climatic condition.[60]

According to technicians from the Ministry of the Environment and Water (MMAyA, for its Spanish acronyms) who carried out geophysical studies in the area and its surroundings, a great deal of the groundwater that moves within the ignimbrite fractures, added to that de-rived from frozen, discontinuous, soils and that from unconsolidated (colluvial-fluvial) and con-solidated (secondary porosity) materials – marked by resistivity anomalies – merges and gives rise to slow subsurface water flows that slowly emerge in the bofedal.[61]

At least 70 springs that are geographically concentrated in four zones have been identified; these have been channeled through secondary open channels that are collector channels lined with stone.[62] It has also been possible to find streams that have not been channeled – making them natural – and that have very slow natural flows that go in different directions or that have stagnant, but clean waters. During winter, these natural streams are covered with ice, unlike the channeled springs, due to the movement of water created artificially by the channels. The springs and natural streams create areas of surface moisture that give rise to the formation of high altitude bofedals.

On the Bolivian side, the total area of the bofedals in the Silala area is of approximately 109,700 m2; as of this date, this piece of data presents some variations, possibly due to the drying or drainage of some of the bofedals.[63] The location and other physical characteristics of these springs are presented in Figure 18.

In the sectors that have not been channeled, it can be observed that the natural outcrops of discharge are very slow, forming short flows of clean water that follow different directions, sat-urating the soil and preventing its degradation. The link between groundwater and the bofedal, makes these fragile ecosystems in the Silala to be classified as ―static bofedals‖.[64]

59 Vice Ministry of Water Resources and Irrigation, ―Technical Report. Second Campaign of Water Sampling for the Hydrochemical and Isotopic Analysis and Diagnosis of the Channels in the Silala Springs‖, 2017, p. 3.
60 MMAyA, Abel Sangueza Antezana, ―Characterization of Water Resources in the South West of the Potosi Department - Municipality of San Pablo de Lipez. Silala Bofedals and Adjacent Areas‖, Volume II, 2016, p. 3.
61 MMAyA, Abel Sangueza Antezana, ―Characterization of Water Resources in the South West of the Potosi Department - Municipality of San Pablo de Lipez. Silala Bofedals and Adjacent Areas‖, Volume II, 2016, p. 34.
62 MMAyA, Abel Sangueza Antezana, ―Characterization of Water Resources in the South West of the Potosi Department - Municipality of San Pablo de Lipez. Silala Bofedals and Adjacent Areas‖, Volume II, 2016, p. 33.
63 SERGEOMIN, ―Study of the Geology, Hydrology, Hydrogeology and Environment of the Silala Springs area‖, 2003. P. 65.
64 MMAyA, Abel Sangueza Antezana, ―Characterization of Water Resources in the South West of the Potosi Department - Municipality of San Pablo de Lipez. Silala Bofedals and Adjacent Areas‖, Volume II, 2016, p. 32.

On the other hand, in sectors where water has been channeled through open canals to secondary collector channels lined with stone, it is possible to observe a constant recharge and the water has been drained in only one direction due to the built channel, without saturating the adjacent soils and causing the degradation of these soils and the bofedal. This anthropic intervention gave rise to the degradation of soils and ecosystems, due to the fact that these soils passed from a state of high content of organic matter to a state of low content of organic matter. This process is unidirectional and irreversible, specifically in the South Bofedal.

The dense drainage network, with channels of different width and length, is found in the South and North Bofedals. The drainage channels have been dug as 2nd and 3rd order branches that collect water from the springs and discharge into the Main Channel. SERGEOMIN (2003) shows that there is a concentration of springs in the area in four zones located on the South Channel, which are detailed below from East to West:

3.4.1. South Bofedal – First Bofedal

The sequence of the Profiles from geophysical surveys with Vertical Electric soundings (VES), obtained between 2000 by SERGEOMIN, and Tomographic Profiles taken by the MMAyA in 2016 and COFADENA in 2017, suggest that the depth of the groundwater that wells up in this first bofedal is shallow and presents saturated surface sediments.

At the eastern end of the South Channel, the springs emerge from the joints present in the underlying ignimbrites, towards sediments or recent soils, forming a first bofedal. The outcropping water saturates the unconsolidated surface sediments forming the a bofedal that has an approximate surface area of 65,200 m2 and is the largest of all Silala Bofedals[65] (see Figure 19).

A total of 19 springs have been inventoried in the area of this bofedal. These have been channeled by the FCAB company with the construction of simple engineering structures (stone masonry) connected to an open collector channel, also made of stone, forming the Southern Channel. This channel runs in a general direction from East to West until its intersection with the North Channel, forming the Main Silala Channel.

65 SERGEOMIN, ―Study of the Geology, Hydrology, Hydrogeology and Environment of the Silala Springs area‖, 2003. P. 27

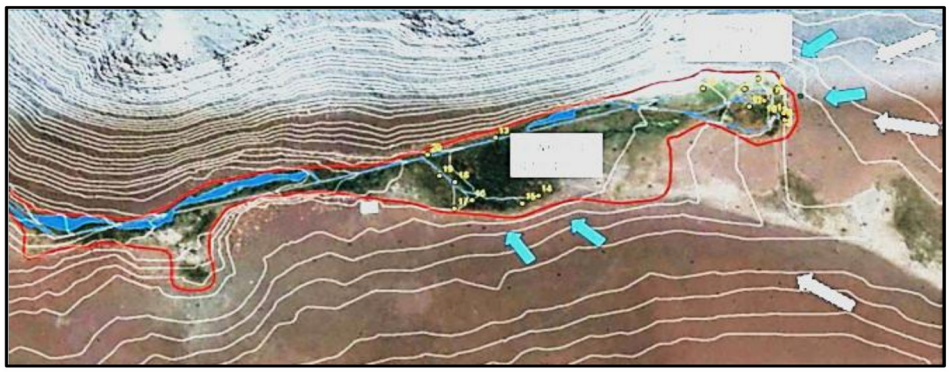
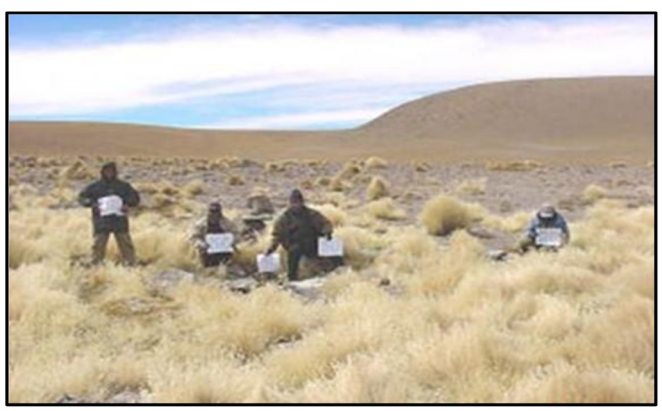


Figure 19. General map of the South Bofedal in which the extent, springs, network of channels and the general directions of the flow are presented.[66]

The flows of the springs in this bofedal vary from 0.25 l/sec at 2.0 l/sec. The electrical conductivity of the water from the springs varies from 240 to 350 µS/cm and the temperature ranges from 14º C to 16º C. There are also several other small springs on the surface of the bofedal that have not been channeled, moistening the soil without any movement of water (See Photograph 6).



Photograph 6. The South Bofedal – First Bofedal.[67]

3.4.2. South Channel – Second Bofedal

The second concentration zone of four to six springs forming a small bofedal in the South Chan-nel (middle part) arises from out-crops of the Silala ignimbrite that form the South Ravine. To its

66 DHI. Provisional Report No. 1. Surface Flows. July, 2017. p. 14.
67 SERGEOMIN, ―Study of the Geology, Hydrology, Hydrogeology and Environment of the Silala Springs area‖,2003. P. 26.

greatest extent it was almost dry (see Photograph 7); today the whole ravine is flooded and it is difficult to see the springs rising from the rocks.

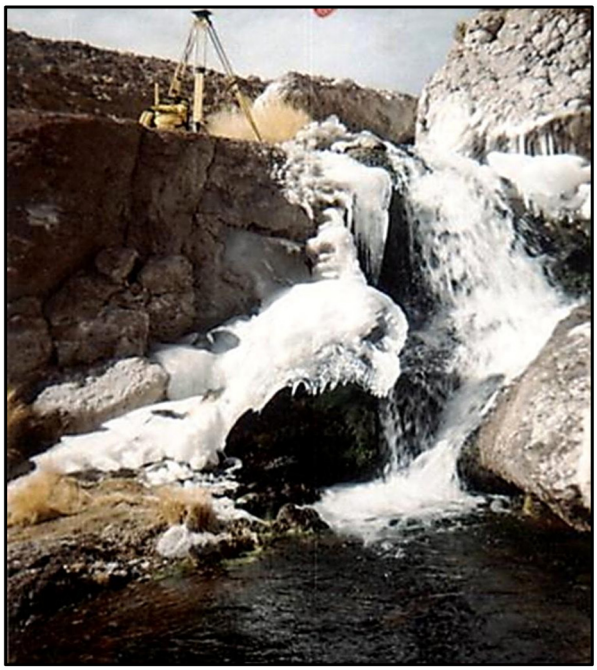


Photograph 7. South Ravine, presenting channelization. 2000.

3.4.3. South Channel – Third Bofedal

The third bofedal of the South Channel begins at the foot of the first waterfall in the South Ravine. The waterfall has an approximate altitude of 3 m and has been formed by a small normal E-W transverse fault that crosses this area (see Photo 8). This bofedal has a surface area of 3,600 m2, begins at an altitude of 4,410 meters above sea level, and presents a total of 18 channelized springs. The occurrence and physical characteristics are similar to those of the South Bofedal.

In this third bofedal, as in the previous bofedals, the emergence of springs is controlled by the jointing and faulting of the ignimbrite rock. In some cases, it is possible to observe up to 3 springs outcropping per linear meter—a high density per space of length. The flow rates of these springs vary from 0.5 to 2.0 l/sec, the temperature ranges from 14º C to 15º C, the average pH is 8.0, and the conductivity varies between 230 and 350 □S/cm. A main open collector channel lined with stone was built in the center of the bofedal. The channels that collect the waters of the outcrops or springs have a shape perpendicular to it.



Photograph 8. Waterfall in the South Ravine and Channel. 2000.

This bofedal has an average of 12 m wide and is located between the walls or cliffs of the ignimbrite rock (Silala ignimbrite II) from 20 to 60 m high. The southern wall or cliff of the ravine is the highest. Along this wall and at about 2 to 3 m from the floor of the ravine, there is a path with two or three outcrops of water that have been covered and sealed with mud and Festuca ortophylla, probably to preserve the path.

Due to the lack of maintenance works or the damage caused by strangers, some stones are missing in the side walls of the South Channel and the water is scattered and dispersed forming puddles or pooled waters, as well as water flowing freely on the ground and the outcropping rocks of the South Ravine.

Near the second waterfall, in the northern wall or cliff of the South Ravine, typical erosion features can be observed, caused by fast moving water flows. These features are found at a height of 2 m from the current level of flowing water and can be interpreted as erosion caused by strong fluvio-glacial flows that occurred thousands of years ago (Tauca phase water) and not as a recent erosion (less than 200 years old) caused by recent fluvial flow.

3.4.4. North Bofedal

The fourth spring concentration area is located in the North Bofedal (see Figure 20 and Photograph 9) with 26 channeled and inventoried springs. Lately, several other channels have been found, such as hidden perforated pipes, embedded in the rock and covered with earth. Most of the springs have been channeled with open collector channels that go SW and form the North Channel. The total area of this bofedal is 40,900 m2 and the first spring outcrops at 4,404 m.a.s.l. The electrical conductivity measured in the springsvaries from 95 to 134 S/cm, the temperature is 1 3º C to 16º C and a pH of7.70 to 8.35 measured in 2003[68] and of 8.19 to 8.52 in 2017.

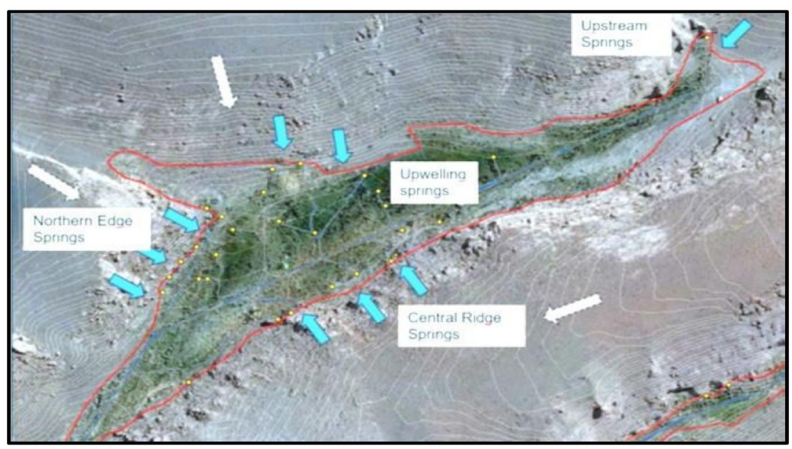


Figure 20. General map of the North Bofedal in which the extent, springs, network of channels and the general flow directions are presented.[69]

68 SERGEOMIN, ―Study of the Geology, Hydrology, Hydrogeology and Environment of the Silala Springs area‖, 2003. P. 29.

69 DHI. Provisional Report No. 1. Surface Flows. July, 2017. p. 13.



Photograph 9. Springs in the North Bofedal. With Stagnant Water, Without Movement.[70]

In the North Bofedal, there are three groups of springs; the first in the head of the bofedal, which is aligned with the second group in the middle and some in the south side of the bofedal and the third group is stuck to the north wall of the bofedal. Also, this bofedal presents 4 old piezometric wells of a depth of 10 m, covered with 2 and 1/2-inch iron pipes. These wells were installed by the FCAB company several years ago. The measurements in these wells show piezometric levels between 0.40 and 0.67 m above the surface.[71]

3.4.5. Main Channel

The Main Silala Channel runs along the length of the Main Ravine, which is a valley with high walls and a flat basal area covered with glacial sediments and a U-shaped cut profile. The walls that surround the ravine are vertical, slightly inclined and constituted by ignimbrite rocks.

The average flow measured in the Main Channel, at the border, is 160-210 l/sec.[72] The water takes bicarbonate water of magnesium and sodium with other alkaline ions.

70 SERGEOMIN, ―Study of the Geology, Hydrology, Hydrogeology and Environment of the Silala Springs area‖, 2003. P. 33.

71 SERGEOMIN, ―Study of the Geology, Hydrology, Hydrogeology and Environment of the Silala Springs area‖, 2003. P. 33.

72 DHI, 2018, Final Report, Annex C Surface Waters p. 12.

DHI states that the flows coming from the springs of the North and South Bofedals represent approximately60% of the total flow of the Main Channel. While the so-called diffuse flows represent the remaining 40%, mainly from the South Channel.[73]

The Main Channel and the other two channels have been built in sections with a straight line trend, with a uniform gradient to accelerate the movement of water and reduce the flow resistance and increase the volume of water directed towards the border with Chile (see Photograph No. 10). However, in many areas, the channel bed is directly below the surface of the underlying bedrock, as a result of the earlier channel coating and there is a leakage into and out of the channel throughout its stretch.



Photograph 10. Main Silala Channel.
Open Channel coated with Ignimbrite rocks. 2017.[74]

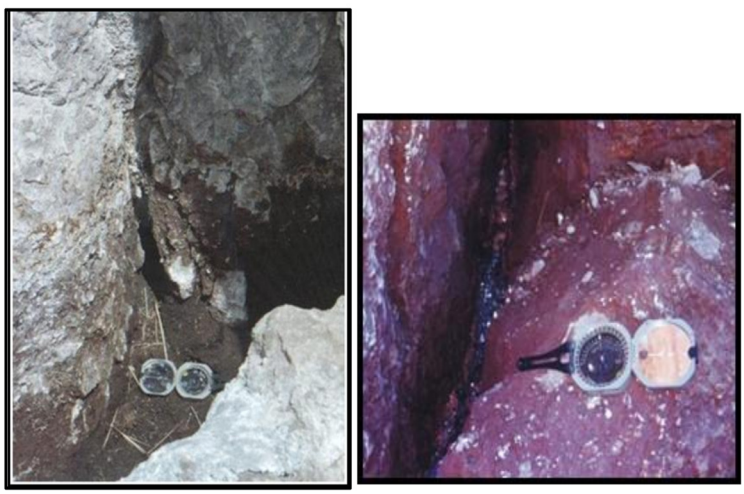
On the Chilean side, the Main Channel receives water from 37 springs,[75] mostly located in the area of the Silala Fault (north wall – right side, downstream) and one or two springs on the south side of the ravine (left, downstream). These springs produce around 110 l/sec of water that are used by the CODELCO contract. In the channel, they converge with around 30% of the waters that come from Bolivia and that are distributed between the two exploitation contracts granted by the Chilean government, FCAB and CODELCO.

73 DHI, Final Report, Product 2. 2018. P. 18.
74 DIREMAR, 2017
75 CM, 2017. Annex II. Arcadis. Detailed Hydrogeological Survey of the Silala River.

Some of the springs in the Silala Main Ravine, with their respective conveyance channels, were inventoried, sampled and photographed in the Chilean sector. Photographs 11 and 12 show the outcrops of groundwater from the Silala Shared Aquifer that flows through the joints of the Silala and Cabana ignimbrite rocks.



Photograph 11. Springs in the Main Ravine on the Chilean side emerging in the joints of the Silala ignimbrite with its collecting canals. 2000.76



Photograph 12. Main Channel on the Chilean side. Springs in the fractured Ignimbrite. 2000.[77]

76 The source is the author‘s.

77 The source is the author‘s.

4. HYDROGEOLOGY

4.1. Hydrogeological researches

The hydrogeological researches completed in the Silala Near Field were entrusted by DIREMAR to DHI international consultants. In turn, DIREMAR procured the services of SERGEOMIN and Maldonado Explorations S.R.L. drilling companies to drill wells and perform tests in order to determine the hydraulic behavior of the hydrogeological units. Twenty-nine points were drilled and 35 vertical pipe piezometers were installed as monitoring points for the groundwater level, allowing the collection of field data related to water quality and sampling for their laboratory analysis. In total, 89 permeability tests were carried out in situ on the boreholes and piezometers. In addition, step tests and 3-day constant flow test were performed in borehole DS-4P of the South Bofedal.

The purpose of the drilling was to collect additional data on groundwater at the Silala Springs and relate it to the geology, hydrology and hydrogeology of the Silala Aquifer, in the Near Field area. This data was also used to develop a Conceptual Hydrogeological Model (CHM), presented by DHI to DIREMAR as the final deliverable of its work. The CHM is the basis of the groundwater flow numerical model. The CHM will not be analyzed here due to its high specialization, and therefore the reader should refer to DHI‘s Final Report of March 2018, Product 2: ―Study of the Flows in the Silala Wetland and Bofedal System‖.
According to DHI, hydrogeological research includes the collection and analysis of the following:

- Piezometer and trial pit drilling and construction;
- Piezometer and borehole development;
- Lithological record of the boreholes;
- Slug tests on the piezometers;
- Packer tests (Lugeon and Lefranc);
- Installation of instrumental and manual water level monitoring equipment;
- Collection and analysis of groundwater samples for hydrochemistry studies;
- Pumping tests of aquifers; and
- Development of a hydrogeological database and initial parameter values for the numerical model.

To obtain the full detail of the hydrogeological research, the reader should refer to DHI‘s works - Product 1
―Groundwater Flows‖ of January 2018. A brief summary of this report is presented below and Figure 21 shows the location of the wells and the hydraulic tests performed on them.

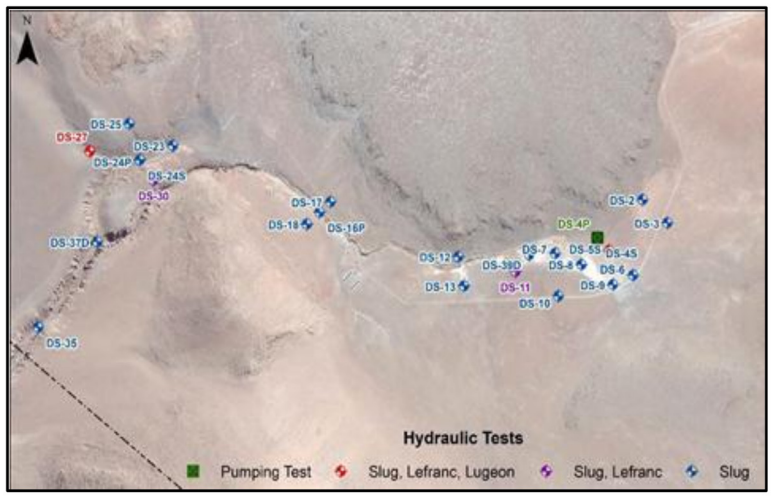


Figure 21. Map of the location of the wells with the hydraulic tests carried out. DHI, 2018.

4.1.1. Piezometer Drilling and Development

The piezometers and test wells were drilled using diamond drilling platforms and a reverse circulation (RC) drilling rig (1992 Mobile B-80-22). The diamond drilling platforms were operated by SERGEOMIN and the Maldonado Explorations S.R.L Company; while the RC platform was operated only by Maldonado. In general, the cores were extracted from the wells and 50 mm diameter PVC Schedule-40 piezometers (although some were 37.5 mm) were installed in the 96 mm wells. Rock chippings and borehole cores were continuously collected and recorded by a field hydrogeologist in the site. The piezometers were developed using compressed air, using the air-lift development method, to extract water volumes from the well. This development method was considered fully satisfactory.

Water quality parameters (pH, electrical conductivity, total dissolved solids, oxidation reduction potential and temperature) were controlled with a manual unit throughout the process. Subsequently, the parameters were controlled in the laboratory.

Figure 22 shows the hydrogeological units with the geometric mean of the measured hydraulic conductivity (K), obtained from small-scale hydraulic tests. The HGU7 - Fault zones (Silala Fault) - is the most important because it is the unit that hosts the largest number of springs.

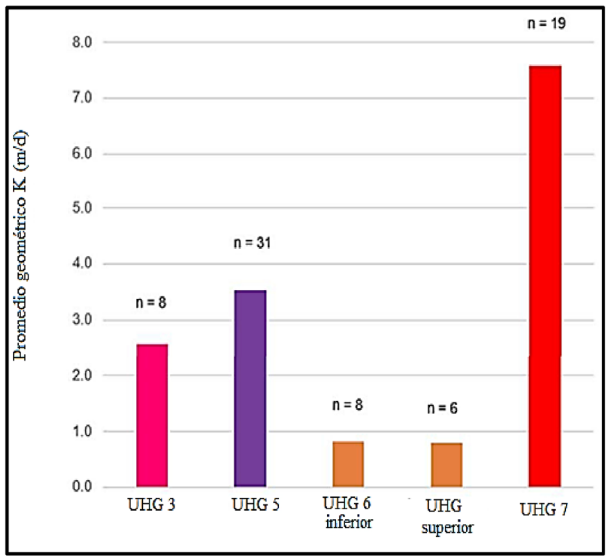


Figure 22. Hydrogeological Units: geometric mean for the measured hydraulic conductivity (K) obtained from small-scale hydraulic tests. HGU7 - Fault Zones.

The hydraulic testing program was implemented in the boreholes to characterize the hydraulic properties of the sub-surface materials. It had a special focus on the ignimbrite rock aquifer. The tests included Slug and Packer tests (Lugeon and Lefranc) and various pumping tests on a larger scale, to apply water stress to a larger aquifer volume.

4.1.2. Slug Tests

A Slug program was implemented to quantify localized hydraulic properties. Slug tests were conducted in wells less than 15 m deep and are generally indicative of fractured ignimbrite. The average arithmetic and geometric values for the Slug tests were 9.12 meters per day (m/d) and 3.12 m/d, respectively. The geometric average for all hydrogeological units evaluated has al-ready been presented in Figure 22.

4.1.3. Packer Tests

The purpose of the Packer tests (Lefranc and Lugeon) is to determine the hydraulic conductivi-ty in the rock and its respective depths. A total of 22 Packer tests were completed, ten of the Lugeon type and twelve of the Lefranc type, within the hydrogeological units.

The results of the twelve Lefranc tests presented average arithmetic and geometric values of 1.11 m/day and 0.065 m/d, respectively. However, many of the tests performed in well DS-11 are inside the overload reservoirs (alluvial and colluvial). When only the

ignimbrite tests are considered for wells DS-5 (33 to 52 m.b.g.s. and 51 to 70 m.b.g.s.) and DS-11 (28 to 46 m.b.g.s. and 44 to 61 m.b.g.s.) the values vary from 1.01 m/d to 1.47 m/d with a geometric mean of 1.24 m/d.

The results of the Lugeon tests in the DS-5P well were significantly different from the Slug and Packer test results for the DS-5S and DS-5P wells because they have significantly higher conductivity values that range from 1.0 m/d to 32 m/d (Slug test in the DS-5S well). The Lugeon tests did not indicate a significant decrease in hydraulic conductivity when the depth is in the upper 100 m of ignimbrite; however, given its limited effectiveness, this conclusion is considered uncertain.

4.1.4. Pumping Test in the Aquifer

The 3-day pumping test was completed to estimate the hydraulic properties on a larger scale than that obtained from the Slug and Lefranc tests. The pumping tests in the aquifer were per-formed in the DS-4P well. Ideally, the scale of the test approximates a representative elemental volume (REV) of the ignimbrite aquifer, allowing estimation of the hydraulic properties of a REV.

Pre-test water level monitoring was performed in wells DS-4P and DS-5P-II and barometric pressure was controlled using a Barotroll installed in the DS-4P wellhead. The barometric efficiency of the fractured rock aquifer in wells DS-4P and DS-5P-II was estimated be-tween 0.79 and 0.84, respectively. This suggests semi-confined conditions in the fractured ignimbrite aquifer explored in these wells.

The step test began with an initial flow rate index of 4.8 l/sec. Subsequent test rates were 9.2 l/sec, 13.2 l/sec and 17.3 l/sec. The maximum flow rate of 17.3 l/sec generated only 5.7 m of reduction and was stable throughout the test scales, indicating that the well could sustain flow rates minimally as high.

4.1.5. Constant Flow Test

A constant flow pumping test was conducted in the DS-4P well to estimate the hydraulic prop-erties of the aquifer bedrock in the Silala Fault zone and to evaluate the possible effects of boundary conditions on the flow system. The discharge rate was reasonably controlled during the test and ranged from 13.0 l/sec to 14.4 l/sec, with an average of 13.8 l/sec. Flow rates were relatively constant during the first 90 minutes of the test, but small increases in frequency were observed at 90 minutes and 500 minutes of the test. The static water level before the start of the test was 4.77 m.

The maximum drawdown measured in the DS-4P well is 4.35 m, which is less than 5% of the saturated thickness of the aquifer (estimated at 95 m). The drawdown curve for the DS-4P well stabilizes rapidly, after which it remains fairly stable.

The maximum drawdown measured in the observation wells (approximately 31 cm) is presented in the deepest piezometers DS-5 (i.e. DS-5P-I and 5P-II) located about 81 m from the DS-4P well. No measurable drawdown was observed in well DS-1, the distal well above the gradient (2.375 m from well DS-4P) with a deeper completion interval (117.9 m.b.n.s. to 137.9 m.b.n.s.), indicating that the radi-us of influence of the test was less than approximately 2.375 meters. Measurable responses were also ob-served in wells DS-3 (25 cm), DS-6 (21 cm), DS-8 (8 cm) and DS-9 (17 cm).

The test generally shows greater drawdown above the gradient and has a radius of influence of approximately 450 m. The greater drawdown to the Northeast may also reflect greater perme-ability along the predominant direction of the fault zone.

4.2. Aquifer Test Analysis Methods

Several independent data analysis methods were chosen due to their being established methods. In addition, the use of independent methods and test types serves as a cross-check of the re-sults, which improves the robustness of the analysis.

4.2.1. Analysis and Data Reports

The analysis and reports of aquifer tests were simplified with Pump Test Software and Slug Aq-tesolv, Version 4.50 Professional, available in Duffield (2007). Manual mode allows the use of professional criteria and knowledge of local conditions when adjusting aquifer test da-ta. Since the automatic mode did not guarantee the most appropriate match, the manual mode was generally used to analyze the data obtained from tests performed on the aquifer.

4.2.2. Pumping Test Results

Stepped drawdown and constant flow tests were used. The results of the stepped drawdown tests produced information on transmissibility, hydraulic conductivity, specific capacity, and maximum yield estimates for the DS-4P well.

4.2.3. Analysis Methods for the Step Test

Data from the step test were used to evaluate the performance of the DS-4P well, to determine the velocity for the constant flow test and the maximum pumping capacity of the well.

Step test results showed that the specific capacity of the DS-4P well changes with pump-ing speed and ranges from 3.02 lps/m, with a discharge of 17.3 lps, to 6.10 lps/m, with a discharge of 4.8 lps. Well efficiency is estimated to be between 57% and 27% for flows be-tween 4.8 lps and 17.3 lps.

4.2.4. Analysis Methods for the Constant Flow Test

The constant flow test estimates the transmissibility, horizontal hydraulic conductivity, storage ca-pacity and specific storage of the geological media tested, as well as the vertical connectivity of the units examined within the different HGU or parts of the same HGU.

The horizontal hydraulic conductivity estimated in a constant discharge pumping test is aver-aged over the saturated aquifer thickness. It is not defined, but it is of at least 95 m; as defined by the saturated interval of the DS-5P-I well, which was drilled at 100 m and presented flow en-try zones at the bottom of the well.

The Cooper-Jacob (1946), Theis (1935) and Moench (1997) methods were applied to constant flow pumping test data. These analytical solutions were chosen because they consti-tute established and peer- reviewed methods appropriate to the conditions found at the site.

The distance drawdown method was applied to simultaneous water level observations from the constant flow pumping test for tests where multiple observation wells were available. Dis-tance drawdown methods provide a general estimate of the hydraulic conductivity on the scale of the distance between the pumping well and all observation wells used in the pumping test. Transmissibility estimates for deep piezometers ranged from 1.405 to 10.470 m2/d and had a ge-ometric mean of 2.611 m2/d. The hydraulic conductivity for the deep piezometer estimates ranged from 14.8 to 110.2 m/d and presented a total geometric mean of 27.5 m/d. Storage esti-mates ranged from 1.9 x 103 to 0.11 x 103 m2/d.

4.3. Water Quality Sampling

The groundwater samples were analyzed by the Ministry of Energy in 2018. The water samples were analyzed for all major ions, in addition to other indicator elements, the results were previ-ously presented in Tables 2 and 3.

4.4. The Silala Aquifer

DHI consulting company developed a three-dimensional geological model using the GeoModeller software (Intrepid Geoscience, 2017) to provide the basis and define the geological characteristics and scope of the various hydrogeological units (HGU). The hydrogeological framework (HGFM) model includes stratigraphic units and structural features. The hydrogeological units were chosen to have unique and distinguishable hydraulic parameters. These units were presented in Table 1 along with their relative unit thicknesses.

The information included in the HGFM model was obtained from several sources, including: geological and site-specific field campaigns, geological maps, cross-sections, inside diameter records,

geophysical data, and a digital terrain surface. Regional geological deformation and structural trends are often expressed on a local scale; however, multiple prominent geological features extend be-yond the Silala Near Field. It was considered necessary to consider a larger scope for the HGFM model, as geological features have a significant impact on sub-regional and local groundwater flow.

The HGFM model was developed from various geological and geophysical data sets. It presents a sum-mary of the Silala geological history and descriptions of hydrogeological units. The surface terrain was developed from a local high-resolution digital elevation model (DEM), based on a reconnaissance performed using drones in the Near Field (DIREMAR/Pix4D, 2016). The initial geological con-tacts were obtained from maps and cross sections produced by SERGEOMIN (2003 and 2017).

The logs of the piezometer wells and the drilling of test wells were used to restrict the subsoil's geological contacts. The well locations and stratigraphic records were imported directly into the GeoModeller software and provided approximate elevations for the geological contacts and relative thickness of the various hydrogeological units (HGU).

In addition, electrical resistivity tomography scans, performed by COFADENA in 2017, were integrated in the development of interpretations. The 28 electrical resistivity tomography scans provided high resolution localized images of the geology of the Silala Near Field. Sub-surface data sets were used during model development to increase model accuracy and development us-ing calibration points.

The scope of model construction was delineated on basis of the inclusion of local and sub-regional geological features relevant to the hydrogeology in the Near Field. Inacaliri Vol-cano, Silala Chico Dome and Silala Fault were of particular importance when developing the HGFM model, as the Silala Channel system passes between Inacaliri Volcano and Silala Chico Dome. Both volcanic bodies are the product of multiple large lava flows that created thick de-posits of compact crystalline rock that exhibit high resistance to physical and chemical weathering. When not altered, these large igneous bodies probably act as hydraulic barri-ers to groundwater flow. Chemical analyses of surface and groundwater from the field sug-gest that the groundwater flow deviates from its expected downward flow path and travels around these intrusive [materials].

Multiple field reports and observations from field visits document significant faults and fractures throughout the Near Field area[78]. Associated fractures and faults were also observed in drill logs and Electrical Resistivity Tomography (ERT) profiles[79]. Not all lineaments are explicitly modeled in the HGFM model. However, the Silala Fault has a significant impact on local hydrogeology and is represented within the model as the HGU7—a normal, almost vertical, northeastern trend fault that runs through the entire domain of the Near Field model.

78 Hausser (2004), SERGEOMIN (2017) and SERGEOMIN (2003).
79 COFADENA, 2017.

Within the area surveyed, several smaller faults and fracture systems are parallel to the Silala Fault which, in turn, reflects structural trends in the region.

Fracturing and subsequent weathering of the rock near the surface have resulted in large areas of fragmented rock debris that probably act as equivalent porous media. An accurate delineation of the Silala Fault was recorded. For the purpose of the HGFM model, it was assumed that the Silala Fault zone was vertical and extended to the bottom of the model scope. The Silala Fault zone was explicitly simulated in the HGFM (as HGU7) and assigned an approximate width of 50 meters to simulate the extensive fracturing and physical weathering that occurs within this zone. For the purposes of the model, the lower ignimbrite layer (Lower HGU6) extends to 4,000 m.a.s.l., although the thickness is currently not defined, but it is believed that the Lower HGU6 is between 300 and 500 meters thick.

4.4.1. Aquifer Storage

DHI‘s reports indicate that specific information on the storage properties of the aquifer, includ-ing storage capacity, specific yield and specific storage, has been defined from the pumping tests performed at DS-4P and the pumping tests in Chile.

During the pumping test in Chile, the Silala Shared Aquifer behaved like a confined aquifer, suggesting that less fractured and lower permeable ignimbrite layers may result in confined conditions at the local level and potentially at the sub-regional level. Similar responses were observed in the DS-4P test, with depth. Storage values calculated from the Chilean tests were within the range measured in the DS-4P test.

4.4.2. Hydrogeochemical Results

The water quality data previously collected from the Silala Spring System was post-processed in graphic representations of water chemistry (Figures 16 to 43). The Stiff diagrams show that the largest ion composition has a polygonal shape with cations to the left and anions to the right, represented as milliequivalents per liter. These diagrams are useful to evaluate how the chemis-try of water varies in space and/or time, such as the South Bofedal in comparison with the North Bofedal, or the water chemistry of the surface piezometer versus the deep one.

The diagrams highlight an obvious contrast in water quality between the North and South Bofedals (see Figure 23). Both bofedals have sodium bicarbonate type water, but the water chemistry is significantly different. The water of the South Bofedals has significantly higher concentrations of bicarbonate, calcium, magnesium, and chloride and much lower bicar-bonate/magnesium ratios. While the North Bofedal has a significantly lower proportion of bi-carbonate, calcium, magnesium, and a higher bicarbonate/magnesium content.

All samples in Bolivia have uniformly high silica concentrations of 22.5 mg/lt (near or in satura-tion) and aqueous concentrations are likely to be controlled by equilibrium with silica gel in ignimbrite fractures. Most dissolved solids, represented mainly

by sodium, bicarbonate and silica, are derived from the reaction with the ignimbrite aquifer and, in the case of bicarbonate, the CO2 derived from the soil.

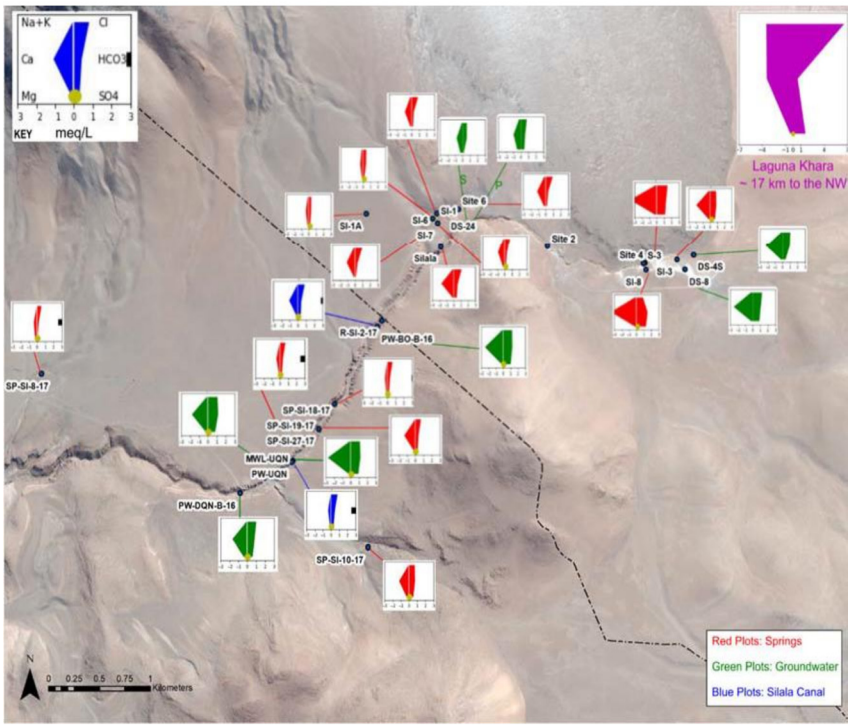


Figure 23: Stiff diagrams for the Springs, Channel and Groundwater of the Silala Near Field. DHI, 2018.

The water mixture of the North and South Springs, in the proportion of their measured percentages in the total flows of the Silala Springs System, of 37% and 63%, respectively, produces water with bicarbonate, magnesium and other ions that are similar to the water quality of the channel near the border. Therefore, it can be said that there is agreement between the approximate proportions of the physical and chemical measurements for the two types; that is to say, these are the water sources.

The lower total dissolved solids, lower bicarbonate/magnesium ratios, and difference in chloride concentrations suggest different sources for water discharge at the North and South Springs. It further suggests that the waters discharged at North Springs have a shorter groundwater flow path and are younger in age.

The results suggest that, during the pumping test, the wells in Chile extracted water from the same aquifer that feeds the South Bofedal. Generally, these waters are indicative of waters with a longer residence time in the subsoil compared to the springs and streams of northern Chile.

Three (3) radiocarbon (14C) samples were collected from the South Bofedal, North Bofedal and one intermediate location by SERGEOTECMIN (2004) and nine (9) samples were collected from the Chilean side of the system. The results were used to estimate the apparent groundwater ages for the Bolivian samples. Thereafter, 25 surface water samples and 9 pie-zometer samples were analyzed for their isotopic analysis at Hydroisotop laboratory.

Conceptually, the radiocarbon dating completed to date suggests a relatively old apparent age in the South Bofedal (±11,000 years) and a significantly younger apparent age in the North Bofe-dal (±1,000). And it is consistent with the conceptualization that recharge occurs at the Inac-aliri Volcano due to the high elevation and, as a result of the much shorter flow path, it has a lower apparent age.

The overall chemistry, the 18O and 2H ratio, and the relative ages of 14C suggest that there are two main groundwater sources. The water that is nearest to the surface and that is younger is associated with shorter groundwater flow paths and probably with local recharge mechanisms. Older water possibly has longer and deeper groundwater flow paths and longer residence times. It is believed that this older and deeper water was recharged further away from the Silala and that it is associated with the flow in the ignimbrite along the Silala Fault zone.

In the upper parts of the Silala springs system, in the south bofedal, there is a presence of semi-confined and confined waters. The ignimbrite bedrock is extensively fractured and brecciated and it is, in some places, filled with fine sand.

As DHI noted, channel flow measurements and springs indicate that the Silala Channel system receives considerable lateral flows, which are not taken into account in spring flow meas-urements. The springs occur in fractured rocks. The flow measurement work showed that the South Channel, to the Southeast of the North Bofedal, was a section that gained a lot of strength (Figure 24) due to the significantly lower elevations of the soil surface in relation to the spring elevations.

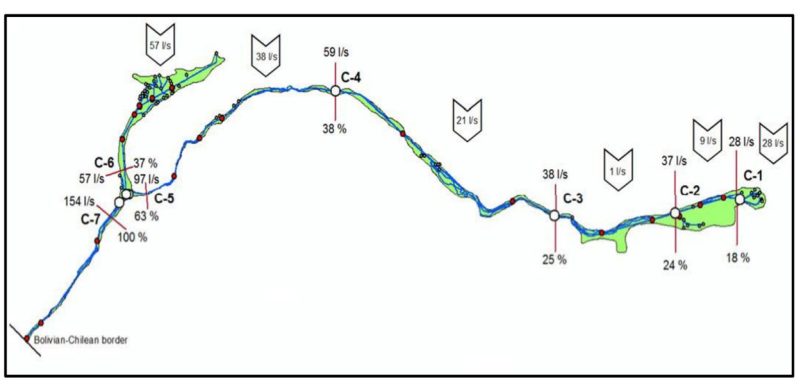


Figure 24. Mapping of flows and net tributaries based on simultaneous measurements of the average channel flow (in l/sec.). DHI, 2017.

4.5. Negra Ravine in the Chilean-Side Silala

In the official visit to the Silala – Chilean sector – by Bolivian geologists, which was scheduled for a whole day, in October 2000, the Negra Ravine was visited in the company of a delegation from the Minis-try of Foreign Affairs of Chile. Back then, it was possible to collect water samples from the springs that emerge in in the Main Ravine, in the Negra Ravine, and from the springs in the ignimbrites that emerge in the area north of the Inacaliri Police Station.

The walls of the Negra Ravine, formed by an EW fault that cuts through the Silala fault, do not exceed 20 m. The soil is saturated by the underground waters that form a bofedal 15 to 20 cm thick, composed of organic material and flora typical of a high altitude bofedal. The bofedal has a surface area that ranges from 2.5 to 3.0 km2 and is in its original state without any channel or artisan artificial works. The out-flowing water in the bofedal does not flow towards the Main Ravine of Silala, despite the existence of a height difference of 120 m from the head of the bofedal to the intersection with the Main Ravine, at a distance of approximately 2.5 km. The intersection is 4,193.6 m high. It is important to indicate that no surface runoff water has been observed flowing from the Bofedal of Negra Ravine, forming a bofedal with re-tained water that feeds a pasture-flora and microfauna that is preserved in its original natural state.

From the head of the ravine at 4,313.7 meters of altitude to 4,234.5 meters, several springs or sur-face streams emerge; many of them emerge from the base of the ignimbrite walls that form the ravine walls. However, due to the limited time available for the survey on the Chilean side, it was not possible to make an inventory of the number of springs that emerge in the bofedal of Negra ravine.

A very specific detail on these springs is given in Annex II of Chile‘s Memorial[80]. In the Main Silala ravine, in the section from the border to the intersection with the Negra ravine, 23 springs were inventoried emerging in a longitudinal space of 508 m at the base of the Silala Ig-nimbrite and forming the walls of the ravine (Annex III describes 37 springs). Twenty of these springs appear on the northern wall of the ravine (right side, downstream) and three on the south wall of the ravine (left side, downstream). The first channelized spring emerges at 4,263 m and is located 212 m from the water control dam on the border (FCAB‘s first intake).

It has been found that the Negra ravine is a ravine with a N33□ W direction without surface flows, formed by a very humid bofedal that intersects the Main Silala ravine at 1,850 m, downstream from the international border. It has an approximate length of 2.5 km, forking out in its upper part and forming two small shallow hollows.

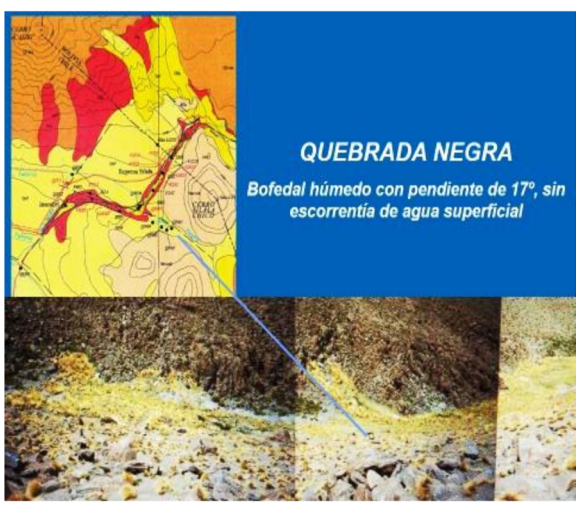
80 CM, 2017. Annex II. Arcadis. Detailed Hydrogeological Survey of the Silala River.

The geology of this ravine is constituted by ignimbrite rocks (Silala ignimbrite) intruded by a dome of dacitic composition (Silala Chico dome). The upwelling groundwater in the bofedal found in the ravine is the result of the action of a fault with a NWW – SEE direction. It was formed by ancient fluvio-glacial flows that benefited from this fault zone with a steep slope. Its soil is sandy with very few boulders of size no larger than 10 cm in length of ignimbrite rock scattered on the surface.

The waters of Negra ravine, from the hydrochemical point of view, are classified as sodium bicarbonate waters. The content of chemical elements evaluated in terms of total dissolved solids (TDS) shows that they are suitable for human consumption and irrigation. Due to their hydrochemistry and physical properties, the waters of the Negra ravine are very similar to the waters of the South Bofedal on the Bolivian side. These are waters that come from the lowest level of the outcropping aquifer.

In summary, the origin of the bofedal in the Negra ravine is related to the saturation of water of Quaternary sediments, analogously to the Silala bofedals on the Bolivian side before the construction of the hydraulic works, which is why, in the event of a flow or active surface runoff, the latter would be minimal, as the bofedal remains intact in its original state. The groundwater flow is convergent to the Main Silala Channel.

The waters of the Main Silala Ravine and the area of the Inacaliri station are similar to the waters of the Bolivian North Bofedal. These waters are sodium carbonate waters.



Photograph 13. Negra Ravine on the Chilean Side with its unmodified Bofedal, October 2000[81]

81 The source is the author‘s.

Photograph 13 shows the Negra ravine with the bofedal of 2.5 km length, which is completely wet and unaltered, formed and fed by the natural outcrops of springs in the base and the floor formed by the aquifer in the Silala Ignimbrite. The gradient of this ravine is greater than 17 degrees and at the end of the slope, at the margin of the bofedal, it has been possible to verify and corroborate that by not having collector channels built by man, there are no surface water flows.

The water samples collected in these two channelized bofedals that are found on the northern skirts of the Inacaliri volcano are a little purer (conductivity 83 - 90 µS/cm) than the waters collected in the 23 springs of the Main and Negra ravines (conductivity 179 - 248 µS/cm.), probably because they are mixed with recent water recharge within the subsurface aquifer.

The results of the physical-chemical analysis of the samples of the Negra ravine are presented in Table No.1. The first two samples are those collected in 2000 during the PIR Program [Spanish acronyms] and the third (SP-SI-10-17) was sampled and analyzed by the Chilean technicians in 2016.[82]

82 CM, 2017. Annex II. Arcadis, 2017. Detailed hydrogeological survey of the Silala river.

5. HYDROCHEMISTRY OF THE SILALA FLOWS

This section of the report provides a description and discussion of the hydrochemistry of the water from the springs, the groundwater, and the channeled surface flows, obtained in four sampling campaigns. Discussions focus on salinity patterns and chemical composition of the types of water analyzed. Also, the composition of the stable isotopes of these waters is presented. The discussion focuses on the differences between the isotopic signatures of the springs and the groundwater, and their possible relationship with the local and regional recharge of the aquifers. Finally, the Carbon-13 and Carbon-14 data are presented and discussed in the context of the conceptual model completed to determine the age of the waters.

In 2017, four field work campaigns were carried out to sample surface water for the hydrochemical and isotopic analysis of the Silala Springs and Channels. This was done by technicians from the Vice Ministry of Water Resources and Irrigation of the Ministry of the Environment and Water.

Figure No. 2 shows a map of locations in which spring sites are presented. The sampling location maps for all four campaigns are presented in Figures Nos. 40 to 43. In situ parameters were measured, including pH, electrical conductivity, and temperature which were then compared with the data obtained in the laboratory. The hydrochemical data is presented in Tables Nos. 2 and 3 of the Sampling Campaigns 3 and 4.

The chemical analysis included cations and larger anions. The anions were determined by ion chromatography (chloride, sulfate, nitrate) (Cl-, SO42-, NO3-) and volumetric titration (bicarbonate) (HCO3), and the cations (sodium, potassium, calcium, magnesium) (Na+, K+, Ca2+, Mg2+) by plasma emission spectrometry (ICP-OES). The chemical analysis was carried out in the laboratory of the Ministry of Energy.

The isotope analysis – entrusted by DIREMAR – included oxygen-18 (18O), deuterium (2H), tritium (3H), carbon-13 (13C), and carbon-14 (14C); these were developed by Hydroisotop company in Germany. The isotopic data for Campaigns 1 and 4 are reported in Tables 5 and 6.

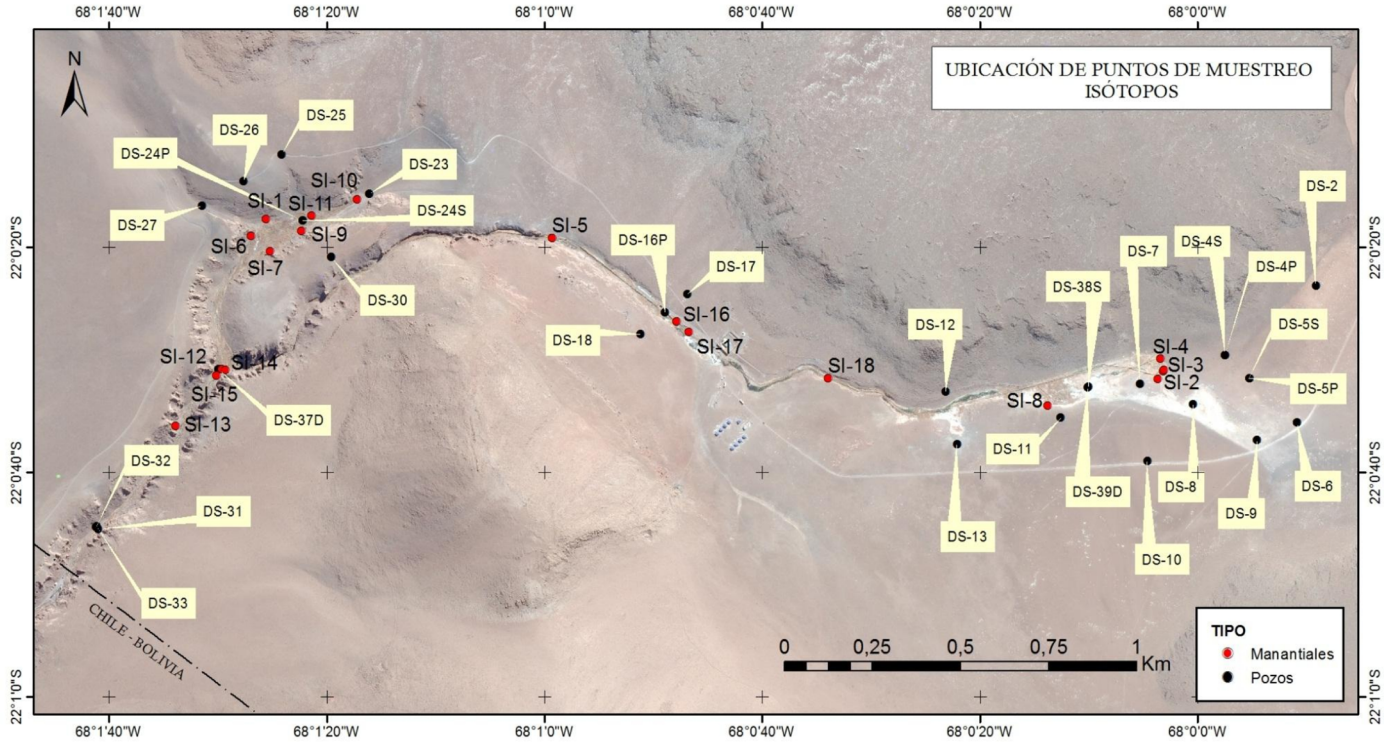


Figure 25. Map presenting the location of the sampling points for the hydrochemical and isotopic analyzes.[83]

[83] Source: DIREMAR, 2018.

Sample No.	Coordinates		Water type	T° C	pH lab.	CE lab.	Alkalinity	Cl	SO_4	HCO_3	Ca	Mg	K	Si	Na	NO_3
	X	Y				µS/cm	mg/l $CaCO_3$	mg/l	mg/l	mg/l	mg/l	mg/l	mg/l	mg/l	mg/l	mg/l
C3 SI-1	600767	7566312	North Spring	13,6	8,52	112,90	1,78	7,22	7,80	28,39	6,89	1,47	1,95	16,06	7,80	1,75
C3 SI-2	603129	7565885	South Spring	15,4	7,90	238,00	6,56	8,65	8,26	84,20	14,18	6,06	2,93	19,45	8,26	1,87
C3 SI-3	603127	7565882	South Spring	14,1	7,90	254,00	0,00	11,21	8,49	100,32	15,54	6,84	3,13	13,61	8,49	2,02
C3 SI-4	603121	7565915	South Spring	14,4	8,01	228,00	0,00	11,21	8,03	80,33	11,88	5,15	2,74	20,30	8,03	1,95
C3 SI-5	601519	7566257	South Channel	13,0	8,98	281,00	12,12	8,84	6,31	94,22	16,98	8,13	3,23	20,91	6,31	0,54
C3 SI-6	600727	7566268	North Spring	16,8	8,42	117,40	0,95	8,74	7,80	24,64	5,86	1,25	1,85	16,34	7,80	1,77
C3 SI-7	600776	7566225	North Spring	18,0	8,32	129,60	0,00	8,93	8,72	38,05	7,59	1,81	1,95	16,63	8,72	1,92
C3 SI-8	602823	7565789	South Bofedal	13,8	7,67	398,00	0,00	12,16	19,04	167,43	30,12	15,33	5,29	27,18	19,04	1,75
C3 SI-9	600859	7566279	North Spring	17,0	8,31	124,30	0,00	9,31	8,49	38,05	7,42	1,68	1,95	14,65	8,49	1,94
C3 SI-10	601006	7566366	North Spring	15,4	8,19	95,20	0,00	5,99	8,26	21,26	4,77	0,78	1,75	17,19	8,26	1,67
C3 SI-11	600887	7566321	North Spring	14,1	8,28	134,00	0,00	5,51	2,53	26,58	4,86	0,74	1,95	17,29	2,53	1,29
C3 SI-12	600633	7565886	Main Channel	12,7	8,78	182,40	3,56	7,13	6,19	51,34	9,53	3,60	2,54	17,47	6,19	1,01
SAMPLES FROM NEGRA RAVINE																
PIR – 1	600473	7563650	Negra Ravine Spring	-	7.4	248.00	77.7	7.39	23.46	129	17.56	8.23	12.00	-	21.0	0.00
PIR – 2	600291	7563666	Negra Ravine Spring	-	7.7	230.00	76.2	5.34	19.34	129	19.15	6.90	8.00	-	21.0	0.00
SP-SI-10-17	600098	7563292	Chilean Negra Ravine spring	13.6	7.9	228.40	75.0	2.16	14.88	99	14.63	6.29	6.68	30.60	11.86	0.22

Table 2. Location of the field parameters and hydrochemical data from the third field campaign and Negra ravine samples. (The source is the author's)

Sample No.	Coordinates		Water type	T° C	pH lab.	CE lab.	Alkalinity			Cl	SO_4	HCO_3	Ca	Mg	K	Si	Na	NO_3
	X	Y				µS/cm	$CaCO_3$ mg/l			mg/l	mg/l	mg/l	mg/l	mg/l	mg/l	mg/l	mg/l	mg/l
C4 SI-1	600767	7566312	North Spring	14,4	8,25	114,2	0,00			4,94	7,74	56,62	9,04	1,46	1,82	17,11	9,38	2,60
C4 SI-2	603129	7565885	South Spring	14,0	7,75	246,0	0,00			6,14	8,98	142,96	16,31	6,13	2,80	21,02	19,08	2,22
C4 SI-3	603127	7565882	South Spring	14,6	7,41	260,0	0,00			6,61	8,98	145,79	17,04	7,05	3,10	22,04	19,08	2,32
C4 SI-4	603121	7565915	South Spring	12,2	7,80	226,0	0,00			5,34	7,74	127,39	14,61	5,40	2,80	20,26	18,09	2,39
C4 SI-5	601519	7566257	South Channel	10,9	8,40	283,0	0,00			4,74	8,98	165,61	19,57	8,97	3,59	22,21	19,08	0,81
C4 SI-6	600727	7566268	North Spring	16,3	8,16	115,4	0,00			4,54	6,91	55,20	8,41	1,51	1,82	17,45	9,68	2,05
C4 SI-7	600776	7566225	North Spring	15,7	8,01	139,0	0,00			5,20	7,46	60,86	9,48	1,95	1,92	17,62	10,68	2,13
C4 SI-8	602823	7565789	South Spring	14,5	7,59	404,0	0,00			5,47	10,08	225,05	32,32	15,81	5,45	31,79	21,07	2,07
C4 SI-9	600859	7566279	North Spring	15,5	8,03	124,7	0,00			5,07	7,05	63,69	8,48	1,56	1,92	16,40	10,48	2,13
C4 SI-10	601006	7566366	North Spring	14,9	8,08	96,3	0,00			4,24	6,01	43,88	7,52	1,13	1,82	17,59	7,89	1,81
C4 SI-11	600887	7566321	North Spring	14,9	8,21	87,7	0,00			4,14	5,94	36,80	7,50	0,94	1,92	17,36	7,29	1,73
C4 SI-12	600633	7565886	Main Channel	13,8	8,31	173,7	0,00			4,87	6,91	89,17	12,66	3,73	2,51	18,16	13,10	1,36
C4 SI-14	600647	7565902	North Channel	14,8	8,19	121,7	0,00			4,80	6,63	63,69	9,20	1,83	1,92	16,06	10,18	1,94
C4 SI-15	600656	7565901	South Channel	12,3	8,44	217,0	0,00			5,20	8,15	123,14	15,87	5,93	2,90	18,95	15,10	1,66
C4 SI-16	601846	7566025	South Channel	13,4	8,44	302,0	0,00			5,40	6,63	168,44	22,22	10,27	3,88	18,30	19,08	1,17
C4 SI-17	601878	7565997	South Channel	13,5	9,00	248,0	20,88			5,74	7,32	83,51	17,41	7,20	3,10	18,55	21,07	0,63
C4 SI-18	602245	7565868	South Channel	14,3	8,98	256,0	14,62			5,17	6,98	107,57	17,12	7,18	3,15	20,04	18,58	0,94

Table 3. Location of the field parameters and hydrochemical data from the fourth campaign

5.1. Analysis of Hydrochemical Results

This section discusses the hydrochemical results associated with water samples collected from springs, wells and surface water in the channels, bofedals and springs of the Silala. The main results of the radioactive isotope and ion analyzes were used in the conceptualization of surface and groundwater flows in the area of the Silala. Some data has been compiled from multiple sources, including SERGEOMIN (2003), the Ministry of Energies (2017) and SERGEOMIN (2017).

5.1.1. Physical-Chemical Characteristics of the Silala Waters

In order to define the most important physical-chemical characteristics of the surface water samples of the Silala springs, the most important ions and some other characteristics were determined. The complete analysis of the water contains its determination of bicarbonate or alkalinity, of chlorine, sulfate, sodium, calcium, magnesium, and the sum of the two as hardness. The electrical conductivity, the dry residue, the pH, as well as the contents of potassium, nitrates, silica, carbonate radical, iron and manganese have been determined. Analysis has also been completed with the determination of arsenic contents, both in the bofedals and in the South and North Channels.

The results obtained are analyzed with recognized graphical methods such as the Stiff, Piper, Schoeller, and Wilcox diagrams. The diagrams are methods of visual differentiation and comparison, which graphically represent the chemical composition of the waters, the coincidences in the classification, and the possible similarities and differences between the different samples.

Due to their hydrochemistry and physical parameters, the waters of the North Bofedal are cleaner and purer than those of the South Bofedal, which apparently come from a deeper level of the Silala Aquifer.[84]

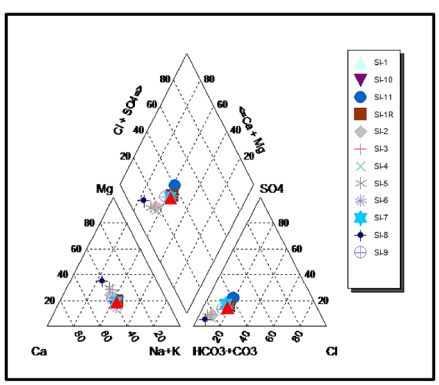


Figure 26. Piper Diagram - Campaign 1.[85]

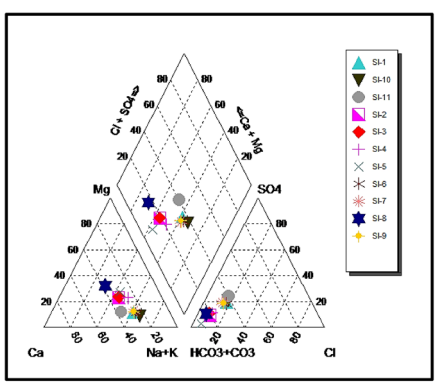


Figure 27. Piper Diagram – Campaign 2.[86]

84 SERGEOMIN, —Study of the Geology, Hydrology, Hydrogeology and Environment of the Silala Springs area‖, 2003. P. 40.

85 The source is the author‘s.

86 The source is the author‘s.

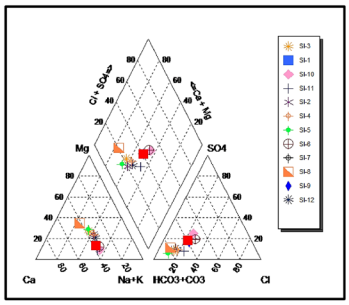


Figure 28. Piper Diagram - Campaign 3.[87]

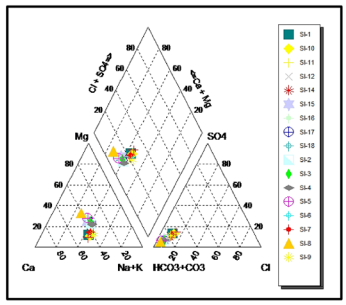


Figure 29. Piper Diagram - Campaign 4.[88]

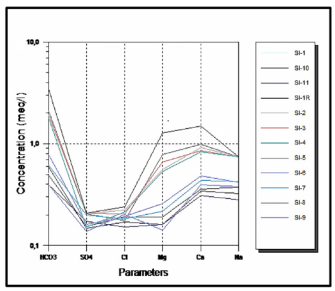


Figure 30. Schoeller Diagram - Campaign 1.[89]

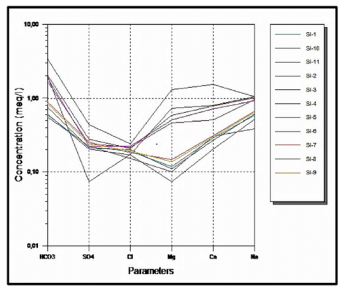


Figure 31. Schoeller Diagram – Campaign 2.[90]

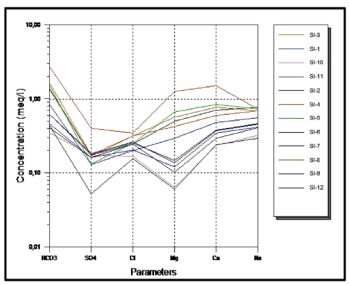


Figure 32. Schoeller Diagram – Campaign 3.[91]

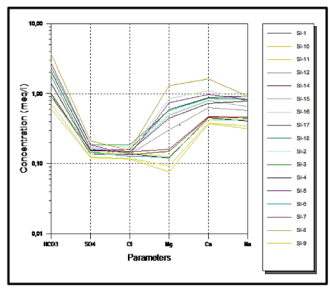


Figure 33. Schoeller Diagram - Campaign 4.[92]

87 The source is the author‘s.
88 The source is the author‘s.
89 88 The source is the author‘s.
90 The source is the author‘s.
91The source is the author‘s.
92 The source is the author‘s.

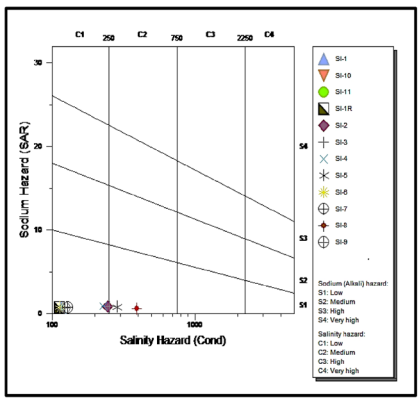


Figure 34. Wilcox Diagram – Campaign 1.[93]

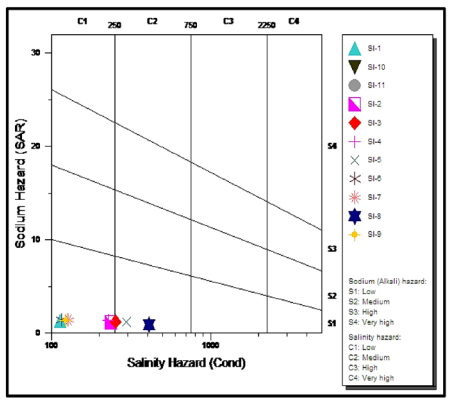


Figure 35. Wilcox Diagram - Campaign 2.[94]

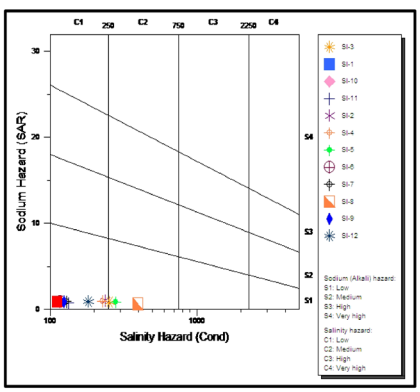


Figure 36. Wilcox Diagram - Campaign 3.[95]

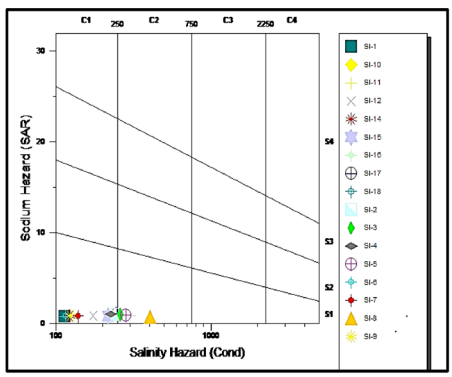


Figure 37. Wilcox Diagram - Campaign 4.[96]

93 The source is the author‘s.
94 The source is the author‘s.
95 The source is the author‘s.
96 The source is the author‘s.

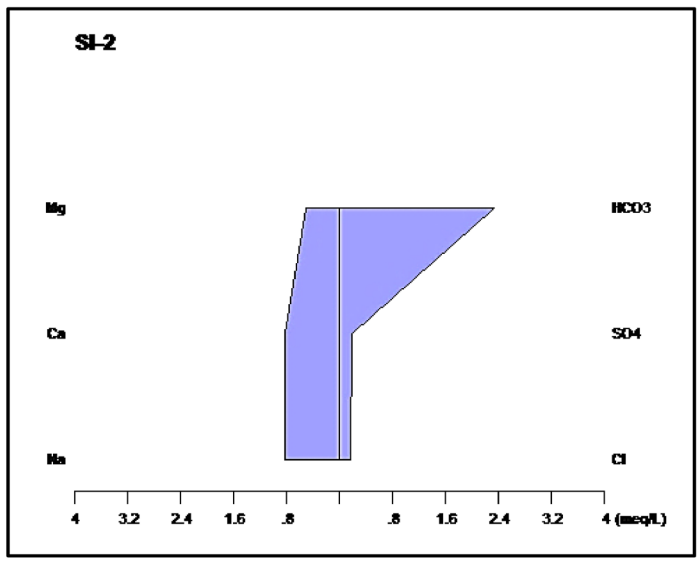


Figure 38. Stiff Diagram of sample Si-2 from the South Bofedal. As a reference sample[97]

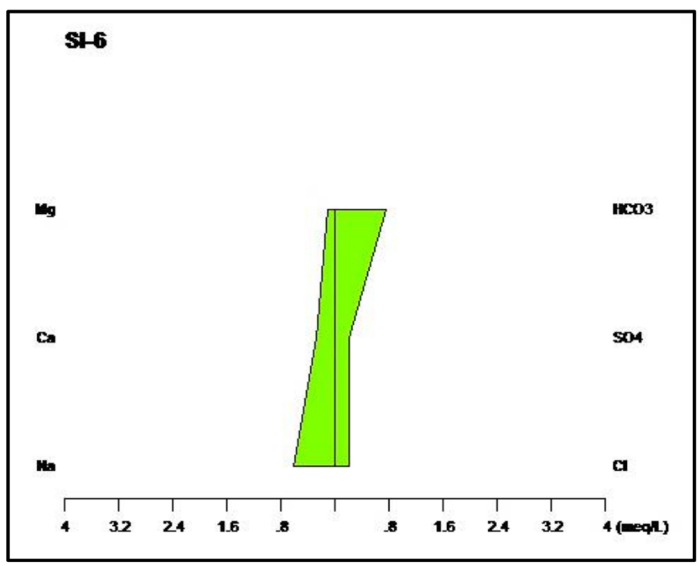


Figure 39. Stiff Diagram of sample Si-6 from the North Bofedal. As a reference sample.[98]

[97] The source is the author's.
[98] The source is the author's.

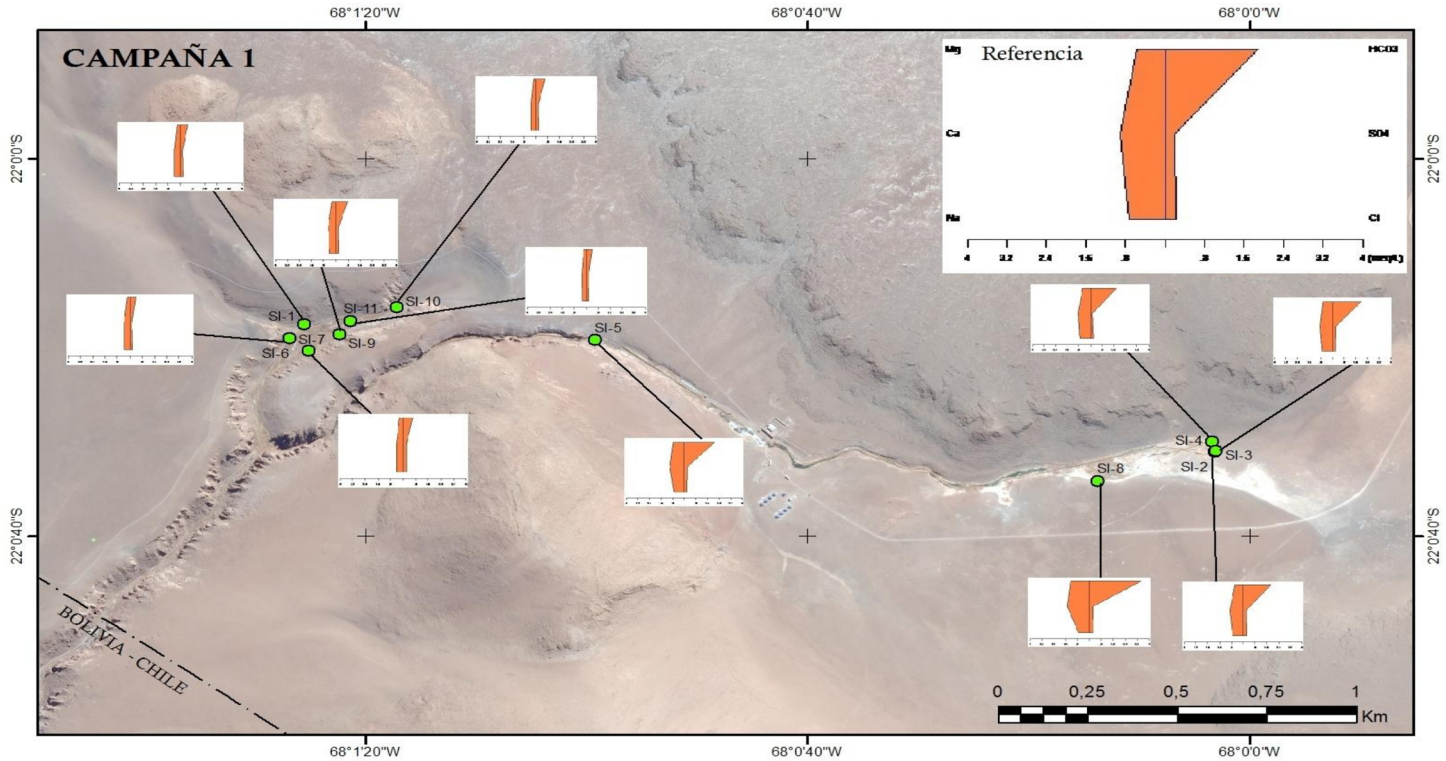


Figure 40. Map of the Springs including the Stiff Diagrams for the Samples from the First Field Campaign in the Silala Near Field[99]

[99] The source is the author's.

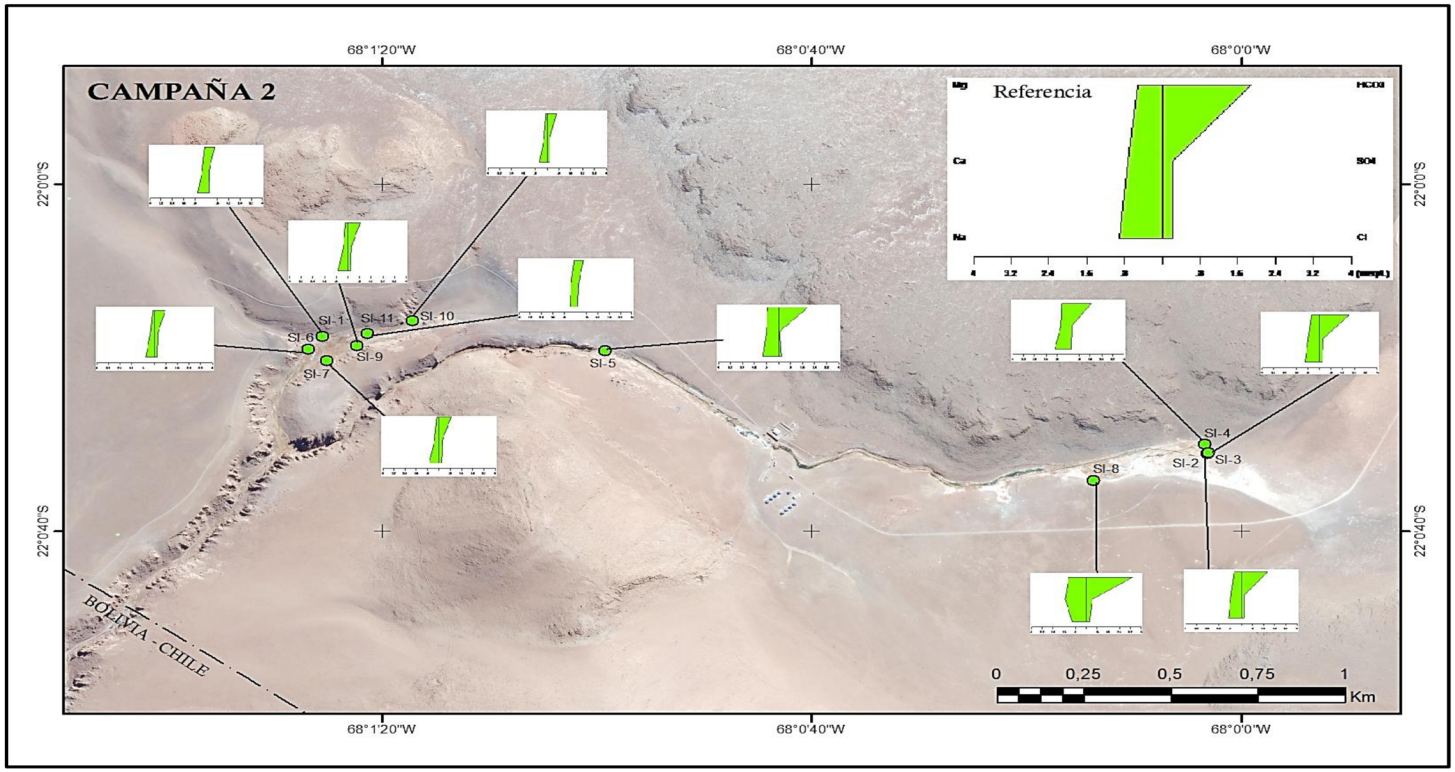


Figure 41. Map including the Stiff Diagrams for the Samples taken in the Second Field Campaign in the Silala Near Field[100]

[100] The source is the author's.

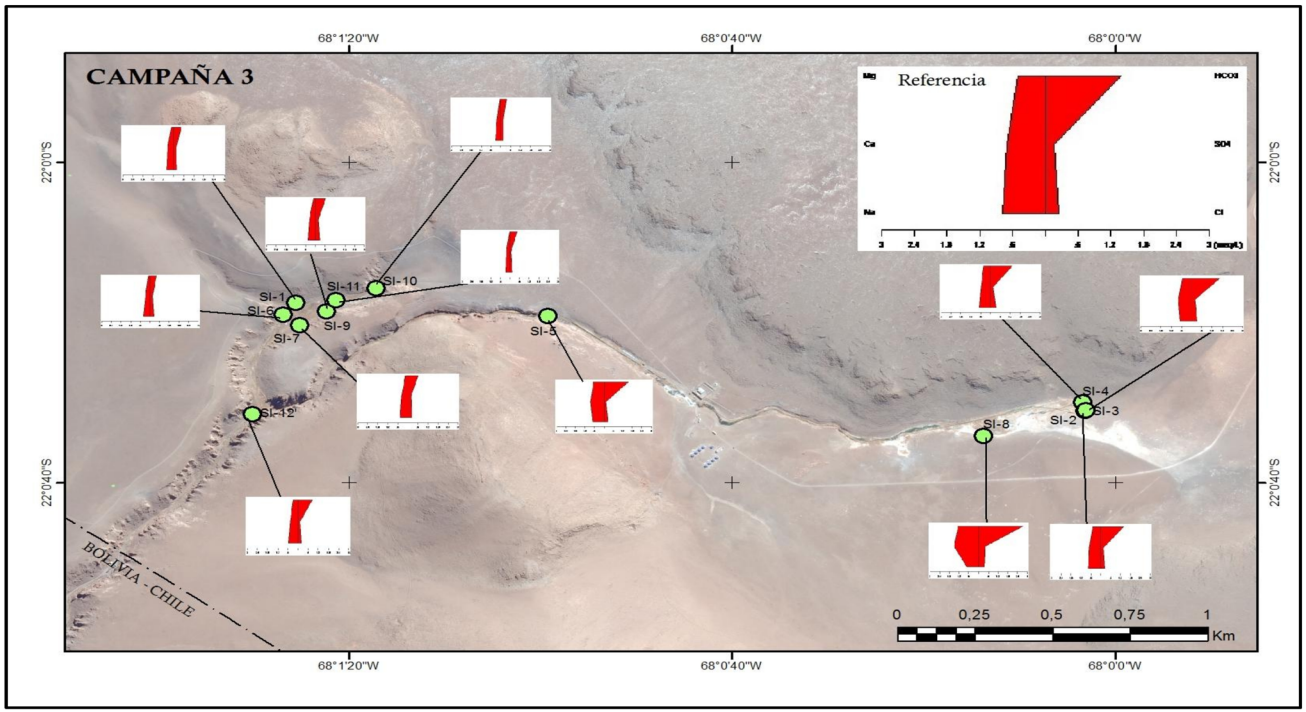


Figure 42. Maps including the Stiff Diagrams for the samples taken from the Third Field Campaign in the Silala Near Field[101]

[101] The source is the author's.

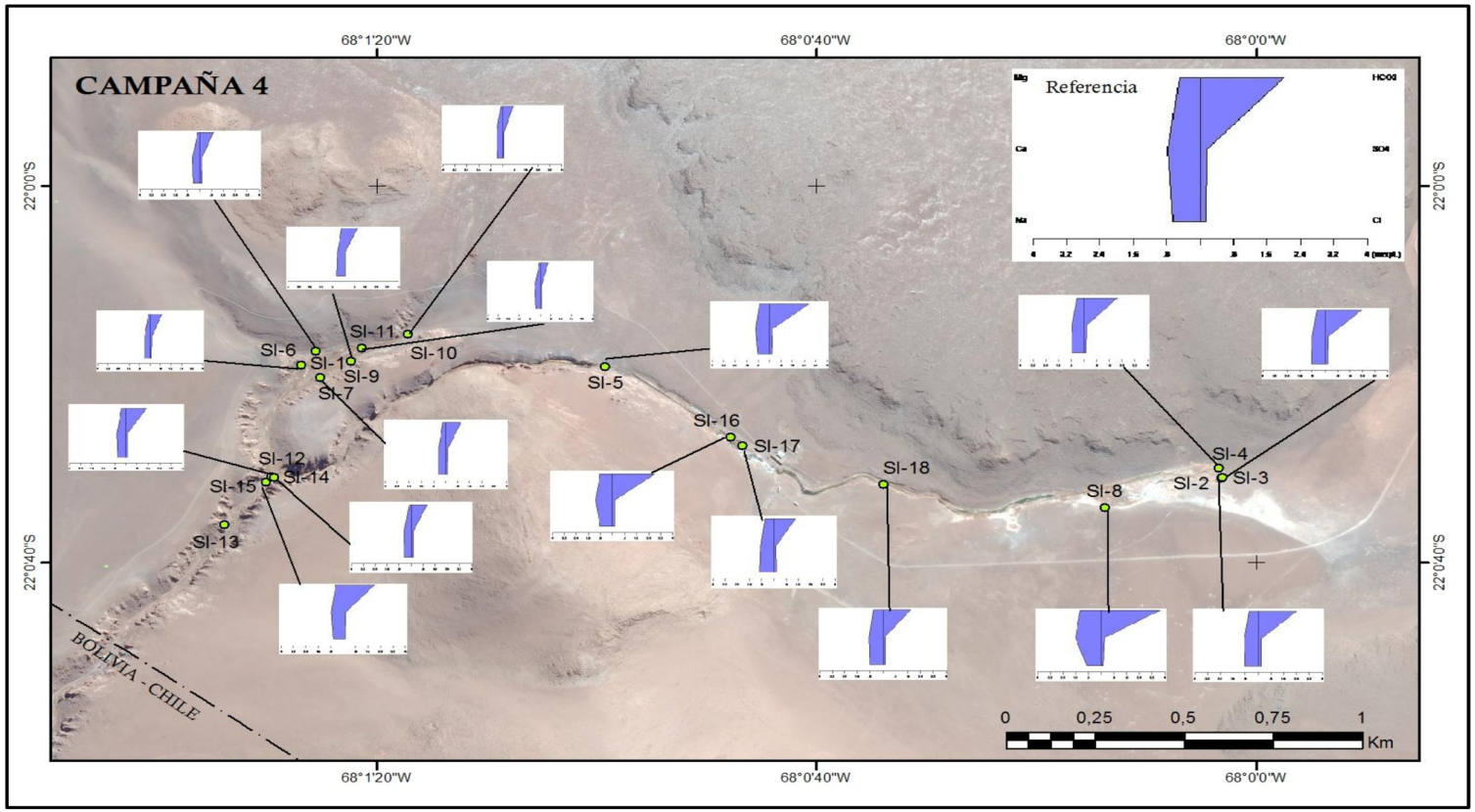


Figure 43. Maps including the Stiff Diagrams for the Fourth Campaign in the Silala Near Field

5.1.2. Water type classification

Piper diagrams show the distribution of cations and anions in a hydrochemical analysis of many samples expressing them as percentages. They are very useful because in them the different samples can be grouped in groups or dispersions on basis of their chemical facies. In contrast, Stiff diagrams show the chemical distribution of anions and cations to determine the type of water in a single sample. Therefore, thanks to the use of the Piper diagrams (Figures 26 to 29) and the Stiff diagrams (Figures 38 to 39), it has been possible to determine that the waters analyzed are of the sodium bicarbonate type. The regulations of the Ministry of Water and Environment indicate that in order for water to be suitable for Type _A' domestic consumption must contain at most 500 mg/l of bicarbonate, and the Silala waters analyzed do not exceed the 208 mg/lt. Regarding the sodium content, the MMAyA provides that Type _A' waters are those with a maximum content of 200 mg/l of sodium. The Silala waters analyzed do not exceed the 95 mg/l. Therefore, it can be concluded that the waters analyzed in the Silala region are Type _A' waters, suitable for any use, including human consumption.[102]

The Schoeller Diagrams (Figures 30 to 33) indicate that the groundwater sampled and analyzed from the Silala Transboundary Aquifer are essentially of a single type, sodium bicarbonate, with small hydrochemical variations and with very narrow variations in physical parameters.

Waters for irrigation purposes are classified with the Wilcox Diagram (Figures 34 to 37). Most of the Silala waters are of type C1S1 and C2S1, corresponding to low salinity and low sodium absorption ratio (SAR). Wilcox diagrams show a medium salinity risk in most samples. Therefore, the waters of the Silala are suitable for the irrigation of all types of soils, without any restriction.

The Stiff diagrams recorded in the location maps of the sampling points (Figures 40 to 43) clearly show the differences in the hydrochemical composition of the groundwater that upwells in the two bofedals (South and North), and in the water transported by the channels that drain them.

The conductivity values of the waters of the South Bofedal show a small difference with respect to the waters of the North Bofedal. Other small differences, including the altitude difference of around 50 m in relation to the sampling points [SIC, the sentence is incomplete].

In summary, the water type of the Silala springs is SODIUM BICARBONATE (Sodium Bicarbonate) with the following characteristics described in Table No. 4:

102 See also the concordant conclusions arrived at in the Tomas Frias Autonomous University Survey, p. 116.

TABLE 4. CHARACTERISTICS OF THE SILALA WATERS

COMPONENT	VALUES	OBSERVATION
Water type	Sodium Carbonate	Piper Diagram
Cations	rNa > rCa > rMg	
Anions	$rHCO_3$ > r Cl > rSO_4	
TDS	111 a 192 mg/lt	
pH	7.40 a 8.35	
Electric conductivity	209 a 398 µS/cm	South Bofedal
Electric conductivity	95 a 120 µS/cm	North Bofedal
Water temperature	13° C a 16° C	
SAR	C1S1 y C1S2	Low salinity and low Na absorption
Hardness	20.97 a 62.92 mg/lt	soft

5.2. Data and Analyses of Environmental Isotopes

This section addressees the assessment of the environmental isotope data collected from the springs and the groundwater in the Silala Near Field. The stable isotopes used in this investigation were Oxygen-18 (18º), Deuterium (2H) and Carbon-13 (13C), while the radioactive isotopes were: Tritium (3H) and Carbon-14 (14C). The stable isotopes, which were part of the water molecule, provide information on the origin of the groundwater and, therefore, are used to evaluate the recharge zones. On the other hand, 3H and 14C provide information on the residence time of groundwater. 13C provides information on the geochemical reactions that can affect dissolved inorganic carbon (DIC) throughout the groundwater flow system.[103]

In the following Table No.5, the results of the samples collected in Campaigns 1 and 4, which were analyzed in the Hydroisotop Laboratory of Germany,[104] have been transcribed. These results will be explained later, in detail.

103 Clark and Fritz, 1997.
104 See Annex: Analysis results from Hydroisotop laboratory.

TABLE 5. RESULTS FROM THE STABLE ISOTOPES OF THE FIRST

Sampling date	ID of the sample	$\delta^{18}O$ VSMOW (‰)	$\delta^{2}H$ VSMOW (‰)	Tritium ^{3}H TU	Carbon - 13 $\delta^{13}C$-TIC (‰)	Carbon -14 ^{14}C-TIC
03.06.2016	C1 Si1	-11.92	-89.9	< 0.6	-9.2	39.56 ± 0.24
03.06.2016	C1 Si2	-12.41	-95.0	< 0.6	-7.5	19.19 ± 0.14
03.06.2016	C1 Si3	-12.49	-95.8	< 0.6	-7.5	18.54 ± 0.14
03.06.2016	C1 Si4	-12.52	-95.9	< 0.6	-8.5	20.38 ± 0.14
03.06.2016	C1 Si5	-12.18	94.5	< 0.6	-7.1	27.17 ± 0.18
03.06.2016	C1 Si6	-11.96	-92.3	< 0.6	-6.8	48.09 ± 0.28
03.06.2016	C1 Si7	-12.02	-91.5	< 0.6	-7.6	38.33 ± 0.22
03.06.2016	C1 Si8	-12.55	-95.3	< 0.6	-6.8	8.13 ± 0.08
03.06.2016	C1 Si9	-12.06	-92.7	< 0.6	-	-
03.06.2016	C1 Si10	-12.00	-91.0	< 0.6	-	-
03.06.2016	C1 Si11	-12.12	-90.6	< 0.6	-	-
12.07.2017	C4 Si1	-12.04	-92.2	< 0.6	-8.6	42.08 ± 0.26
11.07.2017	C4 Si2	-12.52	-96.2	< 0.6	-9.3	13.71 ± 0.12
11.07.2017	C4 Si3	-12.56	-96.3	< 0.6	-7.9	12.43 ± 0.10
11.07.2017	C4 Si4	-12.07	-94.4	< 0.6	-7.9	15.45 ± 0.14
13.07.2017	C4 Si5	-12.16	-93.7	< 0.6	-8.8	17.78 ± 0.14
12.07.2017	C4 Si6	-11.71	-91.6	< 0.6	-6.9	42.54 ± 0.44
12.07.2017	C4 Si7	-11.70	-92.1	< 0.6	-10.2	30.64 ± 0.20
12.07.2017	C4 Si8	-12.32	-96.0	< 0.6	-8.3	5.31 ± 0.08
12.07.2017	C4 Si9	-11.99	-93.1	< 0.6	-10.2	31.53 ± 0.22
12.07.2017	C4 Si10	-11.63	-90.7	< 0.6	-12.0	42.37 ± 0.32
12.07.2017	C4 Si11	-11.73	-89.9	< 0.6	-10.5	28.45 ± 0.20
12.07.2017	C4 Si12	-11.89	-93.1	< 0.6	-10.0	27.99 ± 0.20
12.07.2017	C4 Si14	-11.86	-93.0	< 0.6	-8.8	45.18 ± 0.30
12.07.2017	C4 Si15	12.06	-94.0	< 0.6	-9.8	24.79 ± 0.20

Source: Analyses performed bu the Hydroisotop Laboratory of Alemania. 2018.

5.2.1. Stable Isotopes of Oxygen and Hydrogen

Oxygen has two important stable isotopes (non-radioactive): 16O and 18O, with atomic ratios between 490: 1 and 530: 1,[105] respectively. The most important stable isotopes of hydrogen are: 1H and 2H (Deuterium), with proportions between 1: 5900 and 1: 10,000. In practice, the ratio of the frequency of the oxygen and hydrogen isotopes R is not determined in absolute terms, but in proportion to a standard sample, known as seawater, which is called SMOW (Standard Mean Ocean Water). The ratio between the sample Rm to be determined and the standard sample Rst are expressed as:

$$\delta\ ^{18}O = 1000 \text{ x } R_{m_}R_{st} / R_{st} \quad (\text{in } {}^{0}/_{00})$$

105 Because the scale of 490: 1 is inverted to 1: 5900.

Similarly, for the proportion of 1H and 2H in the determination of δ 2H the standard sample SMOW is also used. In general, for freshwater, the values of δ 18O and δ 2H are negative due to the evaporation of ocean water. The molecules with negative charge come from, with greater preference, pluvial precipitations. The δ2H values of the precipitation samples contain a higher negative content than those of δ 18O, both are proportional to each other according to the ratio:

$$\delta\ 2H = s \times \delta\ 18O + d$$

Which stands for: s = slope and d = excess deuterium

Technical Report 2DA (2018), prepared by the Vice Ministry of Water Resources and Irrigation of the Ministry of the Environment and Water describes the ―Water Sampling Campaign for Hydrochemical and Isotopic Analysis and Diagnosis of Canals in the Silala Springs‖ for the flow samples taken in 2016 and 2017 and analyzed at the beginning of 2018, both for Oxygen-18 (δ 18O) and for Deuterium (δ 2H) in the Hydroisotop Laboratory of Schweitenkirchen, Germany. The results are shown in the following tables and figures.

TABLE 6. ISOTOPIC PARAMETERS (δ 18O) AND (δ 2H) OF THE WATERS OF SILALA

Sampling date	Sample number	Oxigen-18 ($\delta\ ^{18}O$) en $^{0}/_{00}$	Deuterium ($\delta\ ^{2}H$) en $^{0}/_{00}$
03.06.2016	CI SI1	-11,92	-89,90
03.06.2016	C1 SI2	-12,41	-95,00
03.06.2016	CI SI3	-12,49	-95,80
03.06.2016	C1 SI4	-12,52	-95,90
03.06.2016	C1 SI5	-12,18	-94,50
03.06.2016	C1 SI6	-11,96	-92,30
03.06.2016	C1 SI7	-12,02	-91,50
03.06.2016	C1 SI8	-12,55	-95,30
03.06.2016	C1 SI9	-12,06	-92,70
03.06.2016	C1 SI10	-12,00	-91,00
03.06.2016	C1 SI11	-12,12	-90,50
12.07.2017	C4 SI1	-12,04	-92,20
11.07.2017	C4 SI2	-12,52	-96,20
11.07.2017	C4 SI3	-12,56	-96,30
11.07.2017	C4 SI4	-12,07	-94,40
13.07.2017	C4 SI5	-12,16	-93,70
12.07.2017	C4 SI6	-11,71	-91,60
12.07.2017	C4 SI7	-11,70	-92,10
12.07.2017	C4 SI8	-12,32	-96,00
12.07.2017	C4 SI9	-11,99	-93,10
12.07.2017	C4 SI10	-11,63	-90,70
12.07.2017	C4 SI11	-11,73	-89,00
12.07.2017	C4 SI12	-11,89	-93,10
12.07.2017	C4 SI14	-11,86	-93,00
12.07.2017	C4 SI15	-12,06	-94,00

Source: Analyses performed by the Hydroisotop Laboratory of Germany, 2018.

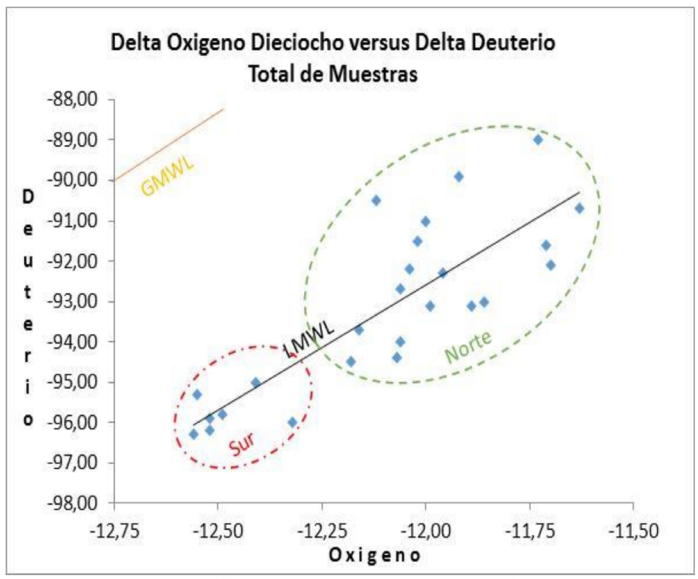


Figure 44. Oxigen-18 ($\delta^{18}O$) ratio versus Deuterium ($\delta^{2}H$) of the total samples

TABLE 7. SAMPLES TAKEN IN 2016

Sample date	Sample number	Oxigen-18 ($\delta^{18}O$) in $^{0}/_{00}$	Deuterium ($\delta^{2}H$) en $^{0}/_{00}$
03.06.2016	CI SI1	-11,92	-89,90
03.06.2016	C1 SI2	-12,41	-95,00
03.06.2016	CI SI3	-12,49	-95,80
03.06.2016	C1 SI4	-12,52	-95,90
03.06.2016	C1 SI5	-12,18	-94,50
03.06.2016	C1 SI6	-11,96	-92,30
03.06.2016	C1 SI7	-12,02	-91,50
03.06.2016	C1 SI8	-12,55	-95,30
03.06.2016	C1 SI9	-12,06	-92,70
03.06.2016	C1 SI10	-12,00	-91,00
03.06.2016	C1 SI11	-12,12	-90,50

Source: Analyses performed by the Hydroisotop Laboratory of Germany, 2018.

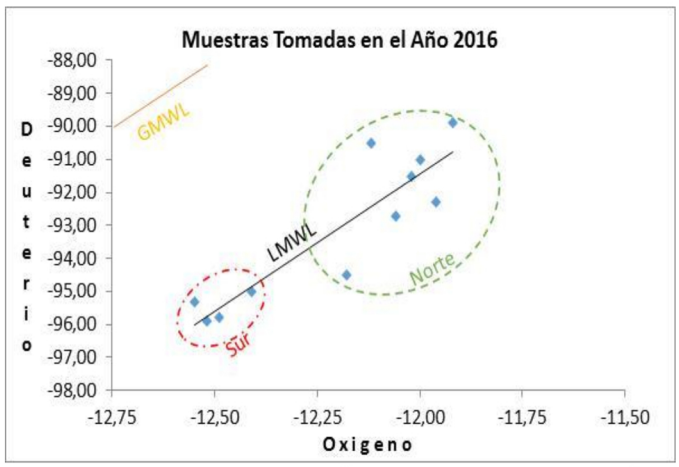


Figure 45. Ratio of the Oxigen-18 ($\delta^{18}O$) samples versus Deuterium ($\delta^{2}H$) Taken in 2016.

TABLE 8. SAMPLES TAKEN IN 2017

Sample date	Sample number	Oxigen-18 ($\delta^{18}O$) in $^{0}/_{00}$	Deuterium ($\delta^{2}H$) en $^{0}/_{00}$
12.07.2017	C4 SI1	-12,04	-92,20
11.07.2017	C4 SI2	-12,52	-96,20
11.07.2017	C4 SI3	-12,56	-96,30
11.07.2017	C4 SI4	-12,07	-94,40
13.07.2017	C4 SI5	-12,16	-93,70
12.07.2017	C4 SI6	-11,71	-91,60
12.07.2017	C4 SI7	-11,70	-92,10
12.07.2017	C4 SI8	-12,32	-96,00
12.07.2017	C4 SI9	-11,99	-93,10
12.07.2017	C4 SI10	-11,63	-90,70
12.07.2017	C4 SI11	-11,73	-89,00
12.07.2017	C4 SI12	-11,89	-93,10
12.07.2017	C4 SI14	-11,86	-93,00
12.07.2017	C4 SI15	-12,06	-94,00

Source: Analyses performed by the Hydroisotop Laboratory of Germany, 2018.

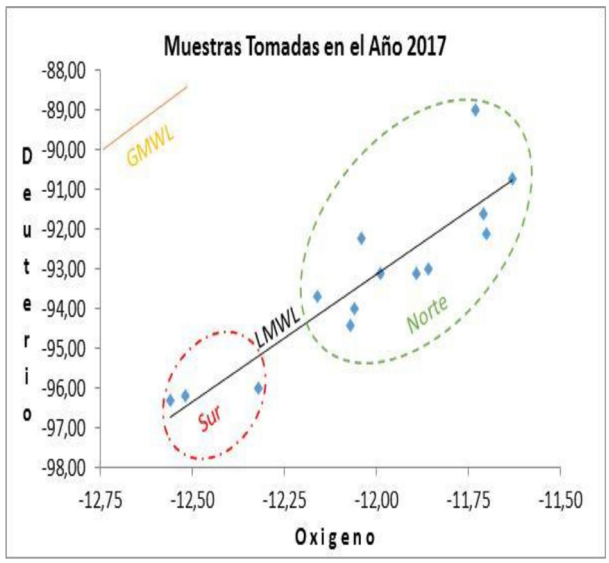


Figure 46. Ratio of the Oxigen-18 ($\delta^{18}O$) samples versus Deuterium ($\delta^{2}H$) Taken 2017.

TABLE 9. RESULTS OF THE STABLE ISOTOPES FROM THE DRILLED WELLS

Sample date	ID of the sample	$\delta^{18}O$ VSMOW (‰)	$\delta^{2}H$ VSMOW (‰)	Tritium ^{3}H TU	Carbon - 13 $\delta^{13}C$-TIC (‰)	Carbon - 14 ^{14}C-TIC
--	DS-27	-	-	< 0.6	-9.2	47.54 ± 0.32
29.12.2017	DS-4P	-12.48	-96.7	< 0.6	-7.9	16.40 ± 0.16
--	DS-4P PUMPING	-12.48	-96.9	< 0.6	-7.2	15.72 ± 0.16
15.11.2017	DS-4S	-12.14	-94.9	< 0.6	-6.2	15.14 ± 0.14
29.12.2017	DS-1	-11.95	-93.4	< 0.6	-8.6	34.31 ± 0.24
20.12.2017	DS-25	-12.09	-91.5	< 0.6	-9.5	63.07 ± 0.38
15.11.2017	DS-8	-12.51	-97.1	< 0.6	-6.7	14.19 ± 0.14
16.11.2017	DS-24S	-11.92	-90.0	< 0.6	-7.5	47.34 ± 0.30
15.11.2017	DS-24P	-11.88	-90.4	< 0.6	-7.0	49.78 ± 0.32

Source: Analyses performed by the Hydroisotop Laboratory of Germany, 2018.

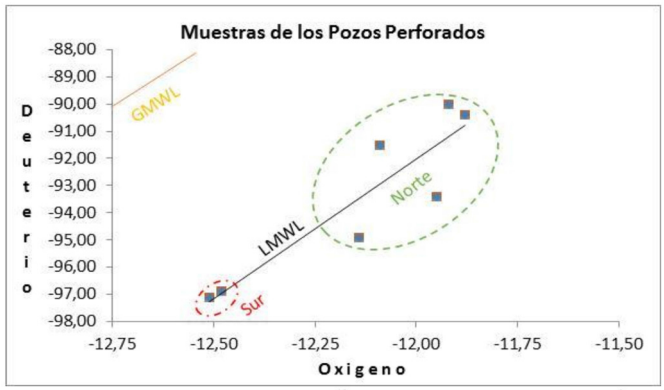


Figure 47. Ratio of the Oxigen-18 ($\delta^{18}O$) samples versus Deuterium ($\delta^{2}H$) in the Samples Taken from the Drilled Wells.

It can be observed that all the points are properly located along a trend line (black), which is crossed by the investigated data. This line represents the so-called _Local Meteorological Water Line (LMWL)‘ which runs parallel to the _Global Meteoric Water Line (GMWL)‘ (mustard) which is located at the upper left side of the figures.

In its passage through the continent the clouds become rain precipitations; that is the moment in which preferably the —heavy‖ molecules of water condense. Therefore, in general, the values of δ 18 O and δ 2H decrease in value, as precipitation occurs in the continental territory.

The low values in the Silala area can be explained and interpreted by the fact that rain and snowfall do not arrive from the Pacific Ocean, which is close to the west and in the vicinity, but is derived from the rainfall from the distant Atlantic Ocean or from the macro-Amazon basin in the east.

The fact that the points that represent the ratio δ 18O and δ 2H are found along the LMWL shows that a rapid and direct infiltration of rainfall to the aquifer occurred during recharge and that the waters of Silala did not endure evaporation before its infiltration. Due to this fact, the idea that the waters come from lagoons found east of the Silala, such as Laguna Blanca or Laguna Khara, can be discarded and excluded. In addition, the figures indicate that there are not any very _light‘ values of δ 18 O outside the LMWL, which would indicate that there is no influence on the waters of Silala with volcanic carbon dioxide content from the interior of the earth. This fact is important in the estimation of water age using the 14C values, which were published in Neumann & Torrez (2005).

Different physical properties, such as evaporation and temperature, modify the composition of the δ 18 O and δ 2 H isotopes in humidity, precipitation and groundwater. The fractionation of isotopes δ 18 O and δ 2 H depends on the temperature. In warmer places and times, more rainwater evaporates, presenting a greater number of _heavy‘ molecules,

because their values are positive; on the contrary, in colder times and places there is an enrichment of ‗lighter' molecules and the values are negative, as in the case of the waters of Silala.

The lower end samples in the LMWL have ‗lighter' values and come from the South Bofedal, the South Ravine and the wells drilled in these two places of the Silala. Thus, it is possible to deduce that this groundwater has been recharged in a much colder time than the current one.

Waters exposed to evaporation as in lagoons, stagnant and bofedal waters experience a fractionation of the oxygen and hydrogen isotopes in a different relationship due to the enrichment of $\delta^{18}O$, with a greater number of ‗heavy' values, due to the fact that these waters were exposed to evaporation.

5.2.2. Stable Isotopes of Tritium

Spring and groundwater data show that the concentration of the stable isotopes of Tritium is zero, indicating that these waters are not recent and are much older than the last 90 years.

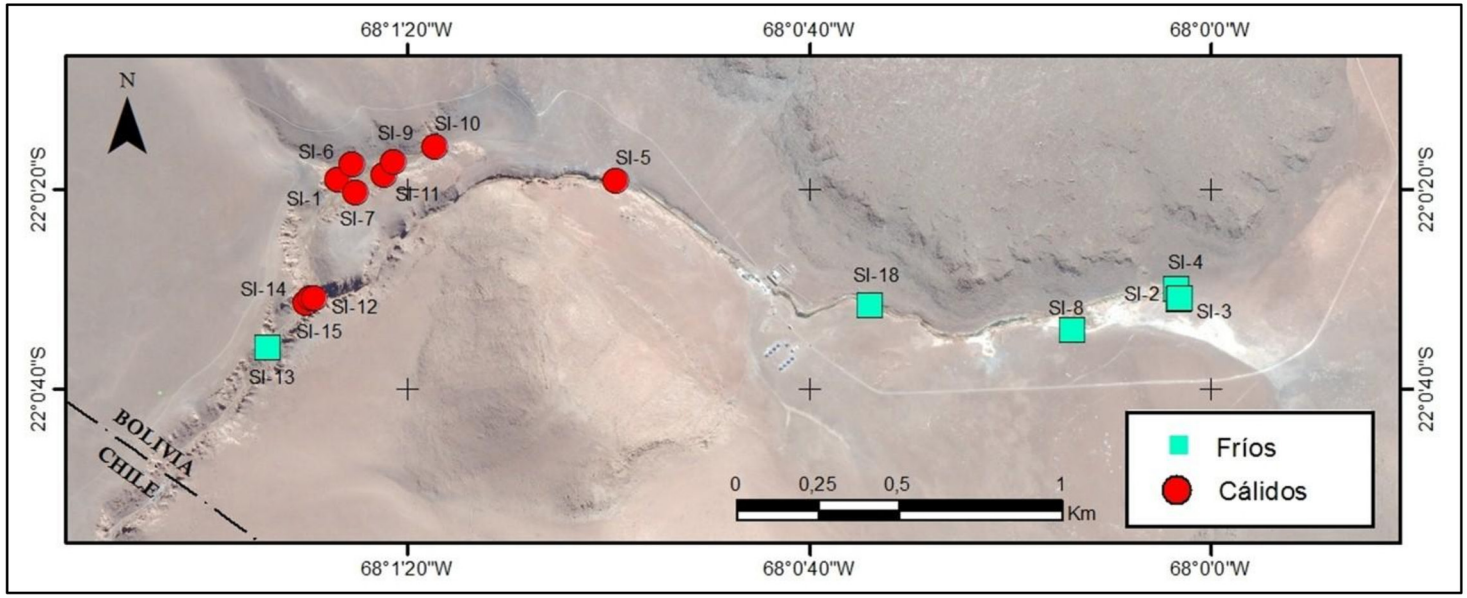


Figure 48. Map with the results of the relation of the frequency of oxygen and hydrogen isotopes – Campaign 4[106]

[106] The source is the author's.

320

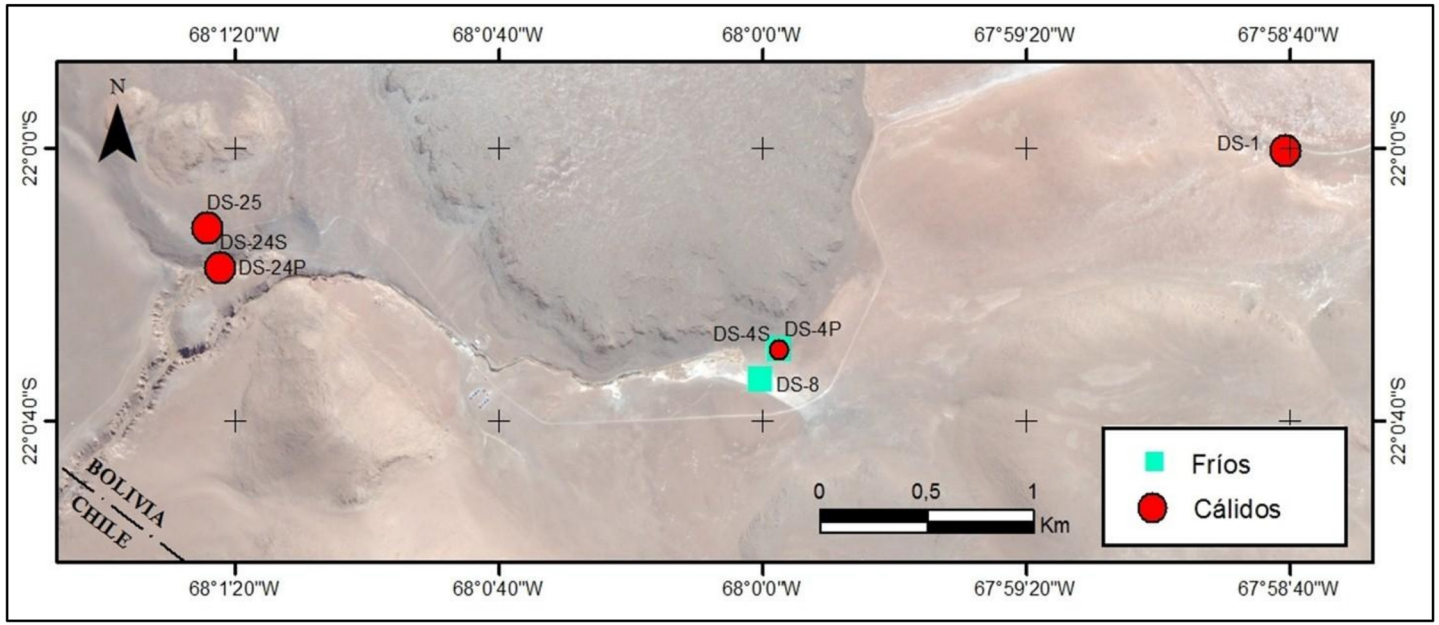


Figure 49. Map with the results of the relationship of the frequency of the isotopes of oxygen and hydrogen from drilled wells (2017).[107]

[107] The source is the author's.

5.2.3. Ratio of the Carbon-13 and Carbon-14 Isotopes

A plot is made to determine a ratio of the Carbon-13 and Carbon-14 isotopes in the waters of the two North and South Bofedals, this determines the ratio between them and allows observing the results obtained. Figure 50 shows the ratio of isotopes per sampling campaign carried out in the Bofedal waters and Figure 51 shows the ratio of wells drilled in the two bofedals.

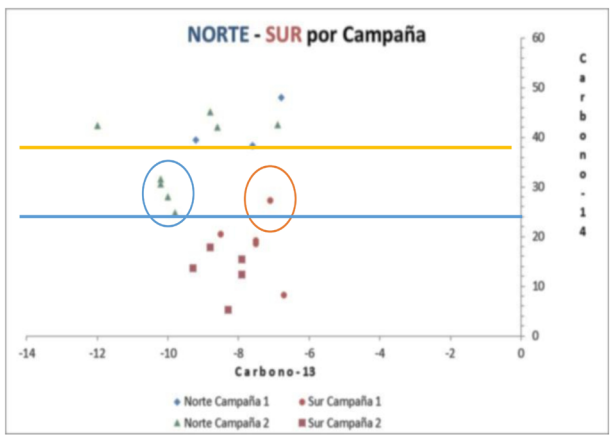


Figure 50. Ratio of carbon-13 and carbon-14 isotopes in the waters of the North and South Bofedals

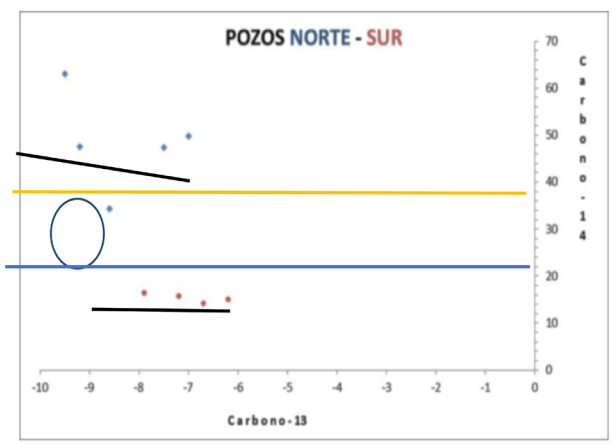


Figure 51. Relationship of carbon-13 and carbon-14 isotopes in waters of nine wells drilled in the two Bofedales North and South

Note: Horizontal blue lines indicate 10,000 years BP of water age.
Horizontal orange lines indicate 5,000 years BP of water age.

As conclusions of the analysis of the Carbon-13 and Carbon-14 isotopes, it can be indicated as a first ratio, that, in both figures, there is a separation of two types of water in the Silala groundwater, both in the waters of the bofedals as in those of the wells. A second ratio is observed, which is the grouping of the groundwater samples based on the sampling campaigns (Campaign 1 and Campaign 2) carried out.

All groundwater samples from the South Bofedal show an age older than 10,000 years BP, except for sample C1 Si5.

Not all groundwater samples from the North Bofedal show an age younger than 5,000 years BP. Some are older than this age.

6. GENERAL CONCLUSIONS

The general conclusions of this report are presented with bullet points to facilitate its explanation and understanding:

On Geology:

- The area of the Silala Springs was geologically formed during the Upper Miocene (7.5 to 8
Myr), when the Silala ignimbrites were deposited. The latter are highly volatile, Neogene pyroclastic flows with a high content of magmatic fragments that are strongly fractured and jointed by tectonic movements caused by the Uyuni-Khenayani fault system, which occurred between 27 to 17 Myr, namely, before the ignimbrites were deposited. A second and strong volcanic activity caused the intrusion of volcanic domes dating back to 5.8 to 6.2 Myr and a third volcanic activity that took place between 1.5 to 1.7 Myr modified the ignimbrite plateaus landscape.

- The volcanic features mentioned above were modified by the subsequent deposition, formation and action of large glacial masses that began 65,000 years BP, until the last glacial maximum of approximately 14,500 years BP. The movement and melting of the glaciers greatly modified the regional geomorphology giving way to the current landscape, that presents an undulating plain, and the formation of characteristic glacial valleys on volcanic cone skirts.

- Glacial melt water action is one of the most notorious local geomorphological features on the rocks in the Silala Ravine, which is a typical example of a ravine formed by the erosive action of glacial waters derived from melting that occurred more than 10,000 years BP.

- The Silala Ravines, on the Bolivian side, are of tectonic origin and were later eroded by the movement of glacial and fluvioglacial Quaternary ice. They show very limited surfaces covered with alluvial sediments and contrast with the Quaternary geology and the ravines on the Chilean side—which are fluvial in origin.

- The ignimbrites outcrop in the Main Silala Ravine, on the Bolivian side, presenting packages of cooling flows, which can be confused with terraces that would supposedly accumulate Quaternary sediments, as on the Chilean side.

- The vertical and almost vertical walls seen in the photographs of the Main Ravine and the trial pit excavated therein are strong evidence of the formation of the ravines by tectonism and movement of glacial ice and fluvioglacial waters.

On Hydrology:

- The surface water flow observed in the Silala Bofedal and Spring System belongs to a constant and consistent flow regime, with a system of springs fed by groundwater contained in the Silala Transboundary Aquifer.
- A probable 234 km2 hydrological basin (Silala Far Field) has been digitally delineated. This basin is likely to allow groundwater to flow from aquifers to the Silala Springs through faults and joints and has been used to evaluate these waters‘ recharge and water balance.

- Based on the surveys carried out within the basin, an average precipitation of 125 mm/year has been estimated for 1969 – 2017: the inter-annual variation of rainfall is very high, ranging from rainfall close to 0 mm/year in 2009-2010 to more than 300 mm/year in 1997 and 1999. Likewise, records of average annual temperature of 2.2 ° C for 1969-2010 have been estimated, with maximum and minimum temperatures between +19.6° C and -19.6° C. The potential evapotranspiration rate (Et0) is 1472 mm/year, with a variation from 2-2.5 mm/day in austral winter months to 5-5.5 mm/day in the summer.

- The average flow measured in the Main Channel, at the border, is 160-210 l/sec. Likewise, it has been observed that the flows coming from the North and South Bofedal springs represent approximately 60% of the total flow of the Main Channel, while the so-called diffuse flows represent the remaining 40%.

On Hydrogeology:

- All the springs that emerge in an artesian way in the Silala area constitute discharges from the Silala Ignimbrite aquifer. In many cases, it is possible to observe springs welling up directly from the joints and fissures. The fine quaternary and recent sediments that cover the ignimbrites are fed and saturated by the water derived from the underlying ignimbrite aquifer, forming bofedals. Two main systems of joint sets have been determined; 67% of them have a NE-SW course and the remaining 23% have a NW-SE course.

- The surface water flow observed in the Silala Spring System belongs to a constant and consistent flow regime of a system of springs fed by potable groundwater stored in different levels of the Silala Aquifer, which is hosted in the highly fractured Silala Ignimbrites (faults and joints).

- The measured hydraulic conductivity and understanding of the ignimbrite aquifer suggest that there is a significant transboundary groundwater flow, which is currently estimated in the approximate order of 230 l/sec. The most representative values of pumping tests completed near the Chilean border would provide excessive transboundary flows of 600 l/sec.

- There are northeast trend structures that include several large faults. These fault zones are brecciated and have a higher hydraulic conductivity than the surrounding materials and are thus interpreted as groundwater transmitters, at great distances (i.e. Far Field

of Silala, or beyond). A network of smaller openings, northwest trend fractures, act as conduits that transmit groundwater following the course of this fault.

- The hydraulic properties (storage values and efficiency) of the ignimbrites and the groundwater head suggest that there are semi-confined conditions at depth and that unconfined conditions persist in shallow piezometers.
- The pumping tests conducted at the South Bofedal indicate the presence of a transmitter ignimbrite aquifer with a large-scale hydraulic conductivity estimated at 18 m/d and a locally higher conductivity within the Silala Fault area (54 m/d). These values are higher than the 6.5 m/d value estimated in the pumping tests in Chile, near the border.

- The general trend for hydraulic conductivity is a large-scale convergence of larger conductivity values measured on a smaller scale. This suggests that transmitter fractures are well connected on a large scale and that, at the scale of the representative elementary volume (REV), they seem to control long-term hydraulic behavior, which approaches a porous medium.

- During the pumping test, the hydraulic behavior of the ignimbrite aquifer included a behavior that does not respond to the Theis method, in the flow of the fracture near the pumping well, but, on larger scales, it behaved as an equivalent porous medium (EPM).

- The Silala Aquifer, hosted in the eruptive igneous rocks of the Silala Ignimbrite unit, has type
A waters from 10,000 years BP in the springs of the South Bofedal and Channel, and from
1,000 years BP in the springs of the North Bofedal. These waters flow in direction to the west, towards Chile in open artificial channels made of stone and mortar.

- The Silala Aquifer is made up of several levels, one of which is regional and emerges in an artesian form—it may be a confined aquifer. The drilling of several exploratory wells could define its real origin, the thickness of the ignimbrites and the underlying rocks.

On hydrochemistry

- According to the Piper, Stiff, Schoeller and Wilcox diagrams, the analyzed waters of the Silala Springs are of the sodium bicarbonate type. According to the regulation of water quality in force in Bolivia since 1997, these waters are fully suitable for human consumption and irrigation; They are of type ―A‖ waters. Likewise, the range of electrical conductivity of the water that emerges in the Silala region varies from 95 to 340 □S/cm. These values correspond to low mineralization waters.

- In the physical-chemical data inventory of the samples collected and analyzed in the Bolivian area of the Silala Springs, both for the surface waters of the springs and the waters conveyed in the three Channels – South, North and Main –, and compared with the samples analyzed in the Chilean works presented in the Chilean Memorial, they manifest the same conditions and conclusions found at the beginning of this century.

• The hydrochemistry of the groundwater that is discharged in the North Bofedal is significantly different from that which is discharged in the South Bofedal. The waters of the North Bofe-dal have lower ages and lower concentrations of dissolved solids and bicarbonate; it is inter-preted that these waters derive from a more localized flow regime.
• The waters of the South Bofedal have older ages, with a greater amount of dissolved solids and bicarbonate concentrations; it is interpreted that these waters derive from the flow found within the Silala Fault zone, which is recharged by a sub-regional to regional flow regime.

• The surface water flow measurements previously analyzed and the hydrogeochemical mixing ratios suggest that most (60-70%) of the groundwater discharged into the sys-tem originates from springs associated with a deeper groundwater flow regime. It is inter-preted that the remaining 30 to 40% comes from more localized flow regimes that are clos-er to the Silala Near Field.

• Knowledge about the origins and age of the groundwater that feeds the springs associated with the area of the Silala Fault is still not very specific. To improve the understanding of these aspects, they should be examined more extensively and using a scale model, e.g. a basin-based model with additional characterization activities.

• Environmental isotopes suggest that the origins of the recharge of deep groundwater and spring water differ significantly. The residence time seems to be the highest in groundwa-ter, shorter in spring water, and intermediate in water samples taken in the Silala channels. In addition, the isotopic analysis suggests that groundwater is regionally recharged.

• In general, the Silala water is sodium bicarbonate water with different degrees of Ca con-tent.
The groundwater is of the bicarbonate calcium type. The chemical data shows that the springs and groundwater are characterized by presenting low salinity. The springs in the upper part of the course tend to be more saline than the springs located in the lower area north of the watercourse. The water has a salinity ratio that is similar to the upper springs.

• The high silicate content of these waters indicates that the main source of the chemical composition of water is the leaching of silicate minerals. The chemical data sug-gests that the springs of the North Bofedal do not constitute a reflection of the groundwa-ter discharge of the deeper aquifer.

• A detailed analysis of the water samples from Negra Ravine in Chile, both due to their physical and chemical properties, shows that they are similar to the waters that well up in the South Bofedal, in Bolivia. In turn, the waters of the Silala Main Ravine in Chile and the Inacaliri Post

area are similar to the waters of the North Bofedal, in Bolivia. They are both sodium carbonate waters.

- Due to the hydrochemistry and the physical parameters of the waters, there are at least two levels of ignimbrite aquifers. A superior one, that forms the South Bofedal, with outcrops at
4,450 m.a.s.l., with an average conductivity of 257 □S/cm that has higher content of Ca, Li and S04. The second level or lower aquifer that emerges at 4,400 m.a.s.l. has an average conductivity of 109 □S/cm and a higher Na content; where the North Bofedal emerges.

- As indicated in the previous paragraphs on geology, hydrogeology and hydrochemistry, it is concluded that groundwater constitutes a transboundary aquifer.

7. BIBLIOGRAPHY

Aravena, R., Suzuki, O., Peña, H., Pollastri, A., Fuenzalida, H., Grilli, A., 1999. Composición isotópica y origen de la precipitación en el Norte de Chile. Geoquímica Aplicada [Isotopic composition and origin of precipitation in Northern Chile. Applied Geochemistry]14 (4), 411- 422.

Argollo J. e Iriondo, 1991, Cuaternario de Bolivia y Regiones Vecinas [Quaternary of Bolivia and Neighboring Regions].

Argollo J. et al. 1987. Geología del Pliocuaternario de Bolivia. Inédito [Geology of the Plioquaternary of Bolivia. Unpublished].

Argollo J. y Mourguiart P., 1995, Climas Cuaternarios en América del Sur [Quaternary Climates in South America], p. 360.

Aravena, R., y Suzuki, O., 1990. Evolución isotópica de ríos en el Norte de Chile. Agua Resources Research [Isotopic evolution of rivers in northern Chile. Water Resources Research], 26 (12), 2887 - 2895.

Arcadis, 2017. Estudio hidrogeológico detallado del río Silala. (Volumen 4, Anexo II) [Detailed hydrogeological study of the river Silala. (Volume 4, Annex II)]

Baby, P., Oller J., Barrios, L., Hérail, G., & Marocco, R. 1990. Un basin en compression d'age oligomiocene dans le sud de l'Altiplano bolivien: Acad'emie des Sciences de France, ComptesRendus des Séances [A basin in compression of oligomiocene age in the south of the Bolivian Altiplano: Academy of Sciences of France, Proceedings of Sessions], series 2, v. 311. P341-347.

Bouwer, H. y R. C. Rice, 1976. Un método de prueba de acuífero para determinar la conductividad hidráulica de acuíferos no confinados con pozos que penetran total o parcialmente, Investigación de Recursos Hídricos [An aquifer test method for determining the hydraulic conductivity of unconfined aquifers with wells that fully or partially penetrate, Water Resources Research], Vol. 12, Nº 3, pp. 423–428.

Chaffaut, I., 1998. Precipitations d'Altitude, Eau Souterraines et Changements Climatiques de L'Altiplano Nord-Chilien. Universite de Paris Sud [Precipitation of Altitude, Underground Water and Climate Change of the North-Chilean Plateu. University of Paris South U.F.R. Scientist D'Orsay] U.F.R. Scientifique D'Orsay, París, Francia.

Clark y Fritz, 1997. Isótopos Ambientales en Hidrogeología [Environmental Isotopes in Hydrogeology]. Lewis Publisher, Nueva York.

Corporación de las Fuerzas Armadas para el Desarrollo Nacional (COFADENA), 2017. Proyecto Estudio Geofísico de los Bofedales del Silala, La Paz, Bolivia: Unidad de Explotación de Recursos Hídricos [Corporation of the Armed Forces for National Development (COFADENA), 2017. Geophysical Study Project of the Silala Bofedales, La Paz, Bolivia: Unit of Exploitation of Water Resources].

Fritz, P., Suzuki. O., Silva. C. y Salati. E., 1981. Hidrología isotópica de las aguas subterráneas en la Pampa del Tamarugal, Chile [Isotopic hydrology of groundwater in Tamarugal Pampa, Chile]. Journal of Hydrology 53, 161-184.

DHI February 2017: Study of the Flows in the Silala Wetland and Spring System, Phase II Product 1 Final Survey, Field Specifications.

DHI February 2017: Study of the Flows in the Silala Wetland and Spring System, Phase I: Product No. 1, Inception Brief.

DHI July 2017: Study of the Flows in the Silala Wetland and Spring System - Second Part Product No. 1: Provisional Report 1, Surface Flows.

DHI, September 2017. Study of Groundwater flows: Provisional Report 4.

DHI November 2017: Contract CDP-I No. 15/2017, Study of the flows in the Silala Wetland and Spring System - Second part Product No. 3: Water balance of the basin aquifer and water and update the measured surface water flow.

DHI March 2018: Contract CDP-I No. 01/2018, Study of the flows in the Silala Wetland and Spring
System -Product No. 2: - 2018, Final Report.

DIREMAR, 2018. Data provided in Excel sheets during data transfer to DHI. Original source to be confirmed with DIREMAR.

DIREMAR/Pix4D, 2016: ―Silala Report.pdf‖, Quality Report of the Digital Elevation Model (DEM)/Digital Terrain Model (DTM) of high local resolution of the Near Field through the use of drones.

Duffield, G., 2007. AQTESOLV Version 4.5, User's Guide. HydroSOLVE, Inc., Reston, VA Espinoza, C., 2017. Evolution of the Springs, La Paz: Sent to the DIREMAR.
Hauser, A. Y., 2004. Morphological, Geological, Tectonic, Hydrogeological and Hydrochemical Context: Morphogenesis, Evolution and Modalities of the Exploitation of the Shared Chilean- Bolivian System of the Silala River, s.l.: Geological and Mining Services of the Government of Chile.

Herrera, C., Pueyo, J., Sáez, A. y Valero-Garcés, B., 2006. Relación de aguas superficiales y subterráneas en el área del lago Chungará y lagunas de Cotacotani, Norte de Chile: Un estudio isotópico. Revista Geológica de Chile [Relationship of surface and groundwater in the area of Lake Chungará and lagoons of Cotacotani, Northern Chile: An isotopic study. Geological Magazine of Chile], 33 (2), 299-325.

Huaranca, Rodolfo, Neumann-Redlin, Christian & Suckov, Alex. 2000. Comunicación provisional sobre la geología e, hidrogeología de los Manantiales del Silala. Aguas Subterráneas y Desarrollo Humano. Memorias del XXXII Congreso IAH y VI ALI-Sud. Mar del Plata, Argentina [Provisional communication on the geology and, hydrogeology of the Springs of Silala. Groundwater and Human Development. Memories of the XXXII IAH Congress and VI ALI-Sud. Mar del Plata, Argentina].

IAEA / OMM, 2015. Red Mundial de Isótopos en las Precipitaciones. La base de datos GNIP [Global Isotope Network in Precipitation. The GNIP database]
(Available in: http://www.iaea.org/water).

Latorre, C., Frugone, M., 2017. Sedimentary history of the Holocene of the Silala River
(Antofagasta Region, Chile). (Volume 5, annex IV). Lewis, 1989.
Magaritz, M., Aravena, R., Pena, H., Suzuki, O. and Grilli, A., 1989. Water chemistry and isotope study of streams and springs in northern Chile. Journal of Hydrology, 108, 323-341.

Ministerio de Energías, 2017. Análisis Físico-Químico de Aguas, La Paz, Bolivia: INSTITUTO BOLIVIANO DE CIENCIA Y TECNOLOGÍA NUCLEAR, CENTRO DE , INVESTIGACIONES Y APLICACIONES NUCLEARES, UNIDAD DE ANÁLISIS Y CALIDAD AMBIENTAL [Physical-Chemical Analysis of Water, La Paz, Bolivia: BOLIVIAN INSTITUTE OF SCIENCE AND NUCLEAR TECHNOLOGY, NUCLEAR RESEARCH AND APPLICATION CENTER, ANALYSIS AND ENVIRONMENTAL QUALITY UNIT].

Neumann-Redlin, Christian & Torrez F., Juan. 2005. Investigaciones hidrológicas, hidroquímicas, e isotópicas en el área de los Manantiales del Silala. SERGEOMIN. Informe Interno no publicado [Hydrological, hydrochemical, and isotopic investigations in the area of the Springs of Silala. SERGEOMIN Internal report not published].

R.C. Smyth and J.M. Sharp, 2006. The hydrology of the tuffs in Heiken, G. ed., Tuffs - Their properties, uses, hydrology and resources. Special Document of the Geological Society of America, 408 pp. 91-111.

SERGEOMIN, 2003. Estudio de Cuenca Hidrográficas: Cuenca manantiales del Silala, La Paz, Bo-livia [Hydrographic Basin Study: Basin springs of Silala, La Paz, Bolivia]

SERGEOMIN, 2003. Mapa Nº 1 Geología, hidrología, e hidrogeología de los Manantiales del Silala Provincia Sur Lípez del Departamento de Potosí s.l.: s. n. [Map No. 1 Geology, hydrology, and hydrogeology of the Springs of the Silala Province South Lípez of the Department of Potosí s.l .: s. n]

SERGEOMIN, 2017: Mapeo geológico estructural del área circundante al manantial del Silala [Structural geological mapping of the area surrounding the Silala spring].

SERGEOTECMIN, 2004. Investigaciones en los Manantiales del Silala – Presentación Silala FISI-CO-QUIMICO ISOTOPOS, La Paz: Informe de investigación interna [Investigations in the Springs of Silala - Presentation Silala PHYSICO-CHEMICAL ISOTOPES, La Paz: Re-port of internal investigation].

SERGOMIN, 2003. Mapa geológico del área del Silala proporcionado por la DIREMAR [Geological map of the Silala area provided by DIREMAR].

SERNAGEOMIN 2017. Geology of the Silala river basin. Volume 5, Annex VI of the Expert Re-ports, International Court of Justice, Controversy on the state and use of the waters of Silala (Chile vs. Bolivia), Report of the Republic of Chile.

Servicio Geológico de Bolivia, Informe sobre la Geología Regional de la parte Sudoccidental de Bolivia [Geological Service of Bolivia: Report on Regional Geology of the Southwestern part of Bolivia], GEOBOL-CONAMAR, 1977. vol. 1 y vol. 2.

Servicio Nacional de Geología y Minería, 1996, Carta Geológica de Bolivia Hoja 5927-6027 Silala- Sanabria, Escala 1: 100 000 [National Service of Geology and Mining. Bolivia Geological Charter Sheet 5927-6027 Silala-Sanabria, Scale 1: 100 000].

Servicio Nacional de Geología y Minería, 2003. Carta Geológica de Bolivia Hoja 5928-6028 Cerro del Inca-Laguna Khara, Escala 1: 100 000 [National Service of Geology and Mining. Bolivia Geological Charter Sheet 5928-6028 Inca Hill- Khara lagoon, scale: 1: 100 000].

Servicio Nacional de Geología y Minería, 2003. Estudio de cuencas hidrográficas-cuenca Pastos Grandes-Cuenca 16 [National Service of Geology and Mining. Study of hydrographic ba-sins- basin Large pastures-basin 16].

Servicio Nacional de Geología y Minería, 2003. Estudio de la geología, hidrogeología y medio am-biente del área de los manantiales del Silala (Proyecto de Integración PIR) Estudio de cuen-cas hidrográficas-cuenca manantiales del Silala cuenca 20. Junio 2000-2001 [National Ser-vice of Geology and Mining. Study of the geology, hydrogeology and environment of the area of the Silala springs (PIR Integration Project) Study of hydrographic basins-basin springs of the Silala 20. June 2000-2001].

Servicio Nacional de Geología y Minería. 2003. Carta Geológica de Bolivia Hoja 5928-6028 Cerro del Inca-Laguna Khara, Escala 1: 100 000. [National Service of Geology and Mining. 2003. Bolivia Geological Charter Sheet 5928-6028 Inca Hill- Khara Lagoon, Scale 1: 100 000].

Servicio Nacional de Geología y Minería. 2003. Estudio de cuencas hidrográficas - Cuenca Pas-tos Grandes-Cuenca 16 [National Service of Geology and Mining. 2003. River basin study – Pastos Grandes basin -basin 16].

Servant et. al., 1995; Sylverstre et. al., 1996, 1999.

Suárez, F., Sandoval, V., Sarabia, A., 2017. River-Aquifer Interactions Using Heat as a Tracer in the Silala River Transboundary Basin. CM. (Volume 5, Annex X).
Tomas Frias Autonomous University. Hydrogeological characterization of the Silala Springs, 2017. Uribe, J., Muñoz, J.F., Gironás, J., Oyarzún, R., Aguirre, E., and Aravena, R., 2015.
Evaluation of groundwater recharge in a closed Andes basin using isotope characterization and
rainfall-runoff model: Salar del Huasco basin, Chile. Hydrogeology Journal, 23, 1535-1551.

Viceministerio de Recursos Hídricos y Riego del Ministerio de Medio Ambiente y Agua, 2017.
Informe Técnico: 2da Campaña de Muestreo de Agua para el Análisis Hidroquímico e Isotópico y Diagnóstico de Canales en los Manantiales del Silala, Bolivia: s. n. [Vice Ministry of Water Resources and Irrigation of the Ministry of Environment and Water, 2017. Technical Report: 2nd Water Sampling Campaign for the Hydrochemical and Isotopic Analysis and Diagnosis of Channels in the Springs of Silala, Bolivia: s. n]

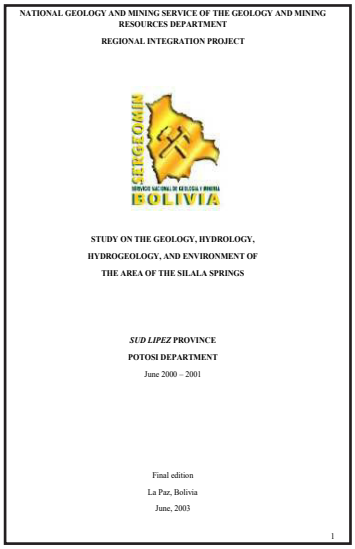
Choque, M.N. Putana Volcano Sheet, Series 1, CGB 41, 1996; Lema, Z., Ramos, C., Richter, DH., et al. Sanabria Sheet SGM I- SGB 43, 1996.

Annex 23.5

Appendix a

SERGEOMIN (National Service of Geology and Mining), Study of the Geology, Hydrology, Hydrogeology and Environment of the Area of the Silala Springs, June 2000-2001, Final Edition 2003

(English Translation)


NATIONAL GEOLOGY AND MINING SERVICE OF THE GEOLOGY AND MINING RESOURCES DEPARTMENT

REGIONAL INTEGRATION PROJECT

SERGEOMIN BOLIVIA

STUDY ON THE GEOLOGY, HYDROLOGY, HYDROGEOLOGY, AND ENVIRONMENT OF THE AREA OF THE SILALA SPRINGS

SUD LIPEZ PROVINCE

POTOSI DEPARTMENT

June 2000 – 2001

Final edition

La Paz, Bolivia

June, 2003

1

Basin N° 20
Study on the geology, hydrology, hydrogeology, and environment of the area of the Silala springs

Sud Lipez Province
Potosi Department

Prepared by:

Dr. Eng. Fernando Urquidi Barrau, Coordinator

Eng. Rodolfo Huaranca Olivera
Eng. Manuel Menacho Leon
Eng. Roberto Salgado Urquidi
Eng. Waldir Soruco Rodriguez
Eng. Julio Torrez Navarro
Eng. Alejandro Vargas Castillo, Assistant in Coordination
Eng. Egr. Nelson Huaranaca Olivera
Eng. Egr. Rene Ramos
Eng. Egr. Grover Salamanca Gutierrez

Eng. Marcelo Claure Zapata, SERGEOMIN's Executive Director
Dr. Jaime Argollo, External consultant
Eng. Joost Reidel, External consultant

Dig. Carlos Huanca Fernandez
Dig. Alejandro Ayarde Ontiveros
Dig. Jhonny Cano Guarachi

La Paz – Bolivia
June, 2001

CONTENT LIST

1. INTRODUCTION
1.1. Location and accessibility
1.2. Objective
1.3. General characteristics
2. REGIONAL GEOLOGY
2.1. Volcanic activity
2.1.1. Silala ignimbrites
2.1.2. Volcanic domes
2.1.3. Stratovolcanoes
2.2. Quaternary and Recent deposits
2.2.1. Glacial activity
2.2.2. Colluvial processes
2.2.3. Alluvial activity
2.3. Geomorphologic features
3. SURFACE GEOLOGY OF THE RAVINES OF THE SILALA WATER SPRINGS AREA
3.1. Formation of the Silala Ravines
3.2. Ravines in formation owing to weathering processes
3.3. Soils in the Silala Ravines
4. HYDROLOGY
4.1. Precipitation
4.2. Temperature
4.3. Evaporation
4.4. Flowrate gauging
5. HYDROGEOLOGY
5.1. Surface waters
5.2. Inventory of groundwater sources
5.2.1. South Canal – South or Oriental wetland
5.2.2. South Canal – Second wetland
5.2.3. South Canal – Third wetland
5.2.4. North Canal – North or Cajones wetland
5.3. Silala Aquifer
5.3.1. Characterization of the Aquifer
5.3.2. Piezometric levels
5.3.3. Recharge
5.3.4. Discharge
6. HYDRO-CHEMISTRY OF THE SURFACE WATERS
6.1. Water sampling
6.2. Classification of the water type
6.3. Age of the water
7. WATERWORKS
7.1. South Canal
7.2. North Canal
7.3. Main Canal

7.4. Desilting Chamber
7.5. Piezometric wells
8. ENVIRONMENTAL ASPECTS
8.1. Introduction
8.2. Surface waters
8.3. Soils
8.4. Flora
8.5. Fauna
8.6. Landscape
8.7. Historical and archeological resources
8.8. Human resources
9. CONCLUSIONS AND RECOMMENDATIONS
9.1. Regional geology
9.2. Geology of the Silala Ravine
9.3. Soils in the Silala Ravine
9.4. Hydrology and hydrogeology
9.5. Environment

TABLES

Table N° 2.1 Stratigraphic column of the study area
Table N° 4.1. Gauging of the Flows of the Silala Canals
Table N° 5.1. Localization of the springs and physical-chemical data
Table N° 5.2. Inventory of the piezometric wells
Table N° 6.1. Location of the water sampling sites
Table N° 6.2. Chemical composition of the Silala waters
Table N° 6.3. Location of groundwater samples for a tritium analysis

FIGURES AND PHOTOGRAPHS

Figure N° 1.1. Location of the study area
Figure N° 4.1. Histogram of monthly average rainfall
Figure N° 4.2. Histogram of monthly average temperature
Figure N° 4.3. Histogram of monthly average evaporation
Figure N° 5.1. Localization of the gauging sites
Figure N° 5.2. Inventory of the springs and piezometric soils
Figure N° 5.3. Localization of the water sampling sites
Figure N° 6.1. Piper diagram
Figure N° 6.2. Wilcox diagram
Figure N° 6.3. Schoeller diagram
Figures Numbers 6.4 to 6.14. Stiff diagrams

Photograph N° 1. Panoramic view of the study area, from south (Bolivia) to west (Chile)
Photograph N° 2. Geological contact between the ignimbrite mantle and lavas, with a panoramic view of the South wetland in the center
Photograph N° 3. Northwest view of the Inacaliri volcano, with its flows of andesitic lava. Negro hill can be seen in the right
Photograph N° 4. Quaternary cover of the South Canal, eastern sight
Photograph N° 5. Ravine in formation owing to weathering processes
Photograph N° 6. Springs that upwell from the South Canal intake
Photograph N° 7. Piezometric well in the North canal of the Silala area, the ignimbrite mantle that delimitates the wetland can be seen in the back
Photograph N° 8. Wetlands with springs delimited by the ignimbrite mantle
Photograph N° 9. Wetland that upwells from the North canal (secondary headrace canal) the ignimbrite mantle can be seen in the back
Photograph N° 10. Panoramic view of the South Canal, the formation of wetlands can be seen in the back
Photograph N° 11. North canal, main water collector
Photograph N° 12. Main canal, with a sight of the desilting chamber
Photograph N° 13. Hydraulic works built for the physical treatment of the water (decanter and desilting chamber)

OFFPRINTS

MAPS

Map N° 1. Regional geological map – at a scale of 1:50,000
Map N° 2. Geological map depicting the location of the Silala Springs and the location of the soil samples – at a scale of 1:5,000
Map N° 3. Hydrological map of the Silala area – at a scale of 1:10,000

SATELLITE IMAGES

Satellite image N° 1. Silala area
Satellite image N° 2. Landsat image of the Silala area – at a scale of 1:50,000
Satellite image N° 3. Spot image of the Silala area – at a scale of 1:50,000



Photograph N° 1. Panoramic view of the study area; to the south of Silala is Bolivia and Chile to west

STUDY ON THE GEOLOGY, HYDROLOGY, HYDROGEOLOGY, AND ENVIRONMENT OF THE SILALA SPRINGS REGION

1. INTRODUCTION

1.1 Location and accessibility

The study area of the Silala Springs is located in Canton Quetena, in Sur Lipez Province of Potosi department. Geographically, it is located in the western mountain range of the Central Andes, within parallels 21°58' and 22°04' south and 67°57' and 68°05' west (Figure N° 1.1.). To the west, it borders the international boundary with the Republic of Chile, crossing landmarks LXXIII, LXIV, and LXXV.

The region can be accessed easily from Laguna Colorada (38 kilometers to the south) by means of two permanent, secondary land roads. The La Paz-Uyuni-Laguna Colorada (Red Lagoon) road is found at an approximate distance of 950 km and is traversable almost all the year, with limited exceptions during rain seasons.

1.2 Objective

The purpose of the present study is to obtain knowledge on the geological, hydrological, and hydrogeological evolution of the Silala study area, which comprises an approximate extent of 150 km2, with an emphasis on the formation and evolution of the Silala ravines, the 79 km2 drainage area of the Silala, and the characterization of the spring waters that well up in the area surveyed.

This study is a component and an integral part of the Regional Integration Project (RIP) of the National Geology and Mining Service (SERGEOMIN, for its acronyms in Spanish) entrusted by the Ministry of Economic Development and the Ministry of Foreign Affairs and Worship.

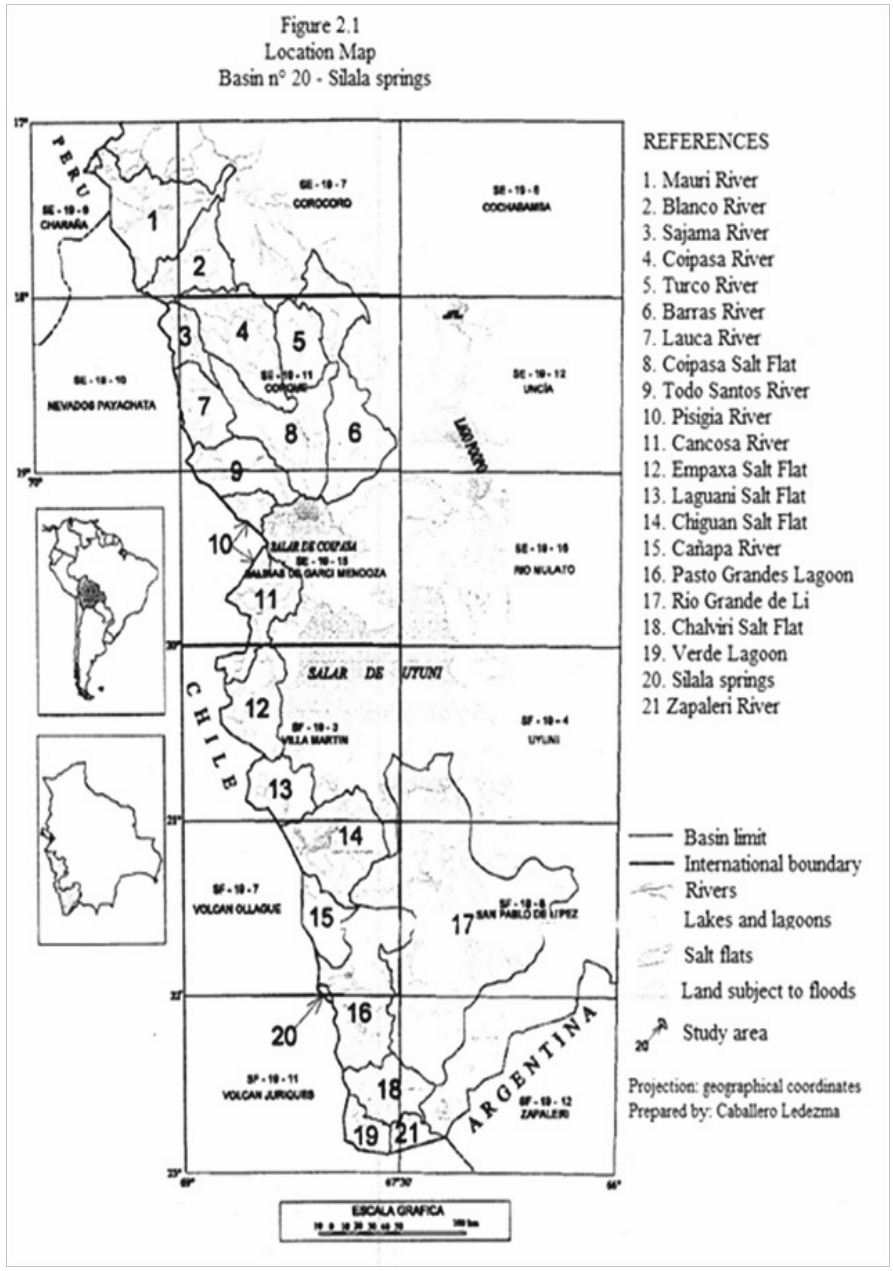
1.3 General characteristics

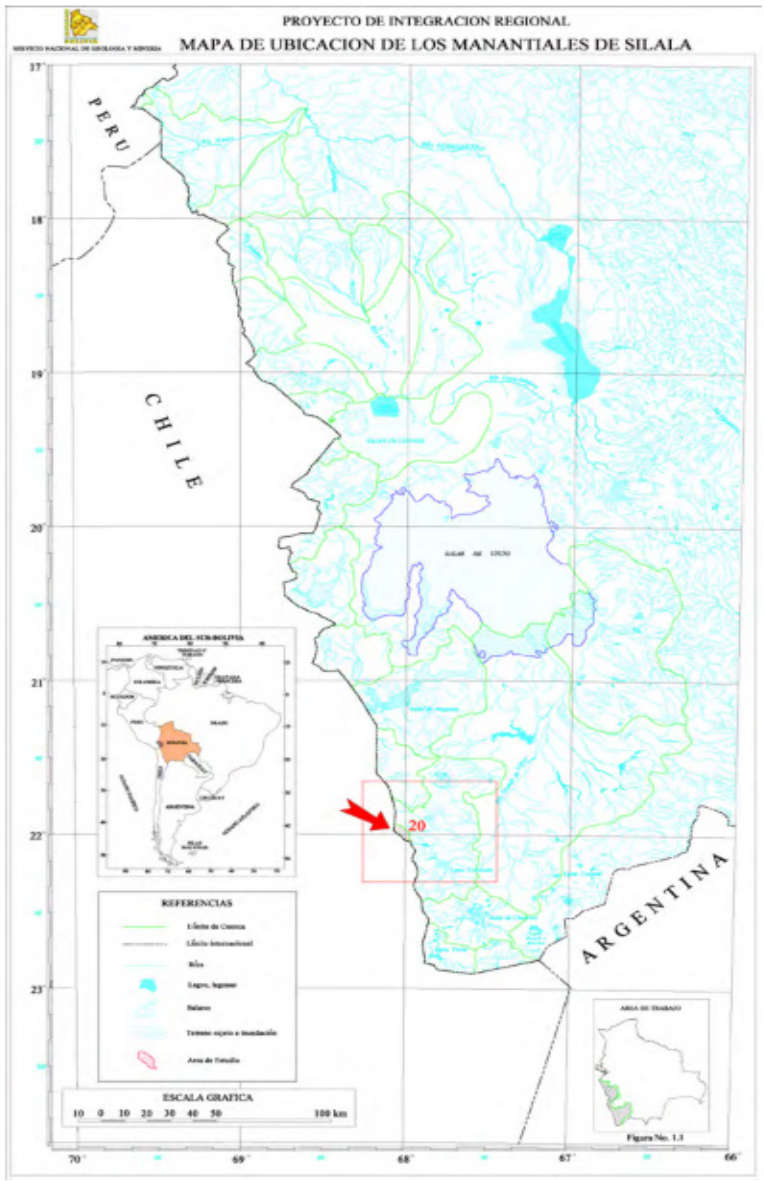
The study area is characterized by a flat-undulating topography, which slopes slightly to the west and is surrounded by domes and stratovolcanoes (Photograph N° 1). The altitudes within the area range from 4,278 meters above sea level (m.a.s.ls), at the boundary that crosses the Main Ravine of Silala, to 5,701 m.a.s.ls, on the top of the Silala Volcano (Satellite Image N° 1).

The study area is characterized by a climate that is common to high mountain desert zones. The flora and fauna are quite limited and characteristic of the western mountain ranges and the Bolivian High Plateau.

This region unpopulated; the closest community is that of Laguna Colorada (22 inhabitants), found 38 Km to the south-east of the study area.

Figure 2.1
Location Map
Basin n° 20 - Silala springs




PROYECTO DE INTEGRACION REGIONAL
MAPA DE UBICACION DE LOS MANANTIALES DE SILALA
PERU
CHILE
ARGENTINA
20
REFERENCIAS
ESCALA GRAFICA
10 0 10 20 30 40 50 100 km
Figura No. 1.1

2. REGIONAL GEOLOGY

The area of the Silala Springs is found in the southern block of the western mountain range and is part of the Central Volcanic Zone of the Andes. The regional geology is dominated by volcanic activities that date back to the Miocene and Recent ages and processes that occurred as a consequence of Pleistocene-Holocene glaciations. Map N° 1 shows a geological mapping of the area at a scale of 1:50,000 and Table N° 2.1. shows a detail of the stratigraphic column. Weathering, erosion, and deposition processes are represented by quaternary and recent unconsolidated sediments that cover vast surfaces of the area. The materials deposited form glacial, fluvioglacial, colluvial, and alluvial deposits formed by polygenic blocks or quarry stones, clasts from different rocks and of different sizes, and fine sediments—as sand and silt.
Tectonism of the study area is influenced by the uplifting and faulting of the Lipez regional block, known as the Cuña Occidental. The major manifestation of this tectonism in the area is the Khenayani faulting system (27 to 17 Myr), which crosses the area with a regional ENE direction, together with adjustment faults that follow the same direction and transversal adjustment faults with EW and WNW directions. The latter have a limited, yet deep extension, and made volcano effusion possible, resulting in the deposition of effusive igneous rocks and pyroclastic debris (Satellite image N° 1) and fractures of basal ignimbrite rocks.
Tectonism, manifested as faulting and jointing of effusive rocks of the area, is of utmost importance for the emergence of the Silala Springs.

2.1 Volcanic activity

The volcanic activity in the area is of significance and begins in the Andean Cycle of the Upper Miocene. During this cycle, volcanic craters, centers, and domes were formed, among which is that of Agua de Perdiz (found outside the study area), which is manifested with the eruption and deposition of a regionally large ignimbrite mantle known as Silala Ignimbrites. These are exposed in the area and are partially covered by lava flows from the stratovolcanoes intruded through them (Photograph N° 2). This is the first effusive phase in the area of study. The most evident volcanic structures, found within and around the area, are the volcanic domes of the Silala Chico and Torito hills, and the Inacaliri and Silala stratovolcanoes, which were formed by the accumulation of products that resulted from extrusive and effusive phases. The first extrusive phase is represented by the formation of volcanic domes. The second effusive phase is represented by andesitic lava flows and lavas of andesitic-dacitic composition.

The formation of volcanic centers as Cerro Negro volcano—the effusive volcanism of which formed deposits of andesitic lava that cover preexisting reliefs—began at the end of the Pleistocene age.

2.1.1. Silala ignimbrites

The regional basement is formed by mantles of consolidated volcanic tuffs denominated Silala Ignimbrites, characterized for having a clear pink, violet color, of a dacitic composition and are composed of plagioclases, quartz, biotite, and hornblende. These correspond to calcalkaline series rich in K2O, and its contents of SiO2 vary between 63% and 66%. The matrix of volcanic glass includes lithic fragments of different types of rocks, predominated by fragments of pumice stone of up to 10 cm of size. Its crushing index varies from 3 to 1. No information is available on its total thickness in the area, given that its basal contact cannot be observed and there is no knowledge on the rock type on which they rest. These are partially welded volcanic tuffs and are strongly fractured and jointed with two defined sets, one predominant dip direction is N40°E and the other N50°W. These ignimbrite mantles have an inclination to the west. According to extrapolated radiometric data from surrounding areas, these ignimbrites have an age of 7.8 ± 0.3 million years (Myr), that is, they date back to the Late Miocene (Choque, 1996; Lema & Ramos, 1996; Richter, et. al., 1992).

2.1.2. Volcanic domes

Silala Chico Hill Volcanic dome

A volcanic body of reduced dimensions emerges to the northwest of the Silala hill; namely, the Silala Chico hill volcanic dome, which intrudes the Silala Ignimbrites. It has a diameter of about 3 Km and culminates at an altitude of 4,849 m.a.s.ls. It is covered by lavas of an andesitic-dacitic, porphyry composition of a dark grey color, with 88% to 90% of plagioclases (andesine-labradorite) and 4% to 10% of pyroxene. Dating made on basis of samples collected by the PIR have found that the Silala Chico hill volcanic dome has an age of 6.04 ± 0.07 Myr.

Cerro Negro Hill volcanic dome

This volcanic body is found on the edge of the study area, in the northwestern sector. It has a basal diameter of 2 Km and an approximate altitude of 5,200 m.a.s.ls. It is formed by andesitic rocks of a light grey color.

Torito volcanic dome

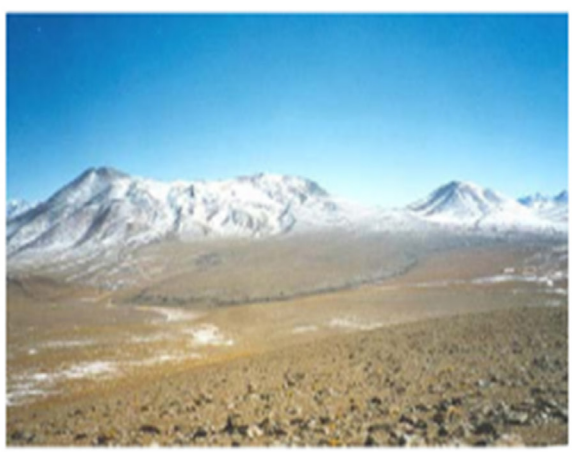
This dome is found in the eastern sector of the study area. It has a dacite and andesite composition and an approximate altitude of 4,900 m.a.s.ls. Its basal diameter is of approximately 1.6 Km.

TABLE 2.1
STRATIGRAPHIC COLUMN OF THE SILALA SPRINGS

ERA	AGE	PERIOD	LITHOLOGY	DESCRIPTION OF GEOMORPHIC PROCESSES	YEARS
CENOZOIC	QUATERNARY	HOLOCENE		STABILITY OF THE RELIEF DRY CLIMATE	
			ALLUVIAL DEPOSITS COLLUVIAL DEPOSITS FLUVIOAL-GLACIAL DEPOSITS	RELIEFS CHARACTERISTIC OF QUATERNARY SEDIMENTS WETLANDS EMERGENCE OF WETLANDS	10,000 years BP
		PLEISTOCENE	ALLUVIAL DEPOSITS COLLUVIAL DEPOSITS FLUVIOAL-GLACIAL DEPOSITS	FORMATION OF VALLEYS AND RAVINES ALLUVIAL RELIEFS MORAINIC RELIEFS GLACIATION	14,000 years BP 65,000 years BP
			BASIC ANDESITIC LAVA	FORMATION OF STRATOVOLCANOES SLIGHT MODIFICATIONS OF PALEORELIEFS	<10 Myr.
			Erosion surface		1,6 Myr.
	NEOGENE	PLIOCENE	ANDESITIC TO DACITIC LAVAS	FORMATION OF THE *INACALIRI* AND SILALA STRATOVOLCANOES	1,9 Myr.
				TECTONIC STABILITY FORMATION OF PALEOSOLS SEGMENTATION AND FORMATION OF VALLEYS EROSION PROCESSES	
			Erosion surface		5,3 Myr.
		MIOCENE	ANDESITIC-DACITIC LAVA (5.94Myr.) ADESITIC LAVA (6.04 Myr) SILALA IGNIMBRITES (highly fractured) (7.8 Myr.)	*INACALIRI* VOLCANO (phase I) *SILALA CHICO* VOLCANIC DOMES, *NEGRO* VOLCANO, AND *TORITO* HILL	



Photograph N° 2. Geological contact between the ignimbrite mantle and lavas, with a panoramic view of the South wetland in the center



Photograph N° 3. Northwest sight of the Inacaliri volcano, with its flows of andesitic lava. *Negro* hill can be seen in the right

It is estimated that these two volcanic domes date from the Upper Miocene, just as the Silala Chico volcanic dome and the first extrusive event of the Inacaliri volcano.

2.1.3. Stratovolcanoes

Inacaliri volcano

This volcano has an approximate basal diameter of 10 Km, culminates at a height of 5,570 m.a.s.ls, and is characterized by two effusive events.

The first volcanic event is represented by the effusion and deposition of andesitic lava of a dark gray color, similar, or relatively subsequent, yet occurring within the same volcanic event, to the rocks of Silala Chico Hill dome, with a radiometric age of 5.84 ± 0.09 Myr, as determined by the PIR (Uribe, Com. Per.). The radiothermal age of the second event is similar to that of the Silala volcano, dating from the Upper Pliocene between 1.9 Myr (Lema & Ramos, 1996) and 1.48 ± 0.02 Myr.

The second effusive event covers up the volcanic cone of the first event. A well preserved crater can be observed in the upper part of the volcano. This last volcanic activity discharged a flow of andesitic lava, a little more basic than that of the Silala volcano, covering the preexisting reliefs (photograph N° 3). The lava is composed of 80% of plagioclases and 18% to 19% of hornblende.

Silala Volcano

The Silala volcano is found on the southeastern edge of the study area. Its diameter is of 14 Km and its height is of 5,700 m.a.s.ls. Its slope varies, from the bottom to the top, between 12% to 40%. The rocks that form this volcano consist of andesitic-dacitic porphyritic lavas and of a dark grey color to a sky-blue one, characterized by 70% of plagioclases (andesine-labradorite) and 28% of pyroxene. They rest on the Silala pyroclastic flows and present a typical shallow radial paleodrainage. The age of the Silala volcano, as determined by the PIR Project, is of 1.74 ± 0.02 Myr.

2.2 Quaternary and Recent deposits

Unconsolidated deposits, or Quaternary and Recent soils cover approximately 30% of the surface of the area, and are represented by well-defined weathering, erosion, and deposition processes. The characteristics and composition of the soils sampled and analyzed from the Main Ravine and the North and South Silala Ravines are summarized in the present survey.

2.2.1 Glacial activity

The glacial activity, together with volcanic activity and weathering, shaped the geomorphological formations currently present in the region and is characterized by erosion and accumulation geoforms in the southern part of Inacaliri volcano

It is characterized by the main types of glacial erosion, as the formation of cirques and the deepening, enlargement, and widening of preexisting valleys, and has formed new potential watercourses, as those of the Silala Ravines. The forms of secondary accumulation, on the other hand, consist of lateral and terminal moraines and fluvioglacial deposits. Due to the geomorphological features of the glacial deposits in the area of study, the latter can be correlated with the last glaciation of the mountain ranges and the Bolivian high plateau (Argollo et al., 1987 and Argollo, 1991), which began approximately 65,000 of years BP.

Three groups of moraines encased in glacial valleys can be observed. The outermost or most distal one is located at an approximate height of 4,500 and corresponds to the Last Glacial Maximum, which occurred 14,500 years BP in the Central Andes (Argollo, J. 1991). Its age of origin was determined in other studies via radio-carbonic methods, mainly in peats and shells, for both the western and eastern mountain ranges. The second moraine is located at 4,670 m.a.s.ls and the last one at 4,800 m.a.s.ls, and correspond to the tardiglacial age.

Simultaneously, lengthy cryogenic flow tongues have been found in areas where there is no glacial activity, above the 4,700 m.a.s.ls. The frontal lobes of these can reach heights of up to 4 meters. These processes are not active at present.

Other intermediate, or combined formations consist of fluvioglacial sediments that are present as accumulations of a relatively heterogeneous granulometric composition. These sediments reach the outlets of glacial valleys that surround the stratovolcanoes and the Silala Ravines.

The fluvioglacial sediments that are found on the base of the Main, North, and South Ravines are detailed in the Soil Survey of the Silala area ravines.

2.2.2 Colluvial processes

The colluvial sediments, or deposits are located in different zones of the area and cover gentle slopes. These deposits present a quiet incipient sedimentary structure and are heterometric, and frequently polygenic.

2.2.3 Alluvial activity

Alluvial activity is represented by fluvioglacial water runoffs that gave place to types of erosion and accumulation 10,000 years BP. It is possible to observe alluvial fans of great dimensions, reflecting climatic conditions and amounts of water runoff that are completely different from the current ones. Other alluvial accumulation forms in the study area are alluvial plains characterized by red paleosols developed on ignimbrites that date back to 7.8 Myr and on andesitic-dacitic lava dating back to 1.7 Myr. In cases where springs emerge on the surface

they materialize as wetlands formed as a result of the influence of standing waters on sandy-clayey material, ranging from fine to medium grains, particularly on the upper part of topographic depressions, where the slopes are gentle, or simply don't exist. These are wetlands characteristic of highland areas.

2.3 Geomorphological features

The current geomorphological features of the Silala area were modelled 7.8 Myr ago. They began with the deposition of volcanic tuffs from the Silala Ignimbrites during the Upper Miocene over rocks that presumably date back to the Paleozoic basement, or the Lower Miocene, forming traditional plateaus with vertical hillsides and drainage systems that are not perceptible at present. These plateaus endured rough geomorphic alterations owing to the intense jointing and the degree of welding of the ignimbrites, together with, of course, the weathering action of the movement and melting agents of the glaciers, extreme temperature changes, and the wind. This resulted in the formation of cliffs that surpass the 100 meters of altitude, and red-colored paleosols in the region. These plateaus were subsequently covered by lava flows that conceal some of the original features of the ignimbrites and paleosols. Thereafter, the whole regional structural package rose slightly approximately 1.7 to 1.9 Myr (Lema & Ramos, 1996), presenting small inclinations to west, in parallel to the intrusion of volcanic cones and the formation of stratovolcanoes. Based on the ages obtained by the RIP, these geomorphic features might have been altered by a third volcanic event that took place 1.4 Myr ago.

During the glaciations that occurred 14,500 years BP, i.e. in the Last Glacial Maximum of the Central Andes mountain range, the geomorphic features were strongly altered by the movement and melting of the glaciers, resulting in the formations of lakes, lagoons, and salt flats throughout the Bolivian high plateau, as well as the formation of deep valleys, as the Silala.

Glaciation melting activity is one of the geomorphological features that have had the most notorious effects on the formation of the Silala ravine—a feature that was formed 10,000 years BP, or more. Ravines began forming at the end of this glacial episode (the tardiglacial). These are a typical example of the effects of meltwater, which occur predominantly on weaker zones of outcropping rocks, in this case the Silala Fault and the E-W transversal adjustment faults. However, the current design of the Main Ravine, characterized by a U-shaped geomorphic transversal cut with vertical lateral hillsides (15 to 100 m of altitude and 40 m of width) and a flat base, is the result of the combination of several weathering factors and not just fluvioglacial action. It is worth noting that since the Holocene, the depth and width of Silala Ravine do not have a relation with the amount of water that could flow within; in other words, there is a notorious geomorphic imbalance.

It is also important to note that the meltwater also constituted the main recharge of the groundwater that is currently stored in the ignimbrite rocks that date back to the Miocene, giving place to the formation of an acquirer that might either be confined or unconfined and that now upwells in the Silala springs.

During the Holocene, the climate became arid and desert-like—very similar to the current one. The surface water flows and runoffs reduced progressively, or even disappeared. The geomorphic features modelled from this period to the present are mainly the result of wind action and daily thermal differences. The effects of pluvial action on these features is almost nil.

The water that originates from a groundwater aquifer and that emerges as springs can only run on the surface, or through the ravines, when the discharge rate is high enough to defeat the high degree of evaporation, the infiltration occurring on the different types of soils on which water will run, and the relatively lower slopes.



Photograph N° 4. Quaternary cover of the South Canal, eastern sight

3. SURFACE GEOLOGY OF THE RAVINES OF THE SILALA WATER SPRINGS AREA

A detailed work on the soils and the jointing of the ignimbrite cliffs (Map N° 2) was carried out along the ravines where the canals were built to collect and direct the waters of Silala Springs. The soils are sandy, and contain different sizes of silt, clastic rocks, and quarry stones, which are characteristic of fluvioglacial deposits. The soil profiles of the Silala Ravines do not have defined horizons and do not present gradation, or visible depositional levels (photograph N° 4). There is no visible evidence of alluvial sequential deposition.

In the flat parts of the ravines, where the surface springs emerge, the soils are hydromorphic and tend to form wetlands with a horizon composed of organic material and that surpasses the 10 to 15 cm of thickness. In other regions, they are reduced to underlying sandy-loamy packages.

At the base of the Main Ravine's soils, there is a great amount of clastic rocks or quarry stones of a diameter of 30 cm, and many others of a bigger size. Glacial striations were observed on some of these quarry stones, evidencing a fluvioglacial transport and erosion. There are also traces of eolian and mechanical weathering processes in the rock formations present in the ravines, with an accumulation of angular and sub-angular shaped ignimbrite boulders and quarry stones deposited on the surface of the ravines.

3.1. Formation of the Silala Ravines

The Silala Ravines are a characteristic example of ravines formed as a result of the action of faults, giving place to a zone of weakness and to the combined erosive action of fluvioglacial waters and mechanical weathering in this weak zone. The fluvioglacial flow derives from the melting that took place at the end of the glacial era that dates back to more than 10,000 years BP.

The ravine of the Main Canal and the ravines of the South and North Canals (which follow a N50°E and N40°W direction, respectively) originally constituted shallow depressions in the Silala ignimbrite rock, which were formed along faults and weaker levels of strongly jointed rocks. The coinciding course of these depressions is confirmed by the study carried out on the joint system of the area. The weakness zones eroded and became deeper following a strong fluvioglacial erosion and their bottom became wider as a result of a strong weathering caused by the great daily differences in the temperature, forming U-shaped valleys.

At present, there are no active natural fluvial activities. The soil surface of the ravines is covered with sediments and different sizes of clasts of ignimbrite rocks which have not been removed owing to the absence of natural water flows. All of the clasts observed are sub-rounded, angular, and sub-angular, and there is a scarce presence of rounded clasts. This is a notorious indication that, since their formation, the ravines have not received any apparent natural surface runoff.

3.2. Ravines in formation owing to weathering processes

Sudden and marked temperature changes between the day and night in the study area give place to a second strong fracturing in the outcrops of ignimbrite mantles in the zones that present less weakness due to thermal differences (mechanic expansion and contraction processes), which complement the already strong jointing of the area. Wind erosion also contributes to this process. All these weathering processes form small ravines perpendicular to the main ravines, without or with limited contribution of alluvial processes. At least twelve of these ravines in formation were observed in the Ravine of the Main Canal (photograph N° 5) and others in the two ravines of the North and South Canals.

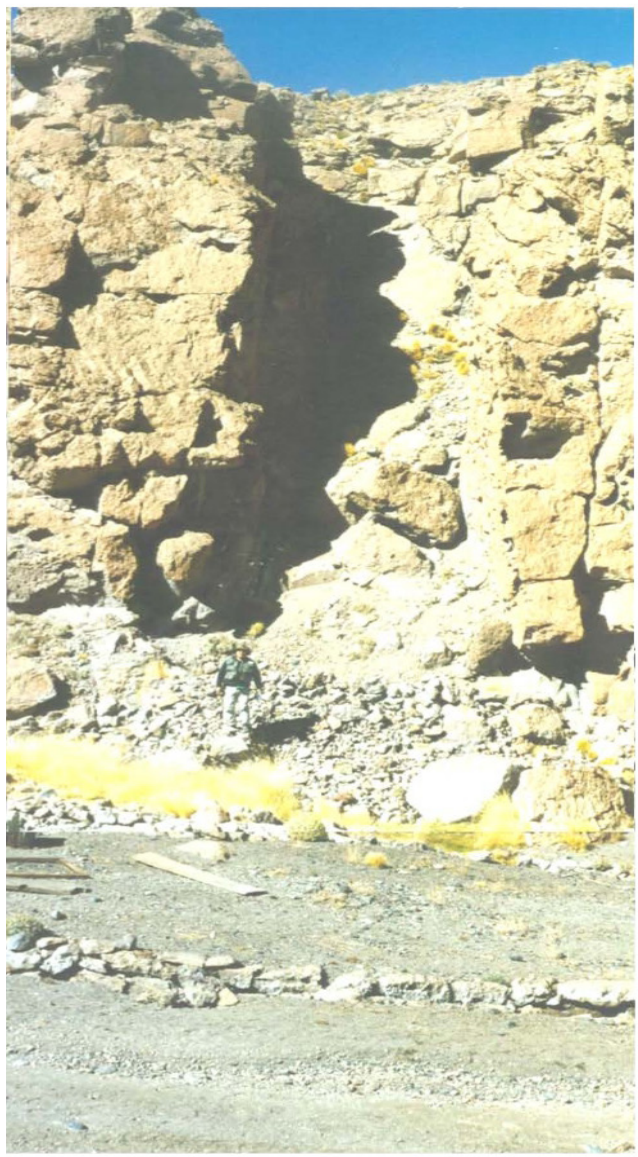
3.3. Soils in the Silala Ravines

This specific study of the Silala Ravines soils was carried out due to the importance of knowing the soil profiles, texture, composition, and constitution of these ravines. Four boreholes were dug in the Main Ravine and samples were taken every 10 cm of depth. Other four boreholes were also excavated in the North and South Ravines and in their respective wetlands. This detailed study, which includes the granulometric results obtained, is part of the Study on the Soils of the Silala Ravine.

The results of the granulometric study show that the grains of clasts and sands of the soils present sub-rounded edges. Very few clasts are rounded. This is an indication of the absence of significant surface runoff flows following the movement and deposition of the fluvioglacial sediments.

The analysis of the soil profiles of the Silala Ravine soils shows that the former are hydromorphic, and present a non-graded sequence of angular clasts of the parent rock, semi-angular sand grains, silt and thin horizons of organic material. The soil profile is not developed and is characteristic of high-altitude mountain soils of fluvioglacial origin. There are no traces of recent fluvial movement. No clear graded deposition of the materials that constitute the soil has been observed.

The granulometric study evidences grading that is typical of soils formed by fluvioglacial sediments, with clasts and angular grains, and an absence of clasts, gravel, and rounded sand grains.



Photograph N° 5. Ravine in formation as a result of weathering processes

4. HYDROLOGY

Owing to the significant climate changes registered 10,000 years BP, there are no hydrological systems in the study area. Climate becomes extremely dry and rainfall extremely scarce, or inexistent (Risacher, 1976; Argollo, 1995). The landscapes and structures observed in the area of study, and particularly in the Silala Ravine do not present active fluvial erosion. Thus, the river course depicted in the topographical charter of the Military Geographical Institute—Sheet 5927-I, Series H731, Silala Chico hill at a scale of 1:50.000—does not obey to the factual reality. Ravines constitute evident topographic depressions that can be observed in both aerial photographs and satellite images, with relatively vertical hillsides and horizontal plateaus, but characterized by the absence of active natural watercourses.

The area does not have a meteorological station. The hydrological parameters described below correspond to the Laguna Colorada meteorological station, which has a 13-year log history (1985-1997). This station is found 38 km to the SE of the study area.

According to oral information obtained from the rangers of the area, the FCAB enterprise had installed portable pluviometers in the Silala. During the completion of the present work, however, none of those instruments were found and it was thus not possible to obtain historical pluviometric data from them.

4.1. Rainfall

The monthly distribution of average rainfall is unimodal (Figure N° 4.1.). The rainfall season begins in December and lasts until March. This season represents the 80% of the total annual rainfall, with a maximum of 21.4 mm in January. The dry period takes place between April and November, with a minimum of 0.0 mm in July. The average annual rainfall for the 1983-1995 period is of 59.1 mm.

There is no meteorological data on snowfall, but it is estimated that the latter might increase pluvial precipitation data by 15 to 20%.

4.2. Temperature

The monthly distribution of monthly average temperatures is also unimodal (Figure N° 4.2.) The maximum temperatures are registered from December to March; the highest average temperature is of 3.9° C, in December. The lowest temperatures are observed from April to August, recording average temperatures that range from 0 to 4.0° C. The annual average of highest temperatures is of 14.2° C and the annual average of lowest temperatures is of -15° C; both these averages provide an approximate variation range of 29° C.

4.3. Evaporation

The monthly distribution of evaporation is also unimodal (Figure N° 4.3). The highest average evaporation rates are recorded between September and March, with values that vary from 78 mm in September to 113 mm in December.

The period of the year in which the lowest evaporation rates are recorded is between April and August; the lowest average evaporation rate was recorded in June, 36 mm.

In general, the months in which the highest evaporation rates are recorded coincide with those in which the highest temperatures are recorded, and those recording the lowest evaporation rates coincide with those recording the lowest temperatures. The relation between evaporation and rainfall is direct in some months. For instance, from April to August, when the lowest rainfall rates are recorded, evaporation is also low; from December to March, on the other hand, when rainfall rates are high, evaporation is also higher. This leads to the conclusion that during high precipitation seasons, rain is more likely to evaporate.

In the study area, average evaporation for the 1985-1997 period is of 914 mm, which means that evaporation is fifteen times higher than the rainfall registered, which is why it is necessary to consider this aspect for water balance calculations.

4.4. Flowrate gauging

In the South Wetland, the Silala Springs emerge on a relatively flat plateau formed by sandy hydromorphic soils that lack defined profiles and rest on the Silala Ignimbrites, forming wetlands. Springs also emerge in the three ravines, i.e. in the Main Ravine that prolongs towards Chile, and in the other two shallow ravines named North Ravine and South Ravine. The wetlands and ravines were canalized, after the waters were granted in concession to the FCAB in 1908, by means of open conveyance and abstraction canals covered with stone and mortar. These canals cross the ravines and have been denominated as the Main, North, and South Canal.

The North Canal follows a N-S direction, draining the North, or Cajones Wetland. The South Canal follows an E-W-SW direction, draining the South, or Oriental Wetland. Throughout the ravines, these two canals form a Y-shaped design, the two bifurcations of which merge and form a single canal that drains the waters, directing them to the international boundary with Chile (Map N° 2) and forming the Main Canal, which was built in the Main Silala Ravine.

The springs that emerge in the north hillside of the South Ravine have been canalized to utilize their waters; however, the water that wells up in the south hillside has been sealed and covered with mud and paja brava (Festuca orthophylla), presumably by employees of the Antofagasta-Bolivia Railroad Company (FCAB, for its acronyms in Spanish) while looking after the canals so as to avoid erosion in the path parallel to the canal. The upwelling waters in the left hillside (downstream), or to the south of the Main Ravine, have not been canalized and have also been covered and sealed with mud and paja brava to prevent runoff. Upwelling water cannot be observed in the north or right hillside (downstream) of the Main Ravine.

It is important to note that most of the upwelling springs in the Main Ravine, on Chilean side, are located in the north hillside of the ravine; only two of them are located in the south hillside.

The gauging of water flows was carried out in different months of the year and in three sites: a) North Canal, b) South Canal, and c) Main Canal, using Cipolletti weirs built by the Railroad Company in the canals, together with one measurement made with a propeller, recoding the rates presented below in Table N° 4.1.

TABLE 4.1
FLOW GAUGING OF THE SILALA CANALS

	Water flow calculated in liters per second (l/sec)				
	July	September	October	November	Average
North Canal	38	40	43	47	42
South Canal	82	110	176	91	115
Main Canal	120	164	219	153	164

Note: The indicated months correspond to 2000.

The flow measurement by sections in the three canals resulted in the following:

The average flowrate measured in the main section of the South Canal before the water falls is of 40 l/sec (measurement made in the intersection of the canal and the road).

The average flowrate measured in the South Canal before the intersection of the South and North Canals is of 129 l/sec.

The average flowrate measured in the North Canal is of 42 l/sec.

The average flowrate measured off the border, in the Main Canal, is of 164 l/sec.

Station: *Laguna Colorada* 22°13' South Latitude
Province: *Sud Lipez* 67°42' West Latitude
Recording period: 1983 to 1995 4,278 m.a.s.ls

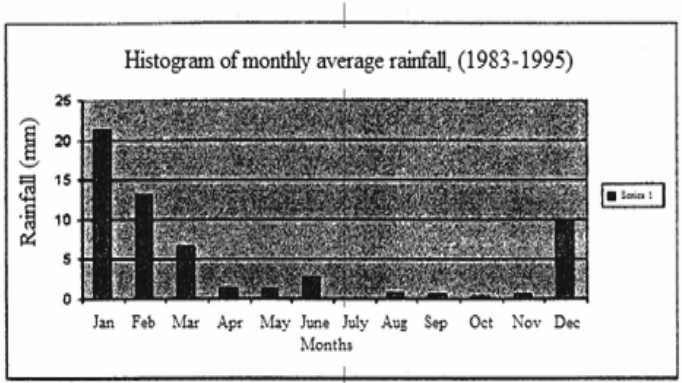


Figure 4.1

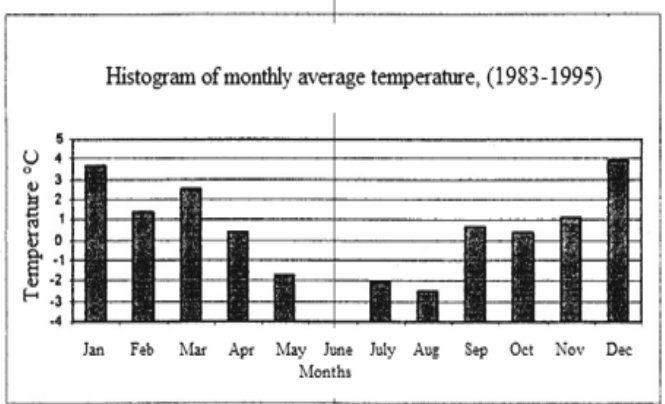


Figure 4.2

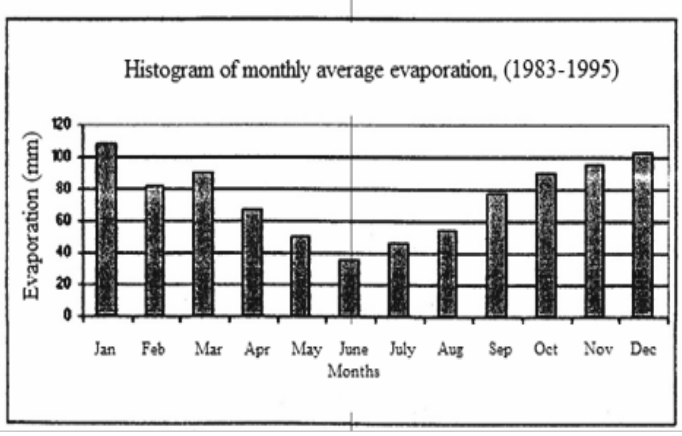


Figure 4.3

5. HYDROGEOLOGY

5.1. Surface waters

Basically, there are no surface water flows in the whole area of study. The only flow found is the one driven through the canals built at the beginning of the XX century, after the Concession for the Use of Waters was granted to the Antofagasta-Bolivia Railroad Company. The scarce rainfall does not allow the formation of surface runoff that might result in the formation of rivers, brooks, or others, be perennial or temporal. The scarce amount of water generated from the melting of snowfall deposited in the volcanoes either evaporates or is absorbed in the colluvial and alluvial sediments that cover their sides, without allowing any surface runoff.

The Laguna Blanca and Laguna Chica lagoons do not constitute actual bodies of water, but rather dry topographical depressions that have no surface water. The surface of Laguna Blanca is covered with 2 to 20 cm clasts of chert, or amorphous quartz, which give that lagoon that whitish color that can be observed in satellite images and aerial images.

5.2. Inventory of groundwater sources

With the objective of assessing the quantity and quality of the groundwater sources, a detailed inventory of the number of springs (photographs N° 6, 7, and 8) has been carried out for this report. The location of the water springs that well up in the wetlands and the ravines of the study area was carried out by technicians of the SETMIN by means of a detailed topographic survey presented in Map N° 2. To localize each groundwater source, the SETMIN used a GPS system with first-order accuracy.

Conductivity transmitters and digital pH equipment were used to measure the physical parameters of the water, together with flow gauging made with small propellers in almost all springs inventoried.

One of the purposes of this study is to establish the number, location, origin, and physical and hydro-chemical characteristics of the springs of the groundwater that wells up in the Silala area.

It has been found that there are at least 70 springs that are geographically concentrated in four zones and that have been canalized with the aid of open abstraction canals made of stone. Also, it has been found that some springs, that either have slow natural flows that follow different directions, or present standing, yet clean, waters, have not been canalized. In winter, these springs are covered with snow, unlike the canalized springs. The springs form surface humidity zones, which in turn form wetlands.

The total current surface area of the Silala wetlands is of 108,700 m2. The location, flowrate, and other physical characteristics of 44 springs are detailed in Table N° 5.1.



Photograph N° 6. Springs that upwell in the South Wetland



Photograph N° 7. Piezometric well in the North canal of the Silala area, the ignimbrite mantle that delimitates the wetland can be seen in the back

In the area, the springs concentrate in four main zones or wetlands (Figure N° 5.1) that are detailed below, from east to west:

5.2.1. South Canal – South, or Oriental Wetland

In the eastern, or oriental, edge of the South Canal, the springs well up from underlying ignimbrites towards Recent sediments or soils. The upwelling water saturates unconsolidated surface sediments forming the South, or Oriental wetland, which has a surface area of 65,200 m2 and is the biggest of all Silala wetlands. A total of 19 springs have been inventoried. These have been canalized with the construction of simple engineering works (stonemasonry) that comprise open canals that drive the waters to an open collector canal, forming the so-called South Canal. The South Canal follows an East-West direction until its intersection with the North Canal.

The first canalized spring wells up at an altitude of 4,450 m.a.s.ls. The flowrates of the canalized springs in this wetland vary from 0,25 l/sec to 2 l/sec. The electric conductivity of the groundwater varies from 240 µS/cm to 350 µS/cm and the temperature varies from 14°C to 16°C. Other springs that have not been canalized can also be observed on the surface of the wetland.

5.2.2. South Canal – Second Wetland

The second zone where four springs concentrate in the South Canal results from the upwelling of small amounts of water in the bed, or bottom of the Silala Ignimbrites and also forms a small wetland—which is almost dry in its entirety.

5.2.3. South Canal – Third Wetland

The third wetland of the South Canal begins at the foot of the first waterfall, which has an approximate height of 3m and has been formed by the E-W fault that crosses the area. This wetland has a surface area of 3,607.5 m2, begins at an altitude of 4,410 m.a.s.ls, and comprises a total amount of 18 springs—all of which are canalized. Its occurrence and physical characteristics are similar to those of the South, or Occidental Wetland.

In this third wetland, similar to the above mentioned ones, the occurrence of springs is controlled by the jointing and faulting of ignimbrite rocks. In some cases, the upwelling of up to three springs per lineal meter can be observed—a high density considering space and longitude. The flowrates of these springs vary from 0,5 to 2,0 l/sec, their temperature varies from 14°C to 15°C, and their pH is of 8. The canals that collect waters from upwelling waters or springs are perpendicular to a chief open collector canal that crosses the center of the wetland.

TABLE 5.1
LOCATION OF THE SPRINGS

Nº	UBICACIÓN	ESTE	NORTE	FECHA	Conduc. (mm/cm)	Tem. (°C)	pH	Caudal (l/s)	Procedencia
M-1	Sitala Norte	601195	7566790	5/26/00	94	13.00	7.86	0.5	Cuaternario
M-2	Sitala Norte	601075	7566700	5/26/00	121	15.40	8.15	2.4	Cuaternario
M-3	Sitala Norte	601043	7566740	5/26/00	127	15.90	8.28	3.5	Cuaternario
M-4	Sitala Norte	601010	7566735	5/26/00	124	16.10	8.56	12	Cuaternario
M-5	Sitala Norte	600950	7566750	5/26/00	122	16.00	8.45	7.1	Cuaternario
M-6	Sitala Norte	601060	7566640	5/26/00	126	15.90	8.13	0.25	Ignimbrita Sitala
M-7	Sitala Norte	600920	7566780	5/26/00	107	15.00	8.11	3.5	Cuaternario
M-8	Sitala Norte	600900	7566710	5/26/00	118	16.00	7.87	1.5	Cuaternario
M-9	Sitala Norte	600840	7566650	5/26/00	124	16.10	8.16	10	Cuaternario
M-10	Sitala Norte	600830	7566640	5/26/00	126	16.20	8.05	5.8	Ignimbrita Sitala
M-11	Sitala Norte	600875	7566675	5/26/00	111	16.50	7.97	16	Ignimbrita Sitala
M-12	Sitala Norte	600885	7566670	5/26/00	102	16.80	7.25	0.5	Cuaternario
M-13	Sitala Norte	600865	7566665	5/26/00	95	17.50	7.00	1	Cuaternario
M-14	Sitala Norte	600900	7566550	5/26/00	116	15.40	8.30	0.25	Cuaternario
V-1	Sitala Sur	601050	7566460	5/27/00	129	15.80	8.23	2	Ignimbrita Sitala
V-2	Sitala Sur	601055	7566462	5/27/00	130	15.50	8.39	1	Ignimbrita Sitala
V-3	Sitala Sur	601057	7566463	5/27/00	130	15.50	8.39	0.5	Ignimbrita Sitala
V-4	Sitala Sur	601100	7566500	5/27/00	128	15.70	8.35	0.5	Ignimbrita Sitala
V-5	Sitala Sur	601105	7566504	5/27/00	126	15.60	8.34	0.5	Ignimbrita Sitala
V-6	Sitala Norte	601140	7566730	5/27/00	145	14.90	8.50	1	Ignimbrita Sitala
V-7	Sitala Norte	601145	7566733	5/27/00	145	14.90	8.50	0.5	Ignimbrita Sitala
V-8	Sitala Sur	601185	7566570	5/27/00	167	14.60	8.23	0.5	Ignimbrita Sitala
V-9	Sitala Sur	601190	7566570	5/27/00	167	15.00	8.20	0.25	Ignimbrita Sitala
V-10	Sitala Sur	602900	7566187	5/29/00	260	13.70		0.25	Cuaternario
V-11	Sitala Sur	602900	7566188	5/29/00	255	15.70		2	Cuaternario
V-12	Sitala Sur	602900	7566189	5/29/00	253	16.00		1.5	Cuaternario
V-13	Sitala Sur	602675	7566200	5/29/00	251	15.90		0.5	Cuaternario
V-14	Sitala Sur	602674	7566200	5/29/00	250	15.40		0.25	Cuaternario
V-15	Sitala Sur	602823	7566200	5/29/00	240	15.70		0.25	Cuaternario
V-16	Sitala Sur	602822	7566200	5/29/00	237	15.70		0.25	Cuaternario
V-17	Sitala Sur	602800	7566215	5/29/00	248	15.20		0.5	Cuaternario
V-18	Sitala Sur	602800	7566225	5/29/00	258	14.20		2	Cuaternario
V-19	Sitala Sur	602820	7566250	5/29/00	230	15.30		2	Cuaternario
V-20	Sitala Sur	602815	7566249	5/29/00	230	15.10		0.25	Cuaternario
V-21	Sitala Sur	602805	7566251	5/29/00	225	14.10		0.5	Cuaternario
V-22	Sitala Sur	602790	7566254	5/29/00	218	12.10		0.5	Cuaternario
V-23	Sitala Sur	602710	7566130	5/29/00	350	7.10		0.5	Cuaternario
V-24	Sitala Sur	602695	7566129	5/29/00	370	5.00		0.5	Cuaternario
V-25	Sitala Sur	602673	7566127	5/29/00	412	16.00		0.5	Cuaternario
V-26	Sitala Sur	602595	7566180	5/29/00	278	14.80		0.25	Cuaternario
V-27	Sitala Sur	602000	7566470	5/29/00	357	13.80		0.2	Cuaternario
V-28	Sitala Sur	601975	7566450	5/29/00	370	14.00		0.5	Cuaternario
V-29	Sitala Sur	601974	7566450	5/29/00	365	13.80		0.25	Cuaternario
V-30	Sitala Sur	601930	7566496	5/29/00	364	14.00		0.5	Cuaternario

The wetland has an approximate width of 12 m and is found between walls, or cliffs of ignimbrite rocks (Silala ignimbrite) of 20 to 60 m of height. The wall, or cliff located to the south is the highest. A pathway presenting some upwelling water can be found along this wall, at 2 to 3 m from the bottom of the ravine. Said pathway has been covered and sealed with mud and paja brava, surely to preserve it.

Due to inadequate maintenance, some rocks that used to cover the lateral walls of the South Canal have now disappeared and the water is thus spilled and dispersed forming large puddles, or pooled waters.

Some of the traits characteristic of erosion caused by fast-moving water flows can be observed near the second waterfall, in the South Ravine's northern hillside, or cliff. These traits are visible at an altitude of 2 m from the current flow level and can be interpreted as erosion caused by strong fluvioglacial flows that occurred thousands of years ago, rather than as recent erosion (200 years BP) caused by recent pluvial flows.

5.2.4. North Canal – North, or Cajones Wetland

The fourth zone where springs congregate is found in the North, or Cajones Wetland, which consists of 26 canalized and inventoried springs. The springs have been canalized with the help of open canals, forming the North Canal. The total surface area of this wetland is of 40,908.8 m2 and the first spring upwells at 4,404 m.a.s.ls. The electric conductivity measured in the springs varies from 95 to 120 µS/cm, the temperature varies from 13° C to 16° C, and the pH varies from 7.70 to 8.35.

There are four 10cm-deep piezometric wells encased with 2 ½ inch iron pipes in the North Wetland. These wells were set up by the Antofagasta-Bolivia Railroad Company several years ago. The measurements made in these wells point to piezometric levels of 0.40 to 0.67 m above the surface.

5.3. Silala aquifer

5.3.1. Characterization of the Aquifer

On basis of the geological, hydrological, hydrogeological, and geophysical data at hand, in the absence of appraisal-well data, the following conclusions on the characterization of the Silala aquifer can be drawn:

The aquifer found in the Silala area is formed by the Silala Ignimbrites, and possibly by underlying geological formations that do not outcrop in neither the study area nor the region. The Silala ignimbrites are highly fractured and jointed. They outcrop in different regions of the area of study, owing to a varying erosion of volcanic rocks and to faults that have formed ravines that have been widened by fluvioglacial processes. The ignimbrites, due to their low degree of welding and high fracturing levels, allow the aquifer to have an effective transmissibility and permeability.

LOCALIZATION OF GAUGING SITES

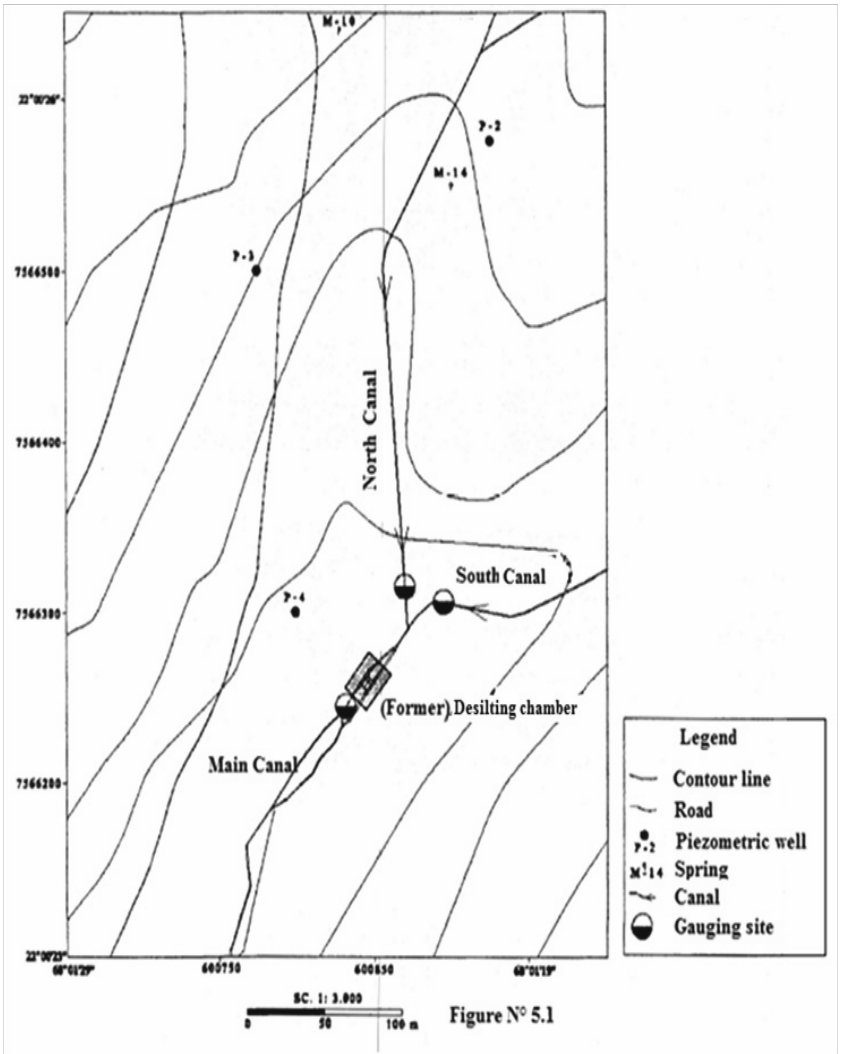
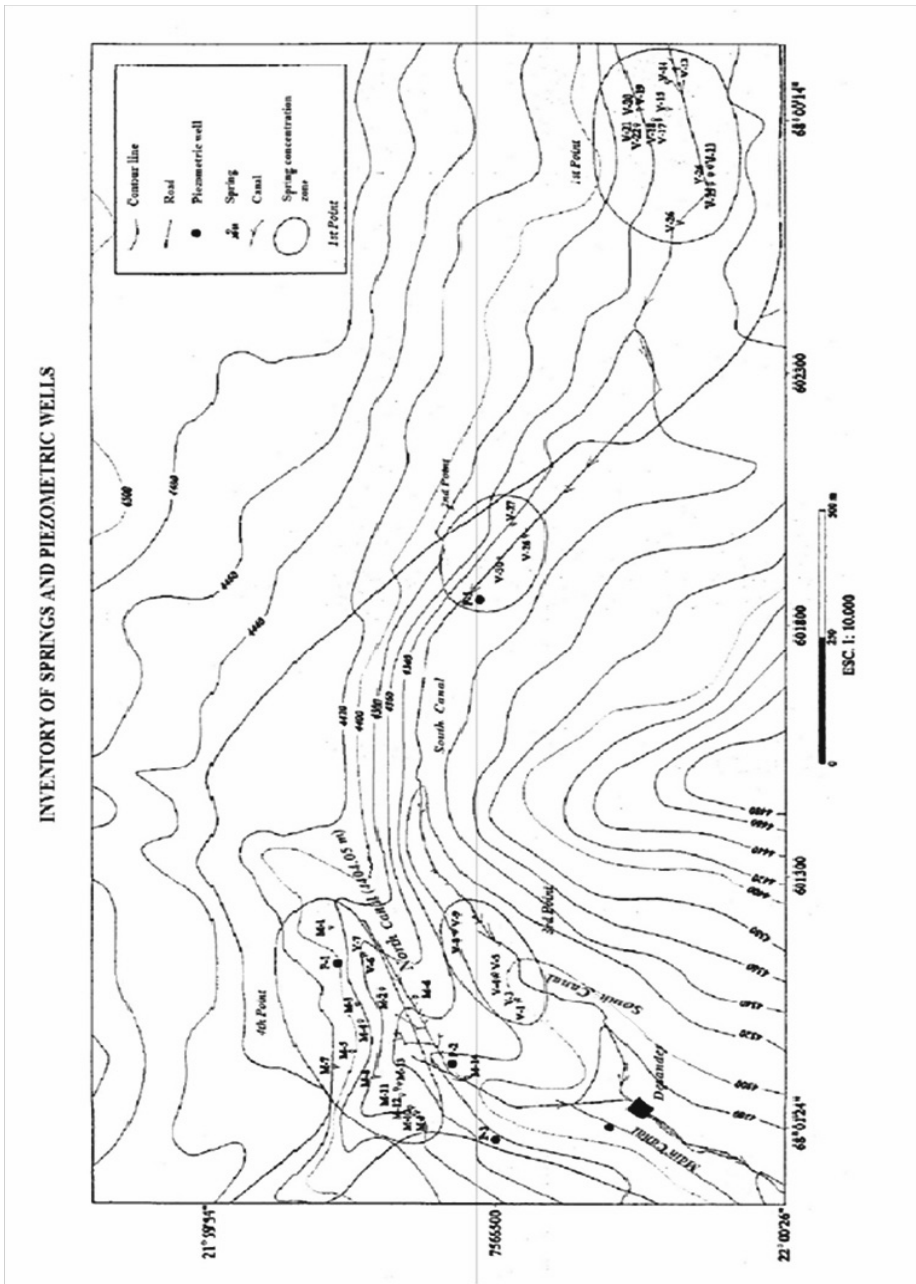
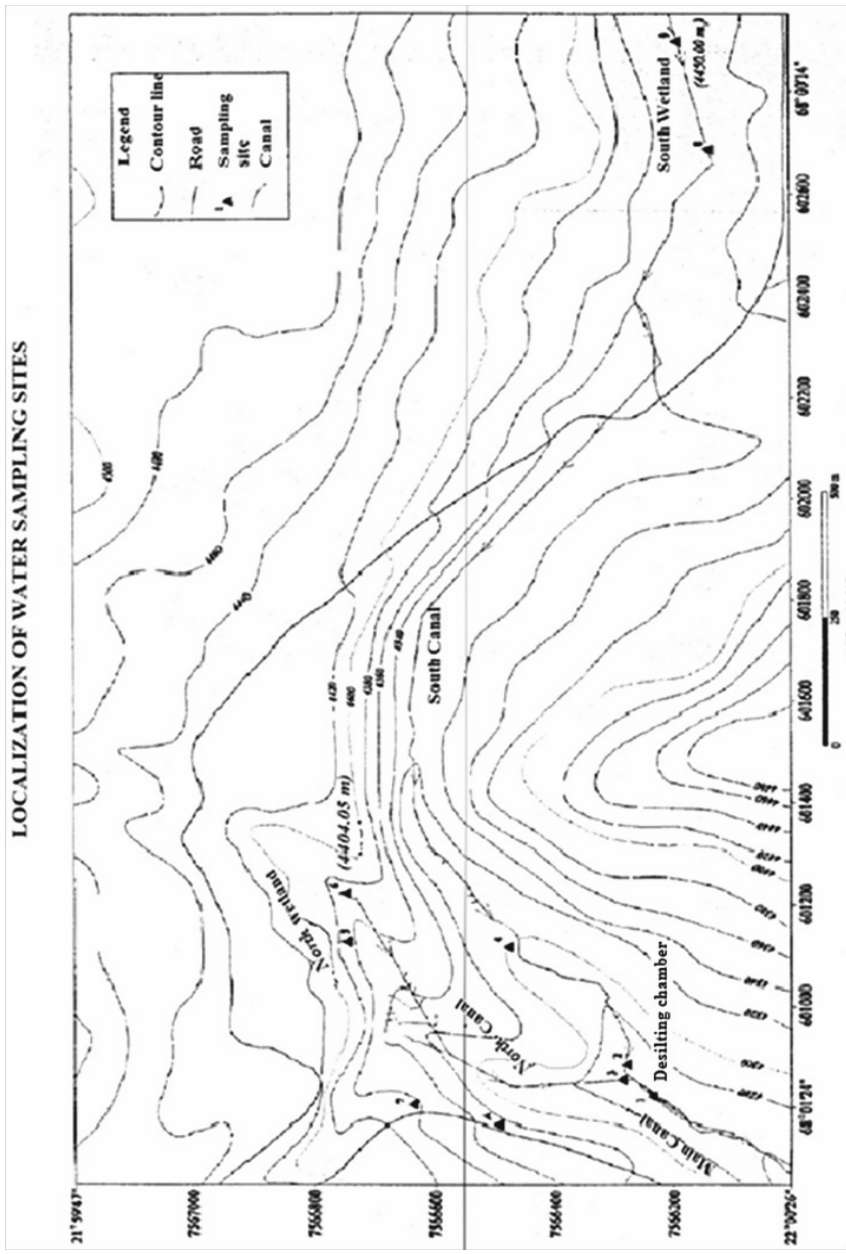


Figure N° 5.1


INVENTORY OF SPRINGS AND PIEZOMETRIC WELLS
Contour line
Road
Piezometric well
Spring
Canal
Spring concentration zone
1st Point
2nd Point
4th Point
South Canal
Main Canal
Diplomadero
ESC. 1: 10,000
21°39'34"
22°00'26"
68°01'14"
68°01'24"
7565500
601800
602300
601300


LOCALIZATION OF WATER SAMPLING SITES
Legend
Contour line
Road
Sampling site
Canal
South Canal
North Canal
Main Canal
Desilting chamber
North wetland
South Wetland
(4404.05 m)
(4450.00 m)

366

INVENTORY OF PIEZOMETRIC WELLS

N°	Location	East	North	Date	Depth (m)	Diameter (inches)	N.E. (m)	m.s.b.p.	Conductivity (mS/cm)	Temp. (°C)	p.H.	Flowrate (l/s)	Obs.
P-1	North Silala	601125	7566775	5/26/00	10.27	2 1/4"	surgent	0.67	88	15.7	8.03	0.25	Sample N° 5
P-2	North Silala	600925	7566575	5/26/00	10.15	2 1/4"	0.19	0.45	78	17	8.48		
P-3	North Silala	600775	7566500	10/24/00	9.75	2 1/4"	2.17	0.75	227	7	8	0.1	Silala Chile 7
P-4	North Silala	600800	7566300	5/26/00	10	2 1/4"	0.20	0.40	115	9.1	8.4		
P-5	South Silala	601850	7566530	5/29/00	5.95	2 1/4"	0.46	0.46	342	6.2			



Photograph N° 8. Wetlands with springs delimited by the ignimbrite mantle

Of the aquifer [sic]. Two main systems of joint-sets have been found: 67% percent of them follow a NE-SW direction and the remaining 23% follow a NW-SE direction.

All of the springs that well up in an artesian manner in the Silala area constitute discharges from the Silala Ignimbrites aquifer. In many cases, it is possible to observe springs that upwell directly from the joints and cracks (Photograph N° 9). The Quaternary and Recent fine sediments that cover the ignimbrites are fed and saturated by the water discharged from the underlying ignimbrite aquifer, forming wetlands.

The Silala aquifer is a regional aquifer that emerges to the surface

in an artesian manner in both Bolivia and Chile, and it might be either a confined or unconfined aquifer—it would be necessary to drill at least two appraisal-wells to define its true origin, the thickness of its ignimbrites and underlying rocks, and the aquifer level or levels. Pumping tests would also be required to determine the permissible discharge levels.

Owing to the hydro-chemistry and physical parameters of the waters, there seem to be two levels of ignimbrite aquifers; an upper one, forming the South, or Oriental wetland, with upwelling waters at 4,450 m.a.s.ls, an average conductivity of 257 µS/cm, and a higher content of Ca, Li, and S04; and a lower aquifer level, springing up at 4,400 m.a.s.ls, with an average conductivity of 109 µS/cm, and a higher content of Na. This is the level at which the North or Cajones wetland wells up.

Contamination has not been detected in the waters that well up from the aquifer.

5.3.2. Piezometric levels

The static piezometric levels of the aquifer vary from 0.40 to 0.67 meters above the surface level, can be considered artesian wells, and are encased by underlying permeable layers. These measures were taken from the piezometric wells set up years ago in the North wetland. Table 5.2 shows the location and detail of the parameters measured in the five piezometric wells found in the Silala. The piezometer of the Third Wetland found in the South Ravine has a depth of 6m and presents a static groundwater level of 0.80 meters above the surface. According to all the data obtained—which matches the geophysical data—it has been established that the groundwater flow predominantly follows an East to West direction and that the aquifer presents high pressure that increases in the same direction.

The permanent upward flow strongly suggests that there is a hydraulic connection within the Silala Ignimbrites, or with a lower permeable layer.

The third piezometer set up in the North Wetland does not present upwelling waters and is located in a zone of the wetland (which is dry) that does not present springs. The depth of the water measured in this piezometer is found at 2m from the surface. This behavior of the aquifer is possibly due to the fact that the ignimbrites found in this region are not highly fractured, unlike other regions of the Silala, or to their being found on the other side of the Silala Fault.

5.3.3. Recharge

Considering that pluvial precipitation is of 60mm/year and that the recharge area of the aquifer is of approximately 75 km2 (see Map N° 1), there would be an approximate volume of 5.5 million cubic meters available for infiltration towards the aquifer. Bearing in mind other parameters such as:

An infiltration factor of 20%, which is extremely high, as the aquifer’s recharge parameter.

Albeit it is known that evaporation is 15 times higher than rainfall, it can be inferred that the remaining 80% of precipitation constitutes the parameter of total losses to evaporation and evapotranspiration.

With these parameters, it is possible to determine that the current discharge volume of 164 l/sec, on the Bolivian side only, could not be sustained with the infiltration volume calculated, which would result in a discharge of about 38 l/sec. As a result, discharge/recharge from meteoric waters in the Silala ignimbrite aquifer is completely improbable.

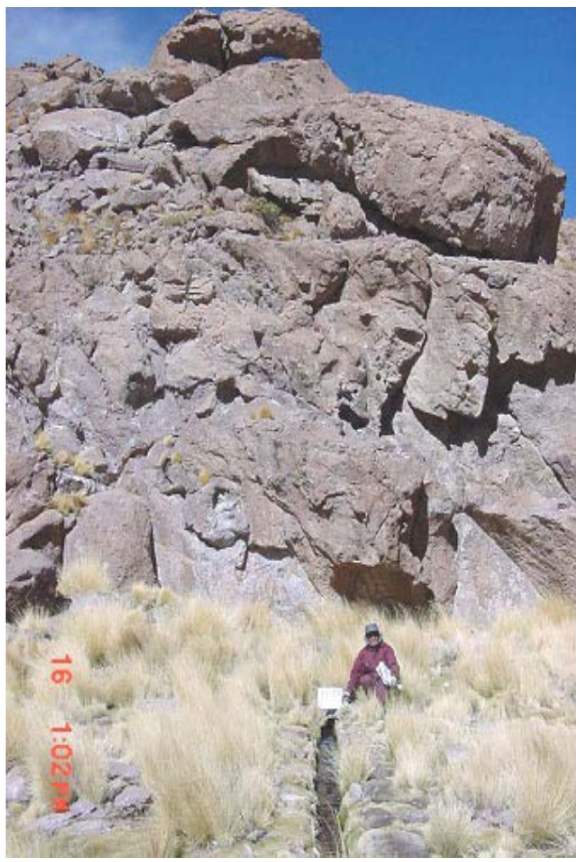
A recharge area 4.3 times bigger than the recharge area of the Silala would be needed, assuming that the recharge comes from pluvial precipitation.

In principle, *Khara* lagoon, found at 17 km to the NE of the Silala, was analyzed as a possible recharge source. The altitude of this lagoon, however, is the same as that of the upwelling springs found in the head of the South Canal. As a result, it is not likely that this lagoon recharges the aquifer. The lagoon is probably a surface manifestation of the Silala aquifer, draining to the east. The lagoon could also be the result of the combined recharge of other aquifers, apart from the Silala.

5.3.4. Discharge

In the Silala area, the aquifer is discharged through the joints and cracks of ignimbrite rocks found throughout the faulting zones, forming springs. Most of the springs well up towards fine-grained quaternary (Recent) sediments composed of lime, sand, and organic material deposited on flat zones, impregnating these sediments and forming wetlands.

The gentle slopes, high evaporation, and evapotranspiration, together with the low-rate of rainfall, and the composition and constitution of the ravines' soils, make free runoff along the ravines, forming continuous brooks or rivers, completely improbable. Currently, the aquifer's average discharge flow, which crosses Bolivia and is driven into Chile by means of open canals built by the FCAB for that specific purpose, is of 164 l/sec, at a measurement range that varies between 120 l/sec and 179 l/sec.



Photograph N° 9. Wetland that upwells from the North Canal (secondary headrace canal). The ignimbrite mantle can be seen in the back

6. HYDRO-CHEMISTRY OF SURFACE WATERS

6.1. Water sampling

For the purpose of characterizing the hydro-chemical quality of the waters that well up in the Silala region, a systematic sampling was carried out in nine points, covering the entire area of the springs (Map N° 2). Some of these points were sampled in successive visits to the study area. The location and characteristics of the sampled points is presented in Table N° 6.1. The samples were analyzed in the Water Laboratory of the Mining and Environment Department of SERGEOMIN, in the city of Oruro.

6.2. Classification of the water type

The range of electric conductivity of the water that wells up in the Silala region varies from 95 to 340 μS/cm. These values correspond to low-mineralization water, in accordance with the Bolivian Rules and Standards of the Ministry of Sustainable Development and Environment (MDSMA, for its acronyms in Spanish), which are in force in Bolivia since 1997.

According to the Piper Diagram (Figure N° 6.1) and the Stiff Diagrams (Figures 6.4 to 6.14), the waters analyzed constitute sodium bicarbonate waters. The MDSMA rules establish that Type A waters apt for domestic consumption must contain a maximum of 500 mg/l of bicarbonate and the Silala waters do not surpass the 208 mg/l. In regard to sodium content, the MDSMA rules provide that Type A waters contain a maximum of 200 mg/l; the waters analyzed in the Silala do not surpass the 95 mg/l. As a result, it is possible to conclude that the analyzed waters in the Silala region constitute Type A waters, apt for every use, including human consumption.

The waters destined for irrigation are classified in the Wilcox Diagram (Figure N° 6.2). Most of these waters are C1S1-type, and present a low salinity and low sodium absorption ratio (SAR). The Silala waters are apt for the irrigation of every type of soil. The M-8 sample is of the C2S1-type, with a slight increase in salinity (medium-salinity) and a low value of SAR. The water taken from this sampling point has a certain restriction for heavy soils. It is possible that this sample was contaminated when testing, or analyzing it.

The Schoeller Diagram (Figure N° 6.3) indicates that the sampled waters from the Silala aquifer are essentially of a single type, i.e. sodium bicarbonate waters, with slight hydro-chemical variations and minor variations in physical parameters.

The Stiff diagrams (Figures N° 6.4 to 6.14) confirm that the water type of the Silala springs are sodium bicarbonate waters.

TABLE 6.1
LOCATION OF THE WATER SAMPLING POINT

N°	Location	Date	Time	Source type	UTM East	UTM North	Conductivity (µS/cm)	Temp. (°C)	Flowrate (l/s)	Observations
1	Silala	06/01/2000	11:15	Intake (Canal)	600810	7566000	187	13	150	Total flowrate of the basin
2	South Silala	06/01/2000	11:15	South Canal	600890	7566300	218	12.5	90	Total flowrate of the south branch
3	North Silala	06/01/2000	11:15	North Canal	600863	7566310	120	14.6	60	Total flowrate of the north branch
4	South Silala	06/01/2000	11:40	Upwelling waters	601105	7566504	199	13.7	0.5	Fracture Upwelling waters (V-5)
5	North Silala	06/01/2000	12:10	Well	601125	7566775	88	15.3	0.25	Piezometric well (P-1)
6	North Silala	06/01/2000	12:25	Upwelling waters	601195	7566790	101	10	0.5	Headwaters of the north branch (M-1)
7	North Silala	06/01/2000	12:40	Upwelling waters	600830	7566640	127	16	5	Fracture Upwelling waters (M-10)
8	South Silala	06/01/2000	13:00	Wetland	602685	7566130	360	13.7		Wetland
9	South Silala	06/01/2000	13:30	Upwelling waters	602900	7566189	251	15.9		Headwaters of the south branch (V-12)
M	South Silala	24/10/2000	10:30	Well	600775	7566500	233	16	0.*	Piezometric well (P-3)

TABLE 6.2
CHEMICAL COMPOSITION OF THE SILALA WATERS

No	pH	Conduc. µS/cm	T S D Mg/L	Sól. Susp. mg/L	T. Hardness mg/L CaCO3	HCO3 mg/L	CO3 mg/L	SO4 mg/L	Cl mg/L	Na mg/L	K mg/L	Ca mg/L	Mg mg/L	Mn mg/L	Li mg/L	Fe mg/L
1	7.65	176.00	149.00	6.00	46.94	106.00	0.00	9.05	7.16	23.00	2.50	10.80	4.85	0.04	0.09	0.04
2	7.70	112.00	111.00	5.00	20.97	68.93	0.00	7.82	7.16	20.00	1.90	6.60	1.09	0.05	0.06	0.05
3	7.90	207.00	177.00	5.00	58.43	131.76	0.00	9.47	8.95	25.80	2.90	12.80	6.43	0.11	0.12	0.11
4	7.70	124.00	111.00	5.00	23.97	69,93	0.00	11.11	7.16	20.00	1.90	6.60	1,82	0.06	0.07	0.06
5	8.35	95.00	114.00	9.00	22.97	50.02	0.00	4.12	7.16	15.00	2.00	6.40	1.70	0.01	0.02	0.04
6	7.40	96.00	119.00	8.00	18.48	56.12	0.00	9.05	7.10	18.00	2.00	5.40	2.00	0.01	0.03	0.37
7	7.70	120.00	118.00	4.00	23.47	75.03	0.00	9.47	7.16	23.00	2.00	6.40	1.82	0.01	0.06	0.06
8	7.50	340.00	277.00	13.00	119.85	218.99	0.00	13.99	7.16	30.00	5.10	25.40	13.71	0.01	0.15	0.25
9	7.55	237.00	192.00	8.00	62.92	150.06	0.00	11.94	7.52	29.00	3.10	11.40	4.12	0.02	0.16	0.10
M	7.50	227.00	114.00	8.00	34.87	137..25	0.00	11.11	8.90	38.00	9.00	8.97	2.42	0.20	0.00	0.06

TABLE 6.3
LOCATION OF GROUNDWATER SAMPLES FOR TRITIUM ANALYSIS

No	Location	Field Data					Obs.
		Sampling date	Conduct. MS/cm	Temp. °C	pH	Flowrate l/S	
1	Silala	5/27/01	209	12	8.39	150.0	Main Canal
4	South Silala	5/27/01	132	14	8.67	0.5	Spring
5	North Silala	5/27/01	132	15.3	8.99	0.5	Spring
7	North Silala	5/27/01	131	16.1	9.21	5.0	Spring
9	South Silala	5/27/01	304	16	8.8	1.0	Spring
10	South Silala	6/27/01	187	13	8.4	35.0	Spring

The Stiff diagrams, as well as the conductivity values for the waters of the South, or Oriental wetland, present a slight difference in relation to the waters of the North, or Cajones wetland. These small differences, added to a difference in altitude of approximately 50m, with respect to the sampling sites, leads to the assumption that there might be different levels of water inside the aquifer. This assumption can only be confirmed by drilling appraisal boreholes, making geophysical "down hole" measurements, and carrying out detailed hydro-chemical analyses.

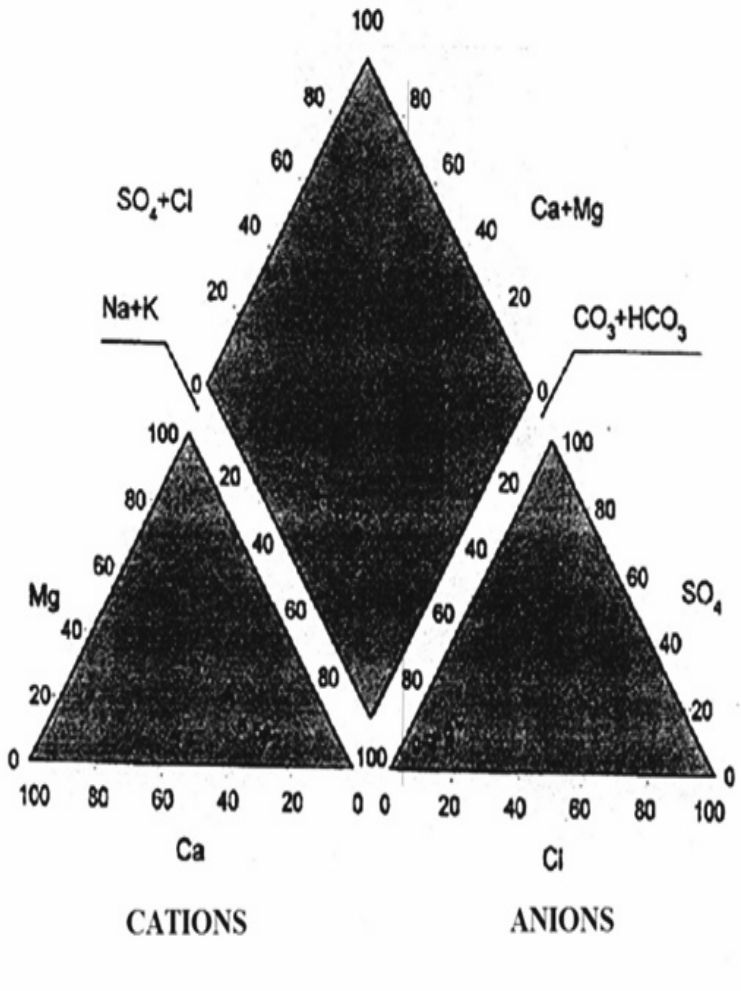
Due to their hydro-chemistry and physical parameters, the waters of the North Wetland are even cleaner and purer than those of the South Wetland, in spite of the fact that they apparently emerge from a deeper level of the Silala aquifer.

Another interpretation for this minor difference related to the water quality is that the southeast block of the Silala Fault is found at a higher altitude than the northwest block; thus, the waters of the South Wetland would be coming from a somewhat deeper level of the aquifer found in the southeast block of the fault and the waters from the North wetland would come from a higher water level than that found in the northwest block.

6.3. Water age

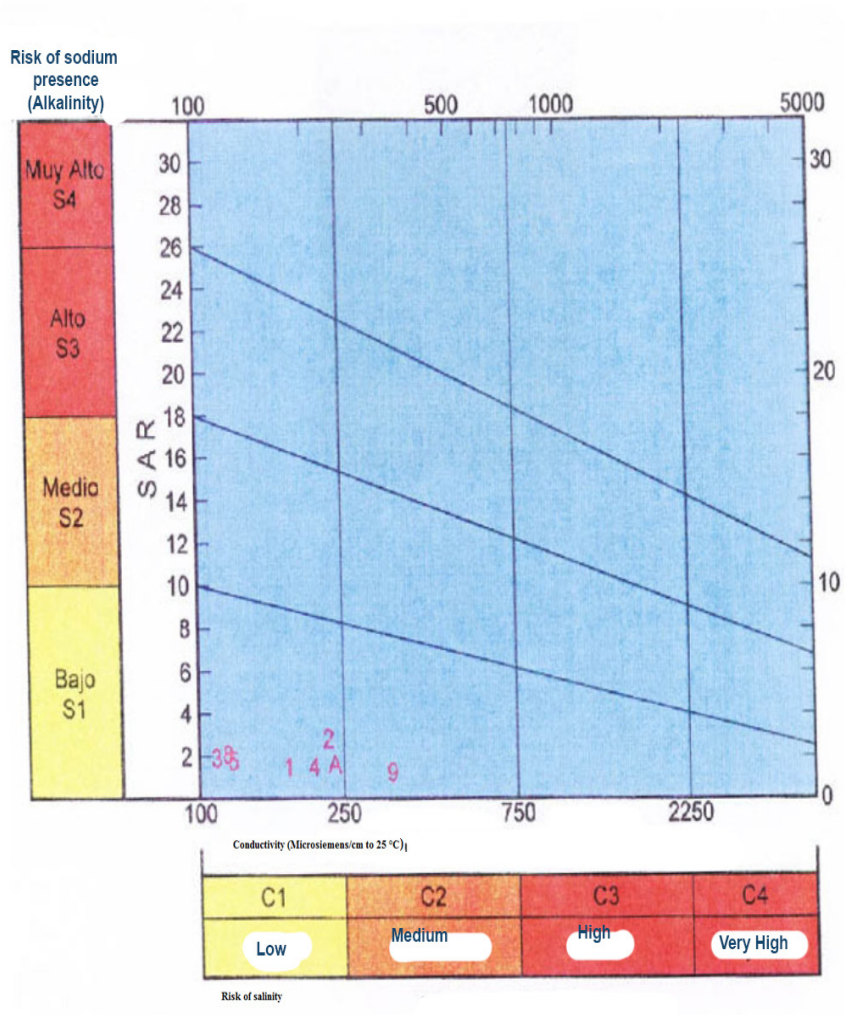
For the purpose of determining the water age of the Silala aquifer, nine samples (Table N° 6.3) were taken and analyzed in the laboratories of the *Federal Institute for Geosciences and Natural Resources of Hannover*, Germany, which reported the following, "unfortunately, the research made with the water samples from the Silala springs have only demonstrated that the said waters are at least 40 years old. In order to count on a more exact finding of the age of these waters, samples for a Carbon-14 analysis—which is time-consuming and cannot be carried out in Bolivia at present—should have been taken. However, we know that the tritium analyses, recharge time, and the emergence of the waters of the springs date back to at least 40 years ago. The conclusion is that the waters from the Silala Spring probably date back to a pluvial period, for instance, the one that took place during the Tauca phase, approximately 8,500 years ago."

PIPER DIAGRAM



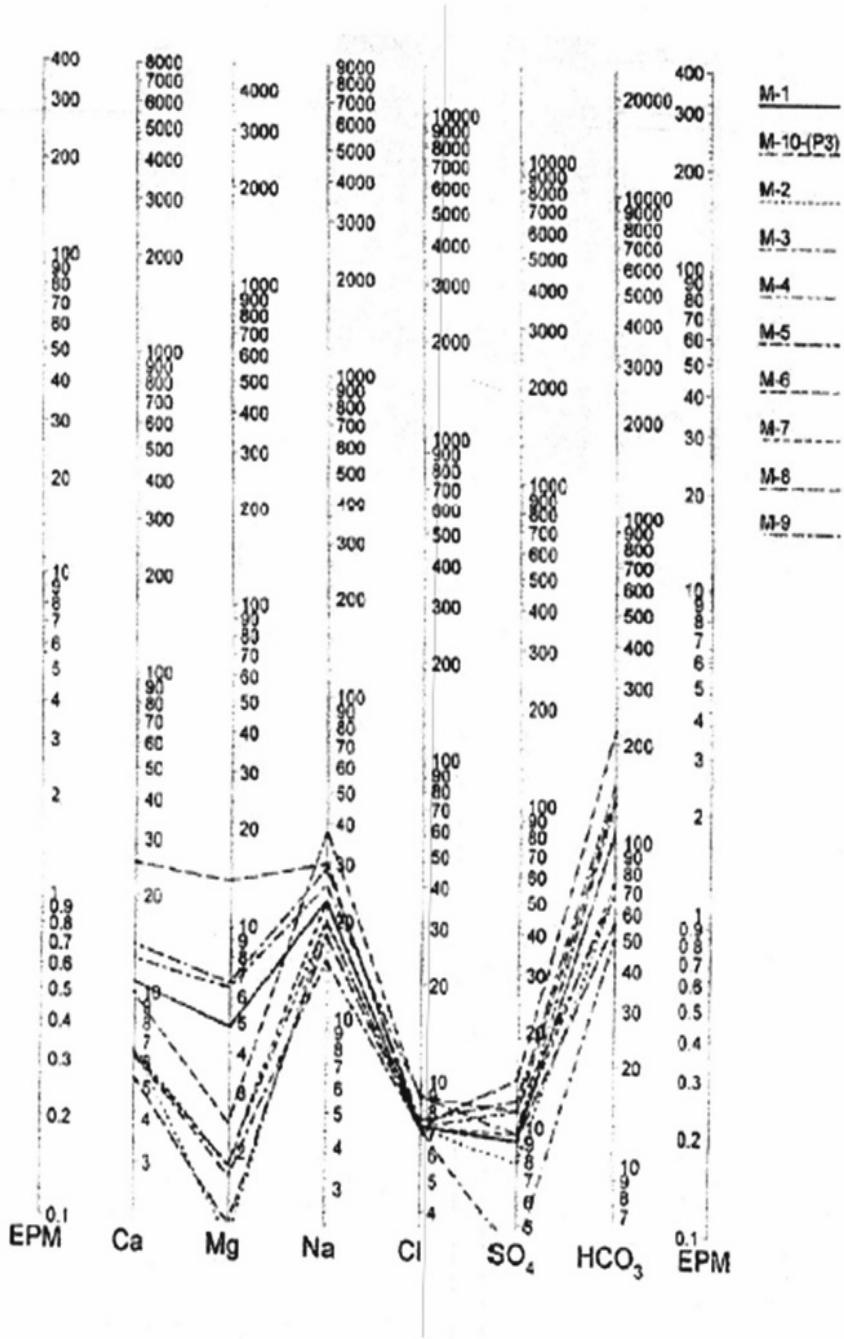
1 M-1
2 M-10-(P3)
3 M-2
4 M-3
5 M-4
6 M-5
7 M-6
8 M-7
9 M-8
A M-9

WILCOX DIAGRAM



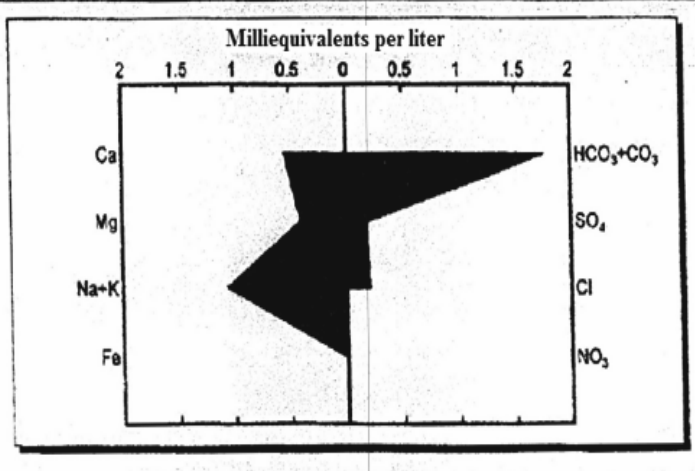
1 M-1
2 M-10-(P3)
3 M-2
4 M-3
5 M-4
6 M-5
7 M-6
8 M-7
9 M-8
A M-9

SCHOELLER DIAGRAM



STIFF DIAGRAM

Code: M-1 Silala



CATIONS					
	Ca	*Mg*	*Na*	*K*	*Fe*
Milliequivalents per liter	0.5389	0.3990	1.0005	0.06393	0.0021
Milligrams per liter	10.80	4.85	23.00	2.50	0.04

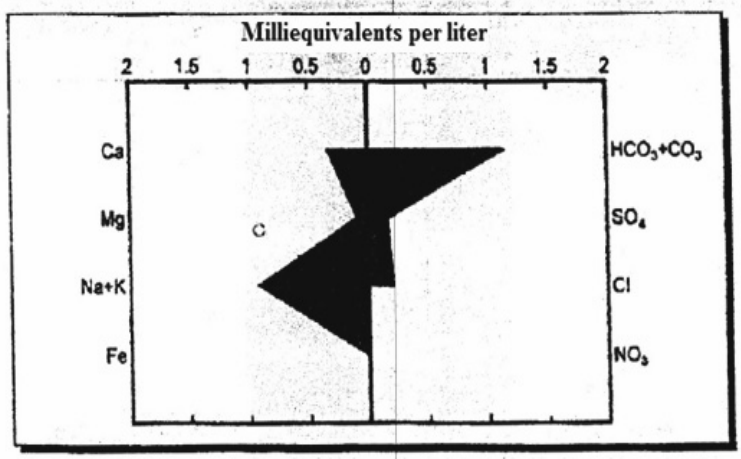
ANIONS					
	HCO3	*CO3*	*SO4*	*Cl*	*NO3*
Milliequivalents per liter	1.74390	0.0000	0.18842	0.20198	
Milligrams per liter	106.40	0.00	9.05	7.16	

Mn	NO2	PO4	F	B	SIO2
0.0000					
TDS	Hardness	Alkalinity	Conductivity	pH	SAR
149.00	46.9	1.7	176.00	7.65	1.4610

Water type: *Sodium bicarbonate*

STIFF DIAGRAM

Code:	M-2 Silala



CATIONS					
	Ca	*Mg*	*Na*	*K*	*Fe*
Milliequivalents per liter	0.3293	0.0897	0.8700	0.04858	0.0027
Milligrams per liter	6.60	1.09	20.00	1.90	0.05

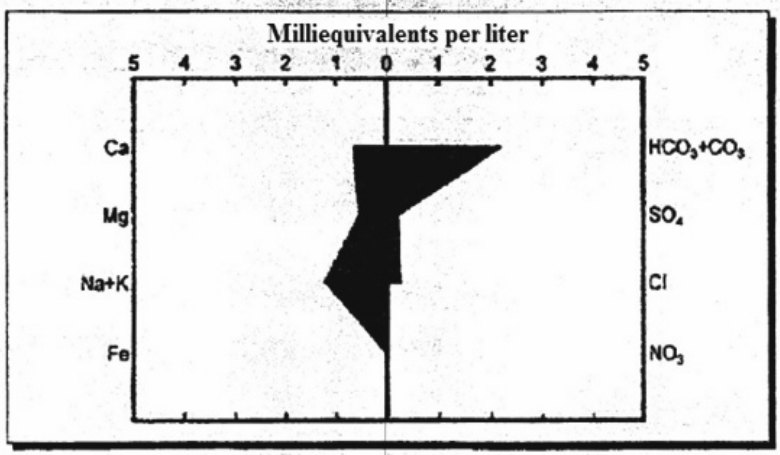
ANIONS					
	HCO3	*CO3*	*SO4*	*Cl*	*NO3*
Milliequivalents per liter	1.12976	0.0000	0.16281	0.20198	
Milligrams per liter	68.93	0.00	7.82	7.16	

Mn	NO2	PO4	F	B	SiO2
0.0000					
TDS	Hardness	Alkalinity	Conductivity	pH	SAR
111.00	21.0	1.1	112.00	7.70	1.9008

Water type:	*Sodium bicarbonate*

STIFF DIAGRAM

Code: **M-3 Silala**



CATIONS	*Ca*	*Mg*	*Na*	*K*	*Fe*
Milliequivalents per liter	0.6387	0.5289	1.1223	0.07415	0.0064
Milligrams per liter	12.80	6.43	25.80	2.90	0.12

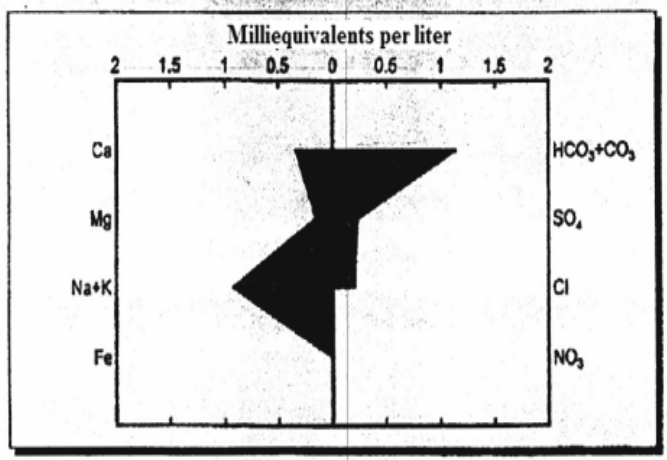
ANIONS	*HCO3*	*CO3*	*SO4*	*Cl*	*NO3*
Milliequivalents per liter	2.15955	0.0000	0.19717	0.25248	
Milligrams per liter	131.76	0.00	9.47	8.96	

Mn	NO2	PO4	F	B	SIO2
0.0000					
TDS	**Hardness**	**Alkalinity**	**Conductivity**	**pH**	**SAR**
177.00	58.4	2.2	207.00	7.90	1.4688

Water type: ***Sodium bicarbonate***

STIFF DIAGRAM

Code:	M-4 Silala



CATIONS					
	Ca	Mg	Na	K	Fe
Milliequivalents per liter	0.3293	0.1497	0.8700	0.04858	0.0032
Milligrams per liter	6.60	1.82	20.00	1.90	0.06

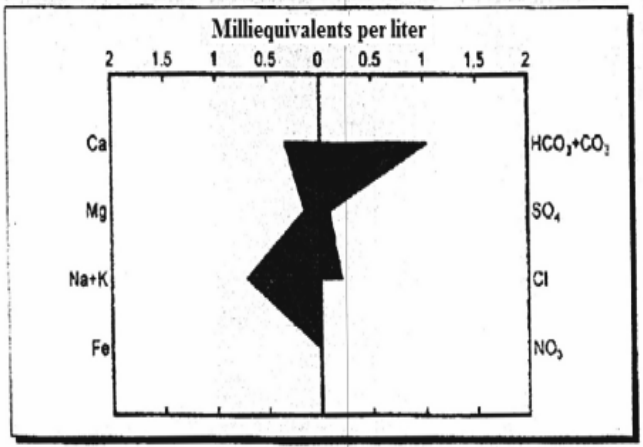
ANIONS					
	HCO3	CO3	SO4	Cl	NO3
Milliequivalents per liter	1.12976	0.0000	0.23131	0.20198	
Milligrams per liter	68.93	0.00	11.11	7.16	

Mn	NO2	PO4	F	B	SIO2
0.0000					
TDS	Hardness	Alkalinity	Conductivity	pH	SAR
111.00	14.0	1.1	124.00	7.75	1.7776

Water type:	Sodium bicarbonate

STIFF DIAGRAM

Code: M-5 Silala



CATIONS	Ca	Mg	Na	K	Fe
Milliequivalents per liter	0.3194	0.1398	0.6525	0.05114	0.0021
Milligrams per liter	6.40	1.70	15.00	2.00	0.04

ANIONS	HCO3	CO3	SO4	Cl	NO3
Milliequivalents per liter	0.81983	0.2000	0.08578	0.20198	
Milligrams per liter	50.02	6.00	4.12	7.16	

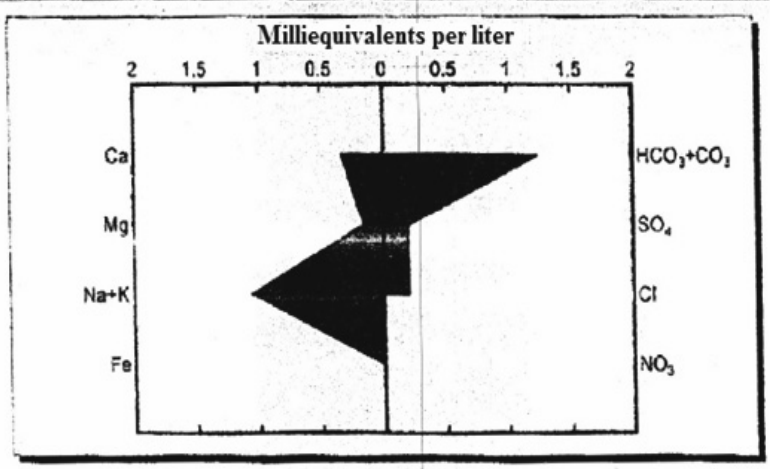
Mn	NO2	PO4	F	B	SIO2
0.0000					
TDS	Hardness	Alkalinity	Conductivity	pH	SAR
114.00	23.0	0.8	95.00	8.35	1.3617

Water type: Sodium bicarbonate

DIAGRAM 6 IS MISSING

STIFF DIAGRAM

Code: **M-7 Silala**



CATIONS	*Ca*	*Mg*	*Na*	*K*	*Fe*
Milliequivalents per liter	0.3194	0.1497	1.0005	0.05114	0.0032
Milligrams per liter	6.40	1.82	23.00	2.00	0.06

ANIONS	*HCO3*	*CO3*	*SO4*	*Cl*	*NO3*
Milliequivalents per liter	1.22974	0.0000	0.19717	0.20188	
Milligrams per liter	75.03	0.00	9.47	7.16	

Mn	NO2	PO4	F	B	SIO2
0.0000					
TDS	Hardness	Alkalinity	Conductivity	pH	SAR
118.00	23.5	2.0	120.00	7.70	2.0659

Water type: ***Sodium bicarbonate***

DIAGRAMA DE STIFF

Código	M-8 Silala



Cationes					
	Ca	*Mg*	*Na*	*K*	*Fe*
Miliequivalentes po litro	1.2675	1.1278	1.3050	0.13041	0.0134
Miligramos por litro	25.40	13.71	30.00	5.10	0.25

Aniones					
	HCO3	*CO3*	*SO4*	*Cl*	*NO3*
Miliequivalentes por litro	3.58925	0.0000	0.28127	0.20198	
Miligramos por litro	218.99	0.00	13.99	7.16	

Mn 0.0000	NO2	PO4	F	B	SIO2
TDS 277.00	Dureza 119.9	Alcalinidad 3.6	Conductividad 340.00	pH 7.50	SAR 1.1925

Tipo de Agua	*Sodium Bicarbonate*

DIAGRAMA DE STIFF

Código	M-9 Sitala



Cationes					
	Ca	*Mg*	*Na*	*K*	*Fe*
Miliequivalentes po litro	0.7086	0.5487	1.2615	0.07927	
Miligramos por litro	14.20	6.67	29.00	3.10	

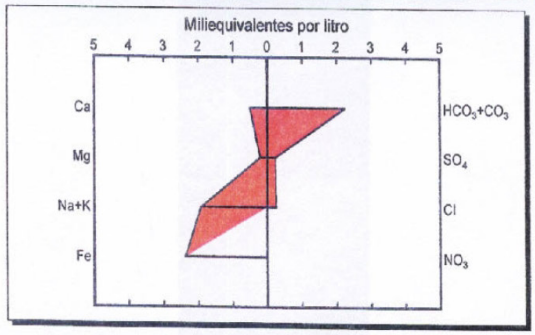
Aniones					
	HCO3	*CO3*	*SO4*	*Cl*	*NO3*
Miliequivalentes por litro	2.45948	0.0000	0.24859	0.21214	
Miligramos por litro	150.06	0.00	11.94	7.52	

Mn	NO2	PO4	F	B	SIO2
TDS 192.00	Dureza 82.9	Alcalinidad 2.5	Conductividad 237.00	pH 7.55	SAR 1.5911

Tipo de Agua	*Sodium Bicarbonate*

DIAGRAMA DE STIFF

Código	7-Silala-P3



Cationes					
	Ca	*Mg*	*Na*	*K*	*Fe*
Miliequivalentes po litro	0.4975	0.1991	1.6530	0.25570	2.3637
Miligramos por litro	9.97	2.42	38.00	10.00	44.00

Aniones					
	HCO3	*CO3*	*SO4*	*Cl*	*NO3*
Miliequivalentes por litro	2.24953	0.0000	0.23131	0.25107	
Miligramos por litro	137.25	0.00	11.11	8.90	

Mn	NO2	PO4	F	B	SIO2
0.0073					
TDS	Dureza	Alcalinidad	Conductividad	pH	SAR
159.00	34.9	2.3	227.00	7.50	2.8009

Tipo de Agua	*Sodium Bicarbonate*

7. HYDRAULIC WORKS

At SERGEOMIN's request, the Mining Technical Service (SETMIN, for its acronyms in Spanish) measured and mapped a total of 3,695m open abstraction canals and secondary conveyance canals. The abstraction canal has an average width of 0.8 meters and an average depth of 0.5m.

The difference between the height measured by the SETMIN, from the eastern edge of the South Canal to the point where the Main Canal meets the international border with Chile is of 114,21 meters. Where the Silala ignimbrites outcrop in the cliffs of the South Canal's South Ravine, it has also been found that there are areas that have been drilled and blown up with explosives, surely to improve the discharge and flow of groundwater.

The main structures that drive the waters towards the Chilean border comprise open abstraction canals that converge with the main canal. The dimensions of these rectangular canals—base and height—vary from 0.60m by 0.60m in the North and South Canals to 1.00 m by 0.60 on the border line. All the canals are open and covered with stone masonry. Their lateral walls are also covered with stones obtained from the nearby regions, and are coated with mortar in some sections. The masonry works were subsequently cemented in certain places.

The degree of efficiency of these hydraulic works is unknown, but it is estimated at a 40%.

7.1. South Canal

This is an open abstraction canal of a longitude of 2,305m (Photograph N° 10). This abstraction canal is connected with two branched systems of secondary conveyance canals in the area of the South, or Oriental Wetland (Map N° 2); the systematic utilization of the waters that well up in the wetland's springs begins with these conveyance canals until they meet the North Canal.

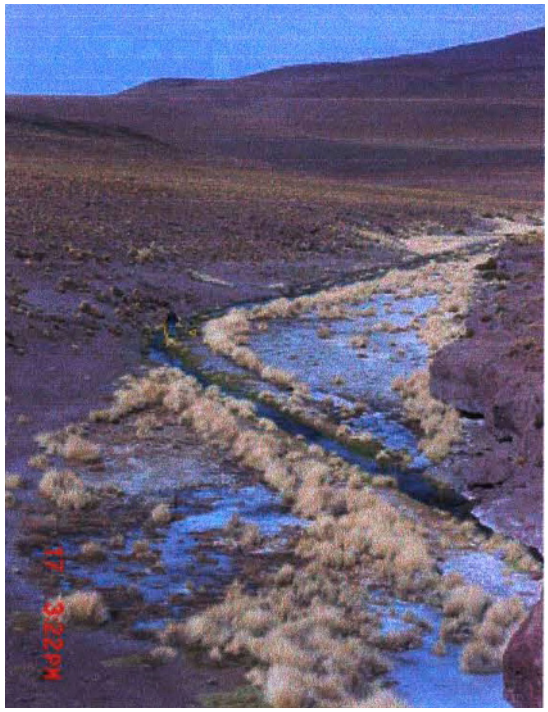
7.2. North Canal

The North Canal is also an open canal of a longitude of 662m, and it shares the same construction characteristics as the South Canal. It was built to collect and drive the water that arises in the springs of the North, or Cajones Wetland (Photograph N° 11).

7.3. Main Canal

The two canals above mentioned converge in the east and merge into a single canal, the Main Canal, which drains water from the Main Ravine (Photograph N° 12). The Main Canal has an extension of 712m from the confluence of the South and North canals, and extends to the border

Photograph N° 10. Panoramic view of the South Canal, the formation of wetlands can be seen in the back





Photograph N° 11. North canal, main water collector



Photograph N° 12. Main canal, with a sight of the desilting chamber



Photograph N° 13. Hydraulic works built for the physical treatment of the water (Decanter and desilting chamber)

with Chile. The flowrates presented in Table 4.1 supra were measured in the outflow points of the North and South Canals—as well as that of the Main Canal—before they merge with one another.

7.4. Desilting chamber

To the west, and 31m downstream from the convergence of the South and North Canals, in Bolivian territory and forming an integral part of the Main Canal, there is a disused structure that was once fed by two canals built in its lateral walls (Photograph N° 13). This structure, made of cemented stone and comprising four cells, served the following purposes: a) as a desilting chamber, or decanter of sediments, or primary water treatment plant; b) as a loading chamber for the 10 to 12-inch steel pipes that came out from it; c) as a control dam for the discharge into the Main Canal. Based on the greenish coloration in its walls, it was possible to conclude that copper sulphate was likely used as the primary compound for water treatment. Two open concrete channels that bypass the main cells are found on both sides of the desilting chamber's external walls. At present, the open concrete channel found on the northwest wall is used and constitutes an integral part of the Main Canal, bypassing the structure.

Superposed to the current open stone canal, there are two 10 to 12-inch of diameter steel pipes that are partially buried and cut, and are completely disused.

7.5. Piezometric wells

Asides from the abovementioned hydraulic works, there are 5 piezometric wells made of 2 ½ inch steel pipes, with an average depth of 10 m. Four of these wells are found in the North Wetland and one in the Third Wetland of the South Ravine. These wells were probably used to carry out piezometric controls of the groundwater during the year, or to improve the groundwater flowrate.

It is important to note that all these hydraulic works were made by Chilean technicians and personnel of the FCAB many years ago and no data or plans on them are available. It is rumored by the local people that there once was a perforated iron pipe buried in the wetlands to increase the groundwater discharge. This suggestion, however, has been refuted by the results obtained through the surface geophysical survey of conductivity carried out in the wetlands and in the Main Ravine.

8. ENVIRONMENTAL ASPECTS

8.1. Introduction

The results obtained in the preliminary baseline environmental study of the Silala area presented in this chapter comprise a compilation of the environmental data obtained to date in the several visits that have been made to the study area.

According to M. Liberman (1986), and the Simplified Map of Bolivia's Ecoregions, the study area falls under the ecoregion classification termed 'Highland Region or Mountain ranges', which corresponds to Uncultivated Semiarid and Arid Meadows, or High Andean Ecosystems, also known as 'Desert-like Puna' [or Puna desertica].

The Ministry of Sustainable Development and Environment has established provisions in its Rules on Water Contamination (Supreme Decree 24176 of December 8th, 1995) that allow comparing the existent, or baseline environmental conditions of the water resources of the Silala area with those governed by the Bolivian legislation.

8.2. Surface water

No surface waterbodies can be found in the Silala area, with the exception of those that well up from the wetlands' springs described in Chapter 5. The so-called Laguna Colorada and Laguna Chica lagoons are dry topographic depressions where no water is present. The surface of the Laguna Blanca is covered by 2 to 20-cm clasts of chert, or amorphous quartz, which give it the whitish color that can be seen in satellite images and aerial photographs.

The body of surface water that is the closest to the region is the Laguna Khara, found at 5.5 km to the NE. The Silala Springs, Laguna Blanca and Laguna Khara seem to be aligned with the path of the Khenayani Lineament. Another surface waterbody is the Laguna Colorada, which is outside the study area and is found 38km to the south of the Silala area.

Contamination effluents have not been detected in the area of study.

8.3. Groundwater

The entirety of the water that flows in the study area originates from underground sources and wells up on the surface as springs, or pooled waters. On basis of the physical and chemical properties of the Silala waters, these are classified as Type A waters, according to the Rules on Water Contamination. These constitute drinking waters that are apt for human consumption with the help of a simple bacteriological disinfection.

The water inflow in the study area is not being monitored in any way.

For a future exploitation of the groundwater resources of the Silala region, it would be strictly necessary to abide by Chapter IV—Preservation of

Groundwater—of the Rules on Water Contamination of the Environmental Law, and to administer, or manage the groundwater aquifers, both upstream and downstream, in a sustainable way.

8.4. Soils

Regionally, the soils of the Silala area present two particularly manifest physiographical forms. The zones that are covered by ignimbrite plateaus, cones, domes, and lava flows are characterized for presenting shallow soils of a brown, reddish-brown color and a light texture that ranges between sandy-loam to clay-loam, which are generally fused with gravel and quarry stones. These soils are vulnerable to erosion, and their use for agricultural ends is highly and manifestly limited.

The alluvial plains and foothills are characterized for presenting shallow soils, of a brown, reddish-brown, greenish color, formed by sandy-loam, clay-loam and clay-sandy loam sediments. They are not generally affected by salinization processes; in places where the latter do have effects on the soil, the reactions vary from neutral to strongly alkaline.

These soils and plateaus are uncultivated. The main limitations to their being used for agricultural purposes have to do with the fact that the soils are unformed and undeveloped, present a total absence of organic horizons, and endure an extremely cold weather characterized by severe frost.

The detailed description of the soils of the North, South and Main Ravines, together with those of the North and South Wetlands is presented in Chapter 3.

8.5. Flora

The flora, or vegetation cover, present in the Silala region is poor, characteristic of the region's ecosystem, and is represented by high altitude wetlands and a community of desert-like bushes. The flora is typical of the West Mountain Ranges and Bolivian High Plateau.

The wetlands are defined as permanently wet meadows that form slightly convex wide compacted cushion plants of a botanical composition that varies depending on the altitude in which they are found and the quality, quantity, and persistence of water. These ecosystems are highly fragile and sensible to any change, mainly in regard to water availability. The flora of the study area is strongly dominated by Juncaceae species represented by Oxichloe Andina and Distichia Muscoides. They are characterized by a low and compact growth, typical of zones with a high phreatic level.

It has been clearly confirmed that there is an absolute connection between the growth, or disappearance of the vegetation cover, or botanical resources and the degree in which water is available.

The wetlands of the Silala region have been highly affected by the construction of water catchment canals. Currently, there are only

vestiges of the original wetlands, which once covered a surface area of approximately 141,200 m2, or 14.1 hectares. The current surface area of the wetlands is only of an approximate 6,000 m2, or 0.6 hectares, and is surrounded by the water catchment works and artificial canals. As a result of this devastation that begun in 1908, the dominant flora species is paja brava (Fetusca Orthophylla), also known regionally as iry ichu. Together with the latter, the other long-grass species present in the area are the Stypa and Festusca spp.

The bushes of the desert-like Puna include several types of Thola (*Parastrephia, Adesmia, and Baccharis spp*). There are also Yareta plants (*Axorella compacta*), which grow sporadically in the slopes of Inacaliri and Silala volcanoes, and seem to have been overexploited. This species is classified as vulnerable in the international list of endangered species.

8.6. Fauna

Fourteen animal species were found to inhabit the study area during the several visits made. All these species are typical of habitats of the Bolivian high plateau and the West Mountain Range, and none of them are endemic, or endangered.

Some of these species are:
- Vicuna (Vicugna vicugna) – Huari – Swalla
- Viscacha or Andean Chinchillidae (Lagidum viscaccia cuvieri)

The following are found among the bird species:
- Pterocnemia pennata, Suri
- Nothoprocta ornata, Pisaka
- Larus serranus, Andean seagull
- Ana Puna, blue beak Puna duck, Chirokankana
- Anas flavirostris, yellow-billed teal, Uncayllu
- Petrochelin andecola, Andean swallow

Lizards of the Liolaemus genus were found among the reptile species, and the batrachian Telmatobius marmoratus among the amphibians observed in the

South Ravine.

The insects observed inhabiting the wetlands were:
- Butterflies
- Horseflies
- Common flies
- Small bees

No fish species have been found in the aquatic habitat of the study area.

8.7. Landscape

The modeling of the region's landscape and study area is intimately related with the different orogenic phases represented by the intrusion and deposition of volcanic rocks from the Miocene and Pliocene, along with the glacial and climatic activities, which acted as erosion and deposition agents during the Pleistocene. The physiographic landscape of the area can be described as wavy plateaus formed by ignimbrite rocks covered by loose sandy sediments, interrupted by mountain ranges formed by volcanoes, and volcanic cones and flows, which are regionally aligned from north to south and appear in positive irregular forms.

Due to its beauty, dominated by the presence of rocks of different colors and textures, the different structures modelled by atmospheric phenomena, mainly the wind and gravity, and the almost complete absence of vegetation, this landscape is denominated the "Natural Japanese Garden".

8.8. Historical and Archeological resources

No historical or archeological resources have been found in the study area. Two rustic houses presenting the characteristics of recent constructions (of the XX Century) have been found, and it is inferred that they were built by llama or cattle raisers. These houses are surrounded by stone walls that form corrals. Contemporary domestic utensils have been found inside them.

There are narrow dirt roads that head up to the slopes of Inacaliri, Silala, and Silala Chico volcanoes, and stone walls were built throughout them. These roads were supposedly used by yareta gatherers, to use yareta as an energy source in the middle of the past century.

No isolated artifacts, or casual findings have been found on the surface of the study area.

8.9. Human resources

There is no human presence in the area—the total human population is nil. The closest human center is found in Laguna Colorada, 38km to the south of the area, where there is a floating population of 22 people that do not have a permanent residence there. These people include the park rangers of the Eduardo Abaroa Andean Fauna National Reserve, and keepers of the ENDE facilities and rest areas for the tourists that stay overnight. In October 2000, seven of these people were women between 18 and 45 years old and 15 men between 20 to 56. Knowledge of and concern for the Silala Springs is almost nil, or of no interest to the population of Laguna Colorada, with the exception of the executives of the Reserve, who have expressed their deep concern for the lack of control and supervision in the Silala.

Laguna Colorada is an overnight and feeding site for tourists crossing from Uyuni to Laguna Verde (the border with Chile) and vice-versa. There are days in which the number of tourists in Laguna Colorada exceeds the fifty people. Most of the inhabitants

of Laguna Colorada work for thirty days in a row in the area, and take seven days of rest in the city of Uyuni.

There are no birth or death records in the study area.

9. CONCLUSIONS AND RECOMMENDATIONS

The study of the geological evolution and hydrological, hydrogeological, and environmental characterization of the Silala area has led to the following conclusions:

9.1. Regional Geology

The area of the Silala Springs was geologically formed during the Upper Miocene (7.5 to 8 Myr), when the Silala Ignimbrites were deposited. The latter were strongly fractured and jointed by tectonic movements caused by the Khenayani Faulting system. A second and strong volcanic activity was then manifested by the formation of volcanic cones (of 5.8 to 6.2 Myr) (the Inacaliri volcano and the Silala Chico, Negro and Torito hills). The third volcanic activity was the formation of stratovolcanoes (Inacaliri and Silala volcanoes) of an approximate age of 1.5 to 1.7 Myr, which resulted in a modification of the landscape of ignimbrite plateaus. The chemical composition of the rocks that resulted from these two last volcanic events are of andesitic-dacitic type. The third volcanic event was the most basic one in terms of chemical composition.

These volcanic features were thereafter modified by the subsequent deposition, formation, and action of large glacial masses that begun 65,000 years BP and extended until the Last Glacial Maximum, approximately 14,500 years BP. Regionally, the movement and melting of the glaciers resulted in major modifications of the regional geomorphology giving place to the current undulated plains landscape and formed valleys typical of glacial regions in the foothills of the volcanic cones. This glacial activity and the glacial meltwater resulted in the deposition of great volumes of Quaternary and Recent sediments.

The soils in the region are sandy, and sandy-loamy, present sub-rounded sand grains in their upper parts and sands with clasts, or quarry stones of up to 40cm in diameter. Locally, the soils present deposition in the surface and in their non-graded sequence of block deposition, together with clasts of different sizes of the parent rock, average sub-angular sand grains, and silt. Some of the soils present features of wind action. Wetlands resting on thin hydromorphic horizons of organic material that lies on fine sandy-loamy material can be found in the places where springs well up to the surface.

9.2. Geology of the Silala Ravine

The action of glacial meltwater is one of the most notorious geomorphological features on the rocks of the Silala Ravine, which is a typical example of a ravine formed by the erosive action of fluvioglacial water resulting from glacier melt dating to more than 10,000 years BP, which benefited from the weak zones caused by faults.

The Main Canal's Ravine and the South and North Ravines, which follow a 50° N to 65° E direction, constituted depressions in the Silala Ignimbrite, which formed throughout planes of weakness formed by the Silala Fault

and the high jointing rate that followed that same direction and dip. This coinciding path is confirmed by the study on the jointing system carried out in the area.

The fluvioglacial erosion of the ravines was thereafter completed by a strong weathering process on the ignimbrite rocks caused by the sharp differences of daily temperature, forming a "U"-shaped ravine, with vertical hillsides and widening the ravines—by up to 40m in the case of the Main Ravine. This process then gave place to a deposition of different sizes of rocks and clasts on the flat surface of the ravines. No active pluvial manifestations have been recorded since this last glacial period ended, all the contrary, the ravines are currently covered with different sizes of blocks, clasts, and sediments, which have not been removed owing to the absence of a natural water flow. All the blocks and clasts observed are angular and there is a complete absence of either rounded, or sub-rounded gravel or clasts.

It is also important to point out that throughout the hillsides of the Silala Ravine, and perpendicular to the latter, it is possible to observe different stages of ravine formation which result from simple mechanical weathering processes, and are not influenced by pluvial processes, or the action of water.

9.3. Soils in the Silala Ravine

These soils, as those of the whole region, are not mature and are composed of fluvioglacial sediments deposited with a non-graded sequence of angular clasts of the parent rock, average sub-angular sand grains, silt, and some thin horizons of organic material. The granulometric survey led to the conclusion that the soil profile is undeveloped, is characteristic of high mountain soils of fluvioglacial origin, and presents no recent pluvial movement. A clearly graded deposition of these materials was not observed. These less thick soils were also observed in the wetlands.

The analysis of soil profiles and the samples collected and analyzed evidence a granulometry typical of fluvioglacial soils, with angular clasts and grains, and a limited presence of rounded, or sub-rounded clast rocks, gravel, and sand. This is a notorious indication that the ravines have not received any significant water flow from any river or brook since their formation, 10,000 years ago.

9.4. Hydrology and Hydrogeology

Basically, there are no active surface waterbodies or courses in the whole area of study. The only active course found is the one that currently drives the waters by means of canals built at the outset of the XX Century. The current hydrological design of the area was modelled by glacial meltwater, and glacier movement and retreat. There is no solid geological evidence of the modification or formation of a recent hydrological network.

The average annual rainfall, recorded in 12 years, is of less than 60 mm and the evaporation rate is 15 times higher. This is evidence of the absence of surface water runoff—not even discontinuous—forming water currents, as rivers, or brooks. Consequently, there is a completely negative and striking hydric imbalance in the area.

The only sources of water in the area are the 70 small groundwater springs that emerge with very slow flows, forming small pooled waters. The springs concentrate in four main zones, two of which form wetlands. The wetlands of the study area cover a surface of 108,700 m2. The spring's flowrates vary from 0.25 l/sec to 2 l/sec and their temperature oscillates between 5 to 16 °C. These are good-quality, uncontaminated Type A waters (according to Bolivian standards).

The main groundwater aquifer of the study area is hosted in the Silala Ignimbrites and possibly in underlying rocks that do not outcrop in the area. This aquifer could be either confined or unconfined and might be fed by uncontaminated fossil waters stored at least 40 years ago. The conclusion, however, is that the Silala Springs waters are quite likely to have originated from a pluvial era, as the one that occurred during the Tauca phase, approximately 8,500 years ago. This aquifer possibly receives only a minimal recharge from current pluvial waters, inasmuch as these are practically nil. There is no other recharge source in the area.

Due to their hydro-chemical and physical properties, the waters that outcrop in the South, or Oriental Wetland are a little different that the waters of the North, or Cajones Wetland—the latter are purer.

Most of the springs found in the wetlands have been abstracted, canalized, and forced by means of a simple engineering work comprising two main open abstraction canals that merge with an additional one before entering the international border. The average flowrate measured in the South Canal, before the waterfall is of 40 l/sec. The average flowrate measured in the South Canal, before it meets the North Canal is of 129 l/sec. The flowrate of the North Canal is of 42 l/sec and that of the Main Canal is of 164 l/sec.

Without the engineering works, it would be really difficult and certainly improbable for the outcropping waters of the Silala Springs to have a natural flow towards the ravines of the wrongly referred to Silala 'River'.

9.5. Environment

A summary of the preliminary environmental baseline of the Silala is presented below:

- There are no surface waterbodies in the study area, with the exception of those that emerge from the springs found throughout the wetlands.
- The waters that outcrop in the Silala wetlands are of Type A, and are uncontaminated.
- The soils and plains are uncultivated. Regionally, the soils of the Silala present two very marked physiographical shapes, in both the ignimbrite plateaus and the alluvial plains. The foothills present shallow soils of a brown, reddish-brown color, and a light texture varying from sandy-loamy to clay-loamy.

- The flora, or vegetation cover present in the study area is poor, and characteristic of the region's ecosystem. It is represented by high altitude wetlands and a community of bushes typical of the desert-like Puna.
- Fifteen animal species have been found to inhabit the study area. All the species observed are common of the habitats of the Bolivian High Plateau and of the West Mountain Ranges—none of them is endemic or endangered.
- Owing to the beauty of its landscape, this region is denominated the "Natural Japanese Garden".
- No historical or archeological resources have been found in the area of study.
- There is no human presence in the area. The total amount of population is nil.

To complete, or complement the present study of the Silala Springs, the following actions and additional works are necessary:

> The drilling of at least four reverse circulation appraisal wells must be scheduled. Two of these wells must be drilled in the surroundings of the South Wetland (Oriental). One will be set up as an observation well and will determine the current and potential production parameters on the basis of a quantification of hydraulic characteristics, and the second one will determine the pumping tests parameters.

> The estimated depth of these wells will be between 300m and 400m, with a minimum bore diameter of 5½ inches. Coating should be used in the first few meters of drilling to avoid possible contamination.

10. BIBLIOGRAPHIC REFERENCES

Argollo, J., Gouze, P., Saliege J.F., & Servant, M., 1987. Fluctuations des Glaciers de Bolivie au Quatemarie Récent. - (in Seminare "Palélacks-Paléoclimats en Amérique Latine et an Afrique" (20.000 ans B.P.- Actuel) [Fluctuations of the Bolivian Glaciers in the Recent Quaternary. - (in Seminary "Palelacks-Paleoclimates in Latin America and Africa (20,000 years B.P.-Present)] ORSTOM, Bondy, Vol. 1: 15 - 17 - Géodinamique,2 (2): 103 - 104.

Argollo, J., 1991. El Cambio Global del Clima y sus Eventuales Efectos en Bolivia. Boletin de la Sociedad Geologica de Bolivia, V. 6 [Global climate change and its eventual effects in Bolivia. Newsletter of the Geological Society of Bolivia, 6th version]: p. 33 - 44, August 1991, La Paz.

Argollo, J., Mourguirat, P., 1995. Paleohidrologia de los Ultimos 25,000 Años en los Andes Bolivianos. Bull. Indt. Fr. Etudes Andinos [Paleo-hydrology of the last 25,000 years in the Bolivian Andes. International Yearbook of Andean Studies]. No. 24 (3). Pages 551 - 562. Paris, France.

Choque M. N. 1996. Hoja Volcan Putana. Escala 1:100.000 [Putana Volcano sheet. Scale: 1:000.000] SGM publication SERIES 1-CGB-41.

Bolivian Military Institute of Geography (IGM, for its acronyms in Spanish), Sheets 927-1; 5928-II; 6028-III; 6027-IV, at a scale of 1: 50,000.
Bolivian Military Institute of Geography (IGM) Sheets S -19-7 Y SF-19-11, at a scale of 1: 250,000.

Lema, Z. J.C., Ramos, C., W. 1996. Zanabria sheet. At a Scale 1:100.000. SGM publication, I-CGB-43.

Montes de Oca, Ismael, 1997. Geografia y Recursos Naturales de Bolivia [Geography and Natural Resources of Bolivia]. Offset Boliviana Ltda. "EDOBOL". La Paz, Bolivia.

PMA, in prep. Base de Datos Radimetricos (DataRad) de Bolivia. Proyecto Andino: Geociencias para la Comunidad Andina [Radiometric Data Base of Bolivia. Andean Project: Geosciences for the Andean Community]. SERGEOMIN. La Paz, Bolivia.

Ricther, D. H., Ludington, S., Soria-Escalante, E. 1992. Geologic Setting of the Geology and Mineral Resources of Altiplano and Cordillera Occidental, Bolivia. U.S. Geological Survey Bulletin 1975, p. 14 - 24.

Risacher, F., 1976. Reconocimiento de Algunos Salares del Altiplano Boliviano: La Paz, Universidad Mayor de San Andres y l'Office de la Reserche Scientifique et Technique [Survey of some of the salt flats of the Bolivian high plateau: La Paz, Higher University of San Andres and The Office of Scientific and Technical Research.

SERGEOMIN, 1966 - 2001. Informes, Boletines, Mapas y Estudios [Reports, Bulletins, Maps, and Studies].

Uribe, H., Per. Com. Datos Radiometricos de Rocas Volcanicas, Programa Multiandino [Radiometric data of volcanic rocks], June 2001, SERGEOMIN.